NASA Contractor Report 159320

NASA-CR-159320
19800024025

Study of Methane Fuel For Subsonic Transport Aircraft

L.K. Carson
G.W. Davis
E.F. Versaw
G.R. Cunnington, Jr.
E.J. Daniels

LOCKHEED-CALIFORNIA COMPANY
BURBANK, CALIFORNIA

CONTRACT NAS-1-15239
SEPTEMBER 1980

National Aeronautics and
Space Administration

Langley Research Center
Hampton, Virginia 23665

FOREWORD

This is the final report of a study on the use of methane as a cryogenic fuel for subsonic transport aircraft. It covers not only the cost and performance implications relative to the aircraft, but addresses the airport facility requirements for the liquefaction and storage of methane as a fuel supply.

The work was done under contract NAS 1-15239 for the NASA Langley Research Center, Hampton, Virginia. Mr. Robert D. Witcofski of the Aeronautical Systems Division was the NASA technical monitor for the study.

The Lockheed-California Company was the prime contractor to NASA and the work was performed in the Commercial Advanced Design Division at Burbank, California. Important phases of the work which required specialization were subcontracted to other organizations. The individuals named below were the principal contributors.

Lockheed-California Company

G.D. Brewer	Study Manager
L.K. Carson	Project Engineer
George Davis	Structures
Edward Versaw	Fuel Systems
Roger Jensen	Weights
J.R. Wilson	Propulsion
L.A. Vaughn	Cost Analysis
C.F. Friend	Aerodynamics
J.J. Rising	Stability and Control

Lockheed Missiles and Space Company, Inc.

George Cunnington, Jr. — Cryogenic Insulation

Air Research Division of the Garrett Corp.

James C. Riple — Heat Exchangers

Institute of Gas Technology

E. J. Daniels — Airport Facility Requirements

N80-21523 # 1

TABLE OF CONTENTS

Section		Page
	Foreword	iii
	List of Figures.	
	List of Tables	
	Summary.	1
	Introduction	4
	Nomenclature	6
1.	Technical Approach	8
1.1	Part One	9
1.1.1	Phase 1: Aircraft design and configuration studies	9
1.1.2	Phase 2: Aircraft fuel system design.	9
1.1.3	Phase 3: Airport requirements	9
1.1.4	Phase 4: Comparative evaluations.	9
1.2	Part Two	10
1.2.1	Phase 5: Extend the methane design study to four additional design ranges.	10
2.	Aircraft Technology Description.	12
2.1	Aerodynamics	12
2.1.1	Technology level	12
2.1.2	Tail sizing requirements	16
2.2	Propulsion	21
2.2.1	Engine cycle selection and installation losses	21
2.2.2	Initial LH_2 engine cycle selection	22
2.2.3	The weight, geometry, and scaling relationship	23
3.	Aircraft Design Development	27
3.1	Configurations	27
3.2	Preliminary Fuel Tank Insulation Concepts and Weight Estimate	

TABLE OF CONTENTS (Continued)

Section		Page
4.	Aircraft Parametric Analysis and Configuration Selection	42
4.1	Performance Analysis of Three Candidate Methane Configurations for the 400 Passenger/10 186 (5500 n.mi.) Payload/Range	42
4.1.1	Safety	54
4.1.2	Thermal Compatibility	56
4.1.3	Operations	61
4.1.4	Configuration selection	61
4.2	Extended Matrix of All Aircraft to Other Payload Ranges	61
4.3	Benefits of Subcooling Fuel	65
5.	Structural Design and Analysis of Methane Fuel Tanks	71
5.1	Tank Structure	71
5.1.1	Structural design criteria	71
5.1.2	Fatigue design criteria	76
5.1.3	Fail-safe design criteria	77
5.2	Tank Design	78
5.2.1	Forward tank	79
5.2.2	Aft tank	98
5.3	Final Design	111
6.	Fuel System	112
6.1	Fuel-Oriented Functions	112
6.1.1	Fuel storage	112
6.1.2	Fueling and defuling	117
6.1.3	Engine fuel supply	120
6.1.4	Liquid methane pump technology	125
6.1.5	Anxiliary power unit fuel supply	125
6.1.6	Fuel transfer	128
6.1.7	Fuel management	128
6.1.8	Fuel jettison	128

TABLE OF CONTENTS (Continued)

Section		Page
6.1.9	Tank vent and pressurization system.	130
6.1.10	Leak detection and vapor purge	137
6.2.1	Fuel level control shutoff valve	146
6.2.2	Ground fueling quick disconnect.	148
6.2.3	Vapor recovery quick disconnect.	150
6.2.4	Absolute tank pressure relief and vent valve	150
6.2.5	Absolute tank pressure regulator	154
7.	Engine-mounted Liquid Methane Heat Exchangers.	155
8.	Fuel Tank Insulation	163
8.1	Design Criteria and Concepts	164
8.1.1	Criteria	164
8.1.2	Concepts	165
8.2	Concept Screening	169
8.2.1	Safety analysis	170
8.2.2	Performance analysis	171
8.2.3	Producibility and operations analysis.	189
8.2.4	Candidate selection	189
8.3	Analysis of Selected Candidate	190
8.3.1	Configuration of candidate system.	190
8.3.2	Analysis method.	193
8.3.3	Analysis results	196
9.	Airport Facility Requirements.	220
9.1	The Conceptual Physical Configuration of the Ground Systems	224
9.1.1	Select a preferred liquefaction cycle and requirements . . .	224
9.1.2	Requirements for LCH_4 storage.	233
9.1.3	LCH_4 distribution and aircraft refueling system requirements	247
9.1.4	LCH_4 processing requirements	262
9.2	Assessment of the Ground System Operating Procedure	271

TABLE OF CONTENTS (Continued)

Section		Page
9.3	Energy consumption of the natural gas feed ground system	274
9.3.1	Energy consumption of the natural gas feed ground system	274
9.3.2	Energy consumption of the substitute natural gas feed ground system	275
9.3.3	Effect of feedgas inlet conditions on fuel gas requirements	277
9.3.4	Energy consumption as a function of degree of subcooling	277
9.4	Estimate of the Capital and Operating Costs of Ground System	281
9.4.1	Economic trade-off analysis (number of liquefaction trains)	281
9.4.2	Capital costs	282
9.4.3	Operating costs	285
9.4.4	Results	286
9.4.5	Additional costs for storing, distributing, and fueling of aircraft with LH_2, LCH_4 and Jet A	287
9.5	Evaluation of the Relative Safety of the LCH_4 Ground System	293
9.5.1	Physical Properties	294
9.5.2	Combustion-related properties	298
9.5.3	Overview of relative hazards	300
9.5.4	Spacing requirement	300
9.5.5	Additional safety standard requirements	303
9.5.6	Possible safety standard changes	303
9.5.7	Federal legislation	304
9.5.8	Review of the LNG industry safety record	306
9.6	Conclusions	307
10.	Technology Development Required	308
10.1	Airport Facility Requirements	308
10.2	Aircraft Component and Systems Developme t	308
10.2.1	Structural element tests	308

TABLE OF CONTENTS (Continued)

Section		Page
10.2.2	Small component tests.	309
10.2.3	Large-Scale tank fabricationand test	309
10.2.4	Pumps and other functional equipment development	309
11	Conclusions.	310
Appendix A	Description of Commercially Available Baseload LNG Liquefaction Processes.	317
Appendix B	Computer Printout Pages for Final Designs of LH_2, LCH_4, and Jet A Aircraft	327
References		345

LIST OF FIGURES

Figure		Page
1	Correlation of life cycle of new transport aircraft with forecasts of oil availability	4
2	Supercritical flow development, Mach 0.83	14
3	Profile drag polar	15
4	Drag rise characteristics	15
5	Configuration 1, horizontal tail sizing summary chart	18
6	Analysis results for Configuration 1, takeoff, engine-out, air minimum control speed vertical tail size requirement	19
7	Cross plot of data for Configuration o, takeoff, engine-out, air minimum control speed vertical tail size requirement	20
8	Effect of fan pressure ratio and bypass ratio on direct operating cost	24
9	Envelope drawing, selected baseline LH_2 and LCH_4 engine	25
10	Methane Configuration 1, all fuel in the fuselage	28
11	Internal wing tank concepts	30
12	Methane Configuration 2, fuel in fuselage plus wing	31
13	Methane Configuration 3, fuel in wing plus pylons	33
14	General range of methane pylon tank	34
15	Summary of fuel tank concepts	37
16	DOC evaluation, configuration 1	44
17	TOGW evaluation, configuration 1	45
18	Airplane cost evaluation, configuration 1	46
19	DOC evaluation, configuration 2	47
20	TOGW evaluation, configuration 2	48
21	Airplane cost evaluation, configuration 2	49
22	DOC evaluation, configuration 3	50
23	TOGW evaluation, configuration 3	51

LIST OF FIGURES (Continued)

Figure		Page
24	Airplane cost evaluation, configuration.	52
25	Composite wing structure and tank concept for liquid methane.	57
26	Temperature gradients and stress level, upper wing surface.	58
27	Growth effects	66
28	Mission capability versus energy	67
29	Sensitivity of DOC to fuel cost, short-range aircraft.	68
30	Sensitivity of DOC to fuel cost, long-range aircraft	68
31	Short range aircraft, 130 passengers/2778 m (1500 n.mi.) . . .	69
32	Design speeds versus altitude.	73
33	Fuselage aftbody limit loads, PLA and abrupt pitching maneuver conditions.	74
34	General arrangement drawing.	79
35	Concept of primary supporting structure for forward tank . . .	80
36	Concept of fail-safe strap reinforcement for forward tank	81
37	General dimensions of forward tank	86
38	Applied ring loads on the forward tank	88
39	Reinforcement ring loading diagrams for forward tank	89
40	Internal loads for reinforcement rings of forward tank	90
41	Section property data for reinforcement rings.	91
42	Compression design allowables for reinforcement rings.	91
43	Pin and trunnion design.	95
44	Typical skin panel for forward tank.	95
45	Fail-safe strap and skin panel oayout for forward tank	96
46	Quadrant panel assembly for forward tank	96
47	Final weld-up of forward tank.	97
48	General design of forward tank for a methane-fueled transport.	99
49	Basic dimensions of aft tank	101

LIST OF FIGURES (Continued)

Figure		Page
50	General design of aft tank for a methane-fueled transport.	113
51	Fuel system schematic.	115
52	Layout-fueling/defuel system	118
53	Refuel panel	119
54	Quick disconnect, ground fueling and vapor return.	121
55	Fuel level control valve	122
56	Fueling shutoff valve.	122
57	Tank isolation valve	123
58	Crossfeed valve assembly	124
59	Fuel-line cross section	125
60	Boost pump assembly and installation	126
61	Engine feed line sizing	127
62	Center of gravity travel with blocked feed line.	129
63	Tank pressure control assembly	131
64	Overboard vent and back pressure valve	133
65	Vent and prssurization system	134
66	Alternate vent installation.	135
67	Vapor efflux rate during refueling	135
68	Vent line sizing	136
69	Leak detector system (integral tank structural details eliminated for clarity).	138
70	Aft tank (integral) insulator.	139
71	N_2 purge system scheumatic	141
72	Purge airflow rate	143
73	Foam purge air drier system.	144
74	Fuel level control shutoff valve	147
75	Ground fueling quick disconnect	149
76	Vapor recovery quick disconnect	151
77	Absolute tank pressure regulator (relief valve and vent valve).	153

LIST OF FIGURES (Continued)

Figure		Page
78	Exhaust emissions from a single aircraft turbojet combustor (reference: NASA TM-73780)	155
79	Absolute tank pressure regulator	156
80	Engine-mounted liquid methane heat exchanger system	157
81	LCH_4 engine fuel and heat exchanger system	158
82	Turbine-cooling air to methane heat exchanger	159
83	Engine oil to methane heat exchanger	160
84	Engine exhaust fuel heater	161
85	Schematic of insulation concepts	166
86	Vacuum system for evacuated microsphere insulation system no. 5	167
87	Purge system for external GH_2 purged insulation system no. 6	168
88	Thermal conductivity of candidate insulations	174
89	Comparison of six insulation concepts for the aft fuselage tank	176
90	Comparison of internal insulations for the wing tanks	177
91	Forward tank - Configuration 1, polyurethane foam (Stepan foam)	178
92	Aft tank, Configuration 1, polyurethane foam (Stepan foam)	179
93	Stepan foam - Configuration 1	180
94	Forward tank, Configuration 1, microsphere insulation 68.9 kg/m^3 (4.3 lb/ft^3) with 5 mil SS jacket - M_i includes 92.7 kg (200 lbs) for vacuum system	181
95	Aft ank, Configuration 1, microsphere insulation 68.9 kg/m^3 (4.3 lbs/ft^3) includes 5 mil SS VAC jacket plus 92.7 kg (200 lb) for vacuum system	182
96	Configuration 1, microsphere insulation forward and aft tanks	183
97	Forward tank, Configuration 1, PPO 38.4 kg/m^3 (2.4 lb/ft^3) internal foam	184
98	Aft tank, Configuration 1, PPO 38.4 kg/m^3 (2.4 lb/ft^3) internal foam	185

LIST OF FIGURES (Continued)

Figure		Page
99	Configuration 1, internal PPO foam	186
100	Internal wing tank, Configuration 2, PPO internal foam	187
101	Pylon tank, Configuration 3, external Stepan foam.	188
102	Pylon tank, Configuration 3.	189
103	General dimensions of forward methane tank	191
104	Aft tank configuration	192
105	Forward tank insulation.	192
106	Aft tank insulation - cylindrical section.	193
107	Tank insulation and vent model for analysis of selected candidate	195
108	Mass of fuel vented on ground and in-flight and mass evaporated in-flight as a function of insulation thickness for 145 kPa (21 psia) saturated liquid fill.	198
109	Mass for fuel vented on ground and in-flight and mass evaporated in-flight as a function of insulation thickness for 124 kPa (118 psia) saturated liquid fill	199
110	Mass of fuel evaporated and vented as a function of primary insulation thickness for 103 kPa (15 psia) saturated liquid fill, aft tank	200
111	Sum of weights of insulation and fuel evaporated in-flight as a function of insulation thickness and liquid saturation pressure at fill	202
112	Mass of fuel evaporated and vented as a function of insulation thickness for 145 kPa (21 psia) saturated liquid fill, forward tank	203
113	Mass of fuel evaporated and vented as a function of insulation thickness for 124 kPa (18 psia) saturated liquid fill, forward tank	203
114	Mass of fuel evaporated and vented as a function of insulation thickness for 103 kPa (15 psia) saturated liquid fill, forward tank	204
115	Sum of insulation and fuel evaporated during flight weights and functions of insulation thickness and fill condition (P_{SAT})	205
116	Aft tank pressure and liquid temperature histories, 124 kPa (18 psi) fill, t_{ip} = 2.54 cm (1.0 inch).	206

Figure		Page
117	Aft tank pressure and liquid temperature histories, 124 kPa (18 psia) fill, t_{ip} = 5.08 cm (2.0 inch)	206
118	Aft tank pressure and liquid temperature histories, 124 kPa (18 psia) fill, t_{ip} = 7.62 cm (3.0 inch)	207
119	Aft tank pressure and liquid temperature histories, 103 kPa (15 psia), t_{ip} = 2.54 cm (1.0 inch).	207
120	Aft tank pressure and liquid temperature histories, 103 kPa (15 psia) fill, t_{ip} = 5.08 cm (2.0 inch)	208
121	Aft tank pressure and liquid temperature histories, 103 kPa (15 psia) fill, t_{ip} = 7.62 cm (3.0 inch)	209
122	Forward tank pressure and liquid temperature histories, 145 kPa (21 psia) fill, t_i = 6.35 cm (2.5 inch).	
123	Forward tank pressure and liquid temperature histories, 124 kPa (18 psia) fill, t_i = 6.35 cm (2.5 inch)	210
124	Forward tank pressure and liquid temperature histories, 69.0 kPa (10 psia) fill, t_i = 6.35 cm (2.5 inch)	212
125	Comparison of feed line weights (inner line weight not included	215
126	Engine feed line 3.18 cm (1 1/4 inch) Stepan foam BX250A outer cover = ϵ 0.1.	218
127	Tank fill and vent lines, Stepan foam BX250A outer cover = ϵ 0.1.	219
128	Major facilities for SFO ground system	224
129	Relative annual cost of liquefaction cycles.	236
130	LCH_4 production versus demand cycle (single train liquefaction).	238
131	LCH_4 production versus demand cycle (dual train)	240
132	Storage tankage capacity requirements as a function of liquefaction train capacity	241
133	Unit costs of LCH_4 storage tank.	242
134	Storage tank cost versus insulation thickness.	243
135	Maximum storage tank steady-state boil-off versus insulation thickness	245
136	Ground system direct operating cost versus insulation thickness	245

LIST OF FIGURES (Continued)

Figure		Page
137	Insulation thickness versus direct operating cost at different fuel gas costs.	246
138	Typical LCH_4 hydrant pit	248
139	Flow schematic, hydrant fueling.	249
140	Distribution loop concept plan	250
141	Expansion joint with concrete enclosure.	257
142	Cost of LCH_4 transport by pipeline, truck, and rail tank car	259
143	Average cost of LCH_4 transport	262
144	LCH_4 boil-off vs. LCH_4 temperature and aircraft tank design pressure.	265
145	Refrigeration horsepower requirements for subcooling	266
146	Subcooling concept	267
147	Liquid N_2 subcooler.	268
148	Conceptual ground.	272
149	Natural Gas System energy consumption.	275
150	Substitute natural gas system energy consumption	276
151	Effect of feedgas temperature and pressure on fuel-gas requirements.	278
152	Quantity of LN_2 required for LCH_4 subcooling	278
153	Quantity of makeup LN_2 required for LCH_4 subcooling.	279
154	Ground system electricity requirement as a function of subcooling.	280
155	Liquefaction train direct cost vs. design capacity	282
156	Total cost of liquefaction and storage as a function of number of liquefaction trains.	283
157	Air separation plant and subcooler direct cost as a function of degree of subcooling	288
158	Total capital investment as a function of degree of subcooling and feedgas cost	290
159	Total annual operating cost of ground system as a function of feedgas cost and subcooling	293
160	Effect of temperature on specific gravity of methane vapor.	295

LIST OF FIGURES (Continued)

Figure		Page
161	Effect of temperature on specific gravity of hydrogen vapor	296
162	Plan view of the LCH_4 storage tanks.	301
163	Dike or impounding wall proximity to containers (reference 71)	302
164	Aft tank installation.	311
165	General design of aft tank for a methane - fueled transport.	313
166	Propane precooled MCR process - schematic (refernce 36). . .	319
167	Natural gas processing scheme incorporating the PRICO process.	320
168	Prico Process (Reference 42)	322
169	Phillips improved optimized cascade liquefaction cycle (reference 28)	324

LIST OF TABLES

Table		Page
1	Summary of Study Results	2
2	Properties of Candidate Fuels	5
3	Extended Matrix of Methane Transports	10
4	Basic Guidelines for Design of Methane, Hydrogen and Jet A Aircraft	11
5	Baseline Hydrogen Engine Characteristics at Cruise	22
6	Baseline Engine Characteristics SLS, Uninstalled Standard Day	26
7	Theromodynamic Design Parameters for Methane Engine	26
8	Pylon Tank Volume Allowances	35
9	Preliminary Insulation System Weights for the Baseline Configuration 1	39
10	Comparison of Candidate Methane Configurations	53
11	Hydrogen, Methane and Jet A Fueled Transport Configurations	55
12	Runway Lengths of World's Major Airports	62
13	Principal Operating Constraints for All Aircraft	63
14	Summary of Study Results	64
15	Percentage Reduction of Cost and Weight Factors Gained by Increasing TOFL and Approach Speed of 400 PAX/10 186 km (5500 n.mi.) Aircraft	65
16	Initial Values, Design Weight Summary	72
17	Methane Tank Operating Pressures	75
18	Combined Loads and Internal Pressure Criteria	77
19	Circumferential Design Stresses	78
20	Forward Tank Design Pressures	82
21	Minimum Skin Thicknesses for Forward Tank(1) (Excludes Damage Tolerance Conditions)	84

LIST OF TABLES (Continued)

Table		Page
22	Fail-Safe Requirements Forward Tank	85
23	Summary of Skin Thickness and Fail-Safe Strap Requirements for Forward Tank	86
24	Structural Analysis of Reinforcement Ring for Forward Tank.	92
25	Aft Tank Design Pressures	102
26	Point Design Internal Load Environment for Aft Tank	103
27	Minimum Skin Thickness Requirements for Aft TAnk	104
28	Fail-Safe Requirements of Aft Tank, Circumferential Damage Condition.	105
29	Shell Strength Requirements of Aft Tank	107
30	Frame Stiffness Requirements for Aft Tank	109
31	Frame Strength Requirements for Aft Tank	109
32	Frame and Hoop Strap Fail-Safe Requirements for Aft Tank.	110
33	Summary of the Frame and Hoop Strap Requirements for Aft Tank.	111
34	Weight and Balance Data Baseline Configurat 1	130
35	Air Purge System Weight EStimate.	145
36	Pressure Regulator Design Parameters.	154
37	Liquid Methane Heat-Exchanger Design Conditions	163
38	Candidate Insulations Analyzed for each of four Tank Configurations	169
39	Safety Ranking Criteria	170
40	Mission Fuel Schedule	172
41	Data Sources for Properties for Insulation Concepts	173
42	Screening Analysis.	190
43	Analysis Program Parameters	194
44	Summary of Fuel and Insulation Weights as a Function of Insulation Thickness and Fuel Saturation Pressure at fill .	201
45	Forward Tank - Summary of Fuel and Insulation Weight as a Function of Insulation Thickness and Fuel Saturation Pressure at Fill.	209

LIST OF TABLES (Continued)

Table		Page
46	Aft Tank Wall Temperature Distribution ^{o}K (^{o}R)	211
47	Aft Tank Vapor Barrier and Fuselage Exterior Temperature Distributions ^{o}K (^{o}R)	213
48	Forward Tank Wall Temperature Distribution for 15 percent Liquid Level t_{ip} = 5.08 cm (2.0 inch).	214
49	Inputs and Outputs of the Ground System	222
50	Preliminary Estimate of Liquefaction Facility Design Capacity	225
51	Cryogenic Heat Exchangers	230
52	List of Compressors and Drivers	231
53	Cost Estimate, Cascade Cycle.	234
54	Cost Estimate, Propane-Precooled Multicomponent	234
55	Cost Estimate, Multicomponent Cycle	235
56	Cost Estimate, Expander Cycle	235
57	Comparison of Liquefaction Cycles	236
58	LCH_4 Demand to be Met from Storage (Single Train)	238
59	LCH_4 Demand to be Met From Storage (Dual Train)	240
60	Cost Components of Aluminum, Double-Wall Aboveground Tankage for LCH_4.	243
61	LCH_4 Trailer Truck Requirements	260
62	Cost of Truck Transport of LCH_4	261
63	Cost of Pipeline Transport of LCH_4.	261
64	Summary of Actual Vapor Losses in Conceptual System KG(LB)/YR	272
65	Estimated Energy Consumption of LCH_4 Ground System With Natural Gas Feed	276
66	Equipment Requirements for Subcooling Concept	279
67	Cost Assumption, LCH_4 Ground System	284
68	Equipment List of Major Items: LCH_4 Ground System.	285
69	Equipment List of Major Items: LCH_4 Ground System.	286
70	Annual Operating Costs, LCH_4 Ground System, Natural Gasfeed, No Subcooling.	291

LIST OF TABLES (Continued)

Table		Page
71	Annual Operating Costs, LCH_4 Ground System, Substitute Natural Gasfeed, No Subcooling	292
72	Physical Properties of Methane and Hydrogen.	294
73	Combustion-Related Properties of Methane and Hydrogen. . .	298

SUMMARY

This investigation was an assessment of the potential of liquid methane as an alternate fuel for subsonic commercial transport aircraft. This study is the fifth of a series which follows those shown as References 3, 4, 5 and 6 which investigated the use of liquid hydrogen as a cryogenic fuel. The base line LH_2 and Jet A transports developed in the referenced series of reports have been brought forward into this study so that a comparison of the technical benefits and performance of all three alternate fueled aircraft could be presented as in table 1.

Other specific technical purposes of this work were:

- To determine a suitable methane fueled aircraft configuration (Sections 3 and 4)
- Provide a concept and structural analysis of methane cryogenic fuel tanks (Section 5).
- Establish a fuel system configuration and its functional requirements (Sections 6 and 7).
- Screen the most likely fuel tank insulation materials and analyse the best candidate system (Section 8).
- Determine the airport ground facility requirements for the liquefaction, storage and distribution of methane and estimate the capital investment and annual operating costs (Section 9).

The potential of subcooling the liquid methane to reduce fuel losses, reduce tank insulation weight and to favorably influence DOC is discussed in four parts:

- Section 4.3 - The effect on aircraft weight and DOC. The fuel cost contained in this DOC was assigned by NASA at the beginning of the study.
- Section 8.3.3 - Subcooling as a variable in the thermal analysis of the tank insulation system.
- Section 9.5 - Subcooling as a factor in the capital and operating costs of the airport liquefaction, storage and distribution facilities.
- Section 11 - Conclusions regarding subcooling.

The net result of these investigations is that the cost of subcooling outweighs the aircraft DOC benefits by a factor of 2 to 1 and, therefore, it has not been incorporated into the airplane design. This latter DOC includes the fuel cost to the airline as loaded aboard the aircraft. It

TABLE 1. - SUMMARY OF STUDY RESULTS

(All aircraft cruise at Mach 0.85 with 2438 m (8000 ft) TOFL and 250 km/hr (135 knots) approach speed)

	Units	Short Range 130 pax 2778 km (1500 n.mi.)			Medium Range 200 pax 5556 km (3000 n.mi.)			Medium Range 400 pax 5556 km (3000 n.mi.)		
		LH_2	LCH_4	Jet A	LH_2	LCH_4	Jet A	LH_2	LCH_4	Jet A
Wing Loading	$\frac{kg}{m^2}$ $\left(\frac{lb}{ft^2}\right)$	493.6 (101.1)	521.9 (106.9)	537.0 (110.0)	513.6 (105.2)	574.0 (117.5)	598.0 (122.5)	512.6 (105.0)	564.8 (115.7)	586.8 (120.2)
Thrust/Weight	$\frac{N}{kg}$ (-)	3.75 (0.382)	3.63 (0.370)	3.63 (0.370)	3.29 (0.335)	3.13 (0.319)	3.25 (0.331)	3.14 (0.320)	3.02 (0.308)	3.13 (0.319)
Gross Weight	kg (lb)	45 510 (100 340)	50 060 (110 360)	48 480 (106 880)	79 600 (175 490)	93 790 (206 770)	90 160 (198 770)	143 330 (315 990)	168 770 (372 070)	167 080 (368 360)
Block Fuel	kg (lb)	2 011 (4434)	4 803 (10 588)	5 784 (12 752)	6 482 (14 291)	16 772 (36 976)	19 130 (42 126)	10 850 (23 197)	27 760 (61 198)	32 700 (72 101)
OEW	kg (lb)	29 780 (65 650)	30 400 (67 015)	27 540 (60 721)	51 540 (113 628)	53 720 (118 441)	47 300 (104 291)	90 340 (199 167)	95 350 (210 214)	87 700 (193 422)
Wing Area	m^2 (ft^2)	92.2 (993.0)	95.9 (1032.0)	90.3 (972.0)	155.0 (1668)	163.5 (1760)	150.8 (1623)	279.5 (3009)	298.8 (3216)	284.8 (3066)
Span	m (ft)	30.4 (99.8)	31.7 (104.1)	31.5 (103.4)	38.4 (125.9)	39.7 (130.1)	38.3 (125.8)	51.5 (169.1)	53.6 (175.9)	52.7 (172.9)
Fus. Length	m (ft)	41.7 (137.0)	40.6 (133.2)	34.4 (113.0)	52.7 (173.0)	51.8 (170.0)	44.1 (144.7)	64.0 (210.0)	61.0 (200.0)	60.0 (197.0)
SFC (Cruise)	$\frac{kg}{hr}$/daN $\left(\frac{lb/hr}{lb}\right)$	0.206 (0.202)	0.503 (0.493)	0.613 (0.601)	0.206 (0.202)	0.501 (0.491)	0.610 (0.598)	0.206 (0.202)	0.501 (0.491)	0.611 (0.599)
L/D (Cruise)	- (-)	16.13 (16.13)	17.74 (17.74)	17.58 (17.58)	15.82 (15.82)	16.54 (16.54)	16.87 (16.87)	17.10 (17.10)	18.21 (18.21)	18.54 (18.54)
Thrust/Engine	N (lb)	85 250 (19 165)	90 810 (20 417)	87 950 (19 773)	65 380 (14 698)	73 350 (16 490)	73 160 (16 448)	116 890 (25 279)	127 440 (28 650)	130 670 (29 377)
TOFL	m (ft)	2 442 (8011)	2 397 (7863)	2 350 (7711)	2 104 (6902)	2 436 (7991)	2 444 (8017)	2 194 (7199)	2 441 (8010)	2 441 (8009)
APP Speed	$\frac{m}{s}$ (Keas)	69.4 (135)	69.4 (135)	69.4 (135)	69.4 (135)	69.4 (134.9)	69.4 (134.9)	69.6 (135.3)	69.4 (135)	69.4 (135)
Price/Aircraft	$\$10^6$ $(\$10^6)$	15.77 (15.77)	15.89 (15.89)	14.43 (14.43)	25.20 (25.20)	25.95 (25.95)	23.17 (23.17)	39.22 (39.22)	40.61 (40.61)	37.60 (37.60)
DOC	$\frac{Cents}{Seat\ km}$ $\frac{Cents}{Seat\ n.mi.}$	1.312 (2.429)	1.187 (2.199)	1.231 (2.179)	1.129 (2.091)	1.040 (1.925)	1.074 (1.988)	0.839 (1.554)	0.761 (1.410)	0.811 (1.501)
Energy Utilization	$\frac{Btu}{Seat\ n.mi.}$ $\frac{Btu}{Seat\ n.mi.}$	667 (1173)	664 (1167)	685 (1203)	699 (1229)	754 (1325)	735 (1292)	585 (1028)	624 (1096)	629 (1106)

	Units	Mach 0.85 Cruise 8000 ft TOFL and 135 knots Approach Speed			Effect of Extending TOFL and Approach Speed To 3200 m (10 500 ft) and 259 $\frac{km}{hr}$ (140 knots)			Very Long Range Aircraft at TOFL and Approach Speed of 5486 m (12000 ft) and 259 $\frac{km}{hr}$ (140 knots)		
		Long Range 400 pax 10 186 km (5500 n.mi.)			Long Range 400 pax 10 186 km (5500 n.mi.)			Very Long Range 400 pax 18 520 km (10 000 n.mi.**)		
		LH_2	LCH_4	Jet A	LH_2	LCH_4	Jet A	LH_2	LCH_4	Jet A
Wing Loading	$\frac{kg}{m^2}$ $\frac{lb}{ft^2}$	568.8 (116.5)	585.8 (120.0)	610.3 (125.0)	581.0 (119.0)	659.1 (135.0)	634.1 (130.0)	634.7 (116.6)	649.3 (133.0)	681.5 (139.6)
Thrust Weight	$\frac{N}{kg}$ (-)	3.20 (0.326)	3.14 (0.320)	3.19 (0.325)	2.97 (0.303)	2.91 (0.297)	2.91 (0.297)	2.69 (0.274)	2.62 (0.267)	2.62 (0.267)
Gross Weight	kg (lb)	168 740 (372 000)	225 580 (497 300)	232 060 (511 600)	167 120 (368 440)	221 570 (488 470)	223 320 (492 320)	249 400 (549 830)	497 770 (1 097 370)	476 230 (1 049 900)
Block Fuel	kg (lb)	21 620 (47 670)	58 980 (130 030)	72 530 (159 900)	21 570 (47 548)	58 900 (129 852)	69 680 (153 607)	50 740 (111 858)	194 750 (429 350)	212 120 (467 641)
OEW	kg (lb)	103 300 (227 750)	116 170 (256 120)	107 360 (236 700)	101 730 (224 280)	112 560 (248 144)	101 890 (224 620)	149 840 (330 346)	231 770 (510 964)	190 880 (420 812)
Wing Area	m^2 (ft^2)	296.8 (3195)	385.0 (4144)	380.2 (4093)	287.6 (3096)	336.1 (3618)	351.8 (3787)	438.1 (4716)	766.5 (8251)	698.7 (7521)
Span	m (ft)	51.8 (170.0)	56.9 (193.1)	58.5 (192.0)	50.9 (166.9)	55.0 (180.5)	56.3 (184.6)	66.2 (217.2)	89.6 (294.0)	87.7 (287.6)
Fus. Length	m (ft)	65.7 (215.6	61.4 (201.3)	60.0 (197.0)	65.7 (215.6)	61.4 (201.3)	60.0 (197.0)	80.5 (264.0)	70.1 (229.9)	68.6 (225.0)
SFC (Cruise)	$\frac{kg}{hr}$ daN $\frac{lb/hr}{lb}$	0.206 (0.202)	0.504 (0.494)	0.615 (0.603)	0.206 (0.202)	0.502 (0.492)	0.612 (0.600)	0.206 (0.202)	0.502 (0.492)	0.613 (0.601)
L/D Cruise	(-)	17.4 (17.4)	19.21 (19.21)	19.13 (19.13)	17.15 (17.15)	18.70 (18.70)	19.00 (19.00)	19.3 (19.3)	21.96 (21.86)	22.84 (22.84)
Thrust Engine	N (lb)	135 000 (30 350)	177 033 (39 800)	185 030 (41 600)	124 140 (27 910)	161 320 (36 269)	162 600 (36 555)	165 530 (37 663)	325 820 (73 250)	311 720 (70 081)
TOFL	m (ft)	2 440 (8006)	2 430 (7973)	2 431 (7976)	3 188 (10 460)	3 180 (10 433)	3 195 (10 482)	3 678 (12 068)	3 636 (11 930)	3 663 (12 019)
APP Speed	$\frac{m}{s}$ (KEAS)	71.0 (138.0)	66.5 (129.3)	65.3 (127.0)	71.9 (139.8)	70.3 (136.7)	66.8 (129.9)	72.0 (140.0)	72.0 (139.9)	72.0 (140.0)
Price Aircraft	$\$10^6$ $(\$10^6)$	43.39 (43.39)	48.10 (48.10)	44.53 (44.53)	42.62 (42.62)	46.59 (46.59)	42.34 (42.34)	58.54 (58.54)	85.21 (85.21)	73.07 (73.07)
DOC	$\frac{Cents}{Seat\ km}$ $\frac{Cents}{Seats\ n.mi.}$	0.869 (1.609)	0.831 (1.538)	0.907 (1.679)	0.859 (1.591)	0.815 (1.510)	0.870 (1.611)	0.982 (1.818)	1.193 (2.209)	1.227 (2.273)
Energy Utilization	$\frac{KJ}{Seat\ km}$ $\frac{Btu}{Seat\ n.mi.}$	636 (1118)	723 (1271)	759 (1334)	634 (115)	722 (1269)	731 (1285)	821 (1443)	1313 (2307)	1224 (2151)

**The 10 000 n.mi. range is actually a 5000 n.mi. radius to a landing and return to point of orgin unrefueled with full payload and reserve fuel at the second landing.

includes the methane plant's current operating costs experienced by the supplier as well as his long term amortization of the initial capital investment.

Other major conclusions of the study are:

- Methane is competitive as an alternate fuel in all major performance factors such as DOC, gross weight, initial cost and energy utilization.

- The mission range in which methane is competitive is, however, limited to ranges of 2778 km (1500 n.mi.) to about 10 186 km (5500 n.mi.). Neither LCH_4 nor LH_2 are competitive with Jet A at the shorter ranges. At the very long ranges, i.e., above 10 186 km (5500 n.mi.), methane becomes noncompetitive to both Jet A and LH_2. The advantages of LH_2 in terms of DOC, weight, cost and energy utilization become even more pronounced at very long ranges.

- The best fuel tank location for the LCH_4 fueled airplane was found to be fore and aft of the cabin in the fuselage as it was in the LH_2 aircraft studied previously.

- The cryogenic tanks for LCH_4 were found to be producible by present methods using an all welded structure of 2219 aluminum.

- Considerations of safety, design complexity and maintenance weighed as heavily in the choice of the LCH_4 aircraft configuration as did the major performance factors.

- The present public controversy about the safety of LNG shipment, storage and handling bears directly and with equal emphasis on the production and distribution of liquid methane at air terminals. It is unlikely, under presently proposed legislation, that the storage of large quantities of liquid methane would be permitted at airports.

- If the question of safety can be satisfactorily resolved, there are no technical barriers in the design of the ground system or of the airplane that would prevent the use of methane as an alternate fuel.

- The cost of LCH_4 delivered in the aircraft tanks amounts to:

	\$ per 10^6 Btu (1976 dollars)
Gaseous CH_4 feedstock	3.000
1600 km pipeline transport	0.500
Liquefaction at airport	1.22
Storage and distribution at airport	0.79
Delivered cost =	5.51

1. INTRODUCTION

The potential of methane as an alternate aircraft fuel has long been recognized. The purpose and motivation of this study comes from recognition that the world's supply of petroleum is being depleted and that after the year 2000 world production is expected to drop off. Figure 1 illustrates two estimates of the anticipated annual world production (Reference 1) with an overlay of time spans typical of the life cycle of a large transport aircraft. For reference, annual production of oil in the United States is shown with its peak occurring in 1970. The extensive overlap of the aircraft operational service beyond the peak of production of even the optimistic projection of world crude oil indicates that the search for the most desirable alternate fuel for transport aircraft must be undertaken vigorously in order to be ready for the inevitable decline in the availability of petroleum-based Jet A fuel.

The recoverable fraction of proven world reserves of the three most abundant natural fuels is, as of December 1977 (Reference 2) estimated to be:

Coal	18.3 to 19.7 x 10^{21}J (17.4 to 18.7 x 10^{18} Btu)
Petroleum	3.26 to 4.00 x 10^{21}J (3.09 to 3.8 x 10^{18} Btu)
Natural Gas	2.41 to 2.82 x 10^{21}J (2.29 to 2.68 x 10^{18} Btu)

This study is predicated upon the assumption that large scale processing facilities are set up for producing methane using coal as a basic resource. The methane would be processed, stored, and distributed in a manner described in Section 9 which was provided specifically for this study by the Institute

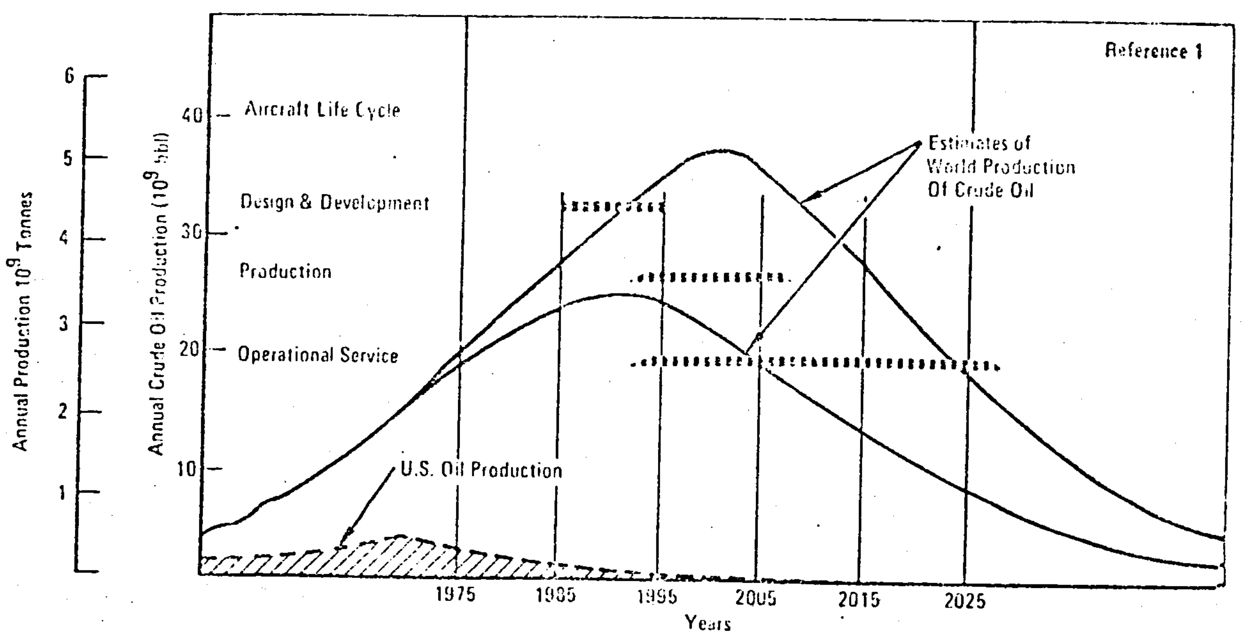

Figure 1. - Correlation of life cycle of new transport aircraft with forecasts of oil availability.

of Gas Technology, Chicago, Illinois, under subcontract. Similarly, the analysis of fuel tank insulation systems and associated analyses were performed for this study by the Thermal Sciences Laboratory at Lockheed Missiles and Space Company, Inc., Palo Alto, California.

The results of the work reported in References 3 and 6 showed that LH_2 fueled aircraft provide significant advantages in mid-range and long range aircraft. Specifically, as the range was increased above 2778 km (1500 n.mi.) the advantage of the LH_2 fueled aircraft gained rapidly in major factors such as gross weight, DOC, runway required and energy utilization, relative to Jet A. The conclusion was that the more energy required for a mission (payload/range), the greater the advantage for a high energy fuel such as LH_2. Even though the fuel volume requirements were much higher for LH_2 because of its low density, the resulting aircraft was still smaller in span and gross weight and had better energy utilization at the greater payload/ranges.

The principal significance of methane as a cryogenic fuel is also in its heating value and density relative to other fuels, see table 2. On a weight basis, as a first approximation, a hydrogen fueled airplane is favored over a methane aircraft by the ratio of the gravimetric heating values, i.e.:

$$\frac{51\ 590}{21\ 500} = 2.40$$

But on a fuel volume basis, methane is favored by the ratio:

$$\frac{567\ 600}{227\ 040} = 2.50$$

These considerations, plus indications that liquid methane might be produced from coal at a lower price and with less expenditure of energy than either LH_2 or synjet, led to the interest in performing this study of LCH_4 fueled aircraft.

TABLE 2. - PROPERTIES OF CANDIDATE FUELS

	Jet A	Methane LCH_4	Hydrogen LH_2
Nominal Composition	$C_{12.19}H_{23.51}$	CH_4	H_2
Molecular Weight	≈170	16.04	2.016
Heat of Combustion			
Gravimetric, MJ/kg (Btu/lb)	42.8 (18 400)	50.0 (21 500)	119.9 (51 590)
Volumetric, GJ/m^3 (Btu/ft^3)	35.3 (949 440)	21.1 (567 600)	8.44 (227 040)
Liquid Density, kg/m^3 (lb/ft^3)	827 (51.6)	422 (26.36*)	70.8 (4.42*)
Boiling Point at 1 Atmosphere, ^oC (^oF)	171 to 267 (339 to 513)	−161 (−258)	−253 (−423)
Freezing Point, ^oC (^oF)	−50 (−58)	−182 (−296)	−259 (−434)
Specific Heat, $J/kg/^oK$ ($Btu/lb/^oF$)	1966 (0.47)	3497 (0.836*)	9663 (2.31*)
Heat of Vaporization, kJ/kg (Btu/lb)	295 (127)	530 (228)	446 (192)

*At Normal Boiling Point

NOMENCLATURE

Ae	=	Effective Cross Section Area
AR	=	Aspect Ratio
ATA	=	Air Transport Association
b	=	Span or Spacing
c_d	=	Section Drag Coefficient
C.G.	=	Center of Gravity
c_n	=	Section Normal Force Coefficient
C_p	=	Pressure Coefficient
CPR	=	Cycle Pressure Ratio
DOC	=	Direct Operating Cost
FAR	=	Federal Aviation Regulation
Fg	=	Residual Strength
f_{me}	=	Fuel Evaporated in Flight
f_{mv}	=	Fuel Vented in Flight
F_{tu}	=	Ultimate Tensile Strength
g	=	Acceleration of gravity
gM_v	=	Fuel vented on the ground (recoverable)
GH_2	=	Gaseous Hydrogen
GCH_4	=	Gaseous Methane
GN_2	=	Gaseous Nitrogen
HHV	=	Higher Heating Value
h	=	Liquid Pressure Head
HP	=	High Pressure
IOC	=	Initial Operating Capability
Jet A	=	Conventional Hydrocarbon Jet Fuel

K_o = Stress Intensity Factor

L/D = Lift to Drag Ratio

LCH_4 = Liquid Methane

LH_2 = Liquid Hydrogen

LHV = Lower Heating Value

LP = Low Pressure

M, M_o = Structural Bending Moment

M = Mach Number

M_D = Design Mach Number

MAC = $\overline{C}$ = Mean Aerodynamic Chord

M.S. = Margin of Safety

M_i = Insulation System Weight

N_x, N_z = Inertial Load Factors

OEW = Operating Empty Weight

pax = Passengers

PLA = Positive Low Angle of Attack

PPO = Polyphenylene Oxide

P_{lim}, P_{ULT} = Limit or Ultimate Load or Pressure

q = Tangential Shear Flow (Stress)

R = Thermal Resistance

S = Wing or Tail Surface Area

SFC = Specific Fuel Consumption

SLS = Sea Level Static (Thrust)

TOFL = Takeoff Field Length

t_i = Insulation Thickness

t_s = Wall or Skin Thickness

TOFL = Takeoff Field Length (FAA)

V_A = Design Maneuver Speed

V_c = Design Cruise Speed

V_D = Design Dive Speed

$\overline{V}_H$ = Horizontal Tail Volume Coefficient

V_s = Stall Speed

$\overline{V}_v$ = Vertical Tail Volume Coefficient

$V_{MC_{Air}}$ = Minimum Air Control Speed

W = Uniform Structural Load

W/S = Wing Loading = $\frac{\text{Aircraft Weight}}{\text{Wing Area}}$

X/C = Chordwise Position in Tenths

ϵ = Emissivity

γ = Reinforcement Efficiency

ρ = Liquid Density or Least Radius of Gyration.

Z = I/C = Section Modulus

1. TECHNICAL APPROACH

The study had five major objectives for determining the potential of methane as a fuel for commercial transports. They were:

- Define the cost, performance, and energy consumption of a commercial transport using liquid methane.
- Define the cryogenic fuel system including the tanks.
- Determine the ground facility complex required and the costs associated with an airport supplying methane for a number of aircraft.

- Compare Jet A, hydrogen, and methane-fueled aircraft on the basis of performance, cost, and energy consumption.

- Define the research and technology advances required to implement the use of methane in commercial transports.

To attain these objectives the work was divided into two parts and a total of five phases.

1.1 Part One

1.1.1 Phase 1: Aircraft design and configuration studies.- Three candidate methane-fueled configurations were selected for preliminary design and evaluation. The bases of the configuration choices were the widest possible range of fuel-tank shapes and locations and determination of their effectiveness as cryogenic fuel containers. All three were evaluated on the basis of L/D, weight, cost, DOC, and safety. Safety and operational aspects weighed heavily in the final choice.

From these three, one configuration was chosen and, with the concurrence of NASA, carried forward for completion of the study. The design payload/range for this airplane was 400 passengers/10 186 km (5500 n.mi.) at 0.85 cruise Mach number which correlates to a previous study of Jet-A- and hydrogen-powered aircraft in reference 3.

1.1.2 Phase 2: Aircraft fuel system design.- The previous work done on hydrogen fuel systems (reference 4) was taken as the baseline design and modified for the differences in temperature, density, and heating values as related to methane. Structural design and producibility and stress analyses were carried out on the chosen tank configuration. An optimum insulation scheme and the effects of subcooling the methane were also investigated.

1.1.3 Phase 3: Airport requirements.- The airport methane processing, storage, and fueling facility requirements were based on San Franciso International Airport (SFO) as an operating site. The quantities of methane required were based on the traffic projections in reference 5. The cost and implications of providing subcooled fuel to the aircraft were included.

1.1.4 Phase 4: Comparative evaluations.- The 10 186 km (5500 n.mi.), 400 passenger, Mach 0.85 methane-fueled aircraft was compared with the equivalent LH_2 and Jet A aircraft as reported in references 3 and 4. It was necessary to update the referenced aircraft because of changes which had been made in the Lockheed computer program (ASSET), used to synthesize and evaluate aircraft performance since the original work was done in 1974-75. In addition, changes had been made to some of the guidelines (refer to section 4.2). The basis of comparison was safety, cost, DOC, performance, and physical parameters.

Subjects for research and technology development were recommended for deficient areas relative to the fuel system and the aircraft.

1.2 Part Two

1.2.1 Phase 5: Extend the methane design study to four additional design ranges.- At about the midpoint of the initial work in the first four-phases, which were for a 400-passenger 10 186 km (5500 n.mi.) airplane, NASA extended the contract work statement to include aircraft designs encompassing all the payload/range combinations which had been evaluated in references 3 and 6. This would provide data for a family of methane transports equivalent in range, payload, and speed to the Jet A and LH_2 transports, derived in 1974 to 1975.

No further work on cryogenic fuel systems, configurations, or airport facilities was required for the additional aircraft. The basis for the methane configuration geometry was to be kept identical to the Jet-A- and LH_2-fueled aircraft except for the physical differences dictated by the density and heating values of methane as a fuel. The additional work provided for a final matrix of airplanes as presented in table 3:

The extended scope then updated the technology and cost factors of the previous LH_2 and Jet A designs from the 1974-75 studies and four new methane design ranges to complete the matrix of three types of differently fueled aircraft at five payload/ranges (table 4).

TABLE 3. - EXTENDED MATRIX OF METHANE TRANSPORTS

(All aircraft cruise at Mach 0.85)

Passengers / Range, km (n.mi)	LCH_4	JET A	LH_2
130 / 2780 (1500)	Added	Update Previous Studies of 1974 – 75	Update Previous Studies of 1974 – 75
200 / 5560 (3000)	Added		
400 / 5560 (3000)	Added		
400 / 10 186 (5500)	Basic Design		
400 / 18 530 (10 000)	Added		

TABLE 4. - BASIC GUIDELINES FOR DESIGN OF METHANE, HYDROGEN AND JET A AIRCRAFT

IOC 1990 – 1995

Advanced Technologies:

- Supercritical aerodynamics
- Composite materials – 50% of airframe structure by weight replaced by composite materials.
- Active controls

Advanced engines:

- Contractor-derived performance for methane, hydrogen and Jet A engines.

Performance Requirements:

- 32.2°C (90°F) day at 304.8 m (1000 ft) for takeoff and landing calculations.
- Engine-out climb gradient $\geqq$ 0.024 for two engine aircraft and $\geqq$ 0.03 for four engine.
- Initial cruise altitude $\geqq$ 10 363 m (34 000 ft) for all
- TOFL and Approach Speeds (all aircraft types) as follows:
- All Aircraft cruise at Mach 0.85

SI UNITS

Passengers / Range (km)	130 / 2778	200 / 5556	400 / 5556	400 / 10 186	400 / 18 520
TOFL (m) APP Speed $\frac{km}{hr}$	2438 250	2438 250	2438 250	2438 250 Also: 3200 259	3658 259

CUSTOMARY UNITS

Passengers / Range (n.mi)	130 / 1500	200 / 3000	400 / 3000	400 / 5500	400 / 10 000
TOFL (ft) APP Speed (knots)	8000 135	8000 135	8000 135	8000 135 Also: 10 500 140	12 000 140

Safety: Equal to or better than current transports.

Other Criteria: Meet all applicable requirements of FAR 25.

DOC Factors:

- Utilization Rate
  - Short Range, 2778 km (1500 n.mi) – 3300 hrs/yr
  - Medium Range, 5556 km (3000 n.mi) – 3600 hrs/yr
  - Long Range, 10 186 km (5500 n.mi) – 4000 hrs/yr
  - Very Long Range, 18 520 km (10 000 n.mi) – 7000 hrs/yr
- 1967 ATA Equations – as modified per reference 4.
- 1976 dollars
- 350 aircraft production base
- Fuel costs

LCH_4 = \$3.79 per GJ (\$4 per 10^6 Btu)

Jet A = \$4.74 per GJ (\$5 per 10^6 Btu)

LH_2 = \$5.69 per GJ (\$6 per 10^6 Btu)

Note: The very long range mission, 18 520 km (10 000 n.mi), is actually a 9260 km (5000 n.mi) radius to a landing and return to the point of origin unrefueled with full payload and reserve fuel at the second landing.

2. AIRCRAFT TECHNOLOGY DESCRIPTION

This study is a follow-on to work that was started on hydrogen-fueled subsonic aircraft in 1974 and this report on methane as a cryogenic fuel follows those shown as references 3 through 6. Taken collectively, those five studies represent an investigation into nearly every aspect of advanced alternate fueled aircraft design, such as:

- Aircraft configurations
- Fuel tank concepts
- Cryogenic insulation concepts
- Fuel system design
- Aircraft operating costs
- Airport requirements for processing and storage including facility costs
- Detailed design and stress analysis of cryogenic aircraft tanks
- Producibility of tank designs
- Major aspects of safety.

Each succeeding study had the advantage of the previous work as a foundation and many detailed investigations could be eliminated, as in the present case for the methane airplane where no optimization process was undertaken for wing sweep, taper ratio, aspect ratio, or thickness ratio since that work was previously done in references 3 and 6 and those values are adopted here. The technology and computational methods used in establishing the aerodynamics of the LCH_4 airplane must be the same as for the LH_2 and Jet A designs to keep comparisons valid, except for any changes that are dictated by the nature of LCH_4 itself. The fuel volume required for methane differs greatly from LH_2 or Jet A for example, because its density and heating value are greatly different. The methane fuel tank insulation thickness is much less and therefore, much lighter than for liquid hydrogen because hydrogen is 91.7°C (165°F) colder. A consistent approach to the study was a matter of first priority throughout, especially in the matter of making comparisons.

2.1 Aerodynamics

2.1.1 Technology level.- The early work done in 1974-75, and cited in reference 3 and 6, was done on the basis of the original Whitcomb findings on supercritical airfoils. Since 1977 preliminary design analyses for advanced aircraft at Lockheed used drag estimation procedures based on a more recent series of wind tunnel tests. That technology level has been designated by Lockheed as "Advanced Potential." The data base includes the representation of a reasonably broad series of configurations rather than just one or two isolated tests. These data are provided in NASA TM X-71996. Reference 100. Recently Lockheed completed tests on two wings designed to the same concept which confirmed the trend and, indeed, indicated slightly lower drag than achieved in the NASA tests when related to equivalent wings.

The use of the advanced potential method of drag estimation results in significant improvement in airplane lift/drag relative to the advanced technology estimation procedure previously employed. This improvement is accomplished by changing only wing section contours while maintaining the same basic airplane geometry (identical airplane component areas and thickness, aspect, and taper ratios).

The drag reduction accompanying the improved lift/drag is explained as follows. The advanced technology airfoil sections promulgated by Dr. Richard Whitcomb and others a few years ago provided a respectable delay in the onset of compressibility drag (approximately Mach 0.045) compared to drag data on wings of aircraft then in production. However, tests of the advanced technology wings (using the same basic geometry) showed considerable drag increase, particularly as the steep portion of compressibility drag rise was approached.

Efforts by Whitcomb and coworkers were then directed toward section contour modifications which would reduce this undesirable drag. This work resulted in the advanced potential family of airfoil sections which have much less additional drag, although a somewhat steeper drag rise Mach number is given up (about 0.015). These airfoils accomplish the drag reduction by means of a flatter "roof-top" pressure distribution as shown in figure 2, compared to the "saddle-back" distributions of the earlier advanced technology sections. The drag reduction shown in figures 3 and 4 is made possible by the lower pressure peaks accompanied by the lighter shocks as the flow advances into the supercritical regime.

A significant difference between the current and advanced potential airfoils is the use of more aft camber to provide a lower drag. This increase in aft chordwise loading produces substantial increases in pitching moment coefficients (up to an increase of -0.1) which must be trimmed by an increased down load on the horizontal tail. This could produce an objectionable drag penalty with earlier aircraft designs having typically forward center of gravity (0.12 to 0.35 $\bar{c}$). The trim losses are minimized by designing tail surfaces to permit more aft center of gravity (0.185 to 0.435 $\bar{c}$). Use of active controls allows an aft center of gravity with minimum increase in horizontal tail size.

The solution to the situation of having the LH_2 and Jet A designs of 1974-75 at an older technology level relative to the LCH_4 designs was to bring them all up to date, and that has been done. Those results are presented in table 1.

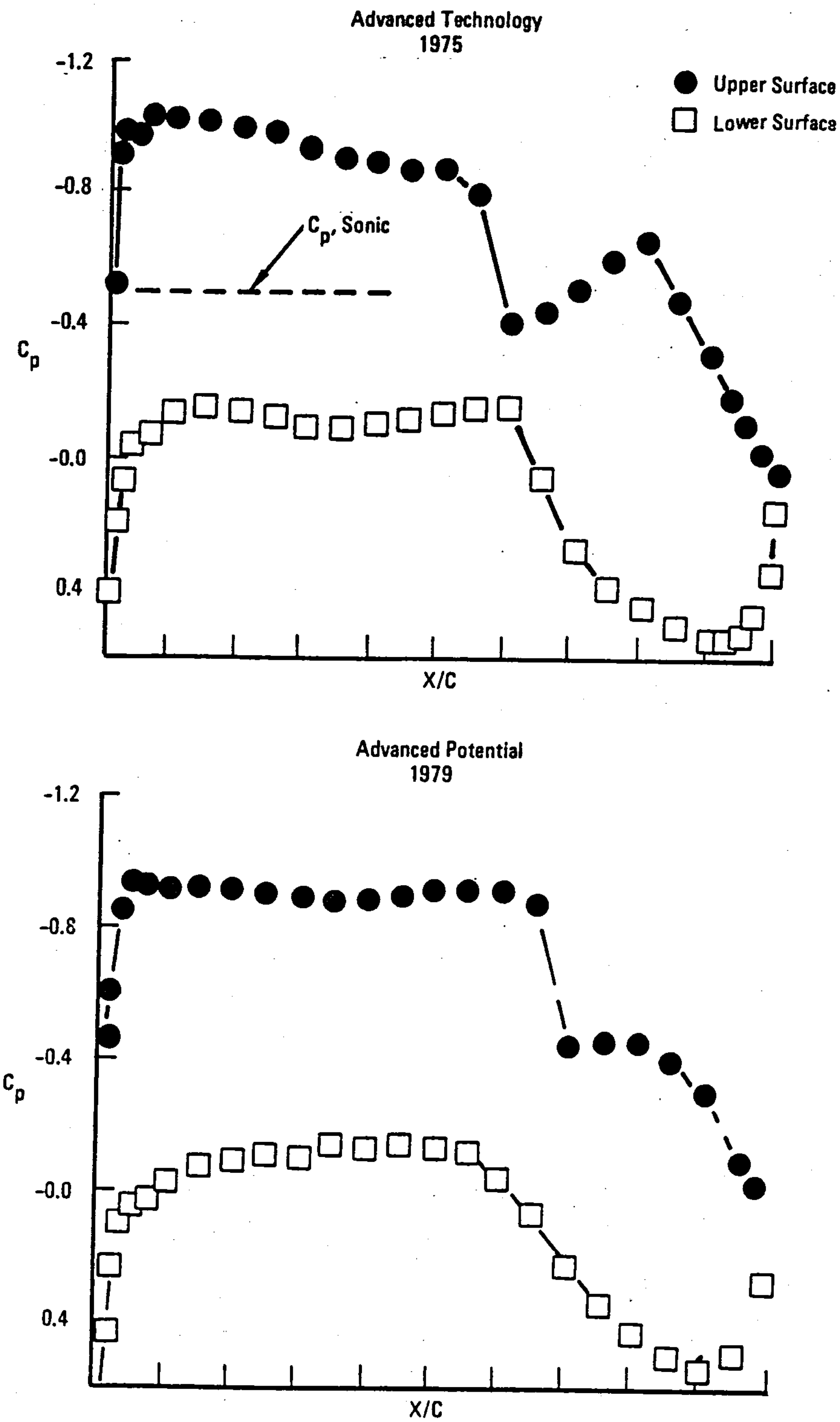

Figure 2. - Supercritical flow development, Mach 0.83.

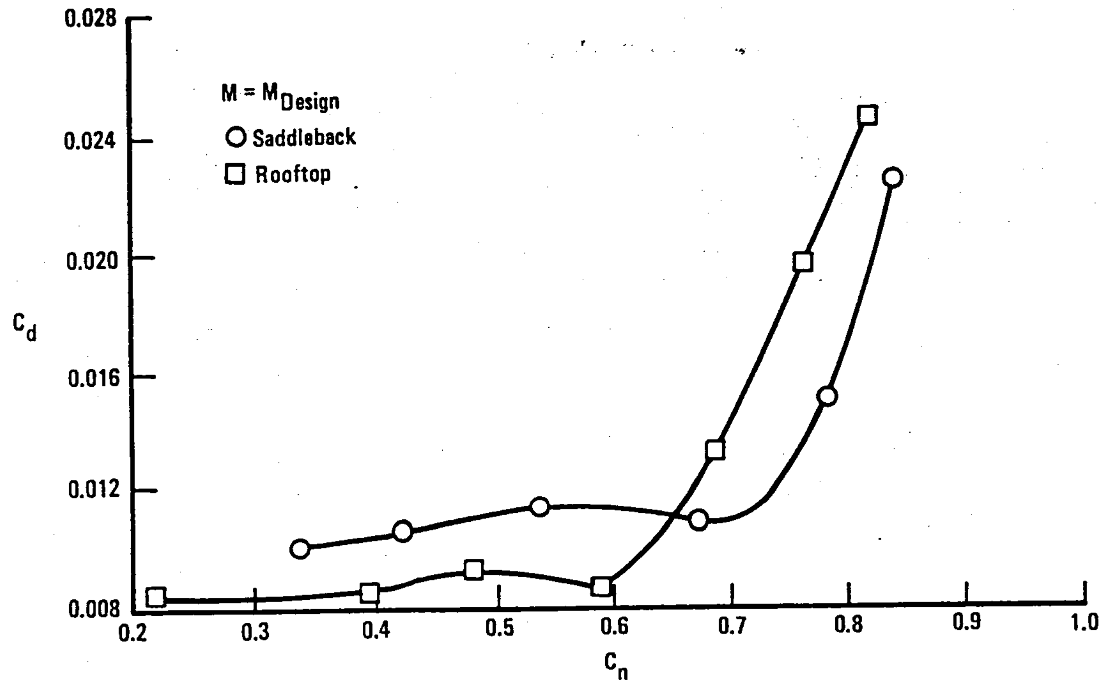

Figure 3. - Profile drag polar.

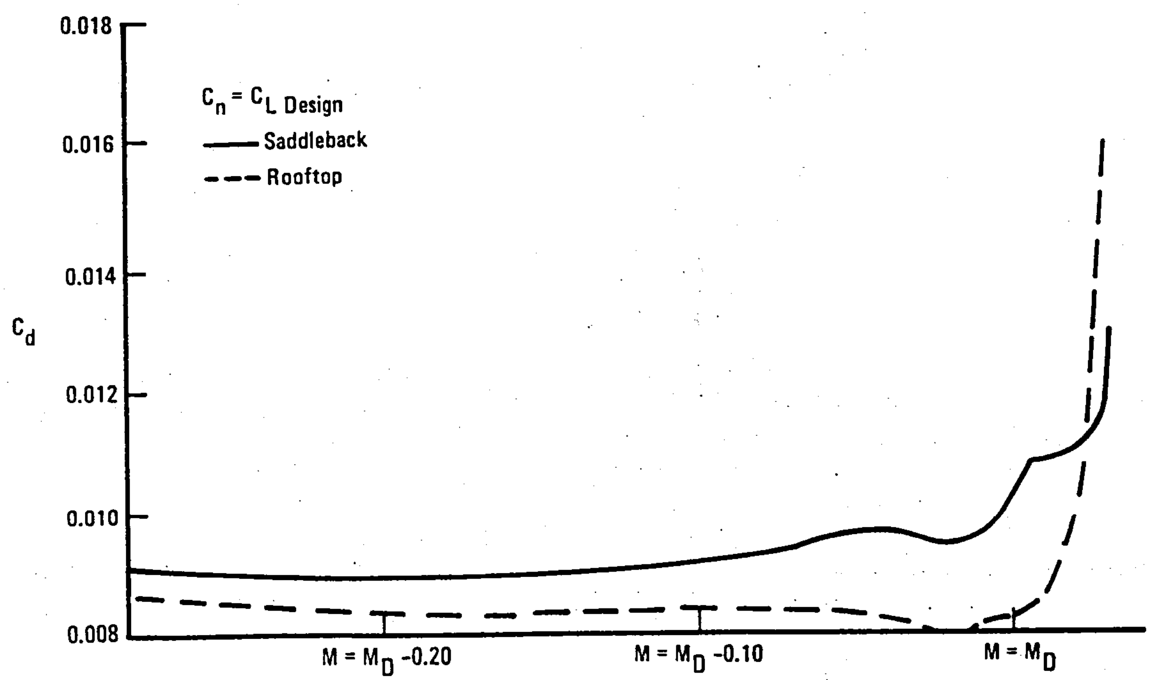

Figure 4. - Drag rise characteristics.

2.1.2 Tail sizing requirements.- The horizontal and vertical tail volume coefficients with the corresponding center of gravity limits were established as follows:

Forward center of gravity limit = 0.185 $\bar{c}$

Aft center of gravity limit - 0.435 $\bar{c}$

Horizontal $\bar{V}_H$ = 0.66 (exposed area)

Vertical $\bar{V}_v$ = 0.055 (exposed area)

Note that the exposed tail area is used to determine the volume coefficients for both tail surfaces. All methane configurations and all LH_2 and Jet A updated aircraft were evaluated on this basis with one exception, and that is the 130-passenger/2778 km (1500 n.mi.) group of airplanes which are twin-engine aircraft. In those cases, the coefficients from the reference 6 study were adopted for consistency. They are:

Horizontal $\bar{V}_H$ = 0.59

Vertical $\bar{V}_v$ = 0.0853

As an illustration, the horizontal tail for the baseline 400 passenger/ 10 186 km (5500 n.mi.) aircraft was sized by the following:

- A total center-of-gravity range of 171.5 cm (67.5 in.) (same as the L-1011).
- At least neutral stability at aft center of gravity
- Control-to-stall at forward center of gravity with maximum landing flaps and idle thrust.
- Takeoff nose wheel liftoff at forward center of gravity with maximum takeoff flaps at $1.05V_{s_{FAA}}$

A constraint on aft center-of-gravity location is that it must be far enough forward of the main landing gear to prevent a "tail-sit" condition at landing touchdown attitudes or at takeoff brake release at light weight. Analysis shows that this margin must be 0.183c for the Methane Configuration 1 (see Figure 10).

The horizontal tail was assumed to be an all-moving surface with a 25-percent chord-geared elevator yielding a usable $C_{L_{max}}$ of ±1.6. This is compatible with that used in reference 3 for tail sizing of the liquid hydrogen subsonic transport. Downwash data for the LH_2 airplane were also used since the aspect ratio of the airplane is the same.

The center-of-gravity limits for the LCH_4 aircraft are dependent on horizontal tail volume coefficient as shown in figure 5. The forward limit is imposed by the requirement for control-to-stall in the landing configuration, and the aft center of gravity limit is defined by the condition for neutral static stability. These data indicate that a volume coefficient (V_H) of 0.66 is required to provide a center of gravity range of 171.5 cm (67.5 in.)

The vertical tail was sized based on the FAA requirement for critical engine-out air minimum control speed ($V_{MC_{air}}$). According to this requirement, $V_{MC_{air}}$ shall not exceed $1.2V_{s_{FAA}}$ for takeoff with bank angle not exceeding 5 deg. However, in practice, the vertical tail is sized for a speed of about $1.09V_{s_{FAA}}$, since the 10.7 m (35-ft) obstacle speed ($\geq 1.2V_{s_{FAA}}$) must also be 10 percent greater than the air minimum control speed.

Vertical tail size must also be evaluated in terms of the requirement for engine-out waveoff at approach speeds. This requirement is applied for the landing flaps configuration but at a higher stall margin: $1.3V_{s_{FAA}}$.

The vertical tail was assumed to be an all-moving surface with no geared rudder, yielding a $C_{L_{max}}$ of ± 1.0.

Air minimum control speed was calculated based on lateral-directional stability and control derivatives of the L-1011 flight training simulator, and the engine thrust decay with speed was estimated based on characteristics for the RB.211-22B power plant.

Results of the air minimum control speed analysis are presented in figure 6. It presents the vertical tail size requirement in terms of speed, weight, and stall margin. The minimum control speed is critical at light weight therefore, these data must be applied at the specified minimum takeoff and landing weights. Minimum operational weights for tail sizing were specified as follows:

- Takeoff with 25 percent payload and 40 percent fuel.
- Landing with 25 percent payload and fuel reserves for an international flight (about 15 percent fuel).

Corresponding weights are 131 544 kg (290 000 lb) for takeoff and 115 668 kg (255 000 lbs) for landing. Observing the data in figure 6 for these minimum takeoff and landing weights, it is apparent that the sizing condition is slightly more critical for takeoff. Figure 7 cross-plots the data in Figure 6 for the takeoff stall margin of $1.09V_{s_{FAA}}$. For the takeoff weight of 131 544 kg (290 000 lb), the vertical tail area required is 10.8 percent of the wing area or a volume coefficient of 0.055 ($\overline{V}_v$).

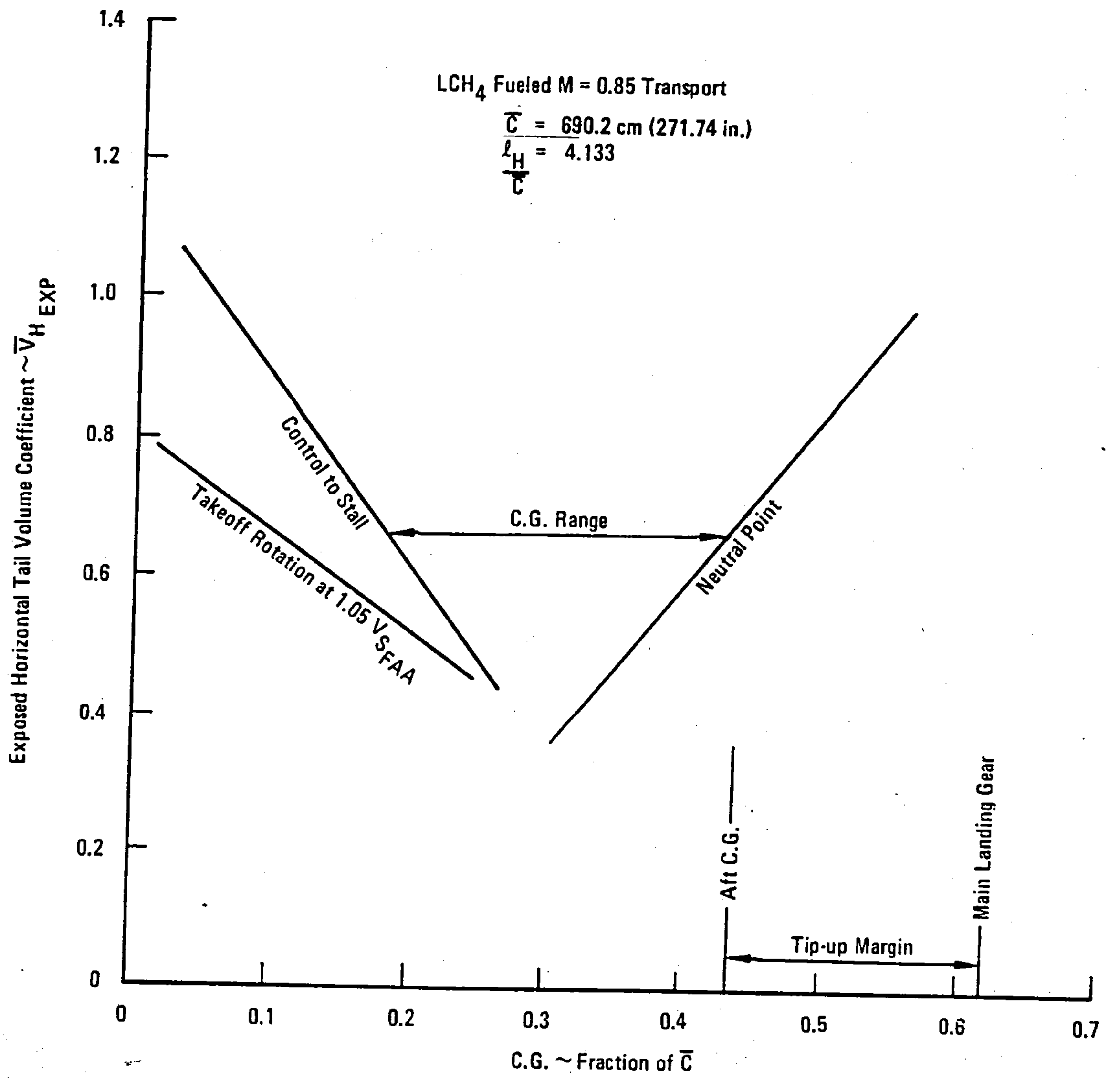

Figure 5. - Configuration 1, horizontal tail sizing summary chart.

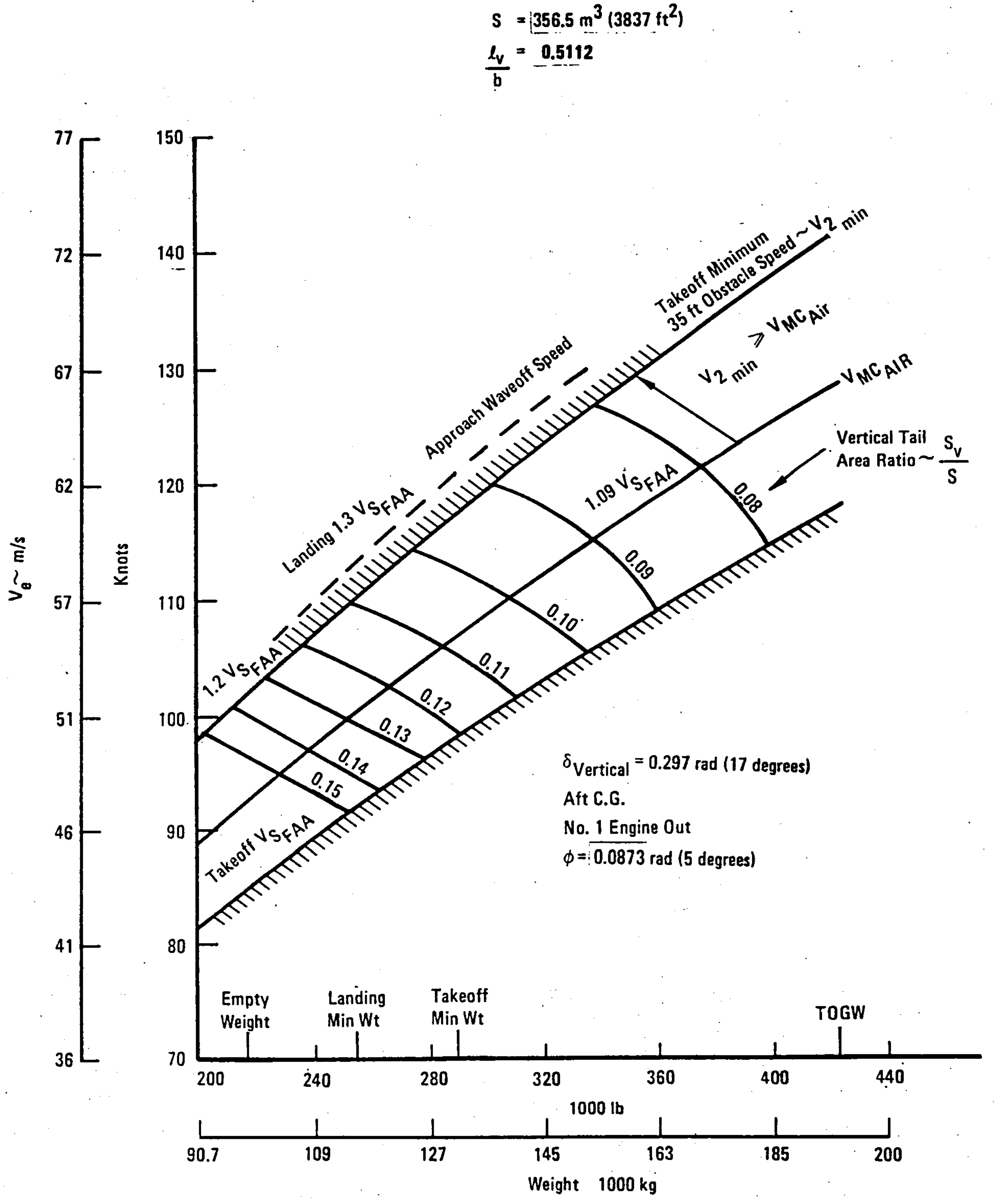

Figure 6. - Analysis results for Configuration 1, takeoff, engine-out, air minimum control speed vertical tail size requirement

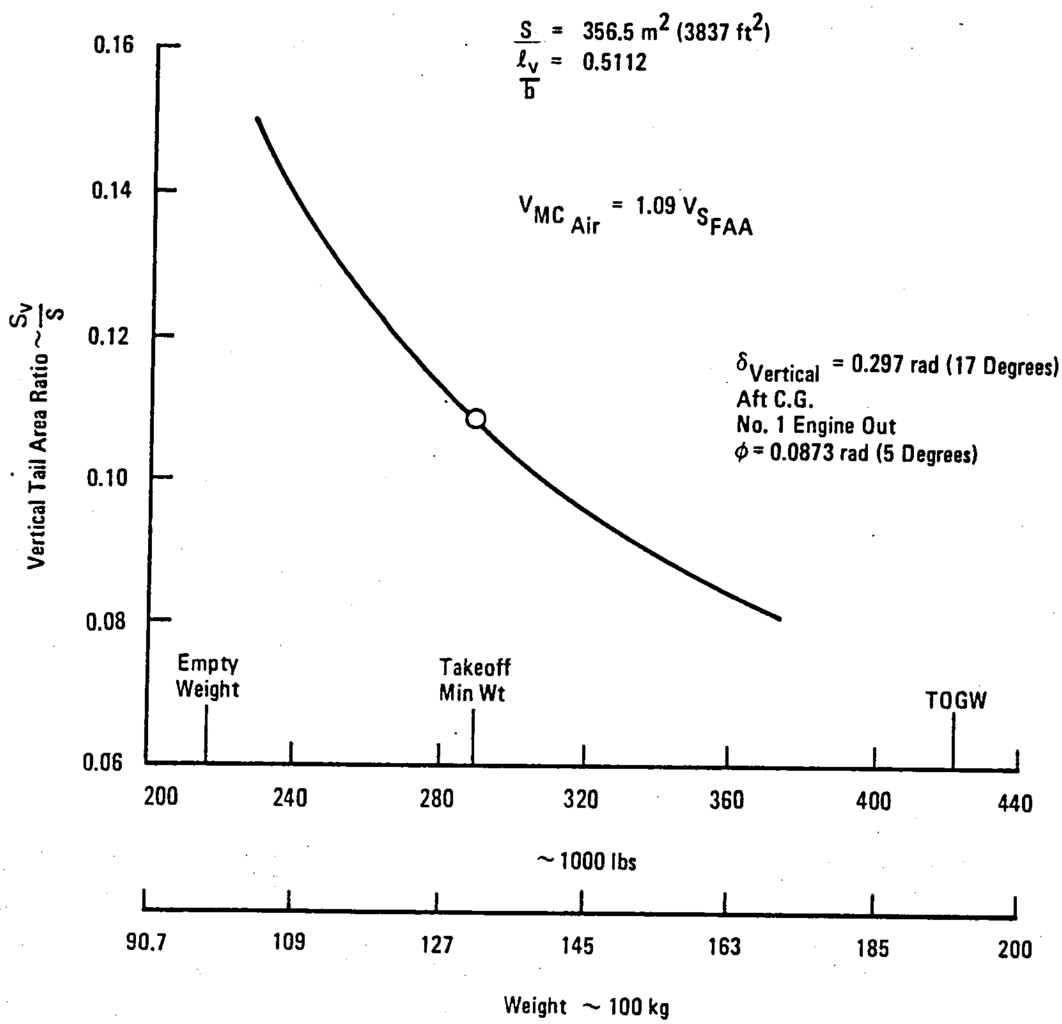

Figure 7. - Cross plot of data for Configuration 1, takeoff, engine-out, air minimum control speed vertical tail size requirement.

2.2 Propulsion

2.2.1 Engine cycle selection and installation losses.- The approach used to select a turbofan cycle compatible with the requirements of the liquid-methane-fueled transport was to investigate the effects of selected concepts on a baseline design. The baseline LH_2 cycle was developed earlier by Lockheed and reported upon in reference 4. Garrett AiResearch reviewed this cycle and found it to be generally consistent with technology projections for 1990; therefore, this cycle was used as a baseline for hydrogen exploitation feasibility studies. Although the baseline values of bypass ratio and fan pressure ratio were later modified as a result of the cycle optimization, the changes had little or no effect on the results of the feasibility studies.

All concepts were evaluated at an assumed initial cruise flight condition of 10 668 m (35 000 ft), Mach 0.85. This flight condition determined engine sizing and was also typical of the cruise condition where the majority of fuel is consumed.

The criteria used for evaluation of the concepts was DOC. The sensitivity of DOC to changes in specific fuel consumption and engine weight was based on a relationship presented in reference 4. The relationship used in the engine study was:

$$\Delta DOC\ (\%) = \frac{\frac{7.75}{10^6}(\Delta\ \text{engine weight}) + 1.332\left(\frac{SFC}{SFC_{base}} - 1\right)}{DOC_{base}} \times 100$$

The change in specific fuel consumption was evaluated using a design-point thermodynamic routine which allowed the various concepts to be modeled. Engine weight for the various concepts was determined by adding the weight of the components associated with each concept to the baseline weight and adjusting the baseline weight for changes in airflow, bypass ratio, and turbine design considerations.

For all cycle investigations, thrust, cycle pressure ratio, turbine inlet temperature, and fan pressure ratio were held constant. Specific thrust (F_N/W_a) was held nearly constant by fixing the energy extraction of the low pressure turbine. This was accomplished by specifying a constant jet nozzle velocity ratio (V_{core}/V_{fan}) in addition to the other constant parameters. Holding specific thrust approximately constant allows the effects of the various concepts to be observed independently of propulsive efficiency changes. It should be noted that holding the jet nozzle velocity ratio and fan pressure ratio constant does not hold specific thrust exactly constant, but it results in only very minor changes in specific thrust and the analytical procedure is greatly simplified. The jet nozzle velocity ratio selected was 1.19 which was based on the original Lockheed cycle.

Installation effects included in the analysis were bleed and horsepower extraction for aircraft systems, inlet total pressure recovery, and exhaust system losses including fan scrubbing drag. Freestream cowl drag and inlet spillage drag were not included. To a first approximation, free-stream cowl drag is a function of specific thrust and therefore, for this analysis, is a constant. Spillage drag at the design point condition is insignificant. Characteristics and installation losses of the baseline-size engine are summarized in table 5.

Cowl drag was accounted for by applying a constant drag coefficient and proportioning to the wetted area of the cowl.

2.2.2 Initial LH_2 engine cycle selection.- The initial LH_2 engine cycle selection proceeded on the basis that a rotor inlet temperature of 1427°C (2600°F) to 1538°C (2800°F) was desirable. The assumption was based on findings that show temperatures above this level require cooling for the low-pressure turbine vanes and blades. Cooling the low-pressure turbine results in significant performance penalties and is expensive. The added mechanical complexity is prohibitive. This assumption was tested later in the reference 4 study through the investigation of a 1760°C (3200°F) engine that used hydrogen to cool the turbine cooling air and thereby minimize the performance penalty.

Baseline engine description: The baseline engine chosen for the initial cycle selection study was a two-spool, separately exhausted turbofan, consisting of the following components:

TABLE 5. - BASELINE HYDROGEN ENGINE CHARACTERISTICS AT CRUISE

Installed Losses and Performance Characteristics	
Performance	
Net thrust, N (lb)	26 689 (6000)
Specific fuel consumption, (kg/hr)/daN ((lb/hr)/lb)	0.2129 (0.2088)
Specific thrust, N/(kg/sec) (lb/(lb/sec))	112 (11.47)
Losses	
Horsepower extraction, kw (hp)	93.2 (125)
Aircraft systems bleed extraction, %	4.1
Inlet total pressure recovery	0.991
Nozzle thrust coefficients	0.995

- Single-stage fan
- Two-stage low-pressure compressor (booster stages)
- Ten-stage high-performance compressor
- Annular combustor
- Axial-cooled HP turbine (single stage)
- Axial-uncooled fan turbine (four to six stages)
- Exhaust regenerator (for fuel heating)
- Separate fan and core convergent exhaust nozzles.

The cycle characteristics of the baseline engine were selected to approximate the cycle used in the feasibility studies discussed in reference 4; however, additional intercomponent pressure drops, cooling flows, and leakage were added.

A study was conducted to define the optimum cycle for the aircraft. This study varied bypass ratio, fan pressure ratio, and overall pressure ratio to find optimum performance, based on the DOC equation presented earlier. Figure 8 summarizes the bypass ratio study. Note that DOC reaches a minimum at bypass ratios between 8 and 11. A realistic single-stage fan is limited to a pressure ratio less than 1.8 (e.g., about 1.7), thereby causing the optimum cycle to occur at a bypass ratio greater than 8. The envelope drawing of the engine is shown in figure 9.

Three heat exchangers are included as part of the methane engine to provide (1) methane cooling of the turbine cooling air, (2) engine oil cooling, and (3) fuel heating. They are described in Section 7.

Basic cycle and performance data are listed in table 6. The thermodynamic design parameters shown in table 7 are the final results of a cycle optimization. They reflect final estimates of component performance, pressure losses, cooling flows, etc. The primary refinements included increases in low-pressure turbine efficiency and nozzle thrust coefficients, compared to those used in the early part of the study.

2.2.3 <u>The weight, geometry, and scaling relationship.</u>- The estimated dry weight of the bare baseline-size engine is 1715 kg (3780 lb). This weight includes engine accessories, i.e., fuel control, fuel pump, lubrication pumps, heat exchangers, and accessory gearbox. Aircraft accessories, inlet, nozzles, fan thrust reverser, and noise suppression are not included. The estimated weight of the inner and outer fan ducts, fan and core nozzles, and fan thrust reverser is 367 kg (809 lb). The total dry weight of the engine exclusive of inlet, aircraft accessories, and noise suppression is 2082 kg (4589 lb).

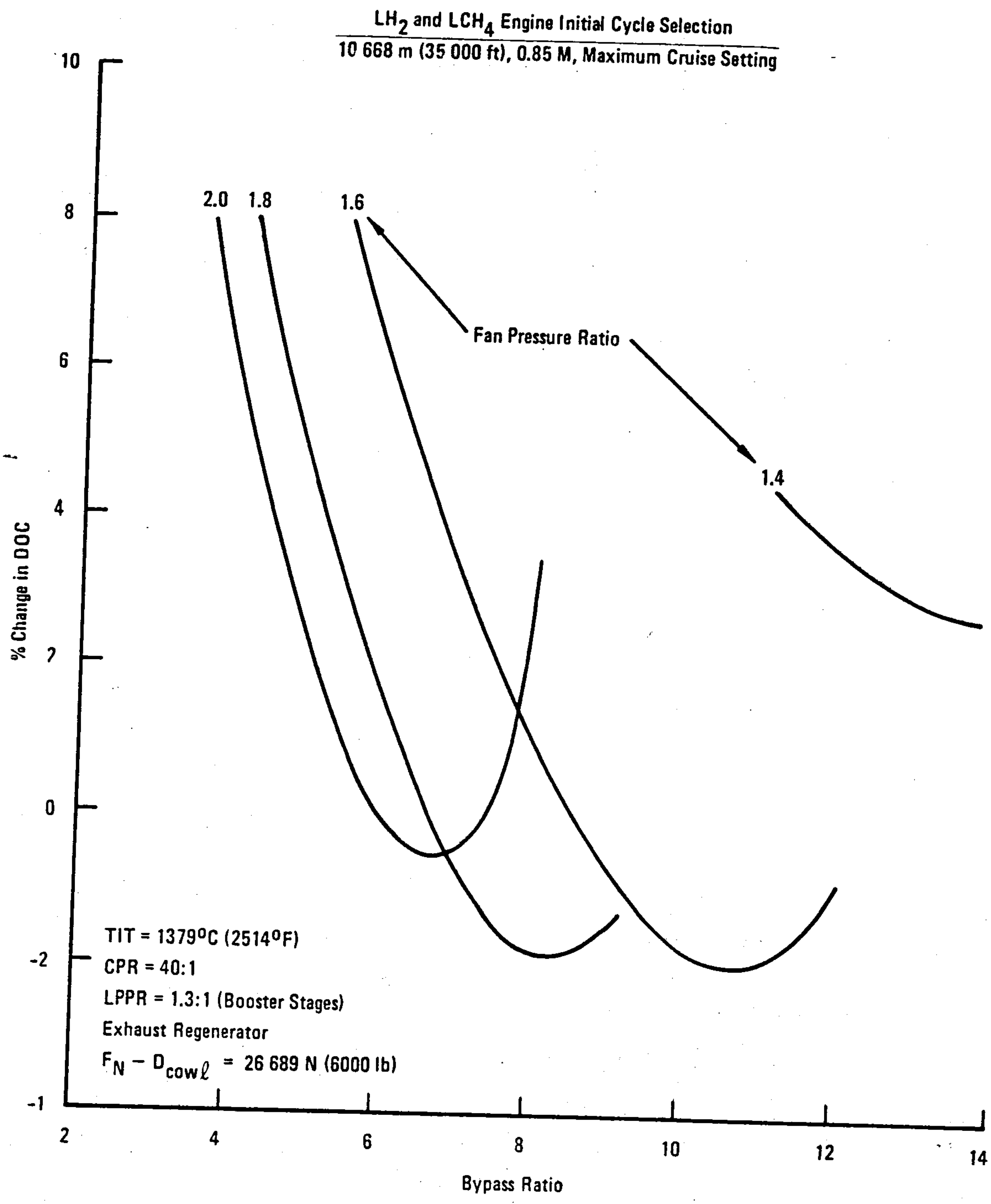

Figure 8. - Effect of fan pressure ratio and bypass ratio on direct operating cost.

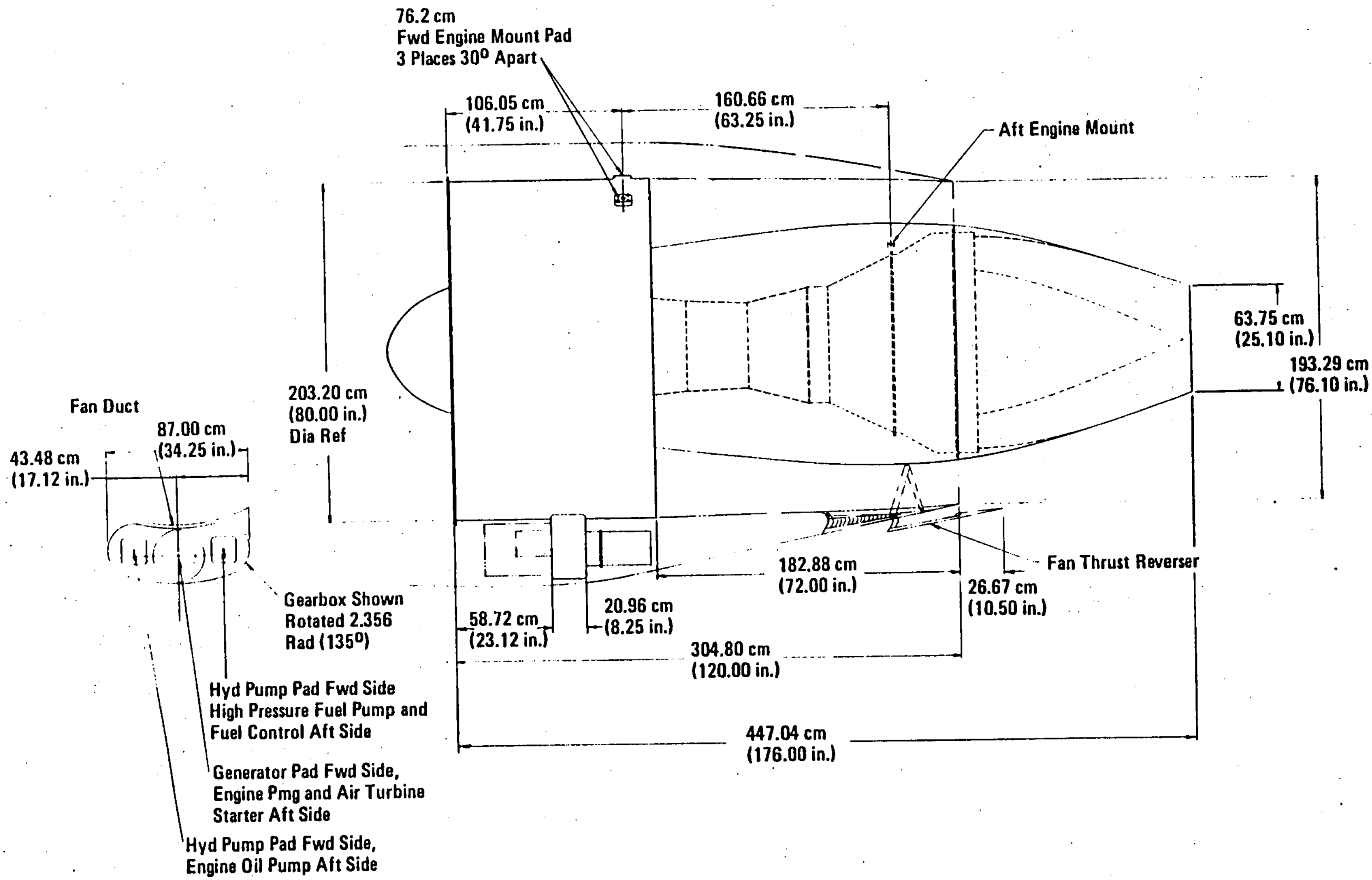

Figure 9. - Envelope drawing, selected baseline LH_2 and LCH_4 engine.

TABLE 6. - BASELINE ENGINE CHARACTERISTICS SLS, UNINSTALLED STANDARD DAY

	LH_2	LCH_4	Jet A
Power Setting	Takeoff	Takeoff	Takeoff
Net Thrust, N (lb)	136 580 (30 706)	136 580 (30 706)	136 580 (30 706)
SFC, $\left(\frac{kg/hr}{daN}\right)$	0.1045	0.2509	0.293
$\left(\frac{(lb/hr)}{lb}\right)$	(0.1025)	(0.2460)	(0.2874)
Bypass Ratio	10.25	10.25	10.25
Fan Air Flow, kg/sec (lb/sec)	485 (1070)	485 (1070)	485 (1070)
Compressor Pressure Ratio	15.5	15.5	15.5
Turbine Inlet Temp, ^{o}C (^{o}F)	1482 (2700)	1482 (2700)	1482 (2700)

TABLE 7. - THERMODYNAMIC DESIGN PARAMETERS FOR METHANE ENGINE

Inlet Recovery	0.991
Fan Efficiency	0.892
Fan Pressure Drop $\Delta P/P$	0.015
Compressor Efficiency	0.862
Turbine Cooling Air, %	3.2
Combustor Efficiency	1.0
High Pressure Turbine Efficiency	0.900
Low Pressure Turbine Efficiency	0.900
Fan Nozzle Thrust Coefficient	0.991
Core Nozzle Thrust Coefficient	0.988

The engine may be scaled within ± 25 percent of its base size according to the following relationships:

$$\text{Scaled Weight} = W_{bl} \left(\frac{\text{Scaled Thrust}}{\text{Base Thrust}}\right)^{1.0}$$

$$\text{Scaled Length} = L_{bl} \left(\frac{\text{Scaled Thrust}}{\text{Base Thrust}}\right)^{0.25}$$

$$\text{Scaled Diameter} = D_{bl} \left(\frac{\text{Scaled Thrust}}{\text{Base Thrust}}\right)^{0.5}$$

3. AIRCRAFT DESIGN DEVELOPMENT

3.1 Configurations

The baseline LCH_4 configuration with all the fuel located fore and aft in the fuselage was adopted from the LH_2 study cited as Reference 3 and is shown in figure 10. This provided a known point of departure for the purpose of comparing a series of design possibilities.

The sequence of the study was to first develop the best configurations out of three general options for the 400-passenger, 10 186 km (5500 n.mi.) payload/range aircraft and to then carry that configuration through to all other payload/ranges. Those options were:

- Configuration 1 - All fuel in the fuselage divided fore and aft.
- Configuration 2 - Maximum fuel in the wing with the balance required in the fuselage fore and aft.
- Configuration 3 - Fuel in the wing plus external pylon tanks.

When "configuration" is spoken of here, it is mostly the fuel system and tank arrangement that is referred to. Outwardly, most of the airplanes are conventional in appearance and do not vary greatly from one to the other. Two exceptions would be the pylon tank version and the 130-passenger/2778 km (1500 n.mi.) airplane. The latter is a twin-engine aircraft because it was presumed that no over-water flights would be made. However, as a twin, it too is outwardly conventional.

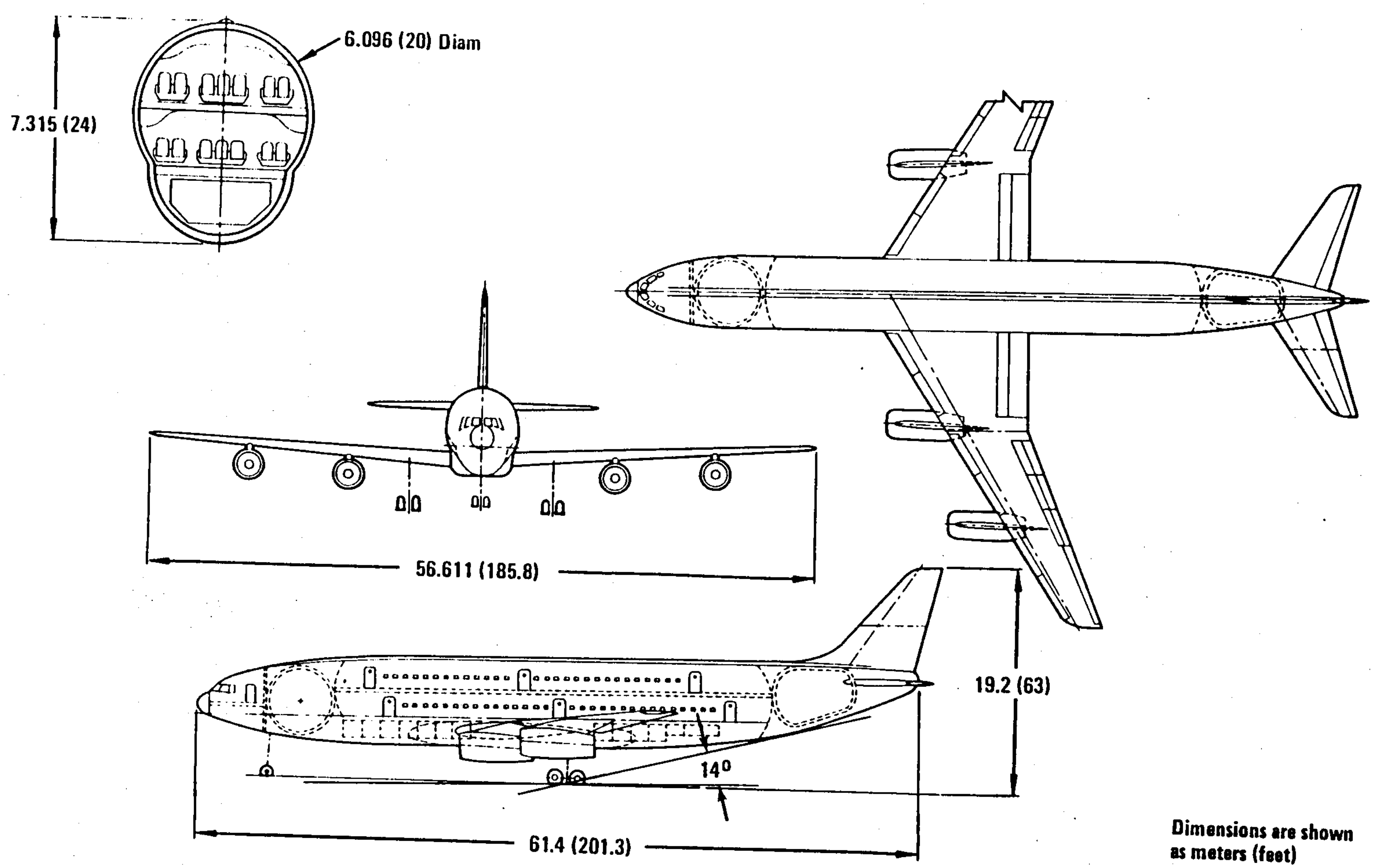

Figure 10. - Methane Configuration 1, all fuel in the fuselage.

Before the second configuration could be accurately sized, a suitable concept for a cryogenic internal wing tank had to be arrived at. Of the three structural concepts for wing tanks shown in figure 11, the design at the bottom of the figure with the graphite epoxy upper and lower surfaces was chosen because of its larger volume capacity. A further improvement for accessibility would be to make every other shear web shown an open span-wise truss, i.e., of the five shear webs shown, make the first, third, and fifth an open truss to increase the size of the fuel bay.

The internal insulation of the composite wing would be polyphenylene oxide (PPO) foam 6.35 cm (2.50 in.) thick. PPO is a proven product, produced by a Netherlands company and used in shipboard LNG containers. It can currently be produced in thicknesses up to 7.62 cm (3 in.) and in a range of densities from 30.4 to 192.2 kg/m^3 (1.9 lb to 12.0 lbs/ft^3).

PPO insulation would have to be laid in sections rather than being blown on and expected to adhere to the tank surfaces. This makes accessibility to the tank interior throughout the wing a prime consideration for installation and inspection of the insulated surfaces. The permeability of the graphite epoxy composite upper and lower surfaces to methane is not viewed as a problem since a thin mylar/aluminum membrane (MAAMF) is visualized at the inner surface of the composite material.

For a cryogenic fuel, it is important to minimize the surface-to-volume ratio of the tanks so that the weight of the structure, its insulation, and the heat transfer to the fuel can be minimized. Because of the very low boiling point of the fuel and the need to reduce boil-off losses, it is advantageous to pressurize the fuel tanks. In this regard, conventional wing tanks are limited to a maximum of approximately 20.7 to 34.5 kPa (3 to 5 psi) above ambient because of the relatively flat tank surfaces. Thus, at altitude, up to 9 percent of the methane might be lost by boil-off (reference 7).

Using the fuel volume afforded by a composite wing concept, it was found that a little less than half of the required volume, 85.2 m^3 (3009 ft^3), could be contained in the total wing bat section between the inboard engines. The remainder, 86.5 m^3 (3056 ft^3), is equally divided between a torus as the forward tank and an aft cylindrical tank, as shown in figure 12.

The torus was introduced for two reasons. It requires about 2.13 m (7 ft) less fuselage length than a sphere, and it provides ready access to the passenger cabin for the crew through the center opening in the event such is desired. For the purposes of preliminary design, the weight difference between the torus and the sphere is negligible. The aft tank, now being smaller than it was in the baseline configuration, can be stowed further aft in the tail section and thereby provides a further reduction in fuselage length of xxx m (11 ft) for a total of 5.49 m (18 ft) overall relative to the first configuration.

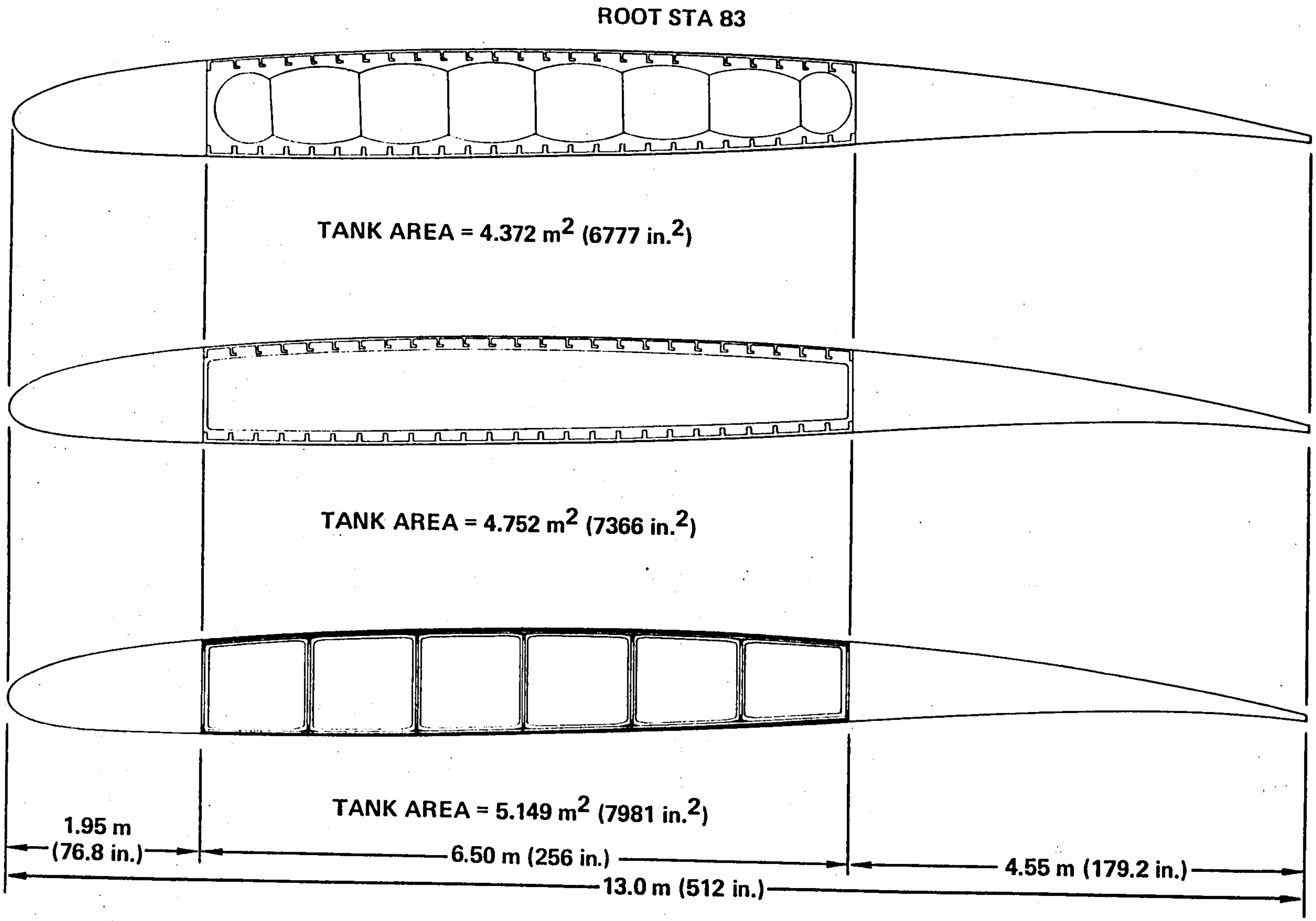

Figure 11. - Internal wing tank concepts.

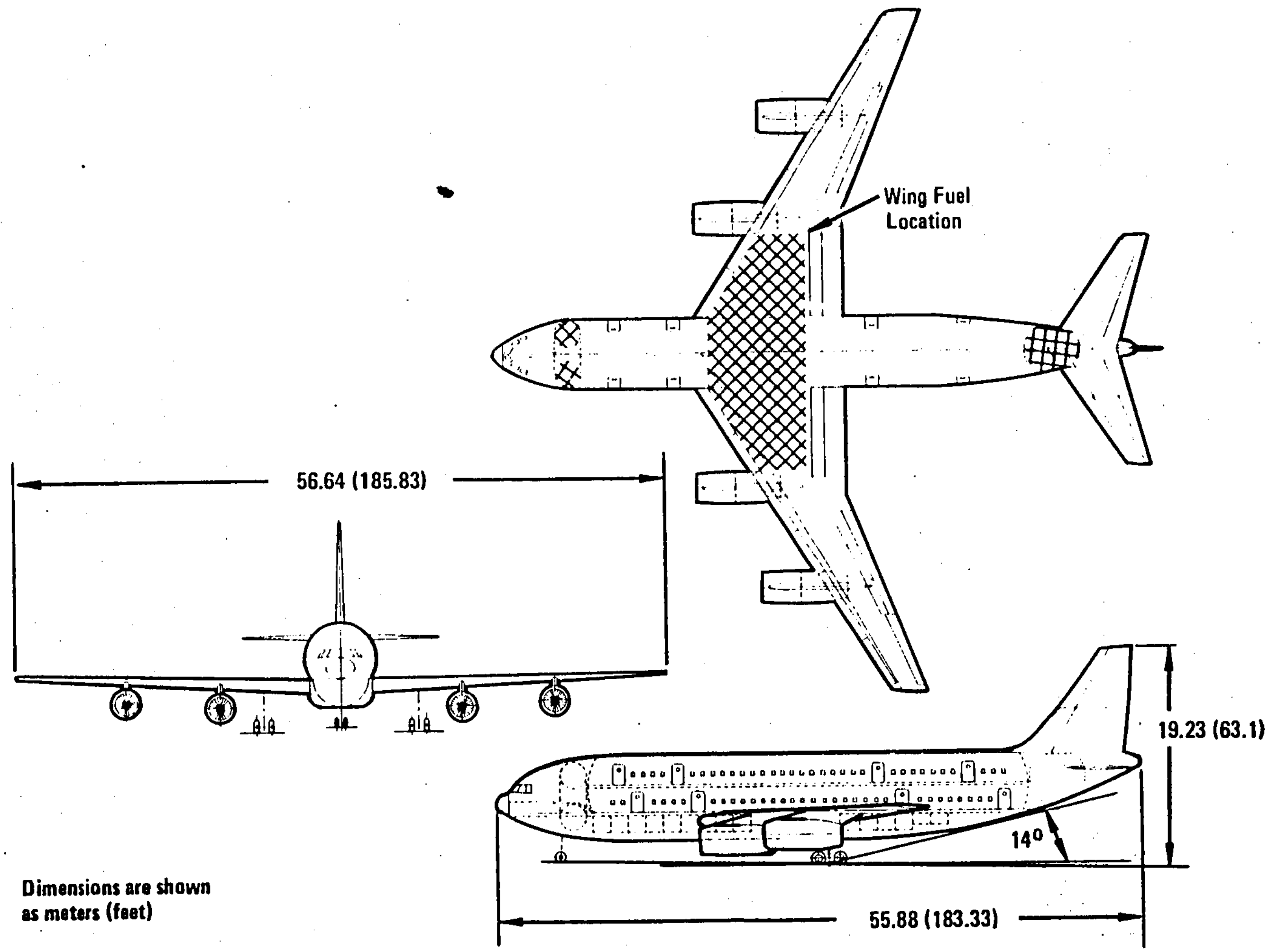

Figure 12. - Methane Configuration 2, fuel in fuselage plus wing.

The third airplane configuration was laid out with all of the fuel removed from the fuselage and contained in the wing and in pylon tanks. This provides the shortest fuselage of all three configurations that can accommodate 400 passengers. As a result, the angle of rotation available for takeoff can go from 0.24 to 0.28 rad (14 deg. to 16 deg.), as shown in figure 13.

The pylon tank configuration and structural concept, figure 14 was adapted from the previous liquid hydrogen configuration (reference 3, figure 63) for the sake of consistency in comparing a methane design that is similar. It is acknowledged that the position of the pylon and tank directly over the engine nacelle is not the right location for the least interference drag at Mach 0.85, and that a better spot is somewhere about midway between the engine nacelles. The best answer to this question can only be arrived at by the aid of a rather substantial wind tunnel program on the aerodynamic integration of the wing/engine nacelle/pylon tank combination.

Initial estimates of the methane load for the 10 186 km (5500 n.mi.) mission showed that 171.6 m^3 (6065 ft^3) of fuel volume would be required. Using the composite wing as shown in figure 11, the wing internal fuel volume between the 0.15 chord and 0.65 chord beam locations was calculated as 85.2 m^3 (3009 ft^3), including the wing center section. The remainder, 86.5 m^3 (3056 ft^3), is divided between the pylon tanks.

The pylon tank geometry was adapted from NASA TR R-100, Configuration 17, which offers a low drag coefficient at Mach 0.85 and a long straight cylindrical center section nearly equal to the wing chord at that location. The front section of the tank is an ellipsoid two diameters in length and the rear an ogive three diameters in length. Having the length in terms of diameters, the volumes of these regular geometric shapes can be expressed as a cubic of one unknown.

Before solving for the required diameter and length, a further step was taken to determine the tank volume in the "as built" condition to accommodate 43.3 m^3 (1528 ft^3) of liquid methane at cryogenic temperature. Table 8 presents volume allowances and conditions for known changes to the tank from its "as built' condition at ambient temperature to obtain the required net fluid volume with ullage at cryogenic temperature.

The correct cubic for the as-built volume is then:

$$\frac{4\pi}{3} D \frac{D^2}{4} + \frac{25\pi}{4} D^2 + \frac{3\pi}{8} D^3 = 46.53 \text{ m}^3 \ (1644 \text{ ft}^3)$$

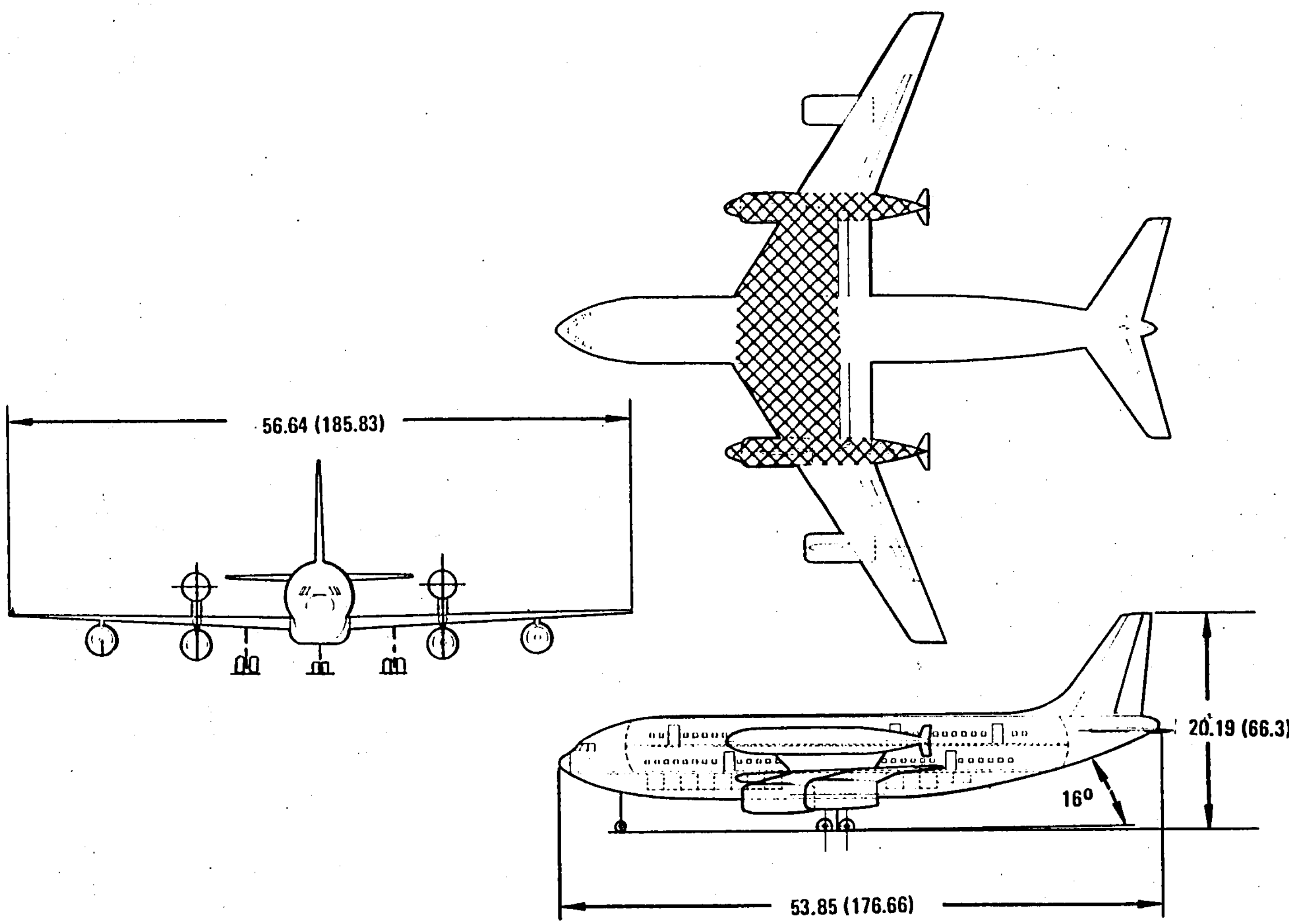

Figure 13. - Methane Configuration 3, fuel in wing plus pylons.

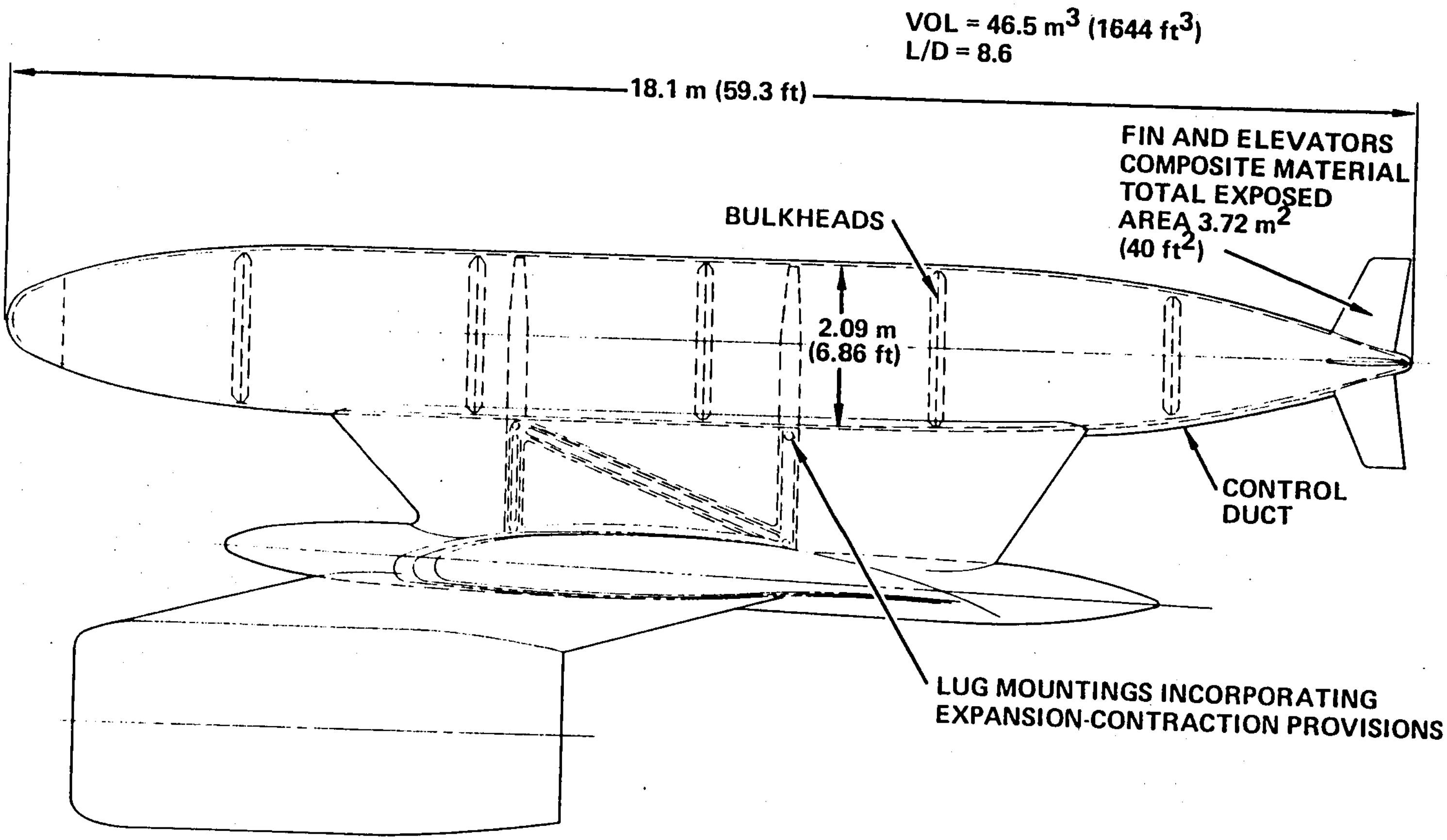

Figure 14. - General arrangement of methane pylon tank.

TABLE 8. - PYLON TANK VOLUME ALLOWANCES

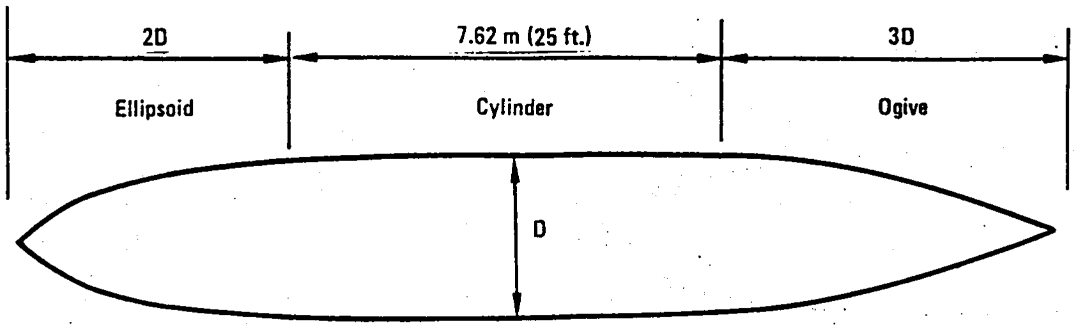

Volume Required = 43.3 m^3 (1528 ft^3)

Condition	% Volume Change
Temperature contraction and pressure change (2219 $A\ell$)	+0.8
Fluid expansion due to density change	+1.4
Internal structure	+0.44
Internal equipment	+0.06
Trapped fuel	+0.30
Ullage	+0.42
Boil-off and pressurant gas	+5.00
Net Change	+7.62%
"As built" volume required	
0.0762 (1528) + 1528 = 1644 ft^3	

$$2.225\ D^3 + 19.6\ D^2 - 1644 = 0$$

$$\therefore D = 2.09 \text{ m } (6.86 \text{ ft})$$

$$\text{Ellipsoid} = 2D = 4.18 \text{ m } (13.72 \text{ ft})$$

Cylinder (equal to chord)
7.62 m (25.00 ft)

Ogive = 3D = 6.27 m (20.58 ft)

Fluid volume length 18.1 m (59.30 ft)

The required tank wall and insulation thickness are added to these dimensions, as shown in figure 14. The inner layer of closed cell foam is Stepan Foam BX250 A with a density of 36.8 kg/m^3 (2.3 lb/ft^3). Next is a MAAMF vapor barrier and then a flexible open-cell foam compressed to 1.78 cm (0.7 in.). On the outside is a Kevlar/syntactic foam wrap for fairing and mechanical protection. This is the same insulation concept as chosen for the integral aft fuselage tank, as shown in figure 106, Section 8. All tank concepts are summarized in figure 15.

Highlights of the pylon tank design include the following features:

- The pylon tank with 43.3 m^3 (1528 ft^3) of liquid methane has about one-sixth the volume of the hydrogen tank and is, by the cube root rule for volumes, only 55 percent as long.

- Although the pylon tanks will need boost pumps for crossfeed, it is visualized that normally the pylon tank would gravity feed to the internal wing tanks. The engines would take fuel from the internal tanks, no pylon tank would ordinarily supply an engine, and therefore, the pylon tanks would be emptied first.

- The elevator on the pylon tank is a controlled flight surface which can be used to aid in trim and in reducing wing moments in torsion. The tank tail surfaces are of composite materials.

- The tank nose is removable for inspection and maintenance access.

- The interior of the tank is insulated in the area where it interfaces with the pylon support structure to reduce heat flow from the warmer support structure to the methane.

- The clearance between the bottom surface of the tank and the upper surface of the wing has been kept about the same as it was for the hydrogen airplane, i.e., about 152.4 cm (60 in.).

- A boot fairing has been added at the wing and pylon intersection to aid in reducing interference drag.

- Bulkhead fuel baffles have been shown which will also aid in stiffening the tank structure.

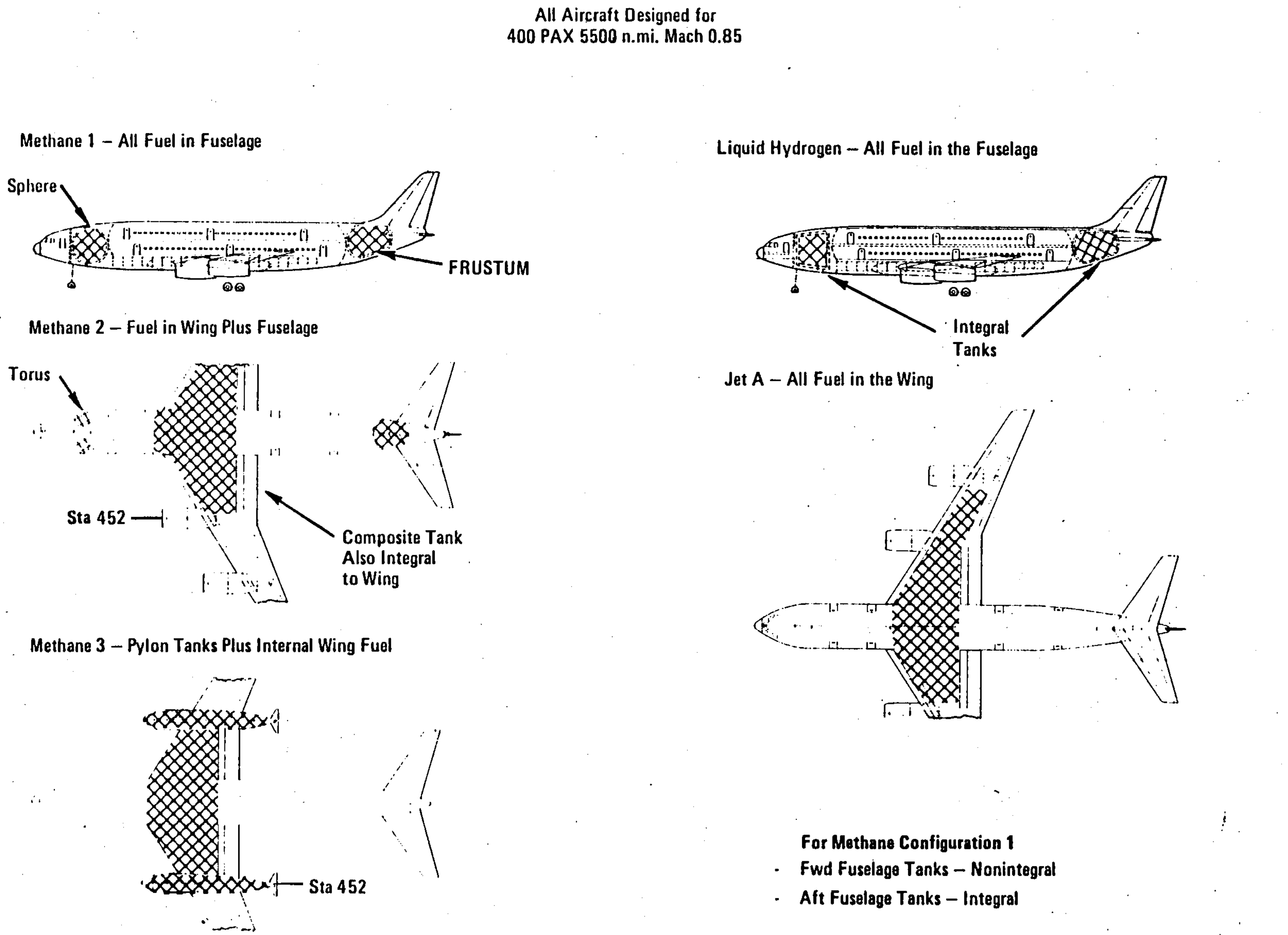

Figure 15. - Summary of fuel tank concepts.

- The following inertia load criteria were applied to the tank suspension system and the fuel in the tank (FAR 25.561):

Upward	n = 2.0
Forward	n = 9.0
Sideward	n = 1.5
Downward	n = 4.5

3.2 Preliminary Fuel Tank Insulation Concepts and Weight Estimate

Before the parametric analysis on the three vehicle configurations could proceed, a preliminary least weight insulation concept had to be arrived at. This was done by applying a heat transfer analysis to the fore and aft tanks of the baseline Configuration 1. For the aft tank the heat transfer analysis includes the insulating value of the open-cell foam-Kevlar fairing, which is used to cover the primary insulation of the conic section. The tank heads have primary insulation only. For the spherical forward tank, primary foam only was used. The results are shown in table 9. Using the criteria of the sum of methane evaporated in flight and the insulation weight, $\Sigma\,(fM_e + M_i)$, the Stepan Foam BX 250A is clearly the lightest for the baseline airplane. It should be noted that the final optimization by computer modeling, as reported in Section 8, provides insulation thicknesses that are slightly less than this initial screening for weight estimating purposes. From these results, the preliminary weights can be accounted for.

For Configuration 1, Stepan Foam BX 250A is the minimum weight system at 1161 kg (2560 lb). No accounting has been made for small changes in fuselage dimensions or ground vent recovery factor. Foam weight includes 0.224 kg/m^2 (0.046 lb/ft^2) for vapor barrier and 0.220 kg/m^3 (0.045 lb/ft^2) for two layers of adhesive.

In Configuration 2, fuel is carried in the wing tanks, including fuselage center section, plus fore and aft tanks in the fuselage.

The wing tanks are graphite-epoxy plus PPO internal foam insulation. Candidate insulation systems are discussed in Section 8.

Required volumes are:

Wing	=	85.2 m^3 (3009 ft^3)
Aft Fuselage Tank	=	43.3 m^3 (1528 ft^3)
Fwd Torus	=	43.3 m^3 (1528 ft^3)
Total		171.8 m^3 (6065 ft^3)

TABLE 9. - PRELIMINARY INSULATION SYSTEM WEIGHTS FOR THE BASELINE CONFIGURATION 1

Symbols:

fM_v – fuel vented in flight

fM_e – fuel evaporated in flight

gM_v – fuel vented on ground (recoverable)

M_i – insulation system weight

Insulation	Optimum t_i cm (in) (a)	fM_e kg (lb) (b)	$\Sigma(fM_e + M_i)$ kg (lb) (c)	gM_v kg (lb) (d)
Stepan Foam Bx 250 * 2.3 pcf				
Aft	5.08 (2.0)	341 (752)	567 (1250)	331 (730)
Fwd	6.35 (2.5)	322 (710)	594 (1310)	322 (710)
Total		663 (1462)	1161 (2560)	653 (1440)
Microspheres Plus VAC System *				
Aft	2.86 (1.125)	228 (503)	624 (1375)	265 (585)
Fwd	3.18 (1.250)	228 (502)	624 (1375)	274 (605)
Total		456 (1005)	1248 (2750)	539 (1190)
Internal PPo * 2.4 pcf				
Aft	7.62 (3.0)	331 (730)	624 (1375)	305 (700)
Fwd	7.62 (3.0)	367 (810)	651 (1435)	342 (755)
Total		698 (1540)	1275 (2810)	647 (1455)

(a) Minimum of $\Sigma(fM_e + M_i)$

(b) Fuel evaporated in flight

(c) Weight of fuel evaporated in flight plus weight of insulation. Does not include open-cell foam or fairing.

(d) Weight of fuel vented on the ground, including cool-down during refueling.

*See Section 8 for discussion of candidate insulation systems.

- Per wing tank

$$\Sigma fM_e + M_i = 1161 \text{ kg } (2065 \text{ lb})$$

$$\Sigma fM_e = 474 \text{ kg } (1045 \text{ lb})$$

$$\Sigma gM_v = 366.5 \text{ kg } (808 \text{ lb})$$

- Total wing

$$\Sigma fM_e + M_i = 1873 \text{ kg } (4130 \text{ lb})$$

$$\Sigma fM_e = 948 \text{ kg } (2090 \text{ lb})$$

$$\Sigma gM_v = 733 \text{ kg } (1616 \text{ lb})$$

The insulation weight is the sum of the PPO plus the internal MAAMF barrier plus two adhesive layers.

For the fuselage tanks, the same t_i was used as for Configuration 1, i.e., aft 5.08 cm (2.0 in.) and forward 6.35 cm (2.5 in.). Aft tank approximate weights are scaled as the volume ratio; however, for the fuel losses of the torus, the optimum t_i is still 6.35 cm (2.5 in.) for Stephan foam and the weights are:

$$\Sigma fM_e = 248 \text{ kg } (547 \text{ lb})$$

$$\Sigma fm_e + M_i = 454 \text{ kg } (1002 \text{ lb})$$

$$\Sigma gM_v = 255 \text{ kg } (562 \text{ lb})$$

The total weight for this configuration is the sum of 1873 kg (4130 lb) for the wing tanks and 454 kg (1002 lb) for the fuselage tank for a total of 2328 kg (5132 lb).

From a tank insulation standpoint, Configuration 2 is poor because the surface-area-to-volume ratios are too high for the torus and the flat wing tanks.

In Configuration 3, fuel is contained in the graphite epoxy wing plus above-wing pylon tanks. The outer fairing and open-cell foam 1.78 cm (0.7 in.) are included as insulation for heat transfer calculations relative to the pylon-mounted tanks. Optimum for the following weights appears to be 5.08 cm (2 in.) of Stepan foam:

$$fM_v = 247 \text{ kg } (544 \text{ lb})$$

$$fM_e = 333 \text{ kg } (735 \text{ lb})$$

$$gM_v = 316 \text{ kg } (698 \text{ lb})$$

$$M_i = 254 \text{ kg } (560 \text{ lb})$$

$$(fM_e + M_i) = 587 \text{ kg } (1295 \text{ lb})$$

From Configuration 2, the wing tank insulation weight is 1873 kg (4130 lb). The pylon tanks have 587 kg (1295 lb) for a total system weight of 2461 kg (5425 lb).

Again, the pylon tank concept is not very efficient thermally. It has a poor shape for thermal optimization. The complete thermal analysis and final optimization process is contained in Section 8.

4. AIRCRAFT PARAMETRIC ANALYSIS AND CONFIGURATION SELECTION

It is worthwhile to state again that the method of the study was to develop the best methane transport configuration from three candidates for the basic payload/range of 400 passengers and 10 186 km (5500 n.mi). This configuration and the resulting fuel system, tanks, and insulation system was then adopted for the other four payload/ranges. Also, the LH_2 and Jet A aircraft of references 3 and 6 studies of 1974-75 were updated to an equivalent technology level so that there would be a consistent matrix of three alternate fueled aircraft at five payload/ranges. The performance of all these aircraft is summarized at the end of this section. The significant parts of the final computer optimization is shown for each alternate fueled airplane in the appendix for the 10 186 km (5500 n.mi.) design range. They are as follows:

- Configuration Geometry
- Weight Summary
- Mission Summary
- Cost Summary
- Parametric Analysis

4.1 Performance Analysis of Three Candidate Methane Configurations for the 400 Passenger/10 186 (5500 n.mi.) Payload/Range

The common characteristics for the methane airplanes were taken from the LH_2 and Jet A studies of references 3 and 6. They are as follows:

Range	10 186 km (5500 n.mi.)
Cruise Mach	0.85
Passengers	400
Aspect Ratio	9
Taper Ratio	0.3
Sweep	0.524 rad (30 deg)
Wing Thickness Ratio	10.0
Tail Volume Coefficients	
Horizontal	0.66 } Based on exposed area
Vertical	0.055 } Based on exposed area
Takeoff Field Length	$\leqq$ 2438m (8000 ft)
Approach Speed	$\leqq 69.4 \frac{m}{s}$ (135 knots)
Initial Cruise Altitude	$\geqq$ 10 363 m (34 000 ft)
Engine-out Climb Gradient	$\geqq$ 0.03

Cost data were based on 1976 dollars and methane fuel was priced at \$4 per 10^6 Btu.

The parametric matrix chosen for optimizing on the basis of DOC was:

Wing Loadings	$\left(\frac{W}{S}\right)$	488 kg/m^2 (100 psf)
		537 kg/m^2 (110)
		586 kg/m^2 (120)
		635 kg/m^2 (130)
		683 kg/m^2 (140)
Thrust to Weight Ratios	$\left(\frac{T}{W}\right)$	2.70 N/kg (0.275 lb/lbm)
		2.94 N/kg (0.300 lb/lbm)
		3.19 N/kg (0.325 lb/lbm)
		3.43 N/kg (0.350 lb/lbm)

This 20-point matrix did not involve any further iteration of aspect ratio, wing sweep, or thickness ratios as they were considered to have been adequately defined by the referenced studies.

The results are shown in parametric form in figures 16 through 24 for each of the three configurations. As can be seen, the "bucket" of the DOC curves is quite flat and significant variations in T/W and W/S can occur with only minor changes in DOC values in the third decimal place. Solving for the point designs of the three configurations on the basis of minimum DOC results in an iterative process of selecting point design values from the curves and confirming that they meet the field-length and approach-speed constraints as closely as possible by detailed analysis in the ASSET computer system.

As indicated by the cross hatching on the back side of the constraint lines on the plots, only those values above the takeoff constraint and also to the right of the approach-speed constraint line can be used. Those below and to the left, on the shaded side of the lines, do not represent valid designs.

Aircraft design parameters based on T/W and W/S values selected from the carpet plots which appeared to provide minimum DOC were input to the computer. The results provided definition of near-optimum versions of aircraft for all three configurations. Table 10 lists values of the significant parameters for the three aircraft.

Configuration 2, which has the lowest DOC in the methane group, has a fuselage that is 18 feet shorter than Configuration 1 because of the ability to carry 53 percent of the methane required in the wing. The use of the torus as the forward fuselage tank rather than the sphere, also contributed to the reduced length. It should be noted, however, that practical aspects

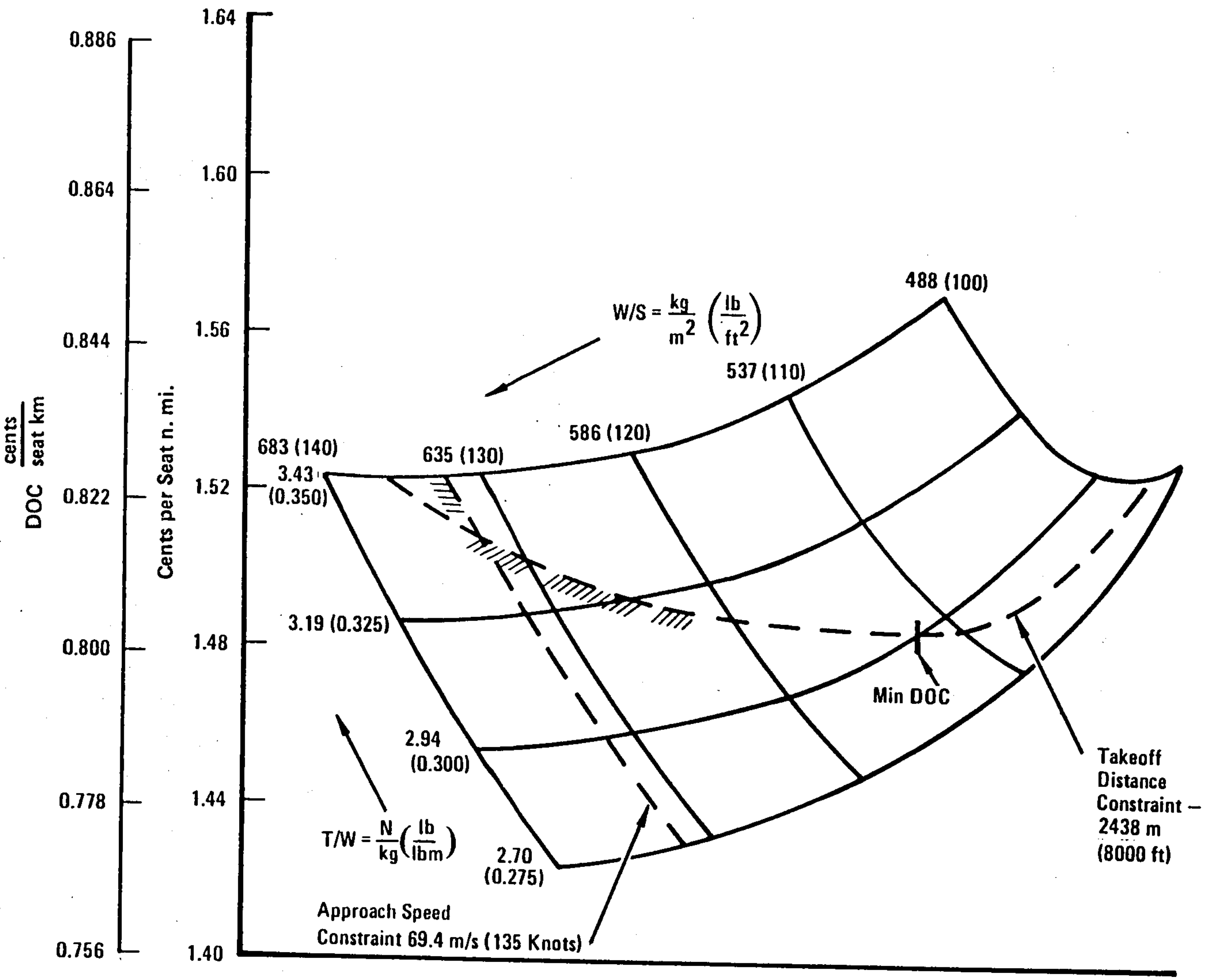

Figure 16. - DOC evaluation, configuration 1.

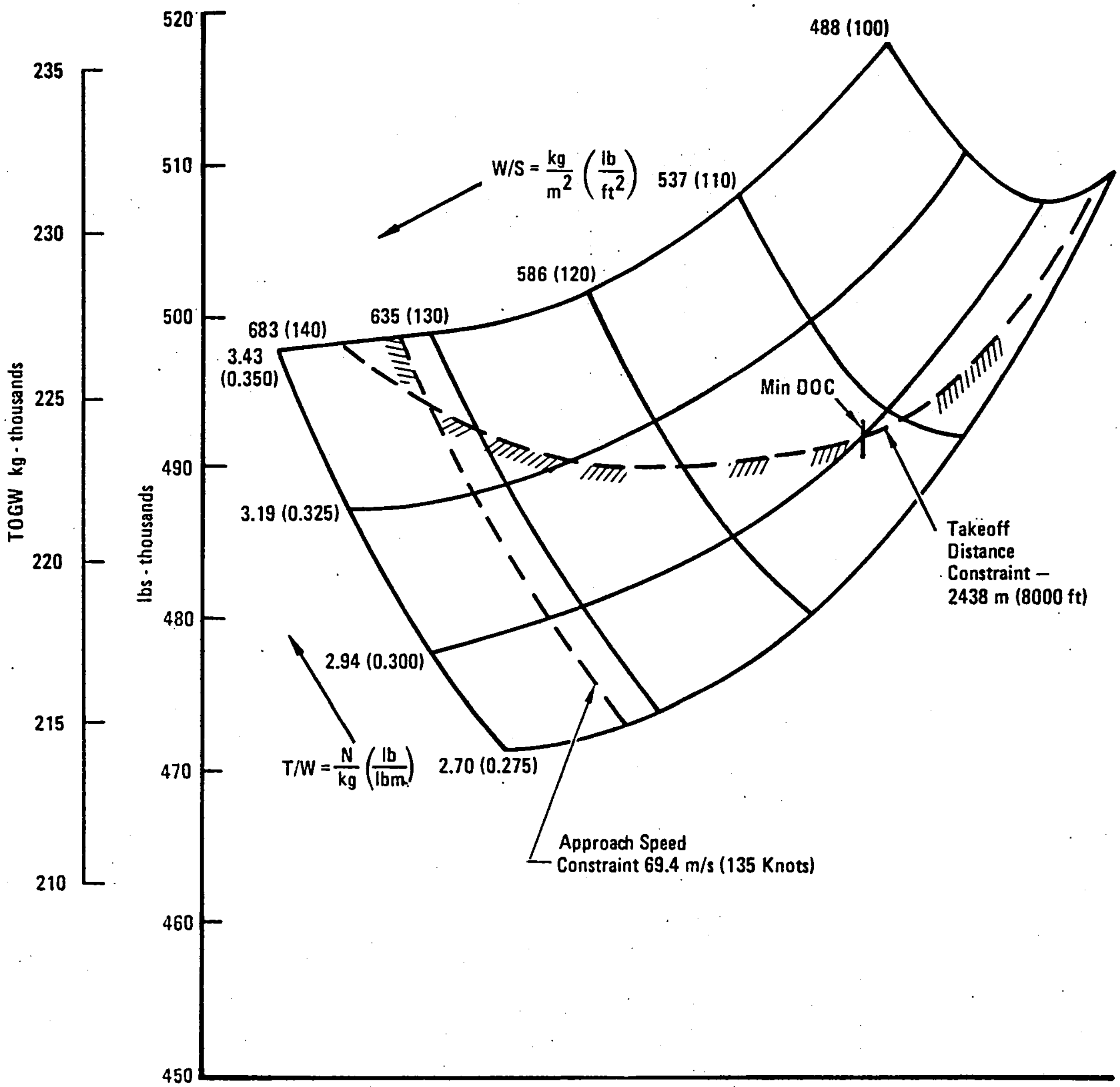

Figure 17. - TOGW evaluation, configuration 1.

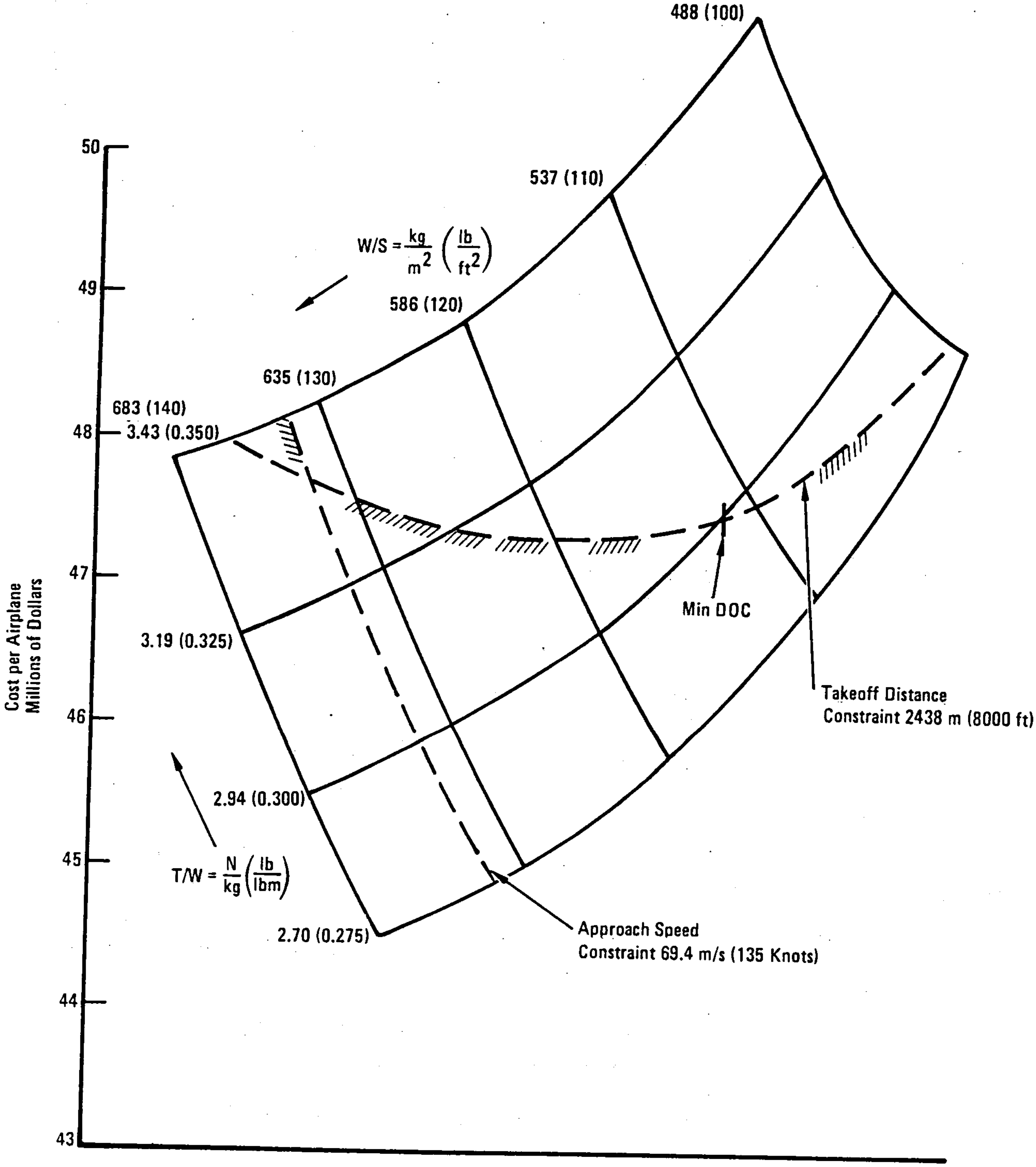

Figure 18. - Airplane cost evaluation, configuration 1.

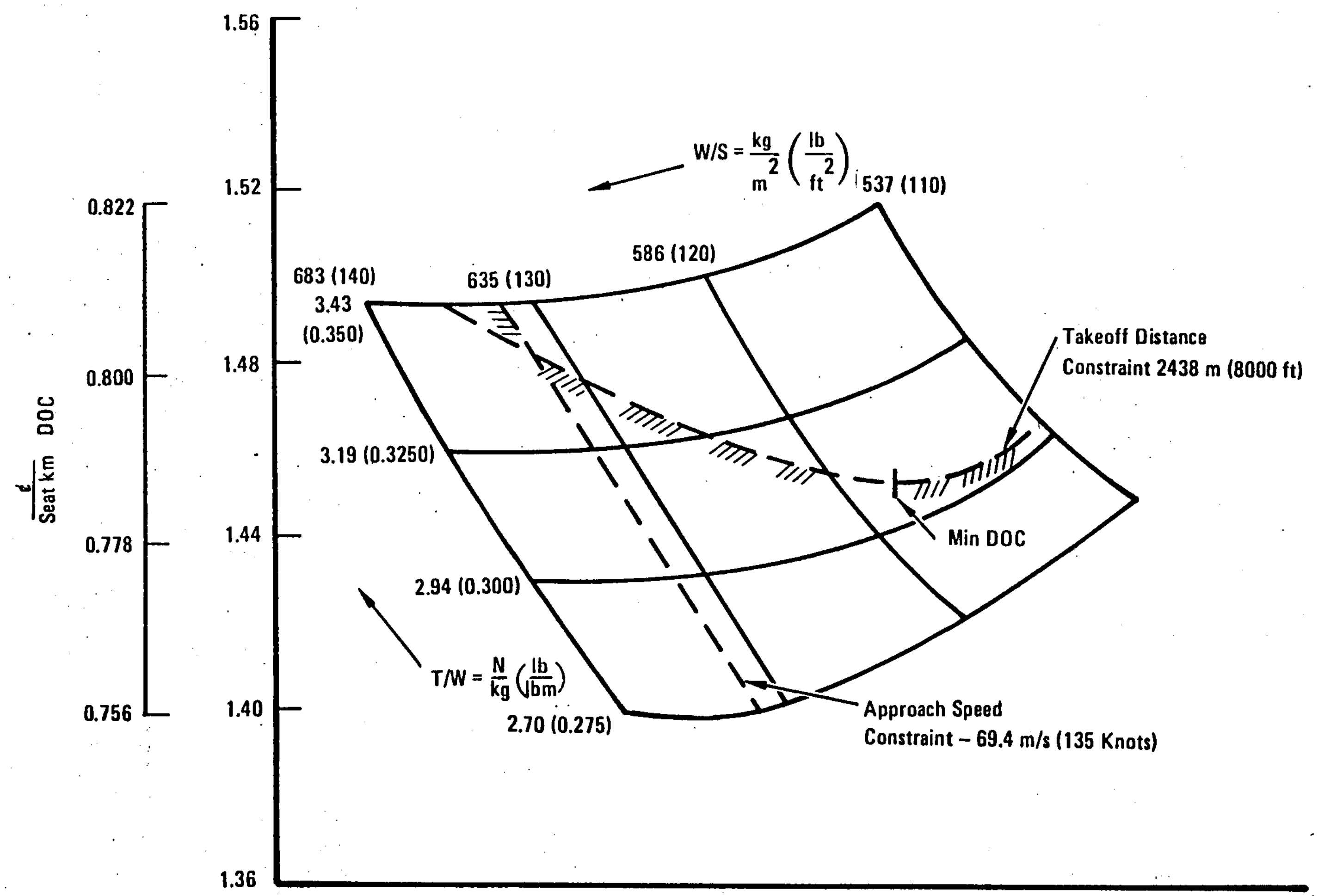

Figure 19. – DOC evaluation, configuration 2.

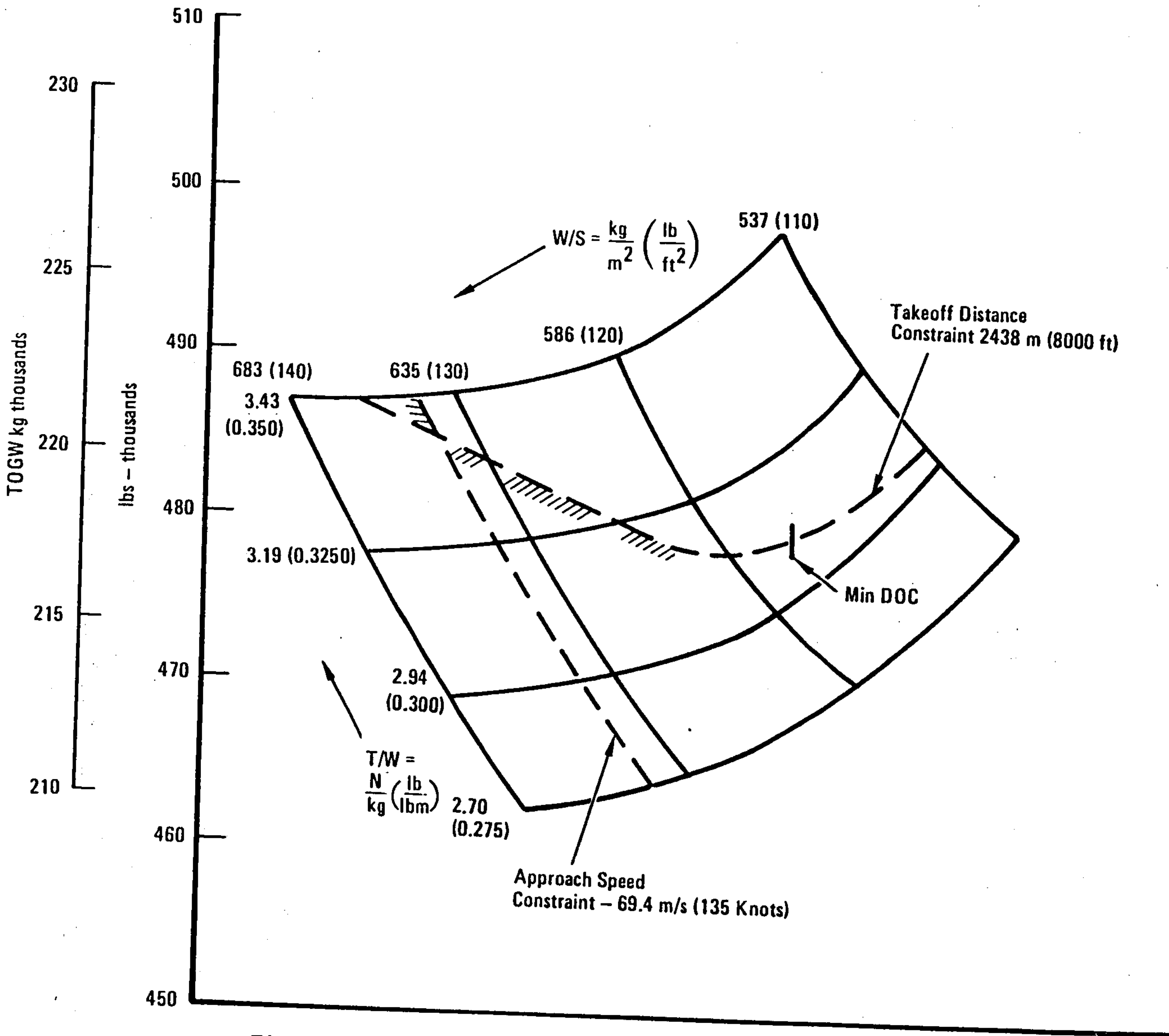

Figure 20. - TOGW evaluation, configuration 2.

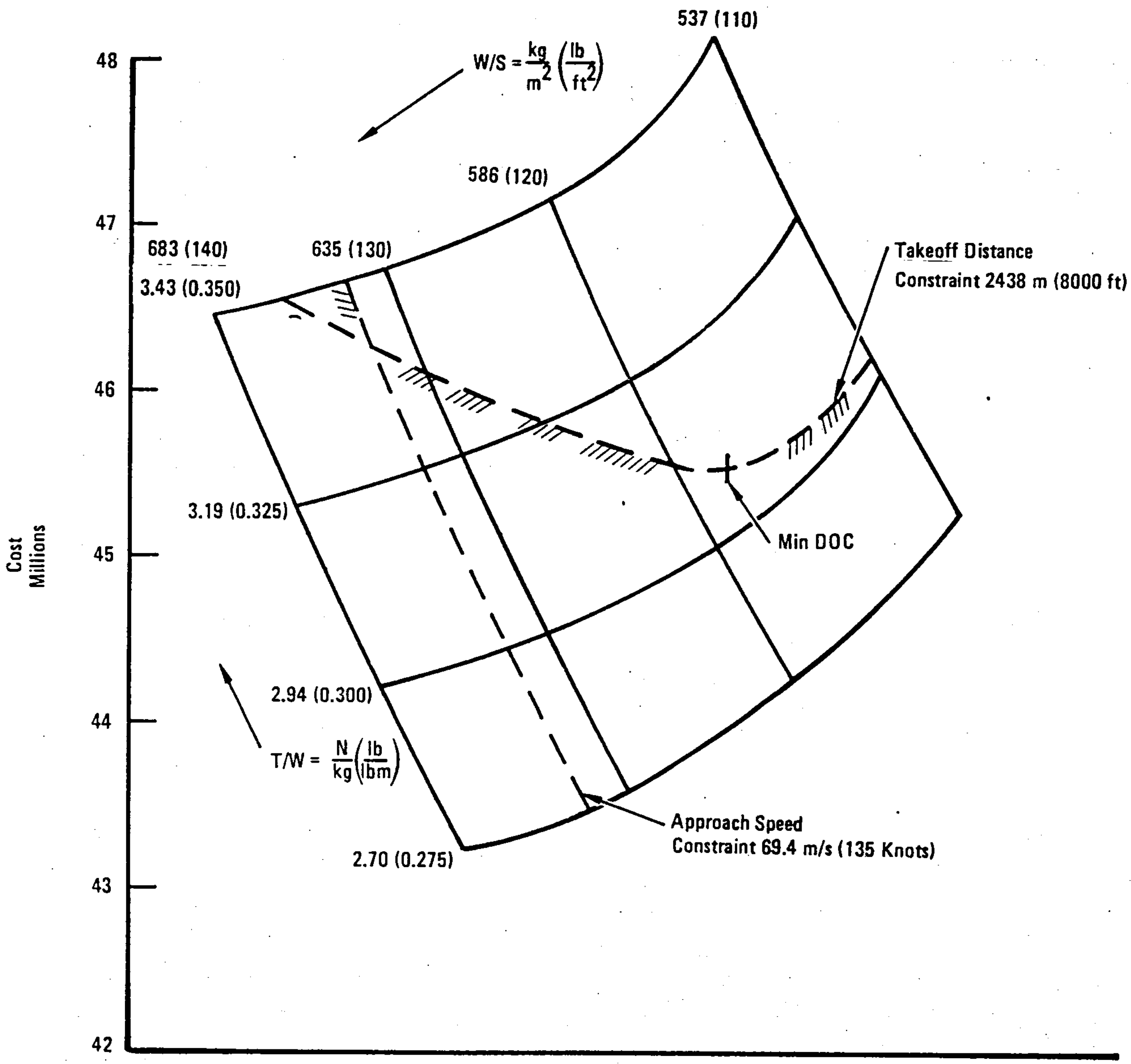

Figure 21. - Airplane cost evaluation, configuration 2.

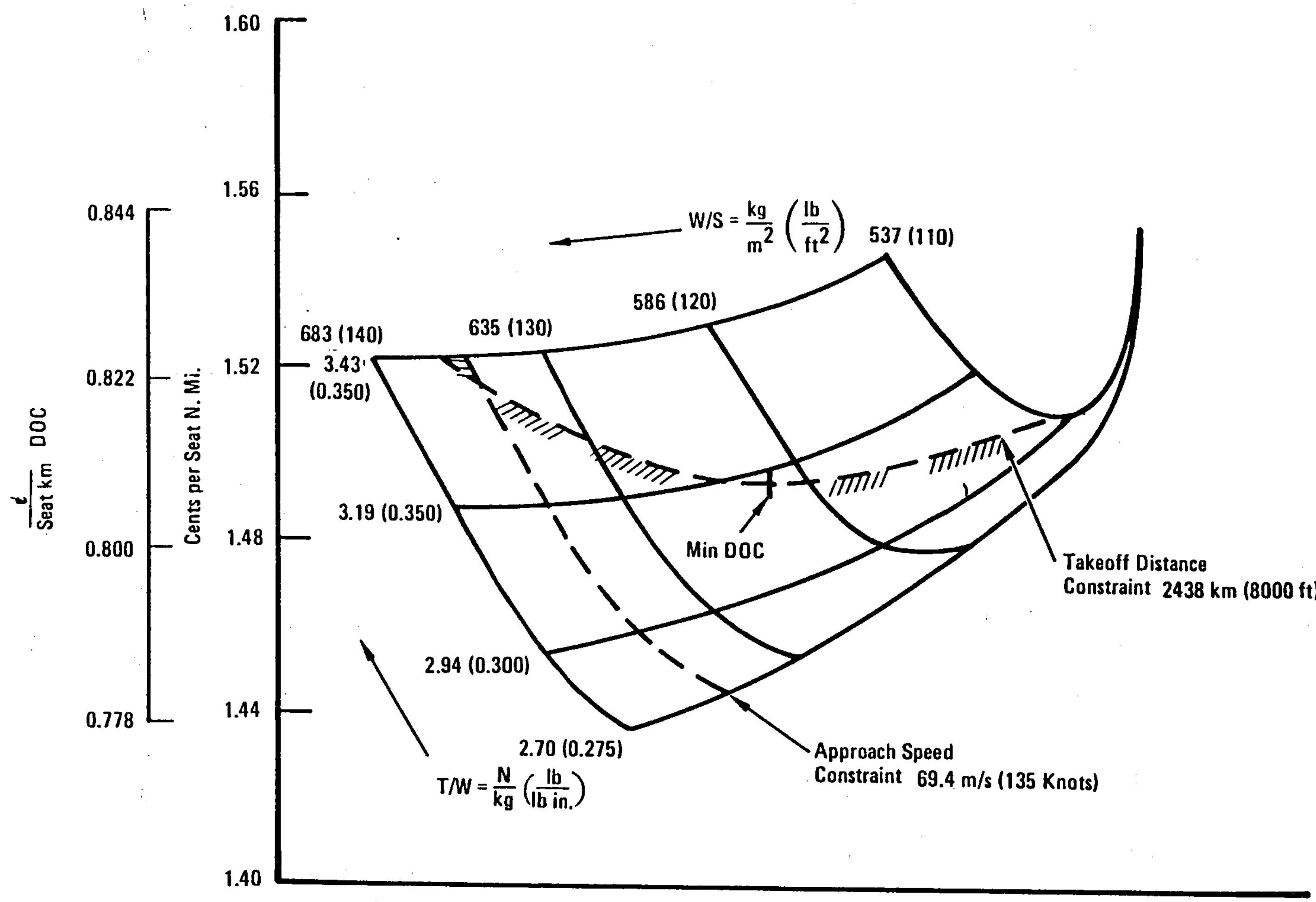

Figure 22. - DOC evaluation, configuration 3.

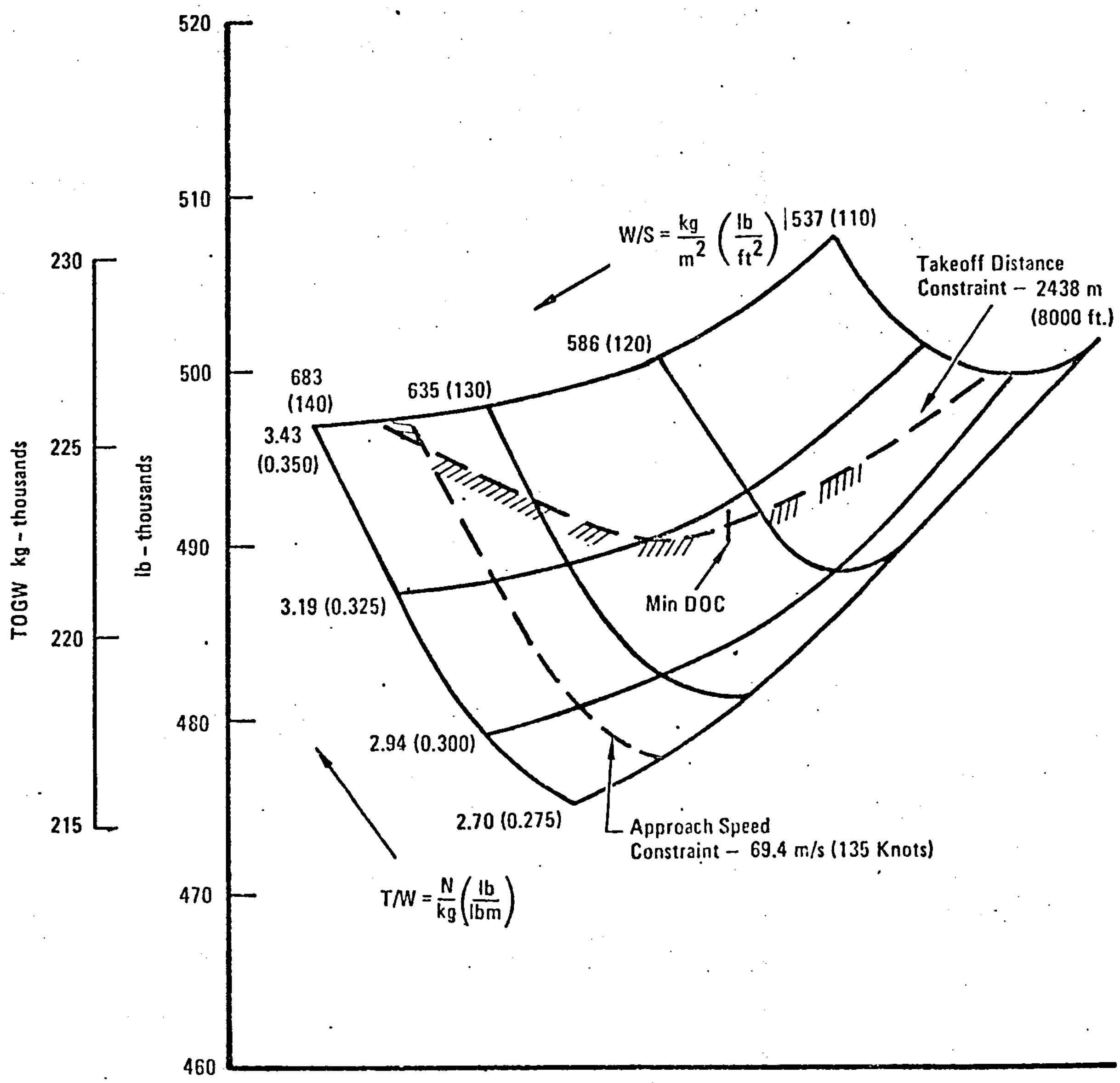

Figure 23. - TOGW evaluation, configuration 3.

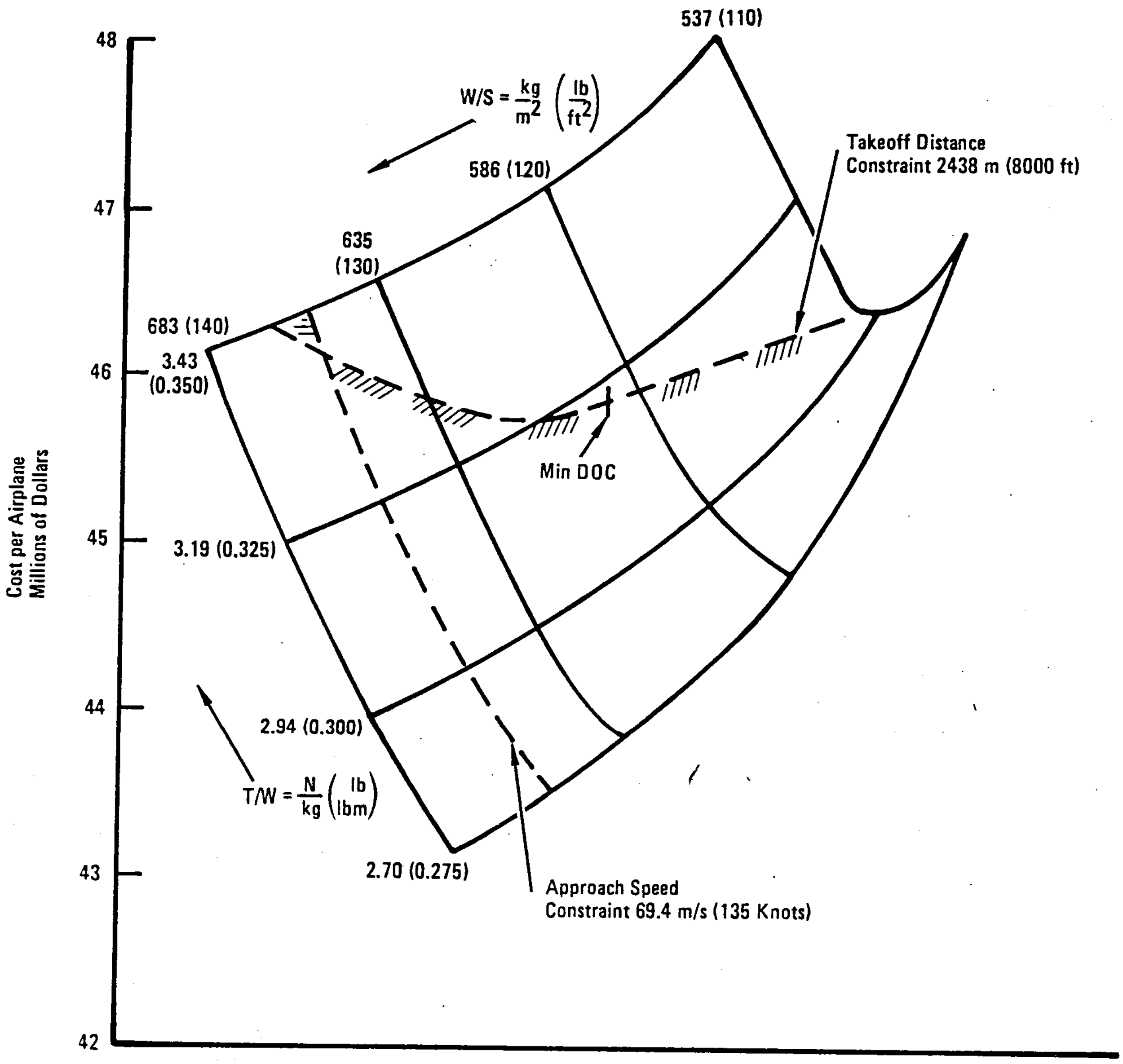

Figure 24. - Airplane cost evaluation, configuration 3.

TABLE 10. - COMPARISON OF CANDIDATE METHANE CONFIGURATIONS

(400 Passengers - 10 186 km (5 500 n.mi.) - Mach 0.85)				
		Configuration 1	Configuration 2	Configuration 3
Gross Wt	kg	224 000	218 200	223 000
	(lb)	(493 900)	(481 000)	(491 700)
Total Fuel Wt	kg	69 040	68 360	72 390
	(lb)	(152 200)	(150 700)	(159 600)
Block Fuel Wt	kg	58 500	58 060	61 690
	(lb)	(129 000)	(128 000)	(136 000)
Operating Empty Wt	kg	115 030	109 900	110 700
	(lb)	(253 600)	(242 300)	(244 100)
Aspect Ratio	-	9	9	9
		(9)	(9)	(9)
Wing Area	m^2	417	385	374
	(ft^2)	(4 490)	(4 147)	(4 030)
Sweep	rad	0.524	0.524	0.524
	(deg)	(30°)	(30°)	(30°)
Span	m	61.3	58.9	58.1
	(ft)	(201)	(193.2)	(190.5)
Fuselage Length	m	61.4	55.9	53.9
	(ft)	(201.3)	(183.3)	(176.7)
L/D Cruise	-	19.11	18.76	19.73
		(19.11)	(18.76)	(17.93)
SFC Cruise	$\frac{kg}{hr}$/daN	0.502	0.503	0.503
	(lb/hr/lb)	(0.492)	(0.493)	(0.493)
Initial Cruise Alt	m	11 582	11 582	11 582
	(ft)	(38 000)	(38 000)	(38 000)
Wing Loading	kg/m^2	537	566	596
	(lb/ft^2)	(110)	(116)	(122)
T/W	N/kg	2.94	3.06	3.15
		(0.300)	(0.312)	(0.321)
Thrust Per Engine	N	164 750	166 890	175 520
	(lb)	(37 040)	(37 520)	(39 460)
FAR T.O. Distance	m	2377	2407	2412
	(ft)	(7 804)	(7 896)	(7 913)
FAR Landing Distance	m	1524	1572	1610
	(ft)	(5 001)	(5 157)	(5 281)
Eng Out Climb Grad	-	0.03	0.0327	0.030
		(0.03)	(0.0327)	(0.030)
Approach Speed	m/s	63.6	65.2	66.4
	KEAS	(123.7)	(126.7)	(129.0)
Weight Fractions				
Fuel	%	30.82	31.32	32.46
		(30.82)	(31.32)	(32.46)
Payload	%	17.82	18.30	17.90
		(17.82)	(18.30)	(17.90)
Structure	%	29.25	28.10	26.94
		(29.25)	(28.10)	(26.94)
Propulsion	%	6.74	6.61	7.34
		(6.74)	(6.61)	(7.34)
Price – Millions	$\$10^6$	47.45	45.68	45.84
	($\$10^6$)	(47.45)	(45.68)	(45.84)
DOC Cents/Seat n.mi.	$/seat km	0.802	0.787	0.807
	(cents/seat n.mi.)	(1.486)	(1.458)	(1.494)
Energy Utilization	kJ/seat km	717	711	756
	Btu/seat n.mi.	(1 261)	(1 251)	(1 330)

of the fuel containment problem, such as the difficulties which will be encountered in providing for pressure-tight sealing of the flat-shaped internal wing tanks, increased boil-off of gaseous methane for a given thickness of insulation, and the effect of increased surface area of the fuel containment system on safety will override this advantage.

The advantage of the reduced fuel volume in the fuselage is only a temporary gain. The much lower total fuel weight required for the hydrogen airplane relative to the methane (by a factor of 2.7, see table 11) overtakes the favorable volume/density characteristics of methane and results in the hydrogen-powered version being smaller in weight, span, and wing area even though the fuselage is longer. It is worth noting that the fuel weight fractions for hydrogen and methane are 15.17 percent and 30.82 percent, respectively, for the same payload, speed, and range.

The appearance of Configuration 1 as the chosen airplane of that group in table 11 rather than the lowest DOC airplane from table 10, Configuration 2, introduces the real basis for screening the methane designs. Had there been overwhelming differences in DOC between the three choices, especially the first two, the decision would have been more clear cut. As it is, the fact that the first configuration DOC is only 1.9 percent higher than the second leads one to look for more compelling reasons for making a choice. It is not reasonable to conclude that the 1.9 percent difference in DOC shown by the analysis will be the real difference for airplanes that might be designed 10 years from now and in service for 20 years beyond that. Rather, the decision should be based on consideration of the practical aspects of the designs, i.e., safety, relaibility, maintainability, producibility, etc.

The pylon tank configuration was eliminated on the basis of having the highest DOC and being thermally inefficient with the combination of flat wing tanks and the long slender pylon tanks. Both are poor shapes for good thermal efficiency. What follows are considerations other than DOC for choosing between the two remaining designs although many of the arguments would also apply to the pylon tank version if it were carried along.

4.1.1 Safety

4.1.1.1 Crashworthiness.- In the 1964 to 1978 time period, United States air carriers worldwide had 31 fatal accidents with 1500 fatalities. Of these 594 (39.6 percent) were due to postcrash fires (reference 8). Prevention of fuel tank rupture and a subsequent fire are predominant design concerns. Controlled breakaway design concepts for landing gear to prevent wing tank rupture alleviates the problem but does not remove the risk of ruptured tanks. Once the gear has sheared off, there are still the pylon-mounted engines to contend with and after that the wing can still break on contact with the ground. Considering the low-spark energy required to ignite methane and its low flammability limit in air, the internal wing tank does not offer much comfort.

TABLE 11. - HYDROGEN, METHANE AND JET A FUELED TRANSPORT CONFIGURATIONS

(400 Passengers - 10 190 km (5 500 n.mi.) - Mach 0.85)

		Hydrogen	Methane Configuration 1	Jet A
Gross Wt.	kg (lb)	168 800 (372 205)	224 000* (493 900*)	232 060 (511 600)
Total Fuel Wt.	kg (lb)	25 600 (56 457)	69 040 (152 200)	84 780 (186 900)
Block Fuel Wt.	kg (lb)	21 620 (47 666)	58 500 (129 000)	72 350 (159 500)
Operating Empty Wt.	kg (lb)	103 300 (227 748)	115 030 (253 600)	107 370 (236 700)
Aspect Ratio	-	9 (9)	9 (9)	9 (9)
Wing Area	m^2 (ft^2)	297 (3 195)	417 (4 490)	380 (4 093)
Sweep	rad (deg)	0.524 (30°)	0.524 (30°)	0.524 (30°)
Span	m (ft)	51.8 (170)	61.3 (201.0)	58.5 (192)
Fuselage Length	m (ft)	65.7 (215.6)	61.4 (201.3)	60.0 (197.0)
L/D Cruise	-	17.36 (17.36)	19.11 (19.11)	19.13 (19.13)
SFC Cruise	$\frac{kg}{hr}$/daN (lb/hr/lb)	0.206 (0.202)	0.502 (0.492)	0.615 (0.603)
Initial Cruise Alt	m (ft)	11 582 (38 000)	11 582 (38 000)	(11 582) (38 000)
Wing Loading	kg/m^2 (lb/ft^2)	569 (116.5)	537 (110.0)	610 (125.0)
T/W	N/kg	3.20 (0.326)	2.94 (0.300)	3.20 (0.325)
Thrust Per Engine	N (lb)	134 990 (30 350)	164 750 (37 040)	185 040 (41 600)
FAR T.O. Distance	m (ft)	2440 (8 006)	2377 (7 804)	2431 (7 976)
FAR Landing Distance	m (ft)	1768 (5 799)	1524 (5 001)	1584 (5 197)
Engine Out Climb Grad	-	0.030 (0.030)	0.030 (0.030)	0.035 (0.0305)
Approach Speed	m/s KEAS	71.2 (138.4)	63.6 (123.7)	65.5 (127.4)
Weight Fractions				
Fuel	%	15.17 (15.17)	30.82 (30.82)	36.53 (36.53)
Payload	%	23.64 (23.64)	17.82 (17.82)	17.20 (17.20)
Structure	%	32.39 (32.39)	29.25 (29.25)	26.32 (26.32)
Propulsion	%	9.07 (9.07)	6.74 (6.74)	5.37 (5.37)
Price – Millions	$\$10^6$ ($\$10^6$)	43.39 (43.39)	47.45 (47.45)	44.53 (44.53)
DOC Cents/Seat n.mi.	cents seat km (cents seat n.mi.)	0.869 (1.609)	0.802 (1.486)	0.907 (1.679)
Energy Utilization	kJ seat km Btu seat n.mi.	637 (1 118)	717 (1 261)	759 (1 334)

(*Fuel system, insulation and tank weights not finalized here.)

The fore and aft fuselage tanks can be provided with energy absorbing mounts and otherwise protected structurally. Their level of safety is higher to the extent that they are not exposed to the breakup of landing gear, wing-mounted engines, and the wing itself. It is very possible that the 30 percent fatality rate due to postcrash fires could be dramatically reduced by the use of fore and aft fuselage tanks.

4.1.1.2 Leak detection and purging.- Extensive compartmentation to isolate potential leak sources would be a basic design directive for any cryogenic-fueled airplane, passenger or cargo. Each such compartment can be continuously purged by ram air in flight. Extensive use of sniffers plus vents and forced-air purging would be a way of dealing with those areas that are likely to leak under ground static conditions.

Obviously, the fewer such potential leak sources there are the better the design. Again, the internal wing tank offers very little but complexity in this regard. If all the fuel can be stored in two locations, such as the fore and aft fuselage tanks, the leak detection and compartment purging can be localized and simplified.

4.1.1.3 Passenger evacuation.- Current regulations require that it be possible to evacuate all passengers in 90 seconds and that doors and slides be provided in such numbers to accomplish this. Evacuation from a methane- or hydrogen-powered airplane should be conventional. Again, the presence or absence of wing fuel tanks bears heavily on passenger safety. If there is a wing fire, obviously passengers cannot evacuate down a slide into it and evacuation is limited to the doors opposite the fire.

4.1.1.4 Engine turbine or fan wheel burst.- Designing for this contingency is another fundamental requirement. Fuel tanks, lines, flight controls, and hydraulics are especially vulnerable. The fuselage tank arrangement would be less vulnerable than wing tanks in this event. The passenger cabin is more vulnerable than the fuselage tanks; however, this hazard is unavoidable in any of the designs and is not a function of the type of fuel used.

4.1.2 Thermal Compatibility

4.1.2.1 Differential thermal expansion.- The introduction of composite materials as a means of designing for light weight in the wing also introduces cryogenic fuel tanks into the area of a mixed composite-aluminum wing structure. The influence of differential expansion depends on materials compatibility and the choice of insulation schemes (figure 25).

If the insulation is inside the tank, as it should be, then the composite upper and lower surfaces are exposed to the same ambient temperatures as the aluminum leading and trailing edge structure. An estimate for illustrative purposes can be made in the following way:

The temperature range would typically be from 48.9°C (120°F) hot day ramp temperature to -53.9°C (-65°F) at altitude (figure 26). The temperature difference between aluminum and graphite epoxy is accounted for by the different solar absorptivity and emissivity of the two materials.

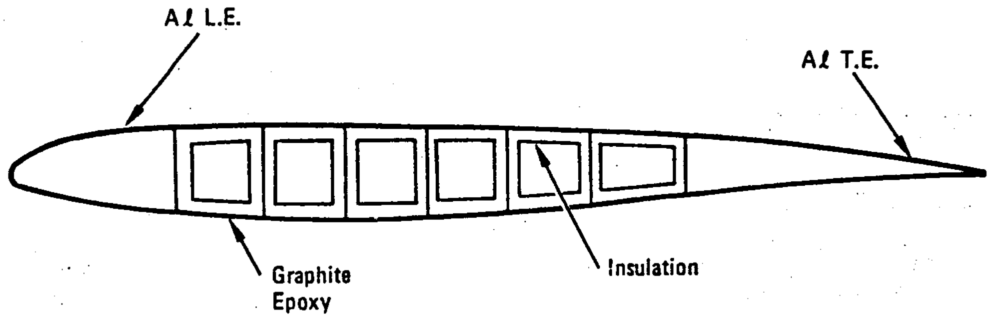

Figure 25. - Composite wing structure and tank concept for liquid methane.

4.1.2.2 Ground soak condition

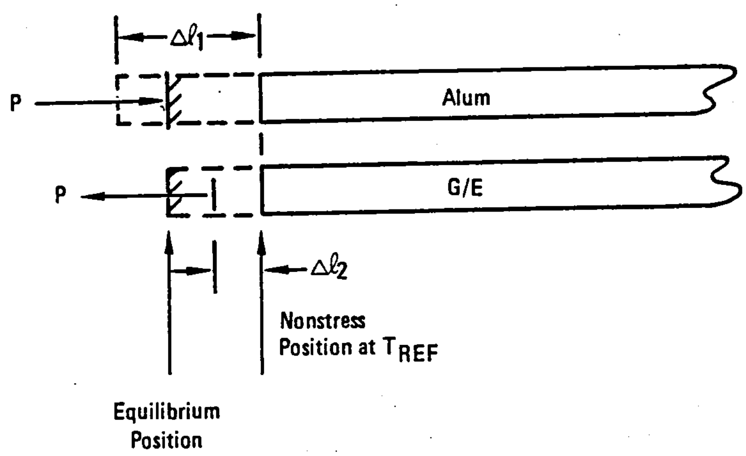

$$\Delta \ell_1 = \alpha_1 \Delta T_1 \ell_1 \qquad \Delta \ell_2 = \alpha_2 \Delta T_2 \ell_2$$

$$\ell_1 \left(\alpha_1 \Delta T_1 - \frac{P}{A_1 E_1}\right) = \ell_2 \left(\alpha_2 \Delta T_2 + \frac{P}{A_2 E_2}\right)$$

$$\ell_1 = \ell_2 = 2.54 \text{ cm } (1.00 \text{ in.})$$

$$P = \frac{\alpha_1 \Delta T_1 - \alpha_2 \Delta T_2}{\left(\frac{1}{A_1 E_1} + \frac{1}{A_2 E_2}\right)}$$

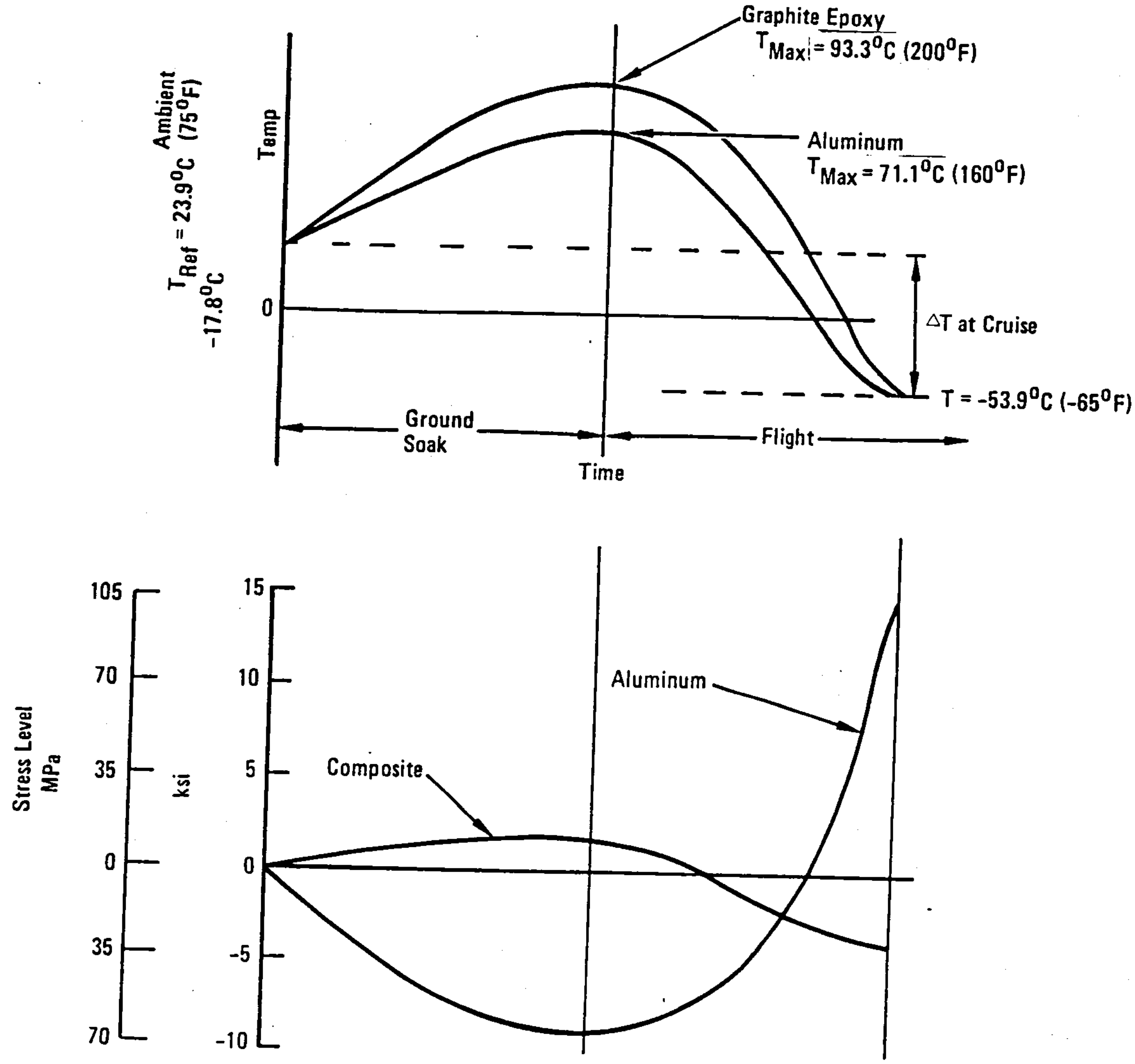

Figure 26. - Temperature gradients and stress level, upper wing surface.

Aℓ Elastic Data

$A_1 = 1.00 \times 0.08 = 0.52\ cm^2$ $(0.08\ in^2)$

$E_1 = 68.95$ G Pa $(10 \times 10^6$ psi)

$\alpha_1 = 23.4 \times 10^{-6}$ cm/cm/^oC $(13 \times 10^{-6}$ in/in/$^oF)$

$A_1E_1 = 0.363 \times 10^6$ kg $(0.8 \times 10^6$ lb)

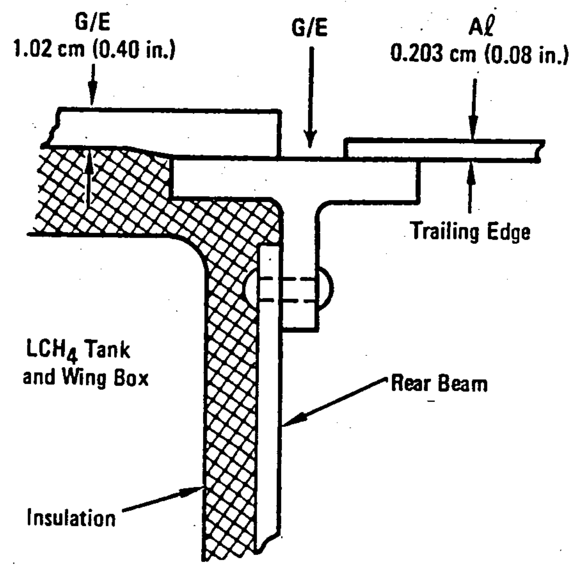

G/E Elastic Data

$A_2 = 1.00 \times 0.4 = 2.58\ cm^2$ $(0.4\ in^2)$

$E_2 = 86.18$ G Pa $(12.5 \times 10^6$ psi)

$\alpha_2 = 1.26 \times 10^{-6}$ cm/cm/^oC $(0.70 \times 10^{-6}$ in/in/$^oF)$

$A_2E_2 = 2.27 \times 10^6$ kg $(5.0 \times 10^6$ lb)

Data are from the USAF "Advanced Composite Design Guide."

In Customary Units:

$$P = \frac{13 \times 10^{-6}\,\Delta T_1 - 0.70 \times 10^{-6}\,\Delta T_2}{1.45 \times 10^{-6}} = 8.96\,\Delta T_1 - 0.483\,\Delta T_2$$

$$\sigma\,(Al) = \frac{P}{A_1} = \frac{8.96\,\Delta T_1 - 0.483\,\Delta T_2}{0.08}$$

$$\sigma\,(G/E) = \frac{P}{A_2} = \frac{8.96\,\Delta T_1 - 0.483\,\Delta T_2}{0.40}$$

4.1.2.3 Midcruise condition.- Cold soaking for a long period at cruise produces a higher stress relative to T_{REF} and the load P is reversed from ground soak as follows:

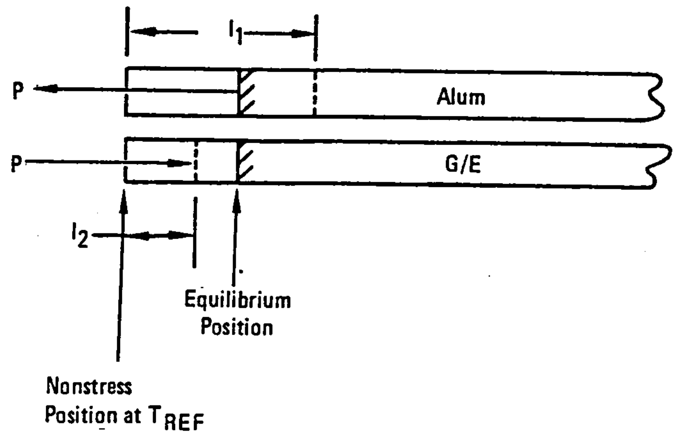

The signs for P in the principal equation become reversed and then one proceeds as above.

$$\ell_1 \left(\alpha_1 \Delta T_1 + \frac{P}{A_1 E_1}\right) = \ell_2 \left(\alpha_2 \Delta T_2 - \frac{P}{A_2 E_2}\right)$$

Omitting the detailed calculations, which are straightforward, the results are:

Condition	ΔT_1 °C (°F)	ΔT_2 °C (°F)	P kg (lb)	δALUM MPa (psi)	δG/E MPa (psi)
End of Ground Soak	(160 - 75) 47.2 (85)	(200 - 75) 69.4 (125)	318 (701)	-60.4 (-8 765)	12.1 (+1752)
Midcruise	(-65 - 75) -77.8 (-140)	(-65 - 75 -77.8 (-140)	538 (1187)	102.3 (+14 840)	-20.5 (-2969)

The graphite epoxy structure is influenced the least because of its greater relative thickness. The above illustration is a simplistic one because no other structural considerations are accounted for but the result shows the magnitude of the stresses created by differential expansion.

The problem is a serious one only if it is ignored; but the design and production complexity are certainly increased by the introduction of a cryogenic fuel tank made of composite material, which also carried primary loads as an integral part of a wing structure that is otherwise aluminum. The induced stress at a level of 102.3 MPa (14 840 psi) would not be allowed to occur. Slip joints could be introduced which would relieve the situation.

4.1.3 Operations.- The nature of cryogenic fuels is such that maintenance and inspection procedures for commerical aircraft will have to be dramatically revised. In the case of wing tanks with internal insulation, access to all internal tank areas for inspection and repair would be necessary. All possible equipment, such as pumps, would be installed so as to be accessible from outside the tanks. Leak checks would be routinely done on the ground and incipient leaks that develop in flight would have to be indicated in the cockpit.

As of now, there is more experience with, and a higher level of confidence in aluminum tanks, spherical or cylindrical, which are centrally located. Certainly, they are more encouraging from a maintenance point of view.

4.1.4 Configuration selection.- Considering all of the foregoing, especially the safety and complexity considerations, the first methane configuration with all fuel in the fore and aft fuselage tanks was adopted with NASA concurrence for completion of the study. That design is used in all of the subsequent sections of the report.

4.2 Extended Matrix of All Aircraft to Other Payload Ranges

This work is an addendum to the basic configuration selection and design of the 400 passenger/10 186 km (5500 n.mi.) mission. For those aircraft, the four major operating constraints were held constant as follows:

Approach speed	69.4 $\frac{m}{s}$ (135 knots)
Takeoff field length	2438 m (8000 ft)
Initial cruise altitude	10 363 m (34 000 ft)
Climb gradient	0.03

It was suggested during the study that the TOFL and the approach speed might be too restrictive in view of the fact that many of the world's major airports have runways that are considerably longer, as shown in table 12.

To examine the effect of varying payload and range as well as the benefit of extending the TOFL and approach speed, the following operating constraints were adopted for an extended matrix of the three alternate fueled aircraft (table 13).

TABLE 12. - RUNWAY LENGTHS OF WORLD'S MAJOR AIRPORTS

City	Longest Runway Available m(ft)
Anchorage	3321 (10 897)
Bogata	3800 (12 467)
Boston	3073 (10 081)
Buenos Aires	3299 (10 824)
Chicago	3536 (11 600)
Frankfurt	3900 (12 795)
Guam	3048 (10 000)
Guayaquil, Ecuador	2440 (8 005)
Hong Kong	3331 (10 930)
Honolulu	3771 (12 371)
Lima	3506 (11 503)
London	3902 (12 802)
Los Angeles	3685 (12 090)
Madrid	4100 (13 451)
Miami	3201 (10 502)
Milan	3927 (12 844)
New York	4442 (14 572)
Panama City	2682 (8 800)
Paris	3900 (12 795)
Philadelphia	3200 (10 500)
Rome	3980 (12 795)
San Francisco	3618 (11 870)
Santiago	3199 (10 496)
Sydney	3962 (12 999)
Tokyo	4000 (13 123)
Washington	3505 (11 500)

*Reference: Jeppesen Airway Manual

The results of varying the TOFL and approach speed are shown in the two adjoining columns of table 14 for the 400-passenger/10 186 km (5500 n.mi.) airplanes. All aircraft were designed to the same technology level and all meet the four principal operational constraints. In addition, they are all minimum DOC airplanes.

TABLE 13. - PRINCIPAL OPERATING CONSTRAINTS FOR ALL AIRCRAFT

Operating Constraint	km (n.mi)	Payload/Range				
		130 Pax 2778 (1500)	200 Pax 5556 (3000)	400 Pax 5556 (3000)	400 Pax 10 186 (5500)	400 Pax 18 520 (10 000)
TOFL	m(ft)	2438 (8 000)	2438 (8 000)	2438 (8 000)	2438 (8 000)	3658 (12 000)
Climb Grad		0.024*	0.03	0.03	0.03	0.03
Init Cruise Alt	m(ft)	10 363 (34 000)	10 363 (34 000)	10 363 (34 000)	10 363 (34 000)	10 363 (34 000)
APP Speed	$\frac{m}{s}$(knots)	69.4 (135)	69.4 (135)	69.4 (135)	69.4 (135)	72 (140)
					and also at 3200 (10 500 ft) 72 (140 knots)	

*The 130 Pax/1500 n.mi airplane is a twin engine aircraft. All others are four engine.

As shown in table 15, all three airplanes are improved by easing the constraints with the LH_2 airplane benefitting the least and the Jet A the most. Adopting the higher approach speed would be a clear choice. The 72 m/s speed is consistent with current operational practice. However, reflection on the proposal to increase the TOFL from 2438 m raises serious doubts about its practicability. Airline flexibility in planning route structures is severely restricted if the field length limit is increased to 3200 m.

The effect of varying payload and range is shown in figures 27 and 28. The significant thing to be noted there and in table 14 is that at the very long range, 18 520 km (10 000 n.mi.) mission, the methane airplane becomes slightly heavier than the Jet A and that the mission energy and energy utilization is slightly higher primarily due to the better L/D of the Jet A airplane, 22.84 as compared to 21.86, or about 4.5 percent. This in turn is due to three design aspects.

The first design aspect is a smaller diameter fuselage for the Jet A aircraft because it carries all the passengers in a single-deck arrangement. This is a consequence of being able to carry all of the fuel in the wing. The LCH_4 fuselage is larger in diameter, 8.02 m (26.3 ft) versus 5.97 m (19.6 ft), so the wetted area of the fuselage is 18 percent greater because of the fuel containment problem with the fore and aft tanks.

TABLE 14. - SUMMARY OF STUDY RESULTS

(All aircraft cruise at Mach 0.85 with 2438 m (8000 ft) TOFL and 250 km/hr (135 knots) approach speed)

Customary Units

		Short Range 130 pax 2778 km (1500 n.mi.)			Medium Range 200 pax 5558 km (3000 n.mi.)			Medium Range 400 pax 5556 km (3000 n.mi.)		
		LH_2	LCH_4	Jet A	LH_2	LCH_4	Jet A	LH_2	LCH_4	Jet A
Wing Loading	$\frac{kg}{m^2}$ $\left(\frac{lb}{ft^2}\right)$	493.6 (101.1)	521.9 (106.9)	537.0 (110.0)	513.6 (105.2)	574.0 (117.5)	598.0 (122.5)	512.6 (105.0)	564.8 (115.7)	586.8 (120.2)
Thrust/Weight	$\frac{N}{kg}$ (-)	3.75 (0.382)	3.63 (0.370)	3.63 (0.370)	3.29 (0.335)	3.13 (0.319)	3.25 (0.331)	3.14 (0.320)	3.02 (0.308)	3.13 (0.319)
Gross Weight	kg (lb)	45 510 (100 340)	50 080 (110 360)	48 480 (106 880)	79 600 (175 490)	93 790 (206 770)	90 160 (198 770)	143 330 (315 990)	168 770 (372 070)	167 080 (368 360)
Block Fuel	kg (lb)	2 011 (4434)	4 803 (10 588)	5 784 (12 752)	6 482 (14 291)	16 772 (36 976)	19 130 (42 126)	10 850 (23 197)	27 780 (61 198)	32 700 (72 101)
OEW	kg (lb)	29 780 (65 650)	30 400 (67 015)	27 540 (60 721)	51 540 (113 628)	53 720 (118 441)	47 300 (104 291)	90 340 (199 167)	95 350 (210 214)	87 700 (193 422)
Wing Area	m^2 (ft^2)	92.2 (993.0)	95.9 (1032.0)	90.3 (972.0)	155.0 (1668)	163.5 (1760)	150.8 (1623)	279.5 (3009)	298.8 (3216)	284.8 (3066)
Span	m (ft)	30.4 (99.6)	31.7 (104.1)	31.5 (103.4)	38.4 (125.9)	39.7 (130.1)	38.3 (125.8)	51.5 (169.1)	53.6 (175.9)	52.7 (172.9)
Fus. Length	m (ft)	41.7 (137.0)	40.6 (133.2)	34.4 (113.0)	52.7 (173.0)	51.8 (170.0)	44.1 (144.7)	64.0 (210.0)	61.0 (200.0)	60.0 (197.0)
SFC (Cruise)	$\frac{kg}{hr}$/daN $\left(\frac{lb/hr}{lb}\right)$	0.206 (0.202)	0.503 (0.493)	0.613 (0.601)	0.206 (0.202)	0.501 (0.491)	0.610 (0.598)	0.206 (0.202)	0.501 (0.491)	0.611 (0.599)
L/D (Cruise)	- (-)	16.13 (16.13)	17.74 (17.74)	17.58 (17.58)	15.82 (15.82)	16.54 (16.54)	16.87 (16.87)	17.10 (17.10)	18.21 (18.21)	18.54 (18.54)
Thrust/Engine	N (lb)	85 250 (19 165)	90 810 (20 417)	87 950 (19 773)	65 380 (14 698)	73 350 (16 490)	73 160 (16 448)	116 890 (25 279)	127 440 (28 650)	130 670 (29 377)
TOFL	m (ft)	2 442 (8011)	2 397 (7863)	2 350 (7711)	2 104 (6902)	2 436 (7991)	2 444 (8017)	2 194 (7199)	2 441 (8010)	2 441 (8009)
APP Speed	$\frac{m}{s}$ (Keas)	69.4 (135)	69.4 (135)	69.4 (135)	69.4 (135)	69.4 (134.9)	69.4 (134.9)	69.6 (135.3)	69.4 (135)	69.4 (135)
Price/Aircraft	$10^6 ($10^6)	15.77 (15.77)	15.89 (15.89)	14.43 (14.43)	25.20 (25.20)	25.95 (25.95)	23.17 (23.17)	39.22 (39.22)	40.61 (40.61)	37.60 (37.60)
DOC	$\frac{Cents}{Seat\ km}$ $\frac{Cents}{Seat\ n.mi.}$	1.312 (2.429)	1.187 (2.199)	1.231 (2.179)	1.129 (2.091)	1.040 (1.925)	1.074 (1.988)	0.839 (1.554)	0.761 (1.410)	0.811 (1.501)
Energy Utilization	$\frac{kJ}{Seat\ km}$ $\frac{Btu}{Seat\ n.mi.}$	667 (1173)	664 (1167)	685 (1203)	699 (1229)	754 (1325)	735 (1292)	585 (1028)	624 (1098)	629 (1106)

		Mach 0.85 Cruise 8000 ft TOFL and 135 knots Approach Speed			Effect of Extending TOFL and Approach Speed To 3200 m (10 500 ft) and 259 km/hr (140 knots)			Very Long Range Aircraft at TOFL and Approach Speed of 5486 m (12000 ft) and 259 km/hr (140 knots)		
		Long Range 400 pax 10 186 km (5500 n.mi.)			Long Range 400 pax 10 186 km (5500 n.mi.)			Very Long Range 400 pax 18 520 km (10 000 n.mi.**)		
		LH_2	LCH_4	Jet A	LH_2	LCH_4	Jet A	LH_2	LCH_4	Jet A
Wing Loading	$\frac{kg}{m^2}$ $\frac{lb}{ft^2}$	568.8 (116.5)	585.8 (120.0)	610.3 (125.0)	581.0 (119.0)	659.1 (135.0)	634.1 (130.0)	634.7 (116.6)	649.3 (133.0)	681.5 (139.6)
Thrust/Weight	$\frac{N}{kg}$ (-)	3.20 (0.326)	3.14 (0.320)	3.19 (0.325)	2.97 (0.303)	2.91 (0.297)	2.91 (0.297)	2.69 (0.274)	2.62 (0.267)	2.62 (0.267)
Gross Weight	kg (lb)	168 740 (372 000)	225 580 (497 300)	232 060 (511 600)	167 120 (368 440)	221 570 (488 470)	223 320 (492 320)	249 400 (549 830)	497 770 (1 097 370)	476 230 (1 049 900)
Block Fuel	kg (lb)	21 620 (47 670)	58 980 (130 030)	72 530 (159 900)	21 570 (47 548)	58 900 (129 852)	69 680 (153 607)	50 740 (111 858)	194 750 (429 350)	212 120 (467 641)
OEW	kg (lb)	103 300 (227 750)	116 170 (256 120)	107 360 (236 700)	101 730 (224 280)	112 560 (248 144)	101 890 (224 620)	149 840 (330 346)	231 770 (510 964)	190 880 (420 812)
Wing Area	m^2 (ft^2)	296.8 (3195)	385.0 (4144)	380.2 (4093)	287.6 (3096)	336.1 (3618)	351.8 (3787)	438.1 (4716)	766.5 (8251)	698.7 (7521)
Span	m (ft)	51.8 (170.0)	58.9 (193.1)	58.5 (192.0)	50.9 (166.9)	55.0 (180.5)	56.3 (184.6)	66.2 (217.2)	89.6 (294.0)	87.7 (287.6)
Fus. Length	m (ft)	65.7 (215.6	61.4 (201.3)	60.0 (197.0)	65.7 (215.6)	61.4 (201.3)	60.0 (197.0)	80.5 (264.0)	70.1 (229.9)	68.6 (225.0)
SFC (Cruise)	$\frac{kg}{hr}$ daN $\frac{lb/hr}{lb}$	0.206 (0.202)	0.504 (0.494)	0.615 (0.603)	0.206 (0.202)	0.502 (0.492)	0.612 (0.600)	0.206 (0.202)	0.502 (0.492)	0.613 (0.601)
L/D Cruise	(-)	17.4 (17.4)	19.21 (19.21)	19.13 (19.13)	17.15 (17.15)	18.70 (18.70)	19.00 (19.00)	19.3 (19.3)	21.86 (21.86)	22.84 (22.84)
Thrust/Engine	N (lb)	135 000 (30 350)	177 030 (39 800)	185 030 (41 600)	124 140 (27 910)	161 320 (36 269)	162 600 (36 555)	165 530 (37 663)	325 820 (73 250)	311 720 (70 081)
TOFL	m (ft)	2 440 (8006)	2 430 (7973)	2 431 (7976)	3 188 (10 460)	3 180 (10 433)	3 195 (10 482	3 678 (12 068)	3 636 (11 930)	3 663 (12 019)
APP Speed	$\frac{m}{s}$ (KEAS)	71.0 (138.0)	66.5 (129.3)	65.3 (127.0)	71.9 (139.8)	70.3 (136.7)	66.4 (129.9)	72.0 (140.0)	72.0 (139.9)	72.0 (140.0)
Price Aircraft	$10^6 ($10^6)	43.39 (43.39)	48.10 (48.10)	44.53 (44.53)	42.62 (42.62)	46.59 (46.59)	42.34 (42.34)	58.54 (58.54)	85.21 (85.21)	73.07 (73.07)
DOC	$\frac{Cents}{Seat\ km}$ $\frac{Cents}{Seats\ n.mi.}$	0.869 (1.609)	0.831 (1.538)	0.907 (1.679)	0.859 (1.591)	0.815 (1.510)	0.870 (1.611)	0.982 (1.818)	1.193 (2.209)	1.227 (2.273)
Energy Utilization	$\frac{KJ}{Seat\ km}$ $\frac{Btu}{Seat\ n.mi.}$	636 (1118)	723 (1271)	759 (1334)	634 (115)	722 (1269)	731 (1285)	821 (1443)	1313 (2307)	1224 (2151)

**The 10 000 n.mi. range is actually a 5000 n.mi. radius to a landing and return to point of origin unrefueled with full payload and reserve fuel at the second landing.

TABLE 15. - PERCENTAGE REDUCTION OF COST AND WEIGHT FACTORS GAINED BY INCREASING TOFL AND APPROACH SPEED OF 400 PAX/10 186 km (5500 n.mi.) AIRCRAFT

Factor		LH_2	LCH_4	Jet A
DOC	%	-1.1	-1.8	-4.1
Weight	%	-0.96	-1.8	-3.8
Cost	%	-1.8	-3.1	-4.9
Block Fuel	%	-0.26	-0.14	-3.9

The second design aspect is the higher fuselage fineness ratio to provide a tail length to meet tail volume requirements for the Jet A airplane. The third design aspect is that the Jet A has a higher aspect ratio wing for minimum DOC.

The sensitivity of DOC to fuel cost is shown for the final designs at two payload/ranges in figures 29 and 30. The baseline DOCs shown there are also shown in table 14.

The twin engine configuration for the short-range, 130-passenger/2778 m (1500 n.mi.) airplane is shown for reference in figure 31. All other configurations are conventional four-engine aircraft; principal characteristics for these aircraft are presented in table 14. Detailed summary sheets for all aircraft in the 400-passenger/10 186 km (5500 n.mi.) range category with a TOFL of 3200 m (10 500 ft) and an approach speed of 140 knots are shown in Appendix B.

4.3 Benefits of Subcooling Fuel

Subcooling of liquid methane can result in lower fuel losses from the aircraft, particularly venting losses during flight. Subcooling will also reduce insulation thickness and system weight and in turn can only be favorable to DOC. The fuel cost savings do not offset the additional capital equipment expense, however; therefore, subcooling has not been added to the aircraft design. Further analysis with supporting data is provided in sections 8.3.3, 9.5 and 11.

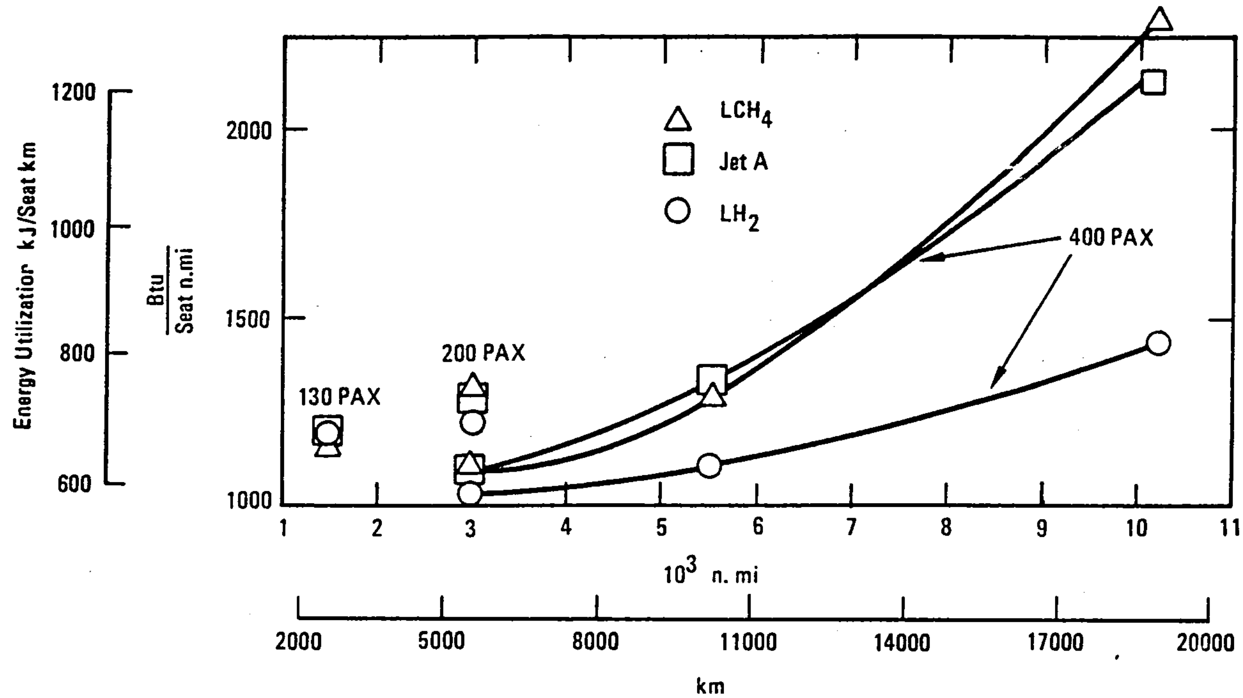

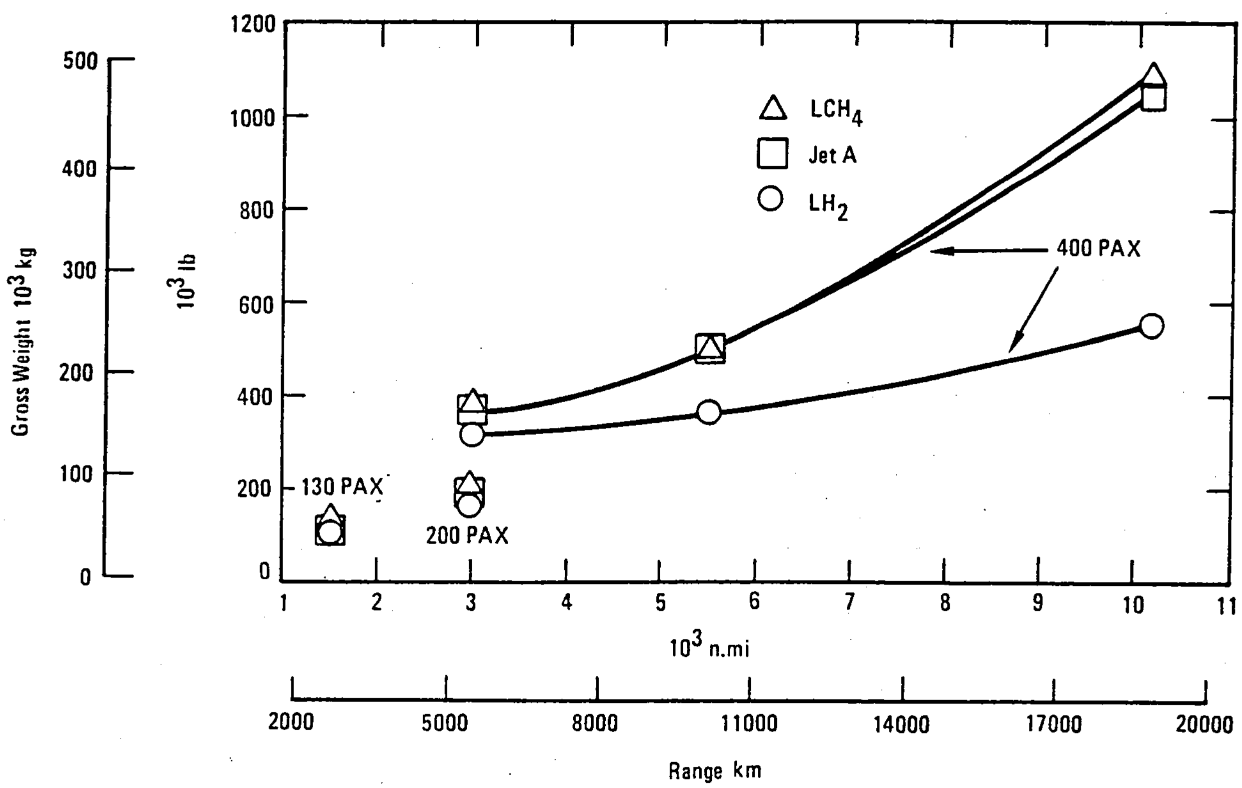

Figure 27. - Growth effects.

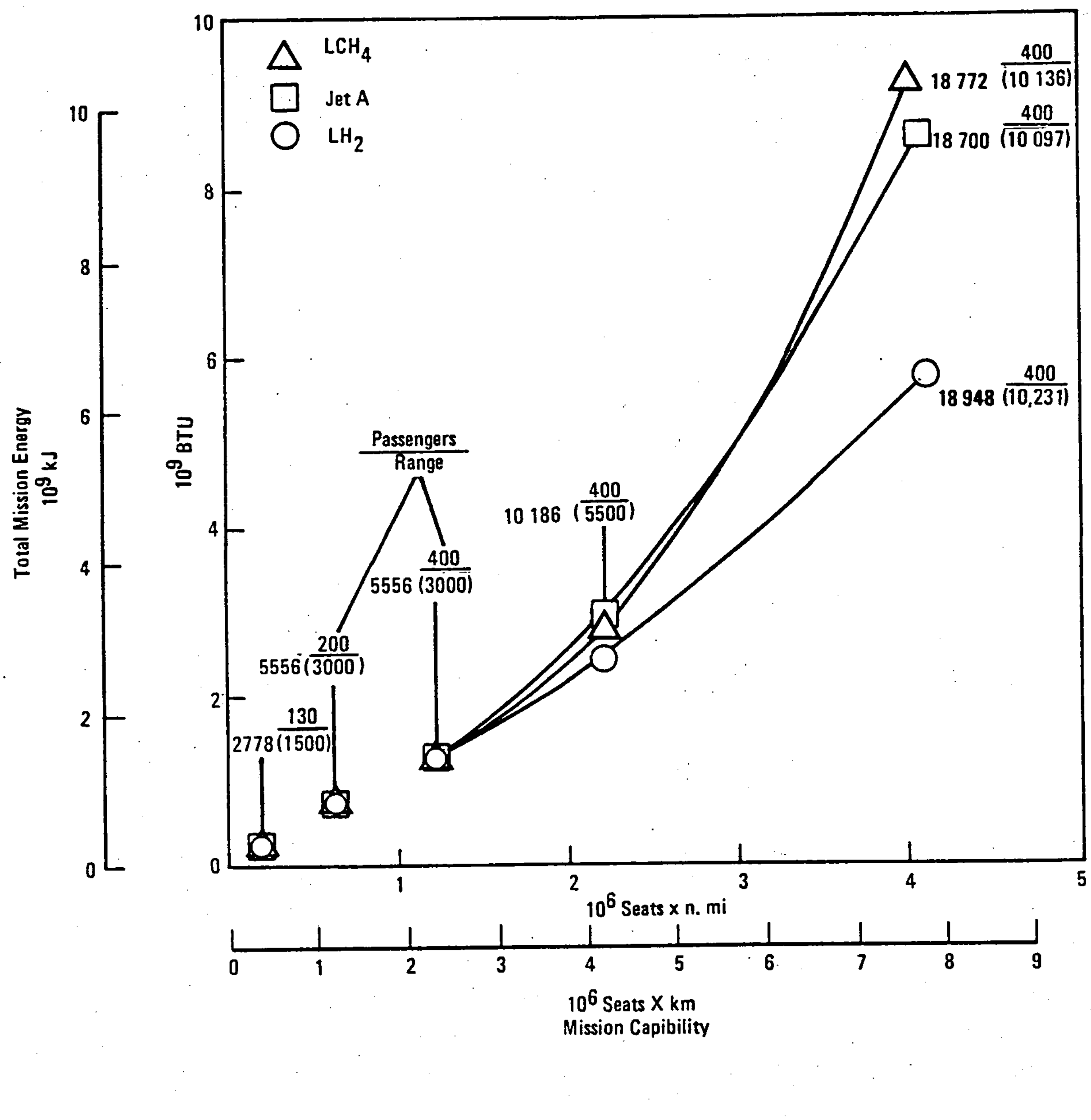

Figure 28. - Mission capability versus energy.

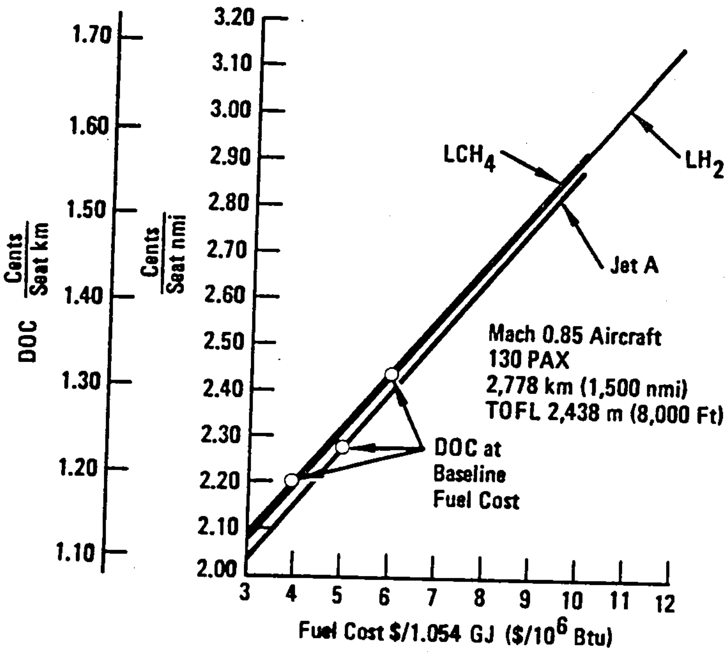

Figure 29. - Sensitivity of DOC to fuel cost, short-range aircraft.

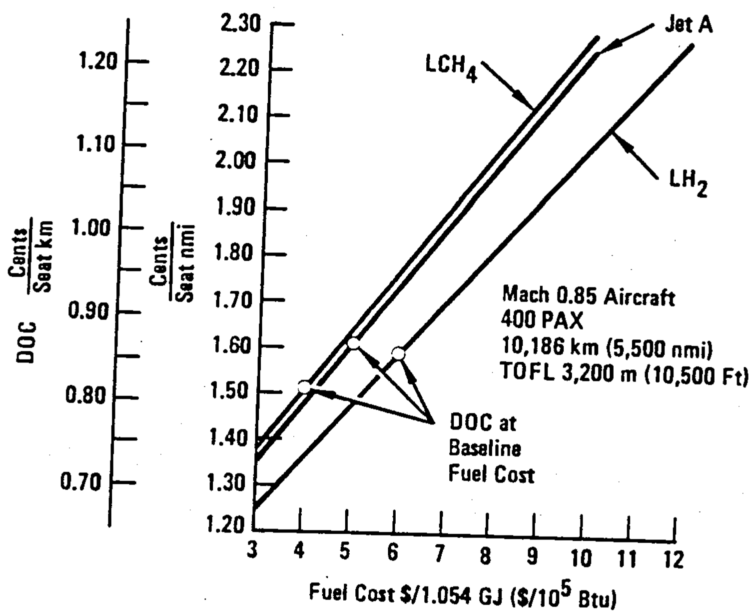

Figure 30. - Sensitivity of DOC to fuel cost, long-range aircraft.

CHARACTERISTICS	WING BASIC	WING TOTAL	HORIZONTAL TAIL EXPOSED	HORIZONTAL TAIL TOTAL	VERTICAL TAIL
AREA/ m^2 (SQ FT)	89.4 (962.5)	100.6(1082.3)	8.75 (94.2)	10.87 (116.97)	12.74 (137.1)
ASPECT RATIO	10.5	———	4.5	4.79	1.6
SPAN /m (FT)	30.6 (100.5)	———	6.28 (20.6)	7.2 (23.66)	4.5 (14.8)
ROOT CHORD/m (IN)	4.5 (176.8)	6.65 (261.8)	2.15 (84.5)	2.37 (93.3)	4.34 (170.9)
TIP CHORD/m (IN)	1.35 (53)	———	0.64 (25.3)	0.64 (25.3)	1.3 (51.3)
TAPER RATIO	0.3	———	0.3	0.27	0.3
MAC /m (IN)	3.2 (126)	———	1.53 (60.2)	1.67 (65.8)	3.1 (121.8)
SWEEP RAD.(DEG)	0.524 (30)	———	0.524 (30)	———	0.524 (30)
T/C ROOT (%)	11.8	———	9	9	9
T/C TIP (%)	8.5	———	9	———	9

RANGE : 2780 Km (1500 NM)
WEIGHT : 48889 Kg (107,800 LB)
PASSENGERS : 130
POWER PLANTS : 2 TURBFANS @ 83 KN (18650 LB)

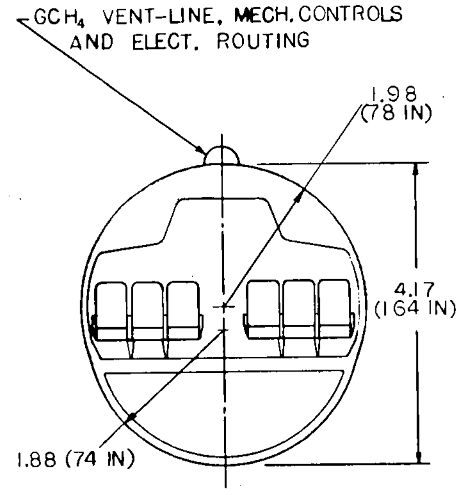

SECTION A A

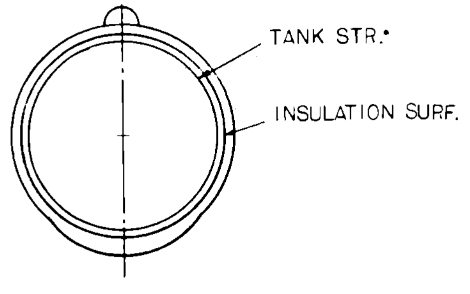

SECTION B - B

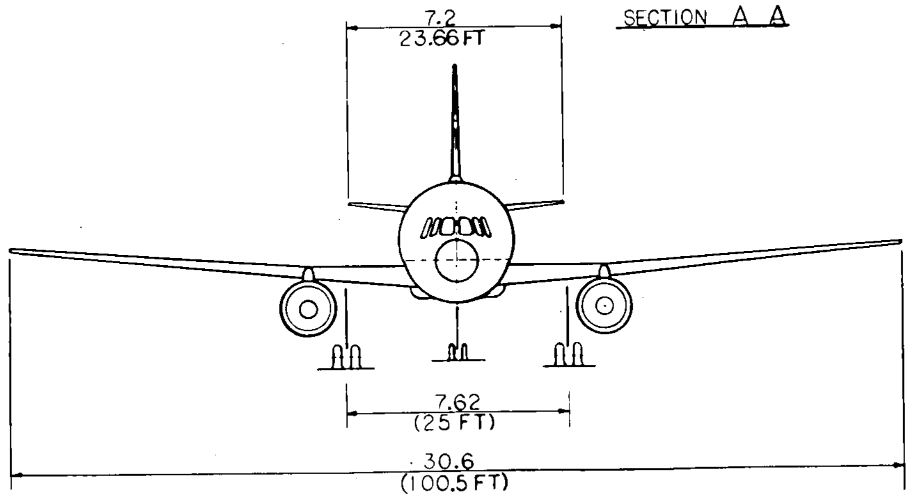

LINEAR DIMENSIONS IN METRES (FT OR IN)

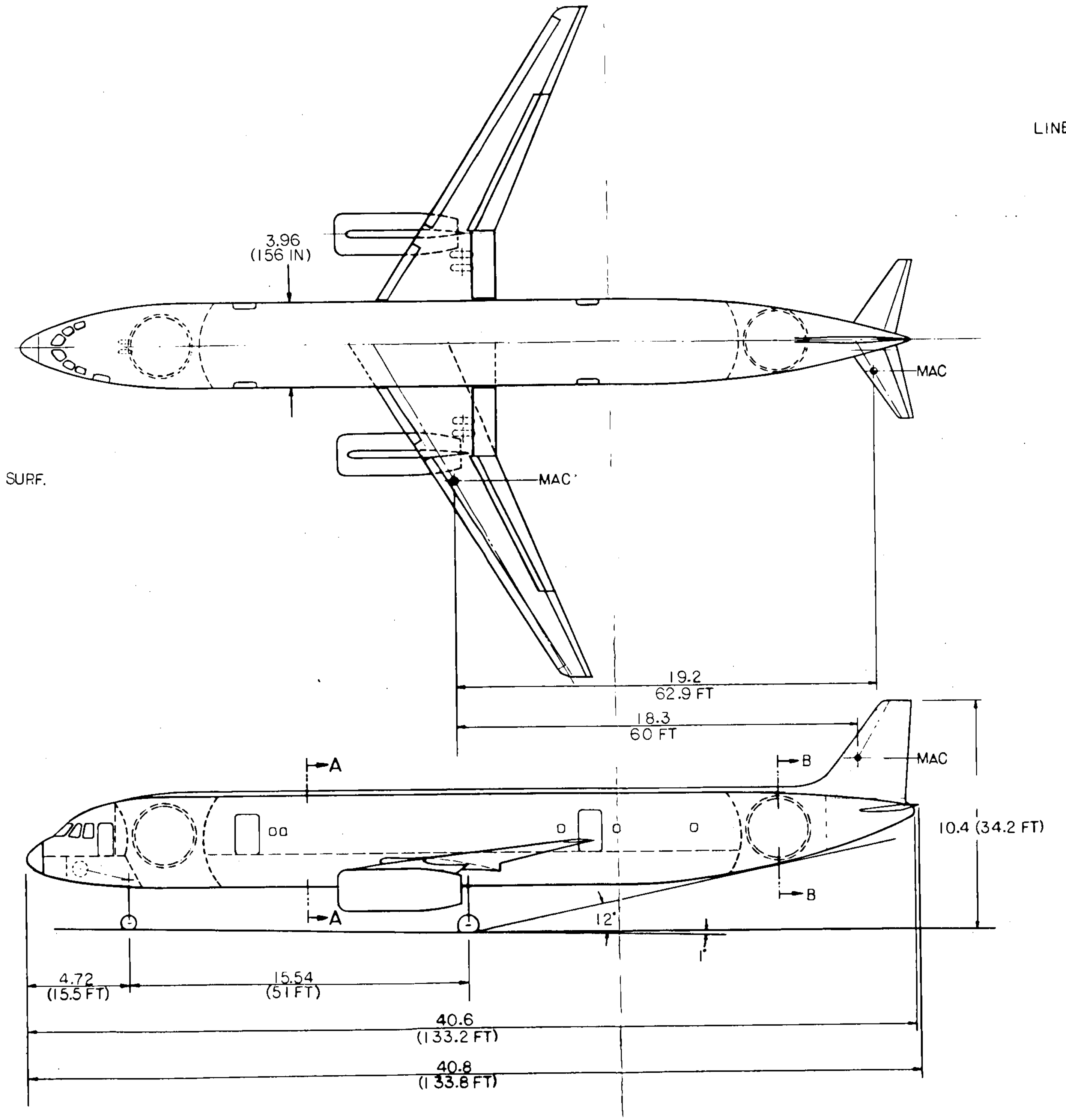

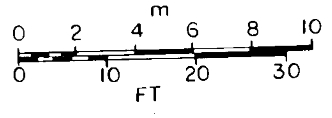

FWD & AFT LCH_4-TANKS 3810 Kg (8400 LB) EACH

Figure 31. - Short range aircraft, 130 passengers/2778 m (1500 n.mi.)

5. STRUCTURAL DESIGN AND ANALYSIS OF METHANE FUEL TANKS

The shape and size of the tanks in this study were determined not only by the fuel quantity required and the tank location but also by the fact that methane is cryogenic. Considerations of the thermal efficiency of the tank shape entered into the appraisal. For the 400-passenger/10 186 km (5500 n.mi.) range aircraft one-half of the fuel required can be carried in the most thermally efficient shape - a sphere. This is an advantage that can be attributed to the density, volume, and heating value characteristics of methane. A spherical forward tank was chosen for the following reasons:

- It has the most thermally efficient shape for a cryogenic fuel
- It provides volumetric efficiency as a container
- The required fuselage diameter is available without further design problems or sacrifices
- It is producible by available methods in the near term

A discussion of the stress analysis and method of fabrication is the best way to describe the concept of the tank. This is only one of many possible design approaches. For the 1990 time period one would have to look at the possibility of making a cryogenic fuel tank out of composite materials, but that task with its added design uncertainties was not addressed during this investigation.

5.1 Tank Structure

A detailed investigation was conducted to establish a feasible design for the LCH_4 fuel tanks. The major design emphasis was placed on the forward tank (which is a spherical tank) because of its dissimilarity in design to those investigated in the hydrogen tank study, reference 4. This section presents results of this investigation. Design criteria and loads are established, major structural components for both the forward and aft tanks are described, and the results of the analyses are presented.

5.1.1 Structural design criteria.- The structural design criteria and loads defined in this section were developed to provide the basis for the evaluation of the candidate tank configurations and a level of structural safety equivalent to current transports for assessing structural mass trends resulting from application of these criteria. Conditions representative of those critical for each component and type of loading have been selected; however, an exhaustive search for absolute maximums has not been carried out.

In general, the criteria are based on the structural requirements of the Federal Aviation Agency FAR 25, with specific criteria being the same as that used for the hydrogen tank study and for the L-1011 aircraft. This section presents the following criteria: basic airplane performance data (airplane mass, design speeds, maneuver envelope, etc.), design pressure, emergency landing, combined loads, fatigue, and fail-safe. In addition, the design loads are presented for four flight conditions.

5.1.1.1 Airplane weight and inertia data.- The loads are based on the design weights shown in table 16. The inertia distribution data was estimated based on these weights and the basic geometry and layout of the configuration. The forward c.g. limit was assumed to be 20 percent MAC. Structural reserve fuel is 7 percent of total fuel, the same criterion as used on the L-1011 airplane.

5.1.1.2 Design speeds.- The design speed-altitude variation is presented in figure 32. It is identical to that for the L-1011 airplane. This figure shows the variation of cruise speed, dive speed and maneuver speed with altitude.

- Design cruise speed, V_c, is the maximum speed at which encounter of high-intensity nonstorm turbulence (U_{de} = 15.2 m/s (50 fps)) must be considered.

TABLE 16. - INITIAL VALUES, DESIGN WEIGHT SUMMARY

Condition	Weight	
	kg	lbm
Maximum Take Off Gross Weight	231 300	510 000
Landing Gross Weight	208 600	460 000
Operating Weight Empty	117 900	260 000
Structural Reserve Fuel	5 400	12 000
Maximum Weight with Structural Reserve Fuel	181 400	400 000
Minimum Flying Weight	123 400	272 000

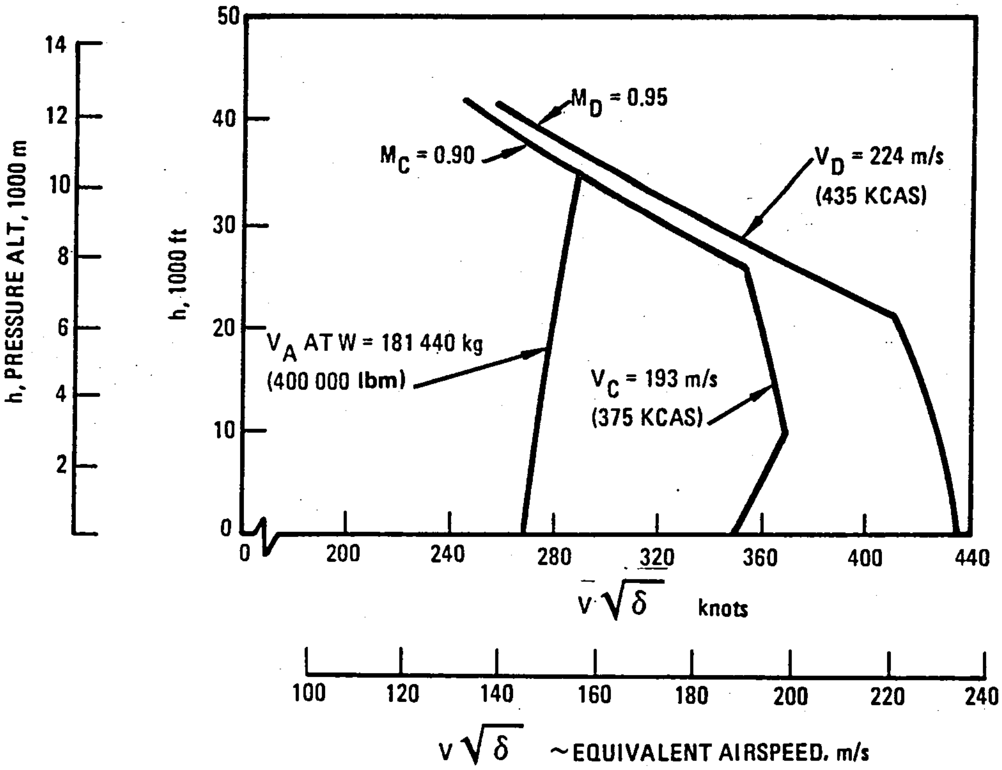

Figure 32. - Design speeds versus altitude.

- Design dive speed, V_D, is established so that the probability of inadvertently exceeding dive speed is extremely remote even while operating at maximum operating speed.

- Design maneuver speed, V_A, is determined from the aircraft stall characteristics. It is very near to the minimum speed at which the design limit load factor can be attained.

5.1.1.3 Maneuver envelope.- The maneuver envelope is a function of weight and altitude. At low speed, the attainable load factor is limited by weight and maximum lift. At speeds above V_A, the allowable maneuver load factor is defined by FAR 25.

5.1.1.4 Design loads.- Based on the results of the hydrogen tank study, reference 4, only those conditions critical for design were investigated for this study. A positive low angle of attack (PLA) and abrupt pitching maneuver conditions are shown in figure 33. The design loads for two other conditions, a negative maneuver and the cruise condition, were approximated for the structural analysis of the tanks.

5.1.1.5 Tank design pressures.- LCH_4 tanks for the baseline aircraft were designed to operate at a nominal pressure of 145 kPa (21 psia). Factors required for cabin pressure (FAR 25) are assumed applicable to the tank design and the cruise altitude is assumed to be 11 600 m (38 000 ft).

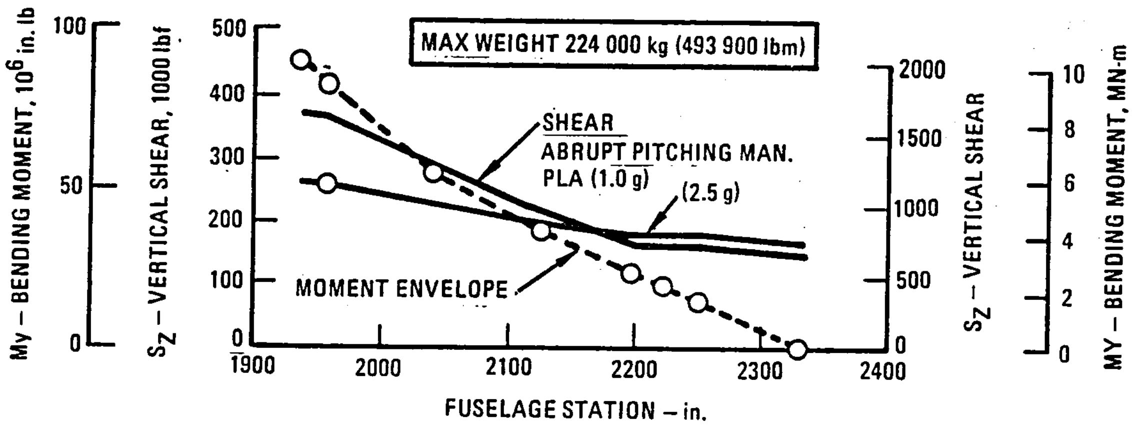

Figure 33. - Fuselage aftbody limit loads, PLA and abrupt pitching maneuver conditions.

$$p = 145 \text{ kPa } (21.0 \text{ psia})$$

The differential pressure (Δp) acting on the tanks is

$$\Delta p = p - P_{at}$$

$$P_{at} = \text{atmospheric pressure}$$

The differential pressure was multiplied by a factor of 1.1 to account for relief valve tolerances to provide an operating pressure. Table 17 presents the operating pressures for the four flight conditions investigated for this study.

$$P_{op} = 1.1\,\Delta p$$

- <u>Differential pressure for combination with limit loads</u> - A limit pressure, equal to the operating pressure plus the inertia head of the fuel, is combined with the limit loads due to maneuver or gusts

TABLE 17. - METHANE TANK OPERATING PRESSURES

Conditions	Alt m (ft)	P_{nom} kPa (psia)	P_{atm} kPa (psia)	ΔP kPa (psi)	P_{op} kPa (psi)
Positive Low Angle	6 700 (22 000)	144.8 (21.0)	42.7 (6.2)	102.0 (14.8)	112.4 (16.3)
Pitch Maneuver	S.L.	144.8 (21.0)	101.4 (14.7)	43.4 (6.3)	47.6 (6.9)
Negative Maneuver	6 700 (22 000)	144.8 (21.0)	42.7 (6.2)	102.0 (14.8)	112.4 (16.3)
Cruise	10 700 (35 000)	144.8 (21.0)	23.4 (3.4)	121.3 (17.6)	133.8 (19.4)

$$p_{limit} = p_{op} + p_{in}$$

- Differential pressure for combination with ultimate loads - An ultimate pressure that corresponds to the limit pressure multiplied by 1.50 was defined for combining with the ultimate loads due to maneuver or gusts.

$$p_{ult} = 1.50 \times p_{limit}$$

- Ground test differential pressure - A proof pressure corresponding to the operating pressure multiplied by 1.33, was specified. No detrimental deformation shall result from this condition.

$$p_{proof} = 1.33 \times p_{op}$$

A burst pressure equivalent to the operating pressure multiplied by 2, was defined. Catastrophic failure of the tank shall not occur.

$$p_{burst} = 2.00 \times p_{op}$$

5.1.1.6 Emergency landing condition.- The following ultimate inertia load factors (FAR 25.561) were applied to the tank suspension system and fuel within the tank. Each load factor was applied on an arbitrary independent condition.

upward: $n = 2.0$

forward: $n = 9.0$

sideward: $n = 1.5$

downward: $n = 4.5$

5.1.1.7 Combined loads criteria.- Flight loads and tank pressure stresses were combined as specified.

- The factor of safety, as defined for the loads and pressures in the foregoing section, was used to combine the loads and form the final stress resultants.

- For compression design, the tensile force produced by the internal pressure was ignored and only the shear and/or compressive forces produced by the external loads were considered.

- For tension design, the sum of the membrane forces produced by the internal pressure and external loads was considered.

- The flight and ground conditions considered are specified in table 18 with the design levels (factors of safety) of the load and pressure environment defined.

5.1.2 Fatigue design criteria.- Fatigue design requirements can be met by limiting the permissible design tension stress of the tank for the ultimate design and operating conditions. The tension allowables for the LCH_4 tanks were based on the results of the LH_2 tank study (reference 4).

The circumferential design stress for the operating condition reflects the fatigue effects of the constant amplitude pressure loading occurring once per flight for the life of the airplane. For the methane tanks, where the surface temperature of the tank at the liquid line is approximately 114 000(-254°F), a circumferential design allowable stress of 117.2 MPa (17 000 psi) was used for the operating condition. This value is approximately 14 percent higher than the 103.4 MPa (15 000 psi) allowable stress currently being used for conventional aluminum transports and is based on the increase in material strength (both yield and ultimate strength) of 2219 aluminum at 114 000(-254°F). The corresponding ultimate design stress level for the biaxially loaded tank wall is 172.4 MPa (25 000 psi), i.e., 1.50 times the operating allowable.

TABLE 18. - COMBINED LOADS AND INTERNAL PRESSURE CRITERIA

Condition	External Loads	Internal Pressure
Operating (Cruise Cond.)	Limit	Limit
Limit Design	Limit	Limit
Ultimate Design	Ultimate	Ultimate
Fail-Safe Design	Limit	Limit
Emergency Landing	Ultimate	Ultimate
Proof Test	–	Proof
Burst	–	Burst

The ultimate circumferential design stress level for uniaxially loaded tank structure, such as frames, was defined by multiplying the current aluminum value of 241.3 MPa (35 000 psi) by the cryogenic temperature correction factor of 1.14. A value of 275.8 MPa (40 000 psi) was used for this study.

A summary of the methane tank design allowables is shown in table 19 which also includes the relative values of the hydrogen system design. The methane allowables are lower in all cases because of the difference in temperature, i.e., the allowable stresses for 2219-T851 increase with decreasing temperature.

5.1.3 Fail-safe design criteria.- The objective of the fail-safe (damage tolerance) design criterion is to ensure that flight safety is maintained in the event of structural damage of reasonable magnitude. Such damage may arise from fatigue as well as accidental impact or other sources.

The tank structure must be capable of supporting the operating pressure loads and appropriate fail-safe loads for accidental damages equivalent to a 30.5 cm (12.0 in.) through-the-thickness crack anywhere in the structure, including members attached to the structure across the damaged section. The

TABLE 19. - CIRCUMFERENTIAL DESIGN STRESSES

Design Condition	Stresses MPa (ksi) LH$_2$ 20 K(-423°F)	Stresses MPa (ksi) LCH$_4$ 114 K(-254°F)
Ultimate Condition		
Tank Wall	255 (37)	172 (25)
Tank Substructure	310 (45)	276 (40)
Operating Condition		
Tank Wall	172 (25)	117 (17)

fail-safe loads shall be equal to the maneuver and gust loads that can reasonably be expected during completion of the flight in which the damage occurred. Fail-safe for the remainder of the structure shall be designed to meet the fatigue and damage tolerance requirements of FAR 25.571.

5.2 Tank Design

The location and shape of the methane tanks are shown in figure 34. The forward tank is a nonintegral tank (i.e., the tank is simply a fuel container and does not participate in the support of the body loads) which is spherical in configuration. The aft tank is an integral design (i.e., tank serves both as a fuel container and also supports the body loads) which is a frustrum of a cone in configuration. Both tanks were considered to be weldments, to reduce the possibility of leakage, and 2219 aluminum was selected for the material system. This alloy was selected because of its ductility of cryogenic temperatures, as well as its weldability, formability, stress corrosion resistance, and its high fracture toughness and resistance to flaw growth (references 9 and 10).

A description of the tank designs and the stress analysis conducted on their major components are presented in the following section. Design criteria and flight loads as specified in the previous section were used as the basis for design.

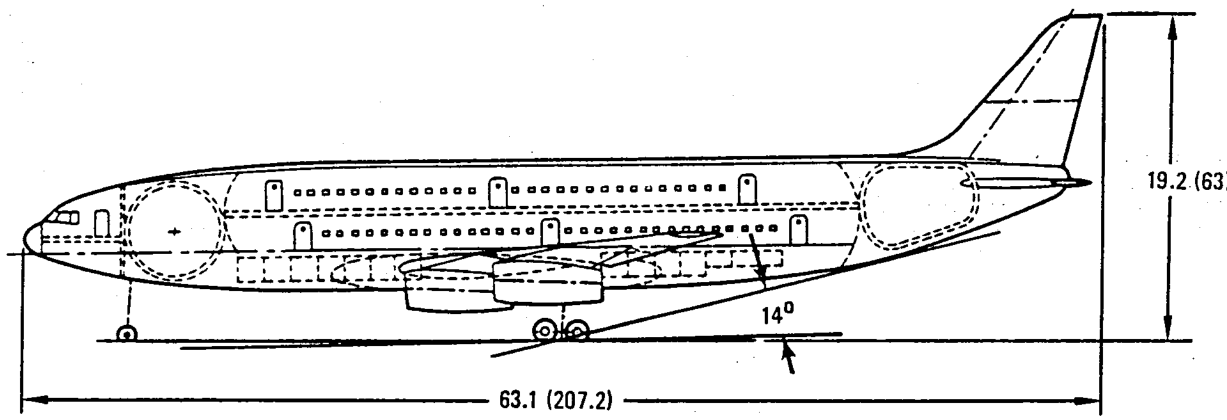

Figure 34. - General arrangement drawing.

5.2.1 Forward tank.- The forward tank design is premised on the criteria defined for the hydrogen tank study (reference 4). Some basic design concepts of this tank are illustrated in figures 35 and 36 with some of the general design requirements listed below:

- The tank is spherical in configuration and is a 2219-T851 aluminum alloy weldment.
- An unstiffened wall configuration is postulated with fail-safe straps provided for damage tolerance capability.
- The nominal tank pressure and pressure schedule as defined in the design criteria are applicable for the design of the forward tank.
- Similarly, the design tension allowables specified in the criteria section are also applicable.

The design pressures are shown in table 20 for the flight conditions and emergency landing condition specified for this study. The limit and ultimate design pressures contain the inertia head component and are displayed at three tank locations, i.e., top, mid, and bottom. These pressures were used to define the minimum tank wall thicknesses.

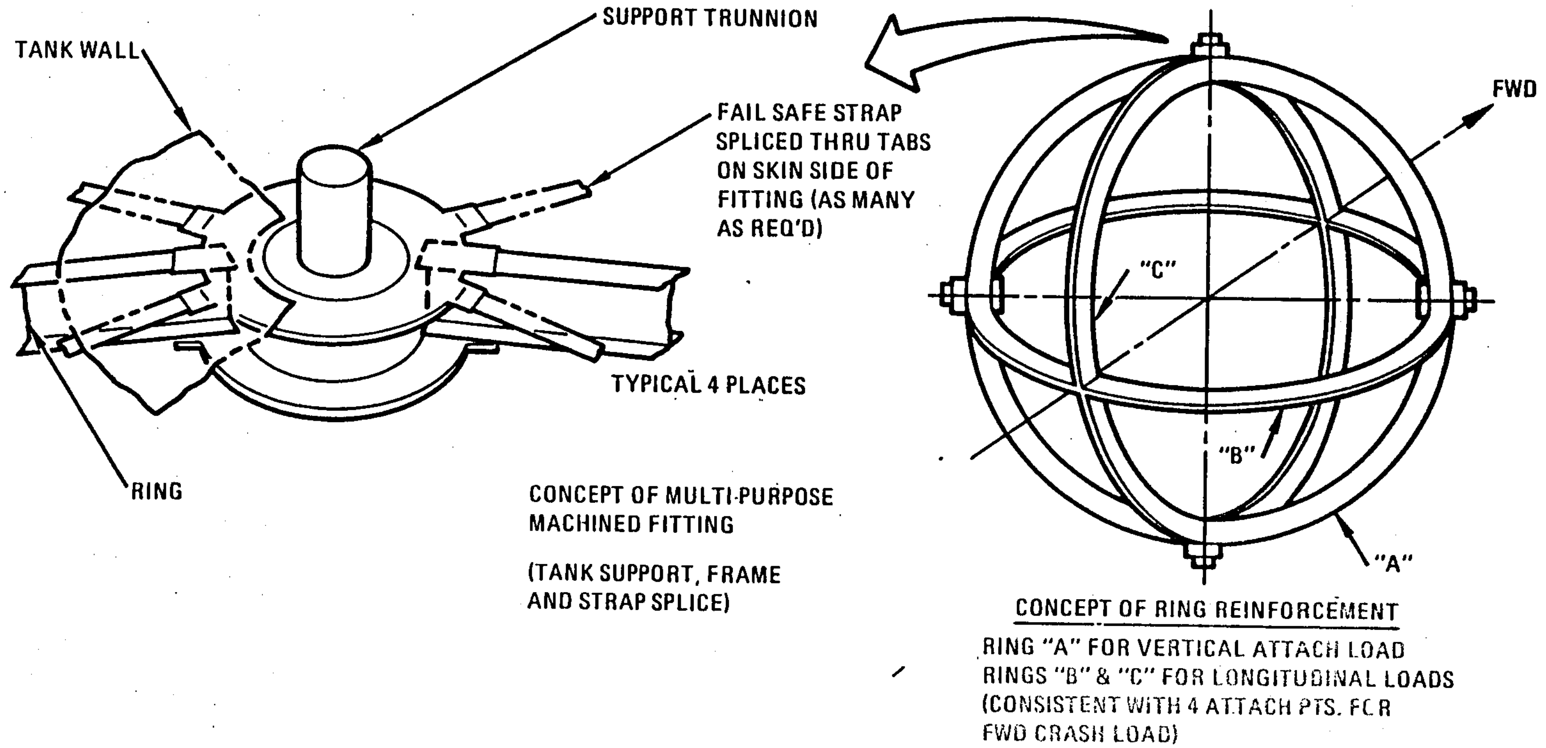

Figure 35. - Concept of primary supporting structure for forward tank.

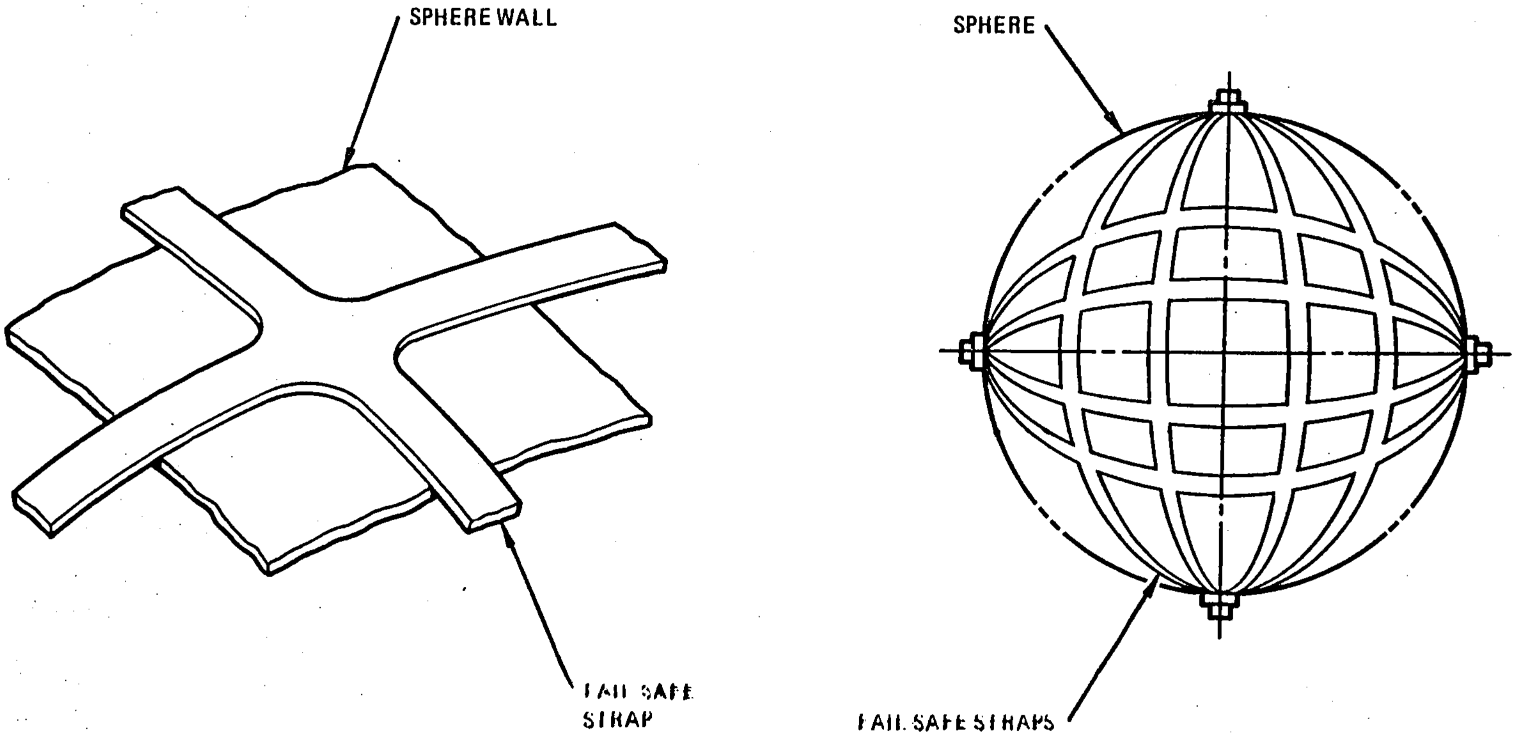

Figure 36. - Concept of fail-safe strap reinforcement for forward tank.

TABLE 20. - FORWARD TANK DESIGN PRESSURES

Flight Condition	Altitude m(ft)	Load[(1)] Factor (Limit) n	Operating[(2)] Pressure p_{op} kPa(psi)	Design Pressure kPa(psi)					
				p_{limit} [(3)]			$p_{ultimate}$ [(4)]		
				Top	Mid	Bottom	Top	Mid	Bottom
Positive Low Angle of Attack (PLA)	6 700 (22 000)	+2.5g	112.4 (16.3)	112.4 (16.3)	141.3 (20.5)	170.3 (24.7)	168.2 (24.4)	212.4 (30.8)	255.8 (37.1)
Pitching Maneuver	Sea Level	+1.0g	47.6 (6.9)	47.6 (6.9)	59.3 (8.6)	71.0 (10.3)	71.7 (10.4)	88.9 (12.9)	106.2 (15.4)
Negative Maneuver	6 700 (22 000)	-1.0g	112.4 (16.3)	135.8 (19.7)	124.1 (18.0)	112.4 (16.3)	204.1 (29.6)	186.2 (27.0)	168.2 (24.4)
Cruise	10 700 (35 000)	+1.0g	133.8 (19.4)	133.8 (19.4)	145.5 (21.1)	157.2 (22.8)	200.6 (29.1)	217.9 (31.6)	235.8 (34.2)
Emergency Landing	Sea Level	+9.0g[(1)]	47.6 (6.9)	- -	- -	- -	176.5 (25.6)	280.6 (40.7)	176.5 (25.6)

(1) All values are limit vertical load factors (n_z) except for the emergency landing value which is an ultimate forward load factor (n_x).

(2) Operating pressures as specified in the structural design criteria.

(3) $P_{limit} = P_{op} + (n_z \rho h)$; where ρh = 11.65kPa/g(1.69 psi/g) one-half depth (radius)
23.24kPa/g(3.37 psi/g) full depth (diameter)

(4) $P_{ultimate} = 1.5 \times p_{limit}$; except for emergency landing condition where $P_{ULT} = 1.5 \times p_{op} + n_x \rho h$

5.2.1.1 Basic shell.- Table 21 presents the results of the membrane sizing of the forward tank and excludes any damage tolerance requirements. This table summarizes the wall thickness requirements for the various design conditions and also specifies an assumed minimum manufacturable wall thickness. The critical criterion is the ultimate design condition where the top of the tank is designed by the negative maneuver condition and the mid and bottom locations are designed by the cruise and PLA conditions, respectively. A gross area tension allowable of 172.4 MPa (25 000 psi) was used for this analysis. The wall thicknesses range from a minimum value of 0.165 cm (0.065 in.) at the top of the tank to a maximum of 0.208 cm (0.082 in.) at the bottom.

A fail-safe analysis was conducted to ensure that the forward tank in the presence of an assumed damaged is capable of supporting 100 percent of the limit load. The analytical methods used for this evaluation are identical to those used for the hydrogen tank study and can be found in reference 11.

The residual strength of the tank was evaluated for several crack lengths with and without fail-safe straps. Table 22 illustrates these results with the first row of calculations at each location reflecting the shell thickness required to sustain a 30.5-cm (12.0-in.) long crack without straps. Wall thicknesses ranged from 0.401 cm (0.158 in.) at the top, to approximately 0.508 cm (0.200 in.) at the bottom location for this unreinforced condition. The remaining calculations on this table present the strap requirements (area and spacing) to maintain a damage-tolerant tank using the wall thickness dictated by the membrane analysis (table 21). Maximum strap areas of 3.55 cm^2 (0.55 $in.^2$) and 2.77 cm^2 (0.43 $in.^2$) are noted at the bottom of the tank for strap spacings of 40.0 cm (15.76 in.) and 27.5 cm (10.84 in.), respectively. Smaller strap areas are indicated for these spacings at the other tank locations. In addition, the effective thickness $\bar{t}$ (sum of the skin thickness and the strap area divided by its spacing) is shown for each spacing analyzed. The straps spaced at 40.0 cm (15.76 in.) appear to offer the least weight design and were chosen for this application.

The results of the skin-sizing and fail-safe analyses are summarized in table 23. These values reflect the maximum skin thickness requirements defined in table 21 for the ultimate design condition and the strap areas specified in table 22 for the limit design fail-safe condition. These analyses are based on the same combinations of flight conditions, but with different factors of safety. The variation of wall thickness and strap area for the forward tank is illustrated in figure 37.

The skin thickness of the shell varies from top to bottom, but is invariant in thickness around the vertical axis. The strap spacing of 40.0 cm (15.76 in.) occurs at the equators of the top and bottom trunnions and the side trunnions, see figure 36. The straps in both of these directions will converge at the trunnions with a sufficient number of straps removed for practical reasons.

TABLE 21. - MINIMUM SKIN THICKNESSES FOR FORWARD TANK(1)
(EXCLUDES DAMAGE TOLERANCE CONDITIONS)

Tank Location	Operating Condition (2)		Ultimate Design Condition (3)		Burst Condition (4)		Emergency Landing Condition (5)		Minimum Manufacturable Wall Thickness	
	p kPa (psi)	t cm (in.)	p kPa (psi)	t cm (in.)	p kPa (psi)	t cm (in.)	p kPa (psi)	t cm (in.)	p kPa (psi)	t cm (in.)
Top	133.8 (19.4)	0.162 (0.064)	204.1 (29.6)	0.165 (0.065)	267.5 (38.8)	0.096 (0.038)	176.5 (25.6)	0.064 (0.025)	-	0.127 (0.050)
Mid	145.5 (21.1)	0.173 (0.068)	217.9 (31.6)	0.178 (0.070)	291.0 (42.2)	0.107 (0.042)	280.6 (40.7)	0.103 (0.040)	-	0.127 (0.050)
Bottom	157.2 (22.8)	0.188 (0.074)	255.8 (37.1)	0.208 (0.082)	314.4 (45.6)	0.114 (0.045)	176.5 (25.6)	0.064 (0.025)	-	0.127 (0.050)

(1) Basic equation

$t = \frac{pr}{2F}$; where : p = design pressure
r = radius = 280.4 cm(110.4 in.)
F = allowable stress

(2) Operating condition, limit cruise pressures

F = 117.2 MPa(17 000 psi.)

(3) Maximum ultimate design pressures

F = 172.4 MPa(25,000 psi.)

(4) P_{burst} = 2.0 x max. lg pressures

$F = 0.90\,F_{tu} = 0.90 \times 427.5$ MPa

= 384.7 MPa(55 800 psi.)

(5) Sea level pressures (ult.) with 9.0g inertia load

$F = 0.90\,F_{tu}$ = 384.7 MPa(55,800 psi.)

TABLE 22. - FAIL-SAFE REQUIREMENTS FORWARD TANK

Tank Location	Limit Load, kN/m (lb f/in.)	Skin Thk. t_s cm (in.)	Strap Spacing b cm (in.)	Crack Length $\ell = 2b$ cm (in.)	Strap Area Ae cm^2 ($in.^2$)	$\frac{2Ae}{t_s}$ cm (in.)	Reinf. Effic. γ	Fg Residual Strength MPa (psi)	$\bar{t}$ (ts + Ae/b) cm (in.)	Applied Stress $N/\bar{t}$ MPa (psi)
Top	190.4 (1 087)	0.401 (0.158)	- -	30.50 (12.0)	- -	- -	1.00	47.6 (6 900)	0.401 (0.158)	47.6 (6 900)
		0.165 (0.065)	40.03 (15.76)	80.09 (31.53)	2.84 (0.440)	34.39 (13.54)	2.72	80.0 (11 600)	0.236 (0.093)	80.7 (11 700)
		0.165 (0.065)	27.53 (10.84)	55.07 (21.68)	2.26 (0.350)	27.36 (10.77)	2.19	77.9 (11 300)	0.246 (0.097)	77.2 (11 200)
Mid	203.8 (1 164)	0.429 (0.169)	- -	30.50 (12.00)	- -	- -	1.00	47.6 (6 900)	0.429 (0.169)	47.6 (6 900)
		0.178 (0.070)	40.03 (15.76)	80.09 (31.53)	3.03 (0.470)	34.11 (13.43)	2.71	80.0 (11 600)	0.254 (0.100)	80.0 (11 600)
		0.178 (0.070)	27.53 (10.84)	55.07 (21.68)	2.39 (0.370)	26.85 (10.57)	2.18	77.2 (11 200)	0.264 (0.104)	77.2 (11 200)
Bottom	239.0 (1 365)	0.503 (0.198	- -	30.50 (12.00)	- -	- -	1.00	47.6 (6 900)	0.503 (0.198)	47.6 (6 900)
		0.208 (0.082)	40.03 (15.76)	80.09 (31.53)	3.55 (0.55)	34.06 (13.41)	2.71	80.0 (11 600)	0.297 (0.117)	80.7 (11 700)
		0.208 (0.082	27.53 (10.84)	55.07 (21.68)	2.77 (0.43)	26.64 (10.49)	2.18	77.2 (11 200)	0.310 (0.122)	77.2 (11 200)

$$Fg = \frac{\gamma}{2} \frac{Ko}{\sqrt{\ell}}$$

Where:

Ko = Stress intensity factor, Ko = 527.4 MPa $\sqrt{cm}$ (48 000 psi $\sqrt{in.}$)

γ = Reinforcement efficiency = 1.00 for unreinforced shell (no straps)

ℓ = Crack length

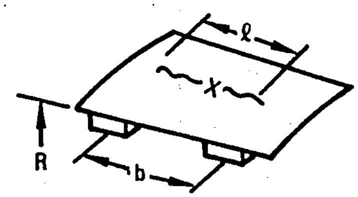

TABLE 23. - SUMMARY OF SKIN THICKNESS AND FAIL-SAFE STRAP REQUIREMENTS FOR FORWARD TANK

Location on Tank	Flt Condition	Skin Thickness: Ult Des Press kPa (psi)	Skin Thickness: t_s Req'd cm (in.)	Fail-Safe Requirement: Limit Des Press kPa (psi)	Fail-Safe Requirement: Strap Spacing cm (in.)	Fail-Safe Requirement: Strap Area cm^2 (in^2)
Top	Negative Maneuver -1.0g 6 700 m (22 000 ft.)	204.1 (29.6)	0.165 (0.065)	135.8 (19.7)	40.03 (15.76)	2.84 (0.440)
Equator	Cruise +1.0g 10 700 m (35 000 ft.)	217.9 (31.6)	0.178 (0.070)	145.5 (21.1)	40.03 (15.76)	3.03 (0.470)
Bottom	Positive Low Angle 2.5g 6 700 m (22 000 ft.)	255.8 (37.1)	0.208 (0.082)	170.3 (24.7)	40.03 (15.76)	3.55 (0.550)

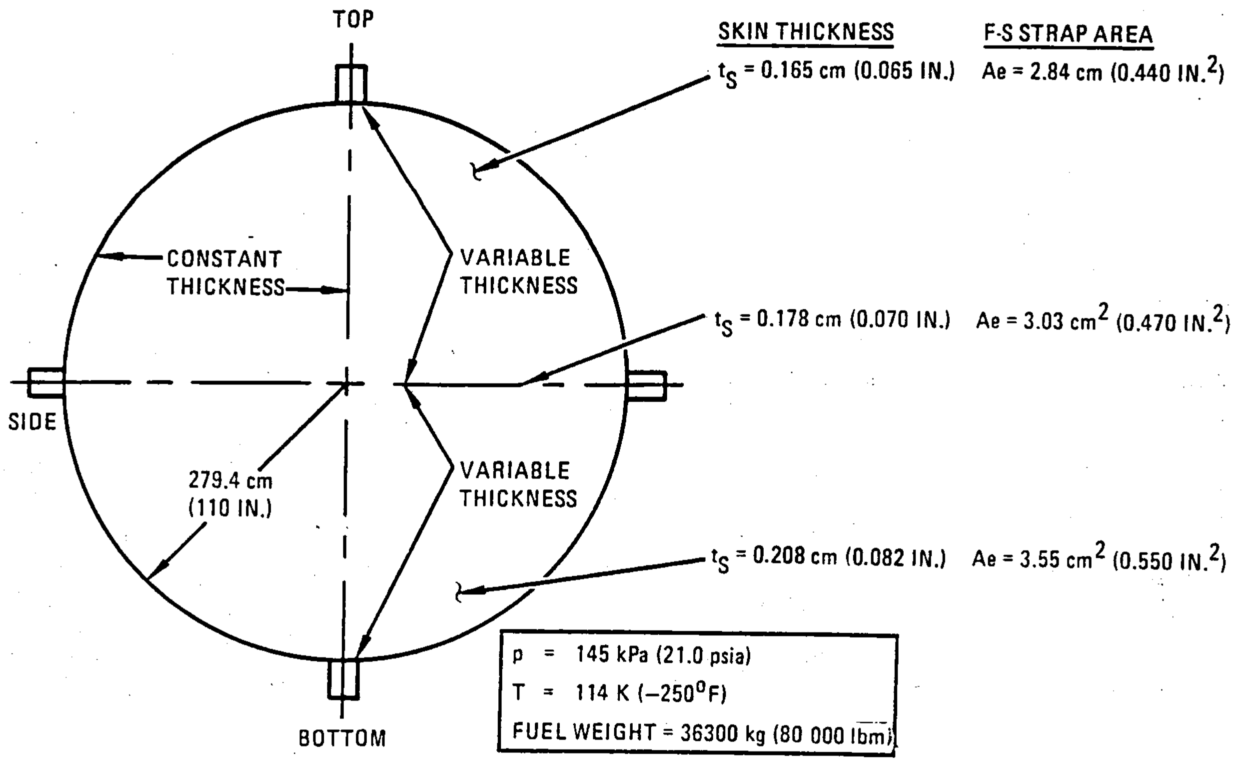

Figure 37. - General dimensions of forward tank.

5.2.1.2 Reinforcement rings.- Three internal rings are used as the basic support structure for the forward tank (figure 35). These rings not only support the shell but also provide trunnion fittings at the poles and sides for supporting the tank within the fuselage. The premised fabrication technique, which is described more fully in a later section, is that of a weldment using 2219-T8511 aluminum alloy extrusions.

The critical design condition for the ring structure is the emergency landing condition as specified by FAR 25.561. The appl ication of the 9-g forward inertia load factor to the weight of a full tank, 36 300 kg (80 000 lbm), results in the most severe design condition for the ring. Figure 38 illustrates the inertia force, n_xW = 3 200 kN (720 000 lbf), applied on the tank and the assumed equally distributed reaction forces at the trunnions. The sketch at the right of this figure presents the forces and moments on a single reinforcement ring. The moments were caused by the offset, 11.4 cm (4.50 in.), between the trunnion reaction point and the frame center of gravity.

Rigid ring theory was postulated for the development of the internal loads within the ring. Formulas for the bending moments, axial forces and shears of closed circular rings were taken from reference 12. By superposition, the individual loading conditions were combined to obtain the final condition. Figure 39 presents the free-body diagrams for these conditions. The first condition reflects a symmetrically supported ring uniformally loaded by the inertia force 800 kN (180 000 lbf), case 19 of reference 12. A ring loaded by two equal and opposite localized couples, M_o, is shown in the second sketch, case 3 of the reference. The third condition reflects a symmetrically supported ring carrying half the inertia force, 801 kN (180 000 lbf) transferred by tangential shear, case 24 of the reference. The last sketch illustrates the final load state obtained by the superposition of the three previous conditions. The axial loads, shears and bending moments on the ring for the combined conditions are shown in figure 40. For clarity, only the forces and moments for one-half of the symmetrically loaded ring are shown.

The rings were subjected to a strength analysis to define the section properties of the cross section at various circumferential locations. An I-section stiffener was employed for the ring configuration. The area A and section modulus Z (I/C) of the stiffener as a function of the flange thickness t_f are shown in figure 41. The stiffener height b_w and flange width $2b_f$ were preselected and held invariant for the analysis at values of 10.2 cm (4.00 in.) and 6.35 cm (2.50 in.), respectively. In addition, the web-to-flange thickness ratio (t_w/t_f) was held constant at a value of 0.70. The ring has larger cross-sectional dimensions (increased height and width, and greater flange thickness) in the vicinity of the trunnion.

The allowable compressive stresses for the complete cross section of the stiffener are presented in figure 42. The ultimate tension strength (F_{tu}) of 2219-T8511 aluminum was used for the tension allowable. Table 24 provides a summary of the results of the ring structural analysis. This table shows the circumferential location being analyzed and the corresponding loads at

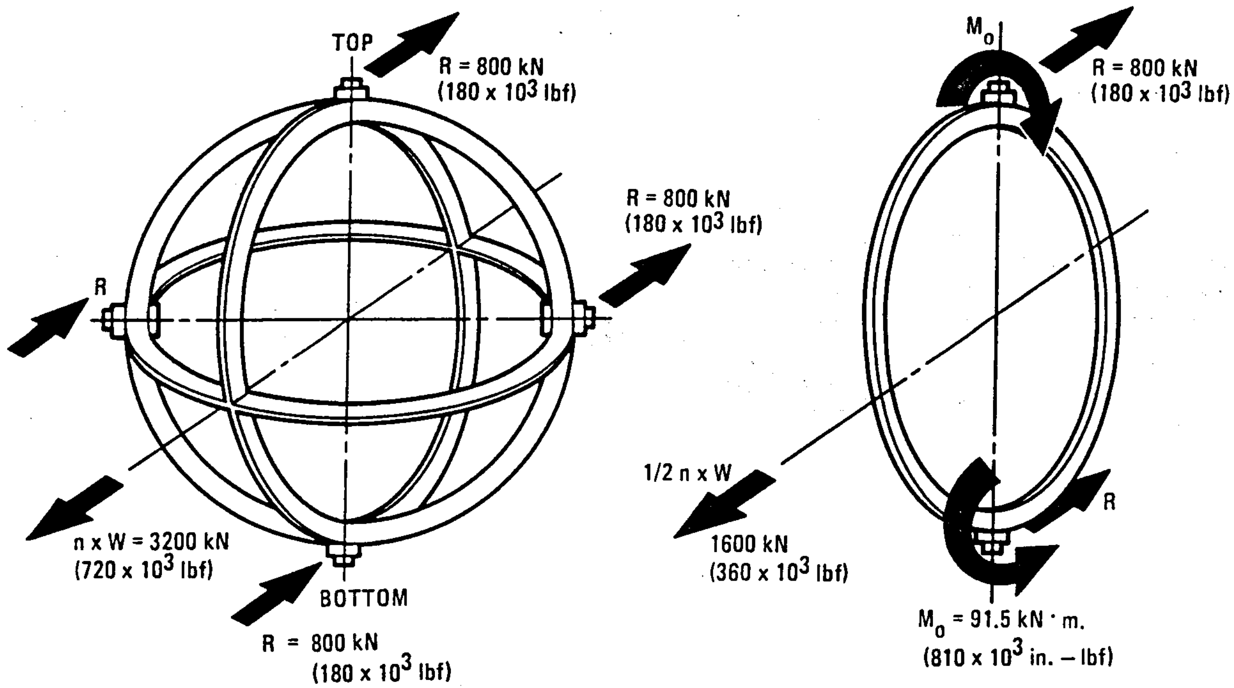

Figure 38. - Applied ring loads on the forward tank.

that location, the required cross-sectional properties of the ring, a summary of the axial and bending stress analyses, and the margin of safety.

5.2.1.3 Pin and trunnion.- A drawing of the tank suspension system is shown in figure 43. The pin has a diameter of 6.99 cm (2.75 in.) and is made from 321 (1/2 hard) stainless steel. The trunnion is fabricated from 2219-T81 aluminum alloy.

The design of these components is dictated by the emergency landing condition as specified in FAR 25.561. The 9-g forward inertia load factor caused the most severe loading condition. The inertia force for a full tank, 3200 kN (720 000 lbf), was equally distributed to the four trunnion i.e., 801 kN (180 000 lbf) per trunnion. The resulting load, shear, and moment diagrams on the pin are:

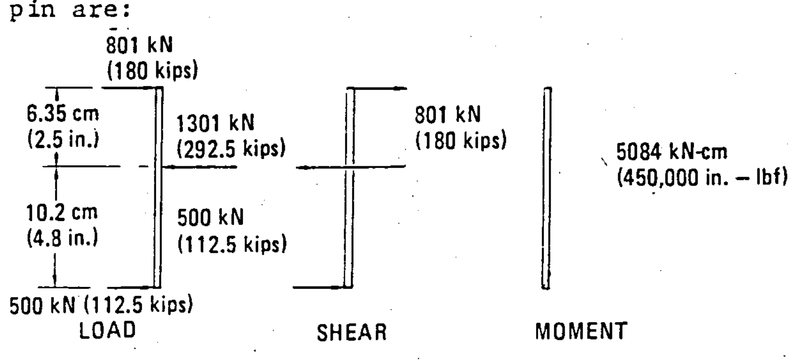

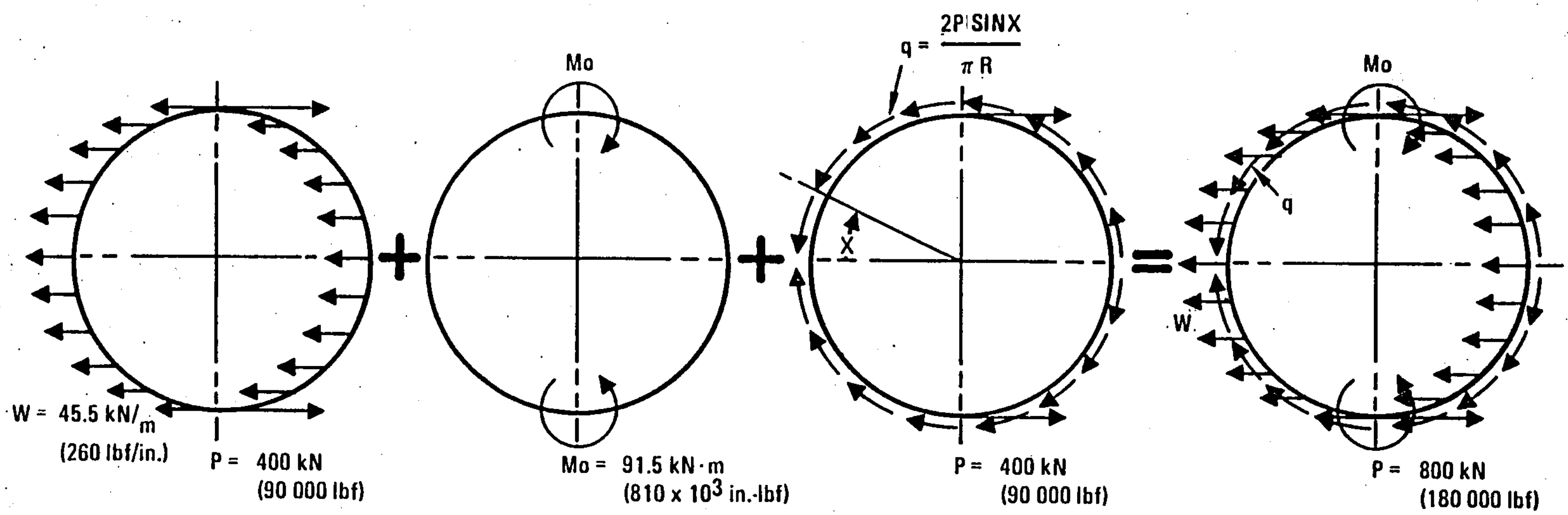

CASE (1)	CASE (2)	CASE (3)	CASE (4)
SUPPORTED AT THE SIDES LOADED BY A UNIFORM LOAD OF W	LOADED BY TWO EQUAL AND OPPOSITE COUPLES	SUPPORTED AT THE SIDES LOADED BY TANGENTIAL SHEAR FORCES	FINAL LOADING

Figure 39. - Reinforcement ring loading diagrams for forward tank.

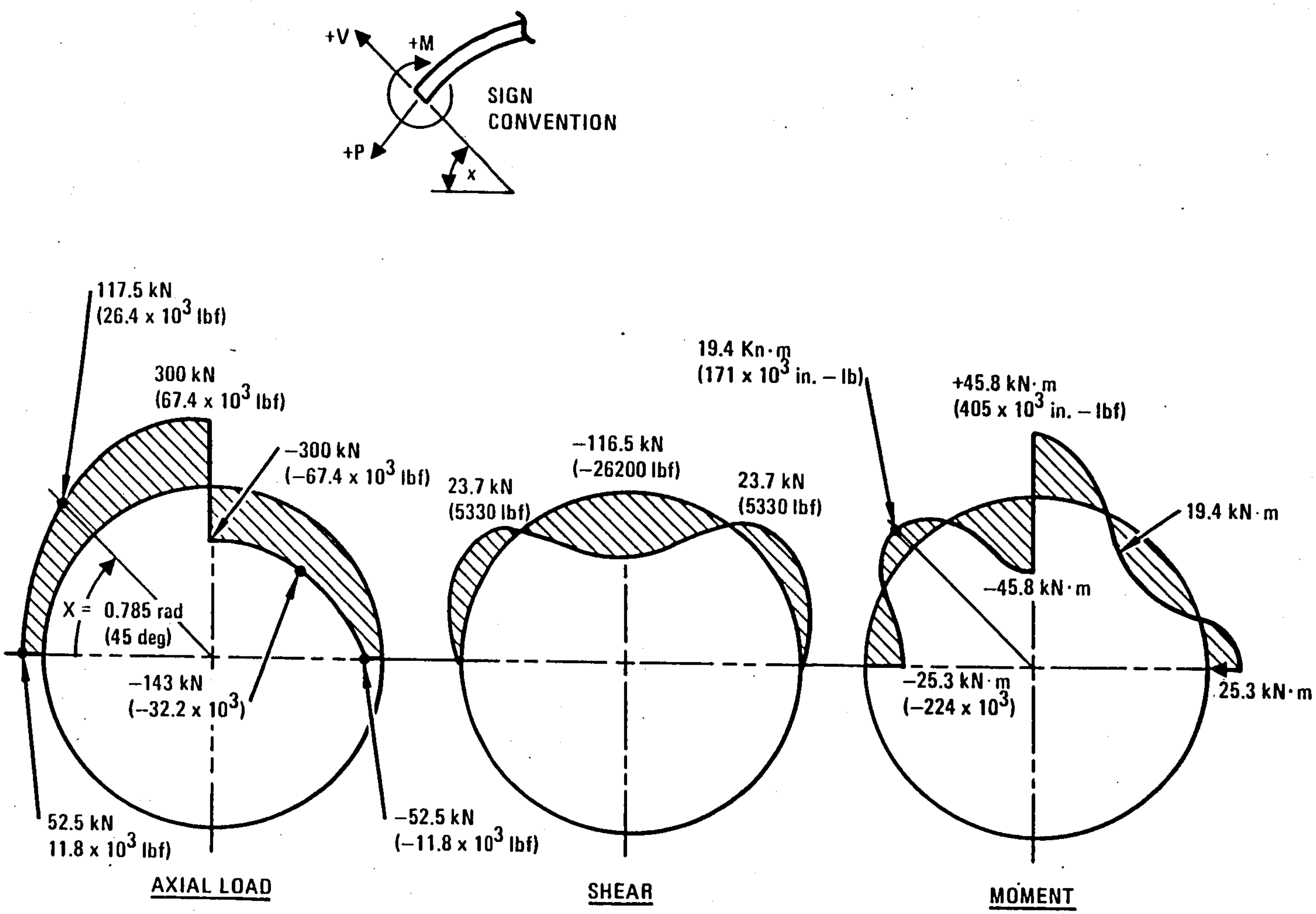

Figure 40. - Internal loads for reinforcement rings of forward tank.

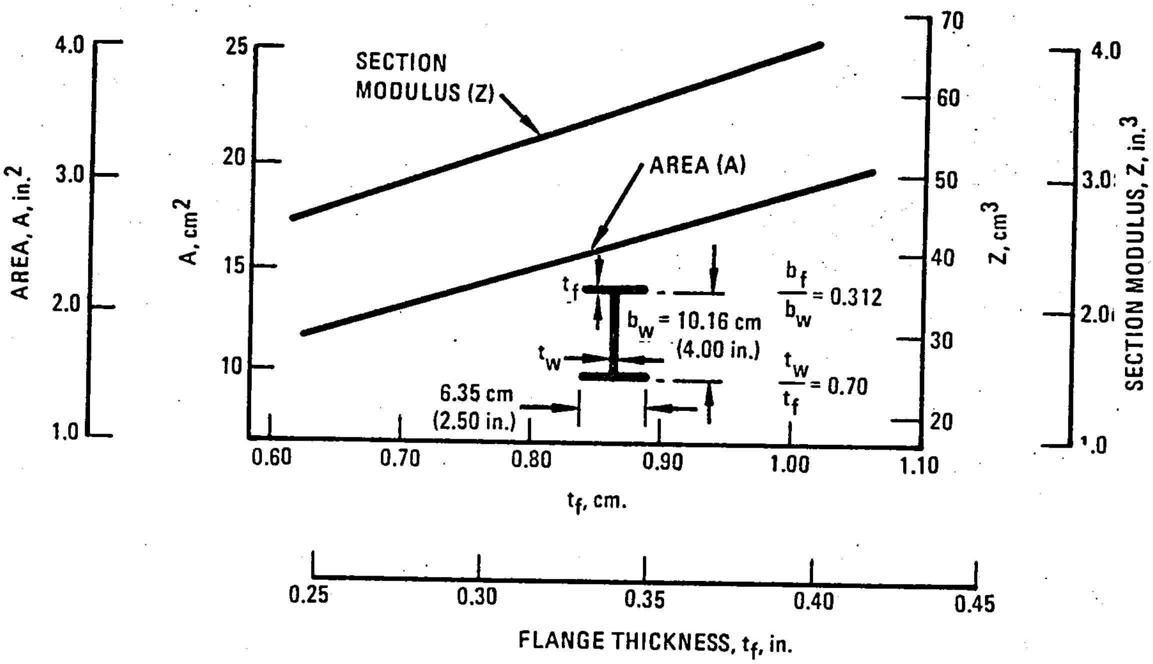

Figure 41. - Section property data for reinforcement rings.

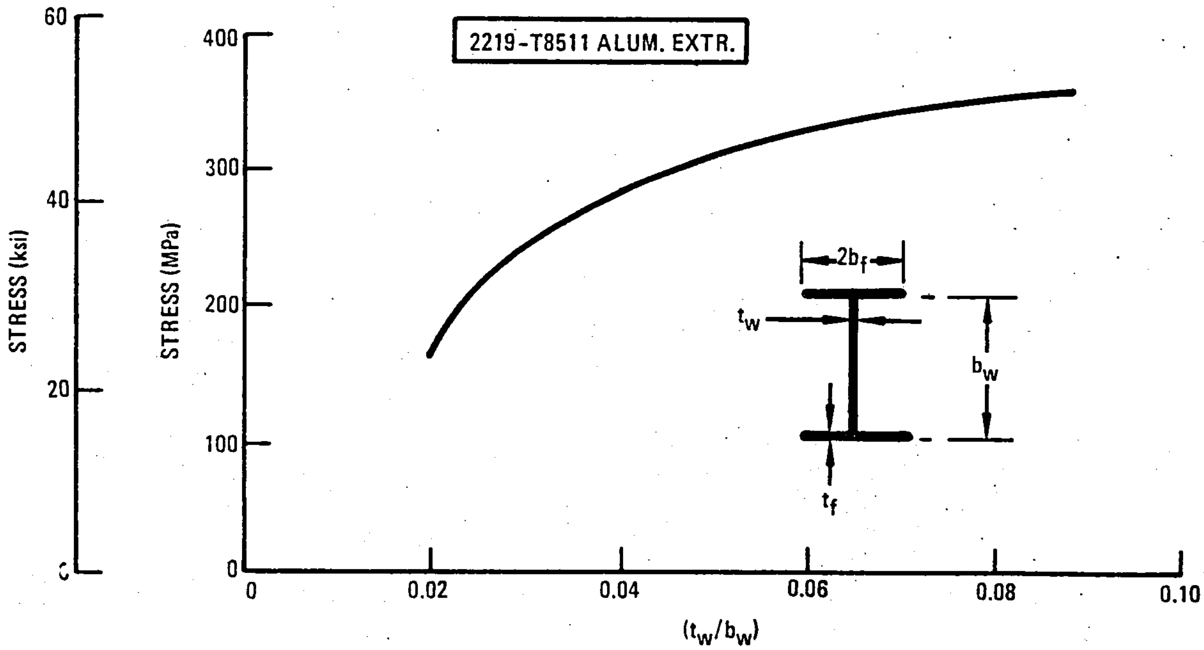

Figure 42. - Compression design allowables for reinforcement rings.

TABLE 24. - STRUCTURAL ANALYSIS OF REINFORCEMENT RING FOR FORWARD TANK

Circum.(1) Location θ rad (deg.)	Internal Loads(1) P kN (lbf.)	V kN (lbf.)	M kN · m (in.-lbf.)	Ring Properties(2) t_f cm. (in.)	t_w cm. (in.)	A cm^2 ($in.^2$)	I/C cm^3 ($in.^3$)	Axial Stress $f_{c,t}$ MPa (ksi)	$F_{c,t}$ MPa (ksi)	$R_{c,t}$	Bending Stress M_u kN · m (in.-lbf.)	R_b	Margin of Safety
0	52.5 (11.8 x 10^3)	0	-25.3 (-224 x 10^3)	0.952 (0.375)	0.665 (0.262)	17.6 (2.73)	62.4 (3.81)	29.6 (4.30)	439.9 (63.8)	0.067	27.12 (240 x 10^3)	0.93	+0.03
0.785 (45)	117.5 (26.4 x 10^3)	23.7 (5 330)	19.4 (171 x 10^3)	0.792 (0.312)	0.554 (0.218)	14.8 (2.30)	53.2 (3.25)	79.3 (11.50)	439.9 (63.8)	0.180	22.82 (202 x 10^3)	0.85	+0.04
1.57^- (90^-)	300.0 67.4 x 10^3)	-116.5 (-26 200)	-45.8 (-405 x 10^3)	1.270 (0.500)	0.635 (0.250)	32.2 (5.00)	141.4 (8.63)	93.1 (13.50)	439.9 (63.8)	0.21	66.32 (587 x 10^3)	0.69	+0.24
1.57^+ (90^+)	-300.0 (-67.4 x 10^3)	-116.5 (-26 200)	45.8 (405 x 10^3)	1.270 (0.500)	0.635 (0.250)	32.2 (5.00)	141.4 (8.63)	-93.1 (-13.50)	-303.4 (-44.0)	0.31	66.32 (587 x 10^3)	0.69	+0.01
2.36 (135)	-143.0 (-32.2 x 10^3)	23.7 (5 330)	-19.4 (-171 x 10^3)	0.952 (0.375)	0.665 (0.262)	17.6 (2.73)	62.4 (3.81)	-81.4 (-11.80)	-333.0 (-48.3)	0.24	27.12 (240 x 10^3)	0.71	+0.05
3.14 (180)	-52.5 (-11.8 x 10^3)	0	25.3 (224 x 10^3)	1.110 (0.437)	0.777 (0.306)	20.2 (3.14)	70.9 (4.33)	-26.2 (-3.80)	-351.6 (-51.0)	0.07	30.8 (272.8 x 10^3)	0.82	+0.11

(1) Circumferential Location

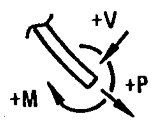

SIGN CONVENTION

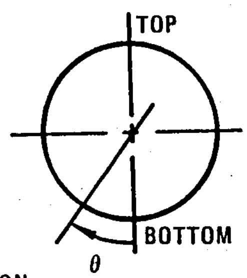

(2) All ring sections have a web height and flange width of 10.16 cm (4.00 in.) and 6.35 cm (2.50 in.), respectively. The exception occurs at θ = 1.57 rad (90 deg.) where the ring height is 12.7 cm (5.00 in.).

(3) The interaction equation for combining the tension and bending stresses is contained in SM53 of reference 13.

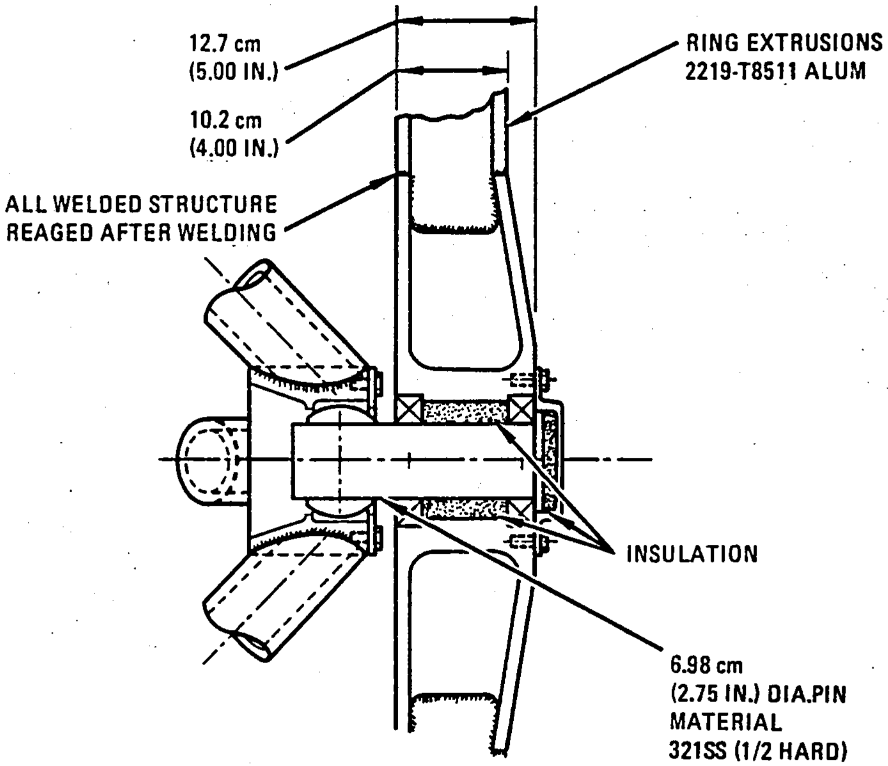

Figure 43. - Pin and trunnion design.

The 6.99 cm (2.75 in.) diameter pin has the following cross-sectional properties

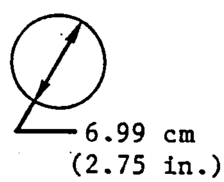

Area (A) = 38.3 cm^2 (5.94 $in.^2$)

Section Modulus (Z) = 33.4 cm^3 (2.04 $in.^3$)

Section Factor (K) = 1.70

The pin was analyzed for the combined bending and shear loads using the plastic bending theory described in reference 13. The bending analysis for the 321 (1/2 hard) stainless steel pin is:

$$F_B = 165.5 \text{ kN/cm}^2 \text{ (240 000 psi)}$$

$$f_b = \frac{M}{Z} = \frac{5084}{33.4} = 152.2 \text{ kN/cm}^2 \text{ (220 000 psi)}$$

the stress ratio in bending is

$$R_b = \frac{f_b}{F_B} = 0.92$$

the maximum shear stress at the neutral axis is

$$f_s = 1.38 \frac{V}{A} = \frac{1.38 \times 801}{38.3} = 28.9 \text{ kN/cm}^2 \text{ (41 800 psi.)}$$

the material strength and stress ratio are

$$F_{su} = 53.1 \text{ kN/cm}^2 \text{ (77 000 psi.)}$$

$$R_s = \frac{28.9}{53.1} = 0.54$$

Using the interaction curve shown in figure 33 of reference 13 the margin of safety is

$$M.S. = \frac{0.94}{0.92} - 1 = +0.02$$

5.2.1.4 Fabrication method.- A method of fabricating the forward tank is discussed in this section. This method is not the only method available but it does present a feasible approach for fabricating a cryogenic tank for the time period under consideration.

The fabrication of the ring support structure is as follows, figure 35:

- Ring C is extruded in two 3.14 rad (180 deg.) sections each about 9.1 m (30 ft.) long. The ends are butt welded to the rim of the trunnion fitting, top and bottom.

- Rings A and B are extruded in four 1.57 rad. (90 deg) quadrants (total of eight pieces) each about 4.6 m (15 ft) long. The ends are butt welded to Ring C or to the trunnion rim as indicated.

The ring frame support structure is the basic building block and is completely fabricated prior to welding on the tank wall segments.

The shell quadrants are built up with two skin panels per 1.57 rad (90 deg) quadrant, a total of 16 panel segments for the sphere, i.e., each panel subtends 0.785 rad (45 deg) at the equator. Each panel segment is stretch formed from the maximum thickness requirement and then chemmilled and trimmed per figure 44.

The fail-safe straps are also formed as panels to match the skin segments. They are stretched formed from the maximum thickness required to mate with the outside diameter of the surface of the skin panel. They are shown in figure 45. The fail-safe straps are then welded to the skin panel.

The next step in this process is to fusion weld two skin segment panels forming a 1.57-rad (90-deg) quadrant as shown in figure 46. A welding tab is used (and removed after welding) to fusion butt-weld the two segments together. Fillet welds are used to attach the ends of the fail-safe straps to the reinforced area of the skin panels. A total of eight quadrant panel subassemblies are required for the tank.

The final assembly is to weld quadrant panel subassemblies to the ring support structure as shown in figure 47. The type of welds and a typical welding sequence are indicated on this figure.

5.2.1.5 Final design.- The general design of the forward tank is shown in figure 48. The major structural components of this spherical tank are shown to illustrate the feasibility of the design. A proposed method of fabrication was described in the previous section.

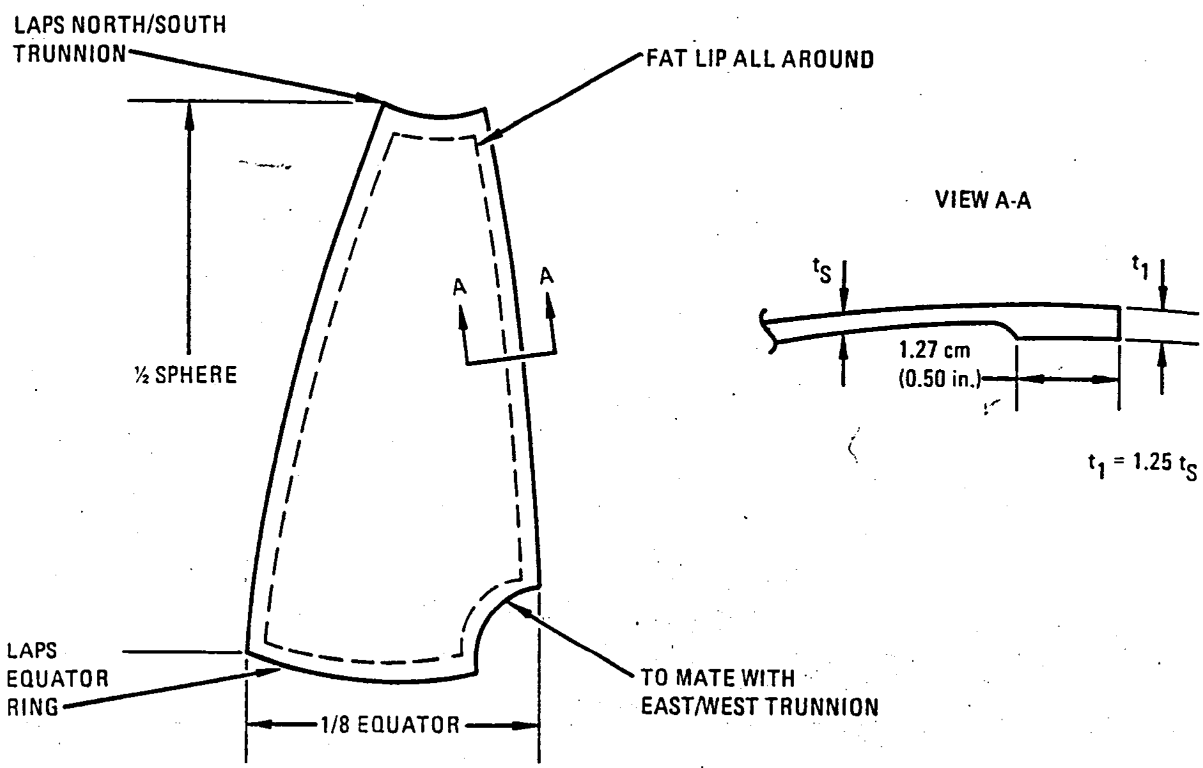

Figure 44. - Typical skin panel for forward tank.

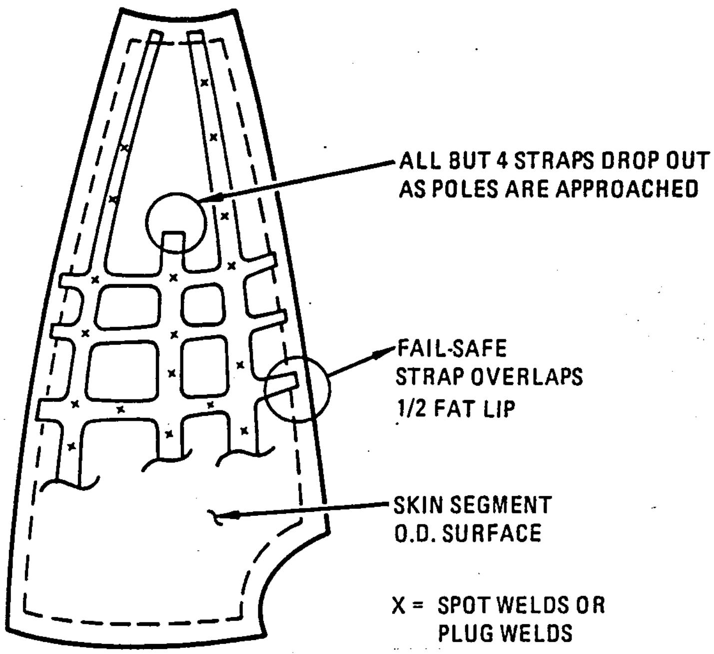

Figure 45. - Fail-safe strap and skin panel layout for forward tank.

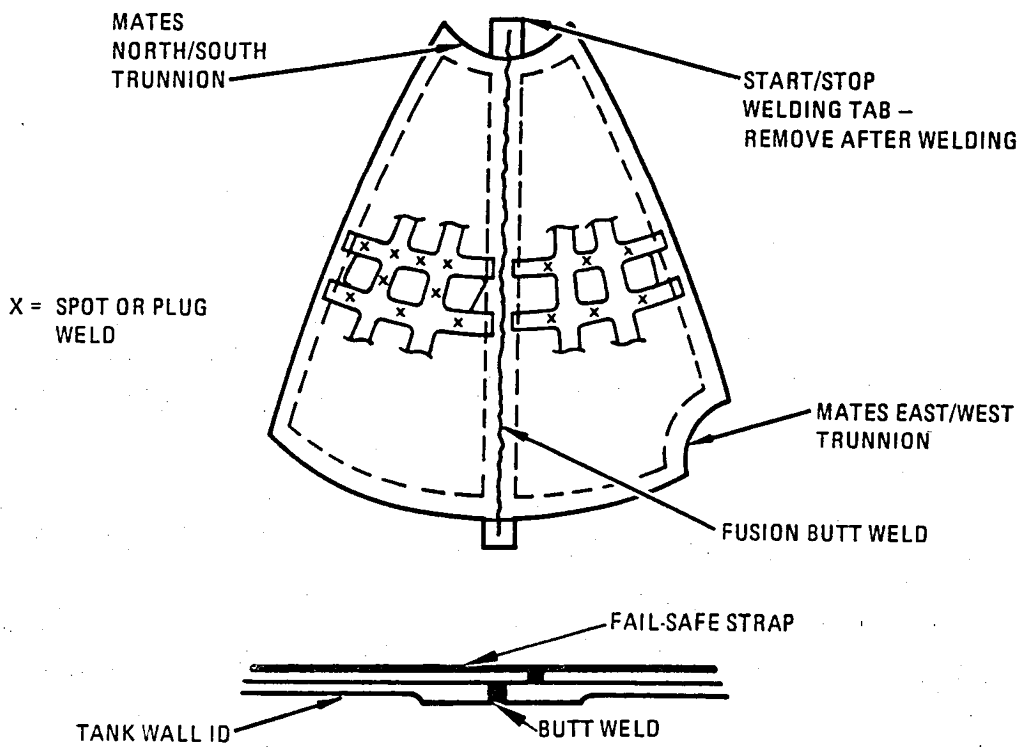

Figure 46. - Quadrant panel assembly for forward tank.

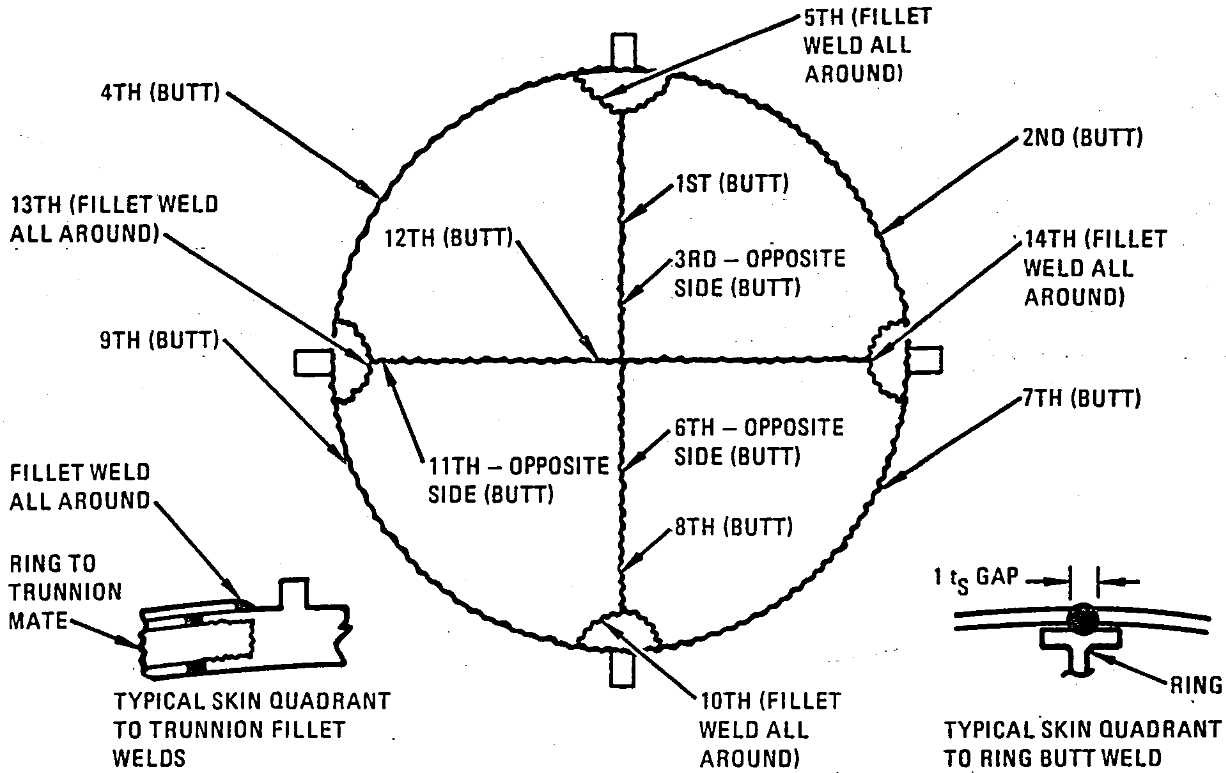

Figure 47. - Final weld-up of forward tank.

The basic shell is an unstiffened wall configuration fabricated from 2219-T81 aluminum alloy sheet. The wall thickness is variable in the meridional direction and constant in the longitudinal direction. The wall thickness ranges from 0.208 cm (0.082 in.) at the lower pole (bottom trunnion) to 0.165 cm (0.065 in.) at the upper pole.

Straps fabricated from 2219-T81 aluminum alloy sheet are spot welded to the external surface of the shell to provide fail-safetiness. These flat straps are made in an integral grid pattern with a variable thickness and a constant width of 7.62 cm (3.00 in.). A grid spacing of 40.0 cm (15.76 in.) is maintained at the equator and the meridian contained in the airplanes X-Z plane.

Internal support for the shell is provided by three internal rings fabricated from 2219-T8511 aluminum extrusions. These rings have an I-section configuration with trunnions provided to support the tank within the fuselage. A solid stainless steel (321 SS) pin is provided at each trunnion to interface with and transfer load to the adjacent fuselage support structure. Bearings in the trunnion, besides their obvious load carrying capabilities, provide a smaller contact area with the tank and reduce the possibility of heat leaks.

5.2.2 Aft tank.- The approach taken in the design of the aft methane tank was to utilize the results of the hydrogen tank study (reference 4), which has the same tank configuration, and modify the design to account for the differences in fuel. A sketch of the general tank design is shown in figure 49 with some of the design features as follows:

- An integral tank design with a conical configuration
- The tank is a 2219-T851 aluminum alloy weldment with an integrally stiffened wall configuration and circumferential rings.
- The nominal tank pressure and pressure schedule as defined in the design criteria are applicable for this design
- Design tension allowables specified in the design criteria section are also applicable

Selective regions on the aft tank were chosen for conducting point design structural analysis. These point design regions correspond to the tank one-quarter and three-quarter span locations (i.e., one-fourth and three-fourths of the distance between the equators of the two closures) and are defined as FS 2038 and FS 2123 on figure 49. Zee-stiffened wall configurations were used on the upper and lower quadrants of the shell at the point design regions. The blade-stiffened configuration was employed on the side quadrants of the shell at these regions.

The design pressures for the aft tank are shown in table 25. The design factors and operating pressures are specified in the design criteria section. The limit and ultimate design pressures contain the inertia head component and are displayed at three circumferential locations at each point design region.

The point design internal load environment is shown in table 26. This table presents the axial and hoop stress resultants (limit) for the two point design regions. The net axial stress resultant is composed of the sum of the axial stress resultants due to the external applied body loads and the internal pressurization. The exception being the maximum net compressive force condition where, as specified in the structural design criteria section, the tension forces due to the internal pressurization are neglected. The internal forces caused by the external bending moment were premised to be reacted at the upper and lower quadrants of the shell; whereas, the shear load is reacted at the side quadrants.

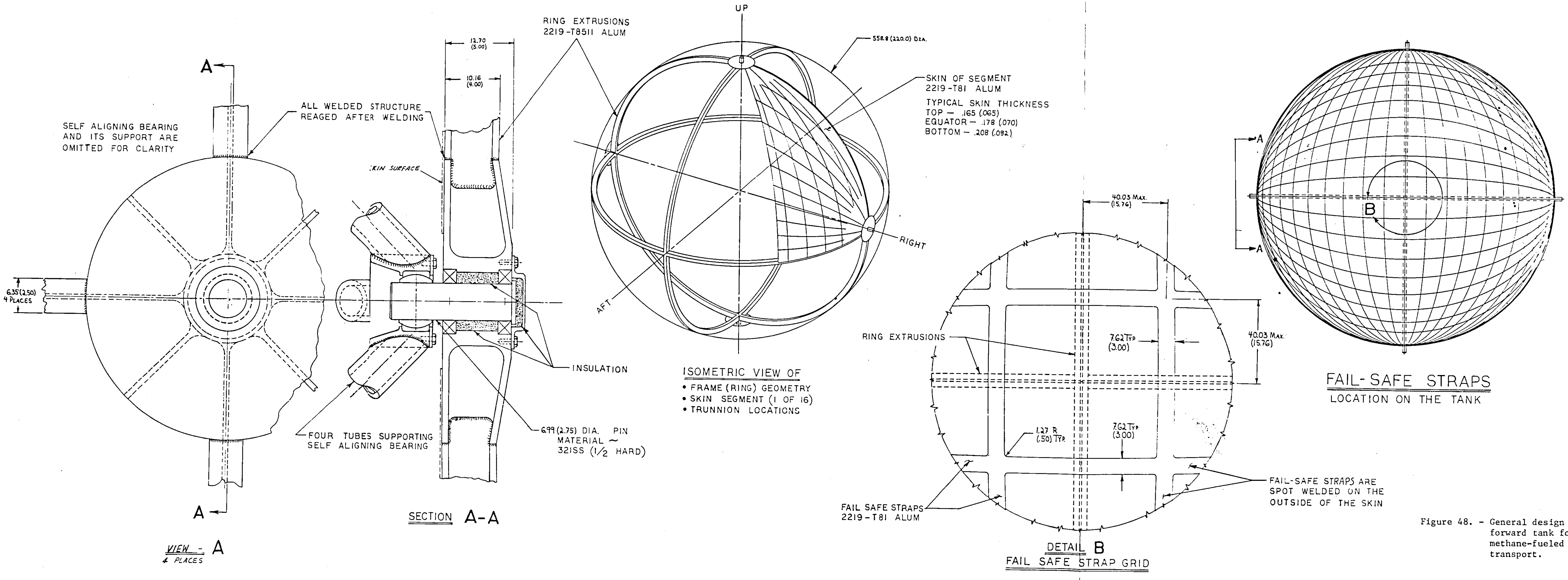

Figure 48. - General design of forward tank for a methane-fueled transport.

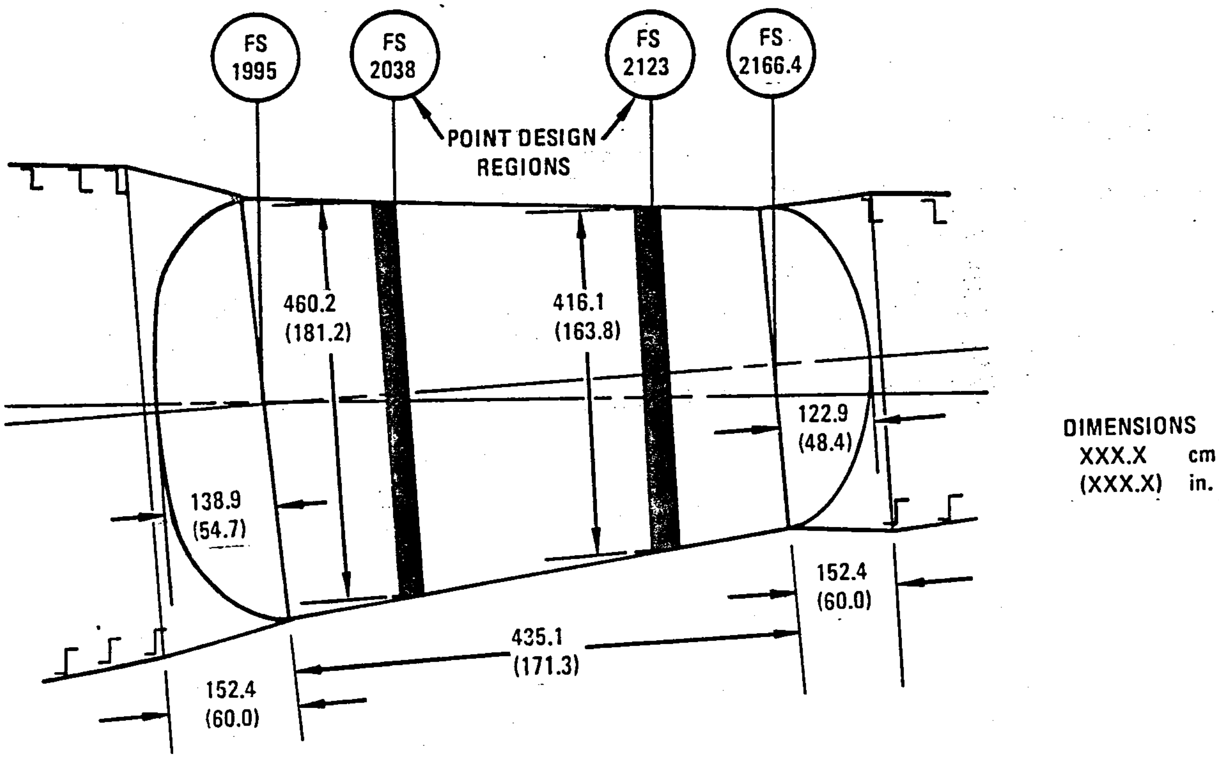

Figure 49. - Basic dimensions of aft tank.

5.2.2.1 Basic shell.- Table 27 presents the results of the membrane sizing of the skin for the aft tank; damage-tolerance requirements were excluded. These data reflect the wall thickness requirements for the various design conditions and also specifies an assumed minimum manufacturable thickness of 0.127 cm (0.050 in.). The critical design condition is the ultimate condition where maximum skin thicknesses of 0.320 cm (0.126 -n.) and 0.282 cm (0.111 in.) are noted on the tank bottom at fuselage stations 2038 and 2123, respectively. At the mid-panel locations, the maximum principal stress was compred to the pertinent design allowable to assess the skin thickness requirements.

The fail-safe criterion as specified in the design criteria was applied to the aft tank to ensure that flight safety is maintained in the event of structural damage. The residual strength of the shell with an assumed circumferential crack was used to define the extensional thickness ($\bar{t}$) of the tank wall and the need for longitudinal fail-safe straps. The longitudinal damage condition which predicates the necessity for hoop straps is described in the frame analysis section. Table 28 displays the results of the cir cumferential damage evaluation. The method of analysis is identical to that used for the forward tank analysis and the limit loads are specified for the

TABLE 25. - AFT TANK DESIGN PRESSURES

REGION	Flight Condition	Altitude m (ft)	Load Factor (Limit) n [(1)]	Operating Pressure p_{op} kPa (psi) [(2)]	Design Pressure, kPa (psi)					
					p_{Limit} [(3)]			$p_{Ultimate}$ [(4)]		
					Top	Mid	Bottom	Top	Mid	Bottom
FS 2038	Positive Low Angle of Attack (PLA)	6 700 (22 000)	+2.5g	112.4 (16.3)	112.4 (16.3)	136.5 (19.8)	160.0 (23.2)	168.2 (24.4)	204.8 (29.7)	239.9 (34.8)
	Pitching Maneuver	Sea Level	+1.0g	47.6 (6.9)	47.6 (6.9)	57.2 (8.3)	66.9 (9.7)	71.7 (10.4)	85.5 (12.4)	100.7 (14.6)
	Negative Maneuver	6 700 (22 000)	-1.0g	112.4 (16.3)	131.7 (19.1)	122.0 (17.7)	112.4 (16.3)	197.2 (28.6)	183.4 (26.6)	168.2 (24.4)
	Cruise	10 700 (35 000)	+1.0g	133.8 (19.4)	133.8 (19.4)	143.4 (20.8)	153.1 (22.2)	200.6 (29.1)	215.1 (31.2)	229.6 (33.3)
	Emergency Landing	Sea Level	+0.9g[(1)]	47.6 (6.9)	–	–	–	238.6 (34.6)	238.6 (34.6)	238.6 (34.6)
FS 2123	Positive Low Angle of Attack (PLA)	6 700 (22 000)	+2.5g	112.4 (16.3)	112.4 (16.3)	133.8 (19.4)	155.8 (22.6)	168.2 (24.4)	200.6 (29.1)	233.7 (33.9)
	Pitching Maneuver	Sea Level	+1.0g	47.6 (6.9)	47.6 (6.9)	56.5 (8.2)	64.8 (9.4)	71.7 (10.4)	84.8 (12.3)	97.2 (14.1)
	Negative Maneuver	6 700 (22 000)	-1.0g	112.4 (16.3)	129.6 (18.8)	121.3 (17.6)	112.4 (16.3)	194.4 (28.2)	182.0 (26.4)	168.2 (24.4)
	Cruise	10 700 (35 000)	+1.0g	133.8 (19.4)	133.8 (19.4)	142.0 (20.6)	151.0 (21.9)	200.6 (29.1)	213.0 (30.9)	226.1 (32.8)
	Emergency Landing	Sea Level	+9.0g[(1)]	47.6 (6.9)	–	–	–	157.2 (22.8)	157.2 (22.8)	157.2 (22.8)

(1) All values are limit vertical load factors (n_z) except for the emergency landing value which is an ultimate forward load factor (n_x).

(2) Operating pressures as specified in Table 6-2.

(3) $p_{Limit} = p_{op} + (n_z \rho h)$; where ρh = 9.51 kPa/g (1.38 psi/g) mid, 19.0 kPa/g (2.76 psi/g) bottom @ FS 2038, and 8.62 kPa/g (1.25 psi/g) mid, 17.2 kPa/g (2.50 psi/g) bottom @ FS 2123

(4) $p_{Ultimate} = 1.5 \times p_{Limit}$; except for emergency landing condition where $p_{ult} = 1.5 \times p_{op} + n_x \rho h$

TABLE 26. - POINT DESIGN INTERNAL LOAD ENVIRONMENT FOR AFT TANK

REGION	Flight Condition	Shell Dimensions: D cm (in.)	Shell Dimensions: h cm (in.)	Shear Flow (Limit)[1][2]: S_z kN (lbf.)	Shear Flow (Limit)[1][2]: q kN/m (lbf./in.)	Axial Force (Limit), N_x[1][2][3] — External Load: M_y MN-m, 10^6 (in-lb.)	External Load: N_x kN/m (lbf./in.)	Pressure Load: Top kN/m (lbf./in.)	Pressure Load: Mid kN/m (lbf./in.)	Pressure Load: Bottom kN/m (lbf./in.)	Net Load: Top kN/m (lbf./in.)	Net Load: Mid kN/m (lbf./in.)	Net Load: Bottom kN/m (lbf./in.)	Hoop Force (Limit), N_θ[5] — Pressure Load: Top kN/m (lbf./in.)	Pressure Load: Mid kN/m (lbf./in.)	Pressure Load: Bottom kN/m (lbf./in.)
FS 2038	PLA	460.2 (181.2)	411.5 (162.0)	-1 023 (-230×10^3)	157.3 (898)	6.418 (56.8)	±431.5 (±2 464)	129.2 (738)	157.1 (897)	184.1 (1 051)	560.8 (3 202)	157.1 (897)	-431.5 (-2 464)	258.7 (1 477)	314.2 (1 794)	368.1 (2 102)
	Pitch. Man.	460.2 (181.2)	411.5 (162.0)	-1 290 (-290×10^3)	198.2 (1 132)	6.418 (56.8)	±431.5 (±2 464)	54.8 (313)	65.8 (376)	76.9 (439)	486.3 (2 777)	65.8 (376)	-431.5 (-2 464)	109.4 (625)	131.7 (752)	153.9 (879)
	Neg. Man.	460.2 (181.2)	411.5 (162.0)	387.0 (87×10^3)	59.4 (339)	-1.932 (-17.1)	±129.9 (±742)	151.5 (865)	140.4 (802)	129.2 (738)	-129.9 (-742)	140.4 (802)	259.2 (1 480)	303.0 (1 730)	280.9 (1 604)	258.7 (1 477)
	Cruise	460.2 (181.2)	411.5 (162.0)	-516.0 (-116×10^3)	79.3 (453)	2.565 (22.7)	±172.5 (±985)	153.9 (879)	165.0 (942)	176.2 (1 006)	326.4 (1 864)	165.0 (942)	-172.5 (-985)	307.9 (1 758)	330.0 (1 884)	352.2 (2 011)
FS 2123	PLA	416.1 (163.8)	373.4 (147.0)	-889.6 (-200×10^3)	151.3 (864)	4.113 (36.4)	±337.1 (±1 925)	116.8 (667)	139.1 (794)	161.9 (925)	453.9 (2 592)	139.1 (794)	-337.1 (-1 925)	233.8 (1 335)	278.3 (1 589)	324.2 (1 851)
	Pitch. Man.	416.1 (163.8)	373.4 (147.0)	-978.6 (-220×10^3)	166.4 (950)	4.113 (36.4)	±337.1 (±1 925)	49.4 (282)	58.8 (336)	67.4 (385)	386.5 (2 207)	58.8 (336)	-337.1 (-1 925)	98.9 (565)	117.7 (672)	134.8 (770)
	Neg. Man.	416.1 (163.8)	373.4 (147.0)	293.6 (66×10^3)	49.9 (285)	-1.232 (-10.9)	±100.9 (±576)	134.8 (770)	126.3 (721)	116.8 (667)	-100.9 (-576)	126.3 (721)	217.7 (1 243)	270.0 (1 540)	252.4 (1 441)	233.8 (1 336)
	Cruise	416.1 (163.8)	373.4 (147.0)	-391.4 (-88×10^3)	66.5 (380)	1.638 (14.5)	±134.3 (±767)	139.1 (794)	147.8 (844)	157.1 (897)	273.4 (1 561)	147.8 (844)	-134.3 (-767)	278.3 (1 589)	295.4 (1 687)	314.2 (1 794)

(1)

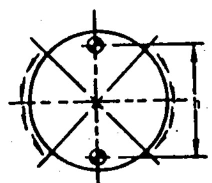

$q = \frac{S_z}{2x.707D}$ (side quadrants)

$N_x = \frac{4M_y}{h\pi D}$ (upper and lower quadrants)

$N_x = \frac{pD}{4}$ (all quadrants)

(2) $S_z = KS_z$ (Pitching Man.)

$M_y = KM_y$ (Pitching Man.)

where:

K = 0.30 Neg. Maneuver

K = 0.40 Cruise

(3) Sign Convention

Positive M = tension loads on upper fibers

Negative M = compression loads on upper fibers

(4) For maximum compressive load condition the tensile forces due to internal pressure are neglected.

(5) $N_\theta = pR$

TABLE 27. - MINIMUM SKIN THICKNESS REQUIREMENTS FOR AFT TANK

REGION	Tank Location	Operating(2)		Ultimate(3)		Burst(4)		Emergency(5) Landing		Minimum Wall Thickness	
		p kPa/(psi)	t cm (in.)(6)	p kPa/(psi)	t cm (in.)(6)	p kPa/(psi)	t cm (in.)	p kPa/(psi)	t cm (in.)	p kPa/(psi)	t cm (in.)
FS 2038	Top	133.8 (19.4)	0.262 (0.103)	200.6 (29.1)	0.267 (0.105)	267.5 (38.8)	0.160 (0.063)	238.6 (34.6)	0.142 (0.056)	–	0.127 (0.050)
	Mid	143.4 (20.8)	0.297 (0.117)	215.1 (31.2)	0.302 (0.119)	286.8 (41.6)	0.173 (0.068)	238.6 (34.6)	0.142 (0.056)	–	0.127 (0.050)
	Bottom	153.1 (22.2)	0.300 (0.118)	239.9 (34.8)	0.320 (0.126)	306.1 (44.4)	0.183 (0.072)	238.6 (34.6)	0.142 (0.056)	–	0.127 (0.050)
FS 2123	Top	133.8 (19.4)	0.236 (0.093)	200.6 (29.1)	0.241 (0.095)	267.5 (38.8)	0.145 (0.057)	157.2 (22.8)	0.084 (0.033)	–	0.127 (0.050)
	Mid	142.0 (20.6)	0.264 (0.104)	213.0 (30.9)	0.269 (0.106)	284.1 (41.2)	0.152 (0.060)	157.2 (22.8)	0.084 (0.033)	–	0.127 (0.050)
	Bottom	151.0 (21.9)	0.269 (0.106)	233.7 (33.9)	0.282 (0.111)	301.9 (43.8)	0.162 (0.064)	157.2 (22.8)	0.084 (0.033)	–	0.127 (0.050)

(1) Basic Equation

$t = \frac{pR}{F}$ p = design pressure
F = allowable stress
R = 230.1 cm (90.6 in.) at FS 2038
208.0 cm (81.9 in.) at FS 2123

(2) Operating condition, limit cruise pressures

F = 117 MPa (17 000 psi.) (Table 6-4.)

(3) Maximum ultimate design pressures

F = 172 MPa (25 000 psi.) (Table 6-4.)

(4) p_{Burst} = 2.0 x max. 1g pressures

$F = 0.90\ F_{tu} = 0.90 \times 427.47$ MPa = 384.7 MPa (55 800 psi.)

(5) Sea level pressures (Ult.) with 9.0g inertia load

$F = 0.90\ F_{tu}$ = 384.7 MPa (55 800 psi.)

(6) Mid panel thicknesses based on principal stress theory.

TABLE 28. - FAIL-SAFE REQUIREMENTS OF AFT TANK, CIRCUMFERENTIAL DAMAGE CONDITION

REGION	Location	Applied Loads (Limit) Cond	Applied Loads (Limit) N_x kN/m (lbf/in.)	Applied Loads (Limit) q kN/m (lbf/in.)	Skin Thickness t_s cm (in.)	Strap Spacing b cm (in.)	Crack Length $\ell = 2b$ cm (in.)	Strap Area A_e cm^2 (in^2)	$\frac{2A_e}{t_s}$ cm (in.)	Reinf. Efficiency γ	Residual Strength F_g MPa (ksi)	$\bar{t}_{min.}$ cm (in.)
FS 2038	Top	PLA	560.8	–	1.17 (0.462)	–	30.5 (12.0)	–	–	1.00	47.78 (6.93)	1.170 (0.462)
			(3 202)		0.267 (0.105)	15.24 (6.00)	30.5 (12.0)	1.935 (0.30)	14.5 (5.71)	1.67	79.98 (11.6)	0.701 (0.276)
	Mid	Cruise	164.9	79.33	0.411 (0.162)	–	30.5 (12.0)	–	–	1.00	47.78 (6.93)	0.411 (0.162)
			(942)	(453)	0.302 (0.119)	–	30.5 (12.0)	–	–	1.00	47.78 (6.93)	0.495 (0.195)
	Bottom	Neg.	259.2	–	0.541 (0.213)	–	30.5 (12.0)	–	–	1.00	47.78 (6.93)	0.541 (0.213)
		Man.	(1 480)		0.320 (0.126)	15.24 (6.0)	30.5 (12.0)	1.290 (0.20)	8.05 (3.17)	1.53	73.08 (10.6)	0.404 (0.159)
FS 2123	Top	PLA	453.9	–	0.950 (0.374)	–	30.5 (12.0)	–	–	1.00	47.78 (6.93)	0.950 (0.374)
			(2 592)		0.241 (0.095)	15.24 (6.0)	30.5 (12.0)	1.935 (0.30)	16.0 (6.3)	1.71	81.70 (11.85)	0.556 (0.219)
	Mid	Cruise	147.8	66.55	0.363 (0.143)	–	30.5 (12.0)	–	–	1.00	47.78 (6.93)	0.363 (0.143)
			(844)	(380)	0.269 (0.106)	–	30.5 (12.0)	–	–	1.00	47.78 (6.93)	0.424 (0.167)
	Bottom	Neg.	217.7	–	0.455 (0.179)	–	30.5 (12.0)	–	–	1.00	47.78 (6.93)	0.455 (0.179)
		Man.	(1 243)		0.282 (0.111)	15.24 (6.0)	30.5 (12.0)	1.290 (0.20)	9.14 (3.6)	1.56	74.46 (10.8)	0.366 (0.144)

(1) $F_g = \frac{\gamma}{2} \frac{K_0}{\sqrt{\ell}}$

where:

γ = Reinforcement Efficiency

= 1.0 for no strap condition

K_0 = Stress intensity factor, 52 700 kPa $\sqrt{m}$, 48 000 psi $\sqrt{in}$

ℓ = Crack length

(2) $\bar{t}_{min.}$ = Maximum value of thickness required to satisfy:

f (principal) = F_g

or

$t_s + (\frac{A_e}{b})$ min

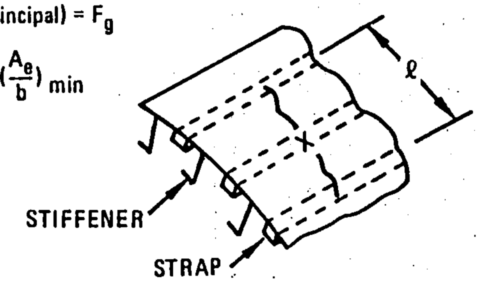

critical design conditions. Minimum axial extensional thicnkesses were defined using the skin thicknesses (t_s) from the prior membrane analysis and for an unstiffened panel configuration (i.e., pure monocoque wall). The upper row at each location on this table reflects the latter condition. Axial extensional thicknesses (including the equivalent thickness of the fail-safe straps) ranging from 0.404 cm (0.159 in.) to 0.701 cm (0.276 in.) were defined for the stiffened wall concept at FS 2038. The corresponding values at FS 2123 were 0.365 cm (0.144 in.) to 0.556 cm (0.219 in.)

Using the cross-sectional data resulting from the prior membrane and fail-safe analyses, the strength requirements were evaluated and are presented in table 29. The top and bottom of the shell were analyzed for their maximum tension and compression conditions using the equations referenced in the footnotes of this table. For the compression analysis, both general and local instability (reference 14) failure modes were investigated; whereas, for the tension condition, an ultimate gross area fatigue allowable of 310.3 MPa (45 000 psi) was used.

The mid-panels were analyzed for the maximum combined stress and shear instability failure modes which are described in the footnotes of table 29. The maximum principal stress for the combined stress state was defined and compared to the ultimate gross area fatigue allowable. For the shear analyses, the general instability stresses were based on simply supported, orthotropic plate theory described in reference 15. The local shear instability stress was based on the failure of the skin between the stiffeners with simply supported, infinitely long plate theory used, reference 13.

All cross-sectional properties as defined for the shell by the previous fail-safe analysis (table 28) were sufficiently strong and met the strength requirements. The exception being the bottom of the shell at both point design regions which required additional material to sustain the applied loads.

5.2.2.2 Frames.- Representative sheet metal frames were sized for application to the aft methane tank. Typical frame designs were evaluated for strength, stiffness, and damage tolerance (i.e., ability to arrest a longitudinal crack in the tank wall). A frame spacing of 108.7 cm (42.8 in.), four equal increments between the tank forward and aft closures, was preselected based on the results of the hydrogen tank study, reference 4. This referenced study indicated that a minimum-weight design integral tank results at frame spacings in the vicinity of 127 cm (50.0 in.).

TABLE 29. - SHELL STRENGTH REQUIREMENTS OF AFT TANK

REGION	Location	Thickness Data				Cond.	Applied Stresses (Ult)(1)				Tension Analysis(2)			Compression Analysis(3)					Shear Analysis(4)						
		t_{Skin} cm (in.)	$\bar{t}_{Strap}$ cm (in.)	$\bar{t}_{Stiff}$ cm (in.)	$\bar{t}_{Total}$ cm (in.)		N_x kN/m (lbf/in)	q kN/m (lbf/in.)	f_x MPa (ksi)	f_{xy} MPa (ksi)	f_p MPa (ksi)	F_t MPa (ksi)	M.S.	(L/ρ)	F_{col} MPa (ksi)	K_c	F_{cc} MPa (ksi)	M.S.	D_1 kN-m (lbf-in)	D_2 kN-m (lbf-in)	$F_{xy,cr}$ MPa (ksi)	(b/t)	K_s	$F_{xy,cc}$ MPa (ksi)	M.S.
FS 2038	Top	0.267 (0.105)	0.127 (0.050)	0.307 (0.121)	0.701 (0.276)	Neg. Man.	-194.9 (-1 113)	–	-27.6 (-4.0)	–	–	–	–	55.8	-235.1 (-34.1)	5.0^+	-101.4 (-14.7)	+ Large	–	–	–	–	–	–	–
						PLA	841.1 (4 803)	–	119.3 (17.3)	–	119.3 (17.3)	310.3 (45.0)	+ Large	–	–	–	–	–	–	–	–	–	–	–	–
	Mid	0.302 (0.119)	–	0.193 (0.076)	0.495 (0.195)	Pitch. Man.	98.8 (564)	297.4 (1 698)	19.99 (2.9)	98.60 (14.3)	108.9 (15.8)	310.3 (45.0)	+ Large	–	–	–	–	–	0.185 (1.64×10^3)	86.60 (766.5×10^3)	170.3 (24.7)	51.7	4.84	112.4 (16.3)	+0.14
						Cruise	247.4 (1 413)	119.1 (680)	49.99 (7.25)	39.3 (5.7)	71.71 (10.4)	310.3 (45.0)	+ Large	–	–	–	–	–	–	–	–	–	–	–	–
	Bottom	0.320 (0.126)	0.084 (0.033)	0.096 (0.038)	0.500 (0.197)	Neg. Man.	388.8 (2 220)	–	77.91 (11.3)	–	77.91 (11.3)	310.3 (45.0)	+ Large	–	–	–	–	–	–	–	–	–	–	–	–
						PLA	-647.3 (-3 696)	–	-129.6 (-18.8)	–	–	–	–	68.0	-154.4 (-22.4)	4.5	-131.7 (-19.1)	+0.02	–	–	–	–	–	–	–
FS 2123	Top	0.241 (0.095)	0.127 (0.050)	0.188 (0.074)	0.556 (0.218	Neg. Man.	-151.3 (-864)	–	-26.89 (-3.9)	–	–	–	–	56.2	-234.4 (-34.0)	5.0^+	-84.81 (-12.3)	+ Large	–	–	–	–	–	–	–
						PLA	680.9 (3 888)	–	122.7 (17.8)	–	122.7 (17.8)	310.3 (45.0)	+ Large	–	–	–	–	–	–	–	–	–	–	–	–
	Mid	0.269 (0.106)	–	0.155 (0.061)	0.424 (0.167)	Pitch. Man.	88.3 (504)	249.6 (1 425)	20.68 (3.0)	92.39 (13.4)	103.4 (15.0)	310.3 (45.0)	+ Large	–	–	–	–	–	0.131 (1.16×10^3)	74.74 (661.5×10^3)	156.5 (22.7)	56.6	4.84	100.7 (14.6)	+0.09
						Cruise	221.7 (1 266)	99.8 (570)	52 26 (7.58)	37.23 (5.4)	71.71 (10.4)	310.3 (45.0)	+ Large	–	–	–	–	–	–	–	–	–	–	–	–
	Bottom	0.282 (0.111)	0.084 (0.033)	0.096 (0.038)	0.462 (0.182)	Neg. Man.	326.6 (1 865)	–	70.33 (10.2)	–	70.33 (10.2)	310.3 (45.0)	+ Large	–	–	–	–	–	–	–	–	–	–	–	–
						PLA	505.8 (-2 888)	–	-109.6 (-15.9)	–	–	–	–	66.0	-164.1 (-23.8)	4.8	-108.9 (-15.8)	+0.00	–	–	–	–	–	–	–

(1) Applied stresses (ultimate)

$f_x = N_x/\bar{t}_{Total}$; $f_{xy} = q/t_s$

(2) Tension Analysis

Maximum Principal Stress $(f_p) = (f_x/2) + \sqrt{(f_x/2)^2 + f_{xy}^2}$

Allowable Gross Area Tension Stress (F_t) = 310.3 MPa (45 ksi)

Margin of Safety (M.S.) = $(F_t/f_p) - 1.0$

(3) Compression Analysis

Column Allowable $(F_{col}) = \pi^2 E/(L/\rho)^2$

where:

E = Modulus of Elasticity = 72.39 GPa (10.5 x 10^6 psi)

L/ρ = Slenderness ratio

Local Instability (Reference 7)

$$F_{cc} = \frac{K_c \pi^2 E}{12(1-\nu_e^2)} \left(\frac{t_s}{b_s}\right)^2$$

where:

K_c = Compressive buckling coefficient, per Figure 6-14 of the Reference

ν = 0.32, Poisson's ratio (elastic)

t_s = Skin thickness, in.

b_s = Stiffener spacing, 15.24 cm (6.00 in.)

(4) Shear Analysis

General Instability – Simply supported orthotropic plate (Reference 8)

$$F_{xy,cr} = \frac{32.6}{t_s} (D_1 D_2^3)^{1/4}/L^2$$

where:

D_1, D_2 = Bending stiffnesses, kN-m

L = Frame Spacing, 1.087 m (42.8 in.)

Local Instability – Simply supported, infinitely long plate (Reference 6)

$$F_{xy} = K_s E \left(\frac{t_s}{b_s}\right)^2$$

where:

K_s = 4.84

The frame stiffness requirements were predicated on the criterion developed by Shanley in reference 16, which ensures failure of the skin-stringer panel between frames. The required frame bending stiffness (EI) and the corresponding section properties and equivalent thickness of a typical frame are shown in table 30. In addition, the critical design condition and the shell diameter used in the calculation are included.

The strength requirement of the frames was conservatively postulated on the frames carrying 20 percent of the hoop force of the shell. Using this force and the circumferential design stress for the tank substructure, table 19 of the criteria section, the area requirements were defined and are shown in table 31. The frame cross sectional area was assumed to be circumferentially invariant with the most critical bottom location designing the complete frame. The PLA condition at this location results in frame forces of 120.1 kN 927 000 lbf) and 105.9 kN 923 800 lbf) at FS 2038 and FS 2123, respectively.

The fail-safe criteria for a longitudinal crack damage case impose minimum area requirements on the frames and the necessity for fail-safe straps in the hoop direction. Table 32 presents a summary of the fail-safe analysis conducted during this study. The theory used for this analysis is equivalent to that used on the hydrogen tank study and is presented in reference 11. The basic equation and the therminology used in defining the effective reinforcement area (A_e) of the straps and frames are displayed in the footnotes on table 32. The determination of the effective area of the frame is based on the damage occurring in the skin adjacent to the frame; whereas, the strap area is predicted on the damage occurring at the frame or at a strap (for multiple strap configurations) with the adjacent strap arresting the crack. With reference to table 32, strap spacings from 15.2 cm (6.00 in.) to 36.3 cm (14.3 in.), two straps between frames, were investigated at the two point design regions. Frame area requirements increased as the number of fail-safe straps decreased, whereas, the strap area requirements are fairly insensitive to their spacing. Based on these results, three straps per bay were selected as typical and used in the design.

Table 33 summarizes the frame area requirements due to stability, strength, fail-safe, and minimum gage. The effective thickness of the minimum gage frame reflects the proportions of the typical frame shown in the footnotes of table 30 with a thickness of 0.127 cm (0.050 in.). In addition, the area and effective thickness of the hoop fail-safe straps are shown for the selected spacing. Note that the strength and fail-safe requirements for the frames are identical.

TABLE 30. - FRAME STIFFNESS REQUIREMENTS FOR AFT TANK

Region	Design Condition: Cond.	Design Condition: Mult MN · m (in.-lbf)	Shell Dia., D cm (in.)	Frame Spacing L cm (in.)	$(EI)_f$ MN · cm² (lbf-in.)	I_f cm⁴ (in.⁴)	A_f cm² (in.²)	$\bar{t}_f$ cm (in.)
FS 2038	PLA	9.626 (85.2×10^6)	460.2 (181.2)	108.7 (42.8)	2.820 (4.09×10^6)	16.23 (0.390)	1.68 (0.26)	0.015 (0.006)
FS 2123	PLA	6.169 (54.6×10^6)	416.1 (163.8)	108.7 (42.8)	1.475 (2.14×10^6)	8.49 (0.204)	0.90 (0.14)	0.008 (0.003)

TYPICAL FRAME DIMENSIONS

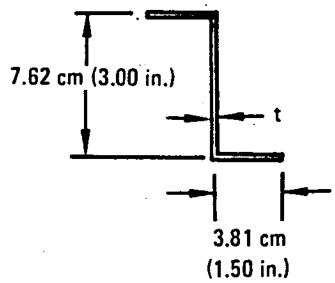

$$(EI)_f = C_f \frac{MD^2}{L}$$

where:

$C_f = 6.25 \times 10^{-5}$ (per Reference 9)

$E = 72.39\ GN/m^2$ (10.5×10^6 psi.)

$A = 6.0t = 0.66I$

$I = 9.0t = 1.50A$

$\bar{t} = \frac{A_f}{L}$

TABLE 31. - FRAME STRENGTH REQUIREMENTS FOR AFT TANK

Region	Design Condition (Ult.): Cond.	Design Condition (Ult.): N_θ kN/m (lbf/in.)	Frame Spacing L cm (in.)	P_f kN (lbf)	A_f cm² (in²)	$\bar{t}_f$ cm (in.)
FS 2038	PLA	552.2 (3 153)	108.7 (42.8)	120.13 (27 007)	4.35 (0.675)	0.041 (0.016)
FS 2123	PLA	486.3 (2 777)	108.7 (42.8)	105.72 (23 766)	3.83 (0.594)	0.036 (0.014)

$P_f = .20\ N_\theta \times L$ (frame force = 20% of membrane force)

$A_f = \frac{P_f}{F}$ where:

F = Substructure Circumferential Design Stress, 276 MPa (40 ksi.)

$\bar{t}_f = \frac{A_f}{L}$

TABLE 32. - FRAME AND HOOP STRAP FAIL-SAFE REQUIREMENTS FOR AFT TANK

REGION	Design Condition		Skin Thick t_s cm (in.)	f_0 (Limit) MPa (psi.)	Frame Spacing L cm (in.)	Straps		Crack Length $\ell = 2b$ cm (in.)	A_e cm^2 (in^2)	Strap Requirement		Frame Requirement	
	Cond.	N_0 (Limit) kN/m (lbf/in.)				No.	Spacing b cm (in.)			A_s cm^2 $(in.^2)$	$\bar{t}_s$ cm (in.)	A_f cm^2 (in^2)	$\bar{t}_f$ cm (in.)
FS 2038	PLA	368.1 (2 102)	0.320 (0.126)	115.0 (16 680)	108.7 (42.8)	6	15.52 (6.11)	31.04 (12.22)	0.606 (0.094)	0.606 (0.094)	0.033 (0.013)	1.497 (0.232)	0.018 (0.007)
	PLA	368.1 (2 102	0.320 (0.126)	115.0 16 680)	108.7 (42.8)	4	21.74 (8.56)	43.48 (17.12)	1.077 (0.167)	1.077 (0.167)	0.041 (0.016)	3.232 (0.501)	0.030 (0.012)
	PLA	368.1 (2 102)	0.320 (0.126)	115.0 (16 680)	108.7 (42.8)	3	27.18 (10.70)	54.36 (21.40)	1.490 (0.231)	1.490 (0.231)	0.041 (0.016)	4.471 (0.693)	0.041 (0.016)
	PLA	368.1 (2 102)	0.320 (0.126)	115.0 (16 680)	108.7 (42.8)	2	36.24 (14.27)	72.49 (28.54)	2.174 (0.337)	2.174 (0.337)	0.041 (0.016)	6.522 (1.011)	0.061 (0.024)
FS 2123	PLA	324.2 (1 851)	0.282 (0.111)	115.0 (16 680)	108.7 (42.8)	6	15.52 (6.11)	31.04 (12.22)	0.535 (0.083)	0.535 (0.083)	0.030 (0.012)	1.606 (0.249)	0.015 (0.006)
	PLA	324.2 (1 851)	0.282 (0.111)	115.0 (16 680)	108.7 (42.8)	4	21.74 (8.56)	43.48 (17.12)	0.948 (0.147)	0.948 (0.147)	0.036 (0.014)	2.845 (0.441)	0.025 (0.010)
	PLA	324.2 (1 851)	0.282 (0.111)	115.0 (16 680)	108.7 (42.8)	3	27.18 (10.70)	54.36 (21.40)	1.316 (0.204)	1.316 (0.204)	0.036 (0.014)	3.948 (0.612)	0.036 (0.014
	PLA	324.2 (1 851)	0.282 (0.111)	115.0 (16 680)	108.7 (42.8)	2	36.24 (14.27)	72.49 (28.54)	1.916 (0.297)	1.916 (0.297)	0.036 (0.014)	5.748 (0.891)	0.053 (0.021)

$$F_{pg} = f_0 = 1.20F_{tu} \left(\frac{2We + \Sigma \frac{A_e}{t_s}}{C_1\ell + 2We} \right) \text{ or rearranging } A_e = \left(\frac{t_s}{2}\right)\left[\frac{f_0}{1.20\,F_{tu}}(C_1\ell + 2We) - 2We\right]$$

(Reference 4)

where:

- $2We$ = An effective width parameter = 1.80
- ℓ = Total crack length, $\ell = 2b$
- F_{tu} = Ultimate tensile strength of the skin material
- C_1 = Longitudinal crack extension parameter for pressurized fuselage panel. A function of the stress intensity factor K_0. $C_1 = 1.055$
- A_e = Effective reinforcement area
- t_s = Skin thickness
- $A_s = A_e = \frac{A_f}{3}$
- $\bar{t}_s = \frac{nA_s}{L}$; $\bar{t}_f = \frac{A_f}{L}$

TABLE 33. - SUMMARY OF THE FRAME AND HOOP STRAP REQUIREMENTS FOR AFT TANK

Region	Strap Requirements			Frame Requirements					
	b cm (in.)	As cm^2 ($in.^2$)	$\bar{t}$ cm (in.)	L cm (in.)	$\bar{t}_{Stab}$ cm (in.)	$\bar{t}_{Str.}$ cm (in.)	$\bar{t}_{FS}$ cm (in.)	$\bar{t}_{Min.}$ cm (in.)	$\bar{t}_{Final}$ cm (in.)
ES 2038	27.18 (10.70)	1.490 (0.231)	0.041 (0.016)	108.7 (42.8)	0.015 (0.006)	0.041 (0.016)	0.041 (0.016)	0.018 (0.007)	0.041 (0.016)
FS 2123	27.18 (10.70)	1.316 (0.204)	0.036 (0.014)	108.7 (42.8)	0.008 (0.003)	0.036 (0.014)	0.036 (0.014)	0.018 (0.007)	0.036 (0.014)

5.3 Final Design

The general design of the aft tank is shown in figure 50. The design of the major structural components of this tank are similar to the integral tank designs of the hydrogen tank study.

The basic shell is conical in configuration with an integrally stiffened wall and supported by internal frames. Elliptical heads of monocoque construction are provided for the forward and aft closures, and the tank divider. The tank is a weldment using 2219 aluminum alloy shapes. The shell incorporates a zee-stiffened wall configuration at the maximum axially loaded upper and lower quadrants with a blade-stiffened configuration being used at the side walls. The skin and stiffener thicknesses vary in the longitudinal direction but are constant in each of the circumferential quadrants. The stiffener pitch and height were held constant at respective values of 15.24 cm (6.00 in.) and 5.08 cm (2.00 in.) for the entire tank.

Damage tolerance capability is provided by adding both longitudinal and circumferential straps to the design. For the circumferential damage case (cracks running in the hoop direction), longitudinal straps are provided between the stiffeners on the upper and lower quadrants of the tank. These straps were spot welded to the shell and have a constant cross-sectional area for each quadrant. The blade-stiffened sidewall panels do not require any straps for this damage case. For the longitudinal damage case, circumferential straps having a constant cross-sectional area of 1.48 cm^2 (0.23 $in.^2$) and a spacing of 27.18 cm (10.70 in.) are provided on the exterior surface of the tank between the internal frames. Internal frames are provided at a spacing of approximately 108.7 cm (42.8 in.). These frames will be fabricated using 2219-T8511 aluminum extrusions with an area of approximately 4.13 cm^2 (0.64 $in.^2$).

6. FUEL SYSTEM

The functional requirements for the fuel system in a methane-fueled airplane are similar in most respects to those of a hydrogen-fueled airplane. Both fuels are cryogens requiring extensive use of insulation for fuel storage and plumbing. Both fuels vaporize readily when exposed to ambient pressures and temperatures encountered by aircraft and become lighter than air at temperatures well below flight ambient. Systems using these fuels require identical treatment for maintenance to preclude ice formation on components and to protect personnel from frostbite when routine hardware repair is necessary. The purpose of this section is to describe the physical characteristics of the fuel system for a methane-fueled subsonic jet transport.

6.1 Fuel-Oriented Functions

The aircraft fuel system consists of all fuel-oriented functions up to the interface with the engine-supplied fuel system. They are illustrated schematically in figure 51 and perform the following functions:

- Fuel storage
- Aircraft fueling and defueling
- Engine fuel supply
- Auxiliary power unit fuel supply
- Fuel transfer
- Fuel management for center of gravity control
- Fuel jettison
- Fuel tank venting and pressurization
- Fuel leak detection and vapor purge

Each of these systems is discussed in the following paragraphs.

6.1.1 Fuel storage.- Fuel is stored in four thermally insulated tanks within the fuselage, figure 10. Each tank is numbered from 1 to 4 corresponding to the engine it normally supplies fuel according to the convention that each engine be fed from an independent source during takeoff and landing. Tanks 1 and 2 form a sphere located between the flight station and the forward end of the passenger compartment. Tank 1 constitutes the left hemisphere which is separated from Tank 2, the right hemisphere, by means of a fore and aft diaphragm. Tanks 3 and 4, which have the form of a modified truncated cone, are located behind the passenger compartment and are separated by a lateral diaphragm. Each tank has a nominal usable fuel capacity of 18 140 kg (40 000 lb) of liquid methane.

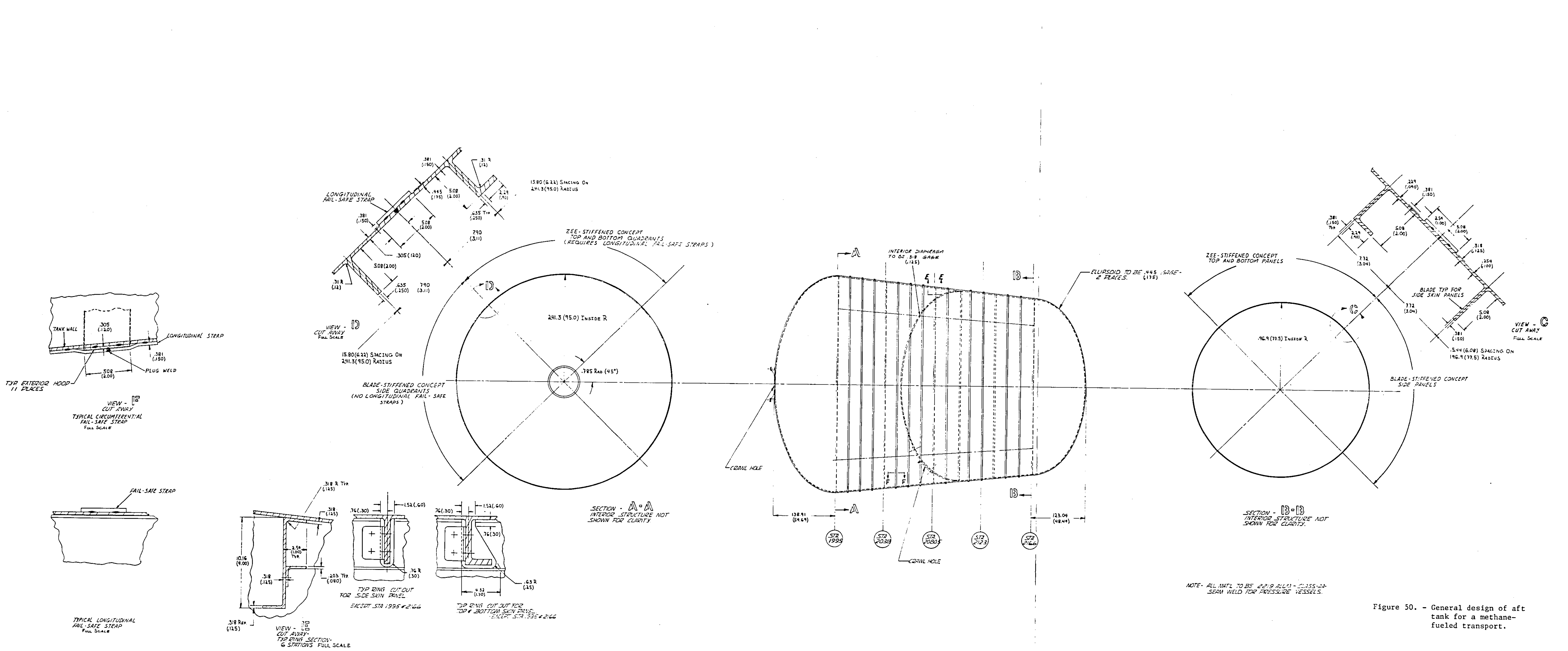

Figure 50. - General design of aft tank for a methane-fueled transport.

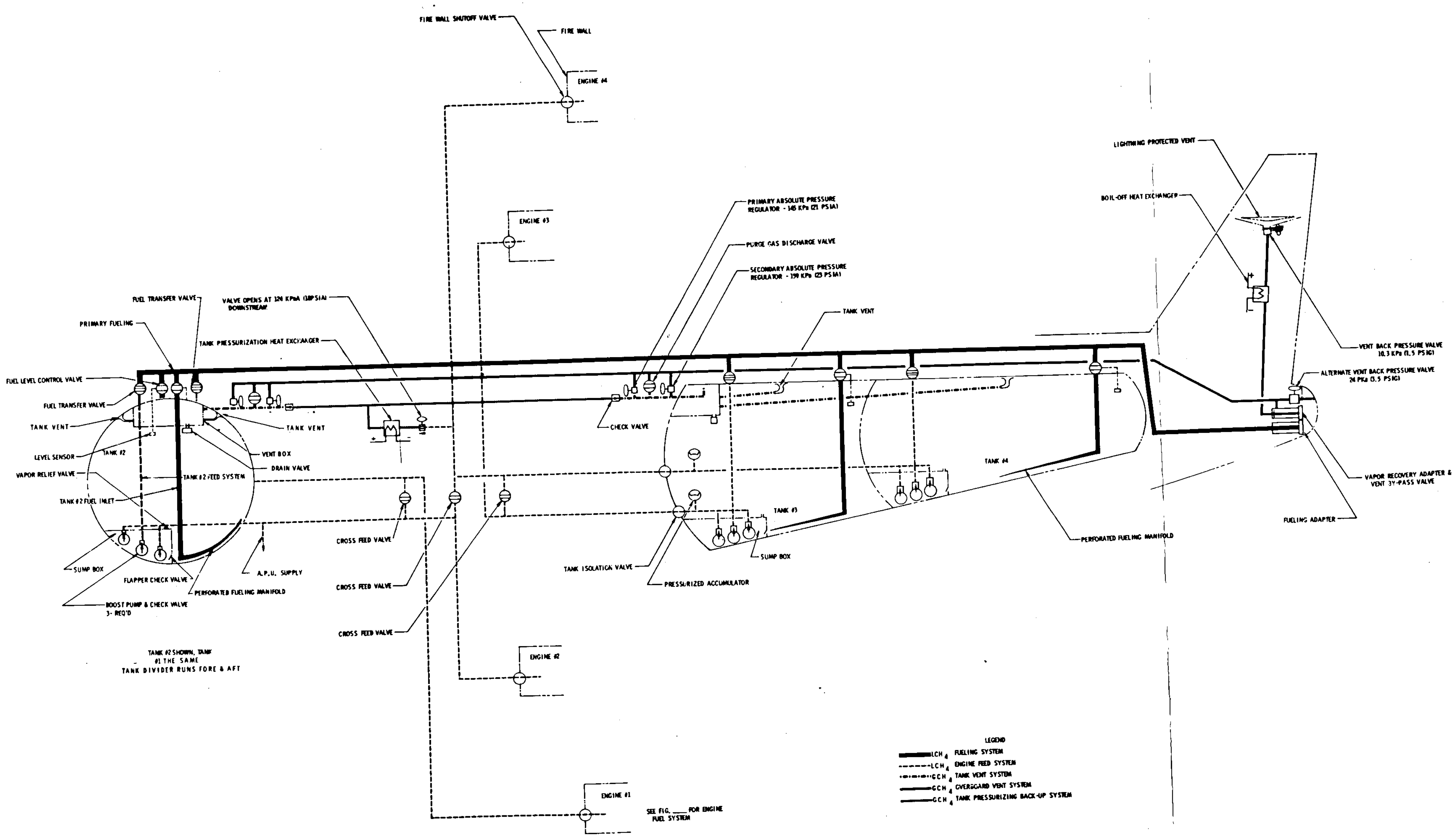

Figure 51. - Fuel system schematic.

The diaphragms separating Tanks 1 and 2 and Tanks 3 and 4 are designed to meet emergency landing condition loads as defined in Paragraph 25.561 of the Federal Aviation Regulations for Transport Category Aircraft. They provide physical separation of the fuel in each compartment but are vented to permit pressure equalization in adjoining tanks.

6.1.2 Fueling and defueling.- The aircraft fueling system interfaces with the airport ground supply through two adapters located at the aft end of the fuselage below the vertical tail, figure 52. One of the adapters receives liquid fuel from the ground supply and the other, the vapor recovery adapter, returns displaced methane gas from the aircraft fuel tanks to the airport liquefaction facility for recycling. The adapters interface with the ground facilities by means of ground fueling and vapor recovery quick disconnects.

The fueling manifold is sized to permit fueling the tanks in 20 minutes from a 15 percent reserve quantity to a nominal total capacity of 72 560 kg (160 000 lb) when the supply pressure at the aircraft interface is 193 kPa (28 psia). This requires a nominally sized 10.16 cm (4 in.) diaphragm fueling manifold extending from the fueling adapter to a wye at the forward fuel tanks. Fuel is conveyed by 5.08 cm (2 in.) lines from the manifold to a point in each tank below the normal reserve fuel level where it is discharged through a series of perforations in the line. The perforations are sized to maintain a low discharge velocity to minimize turbulence in the bulk liquid.

The fuel level control system consists of a shutoff valve actuated by a signal from a level sensor which terminates flow to each tank when it is full. When a given flight requires less than full tanks, the shutoff valves are actuated by a signal initiated by "bugs" on the tank fuel quantity indicators which have previously been set at the desired quantity. The fuel quantity indicators are located in the aircraft fueling panel, figure 53.

Vapor displaced during the fueling operation flows through absolute tank pressure regulators into a common vent line where it is diverted to the vapor recovery adaptor by means of a vent bypass valve built into the adapter and operated by the actuating linkage of the adapter. The absolute pressure regulators prevent flashing of the fuel by maintaining the tank pressure above the saturation pressure of the delivered fuel. The vent lines are sized to accept liquid methane overflow to the vapor recovery adapter without subjecting the tanks to excessive overpressurization in the event that a tank fueling shutoff valve fails to close when the tank is full.

Defueling will be required on very infrequent occasions; e.g., when the tanks must be entered to perform inspection on repair. Defueling is accomplished with both fueling and vapor recovery adapters connected to the airport defueling facility. The fuel transfer and refueling line tank isolation valves are then opened and the fuel level control valves are closed. Operation of the tank boost pumps will start the defueling operation. To maintain tank pressure above outside ambient, some heat may have to be added to the stored methane by means of the fuselage-mounted tank pressurization heat exchanger

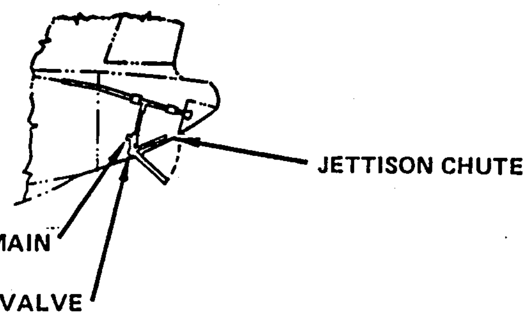

JETTISON ARRANGEMENT
(OPTIONAL)

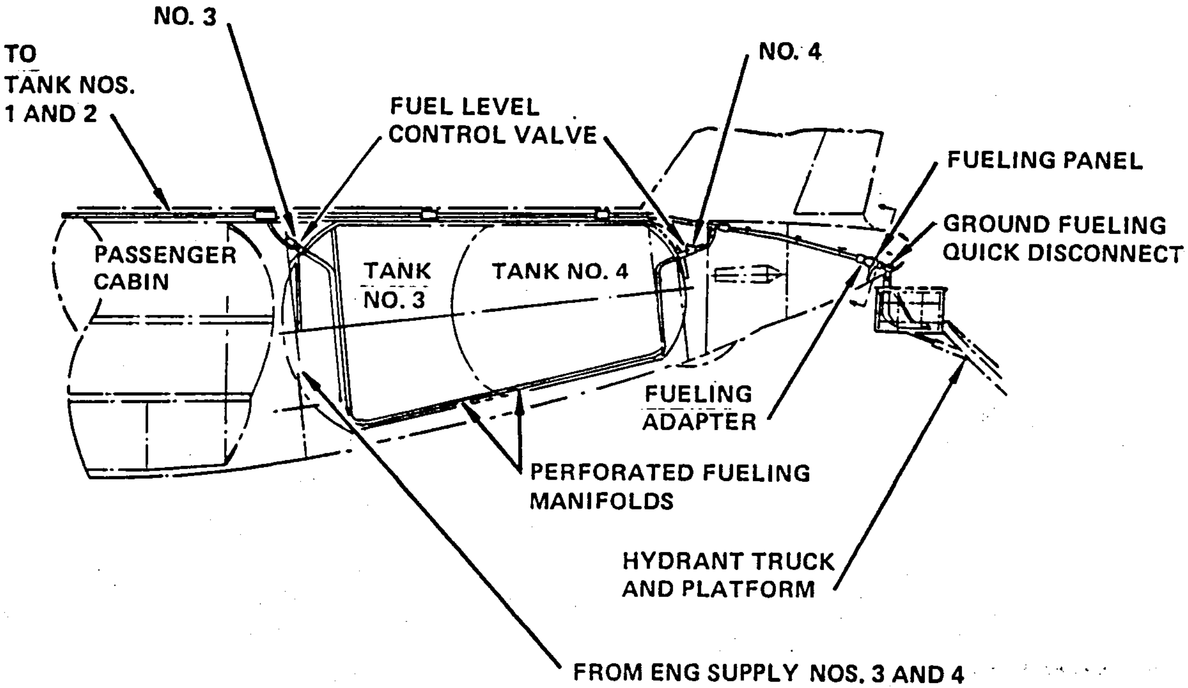

Figure 52. - Layout-fueling/defuel system.

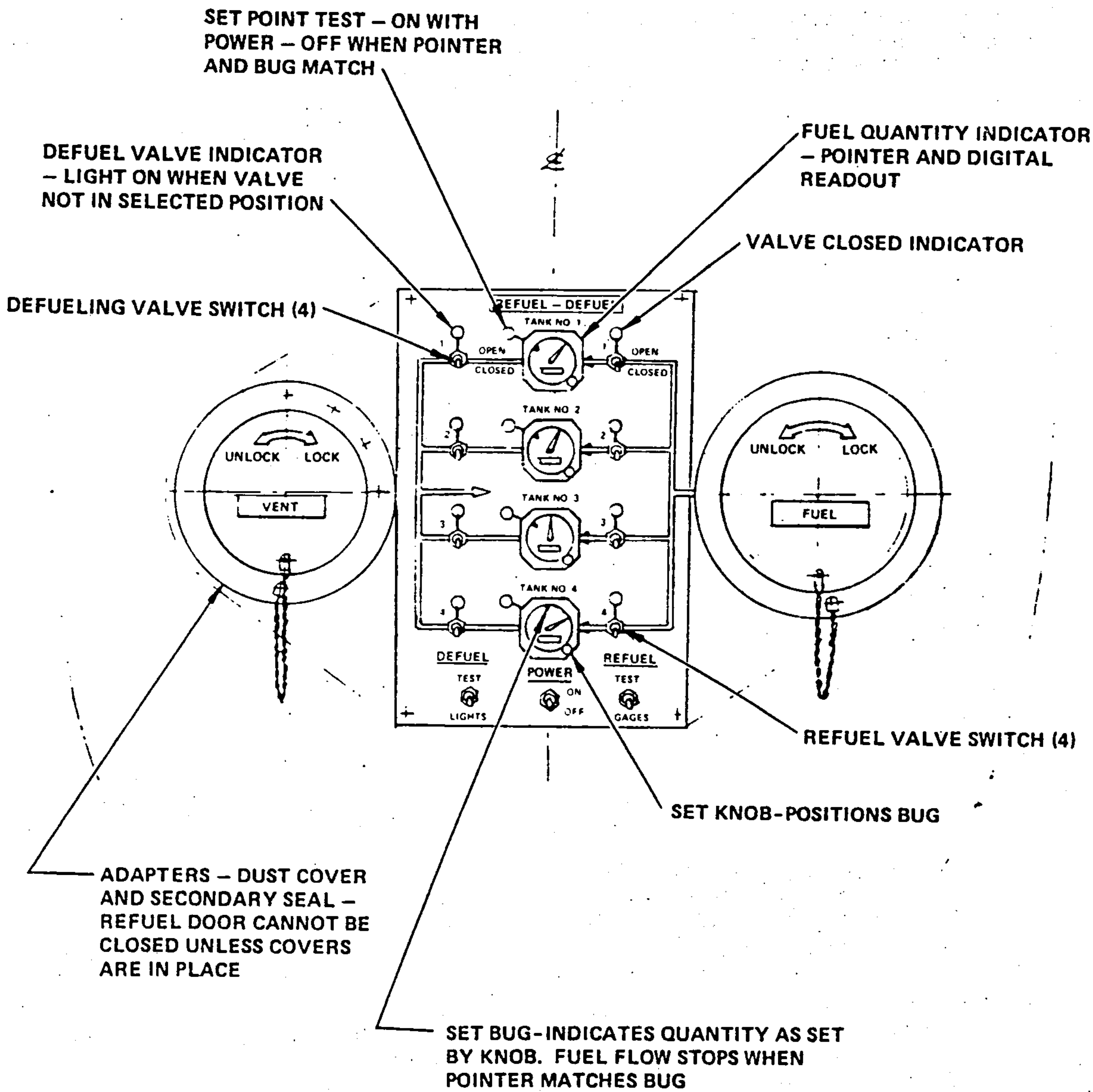

Figure 53. - Refuel panel.

which utilizes a calrod heating element to convert liquid methane to gas. The tanks may be defueled individually or simultaneously.

Those components exposed to liquid methane during fueling and defueling operations are shown installed in figure 52. The ground fueling disconnects are illustrated in figure 54 and the fuel level control shutoff valve in figures 55 and 56. The design requirements for these components are discussed at the end of this section.

6.1.3 Engine fuel supply.- Each engine is normally supplied fuel from its identically numbered fuel tank by opening the tank isolation valve, figure 57, and turning on tank-mounted fuel boost pumps. In the event of engine failure, fuel from the tank which normally supplies the failed engine can be made available to the operating engines by a crossfeed system. A significant feature is the location and arrangement of the crossfeed valves, figure 58. They are contained in one assembly for convenience in servicing and also to preclude long sections of transfer lines which would contain vapor and which, in turn, could result in engine flameout when switching from direct to crossfeed.

Lines leading to the engines are located in the wing box for protection and isolation. The lines are foam insulated within a protecting metal outer tube as shown in figure 59. Evacuated double bellows lines with an outer braided cover are used where required for flexibility.

A surge box located at the low point in each fuel tank houses three boost pumps which supply fuel to each engine, figure 60. The surge box traps fuel in the vicinity of the pumps to minimize unusable fuel, and to ensure its availability during unusual transient maneuvers. The design uses a pressurized accumulator downstream of the pump check valves to preclude engine starvation if the fuel migrates to the top of the surge box during negative or zero g flight.

The design philosophy for the boost pump system is based upon the premise that a single pump failure shall not compromise aircraft safety. In addition, airline operators are reluctant to ground an aircraft if one boost pump in any of its fuel tanks is incapable of being operated. In accordance with this philosophy, each tank in the methane-fueled subsonic transport will incorporate a minimum of three boost pumps. The justification for this conclusion is discussed in the following paragraphs.

Although hydrocarbon-fueled aircraft can take off and climb to cruise altitudes with boost pumps inoperative most of the time, methane-fueled aircraft engines would flame out if the boost pumps failed, due to vaporization in the line with loss of pressure. Hence, the boost pump system must entail a redundancy which precludes loss of thrust from any engine in the event of pump failure immediately after the aircraft becomes airborne. During takeoff and initial climb, this philosophy dictates that one tank supplies one engine, and that two pumps in each tank must be operated simultaneously. Thus, with two pumps operating, a single boost pump failure just after takeoff could not cause a loss of engine thrust. The redundance requirement further dictates that no two pumps within a given fuel tank can be supplied electrical power from the same source.

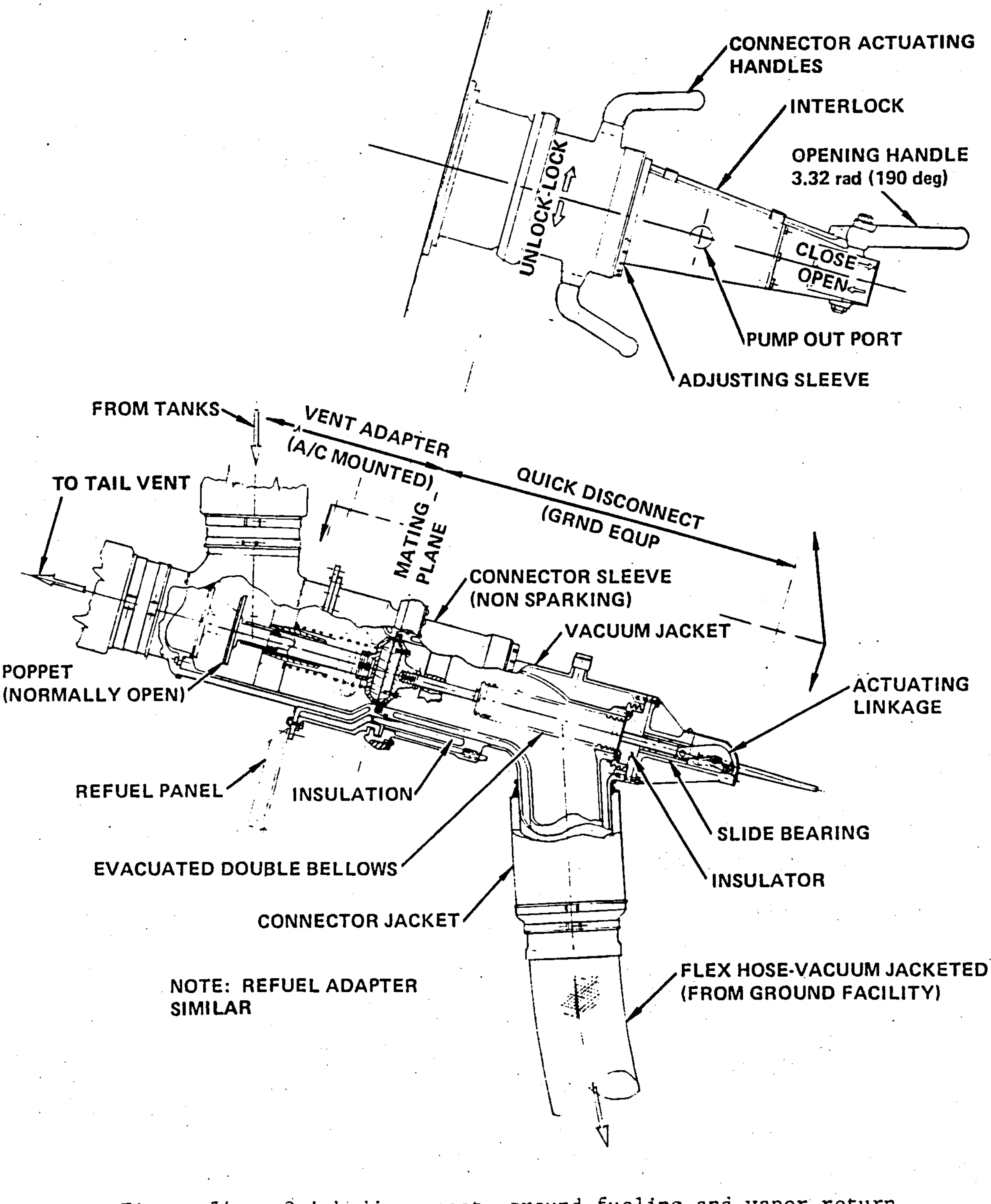

Figure 54. - Quick disconnect, ground fueling and vapor return.

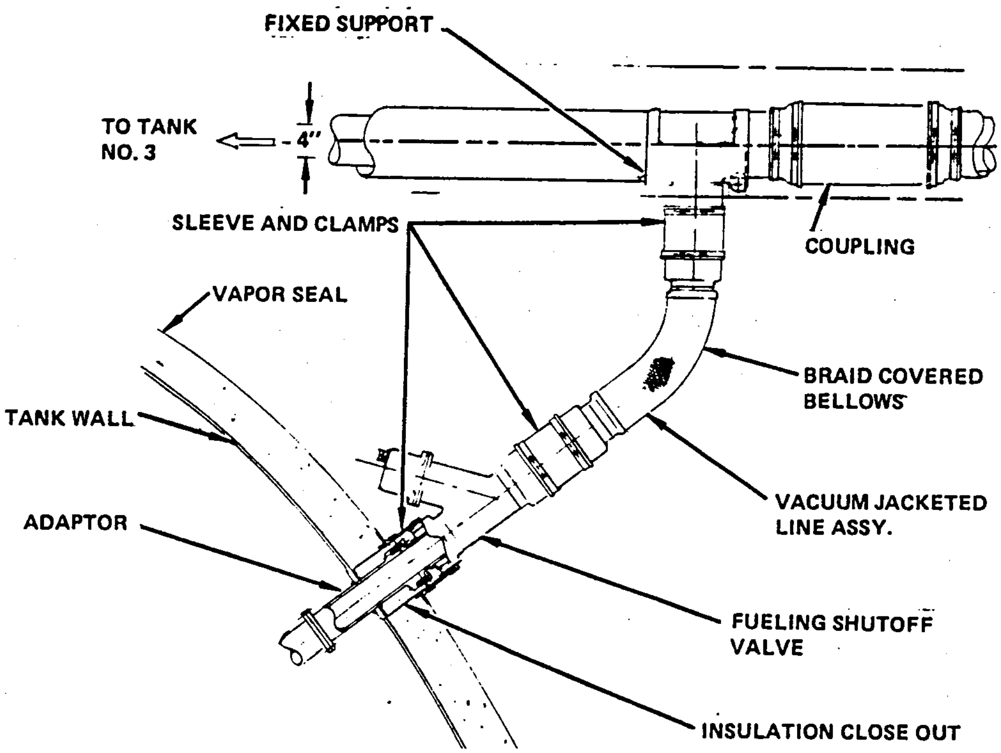

Figure 55. - Fuel level control valve.

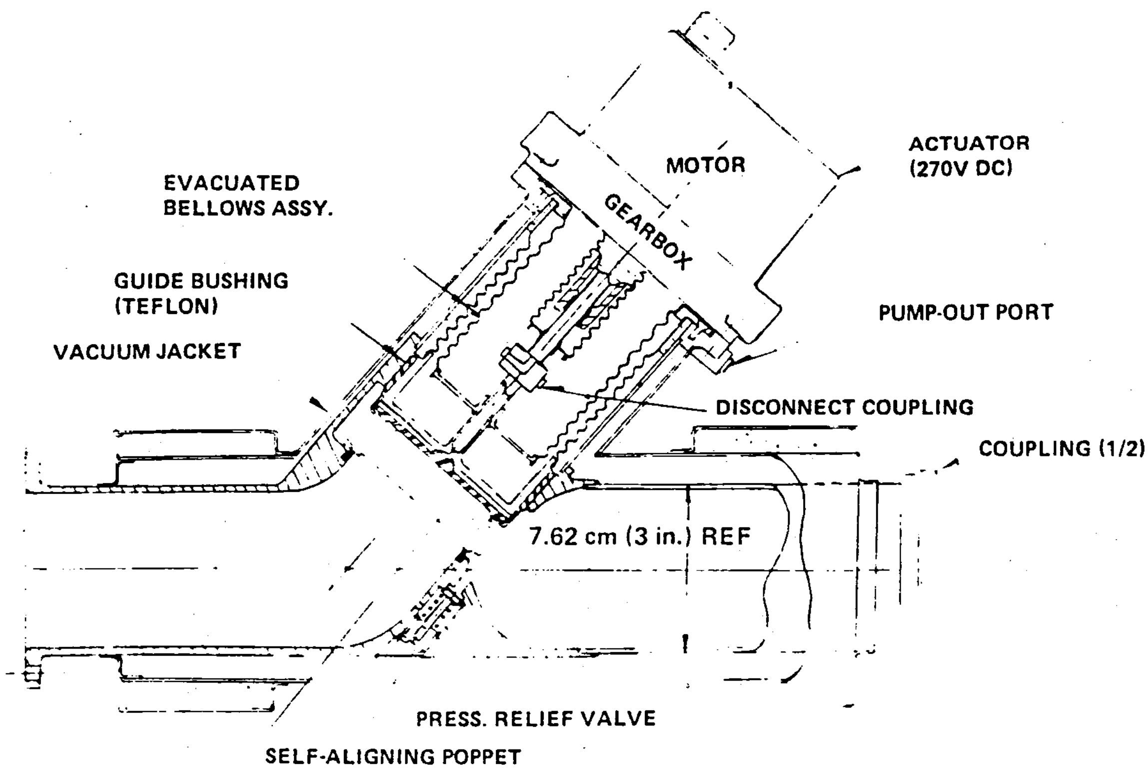

Figure 56. - Fueling shutoff valve.

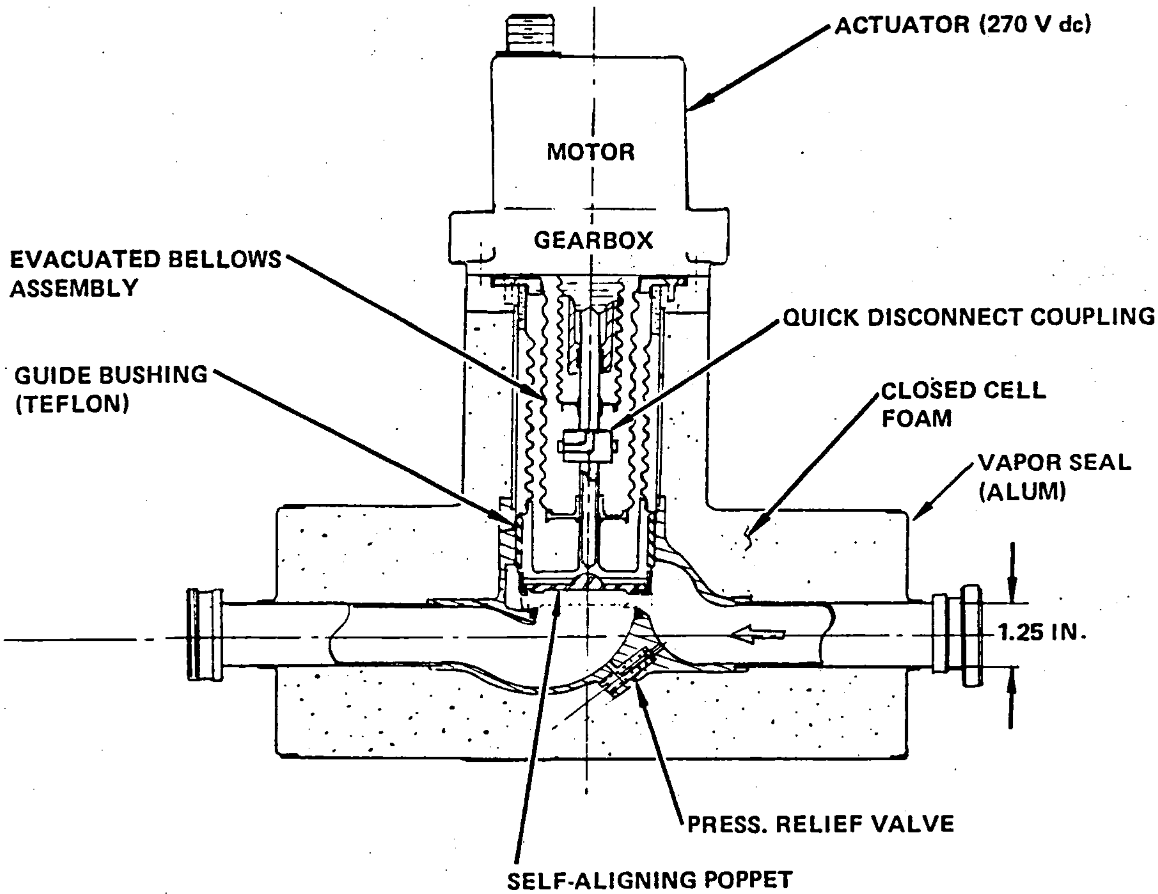

Figure 57. - Tank isolation valve.

Based upon the foregoing, each pump must be capable of supplying fuel at the pressure flow rate required by the engines. Conditions evaluated include:

(a) Takeoff power at sea level

(b) Maximum climb power at sea level and Mach 0.4

(c) Maximum cruise power and Mach 0.85 at 11 582 m (38 000 ft) with one pump supplying two engines

The maximum fuel flow required of each boost pump is established by condition (b). For this condition, a flow rate of 3690 kg/hr (8136 lb/hr) is required for each engine. To ensure that each engine will receive fuel at the required pressure the feed lines are sized by the longest fuel lines: e.g., No. 1 tank to No. 1 engine or No. 4 tank to No. 4 engine. The effect of line size on pressure drop is shown in figure 61. For this airplane, a nominal line diameter of 3.175 cm (1.25 in.) was selected with a line loss of 69.6 kPa (10.1 psi).

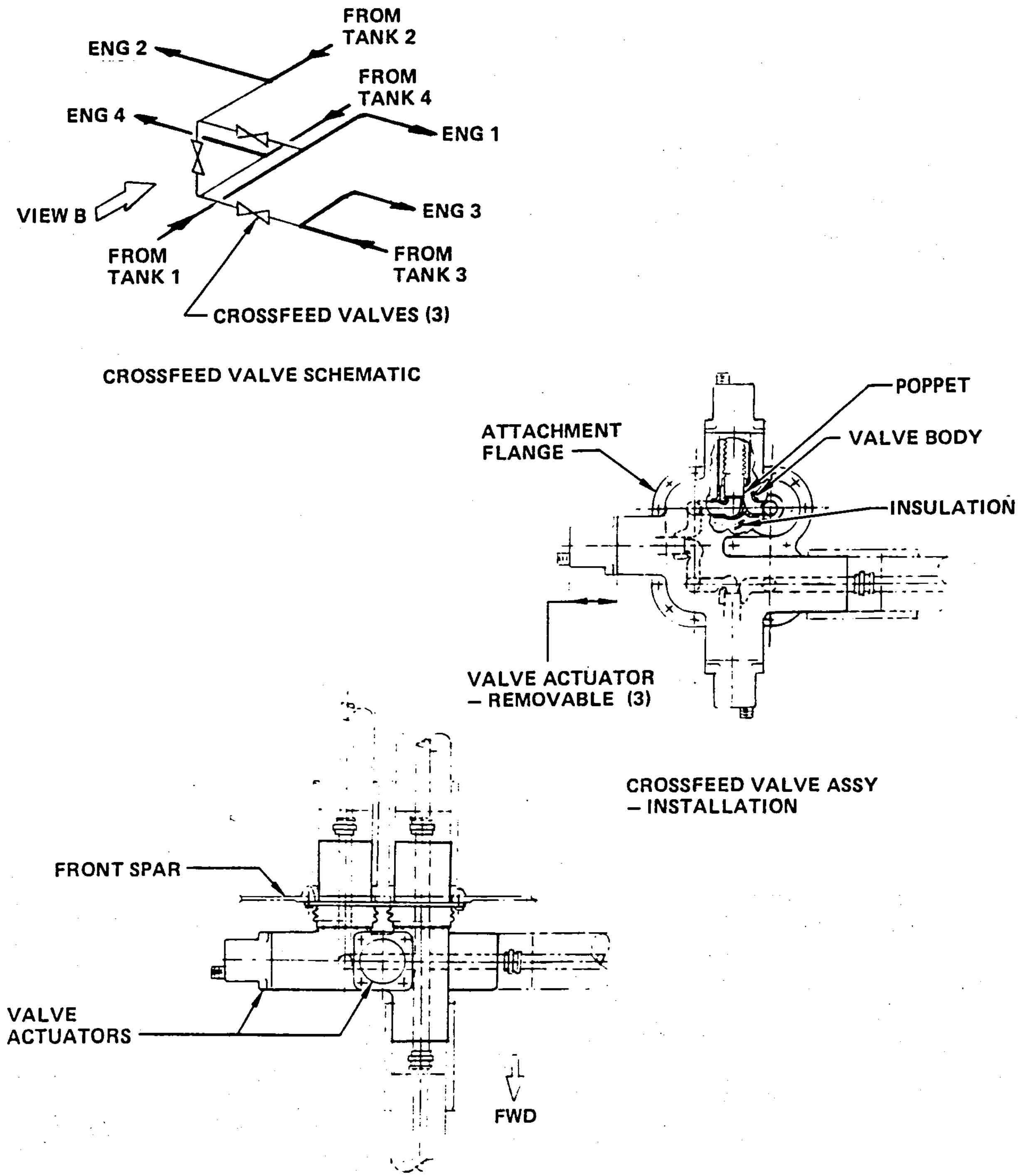

Figure 58. - Crossfeed valve assembly.

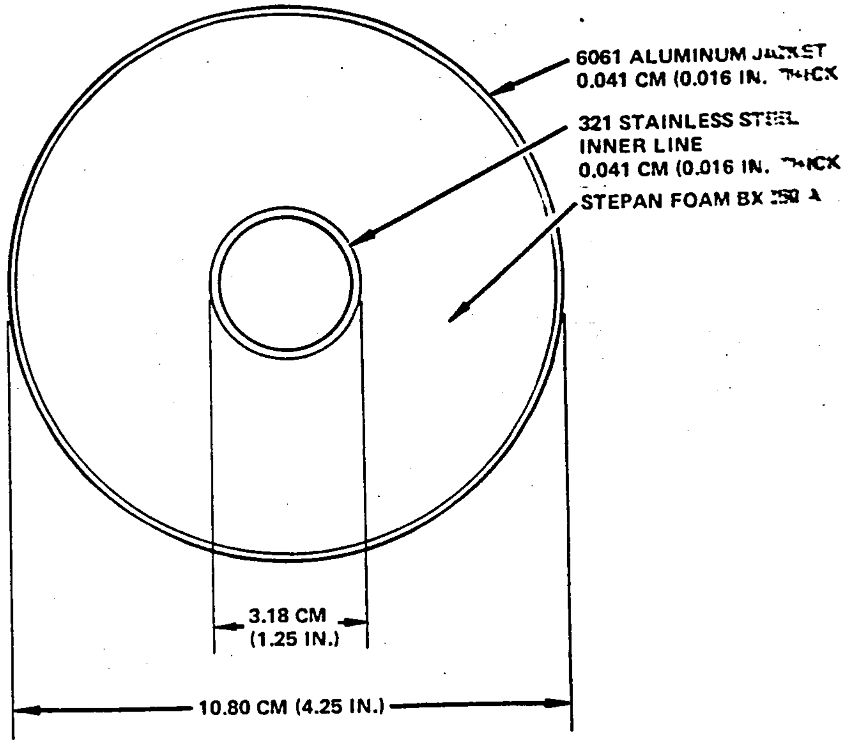

Figure 59. - Fuel-line cross section.

6.1.4 Liquid methane pump technology.- The technology for liquid methane pumps comes directly from the experience of pumping LNG (liquid natural gas). Pressures and flow rates of LNG pumps now reach 34.48 MPa (5000 psi) and 189.3 liters (50 gallons) per minute. This capacity is well over the 144 liters (38 gallons) per minute and 2.76 mPa (400 psi) required for the engine-mounted, high-pressure pump for the methane engine. However, some development is required to obtain flight weight pumps for aircraft application.

Commercial LNG pumps are generally made of 9 percent nickel steel. For aircraft application one could go to 6061 or 5083 aluminum to reduce weight.

As an example of existing capability, AIRCO Cryogenics have provided a pump with a 151 liter (40 gallons) per minute capacity at 11 400 rpm for avionics cooling in the B-1 bomber. The cooling medium is not cryogenic in this application but based on their experince pumping various cryogenic liquids AIRCO believes that with a change of bearings and going to purged labyrinth seals that it could be demonstrated to have an acceptable service life for liquid methane application. There are several pump manufacturers with industrial experience in design, manufacture, and production of LNG pumps.

6.1.5 Auxiliary power unit fuel supply.- The APU is supplied liquid fuel from Tank 2 normally, but also from any tank by crossfeed. During the initial APU startup, before electrical power is available to the tank-mounted boost pumps, it is expected that the normal tank pressure 145 kPa (21 psia) will preclude the need for a separate APU tank-mounted boost pump.

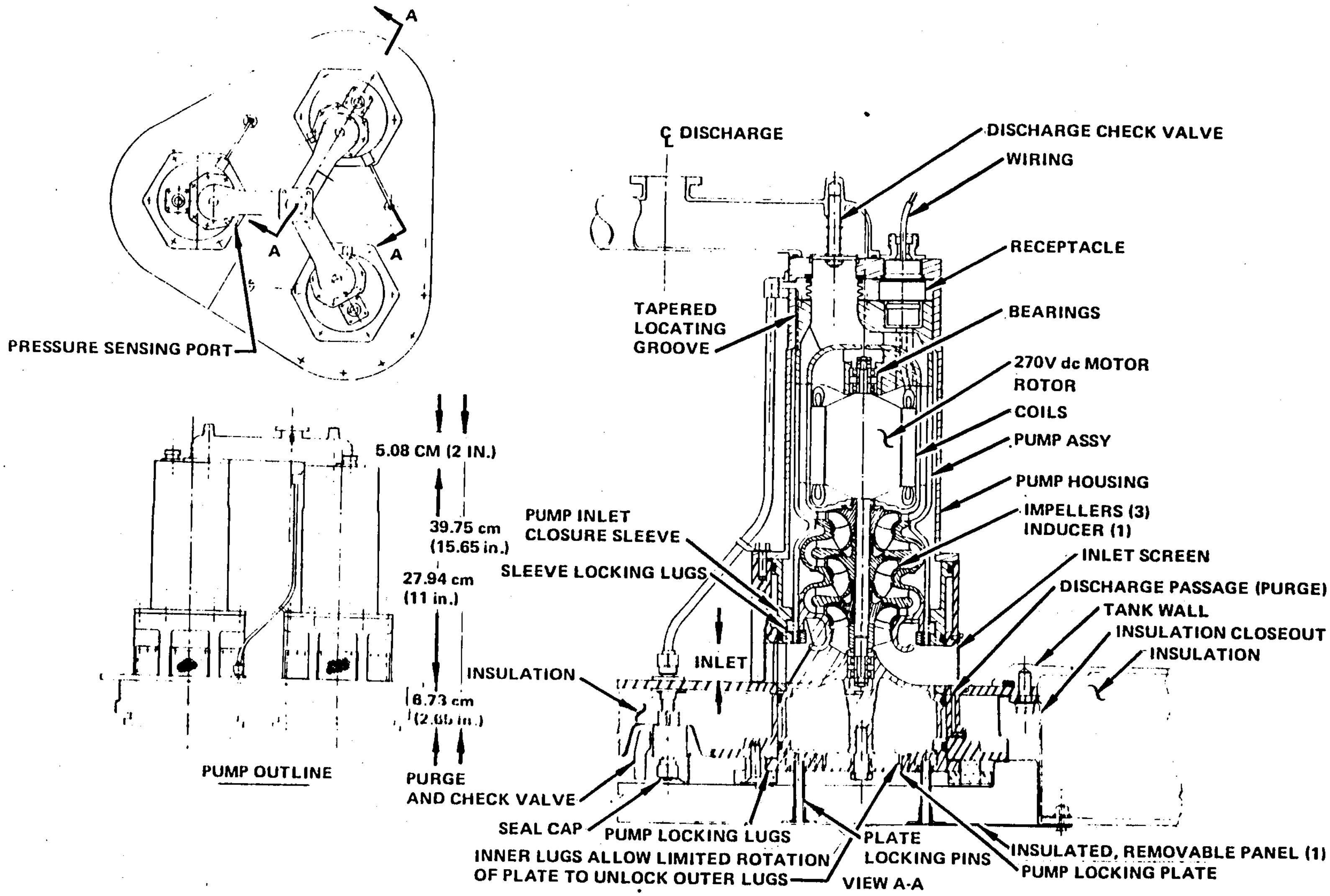

Figure 60. - Boost pump assembly and installation.

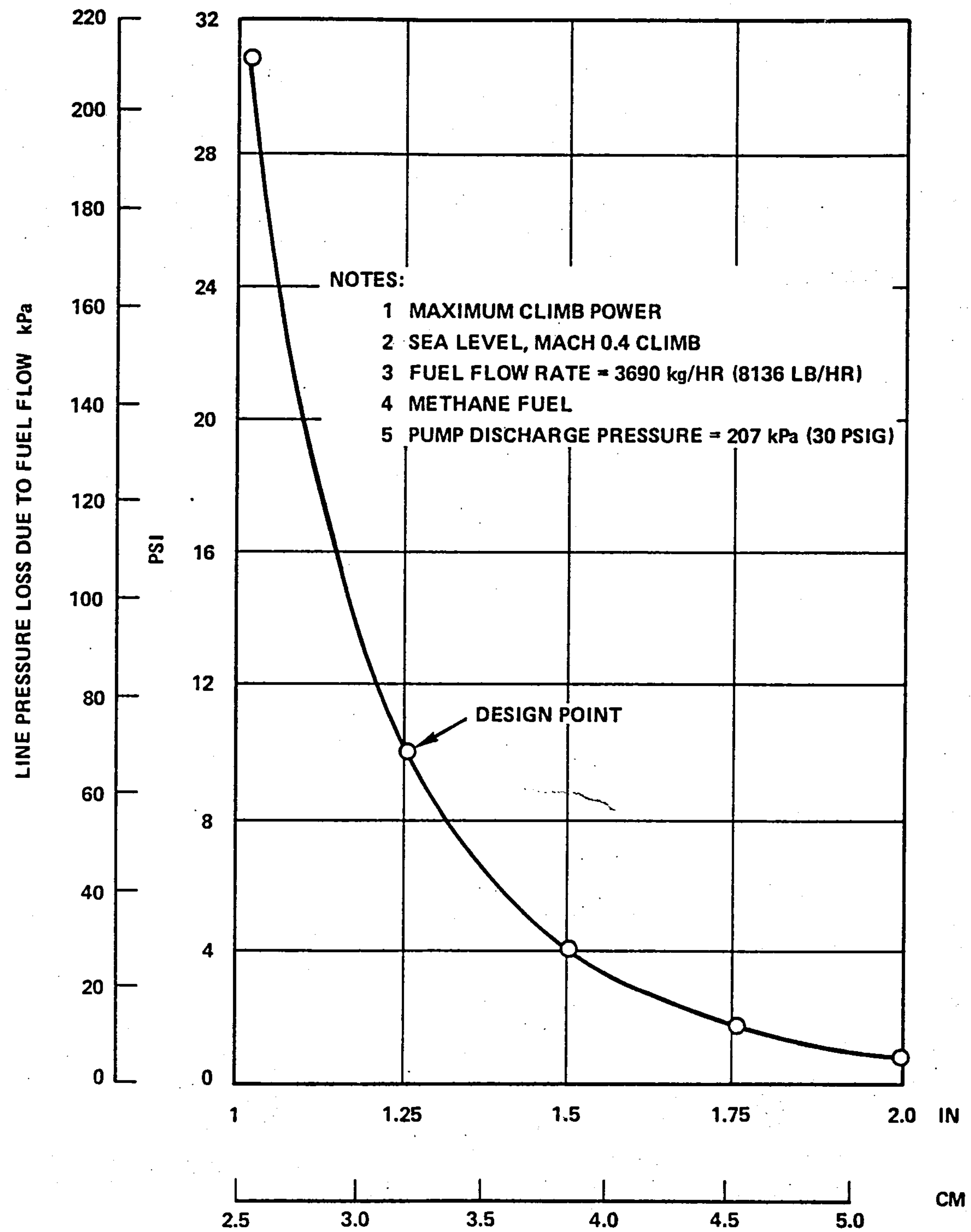

Figure 61. - Engine feed line sizing.

6.1.6 Fuel transfer.- Fuel transfer valves (figure 51) feed into the discharge line from the fuel tank boost pumps and connect with the aircraft fueling manifold. By opening any one of those valves, fuel in the corresponding tank can be transferred to any other tank by opening the fueling valve in that tank. Transfer will continue until the fuel level in the receiving tank reaches the automatic shutoff level when the tank is full. The transfer system precludes trapping of fuel in any one tank if the feed line isolation valve fails to the closed position. Thus the transfer system has the dual function of making all fuel available to all the engines as well as precluding excessive c.g. travel if fuel is trapped in the No. 1 or No. 4 fuel tanks by a closed tank isolation valve.

6.1.7 Fuel management.- The forward and aft locations of the fuel tanks provide a high degree of flexibility in controlling the airplane center of gravity. In normal operation, aircraft balance is maintained by having equal tank capacities with approximately equal moment arms for the forward and aft fuel tanks. To illustrate this point, figure 62 was prepared to show c.g. travel based upon a typical weight and balance sheet. At takeoff, the airplane c.g. is at 37 percent MAC, well within the limits of 26.5 to 43.5 percent MAC at the weight. With normal fuel usage, the c.g. moves forward to 31.3 percent MAC at zero fuel weight creating a minimum requirement for aircraft trim adjustment.

However, c.g. travel can exceed the allowable limits if the system design permits trapping of fuel in any tank as the result of a tank isolation valve failing to the closed position. The consequences of such a design deficiency are not tolerable, as illustrated in figure 62 and table 34 for fuel trapped in the No. 1 or No. 4 tanks while the fuel in the remaining tanks is consumed. Consequently, an alternate path for fuel to be removed from the tank is provided by the fuel transfer system.

An example of the effectiveness of the system is shown in the following. If the fuel valve in Tank 4 fails in the closed position, the corrective action is to open the fuel transfer valve in Tank 4 and close the fuel level control valves in Tanks 1, 2 and 4 only, figure 51. Fuel immediately begins to flow from Tank 4 to Tank 3 through the fueling manifold maintaining Tank 3 full of fuel until all of the Tank 1 fuel is depleted. This does entail some nominal shift in c.g., but the amount does not exceed 2 percent MAC in the forward direction as shown in figure 62. In the other extreme situation, fuel trapped in the No. 3 tank is transferred to the No. 4 tank causing an aft c.g. movement of not more than 2 percent MAC. Fuel trapped in Tank 1 or 2 causes no c.g. shift, because these tanks are mounted side by side and have the same c.g. moment arm. As a result of the transfer system design, c.g. movements with a failed fuel tank isolation valve are always well within the limits specified for normal operation.

6.1.8 Fuel jettison.- Fuel may be jettisoned, at the option of the flight crew, by means of a retractable jettison chute near the airplane tail cone, figure 52. The mast connects with the fueling manifold so that the fuel tank boost pumps can be used by means of the fuel transfer valves to pump fuel overboard down to a prescribed level set by a jettison fuel control sensor.

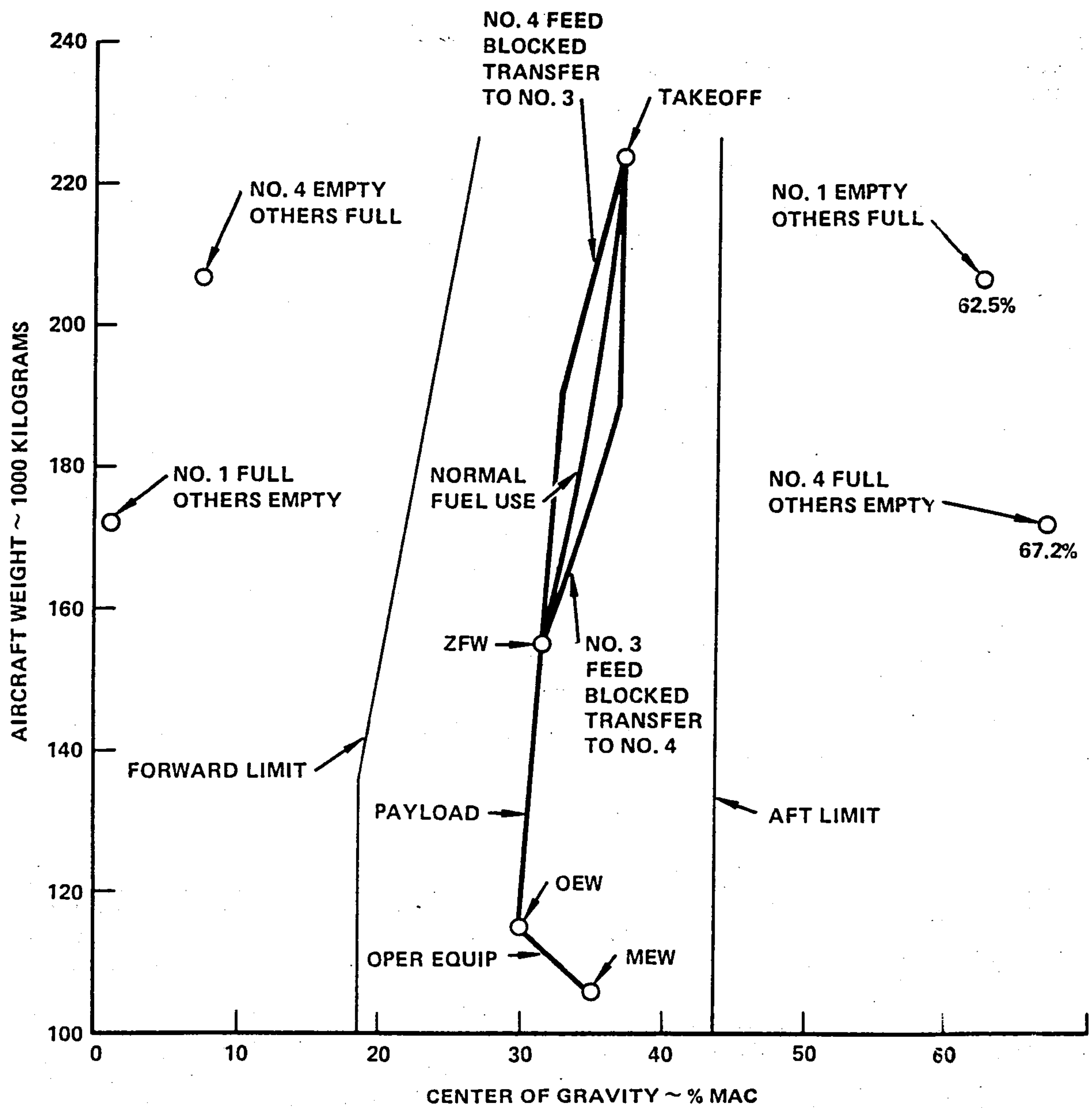

Figure 62. - Center of gravity travel with blocked feed line.

TABLE 34. - WEIGHT AND BALANCE DATA BASELINE CONFIGURATION 1

MAC = 271.7 L.E. MAC at F.S. 1072 Nose at F.S. 0

Condition	C.G. % MAC	Weight kg (lbm)	Moment arm cm (in)
Takeoff	37.0	224 029 (493 900)	2 978 (1 173)
Fuel			
Tank No. 1		17 282 (38 107)	876 (345)
Tank No. 2		17 282 (38 107)	876 (345)
Tank No. 3		17 282 (38 107)	5 105 (2 010)
Tank No. 4		17 282 (38 107)	5 410 (2 130)
Zero fuel weight	31.3	154 901 (341 600)	2 939 (1 157)
Payload – 400 Pax + baggage		36 287 (80 000)	2 972 (1 170)
– Cargo		3 629 (8 000)	2 921 (1 150)
Operational empty weight	29.9	114 985 (253 496)	2 929 (1 153)
Crew and oper. equipment		9 525 (21 000)	2 540 (1 000)
Manufacturer's empty weight	35.0	105 460 (232 497)	2 964 (1 167)

6.1.9 Tank vent and pressurization system.- The forward pair of tanks and the aft pair of tanks have separate pressurization and vent systems but share a common overboard vent system downstream of the pressure regulators, figure 51. Each pair of tanks has a common vent box which maintains an equal ullage pressure on both sides of the diaphragm, separating the fuel in Tanks 1 and 2 and in Tanks 3 and 4. The tanks are maintained at an absolute pressure of 145 kPa (21 psia) by a primary absolute pressure regulator, figure 63, located just downstream of the point where the vent line emerges from each pair of tanks. A secondary pressure regulator set at an absolute pressure of 159 kPa (23 psia) is mounted in parallel with the primary regulator to protect the tank from excessive pressure in the event of failure of the primary regulator. A purge gas discharge valve for use during the initial tank fill and during tank purging for repair or inspection completes the valve assembly at this location. If the tank absolute pressure drops below 124 kPa (18 psia)

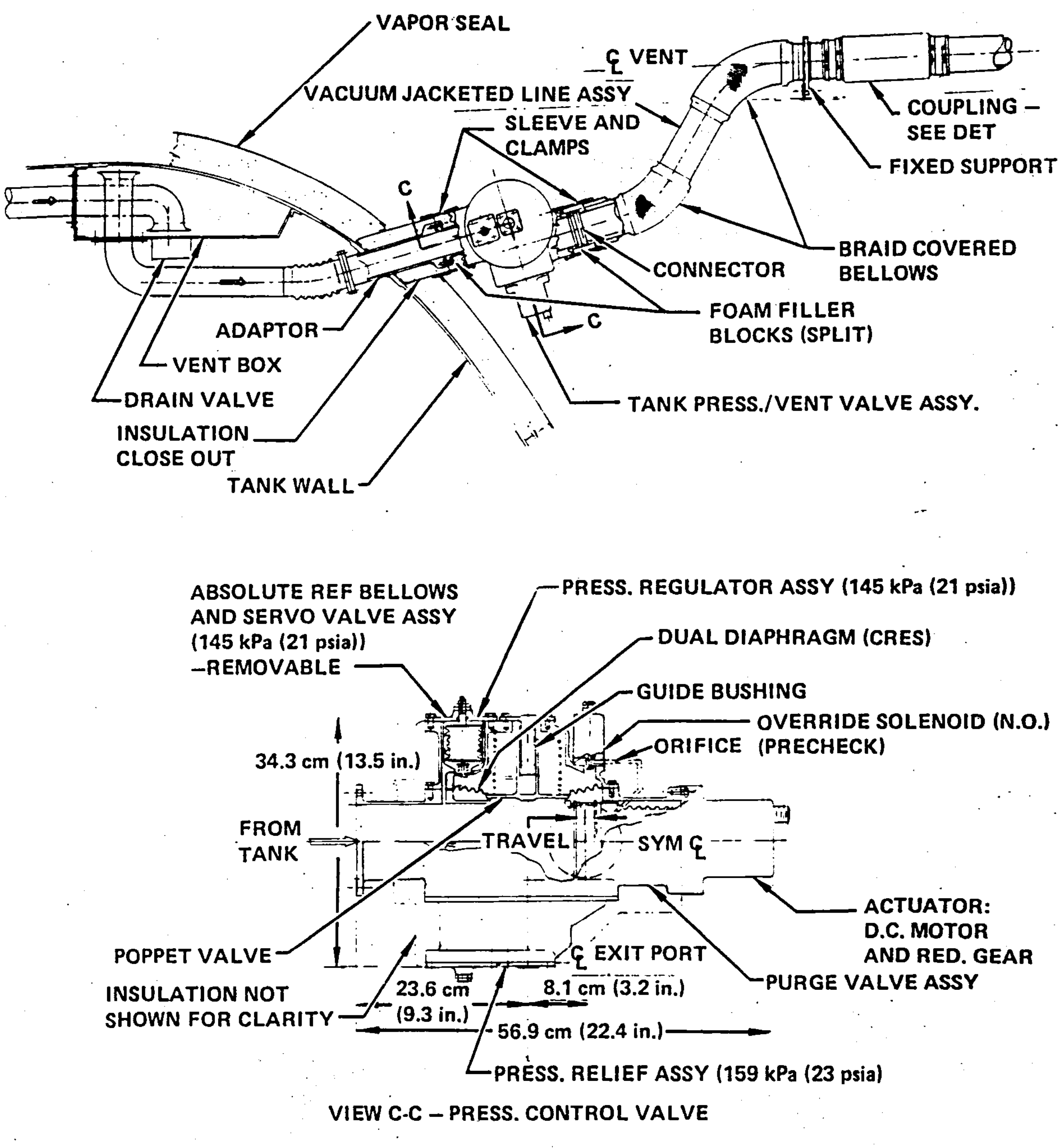

Figure 63. - Tank pressure control assembly.

when the boost pumps are operating, a backup absolute pressure regulator allows liquid flow normally supplied from Tank 4 to be evaporated at the fuselage-mounted tank pressurization heat exchanger (figure 51). Thus tank pressures are always maintained above the minimum level.

Vent boxes located within Tanks 2 and 3 act as liquid traps to preclude liquid from passing overboard through the common vent line during normal operations. A drain valve at the the bottom of each trap allows the liquid fuel to drop down into the tank below when the fuel level is below the float in the drain valve. Each vent box communicates with the tank it serves through a single vent line with its inlet in the ullage bubble above the point of intersection of the fuel surfaces for maximum pitch attitude extremes with full fuel tanks. This represents the simplest and most reliable vent design. If detailed aircraft attitude studies reveal that no single inlet location will always be void of liquid fuel, an alternative design is available which incorporates two inlets in each vent line. The inlet which is remote to the vent box would be open at all times and the inlet near the vent box would be closed by means of a float-operated vent valve when under fuel but open when not covered by fuel. The added complexity of this system is to be avoided, if possible, since it places moving components which would ultimately require maintenance within the fuel tanks.

The common vent line downstream of the absolute pressure regulators serves a dual purpose. In-flight, gas relieved through the pressure regulators is conveyed through the vent line to a lightning-protected overboard vent mounted in the vertical stabilizer, figure 64. The overboard vent assembly includes a servo-operated back-pressure valve set at 10.3 kPa differential (1.5 psig) to prevent air from being drawn into the vent where it could constitute a hazard. During fueling operations, the common vent serves as a means to recover large quantities of boiloff gases by routing them back to the vapor recovery adapter so that they can be recycled by the airport methane liquefaction and distribution system, figure 65. In the event of the failure of the primary vent, an alternate servo operated vent valve, set at 24.5 kPa (3.5 psig) is located in the tail cone area, figure 66. This valve is closed by an override solenoid to prevent opening during fueling.

The vent line must be sized to preclude tank overpressurization during fueling operations. Both vapor and liquid overflow must be considered, vapor because it is present every time the airplane is fueled, and liquid because a failed fueling shutoff valve will permit fuel to flow through the vent line.

During fueling, vapor from all fuel tanks enters the vent line and is conveyed to the vapor recovery adapter. The vapor outflow rate is shown in figure 67. The maximum outflow rate occurs at the end of the fueling operation when vapor at 117^{o}K (211^{o}R) and 145 kPa (21 psia) is released at the rate of 0.078 kg (0.175 lb) per second per tank.

Before a line size selection can be made, however, the effect of a failed fueling valve on vent line pressure drop with liquid fuel overflow must be considered. For this analysis, it is assumed that the fueling valve in the No. 1 tank fails to the open position. For this condition the resulting tank

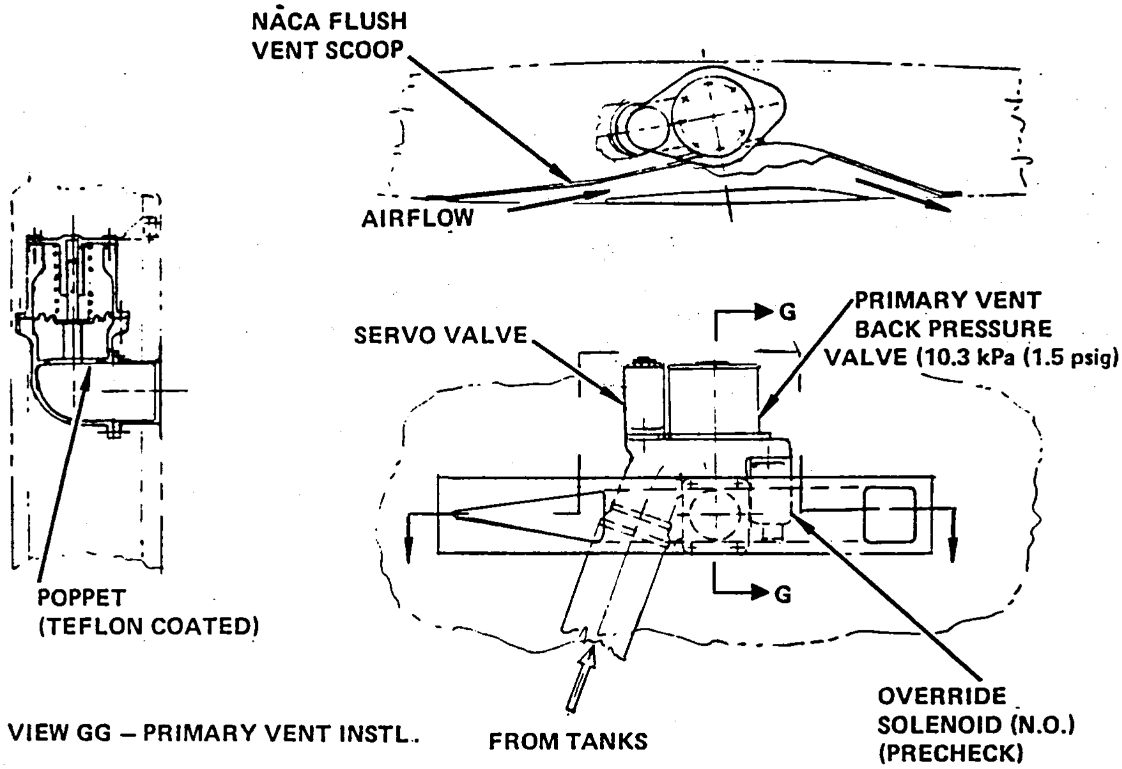

Figure 64. - Overboard vent and back pressure valve.

pressure differential to ambient must not exceed normal operational limits. Refueling at La Paz, Bolivia requires consideration of a 4267m (14 000 ft) refueling altitude. At a cruise altitude of 4267 m (40 000 ft), the differential pressure from the tank 145 kPa (21 psia) to ambient 18.8 kPa (2.73 psia) is 126 kPa (18.27 psig) for normal operation. The absolute pressure in Tank 1 with a failed fueling shutoff valve has been determined assuming liquid fuel overflow out of the tank resulting from a fueling adapter pressure of 193 kPa (28 psia) and a ground vapor return line pressure of 110 kPa (16 psia). This pressure is shown in figure 68 for 7.62 cm (3-in.) and 10.16 cm (4-in.) line diameters. It is apparent that a 7.62 cm (3-in.) manifold is adequate to handle both gaseous venting from all tanks while refueling the aircraft and liquid flow from any one tank if its fueling shutoff valve should remain open after all tanks are full.

After fueling is complete, the fueling and vapor return adapters are both disconnected from the aircraft. Subsequent venting requirements are established by boiloff because of heat leaks through fuel lines and tank insulation. At that time, the maximum gaseous venting efflux is approximately 0.0064 kg/sec (0.014 lb/sec). This flow is discharged through a lightning protected vent located in the vertical tail and communicating with the 7.62 cm (3-in.) vent line through a bypass poppet valve actuated by removing the vapor return fueling adapter, figure 54. A line sized for this boiloff rate would be too small

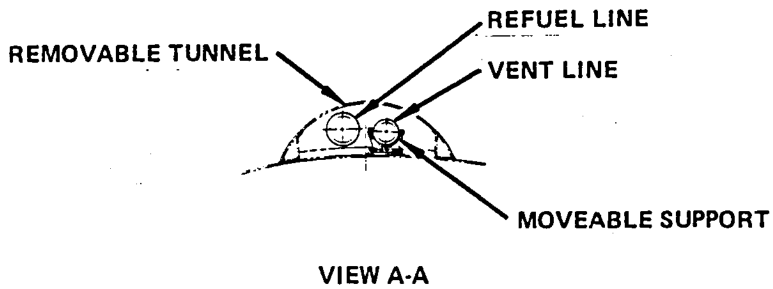

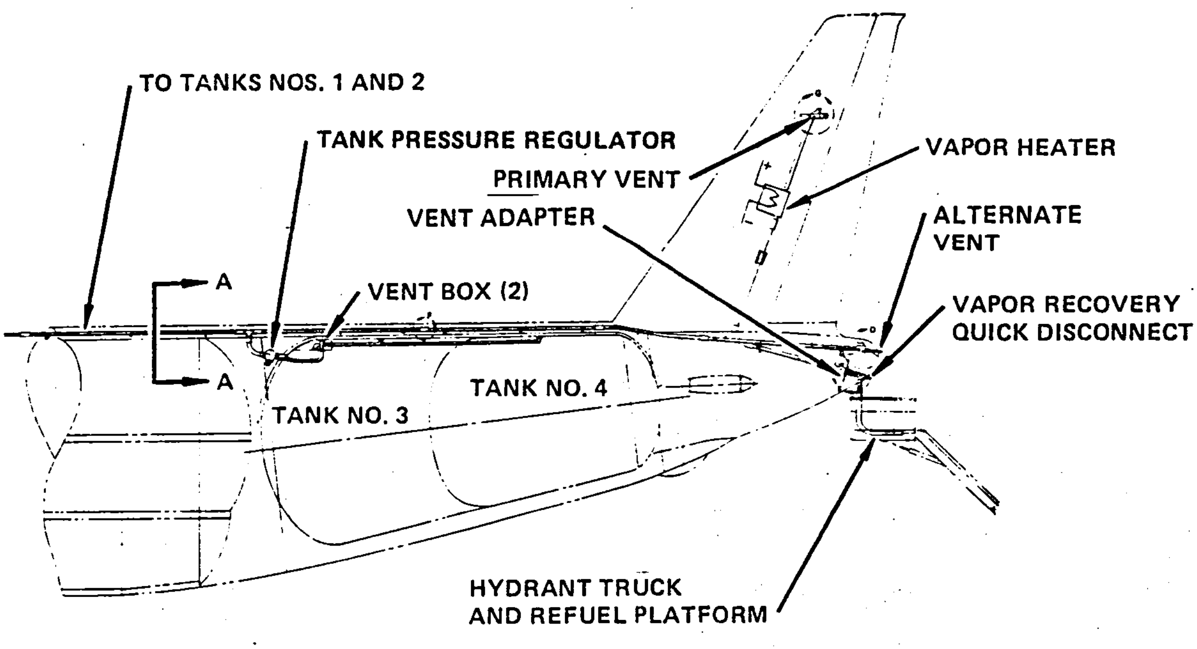

Figure 65. - Vent and pressurization system.

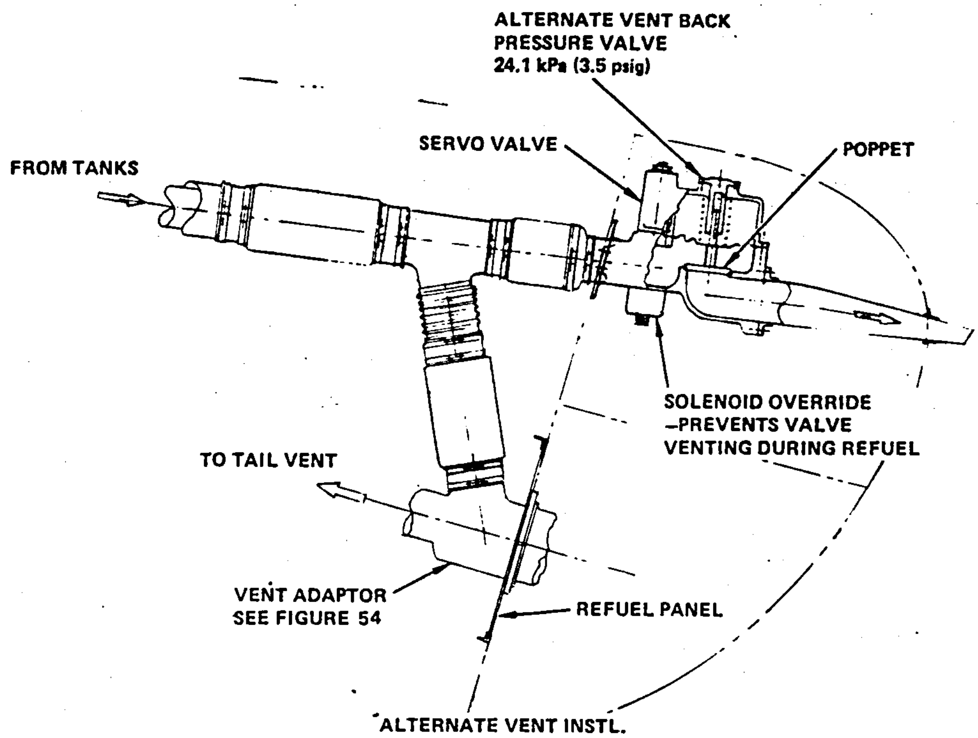

Figure 66. - Alternate vent installation.

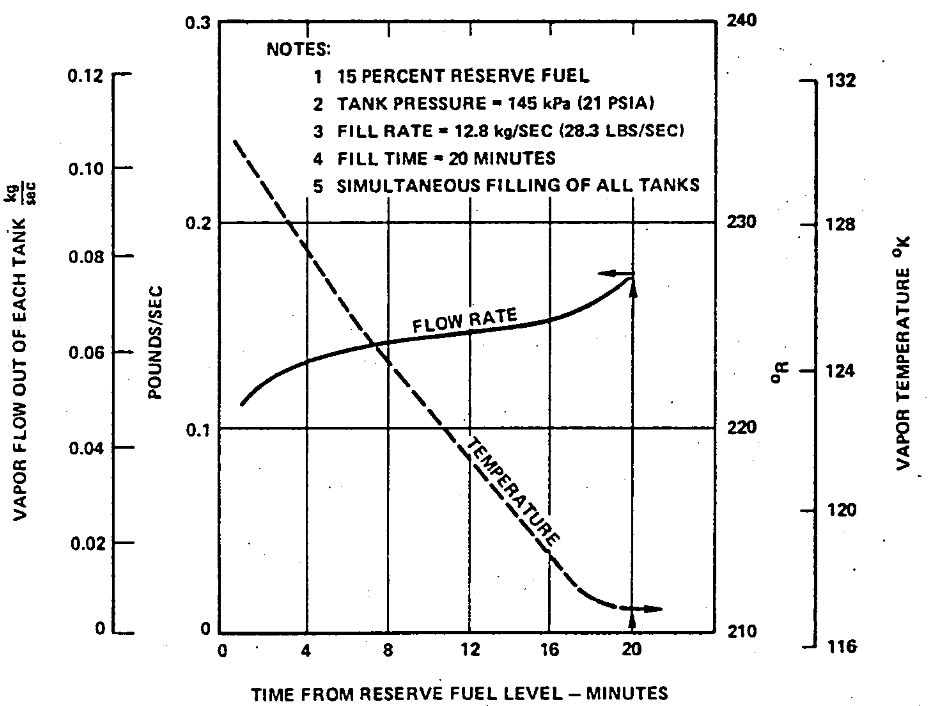

Figure 67. - Vapor efflux rate during refueling.

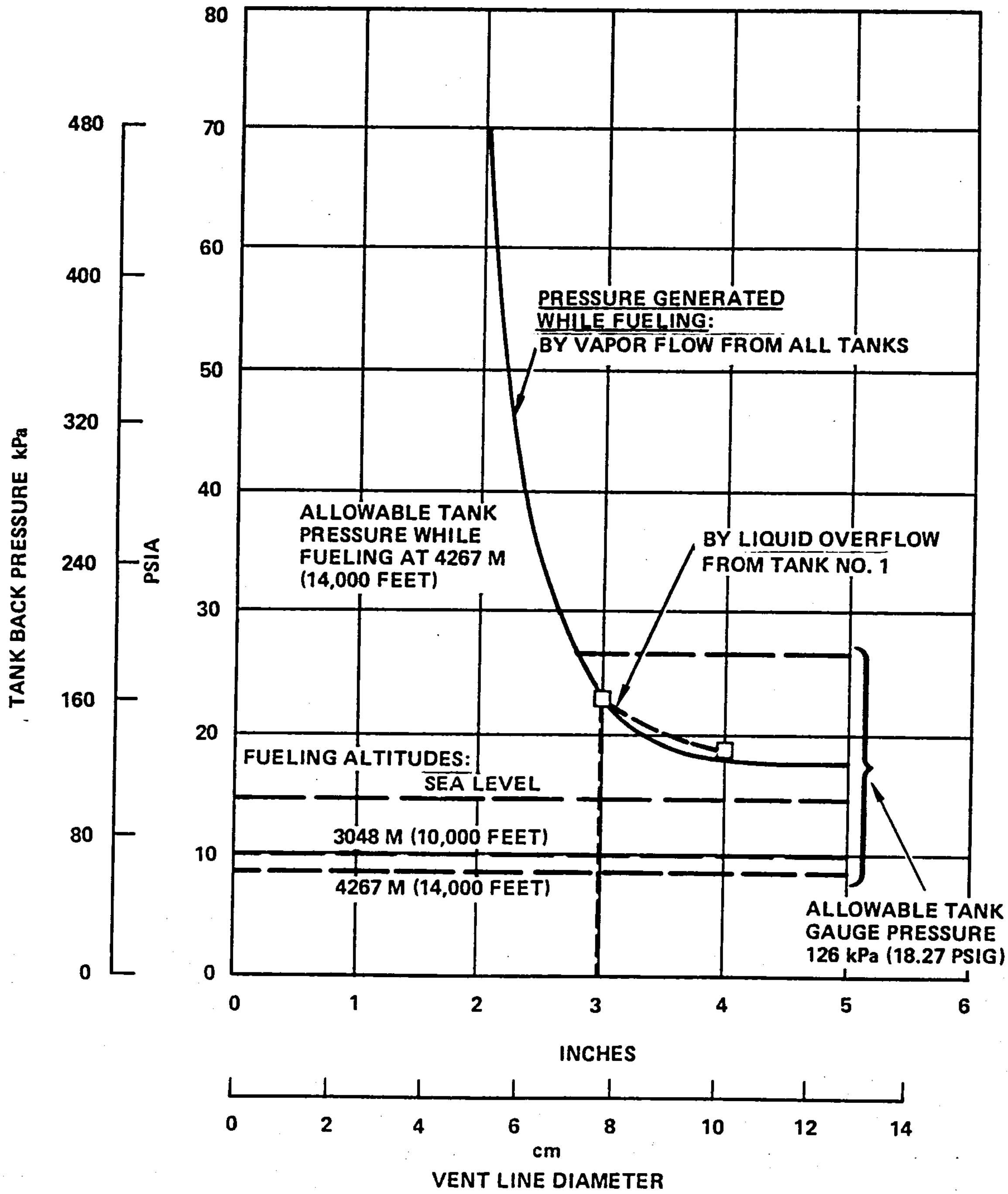

Figure 68. - Vent line sizing.

to be practical (less than 1.27 cm (0.5-inch) in diameter). Hence, an arbitrary line size of 5.08 cm (2 in.) was selected to accommodate an increased vapor boiloff rate that could result from tank insulation damage.

Another factor which must be considered for this vent line is the low temperature of the evolved gases, approximately $117^{\circ}K$ ($211^{\circ}R$). At this temperature, water vapor will condense out of the atmosphere to form ice at the flame arrestor discharge in the lightning protected vent. Hence, it is planned to add heat to the evolved gases to maintain an exhaust temperature above $4.4^{\circ}C$ ($40^{\circ}F$) at all times. The normal heating requirements are very snall, approximately 128.6 kJ/min (122 Btu/min). This heat could be provided by an electrical heating unit mounted in the vertical stabilizer, figure 65.

6.1.10 Leak detection and vapor purge

6.1.10.1 Leak detection.- The detection of small leaks from a methane fuel tank cannot be based upon visual means because the methane becomes a colorless vapor upon exposure to the atmosphere. Visual observation of condensed water vapor from the atmosphere is not a feasible method either, because small leaks of methane can pick up enough heat from the tank insulation and external fuselage skin to be well above the dew point for water vapor. Consequently, other methods which included measuring skin temperatures or sensing the combustibility of the atmosphere surrounding the tank were considered. However, both of these methods require that the leak be conveyed to the detector location. This qualification does not appear to be acceptable for thermal detection but is feasible if a combustibility technique is used.

The method proposed for the methane-fueled airplane is shown in figure 69. Each set of tanks is encased in a blanket of insulation, as illustrated in figure 70. The inner layer of insulation is composed of a closed cell foam (STEPAN BX250A) which is surrounded by a vapor barrier (MAAMF). The foam is bonded to both the tank and vapor barrier to preclude separation as the tank diameter is decreased by cooling during the fueling operation. Longitudinal grooves are cut in the foam adjacent to the tank wall to provide leakage channels to convey leaking methane to a plenum behind the manhole cover at one end of the tank.

To preclude a pressure buildup, the leaking methane is carried overboard through a 1.27 cm (1/2-in.) tube to a drain mast which ensures that the methane is discharged clear of the airplane structure. A pressure relief type check valve prevents air from entering the tube since moisture contained in the air would condense on the tank walls and block the leakage channels. The drain mast contains a flame arrestor to prevent propagation of flames into the tube if leaking methane is ignited by some external source.

A leak detector mounted near the manhole plenum senses the potential combustibility of the leaking methane and triggers a signal to the flight station so that a tank inspection and repair can be initiated at the first opportunity. One type of leak detector incorporating a ceramic bead catalyst which causes a low level of combustible gas oxidation in the presence of air is manufactured by General Monitors, Inc. in Costa Mesa, California. Some developmental effort

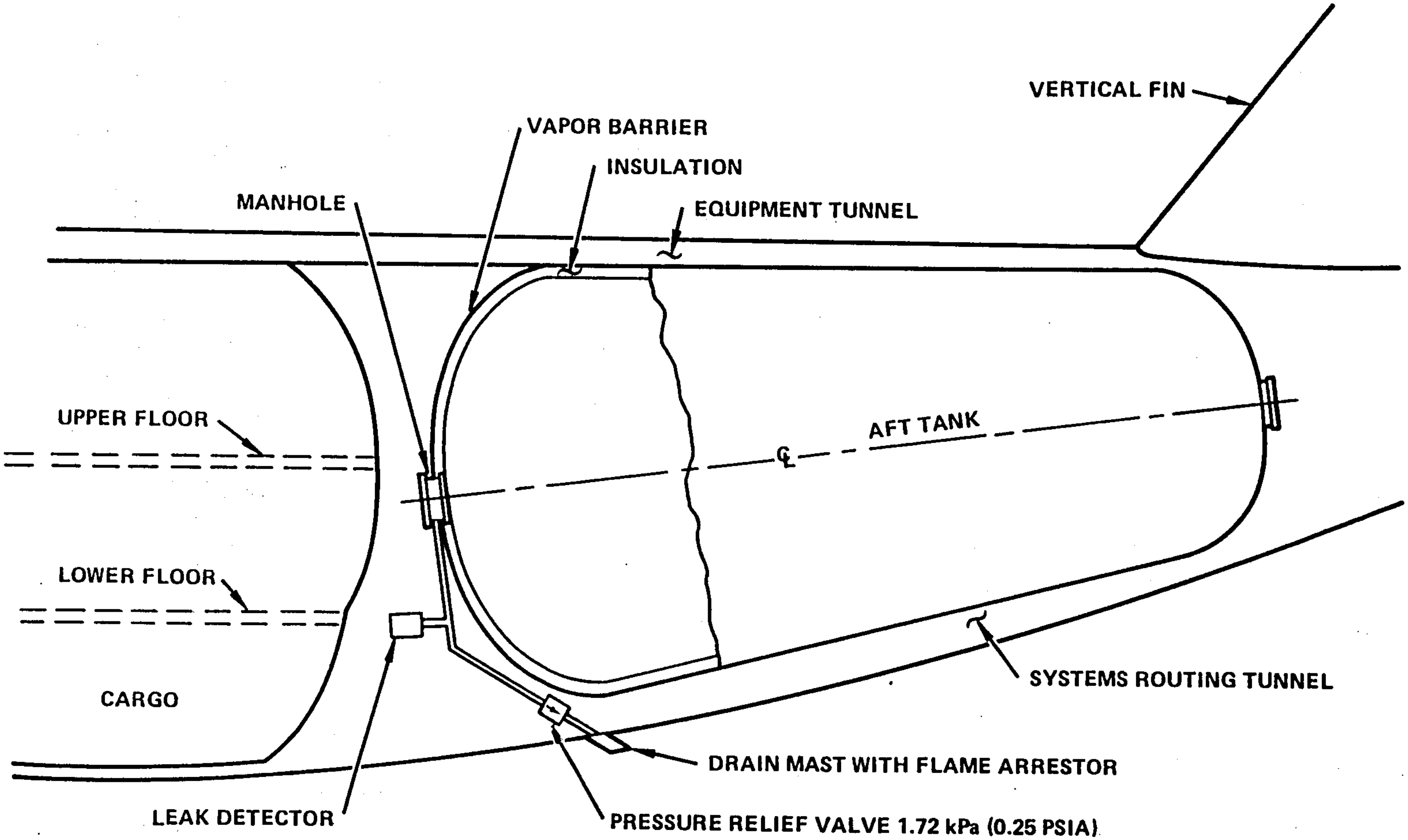

Figure 69. - Leak detector system (integral tank structural details eliminated for clarity).

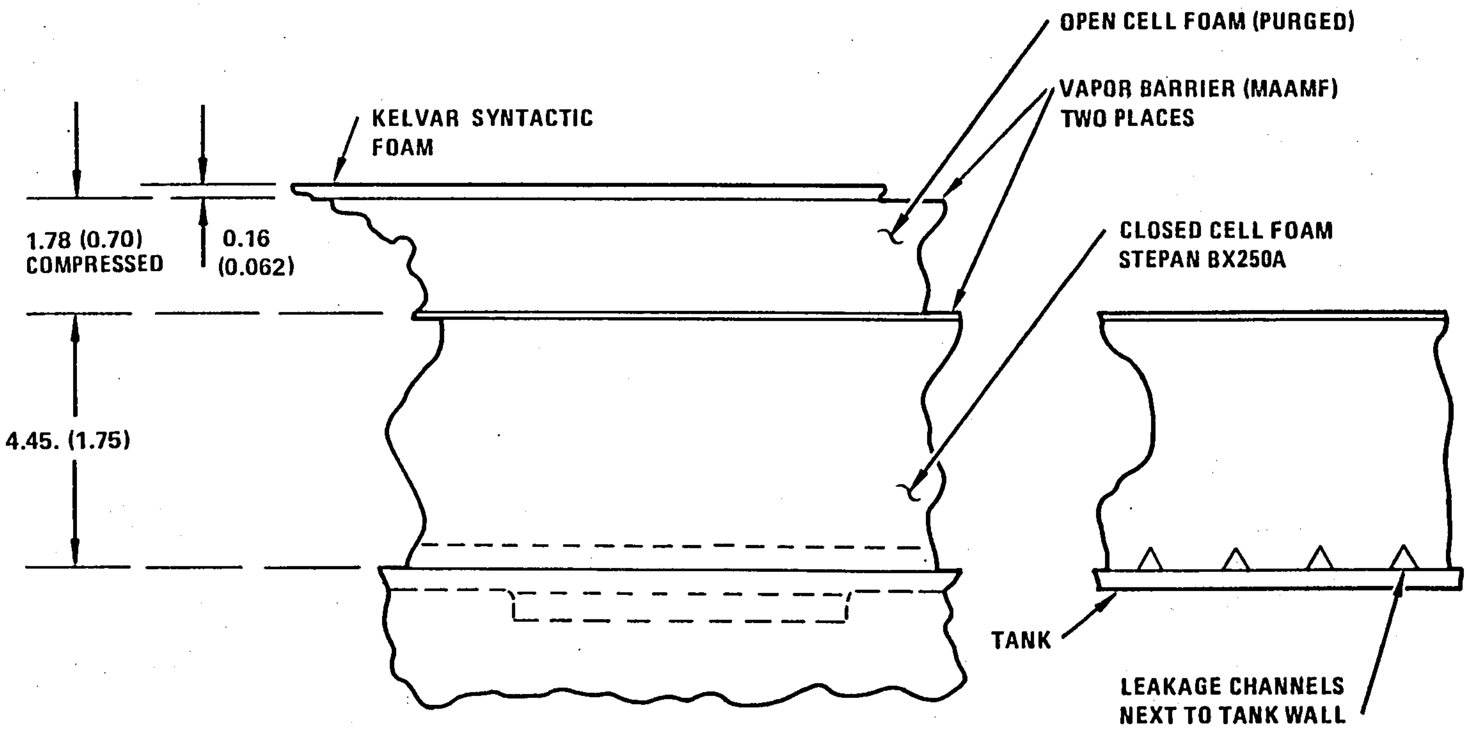

Figure 70. - Aft tank (integral) insulation.

is required to adapt this unit to the variations in ambient pressure attendant to aircraft operation since the unit is normally used for sea level applications.

6.1.10.2 Open cell foam purging.- Figure 70 shows an open cell foam surrounding the tank closed-cell foam insulation. This foam is precompressed by the Kevlar Syntactic Foam outer casing which constitutes the external skin of the airplane in the region of the fuel tanks. The purpose of the precompression is to allow the open cell foam to expand when the tank diameter shrinks, during the filling process, so that the Kevlar outer skin fairing retains its required aerodynamic shape.

The selection of an open cell foam for this application has a dual purpose. Not only does it provide support for the Kevlar skin, but it also serves as a chamber which can be filled with a moisture free gas to preclude a buildup of ice within the cells which would eventually destroy its effectiveness.

In practice, it is not possible to fabricate a Kevlar outer skin which is impervious to moisture-laden air and which can tolerate expected aircraft maintenance activities without developing leaks. Hence, a practical method of maintaining the dry atmosphere is to continually supply the open cell foam with enough dry gas to maintain it slightly pressurized above the outside ambient air pressure. This supply must equal the dry gas leakage rate overboard and be able to maintain the foam pressurized above outside ambient during rapid descents.

Two sources of the dry gas are feasible, stored nitrogen and engine bleed air. A typical nitrogen purge system which stores nitrogen as a liquid and converts it to gas at a regulated pressure differential across the Kevlar skin is illustrated in figure 71. This system is complex and heavy because of the necessity for storing enough liquid nitrogen to complete a given flight plan. A similar system was considered for the liquid hydrogen fueled subsonic transport, reference 4. The weight of such a system applied to the methane fueled airplane has been estimated from the referenced study. It was assumed that the only significant difference in the system weights was in the weight required for storing the nitrogen. The distribution system in both cases is assumed to be identical. The estimate is based upon an 8-hour flight from loading ramp to loading ramp and assumes enough additional nitrogen to climb back to cruise altitude with a 20-percent increase in range.

Weight Breakdown	kg	lb
LN_2	124	273.5
Bottle	10.9	24
Equipment	45.4	100
Plumbing and Shrouds	179.6	396
10% Contingency	23.6	52
Total Hardware	259.5	572.0
Total Hardware Plus LN_2	383.5	845.5

The total weight chargeable to nitorgen storage is 273.5 + 24 = 134.9 kg (297.5 lb). For an 11-hour flight, this weight must be increased to approximately 196.4 kg (433 lb).

An added consideration is the necessity for maintaining a dry atmosphere in the foam during overnight layup time. Assuming an 8-hour-per-day utilization of the airplane, layup time would be 16 hours. This would require a bottle plus nitrogen weight of approximately 378.8 kg (835 lb) if it had to be stored aboard the aircraft.

One possible method of eliminating most of the weight penalty attendant to storing liquid nitrogen is to purge the foam with air which has had its dew point reduced below the lowest temperature the external surface of the tank insulation will experience. In flight, this temperature is -57.8^{o}C (-72^{o}F). Relatively simple compressor, mechanical filter and chemical dessicator systems have been routinely supplying air at even lower dew points for years. These systems incorporate 10.3 to 20.7 kPa (1500 to 3000 psig) air compressors and are used in both military and civil airplane applications for such functions as engine starting, retractable landing gear operation, brake actuation and various other functions which can be actuated by pneumatic systems.

For purposes of this analysis, it is assumed that the purge air in the foam is maintained at 1.72 kPa (0.25 psi) above outside ambient pressure. In level flight, the resulting airflow leakage is as shown in figure 72. If a continuous flow system is used with no stored air, the design flow rate is established by the sea level static leakage flow requirement of 0.006 kg/sec (0.0135 lbs per second). During a descent, the leakage flow must be augmented by an amount which accounts for the increasing ambient pressure at lower altitudes. This pressurization airflow is also shown in figure 72 for a normal maximum rate of descent. The peak pressurization requirements at 8992 m (29 500) and at 3810 m (12 500 feet) occur because the descent profile results in a maximum rate of change in ambient pressure per unit time at these altitudes during descent, the purge air supply system must be capable of supplying the sum of the leakage and pressurization airflow requirements. To ensure this capability, the supply system air compressor inlet receiver cooled engine bleed air which is regulated to approximately 1.72 kPa (0.25 psia), thereby increasing the system flow capacity well above the sea level flow rate. If the peak requirements during descent exceed the air supply capability momentarily, air at a pressure of 10.3 kPa (1500 psia) can be stored in air bottles to be released at that time.

A schematic diagram of the system is shown in figure 73. The system employs a three-stage 10.3 kPa (1500 psig) reciprocating air compressor with the output from each stage cooled by ambient air. A final stage of cooling uses the output of an expansion turbine to reduce the air temperature out of the compressor to 4.4^{o}C (40^{o}F) to maximize the effectiveness of a mechanical filter and chemical dessicator which dries the air to a dew point of approximately -73.3^{o}C (-100^{o}F). The final stage of cooling incorporates a thermal bypass on the cooling air side to maintain the temperature at the 4.4^{o}C (40^{o}F) level and ensure that no water freeze-out occurs in the mechanical filter. The exhaust cooling air from the final stage of cooling has a dew point of approximately

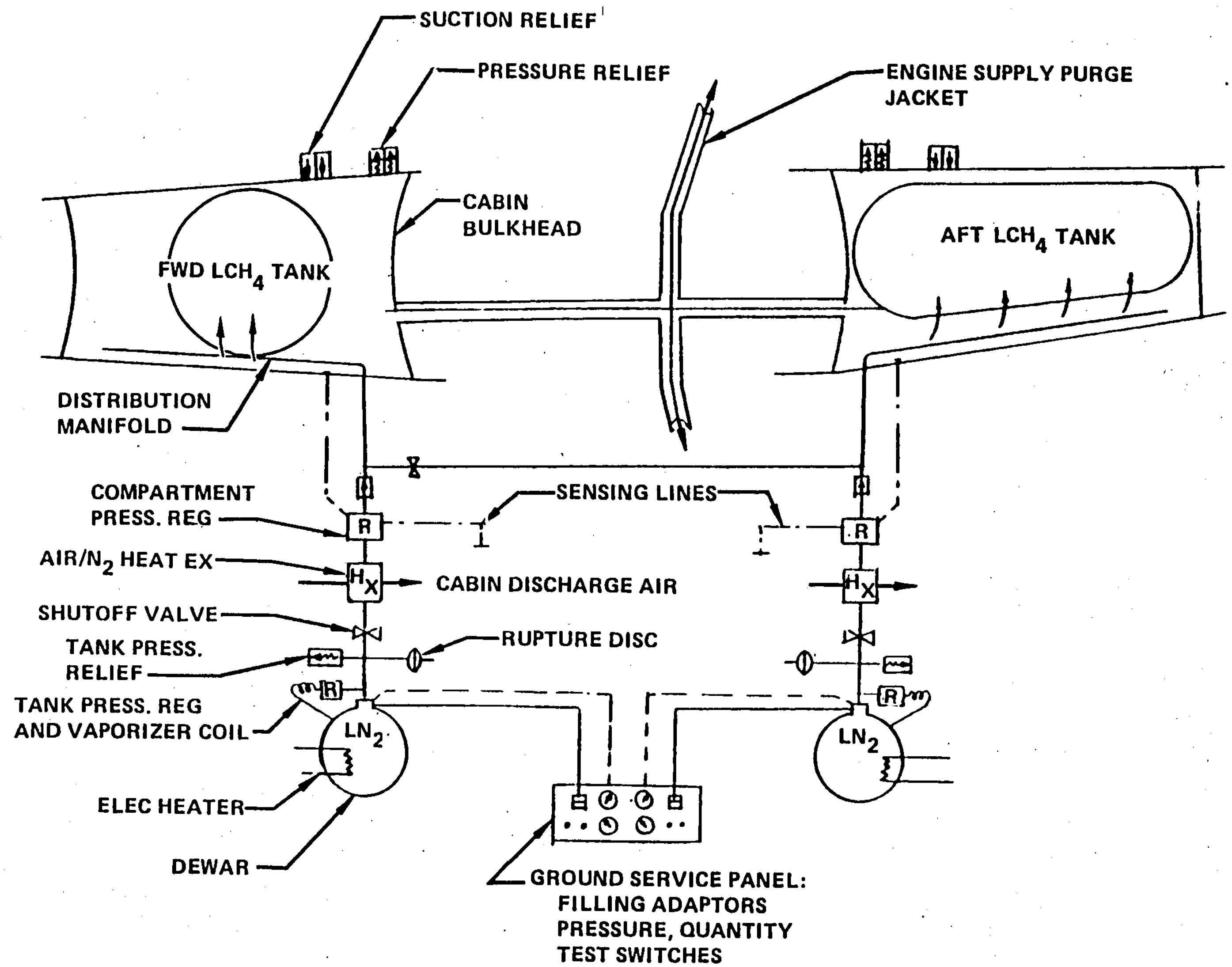

Figure 71. - N_2 purge system schematic.

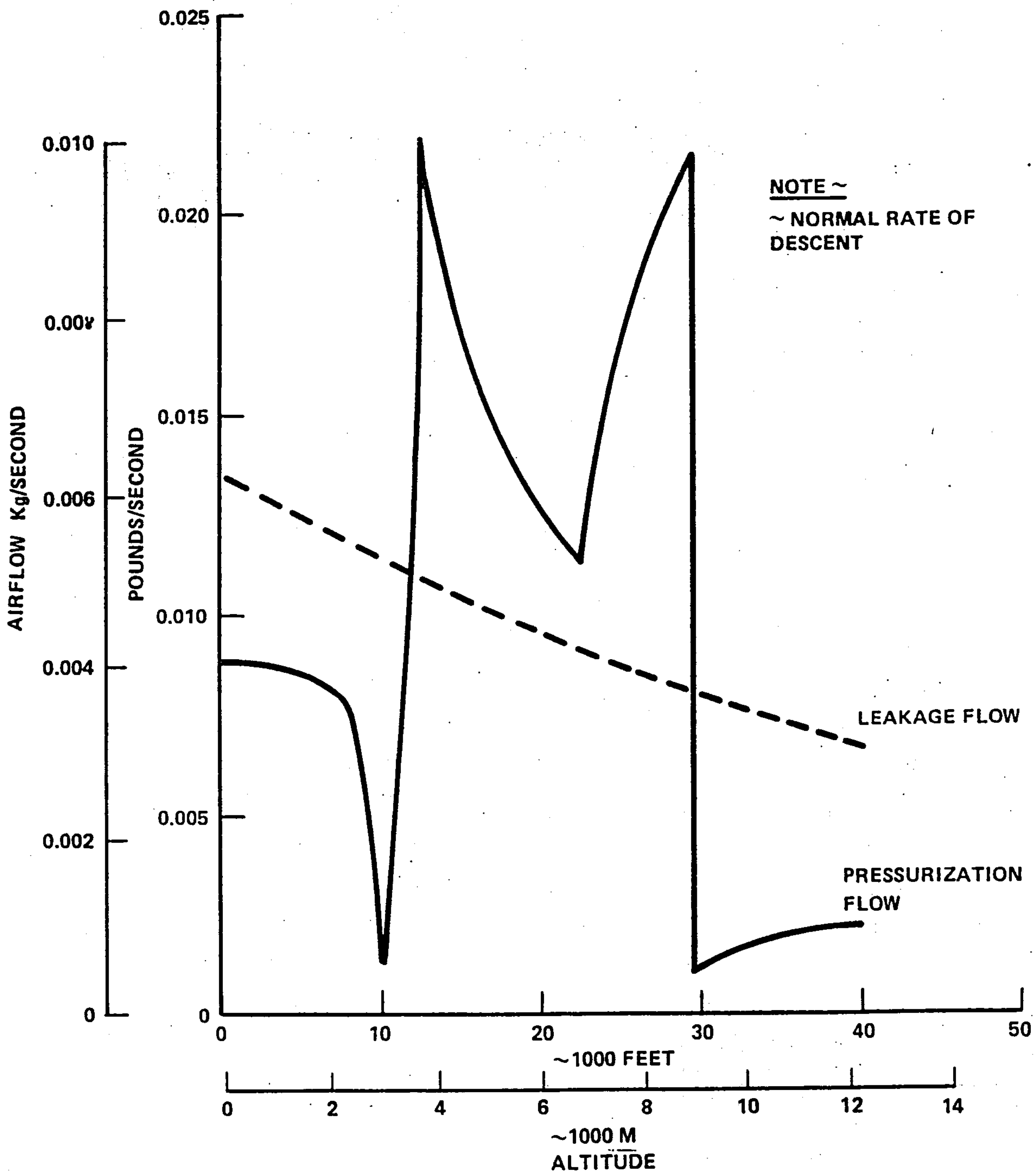

Figure 72. - Purge airflow rate.

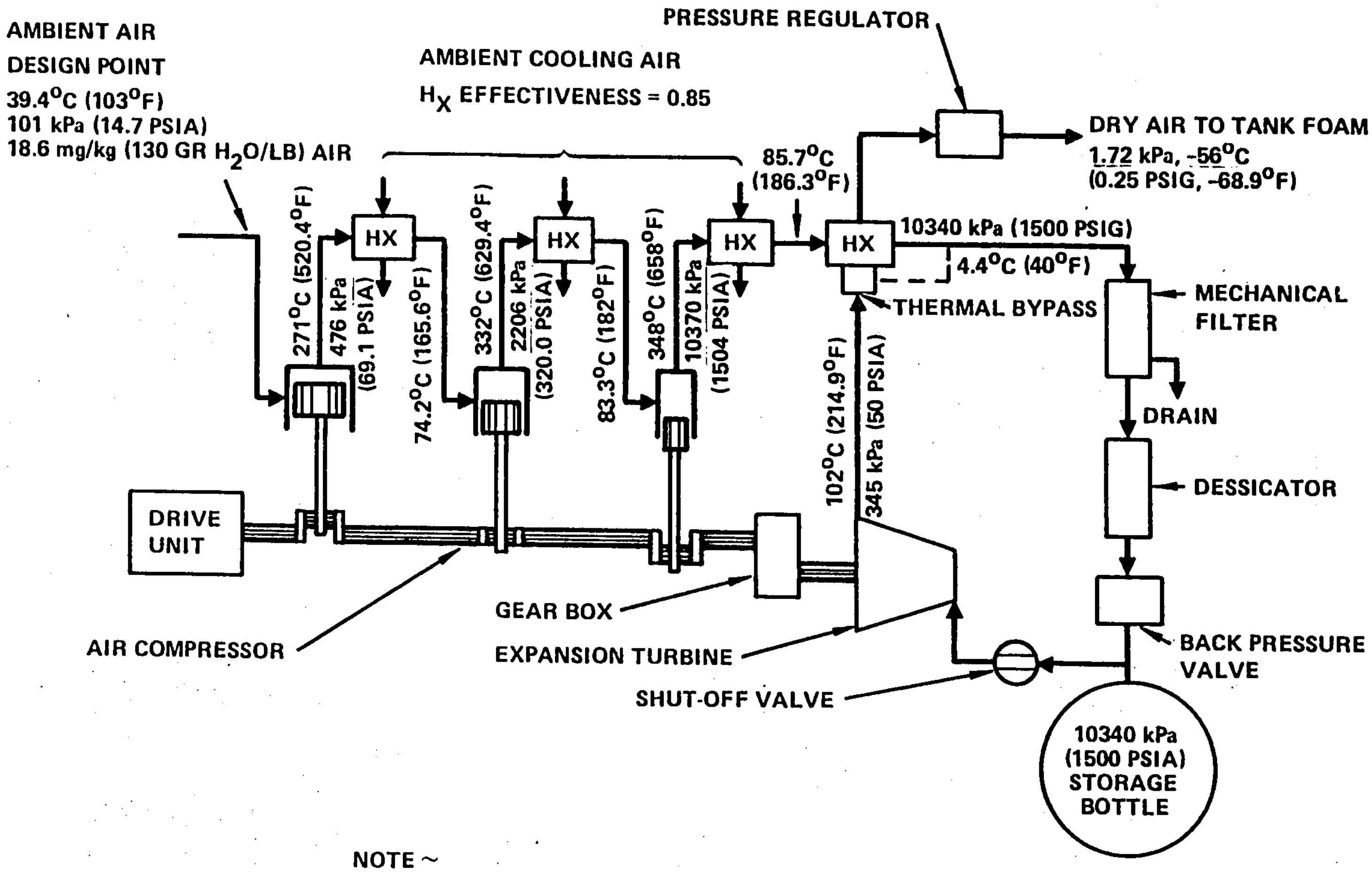

NOTE ~

SEA LEVEL UNPRESSURIZED PERFORMANCE SHOWN

Figure 73. - Foam purge air drier system.

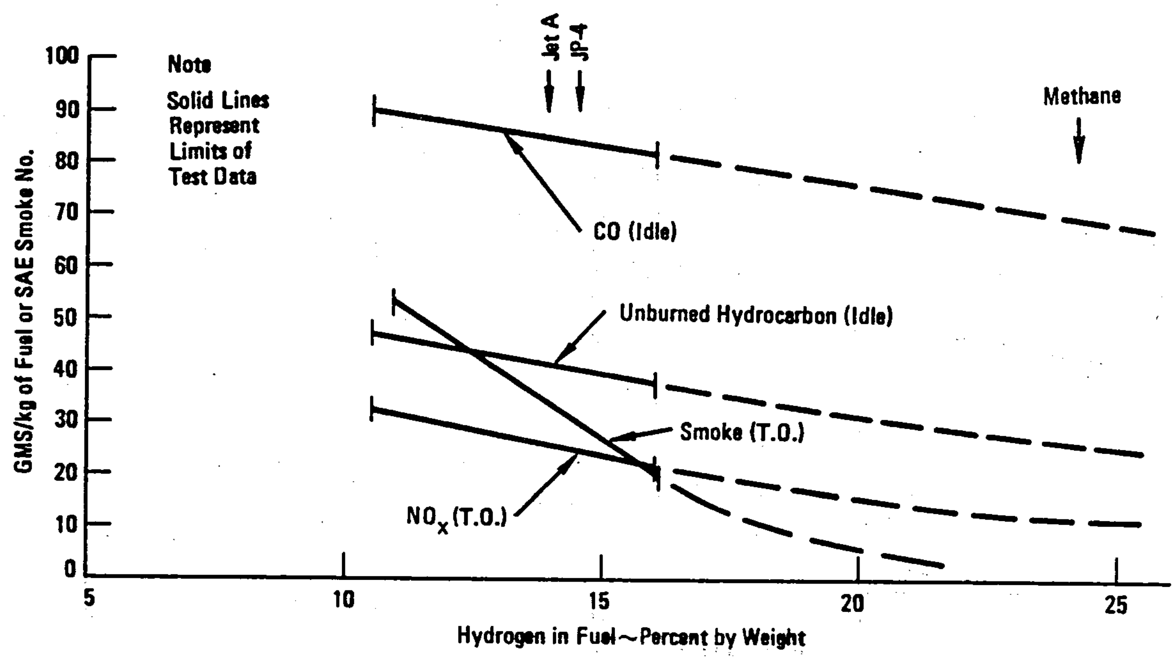

Figure 79. - Exhaust emissions from a single aircraft turbojet combustor (reference 101 NASA TM-73780)

positions of conventional Jet A and JP-4 fuels on the chart are shown for comparison. Although the absolute pollutant level for methane is somewhat questionable, it is obvious that burning methane will significantly reduce the contribution of aircraft to air pollution.

7. ENGINE-MOUNTED LIQUID METHANE HEAT EXCHANGERS

The turbine cooling air and oil cooler, heat exchangers, and the engine exhaust to fuel heater are all engine mounted as they were on the liquid hydrogen airplane of reference 4. The one exception to similarity between the two systems is that the ECS exchanger is not included in the methane system, because it cannot operate as a heat source to the engine exhaust exchanger in this system. This situation is illustrated in figure 80. The general arrangement on the engine is shown in figure 81.

Briefly, the key points of the analysis were arrived at in the following way: At 2.76 MPa (400 psia) and 677°K (1219°R), the enthalpy required is 2463 kJ/kg (1059.8 Btu/lb). The total change in enthalpy will be from the stored temperature of 117°K (210°R) to 1219°R (759°F).

In customary units: $\Delta H = (731.3 - 132.2) + (-1059.8 - (-)1308.7)$

$$= 599.1 + 248.9 = 848 \text{ Btu/lb}$$

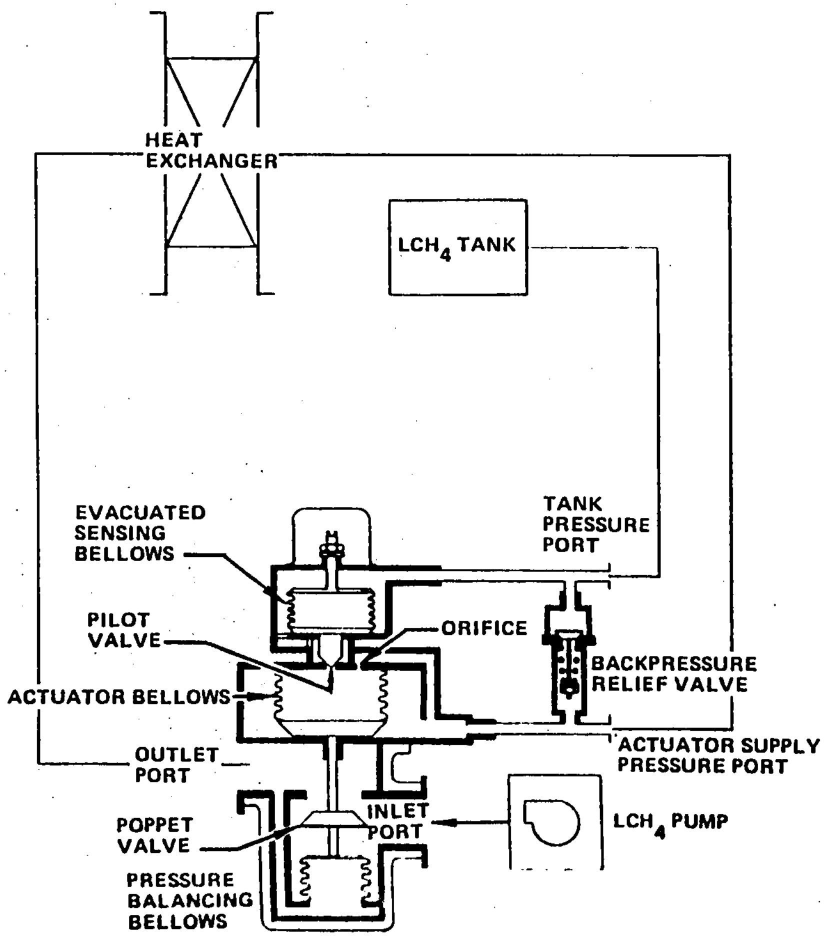

Description:

This unit is a poppet type absolute pressure regulator valve designed for cryogenic service. The valve regulates the pressure in a remotely located liquid methane tank by controlling the amount of fluid passing through the unit. The flow passes through the unit twice, once in the form of liquid and the second time in the from of gas.

Operation:

The liquid methane is routed from the inlet port through the normally open poppet valve to the outlet port. The outlet port is directed to a heat exchanger where the liquid is gasified. The gaseous methane is directed back to the unit to the actuator supply pressure port to a normally closed backpressure relief valve, to the external side of the actuator bellows, through an orifice to the internal side of the actuator bellows, and to a normally closed pilot valve.

As the pressure to the actuator supply pressure port continues to rise, the backpressure relief valve opens and bleeds off flow to the tank pressure port. The backpressure relief valve maintains the pressure at a predetermined value above the tank pressure port. Since the tank pressure port is connected to the methane tank it also provides a means of sensing the tank pressure to the evacuated sensing bellows.

As the tank pressure rises to calibrated setting of the evacuated sensing bellows, the evacuated sensing bellows moves to open the pilot valve which bleeds off the internal pressure of the actuator bellows. The flow into the actuator bellows is restricted by an orifice which creates a pressure differential across the actuator bellows, causing the poppet valve to modulate towards the closed position. This reduces the liquid flow through the heat exchanger, and reduces the pressure to the actuator supply pressure port. In turn, this action reduces the flow into the tank, to limit the tank pressure to the desired absolute valve.

The poppet is inlet pressure balanced by a bellows of identical area of the poppet valve and is exposed to the same differential pressure as the poppet but with a force reaction in the opposite direction. The exterior of the unit is insulated to limit the heat transfer into the flow media.

Figure 78. - Absolute tank pressure regulator.

6.2.5 Absolute tank pressure regulator.- The absolute tank pressure regulator is required to sense the tank absolute pressure, and supply methane as required to a vaporizing heat exchanger (boiler) to generate vapor for tank pressurization, if normal tank boil-off is not sufficient to maintain tank pressure at the primary relief valve absolute pressure level, table 36.

A schematic diagram and description of the valve design and operation are presented in figure 78.

TABLE 36. - PRESSURE REGULATOR DESIGN PARAMETERS

	Liquid Side	Gas Side
Rated flow	0.02 kg/sec (0.050 lb/sec)	0.02 kg/sec (0.050 lb/sec)
Pressure drop	1.77 kPa (0.256 psid)	77.33 kPa (11.22 psid)
Operating pressure	272.3 kPa (39.5 psia)	262.0 kPa (38.0 psia)
Regulated pressure	–	124 kPa (18.0 psia)
Duct diameter	0.960 cm (0.378 in)	0.960 cm (0.378 in)
Estimated MTBF	40 000 hr	

6.3 Environmental Emissions

In their efforts to control air pollution, the Environmental Protection Agency (EPA) instituted the control of aircraft engine exhaust emissions in 1974 when limits were applied to engine exhaust smoke. The EPA currently is negotiating with industry to establish and apply reasonable limits to gaseous exhaust emissions from aircraft engines consisting of oxides of nitrogen (NO_x), carbon monoxide (CO), and unburned hydrocarbons. These controls are expected to be in force as early as 1981; consequently, the aircraft engine industry has been trying to develop the technology and hardware necessary to meet them.

Emissions reduction by hardware changes are limited and depend to a large degree upon the type of fuel used. In this regard, clean-burning combustion research programs by the National Aeronautics and Space Administration (NASA) have revealed that the level of harmful exhaust emissions produced during the combustion process is inversely proportional to the percentage by weight of hydrogen in hydrocarbon fuels. This trend is illustrated in figure 79. The most critical conditions for smoke and NO_x production is at takeoff power. For CO and unburned hydrocarbon the most critical condition is at idle power. Hence, emission data for those powers only are shown. Although available test data range from 10.5 percent to 16 percent, the trend at higher hydrogen concentrations is apparent. The curves have been extrapolated in order to anticipate the effect of burning methane fuel on engine exhaust emissions. The

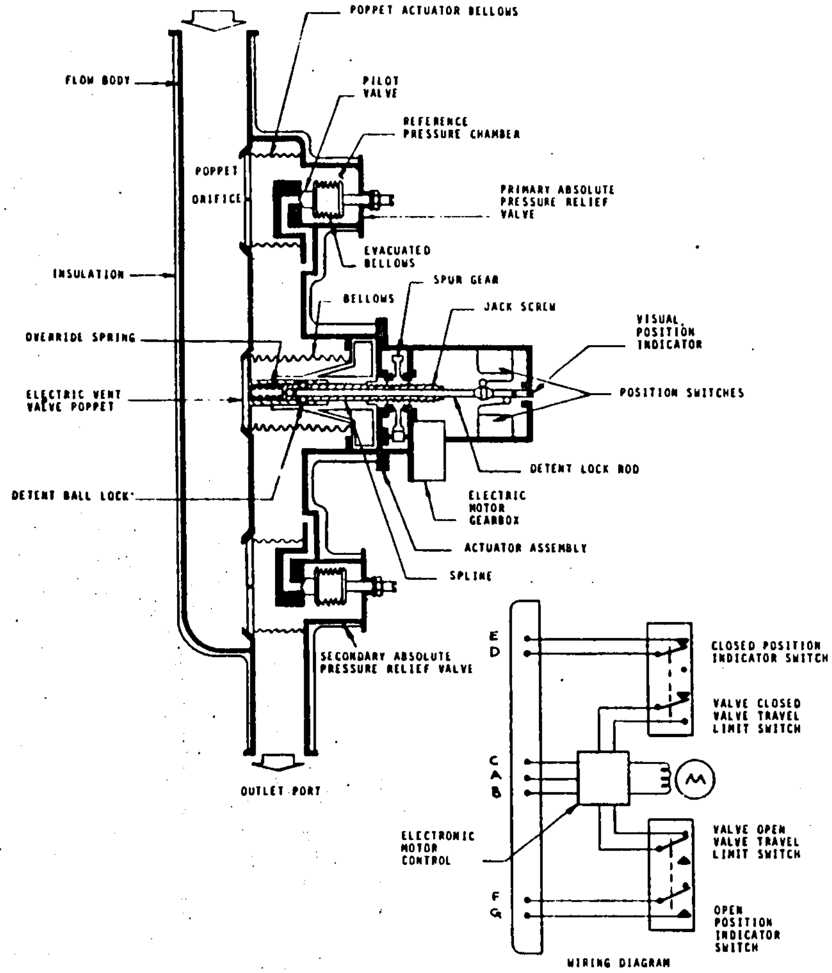

Description:

This unit is composed of a primary and secondary absolute pressure relief valve and an electric motor driven poppet type shutoff valve.

The unit functions to automatically maintain a fixed maximum absolute pressure in an aircraft cryogenic fuel system. The secondary absolute pressure regulator is calibrated above that of the primary to provide back up operation and greater flow capacity in the event of unusual upstream pressure transients. The remotely controlled electrically driven poppet valve can be actuated to bypass both absolute pressure relief valves to provide full venting of the fuel system.

The valve housing is insulated to reduce the heat transfer to the cryogenic flow media. All dynamic seals employ metal bellows to eliminate the need for any sliding seals.

The electric shutoff valve is operated by a reversible brushless electric motor driven actuator assembly. The actuator assembly is replaceable without opening the line. After removing the detent lock rod, the balls are free to decouple from the poppet assembly, allowing complete removal of the jack screw and actuator assembly. The detent lock rod has a tapered end to allow recoupling of the jack screw when reinstalling a new actuator assembly.

All electrical components are located outside of the flow media area.

<u>Pressure Relief Valve Operation</u>:

The primary absolute pressure relief valve poppet is held closed by the preload force in the poppet actuator bellows. When inlet pressure is applied, the orifice admits pressure to the reference pressure chamber and to the evacuated bellows. The evacuated bellows is calibrated so that when the inlet pressure is below the desired actuation point of the primary absolute pressure relief valve, the pilot valve is closed. This results in fluid pressure equalization across the poppet thus keeping the valve closed. As the inlet pressure increases to the desired actuation pressure, the evacuated bellows compresses slightly which moves the pilot valve to vent the reference pressure chamber to the outlet port. The resulting pressure differential acoss the orifice allows the inlet pressure force to overcome the poppet actuator bellows load to open the poppet and allow inlet pressure to vent to the outlet port. The evacuated bellows will respond to increases or decreases in upstream pressure, sensed through the orifice, to modulate the reference pressure chamber and thus the position of the primary relief valve poppet to maintain a fixed maximum upstream absolute pressure.

The secondary absolute pressure relief valve operates identically to the primary device. The evacuated bellows preload of the secondary system is greater than that of the primary device so as to increase the inlet pressure setting at which the device operates. In this way, the secondary valve provides a backup of the primary relief valve in case the primary pressure relief valve malfunctions or cannot accommodate the necessary flow.

<u>Shutoff Valve Operation</u>:

With the motor appropriately energized, the motor torque is transmitted to the spur gear which is threaded to the jack screw. The jack screw is splined to the flow body and coupled to the poppet assembly through the detent ball lock. As the spur gear rotates, the jack screw moves the poppet assembly to the full open or full closed position as desired.

An override spring is incorporated in the poppet assembly to limit the valve sealing force.

A visual position indicator is provided to indicate poppet position. Open and closed position switches are incorporated to limit valve travel and to provide remote position indication.

<u>Electrical Operation</u>:

Energize Pins C & A to close the valve.
Energize Pins C & B to open the valve.
Continuity between Pins E & D valve closed.
Continuity between Pins F & G valve open.

Figure 77. - Absolute tank pressure regulator (relief valve and vent valve).

maintain an absolute tank pressure of 155.1 kPa (22.5 psia). In the event of failure of the primary valve, the secondary valve maintains tank pressure at a higher value, thus revealing the primary valve malfunction. The electric motor shutoff valve is required for use as a purge gas vent valve when initially filling the system.

Significant parameters of the design are:

	Primary Pressure Relief Valve	Secondary Pressure Relief Valve
Rated Flow	0.01 kg/sec (0.022 lb/sec)	0.01 kg/sec (0.022 lb/sec)
Relief pressure	141.3 kPa (20.5 psia)	155.1 kPa (22.5 psia)
Pressure Drop	0.025 kPa (0.1 in. H_2O)	0.025 kPa (0.1 in. H_2O)
Duct diameter	7.32 cm (2.88 in.)	7.32 cm (2.88 in.)

Estimated MTBF is:

Primary pressure relief valve	50 000 hr
Secondary pressure relief valve	50 000 hr
Vent valve	15 000 hr

A schematic diagram and description of the valve design and operation are presented in figure 77.

Referring to the schematic drawings for the pressure relief valves, the operation may be understood as follows: Vapor from the tank bleeds through the poppet orifice into the reference pressure chamber and incurs a pressure drop through the orifice. The pilot valve and partially evacuated bellows bleed vapor from the reference pressure chamber as required to maintain the chamber absolute pressure at a preselected value. The resulting chamber pressure is determined by the design of the pilot valve and partially evacuated bellows, and by the position setting of the adjustment screw. The value of chamber absolute pressure is selected to be such that the resulting pressure force on the main poppet, plus the force of the poppet actuation bellows, is just equal to the desired tank pressure times the main poppet area. If the tank pressure slightly exceeds the desired value, the main poppet will open to a modulated position, thus venting vapor from the tank and thereby limiting further increase in tank pressure.

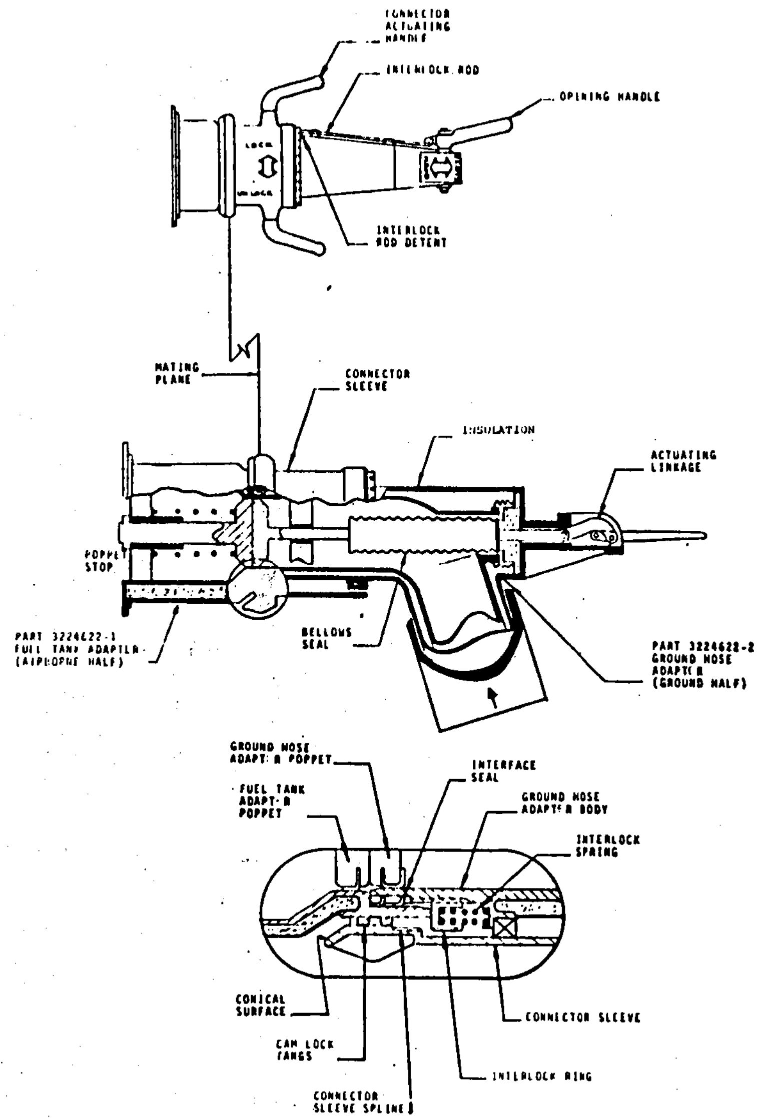

Description

This unit is a manually operated, aircraft fueling, quick disconnect shutoff valve, designed for cryogenic service. The unit consists of an airborne fuel tank adapter and a ground hose adapter.

Both components are insulated to minimize the heat transfer to the flow media. The evacuated double wall bellows seals in the ground hose adapter also contributes to isolate the ambient temperature from the flow media and in addition eliminates the requirement for a sliding shaft seal.

The unit is shown in the closed position, with ground hose adapter fully mated to the airborne fuel tank adapter. Dust caps are provided for use when the two elements are disconnected. Unit tolerances are such that any airborne fuel tank adapter can be mated to any ground hose adapter. The fueling quick disconnect components cannot be interchanged with the vapor recovery quick disconnect components shown in schematic P 3224674.

The design of the unit provides a minimum duct volume between the two halves to eliminate the need to purge the connection prior to opening the valve.

Operation:

To connect the two adapters, the ground hose adapter is manually positioned to the fuel tank adapter. The conical surface on the connector sleeve guides the two halves together so that the cam lock tangs are aligned and the interlock ring is displaced unlocking the connector sleeve from the ground hose adapter body. With the interlock ring in the position shown, the connector sleeve can be rotated in the direction shown. This action advances the cam lock tangs which fully mates the two halves, placing the poppets face to face and seating the interface seal.

When the connector sleeve is rotated to the fully locked position, the interlock rod detent aligns with the interlock rod.

To open the unit, the opening handle is rotated in the direction shown which advances the interlock rod into the detent and through the actuating linkage, displacing the two poppets to the full open position.

To disconnect the unit, the opening handle is first rotated back to the closed position which closes both poppets (as shown) and withdraws the detent on the connector sleeve interlock rod from the detent of the connector sleeve. The connector sleeve can then be rotated to the unlocked position to decouple the unit. As the two halves are separated, the interlock ring is spring loaded back into the connector sleeve spline preventing rotation of the connector sleeve.

The interlock ring prevents inadvertent rotation of the connector sleeve and subsequent opening of the ground hose adapter (by opening handle rotation) when not properly mated to the fuel tank adapter. The interlock rod prevents accidental decoupling of the unit when the valve is in the open position.

Figure 76. - Vapor recovery quick disconnect.

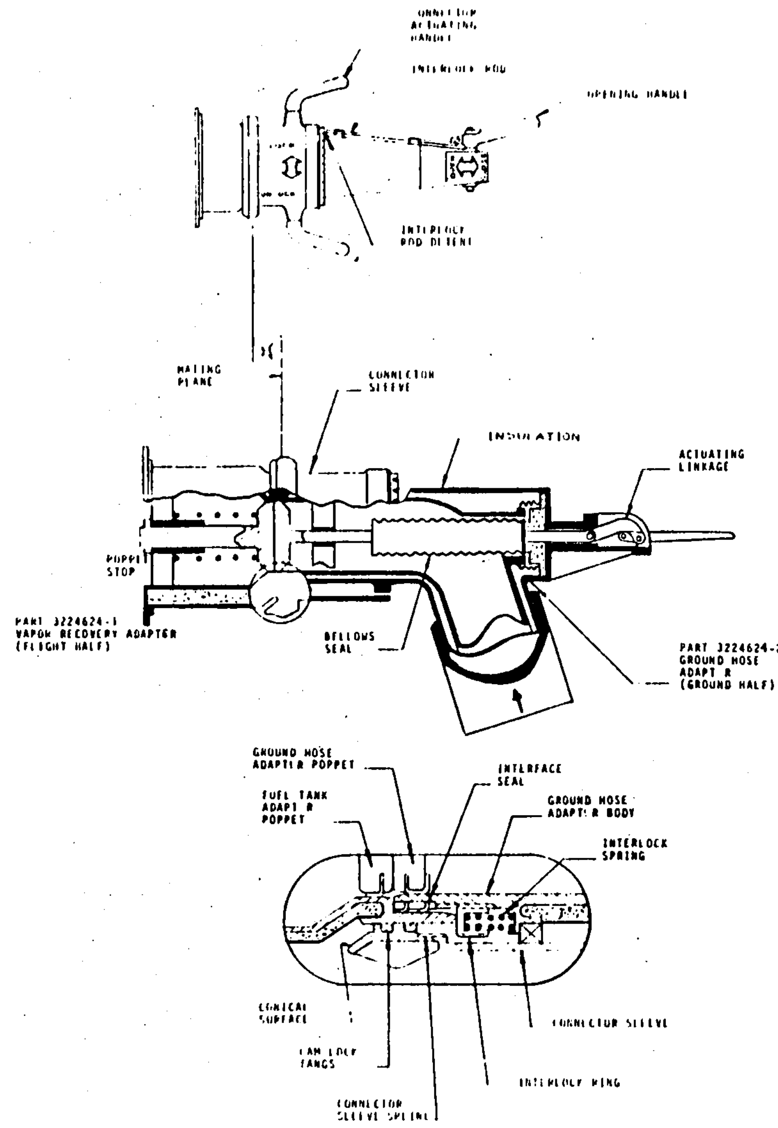

Description

This unit is a manually operated, vapor recovery, quick disconnect shutoff valve, designed for cryogenic service. The unit consists of an airborne vapor recovery adapter and a ground hose adapter.

Both components are insulated to minimize the heat transfer to the flow media. The evacuated double wall bellows seals in the ground hose adapter also contributes to isolate the ambient temperature from the flow media and in addition eliminates the requirement for a sliding shaft seal.

The unit is shown in the closed position, with the ground hose adapter fully mated to the airborne fuel tank vapor adapter. Dust caps are provided for use when the two elements are disconnected. Unit tolerances are such that any airborne fuel tank vapor recovery adapter can be mated to any ground hose adapter. The vapor recovery disconnect components cannot be interchanged with the aircraft fueling quick disconnect components shown in schematic P 3224622.

The design of the unit provides a minimum duct volume between the two halves to eliminate the need to purge the connection prior to opening the valve.

Operation:

To connect the two adapters, the ground hose adapter is manually positioned to the fuel tank vapor recovery adapter. The conical surface on the connector sleeve guides the two halves together so that the cam lock tangs are aligned and the interlock ring displaced unlocking the connector sleeve from the ground hose adapter body. With the interlock ring in the position shown, the connector sleeve can be rotated in the direction shown. This action advances the cam lock tangs which fully mates the two halves, placing the poppets face to face and seating the interface seal

When the connector sleeve is rotated to the fully locked position, the interlock rod detent aligns with the interlock rod.

To open the unit, the opening handle is rotated in the direction shown which advances the interlock rod into the detent and through the actuating linkage, displacing the two poppets to the full open position.

To disconnect the unit, the opening handle is first rotated back to the closed position, which closes both poppets (as shown) and withdraws the interlock rod from the detent on the connector sleeve. The connector sleeve can then be rotated to the unlocked position to decouple the unit. As the two halves are separated, the interlock ring is spring loaded back into the connector sleeve spline preventing rotation of the connector sleeve.

The interlock ring prevents inadvertent rotation of the connector sleeve and subsequent opening of the ground hose adapter (by opening handle rotation) when not properly mated to the fuel tank vapor recovery adapter. The interlock rod prevents accidental de-coupling of the unit when the valve is in the open position.

Figure 75. - Ground fueling quick disconnect.

6.2.3 Vapor recovery quick disconnect.- The vapor recovery quick disconnect is a manually operated quick disconnect and shutoff valve assembly, intended for use in vapor recovery during the aircraft fueling operation. The unit consists of an airborne adapter mounted in the aircraft at the fueling interface, and a ground hose adapter mounted at the end of the ground vapor recovery line. Each unit includes an internal valve which is normally seated, preventing flow through the valve, and which is automatically unseated when the two mating units are joined and secured to each other.

It is a design requirement that no hazard to personnel or equipment occurs if ice forms on the units prior to, during, or after the fueling operation, and that the presence of ice on either mating unit does not interfere with the mating process. In addition, it is required that the design of the mating units does not permit ingestion of ice, water or other contaminants into the system during the filling process.

The adapter in the aircraft must be easily replaceable and designed to break away without damage to the aircraft if the supply truck pulls away from the aircraft without disconnecting the supply hose, and that the part of the adapter remaining in the aircraft automatically closes in the event of a break, to preclude the loss of methane.

The quick disconnect must be suitable for manual handling, installation, and control, by personnel wearing the necessary protective gloves and clothing, and the required manual force of installation and actuation must not exceed 22.2 daN (50 lb).

From the safety viewpoint, the ground vapor recovery adapter must be designed to preclude inadvertent mating with the fueling nozzle. Furthermore, complete electrical contact must be established between the two adapters before they are connected, and the contact resistance must not exceed 10 ohms.

Significant parameters of the design are:

Rated flow	0.32 kg/sec (0.70 lb/sec)
Pressure drop	3.45 kPa (0.50 psid)
Operating pressure	137.9 kPa (20.0 psia)
Duct diameter	7.32 cm (2.88 in.)

A schematic diagram, and description of the quick disconnect design and operation are presented in figure 76.

6.2.4 Absolute tank pressure relief and vent valve.- The absolute tank pressure relief and vent valve is an assembly consisting of two tank pressure relief valves and an electric motor driven shutoff valve. One tank pressure relief valve is designated the primary relief valve and is designed to maintain an absolute tank pressure of 141.3 kPa (20.5 psia) and the other tank pressure relief valve is designated the secondary relief valve and is designed to

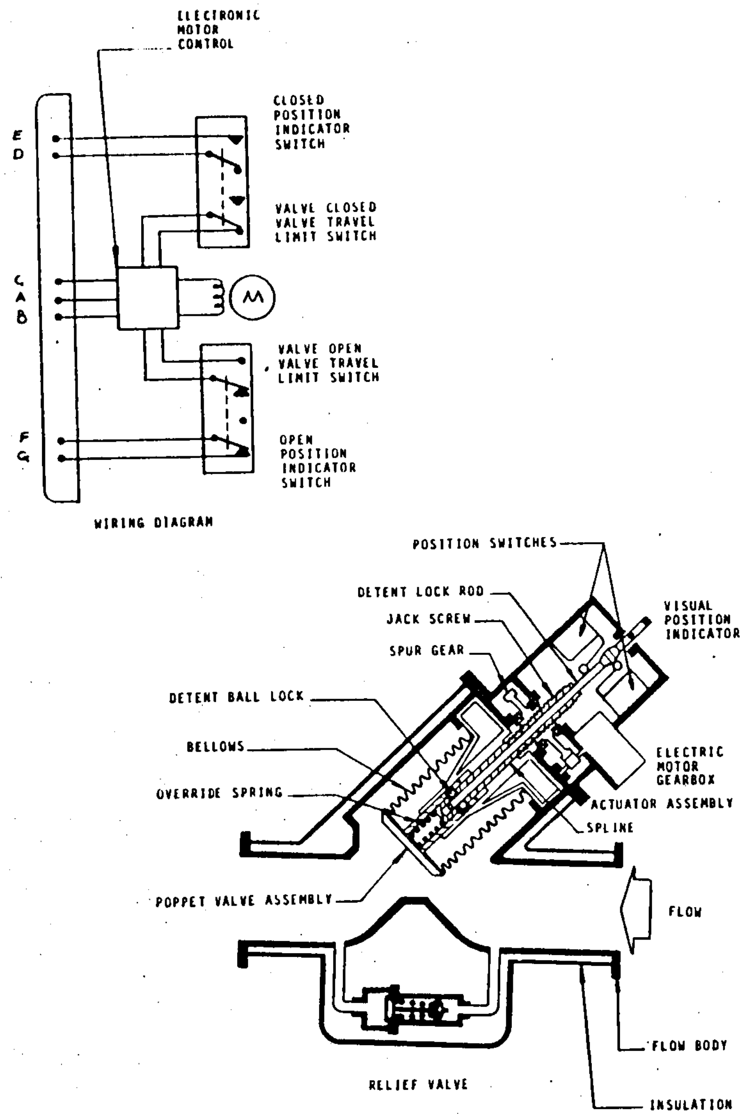

Description:

This is an electric motor operated poppet-type shutoff valve designed for cryogenic operation.

The valve has an insulated flow body to reduce heat transfer to the cryogenic flow media. The flow body has an integral bellows-sealed poppet assembly which eliminates the need for any sliding seals.

The valve is operated by a reversible brushless electric motor driven actuator assembly. The actuator assembly is replaceable without opening the cryogenic line. After removing the detent lock rod, the balls are free to de-couple from the poppet assembly, allowing complete removal of the jack screw and actuator assembly. The detent lock rod has a tapered end to allow re-coupling of the jack screw rod when re-installing a new actuator assembly.

All electrical components are located outside of the flow media area.

Operation:

With the motor appropriately energized, the motor torque is transmitted to the spur gear which is threaded to the jack screw. The jack screw is splined to the flow body and coupled to the poppet assembly through the detent ball lock. As the spur gear rotates,the jack screw moves the poppet assembly to the full open or full closed position, as desired.

An override spring is incorporated in the poppet assembly to limit the valve sealing force.

A visual position indicator is provided to indicate poppet position. Open and closed position switches are incorporated to limit the valve travel and to provide a remote indication when the valve is in the open or closed position.

A pressure relief valve is provided to prevent excessive pressure build-up due to thermal expansion of the flow media when the valve is in the closed position.

Electrical Operation:

Energize Pins C & A to close the valve.
Energize Pins C & B to open the valve.
Continuity between Pins E & D valve closed.
Continuity between Pins F & G valve open.

Figure 74. - Fuel level control shutoff valve.

For this valve and the following selected components to be discussed, the conceptual design, estimates of performance, and MTBF (mean time between failures) are based upon experience with similarly designed equipment. In addition, the nonrecurring design and development costs, and the production costs in the quantity of 350 ship sets plus 20 percent spares were estimated, and the results used as an input to the evaluation of aircraft costs.

6.2.2 Ground fueling quick disconnect.- The ground fueling quick disconnect is a manually operated, aircraft fueling quick disconnect and shutoff valve assembly, intended for use in the aircraft fueling operation. The unit consists of an airborne adapter mounted in the aircraft at the fueling interface, and a ground hose adapter mounted at the end of the ground fueling line. Each unit includes an internal valve which is normally seated, preventing flow through the valve, and which is automatically unseated when the two mating units are joined and secured to each other.

It is a design requirement that no hazard to personnel or equipment occurs if ice forms on the units prior to, during, or after the fueling operation, and that the presence of ice on either mating unit does not interfere with the mating process. In addition, it is required that the design of the mating units does not permit ingestion of ice, water, or other contaminants into the system during the filling process.

It is required that the adapter in the aircraft be easily replaceable and designed to break away without damage to the aircraft if the supply truck pulls away from the aircraft without disconnecting the supply hose, and that the part of the adapter remaining in the aircraft automatically closes in the event of a break, to preclude a spill of methane from the aircraft.

The quick disconnect must be suitable for manual handling, installation, and control by personnel wearing the necessary protective gloves. The required manual force of installation and actuation must not exceed 22.2 daN (50 lb).

From this safety viewpoint, it is required that the ground fueling adapter be designed to preclude inadvertent mating with the vapor recovery nozzle. It is further required that complete electrical contact be established between the two adapters before they are connected, and that the contact resistance does not exceed 10 ohms.

Significant parameters of the design are:

Rated flow	52.2 kg/sec (115 lb/sec)
Pressure drop	34.5 kPa (5.0 psid)
Operating pressure	275.8 kPa (40.0 psia)
Duct diameter	9.86 cm (3.99 in.)

A schematic diagram, and description of the quick disconnect design and operation are presented in figure 75.

$-73.3^{\circ}C$ ($-100^{\circ}F$) and is the purge air for the foam surrounding the tank insulation. The low dew point at sea level ensures that no moisture will condense and form ice in the foam. A pressure regulator senses the pressure in the foam and maintains it at 1.72 kPa (0.25 psig) above outside ambient.

The compressor inlet is supercharged to 172.3 kPa (25 psig) by engine bleed air in flight. To ensure that a sufficient quantity of purge air is available in extremely rapid rates of descent, a pressurized accumulator which contains sufficient air to pressurize the foam to sea level density from an altitude of over 12 192 m (40 000 ft) has been added to the system.

An estimate of the weight of this system is contained in table 35.

This total weight of 86.4 kg (190.4 lb) for supplying dry air to the foam purge distribution system for both flight and layout conditions represents a significant reduction in weight penalty when compared to the 134.9 to 378.8 kg (297.5 to 835 lb) required for storing liquid nitrogen.

TABLE 35. - AIR PURGE SYSTEM WEIGHT ESTIMATE

Component	Weight	
	kg	(lb)
Compressor & Interstage Coolers	11.34	(25.0)
Drive Unit (400 hertz, 200 volt, 3ϕ)	9.07	(20.0)
Expansion Turbine	9.07	(20.0)
Gear Box	9.07	(20.0)
Aftercooler	1.36	(3.0)
Mechanical Filter	6.35	(14.0)
Dessicator	9.07	(20.0)
Backpressure Valve	0.68	(1.5)
Air Storage Bottle	20.87	(46.0)
Shutoff Valve	0.48	(1.05)
Pressure Regulator	0.91	(2.0)
Relief Valve	0.23	(0.5)
Plumbing & Contingencies (+ 10%)	7.85	(17.3)
Total	86.34	(190.4)

6.2 Design Concepts for Major Methane Fuel System Components

Five fuel system components having critical operational requirements or technically challenging design requirements were selected for conceptual design studies. The components studied were:

- Fuel level control shutoff valve
- Ground fueling quick disconnect
- Vapor recovery quick disconnect
- Absolute tank pressure relief and vent valve
- Absolute tank pressure regulator

Operational and performance requirements were established for each selected component based upon the preliminary fuel system analysis. These requirements were used as the starting point for the component conceptual designs and, in some instances, iteration of the requirements was performed to ensure or improve development feasibility.

In addition, some general design requirements were established which applied to all components. These requirements had to do with materials compatibility with methane, materials corrosion resistance, avoidance of dissimilar metals in contact, accessibility of the component for installation and adjustment and, in some cases, means for indicating satisfactory functioning or failure. These general requirements were also considered in the analysis and selection of the individual component design concepts.

6.2.1 Fuel level control shutoff valve.- The fuel level control shutoff valve is an electric motor operated valve, having the purpose of admitting and stopping the flow of fuel to a fuel tank. In addition, it has the special requirement for a pressure relief valve set at 1.25 times the maximum stabilized blocked fueling line pressure to provide for thermal pressure relief of the fueling line after valve closure. Significant parameters of the design are:

Rated flow	13.05 kg/sec (27.5 lb/sec)
Pressure drop	23.2 kPa (3.36 psid)
Operating pressure range	241 to 193 kPa (35 to 28 psia)
Operating temperature range	116.7^{o}K to 328^{o}K (210^{o}R to 590^{o}R)
Duct diameter	5.08 cm (2.00 in.)
Estimated MTBF	15,000 hr

A schematic diagram, and description of the valve design and operation are presented in figure 74.

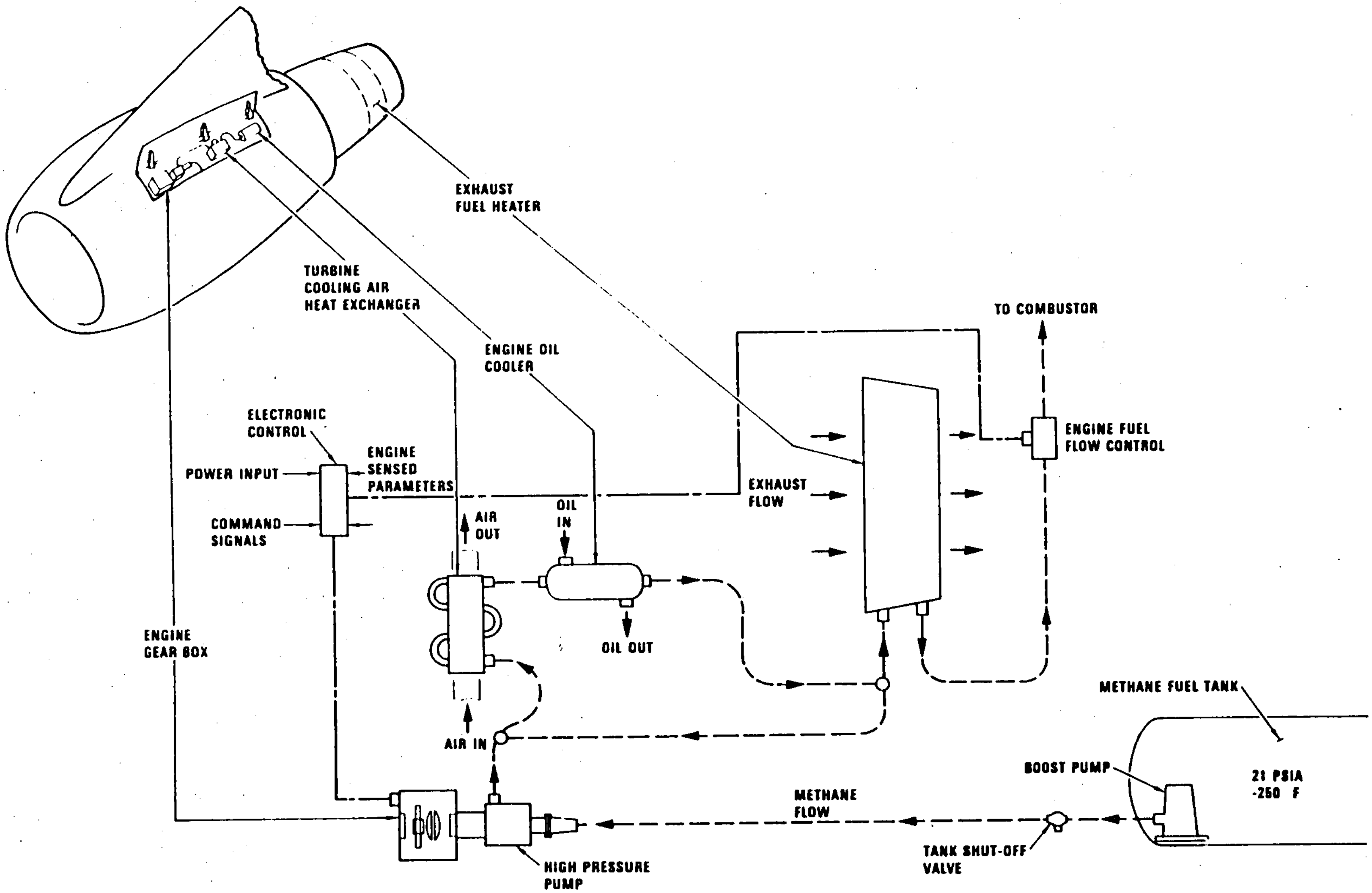

Figure 81. - LCH_4 engine fuel and heat exchanger system.

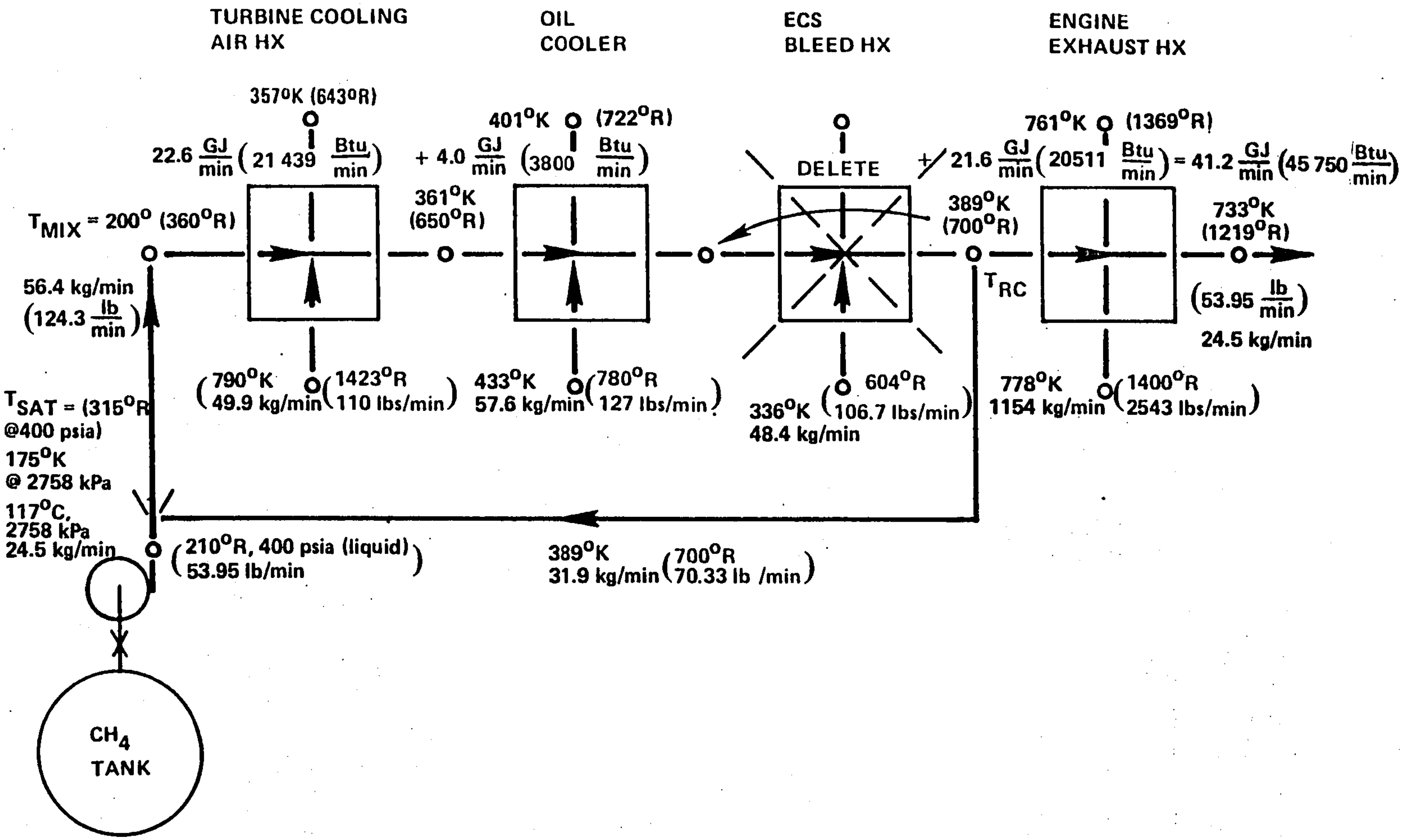

Figure 80. - Engine-mounted liquid methane heat exchanger system.

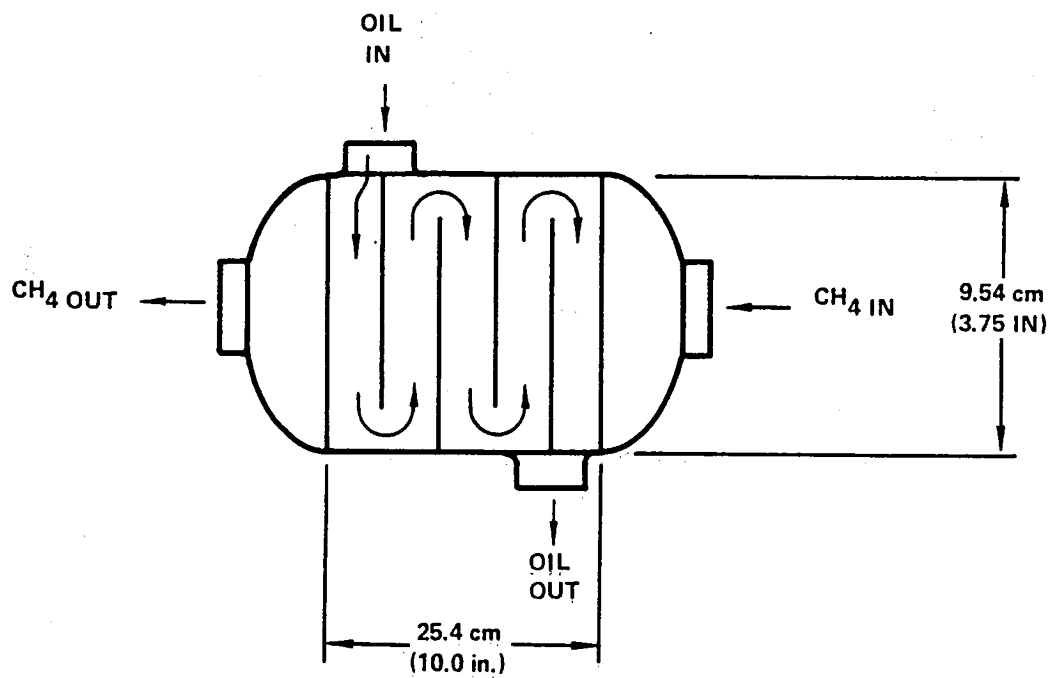

TUBES

TUBE O.D.	0.32 cm (0.125 in.)
TUBE WALL	0.030 cm (0.012 in.)
TUBE MATERIAL	304 CRES
TOTAL NUMBER OF TUBES	528
NUMBER OF METHANE PASSES	1
NUMBER OF OIL PASSES	5
TUBE WEIGHT	2.95 kg (6.5 lb)
TOTAL HEAT EXCHANGER WEIGHT	6.80 kg (15 lb)

Figure 83. - Engine oil to methane heat exchanger.

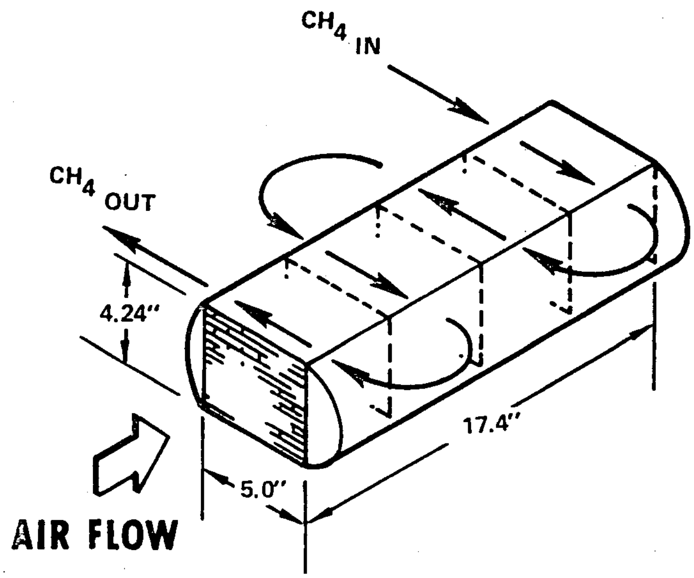

AIRFLOW LENGTH	44.2 cm (17.4 in.)
WIDTH	12.7 cm (5.0 in.)
HEIGHT	10.77 cm (4.24 in.)
FINNED TUBES	
TUBE O.D.	0.64 cm (0.25 in.)
TUBE WALL	0.04 cm (0.016 in.)
TUBE MATERIAL	304 CRES
FIN O.D.	1.27 cm (0.50 in.)
FIN SPACING	0.06 cm (0.025 in.)
FIN THICKNESS	0.010 cm (0.004 in.)
FIN MATERIAL	OFHC COPPER
FIN AND TUBE COATING	NiCr
TOTAL NUMBER TUBES	320
NUMBER METHANE PASSES	4
TUBE WEIGHT	7.71 kg (17.0 lb)
TOTAL HEAT EXCHANGER WT	18.1 kg (40 lb)

Figure 82. - Turbine-cooling air to methane heat exchanger.

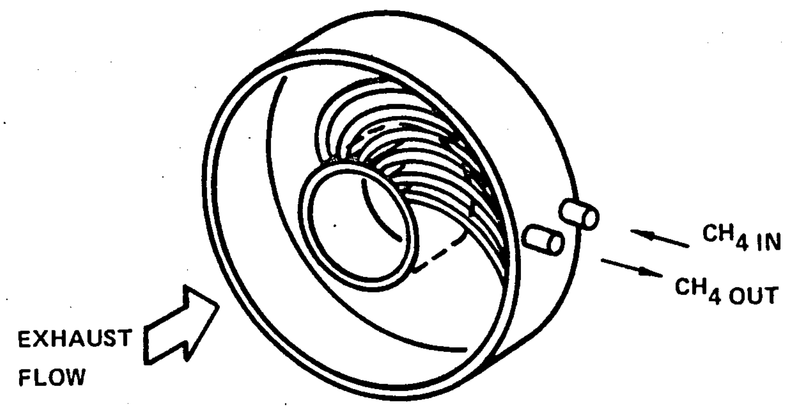

OUTSIDE DIAMETER	126.5 cm (49.8 in.)
INSIDE DIAMETER	56.4 cm (22.2 in.)
AIR FLOW LENGTH	9.53 cm (3.75 in.)
INVOLUTE TUBE LENGTH	56.9 cm (22.4 in.)
CIRCUMFERENTIAL TUBE SPACING	6 DIAMETERS
AXIAL TUBE SPACING	1.25 DIAMETERS
TUBE O.D.	0.478 cm (0.188 in.)
TUBE WALL	0.030 cm (0.012 in.)
TUBE MATERIAL	304 CRES
TOTAL NUMBER OF TUBES	1008
NUMBER OF METHANE PASSES	4
TUBE WEIGHT	19.46 kg (42.9 lb)
TOTAL HEAT EXCHANGER WEIGHT	40.8 kg (90 lb)

Figure 84. - Engine exhaust fuel heater.

The equivalent flow rate of methane as compared to hydrogen is estimated from 15.6°C (60°F) where the lower heating value of methane is 50.0 mJ/kg (21 518 Btu/lb). The change in enthalpy from 15.6°C to 422°C (60°F to 759°F) is estimated at (-1059.8 - (-)1546.2) = 486.4 Btu/lb. Therefore, the total heating value is 21 518 + 486 = 51.1 mJ/kg (22 004 Btu/lb).

Similarly for hydrogen, the LHV is 119.9 mJ/kg (51 590 BTU/lb). The increment from 15.6°C (60°F) to 422°C (759°F) is 5.85 mJ/kg (2516.4 Btu/lb). The total heat value is then 125.7 mJ/kg (54 100 Btu/lb). The relative flow of methane is then:

$$\frac{54\ 100}{22\ 000} = 2.459$$

The hydrogen flow rate in cruise was 9.95 kg/min (21.94 lb/min) so the corresponding methane weight flow is:

$$\text{Weight } CH_4 = 2.459\ (21.94) = 24.47 \text{ kg/min } (53.95 \text{ lb/min})$$

The maximum amount of heat added to the methane is then:

$$\text{Total Heat} = \text{weight X } \Delta \text{ H} - 53.95 \text{ X } 848$$

$$= 106.5 \text{ mJ/kg } (45\ 750 \text{ Btu/min) to reach}$$

$$677^\circ\text{K } (1219^\circ\text{R})$$

The prime reason for the selection of 200°K (360°R) as the mixed recirculation fuel inlet temperature is to prevent the freezing of water condensate in the turbine-cooling air heat exchanger. With the 200°K (360°R) inlet temperature, the minimum tube wall temperature is 323°K (581°R), well above the freezing point of water at 273.3°K (492°R). In addition, the fuel inlet temperature of 200°K (360°R) will keep the methane as a single-phase gas, thus simplifying and eliminating two-phase design uncertainties for the turbine cooling heat exchanger.

The other salient points of the system as shown in figure 8-81 are:

- The methane is all vaporized in mixing.

- The ECS bleed exchanger is eliminated.

- Relative to the hydrogen system, the oil cooler inlet temperature has been raised by 100 degrees to 433°K (780°R) to allow sufficient log mean temperature difference (LMTD) for that exchanger.

- The turbine-cooling air exchanger load was decreased by 15 percent, also to allow sufficient LMTD for the oil cooler.

This system has been used for heat-exchanger sizing. Table 37 is a tabulation of all heat-exchanger design conditions. Figures 82, 83, and 84 show the configurations, flow patterns, and physical characteristics of each.

8. FUEL TANK INSULATION

Previous studies (references 3, 4, and 17) of cryogenically fueled aircraft have proposed a number of insulation concepts for various flight missions. Under the current program, six of the more promising concepts were systematically investigated to derive a system(s) to optimize the LCH_4 subsonic transport aircraft design. Initially, the six concepts were subjected to a screening level of analysis to provide preliminary design data inputs for selection of the preferred aircraft configuration. Once the configuration was established, an in-depth analysis was carried out to optimize the candidate insulation for each aircraft fuel tank.

During the concept screening phase, the six insulation systems were evaluated with regard to safety, performance, producibility, and operational requirements. Five fuel tank geometries were considered in this phase. After selection of the most promising candidate insulation, this system was optimized using a detailed thermodynamic analysis program. Potential performance benefits derived from fuel subcooling were also investigated.

TABLE 37. - LIQUID METHANE HEAT-EXCHANGER DESIGN CONDITIONS

	Turbine Cooling Air HX	Oil Cooler	Engine Exhaust HX
Total Heat Transferred, kJ/min (Btu/min)	22 634 (21,434)	4012 (3800)	21 660 (20 511)
Shell Side Air (Oil) Flow, kg/min (lb/min)	49.9 (110)	57.6 (127)	1144 (2523)
Air (Oil) Inlet Temp., ^oK (^oR)	791 (1423)	433 (780)	778 (1400)
Air (Oil) Outlet Temp., ^oK (^oR)	357 (643)	401 (722)	760 (1369)
Air Inlet Pressure, kPa (psia)	1515.5 (219.8)	–	40.04 (5.81)
Air Pressure Drop $\Delta P/P$ inlet	0.028	–	0.017
Oil Pressure Drop, kPa (psi)	–	112 (16.2)	–
Shell Side Effectiveness	0.734	0.450	0.0442
Tube Side Methane Flow, kg/min (lb/min)	56.38 (124.3)*	56.38 (124.3)*	24.47 (53.95)
Methane Inlet Temperature, ^oK (^oR)	200 (360)	361 (650)	389 (700)
Methane Outlet Temperature, ^oK (^oR)	361 (650)	389 (700)	677 (1219)
Methane Pressure Drop, kPa (psi)	57.9 (8.4)	66.9 (9.7)	17.2 (2.5)
Tube Side Effectiveness	0.272	0.387	0.742

*Recirculation flow of 70.3 lb/min methane required to prevent water condensate from freezing in the turbine-cooling heat exchanger and to avoid two-phase flow on the methane side. Methane temperature before mixing recirculation flow is 210^{o}R (-250^{o}F).

8.1 Design Criteria And Concepts

Selection of the insulation system for a commercial LCH_4-fueled transport aircraft fuel system is constrained by the requirements of maintaining minimum operating costs and achieving a very high level of safety throughout the aircraft lifetime. To realize cost goals, the system must combine lightweight construction with low heat transfer characteristics, the latter consistent with in-flight tank pressurization requirements; have a high reliability, long life cycle; and have development and initial costs commensurate with commercial aircraft practices. Safety considerations must include not only loss of life or aircraft during a flight or ground operation incident, but also failures potentially dangerous to maintenance operations. Design requirements and safety, performance, and operational criteria were established for the fuel containment system of the aircraft. Prior cryogenically fueled aircraft study results and commercial and aerospace experience with cryogenic insulations were used to develop thermal performance data and to evaluate potential problem areas and assess the applicability of each insulation concept.

8.1.1 Criteria.- The general criteria for evaluation and ranking of the insulation concepts are as follows:

- Safety - No single or probable combination of failures will lead to loss of life or aircraft. Assessment of failure modes and their overall impact is to be consistent with current or anticipated safety practices applicable to commercial aircraft in 1990-1995 and to storage and handling of liquid methane. Modes of failure are accidental penetration of exterior surfaces, air or LCH_4 leakage into insulation or aircraft, malfunction of purge or vacuum system and associated control components, toxicity of products in event of external fire.

- Performance - Minimization of aircraft direct operating cost (DOC). DOC is evaluated as a function of system inert weights (including accessories associated with purge/vacuum concepts), fuel vaporized to maintain tank pressure and nonrecoverable fuel loss (vent) weights, system volume, and maintenance requirements (inspection/repair/replacement).

- Producibility - Each system must be designed so it can be fabricated and assembled consistent with aircraft practices.

- Operations - Inspection, servicing, and maintenance requirements and life expectancy should be consistent with current airline operating practices. Costs estimates are for production of 350 ship sets plus 20 percent spares. If costs are competitive, the selection favored the concept with the lowest energy consumption.

8.1.2 Concepts.- Based upon the results of a LH_2-fueled aircraft study (reference 4) six insulation concepts were selected for initial evaluation for application to the LCH_4 aircraft fuel tanks. The insulations were as follows:

1. Internal reinforced closed cell foam (SIV-B Type)
2. Internal open cell foam (PPO)
3. Internal perforated honeycomb
4. External closed cell foam
5. External flexible vacuum jacket, microsphere insulation
6. External GN_2 purged fiberglass

Insulation concepts using helium-purging or combinations of insulations, such as a self-evacuating honeycomb substrate with external foam or GN_2 purged fiberglass, were not considered for this application as liquefaction of air products on the tank wall is not a consideration for the methane case. High-vacuum MLI insulation, as is achieved with a rigid vacuum shell offers no heat transfer benefit for the LCH_4 system. Finally, self-evacuating concepts would not operate with air products as the interstitial gas because of the relatively high temperature for LCH_4 storage. It would be necessary to fill such a system with a higher molecular weight gas which would condense as a solid at the LCH_4 tank wall temperature. Prevention of replacement of this gas by air (noncondensible) diffusion over an extended time period would present a major technology problem.

Figure 85 illustrates the general configuration of each concept. The vacuum and purge systems schematics for the latter two concepts are shown by figures 86 and 87, respectively.

The three basic fuel tank concepts of all fuel in fuselage, fuel in wing plus fuselage and fuel in wing and wing-mounted pylon tanks involve five basic tank configurations. These are:

- Conical aft tank
- Spherical forward tank
- Toroidal forward tank
- High length-to-diameter cylinder (pylon)
- Low depth-to-width rectangular tank (wing).

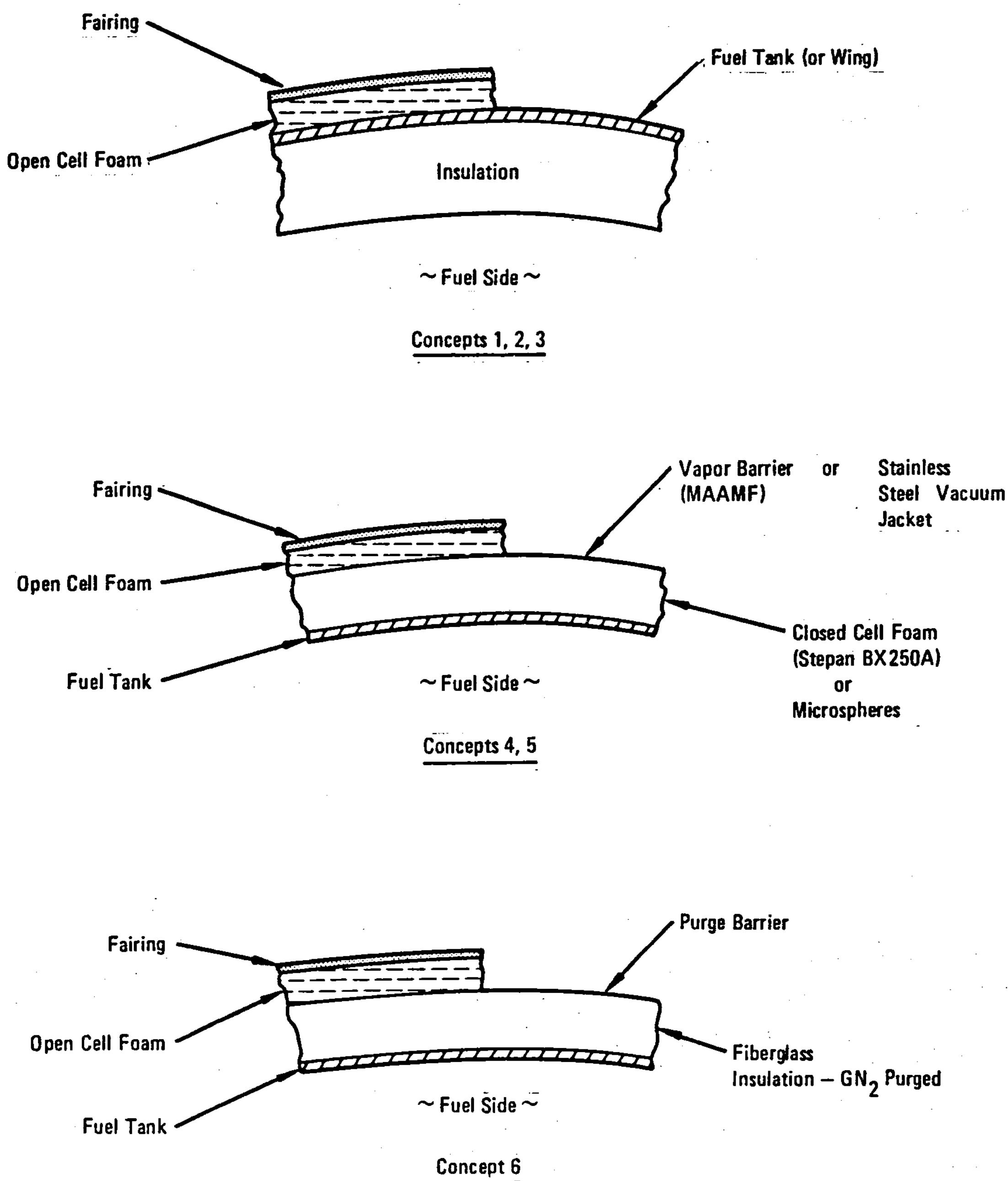

Figure 85. - Schematic of insulation concepts.

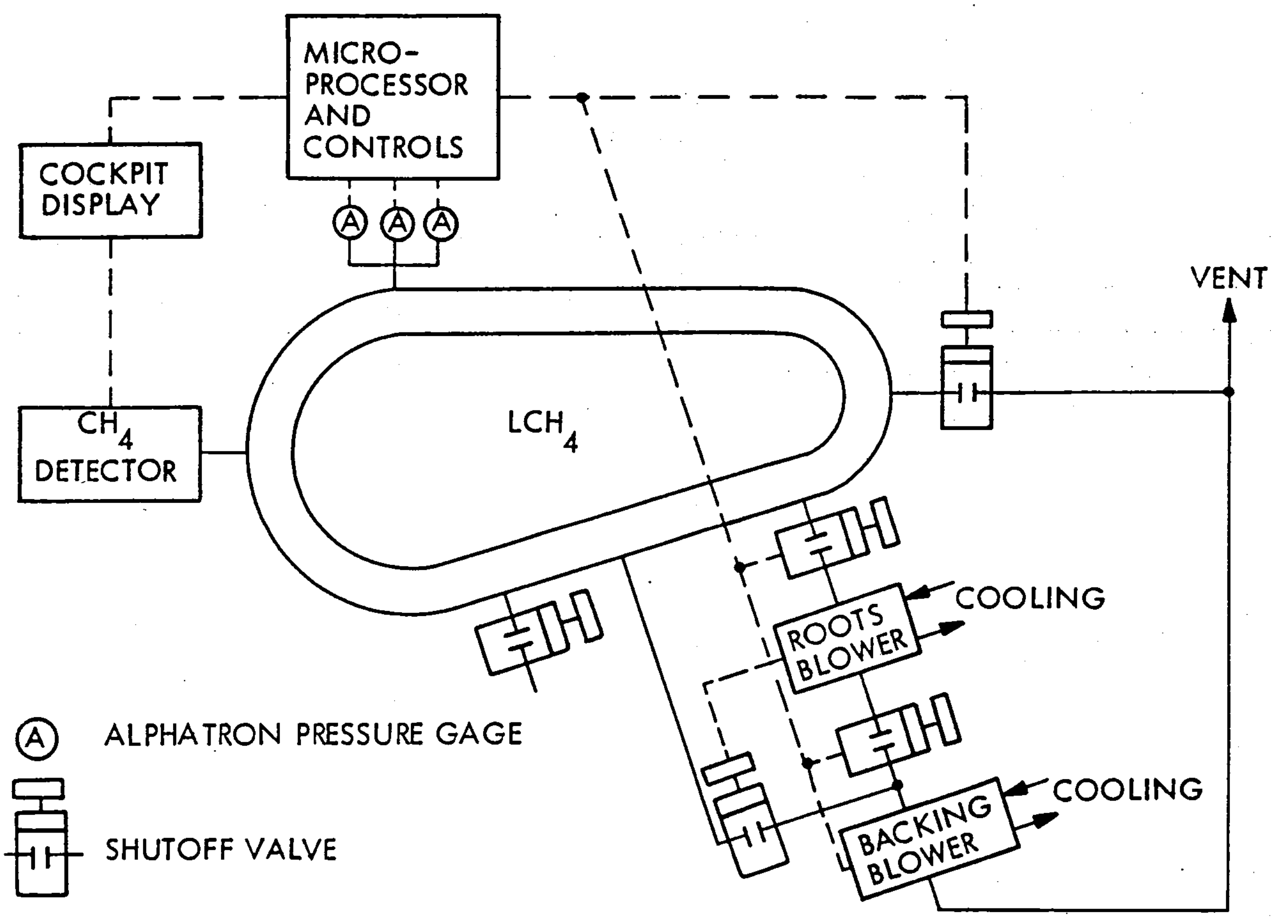

Figure 86. - Vacuum system for evacuated microsphere insulation system no. 5.

All insulations were not analyzed for each tank as producibility and operational considerations preclude some combinations. An internal insulation is required for the wing tanks if reasonable sizes and volumes are to be realized. A nonintegral tank (separate fuel tank with insulation, all contained within the wing structure) presents major installation and servicing problems and also is thermally very inefficient. The latter arises from the very large surface area-to-volume ratio for this tank configuration. Pylon tanks also require a lower thermal conductivity insulation because of their large surface-to-volume ratio. Table 38 presents the insulations analyzed for each type of tank.

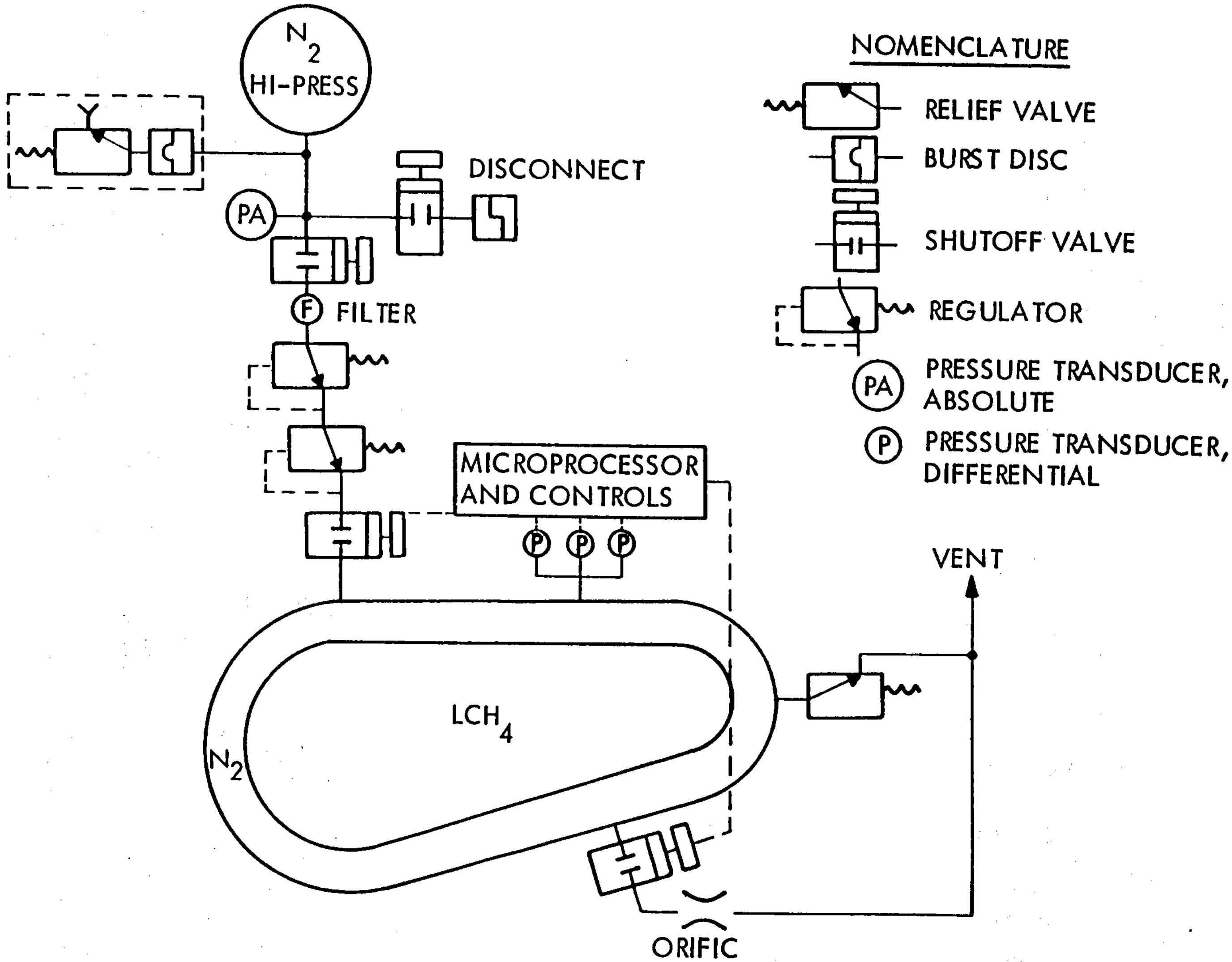

Figure 87. - Purge system for external GN_2 purged insulation system no. 6.

TABLE 38. - CANDIDATE INSULATIONS ANALYZED FOR EACH OF FOUR TANK CONFIGURATIONS

Insulation	Aft Tank	Forward Spherical Tank	Wing Tank	Pylon Tank
Internal Polyurethane (SIV-B)	✓		✓	(a)
Internal PPO	✓	✓	✓	(a)
Internal Honeycomb	✓	(b)	✓	(b)
External Polyurethane	✓	✓		✓
External microsphere	✓	✓		(c)
External GN_2 Purged Fiberglass	✓	✓		✓

Notes (reasons why analysis was not performed):

(a) Very poor thermal performance compared to other systems for this tank
(b) Thermal performance comparable to PPO but more technology development required.
(c) Fabrication of vacuum jacket very costly for this geometry.

8.2 Concept Screening

Each insulation system was analyzed with regard to safety, performance, producibility, and operational requirements. These analyses considered the following parameters:

Safety

- Potential malfunctions
- Leak detection
- Flammability and toxicity
- Inspectability

Performance

- Heat input to fuel (evaporated and vented)
- Weight and volume.

Producibility

- Approach
- Development and manufacturing requirements.

Operations

- Inspection, maintenance, and operational requirements
- Life expectancy.

Results of these studies were then compared to rank each concept for the selection of a candidate for the optimization study.

8.2.1 Safety analysis.- The safety analysis methodology is derived from reference 4 modified to reflect the operating conditions and properties for LCH_4 fuel. It considers four major parameters, shown in Table 39, with a numerical weighting factor assigned to each. The malfunction parameters consider the type of failure (i.e., vacuum jacket leakage), the condition resulting from this failure, its effect on flight operation and aircraft safety, and protective measures that could be provided to overcome or minimize the failure effect. A maximum value of 4 is assigned to the most

TABLE 39. - SAFETY RANKING CRITERIA

Criteria	Ranking Weight*
Malfunction of Component or System	
Barriers	
• Permeability and Leakage	$4(CH_4$, Air) = Total of 8 } For Each Consideration
• Rate of Flow Based Upon ΔP	$2(CH_4$, Air) = Total of 4 } For Each Consideration
• Effect of Thermal Cycles	3
• Resistance to Accidental Penetration	4
Active Systems	3
Leak Detection and Control	
• Time	1
• Sensitivity	1
• Safe Inerting in Service	3
• Safe Inerting for Tank Inspection	3
Flammability and Toxicity	2
Inspectability	
• Tank	1
• Barrier	1
*4 - Maximum Importance: Total of 34 = Maximum Safety	

severe condition with 3, 2, etc. signifying lesser severity. For each severity value (4, etc.) each system is ranked; the lower the number the poorer the performance. For example, failure of the tank wall by a crack would permit GCH_4 to permeate the cells of the external foam which would present a major safety hazard for servicing operations if this leakage is not known to be present. The problem of LCH_4 leakage from the tank is examined in terms of the ability to detect leakage into the insulation and airframe interior (see Section 6 for a leak detection method). A second factor is the potential for removal of methane or inerting of the system during aircraft operation and when it is necessary to remove the fuel tank for maintenance or repair. Flammability of the materials used in the system and the possible toxic products resulting from combustion of a material are the third factors in the analysis. The final factor is how the system design affects the capability to inspect for tank wall or vapor barrier leakage during servicing or maintenance operations.

For purposes of comparison, numerical ranking factors were assigned to each individual parameter. A value of four signifies maximum importance with smaller values indicating safety considerations of lesser impact on aircraft and passenger safety. The ranking scale was selected to give an acceptable value of resolution for comparison between concepts and was consistent with the level of analysis.

The ranking of the six insulation concepts on the basis of table 39 in order of decreasing safety is as follows:

Concept	Ranking Score (100 Max Possible)
Internal Closed Cell Reinforced Foam	69
Internal Open Cell PPO Foam	74
Internal Honeycomb	74
External Closed Cell Foam - MAAMF Barrier*	81
External Evacuated Microspheres	81
GN_2 Purged Fiberglass	75

* With leak detection system of Section 6.

8.2.2 Performance analysis.- A preliminary screening analysis was conducted to evaluate the design mission insulation thickness. Initial tank sizing to determine heat transfer area was based upon a tank volume which would contain the design mission fuel load with 5 percent unusable volume for ullage and internal components. This tank size was used to compute fuel losses for seven segments of a 24-hour period having fuel withdrawal increments, ambient temperatures, and times as shown in table 40. An initial

TABLE 40. - MISSION FUEL SCHEDULE

Segment	Time (hr)		Fuel Fraction	Ambient Temperature	
	Segment	Total	Percent	°K	°R
1. Ground, After Fueling, Engines Off*	0.283	0.283	95	290	522
2. Taxi	0.233	0.516	94.3	290	522
3. Takeoff	0.0817	0.598	93.5	290	522
4. Climb	0.743	1.341	90.5	290	522
5. Cruise	10.273	11.614	54	222	400
6. Descent-Land	0.383	11.997	16	222	400
7. Ground	12.003	24.000	15	290	522
* APU Fuel not Included					

tank pressure of 145 kPa (21 psia) and a minimum allowable pressure of 110 kPa (16 psia) was assumed for the mission. By successive iterations, the tank size and fuel loss converged to give the correct tank dimensions for the design mission fuel requirement. Transient conditions were accounted for by computation of the time constant for each insulation using a stepwise ambient temperature change from ground to cruise and proportioning the cruise and ground segment (5 and 7) into two ambient temperature conditions. This resulted in a gross approximation of heat storage within the system. The initial screening analysis method was used to rank each candidate for each tank type on a relative basis. The highest ranked concepts were then subjected to a detailed analysis to develop absolute performance figures for the final design.

The temperature-dependent properties required for the thermal analysis of the concepts and the sources from which the data were obtained, are as follows:

- Methane - Liquid and vapor phases

  Density

  Compressibility

  Vapor pressure

  Thermal conductivity

  Specific heat

Latent heat of vaporization

Viscosity

Sonic velocity

Properties data were taken from references 18 and 19.

- Tank - Aluminum - 2219 alloy.

  Density (reference 20)

  Thermal conductivity (reference 21)

  Specific heat (reference 20)

- Insulations - Where available, data were taken from the literature for the specific material. In cases where data were not available, the properties were estimated using those of similar materials. Refer to table 41. Figure 88 shows the temperature-dependent thermal conductivity data for several of the insulations considered.

TABLE 41. - DATA SOURCES FOR PROPERTIES OF INSULATION CONCEPTS

Material	Property and Data Source
N_2-filled fiberglass	Thermal conductivity and specific heat; ref. 20
Stepan Foam BX250	Thermal conductivity; ref. 16. Specific heat; ref. 20 for polyurethane
Internal Polyurethane Foam, 3D reinforced	Density and thermal conductivity for GH_2 filled condition; ref. 22
	Specific heat from ratio of foam and glass reinforcement; ref. 20
Internal PPO foam	reference 23
Internal gas-filled honeycomb	Density and thermal conductivity; ref. 24 and 25. Specific heat; extrapolated using ratios of constituents and ref. 20
Microspheres	Density and thermal conductivity; ref. 26 and 27. Specific heat; ref. 20

- Vapor Barrier/Vacuum Jacket - The vapor barrier is the MAAMF construction as follows:

Layer	Material Description
1	1.27×10^{-3} cm (0.5 mil) Mylar, Type A
2	Adhesive
3	1.27×10^{-3} cm (0.5 mil) Aluminum Series 1100.0 Foil

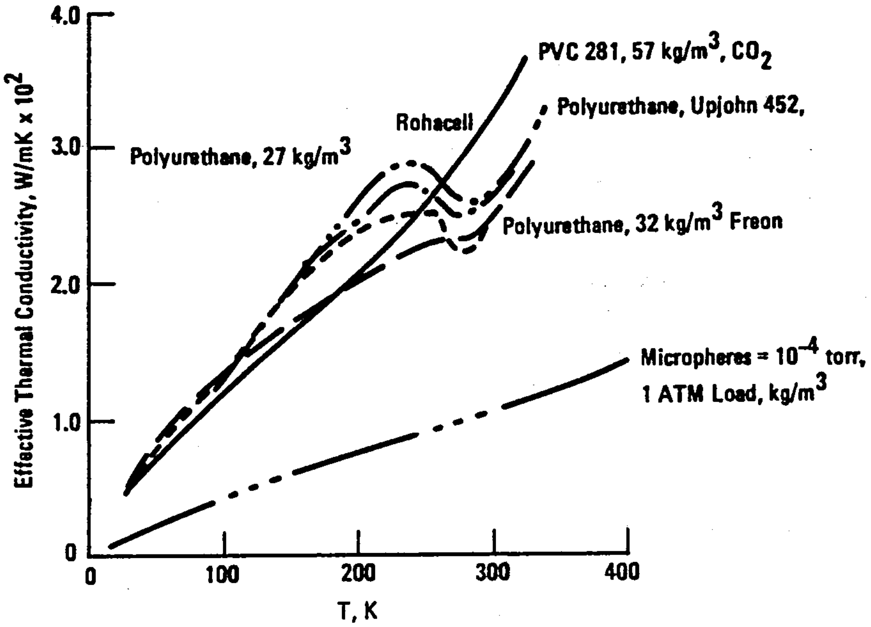

Figure 88. - Thermal conductivity of candidate insulations.

Layer	Material Description
4	Adhesive
5	1.27 to 3.81 x 10^{-3} cm (0.5 to 1.5 mil) aluminum series 1100.0 foil
6	Adhesive
7	1.27 x 10^{-3} cm (0.5 mil) mylar, Type A
8	Dacron or glass net fabric

The total thickness is 12.7 to 15.2 x 10^{-3} cm (5 to 6 mils), and it weighs 0.225 kg/m^2 (0.046 lb/ft^2).

Thermal conductivity of the vapor barriers and the thin 12.7 x 10^{-3} cm (5 mil) stainless steel vacuum jacket was not considered, because the thermal resistances introduced by these components are negligible.

8.2.2.1 Preliminary performance screening.- Initially, the aft tank was subjected to the screening analysis for all six of the insulation concepts to determine the more promising systems for the fuselage tanks. The results of the thickness optimization are shown in figure 89. On the basis of these results, the internal reinforced polyurethane foam was eliminated from further consideration for either fuselage or pylon tanks. Fuel loss plus insulation weights are the greatest for this system and relatively poorer performance would be expected for the pylon tank application because of the very large wetted area-to-volume ratio of this application. This insulation also shows poor performance for the wing tank application, figure 90.

8.2.2.2 Fuselage tank - insulation concept performance.- The fuselage tank geometries investigated in this phase were the cylindrical aft tank and the spherical forward tank. The toroidal tank was not investigated because of the complexity of the thermal analysis for this geometry which was beyond the scope of this program. Four insulations were analyzed for each tank. The internal reinforced foam and the internal honeycomb were not included. As stated earlier, the foam was eliminated because of poor performance. The honeycomb was not evaluated, because its weight versus thickness performance was similar to that for external foam and the development effort required to bring this concept to practicality is estimated to be very large.

The results of the analysis for the external foam, microsphere and internal foam concepts are shown by figures 91 through 99. For the aft tank, the heat transfer analysis includes the insulating value of the open cell foam-Kevlar fairing which is used to cover the conic section. The tank heads have primary insulation only. For the spherical forward tank, primary foam only was used. The symbols used in the figures are as follows:

fM_v - fuel vented in flight

fM_e - fuel evaporated in flight

gM_v - fuel vented on ground (recoverable)

M_i - insulation system weight.

Foam weight includes 0.225 kg/m^2 (0.046 lb/ft^2) for vapor barrier and 0.220 kg/m^2 (0.045 lb/ft^2) for two layers of adhesive. Microsphere weights include 1.03 kg/m^2 (0.21 lb/ft^2) for the vacuum jacket and 90.7 kg (200 lb/tank) for the vacuum system. The PPO weights include a single 7.62 x 10^{-3} cm (3 mil) adhesive layer for bond to the tank wall.

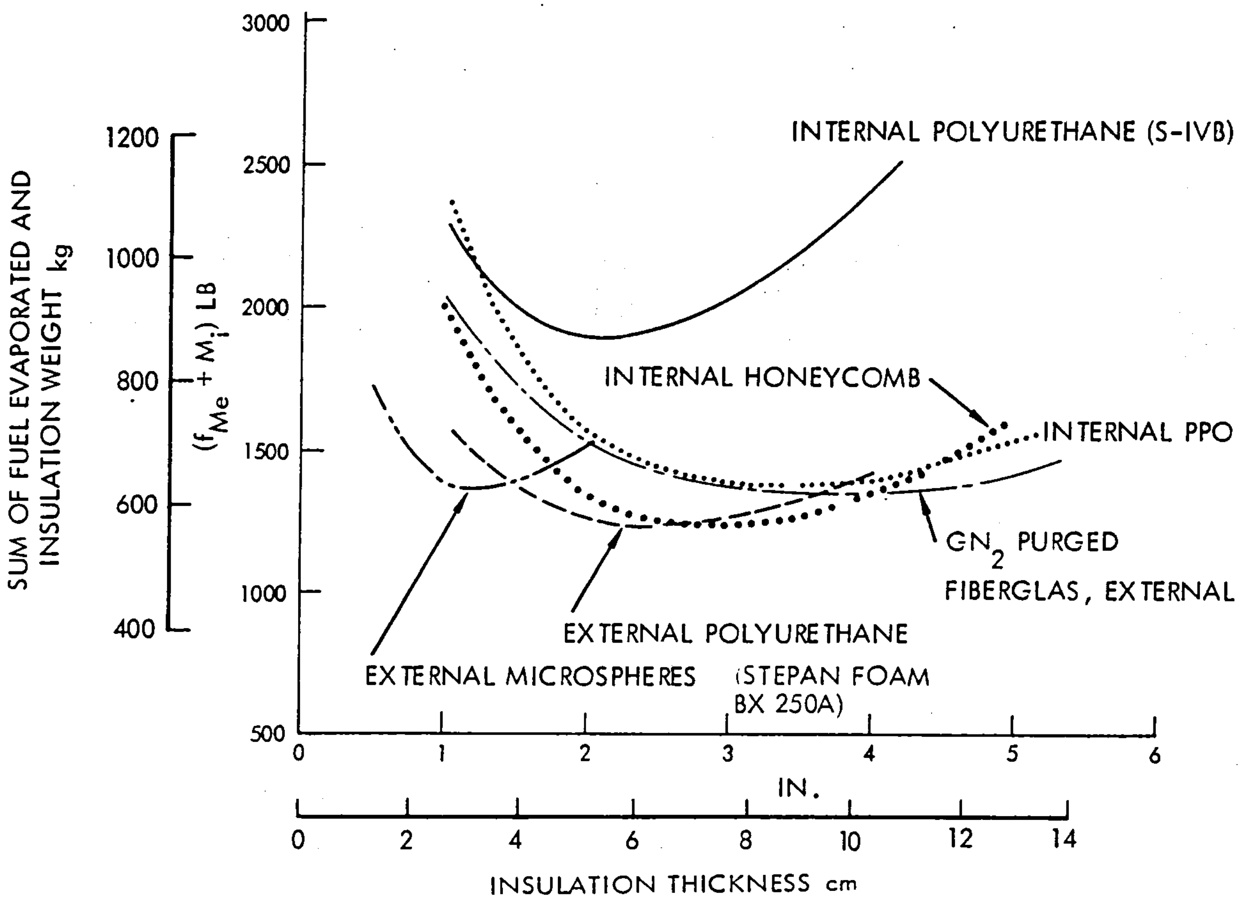

Figure 89. - Comparison of six insulation concepts for the aft fuselage tank.

8.2.2.3 Internal wing tank performance.- The overall performance results for the three candidate internal insulations for the graphite epoxy tank configuration are given in figure 90. The honeycomb and reinforced polyurethane foam were eliminated for the previously stated reasons. The weight performance of PPO as a function of insulation thickness is also shown in figure 100. The optimum insulation thickness is 6.35 cm (2.5 in.), and the sum of the weight of fuel evaporated in flight and the insulation weight is 937 kg (2065 lb) per wing tank.

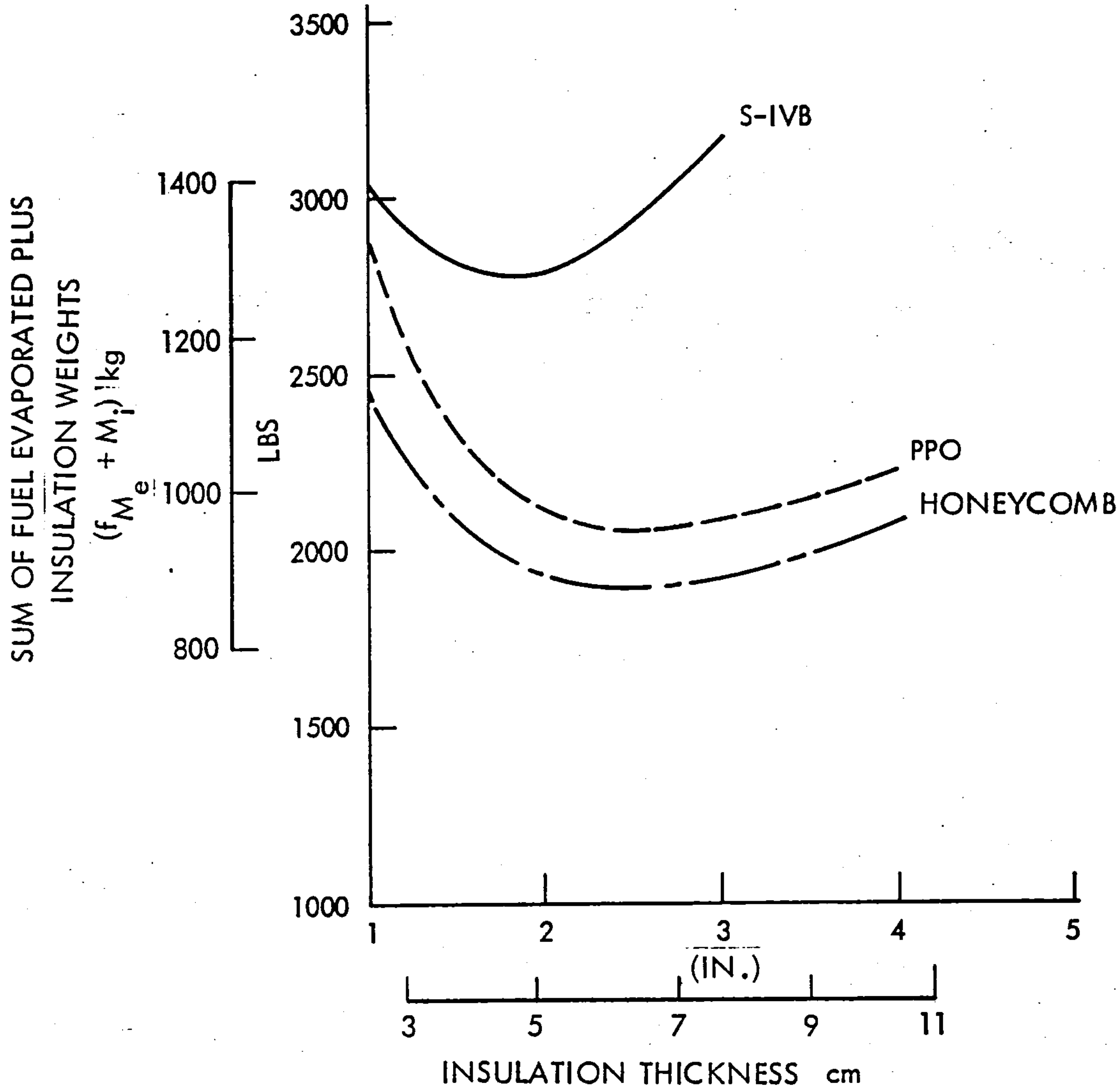

Figure 90. - Comparison of internal insulations for the wing tanks.

8.2.2.4 <u>Pylon tanks</u>.- Two insulations were analyzed for this configuration. The external polyurethane foam showed better overall performance than the gaseous nitrogen-purged fiberglass concept. Internal insulation microspheres were not considered for this application. The former were eliminated because of their relatively poor thermal resistance on this configuration. The microspheres were not included because of their higher bulk density which will significantly increase insulation weight over that of the external foam for this large surface area to volume application. The results of the analysis for the foam concept, which was the minimum weight system, are shown in figures 101 and 102. The GN_2-purged fiberglass concept had a 20 percent weight penalty and a 40 percent thickness penalty compared to the foam.

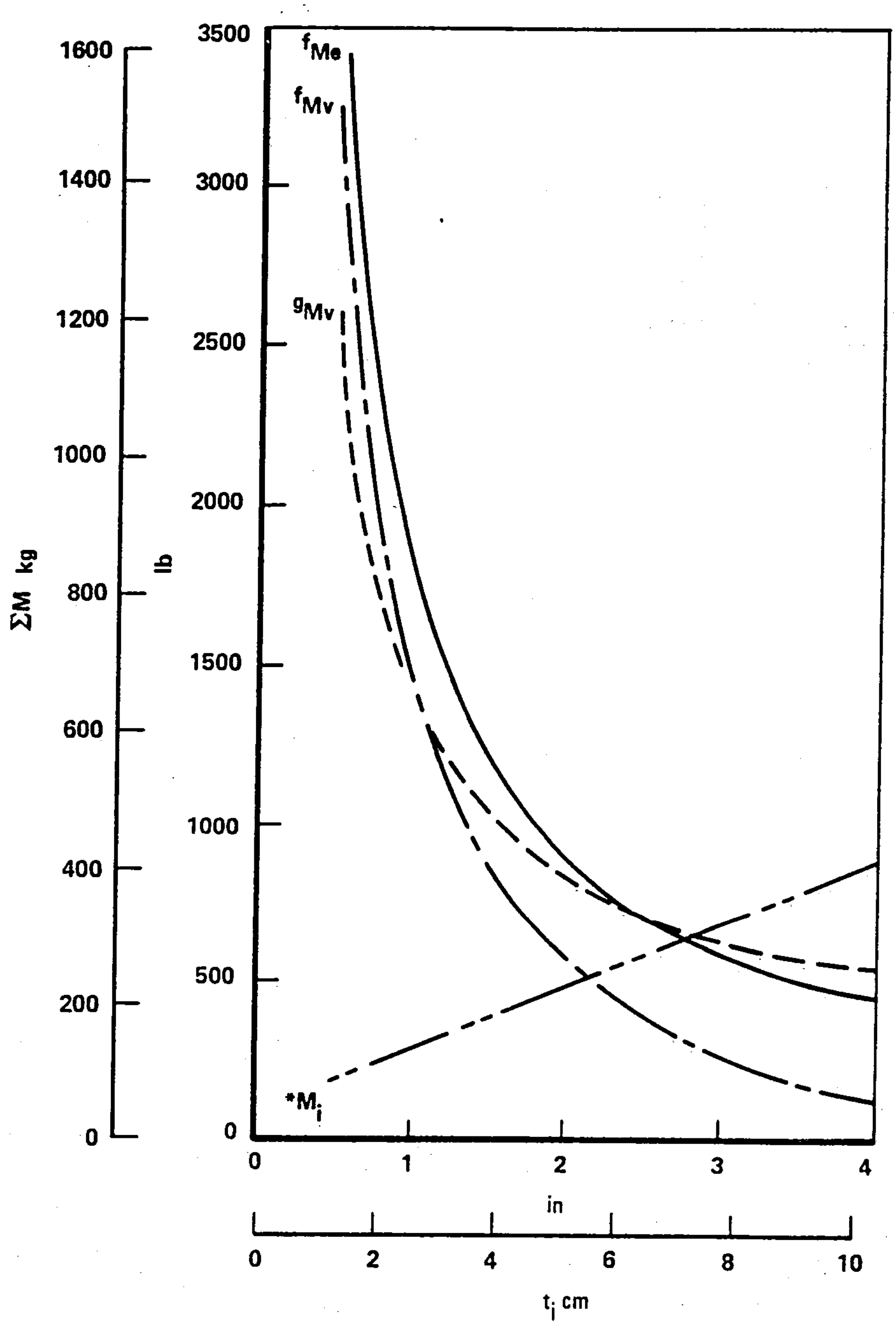

*KEVLAR FAIRING AND OPEN-CELL FOAM WEIGHTS NOT INCLUDED

Figure 91. - Forward tank - Configuration 1, polyurethane foam (Stepan foam).

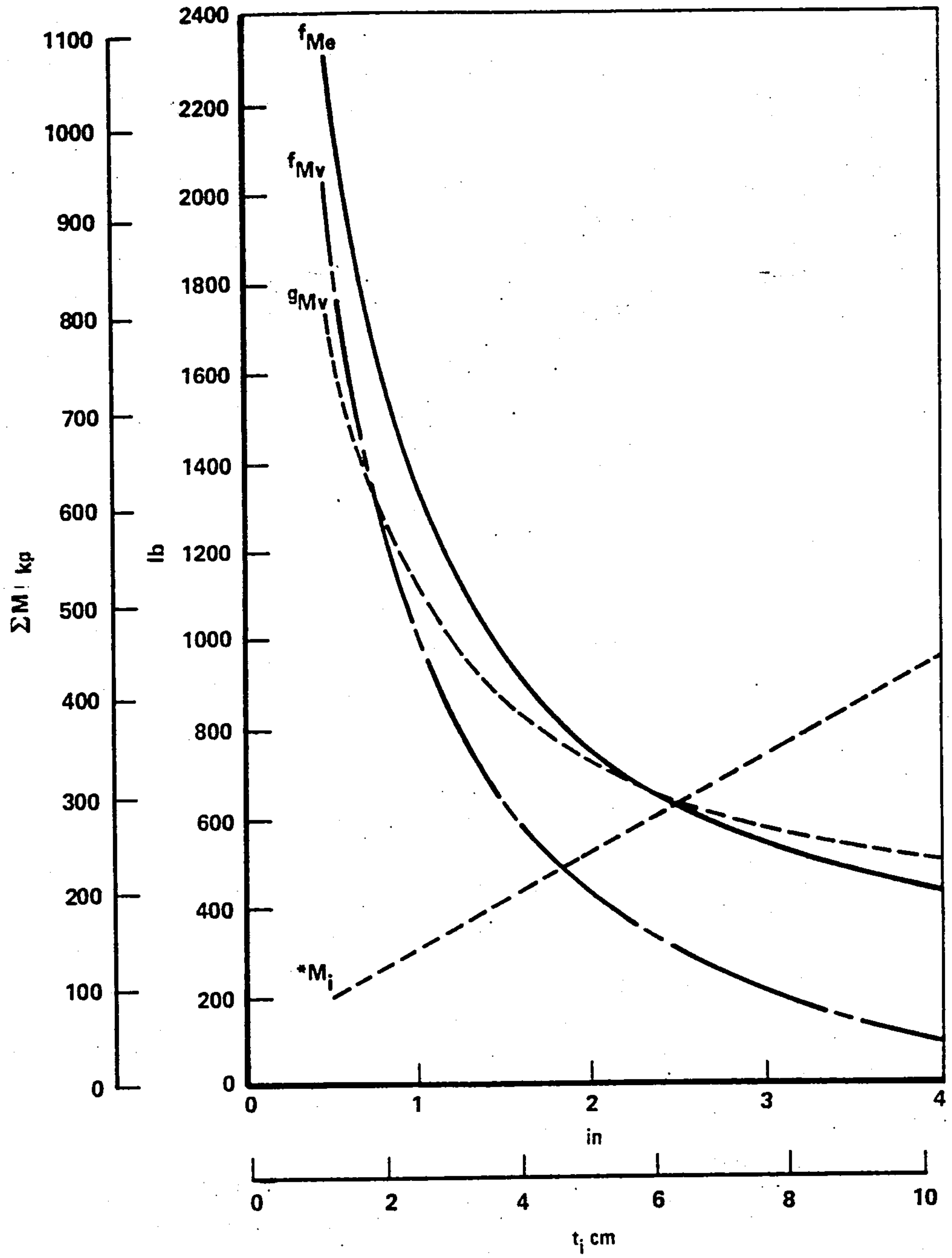

*KEVLAR FAIRING AND OPEN-CELL FOAM WEIGHTS NOT INCLUDED

Figure 92. - Aft tank, Configuration 1, polyurethane foam (Stepan foam).

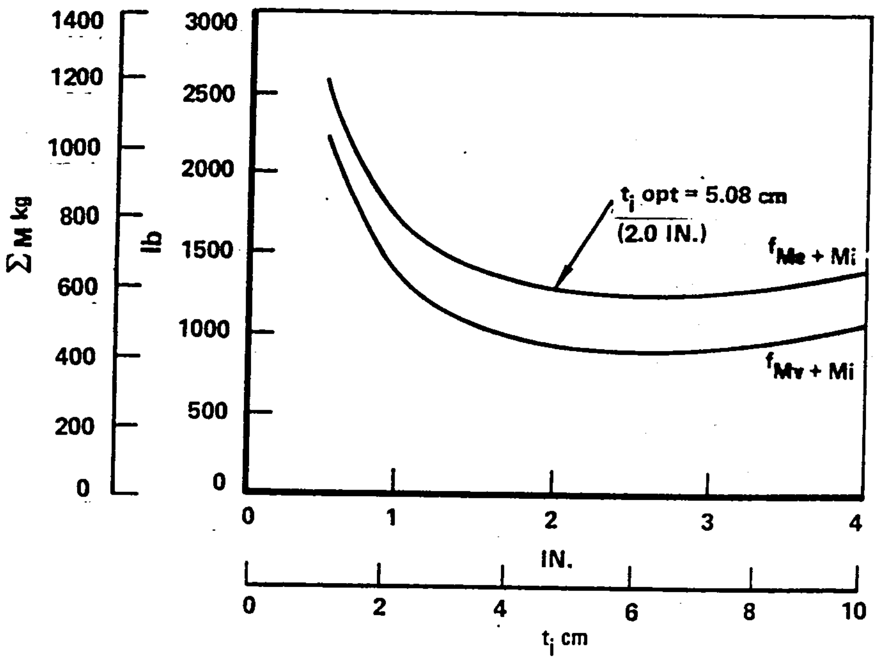

AFT TANK – CONFIGURATION 1

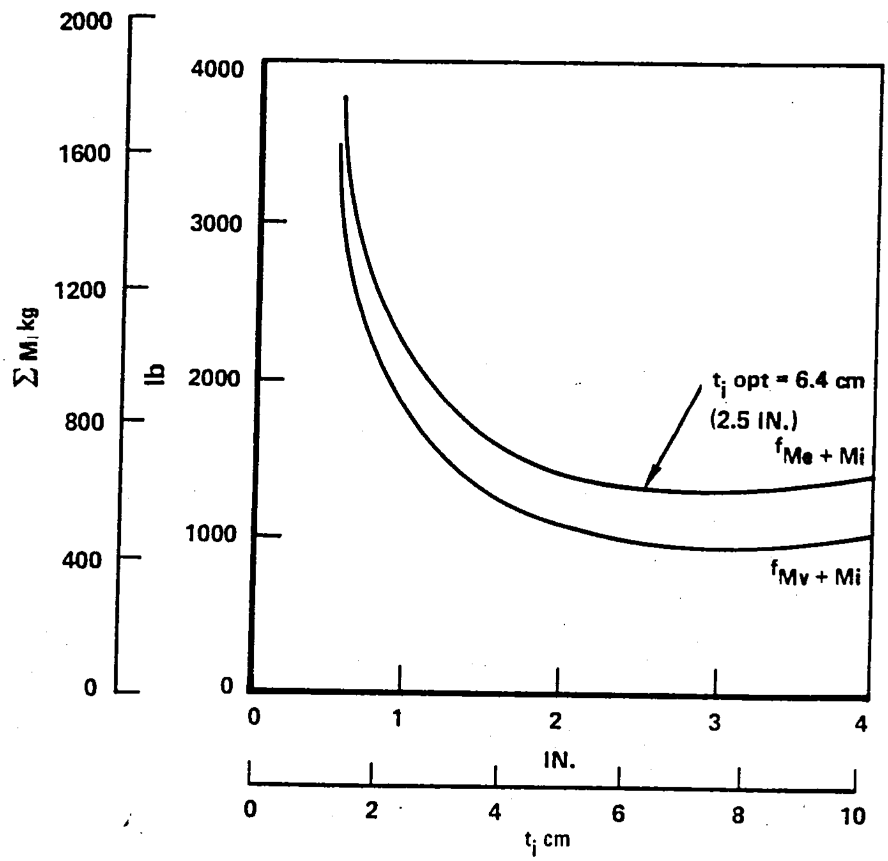

FORWARD TANK – CONFIGURATION 1

Figure 93. - Stepan foam - Configuration 1.

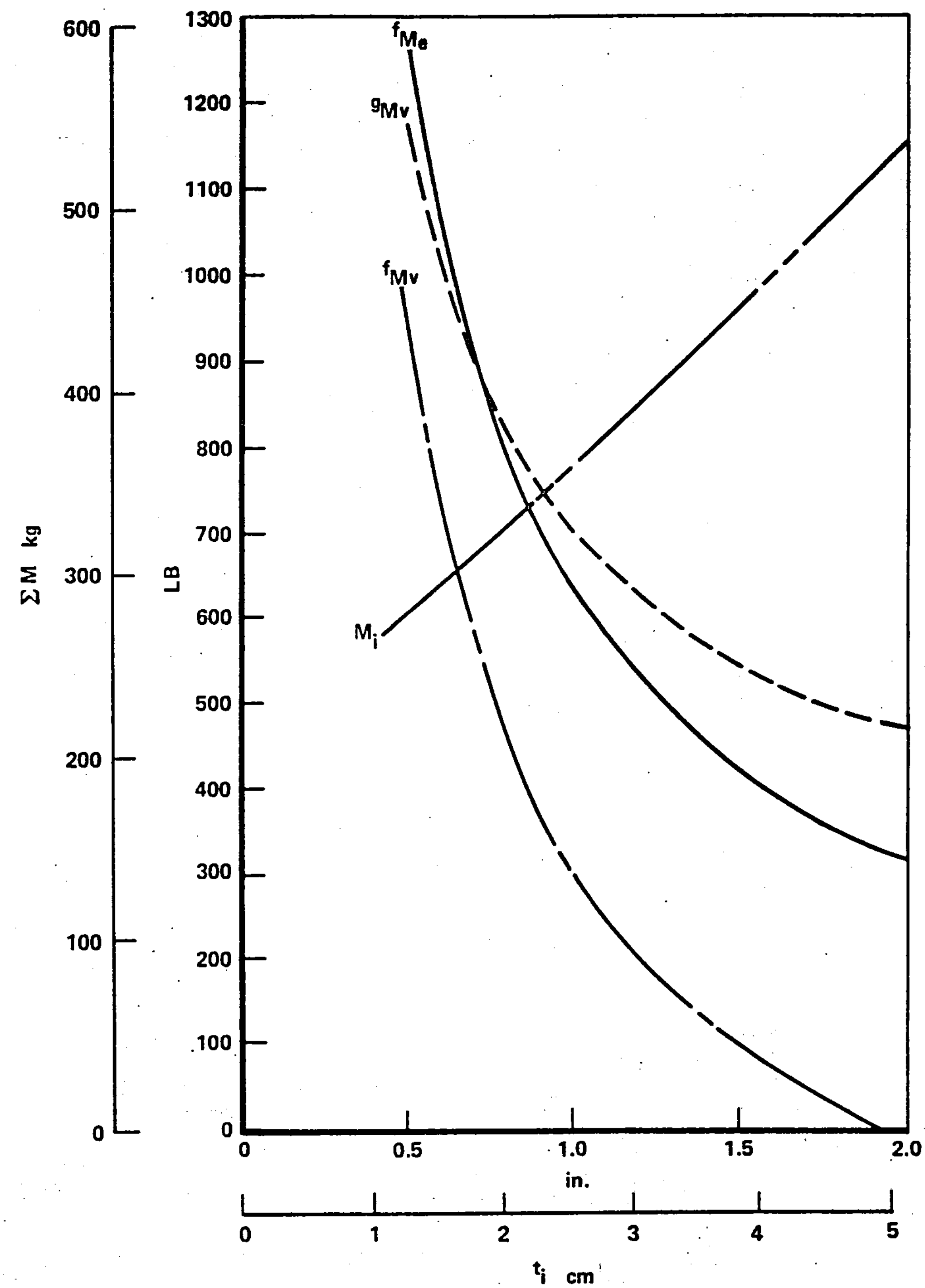

Figure 94. - Forward tank, Configuration 1, microsphere insulation 68.9 kg/m^3 (4..3 lb/ft^3) with 5 mil SS jacket - M_i includes 92.7 kg (200 lbs) for vacuum system.

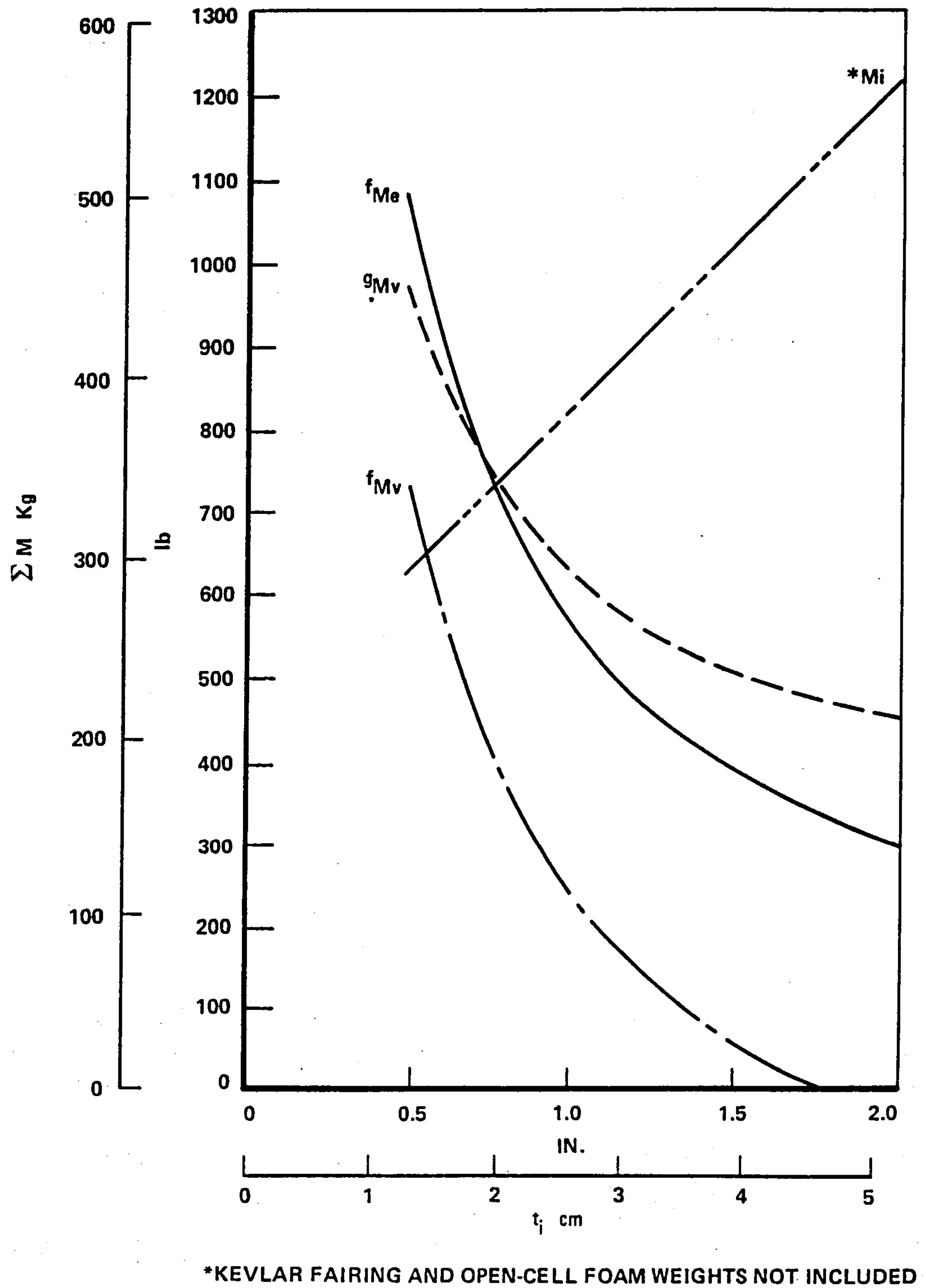

Figure 95. - Aft tank, Configuration 1, microsphere insulation 68.9 kg/m^3 (4.3 lbs/ft^3) includes 5 mil SS VAC jacket plus 92.7 kg (200 lb) for vacuum system.

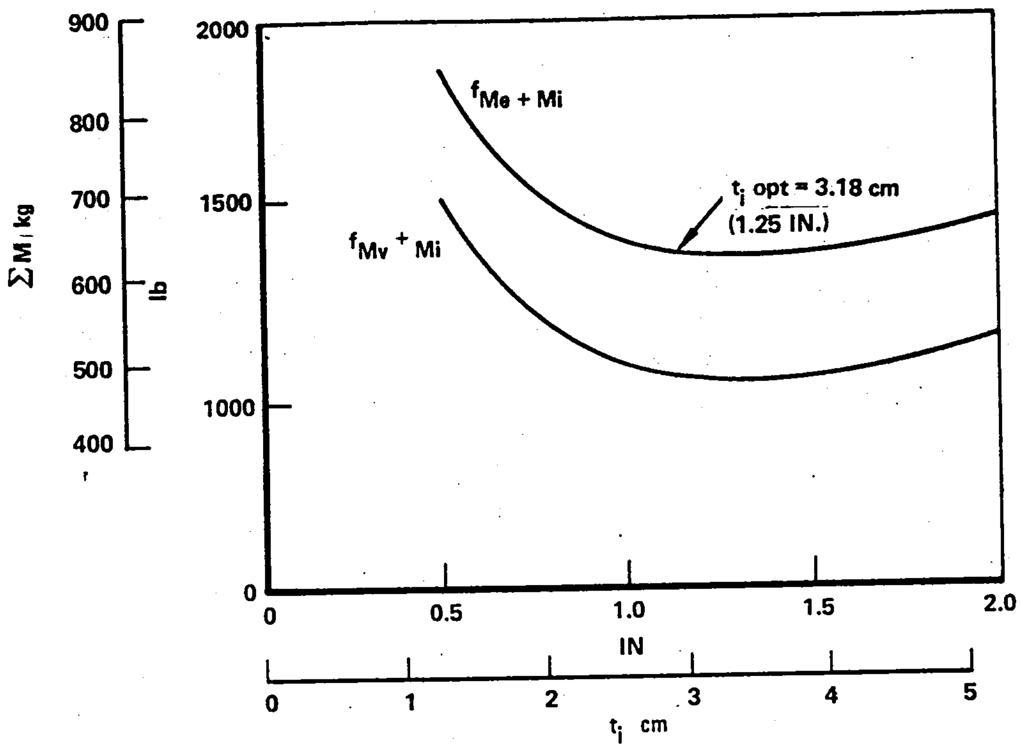

FORWARD TANK – CONFIGURATION 1

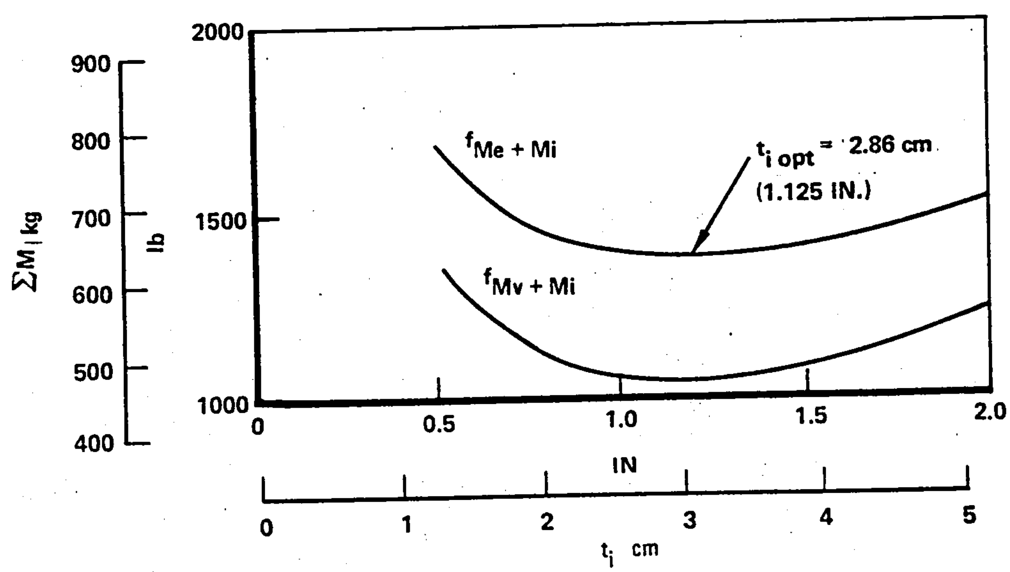

AFT TANK – CONFIGURATION 1

Figure 96. - Configuration 1, microsphere insulation forward and aft tanks.

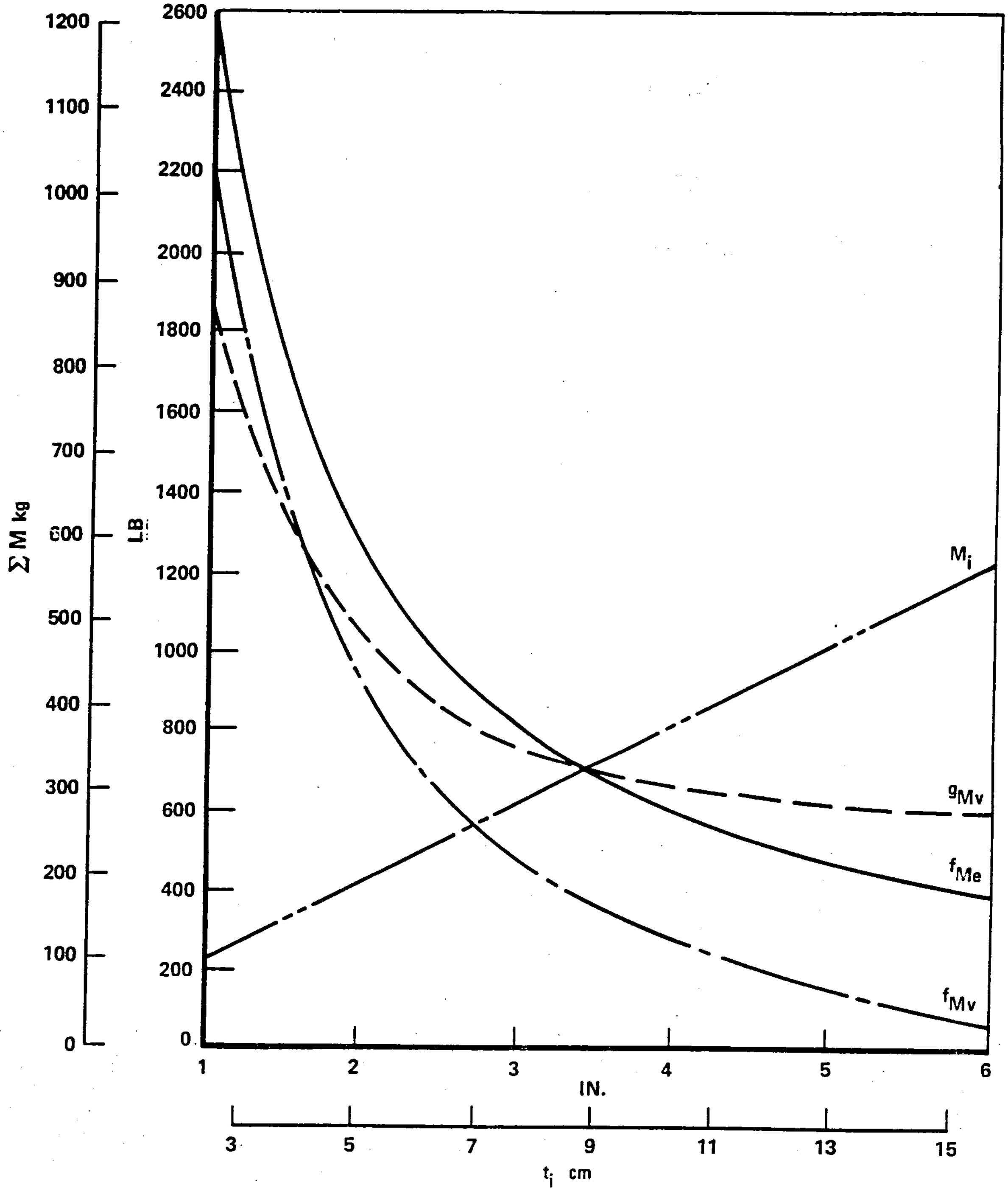

Figure 97. - Forward tank, Configuration 1, PPO 38.4 kg/m^3 (2.4 lb/ft^3) internal foam.

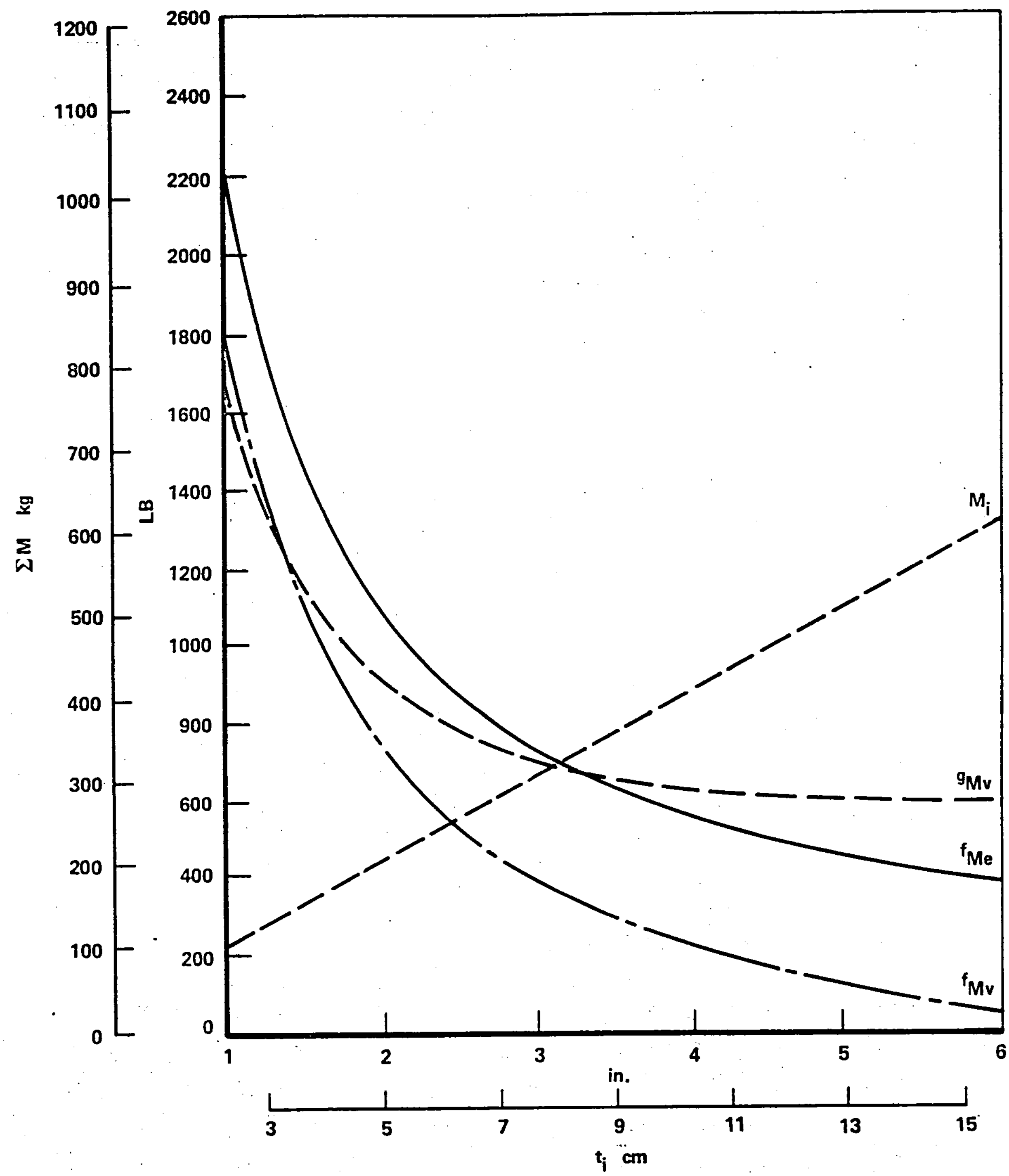

Figure 98. - Aft tank, Configuration 1, PPO 38.4 kg/m^3 (2.4 lb/ft^3) internal foam.

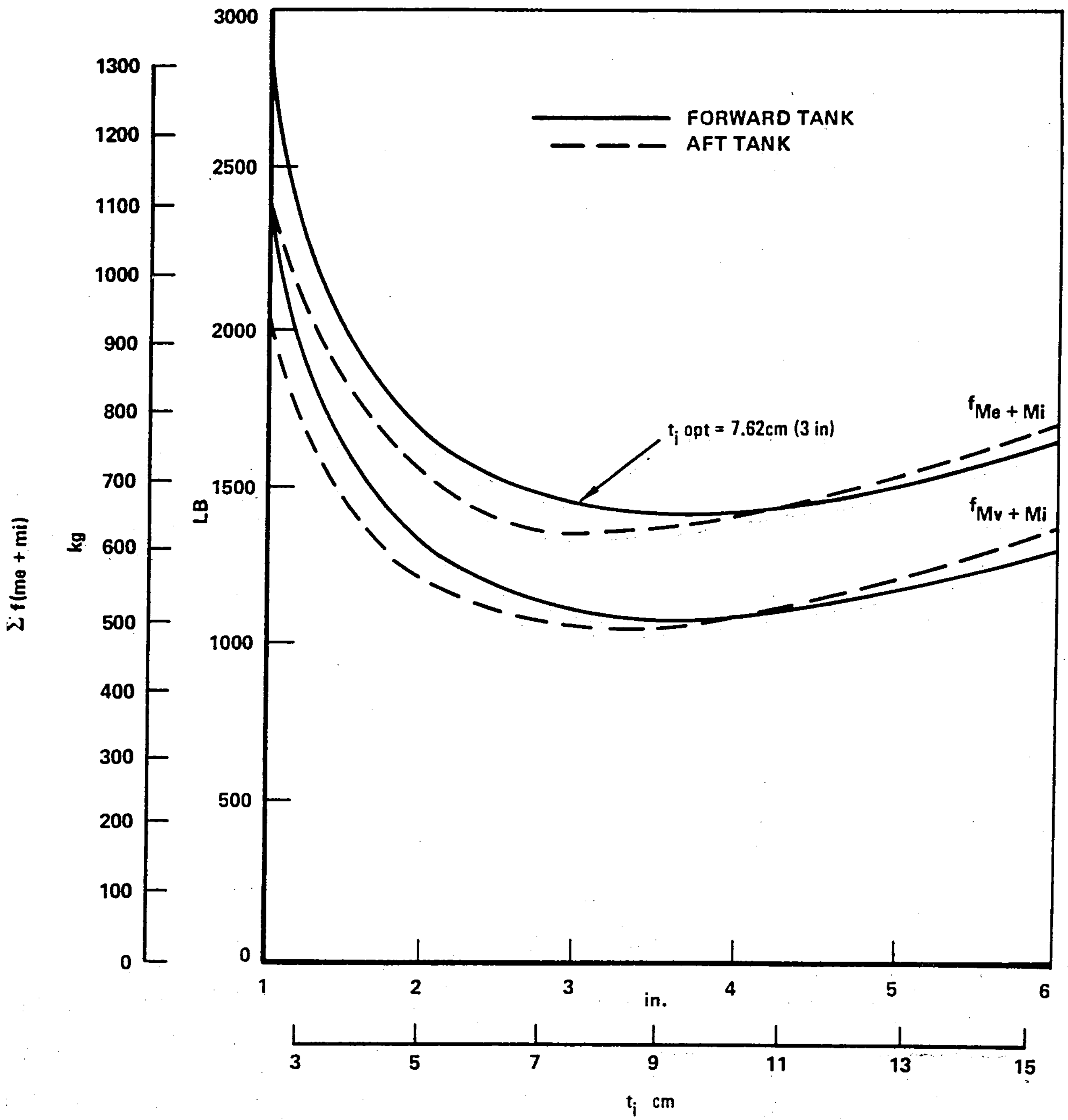

Figure 99. - Configuration 1, internal PPO foam.

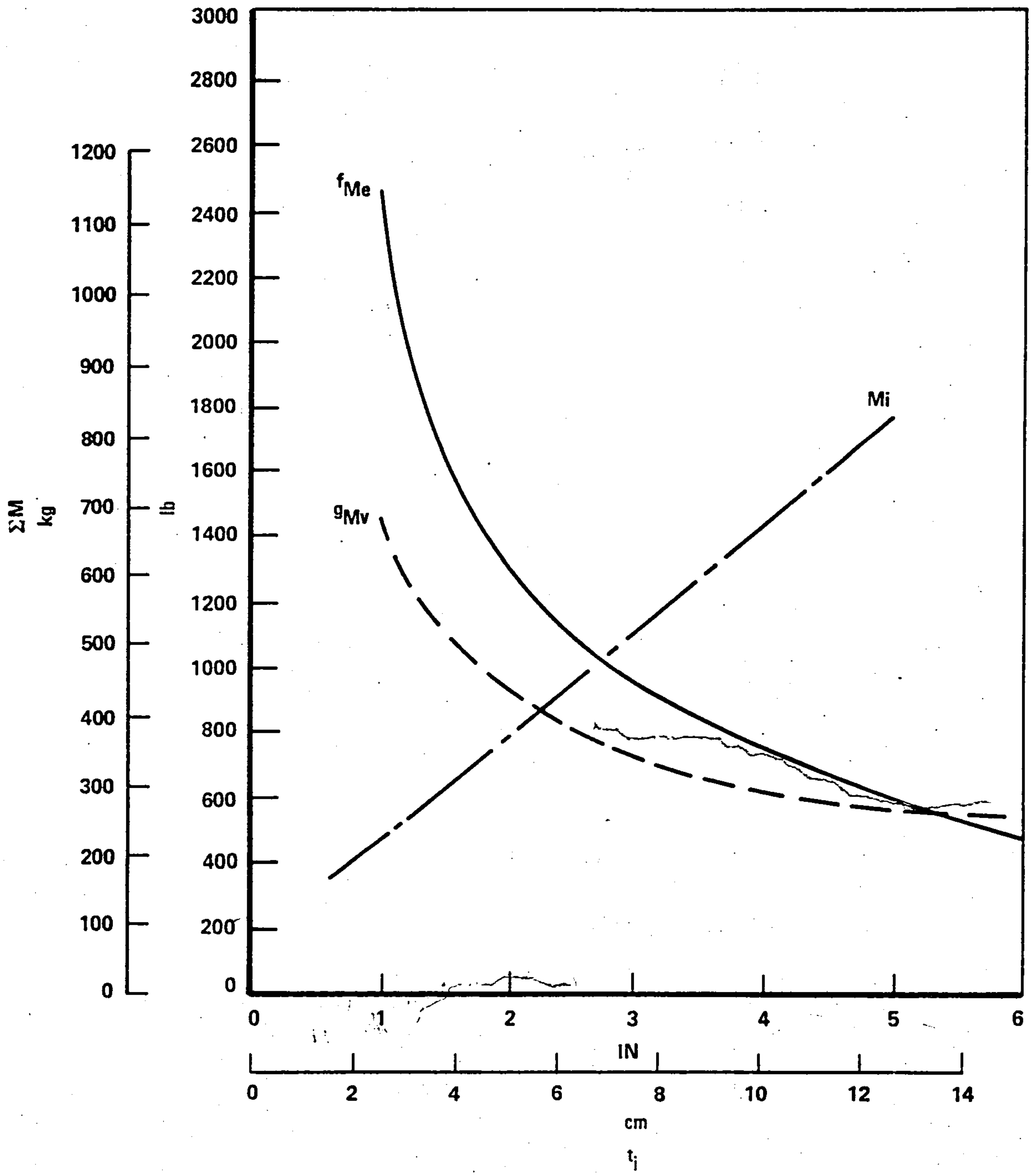

Figure 100. - Internal wing tank, Configuration 2, PPO internal foam.

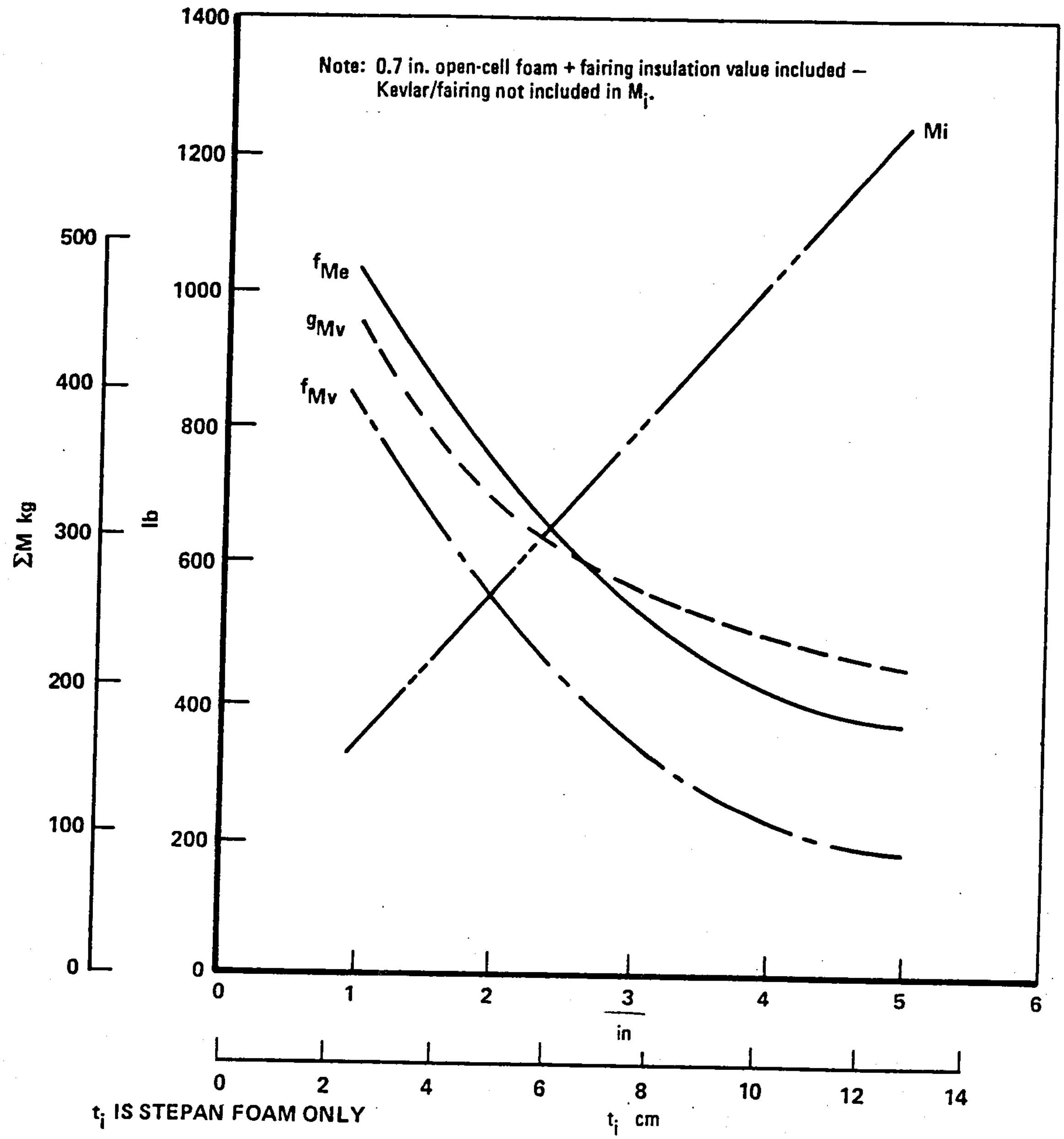

Figure 101. - Pylon tank, Configuration 3, external Stepan foam.

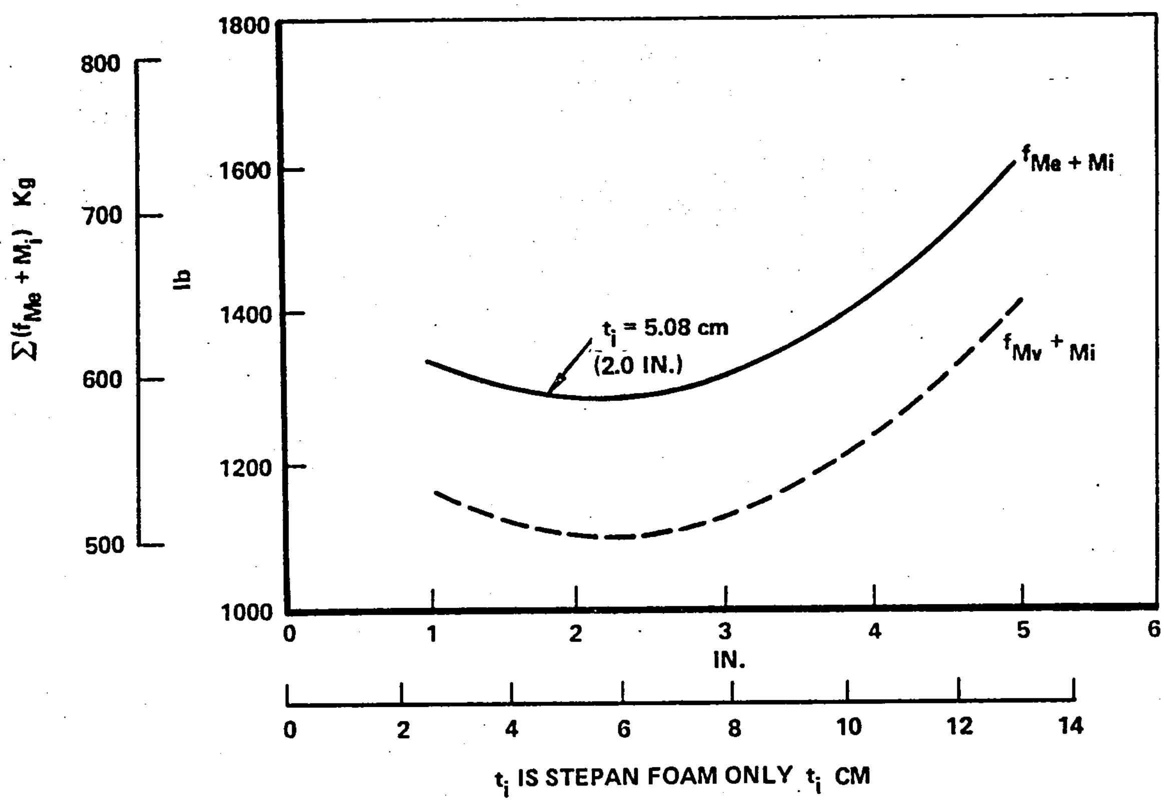

Figure 102. - Pylon tank, configuration 3.

8.2.3 Producibility and operations analysis.- The producibility and operational analysis results were derived directly from reference 4. There is little difference in these criteria among the four more promising candidates. The results of reference 4 were placed in a qualitative type of ranking from 0 to 3, the latter being the highest ranking. The external foam has the highest ranking followed by the microspheres and then the GN_2-purged and PPO foam concepts.

8.2.4 Candidate selection.- The results of the screening analysis are presented in table 42 for the several tank geometries. For the forward and aft fuselage tanks, the external polyurethane foam is judged to be the best candidate, with evacuated microspheres the second choice. The external foam would be the selection for a pylon tank and PPO internal foam for an integral wing tank. The latter two tank configurations, however, have been eliminated on the basis of overall aircraft considerations in Section 3.

TABLE 42. - SCREENING ANALYSIS

Insulation Type	External Closed – Cell Polyurethane			External Evacuated Microspheres			External GN_2 Purged F/G			Internal PPO Foam		
Tank Configuration	Aft	Fwd	Pylon[a]	Aft	Fwd	Pylon[a]	Aft	Fwd	Pylon[a]	Aft	Fwd	Wing[a]
Insulation Thickness cm (inches)	5.08 (2.0)	6.45 (2.5)	5.08 (2.0)	2.87 (1.13)	3.18 (1.25)	–	7.62 (3.0)	8.89 (3.5)	7.11 (2.8)	7.62 (3.0)	7.62 (3.0)	6.45 (2.5)
Insulation Weight kg (lb)	226 (498)	272 (600)	254 (560)	396 (872)	396 (873)	–	419 (923)	437 (963)	409 (902)	293 (645)	284 (625)	427 (940)
Wt. Fuel Vented in Flight kg (lb)	191 (420)	181 (400)	247 (544)	81 (178)	79 (175)	–	128 (282)	121 (267)	147 (324)	179 (395)	213 (470)	341 (751)
Wt. Fuel Evaporated in Flight kg (lb)	341 (752)	322 (710)	333 (735)	228 (503)	228 (502)	–	212 (467)	186 (410)	291 (641)	331 (730)	367 (810)	510 (1125)
Wt. Fuel Vented on Ground kg (lb)	331 (730)	322 (710)	317 (698)	265 (585)	275 (605)	–	241 (532)	233 (514)	227 (500)	318 (700)	342 (755)	367 (808)
$(f_e + m_i)$[b]	$\boxed{567}$ (1250)	e $\boxed{594}$ (1310)	587 (1295)	624 (1375)	624 (1375)	–	631 (1390)	623 (1373)	700 (1543)	624 (1375)	651 (1435)	937 (2065)
Safety Ranking[c]	78			81			75			74		
Producibility[d] Ranking	3.0			2.5			2.0			2.0		

[a] per tank (2 per aircraft)

[b] sum of fuel evaporated in flight and insulation weight

[c] 100 is highest ranking

[d] 3 is highest ranking

$\boxed{e}$ selected candidate

8.3 Analysis of Selected Candidate

The optimum insulation thicknesses for the aft and forward fuel tanks were derived from parametric thermal analysis studies of each tank configuration. Fuel loss weights and insulation system weights were computed as a function of insulation thickness and the saturation temperature of the liquid methane used to fill the tanks at the beginning of a flight. These weights are then translated into DOC for final design optimization (Section 4). The analysis output also included circumferential temperature distributions along the tank wall, within the insulation, and along the vapor barrier and fuselage exterior surface; tank pressure; and vent rate during filling. A description of the insulation system configuration, the analysis method, and the results of the studies are presented in the following subsections.

8.3.1 Configuration of candidate system.- Two tank geometries are used for the fuel tanks; the forward tank is a sphere 5.49 m (18 ft) in diameter with the wall thicknesses as shown by figure 103. A truncated right cone having

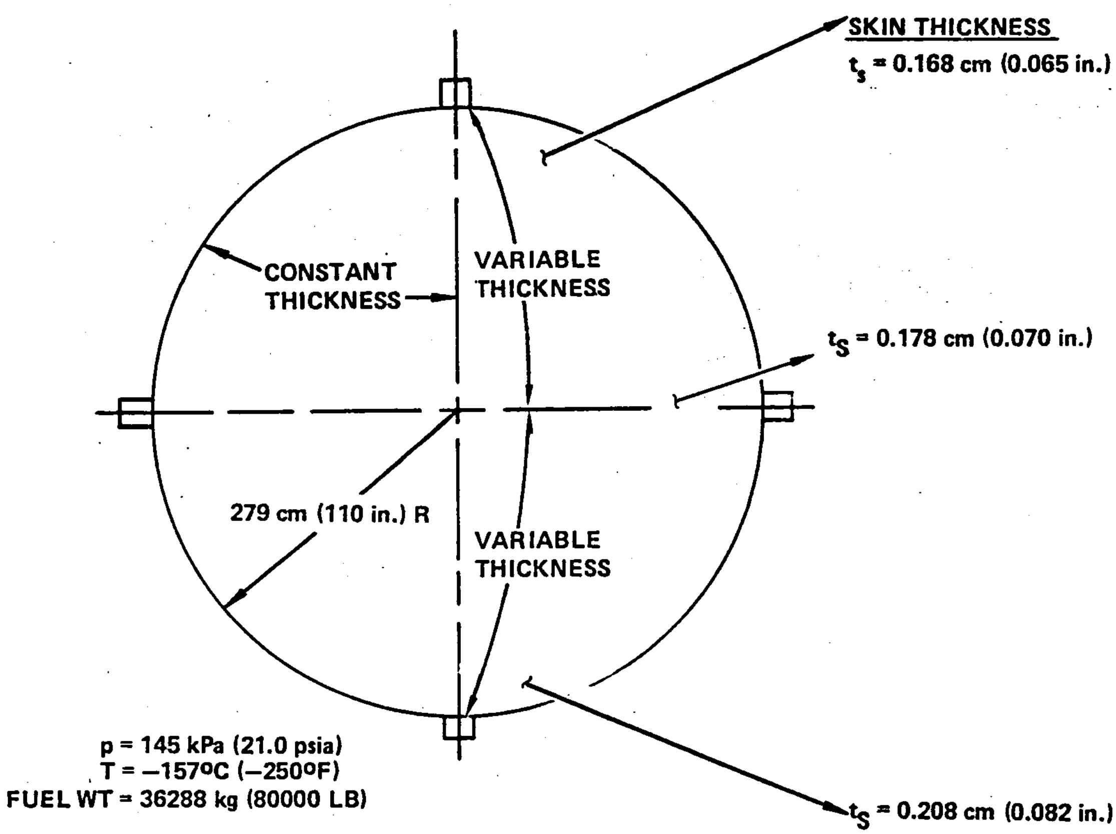

Figure 103. - General dimensions of forward methane tank.

elliptical ends serves as the aft tank, as shown in figure 104. For the parametric studies, the spherical tank was considered to have a uniform wall thickness of 0.183 cm (0.072 in.) and the aft tank a wall thickness of 0.446 cm (0.175 in.). The cryogenic volume of each tank (with fuel in) was evenly divided at 85.8 m^3 (3032 ft^3). Also, the internal bulkhead was not considered in the analysis, and each tank was treated as a single volume of the preceding value. This assumption does not significantly compromise the analysis, as a presumption is made that the internal wall would be adiabatic because fuel quantities would be equal in both compartments.

Forward and aft tank insulations are shown conceptually by figures 105 and 106, respectively. The 36.8 kg/m^3 (2.3 lb/ft^3) closed-cell polyurethane-type foam (Stepan foam BX250A) was selected for both tanks as a result of the screening studies. This foam is covered with a reinforced plastic film-aluminum foil composite (MAAMF) which serves as a vapor barrier to prevent cryodeposition of water vapor within the cell structure during the extended operational life of the aircraft. A second foam insulation is placed between the vapor barrier and Kevlar fuselage fairing in the area of the cylindrical

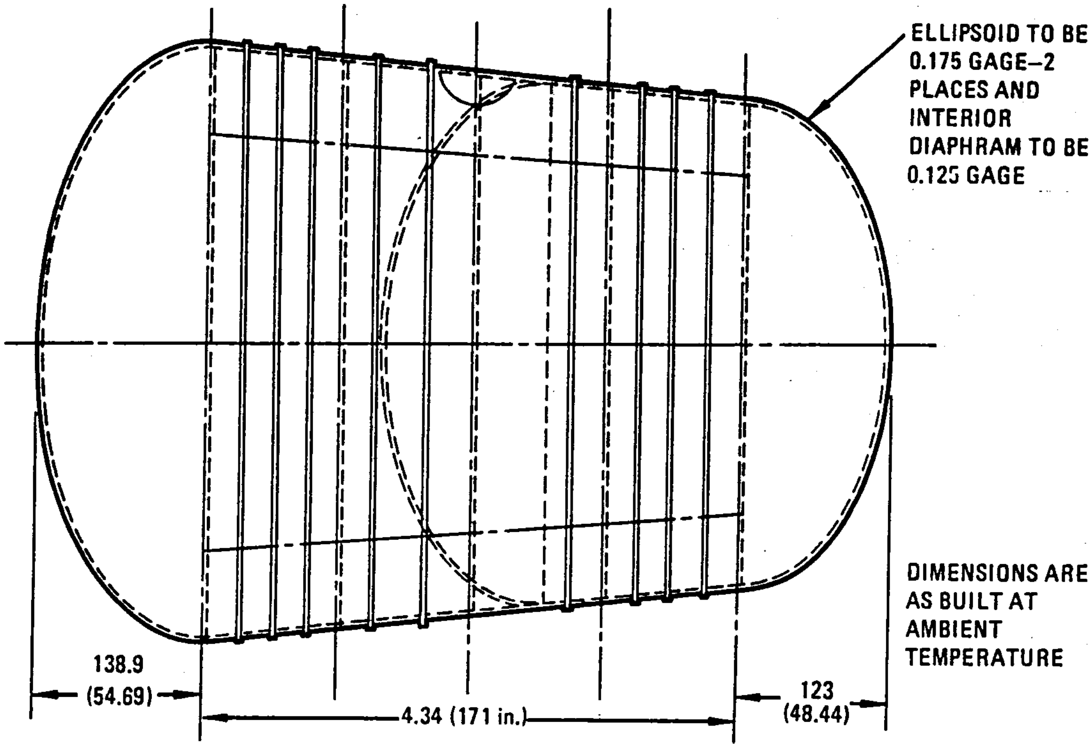

Figure 104. Aft tank configuration.

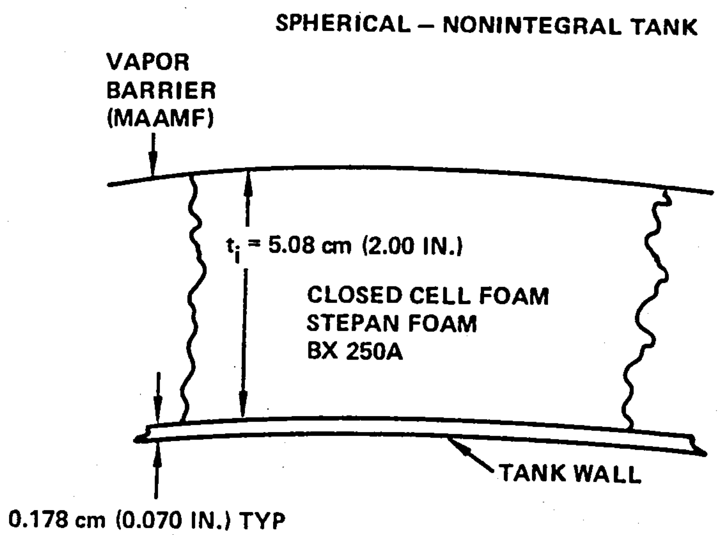

Figure 105. - Forward tank insulation.

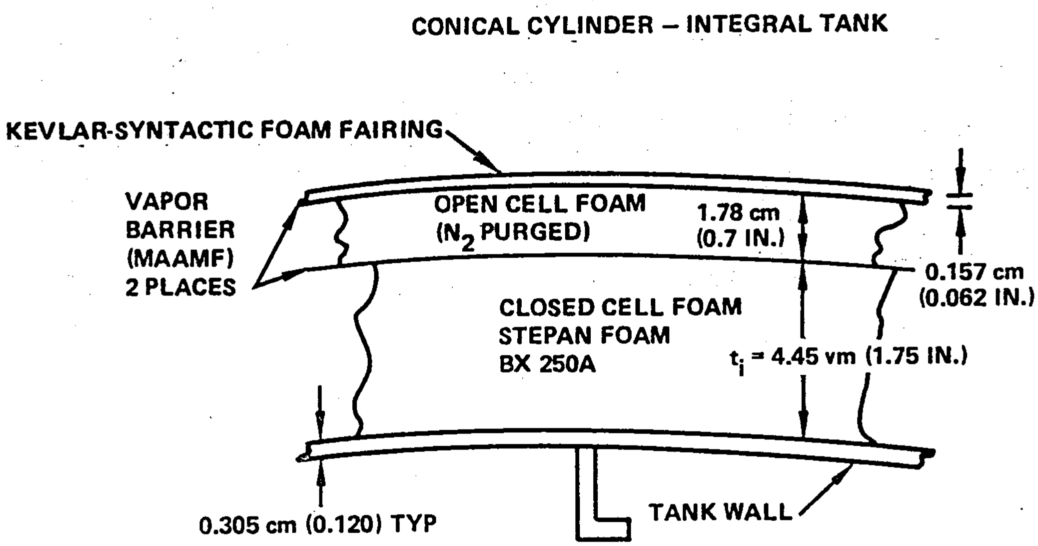

Figure 106. - Aft tank insulation - cylindrical section.

section of the aft tank. This is a low modulus open cell polyurethane type insulation which accommodates the expansion and contraction of the tank wall during temperature and pressure excursions and supports the fairing without distorting the aerodynamic surface. Being of open cell construction, it also permits the purging of this volume with GN_2 for inerting and prevention of cryodeposition of water vapor. The thickness of this secondary foam layer was held constant for the parametric analysis, as its thickness is dictated by dimensional changes rather than heat transfer properties. Its thermal resistance, however, is included in the system thermal model.

8.3.2 Analysis method.- Thermal analysis of the selected candidate was conducted in a transient mode to accurately represent the design mission time-dependent variables of altitude, Mach number and fuel usage. An existing finite difference computer program with subroutines for stratification, filling, draining, pressurization, and boundary layer heat transfer was employed for this effort. In addition to the normal flight mode, a subroutine was included to simulate the effects of severe flight turbulence. This was done using the assumption of complete liquid and vapor phase mixing and uniform liquid wetting of the entire tank wall, all occurring instantaneously, so that thermodynamic equilibrium is reached in the entire volume. Following this equilibration, the stratification process then resumes.

The computer program, THERM, Thermal Analyzer Program, operates for transient heat flow problems by using a forward finite-difference algorithm for solving an analogous R-C electrical network. It is structured to allow maximum flexibility in describing energy transport phenomena unique to a specific application. This specific program computes the parameters given in table 43. Computation is performed in 5-minute time steps of the design mission schedule. The environment temperatures during flight are taken from Standard Atmosphere Tables. Also, the program models both integral and non-integral tanks.

The nodal arrangement used for the fuel tanks is shown in figure 107. The liquid and vapor volumes are divided into 9 and 10 horizontal layers, respectively. The liquid/vapor interface is at the saturation temperature, T_s, corresponding to the tank pressure. Located opposite each liquid and vapor node are a tank wall node, three insulation nodes, and two outer structure nodes for the aircraft fuselage or exterior fairing. The liquid volume consists of eight nodes of increasing thickness down from the surface in the temperature stratified layer of the upper liquid region. The ninth and bottom liquid node correspond to the uniform bulk liquid temperature, T_B, layer at the bottom of a stratified tank that experiences some degree of bottom heating. A form of transient stratification analytical model of reference 28 is used as a subroutine in this program. It was modified to account for the time-dependent changes in the liquid level corresponding to the simulated flight mission.

TABLE 43. - ANALYSIS PROGRAM PARAMETERS

<u>Output:</u>

- Temperature destributions
  - Outer aircraft structure
  - Insulation
  - Tank wall
  - Liquid
  - Vapor
  - Vent gas
- Vent rate/fuel required to maintain tank pressure in design range
- Tank pressure

<u>Input variables:</u>

- Geometry and temperature dependent thermal properties of
  - Aircraft structure
  - Insulation
  - Tank
  - Liquid/vapor
- Fuel load (liquid level) and state at full
- Ambient temperature and pressure and Mach number
- Fuel withdrawl and fill rates
- Mission segment time step/duration
- Quiescent or turbulent, flight at any time into mission

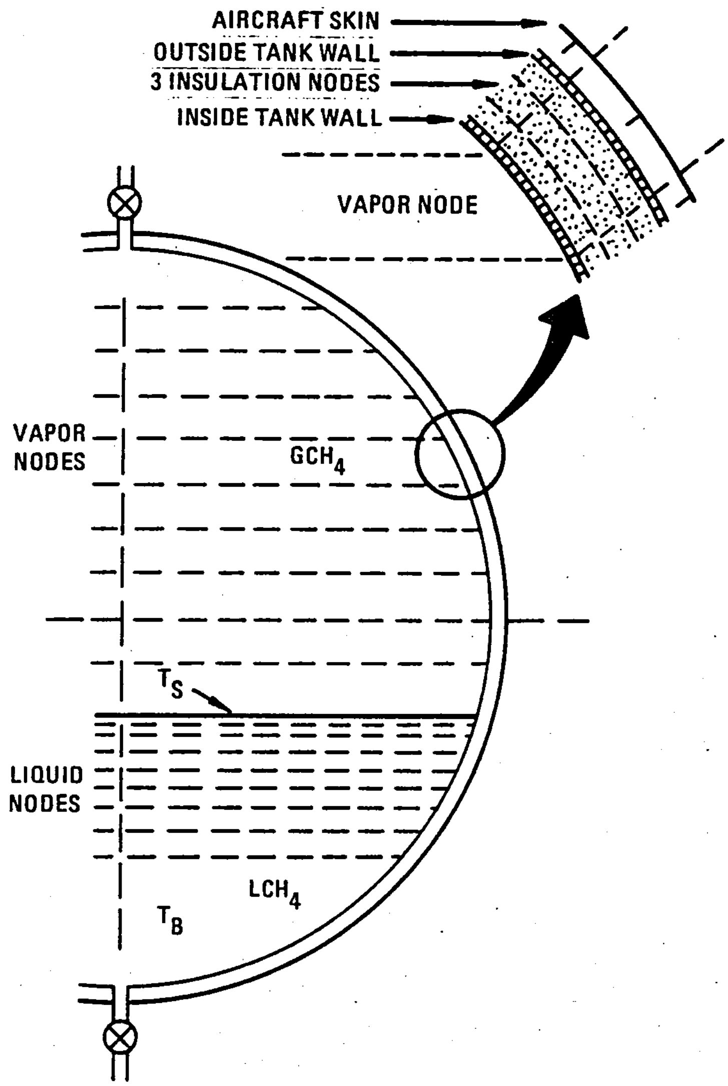

Figure 107. - Tank insulation and vent model for analysis of selected candidate.

The vapor volume consists of 10 horizontal layers in which conduction, convection, mass flow, and radiation effects between the nodes and their surroundings are modeled. The mass, volume, temperature, and pressure of the vapor are computed from a liquid/ullage coupling subroutine that considers the thermodynamics of the two modes of tank pressurization and venting. One mode is represented by a closed tank, self-pressurization model; while the second mode is represented by a constant pressure, continuous tank venting model. This program has the ability to switch between the two tank pressurization and venting modes depending upon the tank heat input, liquid level, liquid withdrawal rates, etc. In this program, a severe flight disturbance that would completely mix the stratified liquid, the vapor, and wet the tank walls can also be simulated. Following this instantaneous event, the liquid restratifies and the tank self-pressurizes and/or vents.

8.3.3 Analysis results. - Fuel losses associated with filling, flight, and ground-hold portions of the aircraft mission were computed for both forward and aft tanks as a function of insulation thickness. These fuel loss parameters are summarized as total fuel vented on the ground, during filling and ground-hold segments, which is recoverable for reliquefaction and nonrecoverable fuel evaporated and vented during flight. Fuel vented for the latter includes taxi and ground time periods between end of filling and start of taxi.

Degree of subcooling of the fuel introduced into the aircraft tanks during fill operations was included as a variable in the thermal performance analysis. The sensible heat term associated with the subcooled liquid reduces the quantity of vapor vented from a tank having a vent valve setting greater than sea level pressure. For isothermal conditions in the liquid, well-mixed, a pressurization system must be included to ensure a positive internal-to-external pressure gradient to avoid the potential for buckling of the lightweight tank or entrance of air into the fuel volume. This leakage problem would also apply to fueling and transfer lines. As discussed in Section 9, inert gas pressurization is difficult because of solubility problems. A bladder or membrane complicates construction, and long-life performance is questionable. By minimizing mixing of the incoming subcooled liquid with the warm liquid remaining in the tank from the previous flight a highly stratified layer can be maintained and ullage pressure is controlled by this liquid surface layer. Mixing of this stratified liquid, such as from encountering severe turbulence during flight, would rapidly decrease ullage pressure which could lead to a negative pressure differential across the tank wall unless a rapid response emergency pressurant system is provided. Because of these considerations, the parametric analysis was conducted with modest subcooling from the baseline fill conditions corresponding to a saturation pressure of 148 kPa (21 psia). This lower limit was a temperature corresponding to 103 kPa (15 psia). One case of filling with liquid corresponding to 69 kPa (10 psia) was examined, and the results, as discussed in Section 8.3.3.3, show the potential for catastrophic failure.

8.3.3.1 Aft tank.- Fuel loss parameters as a function of primary insulation thickness are shown graphically in figures 108 through 110 for tank fill conditions corresponding to liquid saturated at 145, 124 and 103 kPa (21, 18, and 15 psia), respectively. Table 44 presents the fuel losses and insulation weights for representative values of primary insulation thickness. Insulation weights do not include the weights of the open cell foam and Kevlar fairing in the cylindrical region. Insulation thickness on the elliptical ends of the tank is 1.14 cm (0.45 in.) greater than that shown in the figures and table. This increased thickness corresponds to the thermal resistance of the open cell foam and results in a uniform heat flux over the tank wall.

The results of this study yield a slightly thinner optimum insulation thickness than that based upon the initial screening analysis for a 21 psia fill condition. The latter analysis gave a primary insulation (closed cell foam) thickness of 5.08 cm (2.0 in.) in the cylindrical section of the aft tank and 6.35 cm (2.5 in.) for the ends. The more exact analysis predicts optimum thicknesses of 4.45 and 5.59 cm (1.75 and 2.20 in.), respectively. The values of mass vented during ground operations, MVG (out-of-service hold and fueling periods) is essentially in agreement with the values predicted during the screening process. Mass evaporated and vented during flight (MEF and MVF respectively) are less than initially predicted due to the changing tank pressure and liquid stratification during flight (takeoff to landing). The nearly constant values of MVF at $t_{ip} < 8.13$ cm $< (3.2$ in.) is the result of venting during a 15-minute ground-hold period after fill and a 10-minute taxi period where the tank pressure is at the vent valve pressure setting due to liquid-vapor heating during filling.

Filling of the tank with saturated liquid at lower temperatures (corresponding to 124 and 103 kPa (18 and 15 psia) reduces the fuel losses as shown by the comparison in table 44. The most significant advantage of the lower temperature liquid is the large reduction in the amount of fuel evaporated and vented in flight. For 124 and 103 kPa (18 and 15 psia) conditions at t_{ip} = 4.45 cm (1.75 in.) in the venting occurs primarily during taxi. As the rate is small, this fuel might be burned in the engines, and no venting to the atmosphere would be required. Also, for the case of 103 kPa (15 psia) liquid fill venting on the ground after the flight does not occur for 2.5 hours. This could simplify ground-handling operations for both normal and emergency landing conditions.

The sum of mass evaporated in flight and insulation weights (not including open cell foam and fairing) is shown in figure 111. Insulation thickness is an optimum at 4.45 cm (1.75 in.) for 145 kPa (21 psia) conditions. For 124 and 103 kPa (18 and 15 psia) fill conditions, less than 2.54 cm (1 in.) appears to be an optimum on the basis of weight considerations. As discussed in Section 8.3.3.4, a value of t_{ip} = 2.54 cm (1.0 in.) is satisfactory from exterior temperature considerations.

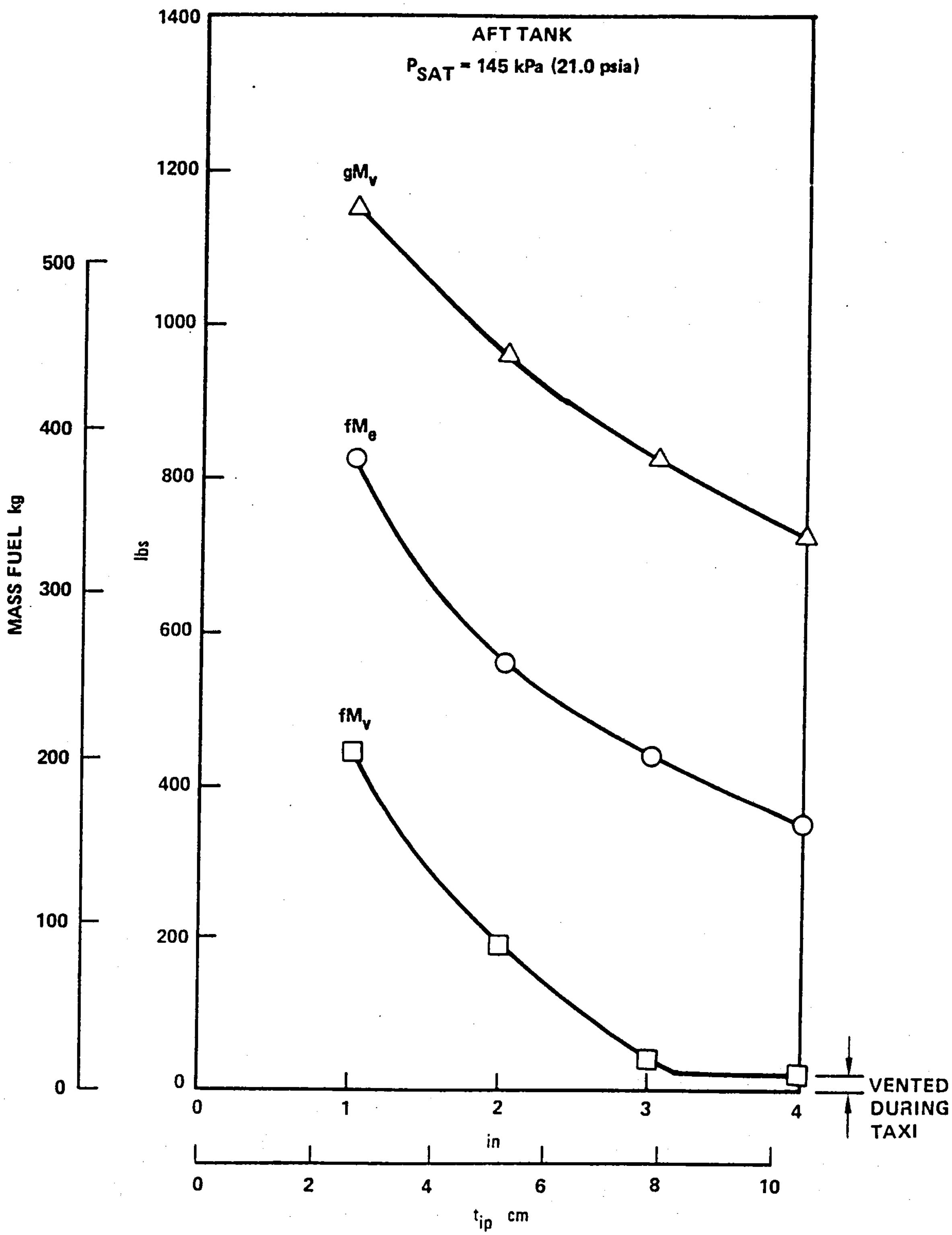

Figure 108. - Mass of fuel vented on ground and in-flight and mass evaporated in-flight as a function of insulation thickness for 145 kPa (21 psia) saturated liquid fill.

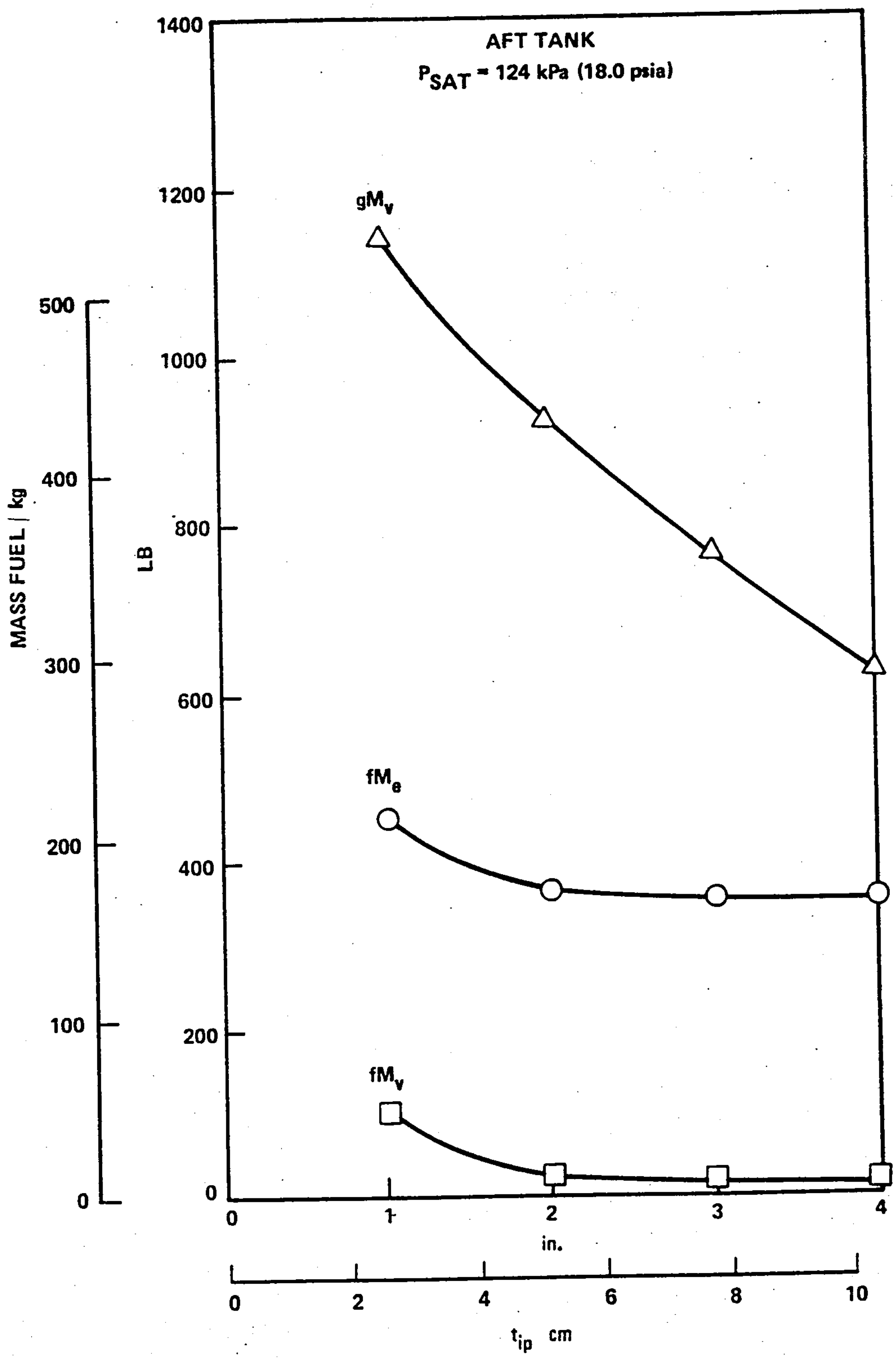

Figure 109. - Mass of fuel vented on ground and in-flight and mass evaporated in-flight as a function of insulation thickness for 124 kPa (118 psia) saturated liquid fill.

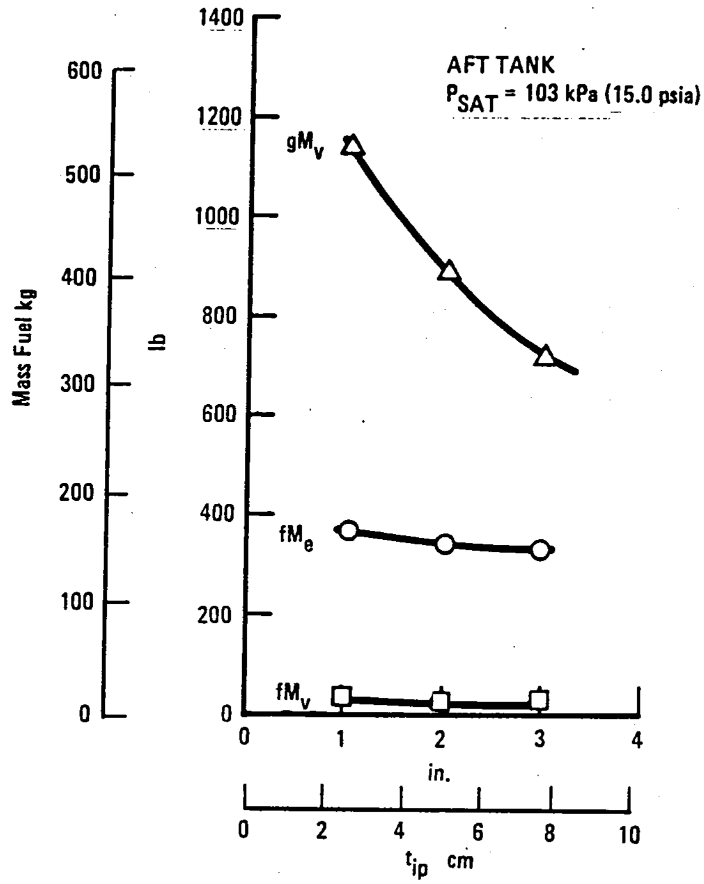

Figure 110. - Mass of fuel evaporated and vented as a function of primary insulation thickness for 103 kPa (15 psia) saturated liquid fill, aft tank.

8.3.3.2 Forward tank.- Figures 112 through 114 present the results of the analysis of the spherical tank for three fill conditions of 145, 124 and 103 kPa (21, 18, and 15 psia), respectively. Weight summaries for representative thicknesses are given in table 45. Insulation thicknesses of 3.81 cm (1.50 in.) and 2.54 cm (1.0 in.) were selected for the aft and forward tanks, respectively. Even with this reduced insulation thickness the spherical tank fuel losses are less than for the aft tank. This is the result of the more favorable wetted area-to-volume ratio for the sphere, particularly at the lower liquid fractions corresponding to the second half of the cruise segment and during the ground period after flight. The influence of lower liquid temperatures for tank filling is similar to that observed for the aft tank.

Again, using the optimization criteria of sum of mass evaporated in flight and insulation weights, the suggested insulation thickness for 21 psia fill conditions is 5.08 cm (2.0 in.). Figure 115 illustrates the weight summation parameter as a function of insulation thickness for the three fill conditions. From a mass loss consideration only, the use of lower temperature

TABLE 44. - SUMMARY OF FUEL AND INSULATION WEIGHTS AS A FUNCTION OF INSULATION THICKNESS AND FUEL SATURATION PRESSURE AT FILL

Saturation Pressure of Fuel at kPa Fill (psia)	145 (21)			124 (18)			103 (15)		
Insulation Thickness cm (in)	2.54 (1)	5.08 (2)	7.62 (3)	2.54 (1)	5.08 (2)	7.62 (3)	2.54 (1)	5.08 (2)	7.62 (3)
Fuel Vented during Ground Hold, kg (lbs)	337 (742.2)	252 (556.6)	197 (433.7)	334 (735.7)	244 (537.9)	174 (383.7)	333 (734.7)	225 (495.2)	154 (338.9)
Fuel Vented during Fill, kg (lbs)	188 (415.5)	184 (404.6)	177 (391.0)	182 (404.1)	176 (388.4)	173 381.1)	184 (404.8)	177 (389.6)	173 (381.9)
Total Recoverable Fuel Vented on Ground, kg (lbs)	525 (1157.7)	436 (961.1)	374 (824.7)	517 (1139.8)	420 (926.3)	347 (764.8)	517 (1139.5)	401 (884.8)	327 (720.8)
Fuel Vented during Flight, kg (lbs)	200 (441.2)	85.7 (189.0)	15.5 (34.2)	41.5 (91.4)	8.16 (18.0)	6.89 (15.2)	10.6 (23.3)	7.8 (17.2)	6.7 (14.8)
Fuel Evaporated during Flight, kg (lbs)	371 (817.0	252 (556.6)	196 (432.0)	206 (454.1)	164 (362.0)	160 (351.9)	167 (368.0)	157 (345.6)	152 (335.2)
Insulation Weight*, kg (lbs)	119 (262.5)	215 (473.8)	311 (684.8)	119 (261.7)	214 (472.8)	310 (684.1)	119 (261.4)	214 (472.7)	310 (684.0)
Σ Weight of Insulation and Fuel Evaporated during Flight, kg (lbs)	490 (1079.5)	467 (1030.4)	507 (1116.8)	325 (715.8)	383 (834.8)	470 (1036.0)	285 (629.4)	371 (818.3)	462 (1019.0)

*Open cell foam plus KEVLAR fairing weights not included.

liquid yields an insulation thickness less than 2.54 cm (1.0 in.). As for the aft tank, this thickness yields acceptable exterior temperatures.

8.3.3.3 Tank pressure control.- A minimum design tank pressure during ground and flight was input into the computer program for system thermodynamic analysis. A minimum design pressure of 110 kPa (16 psia) was selected for these studies. If at any time during the mission tank pressure falls to this value, a subroutine is called in the program to compute the additional amount of fuel which must be vaporized to maintain the design pressure level. This additional vaporized fuel quantity is added to that resulting from heat transfer to the liquid. For the insulation thicknesses investigated for fill liquid temperatures down to 103 kPa (15 psia) saturation conditions, no additional fuel vaporization was required.

For the 145 kPa (21 psia) fill cases the tank pressure varied from 145 to 142 kPa (21.0 to 20.5 psia) from takeoff to landing for 7.62 cm (3 in.) primary insulation thickness. For 6.35 cm (2.5 in.) of insulation, the pressure range was nearly equivalent as shown by figure 116. For 2.54 cm (1 in.) and 5.08 cm (2 in.) of insulation, tank pressure remained above 138 kPa (20 psia) for all times. For lower saturation pressure fill conditions, tank pressure during flight is reduced over that of the 145 kPa (21 psia) case, as illustrated by Figures 116 through 121. Liquid temperatures at the surface and bottom of the tank and the mean liquid temperature are shown as a function of

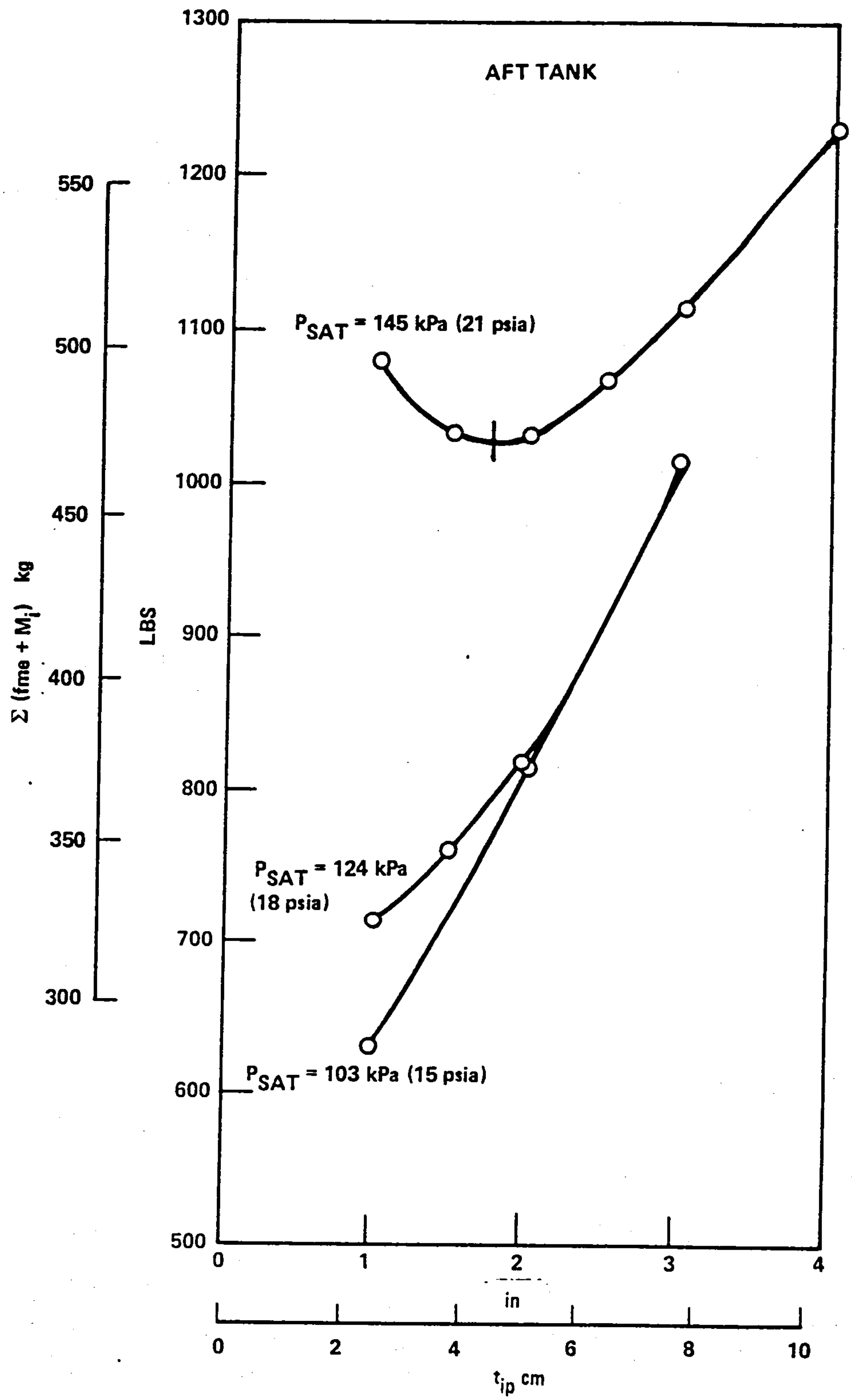

Figure 111. - Sum of weights of insulation and fuel evaporated in-flight as a function of insulation thickness and liquid saturation pressure at fill.

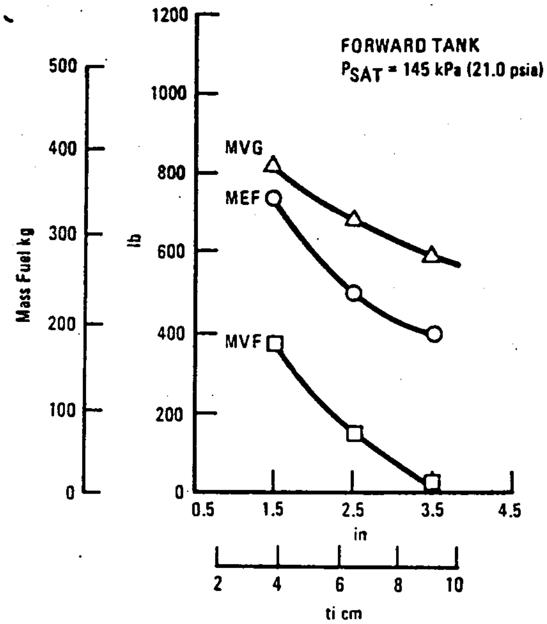

Figure 112. - Mass of fuel evaporated and vented as a function of insulation thickness for 145 kPa (21 psia) saturated liquid fill, forward tank.

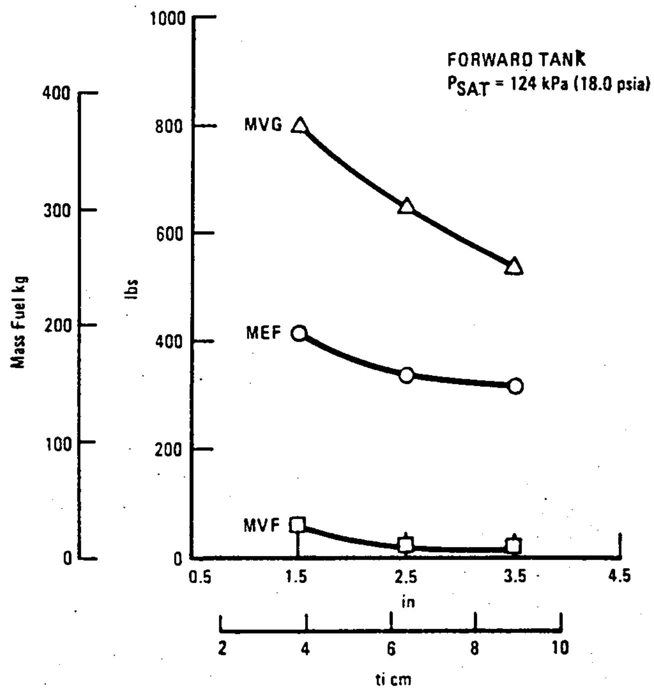

Figure 113. - Mass of fuel evaporated and vented as a function of insulation thickness for 124 kPa (18 psia) saturated liquid fill, forward tank.

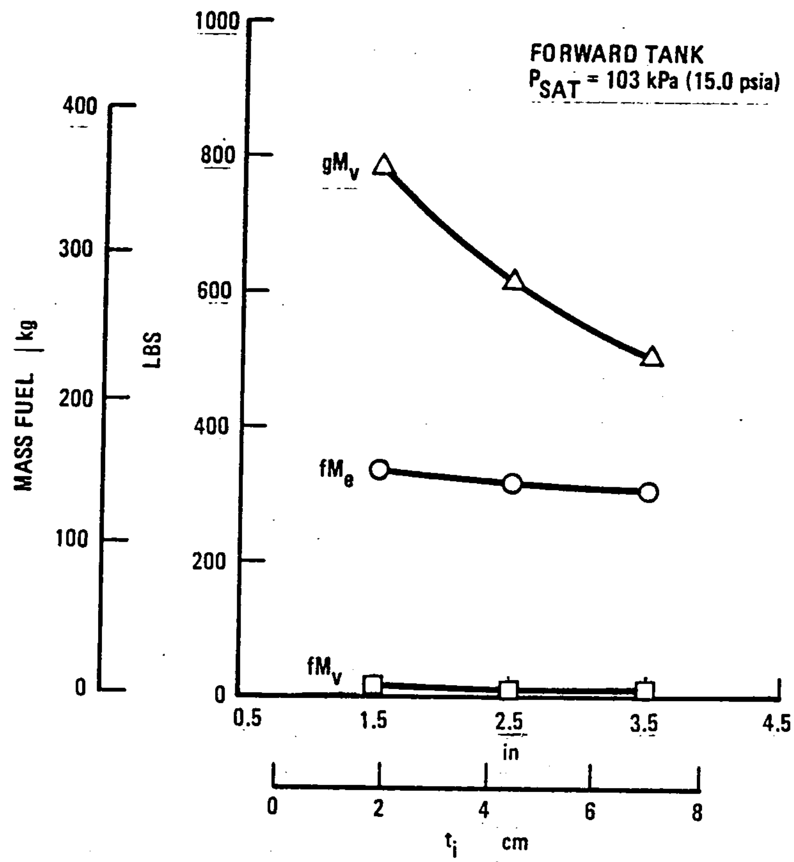

Figure 114. - Mass of fuel evaporated and vented as a function of insulation thickness for 103 kPa (15 psia) saturated liquid fill, forward tank.

insulation thickness, fill conditions, and flight time. The ullage pressure corresponds to liquid surface temperature saturation pressure. It should be noted that the computer program introduces the fill liquid into the bottom of the tank and assumes no forced mixing, i.e., single phase-saturated liquid for fill. Thus, the liquid temperature distributions are not the result of wall heat flux induced stratification, but rather the full model. Separate calculations indicated that stratification of liquid methane would be very small at the wall heat rates considered in this study.

Considering the quiescent fill conditions, tank pressure is described by the upper curve of each figure. If mixing occurs, the intermediate or mean liquid temperature curve defines pressure, as this is the temperature which the fully mixed liquid would experience. For the cases investigated at 124 and 103 kPa (18 and 15 psia) fill conditions, tank pressure for stratified or fully mixed liquid did not fall below the 110 kPa (16 psia) design value.

A similar study was conducted for the forward tank at an insulation thickness of 6.35 cm (2.5 in.) Because of the geometry modeling methodology used for the spherical tank, these data are less accurate than those for the aft tank. They do however, serve to illustrate the pressure trends with fill

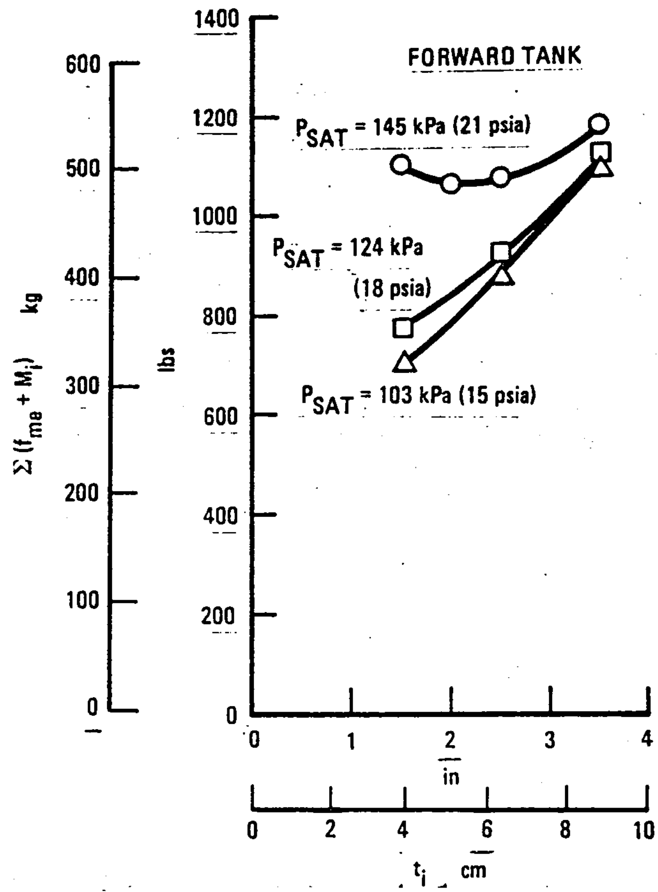

Figure 115. - Sum of insulation and fuel evaporated during flight weights as functions of insulation thickness and fill condition (P_{SAT}).

condition variation. Figures 122 through 124 show liquid temperatures and correspondingly, pressure for fill conditions of 145, 124 and 69 kPa (21, 18, and 10 psia). The fill pressure pressure range was lowered to 69 kPa (10 psia) to find a lower practical value. For 145 kPa (21 psia) for the majority of the flight. The pressure reduction is enhanced in the latter flight period because of the more favorable wetted area-to-volume ratio for the sphere.

A similar increase in pressure reduction over that in the aft tank is seen for 124 kPa (18 psia) fill conditions. For 69 kPa (10 psia) fill conditions, tank pressure at landing is slightly less than the 110 kPa (16 psia) design value. Of more significance, however, is the potential of a dangerously low pressure if complete mixing occurred during takeoff and climb. Mixing could reduce tank pressure to 75.8 kPa (11 psia) which would be less than atmospheric pressure. Although the high degree of subcooling would eliminate in-flight venting and venting on the ground for up to 8 to 10 hours, the potential of catastrophic tank failure eliminated the use of fill liquid saturated at less than 103 kPa (15 psia) from further study.

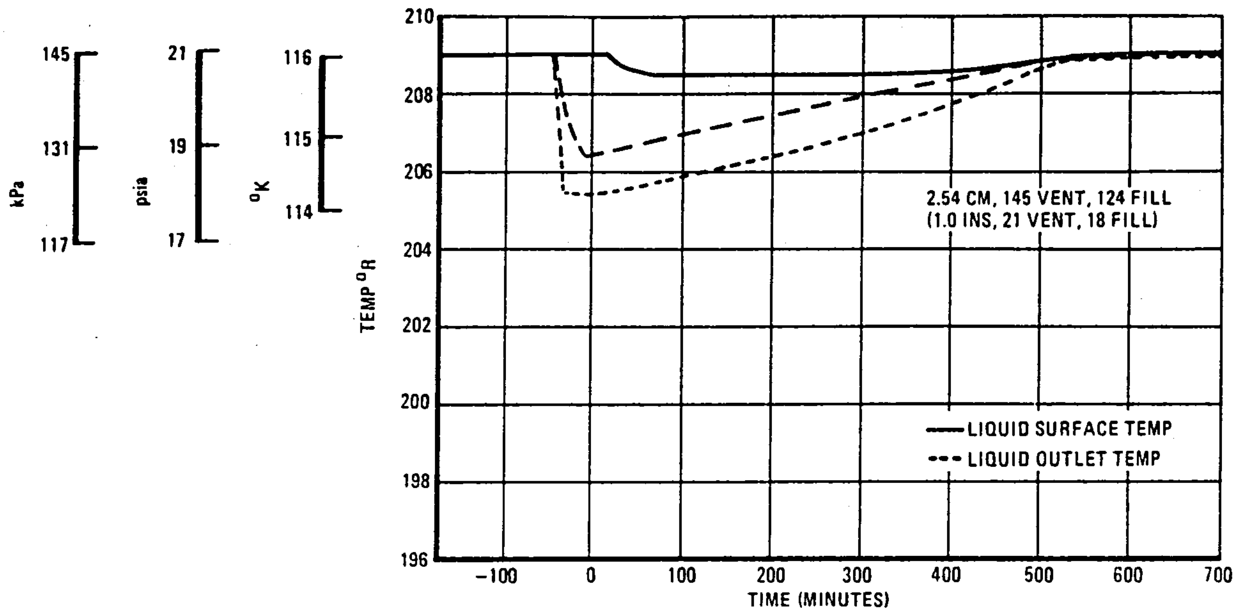

Figure 116. - Aft tank pressure and liquid temperature histories, 124 kPa (18 psia) fill, t_{ip} = 2.54 cm (1.0 inch).

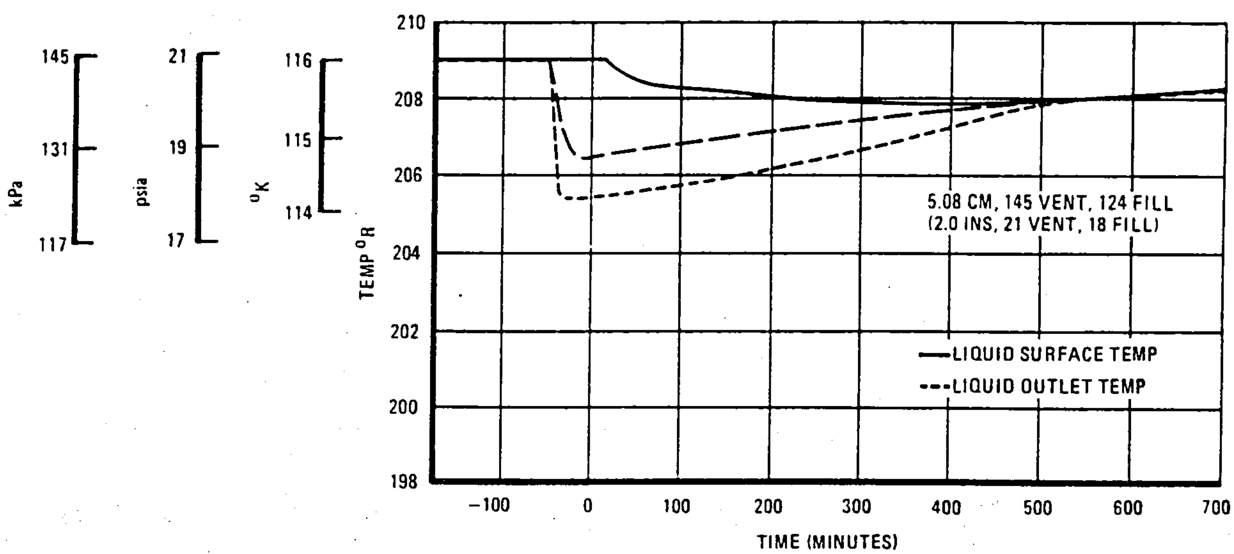

Figure 117. - Aft tank pressure and liquid temperature histories, 124 kPa (18 psia) fill, t_{ip} = 5.08 cm (2.0 inch).

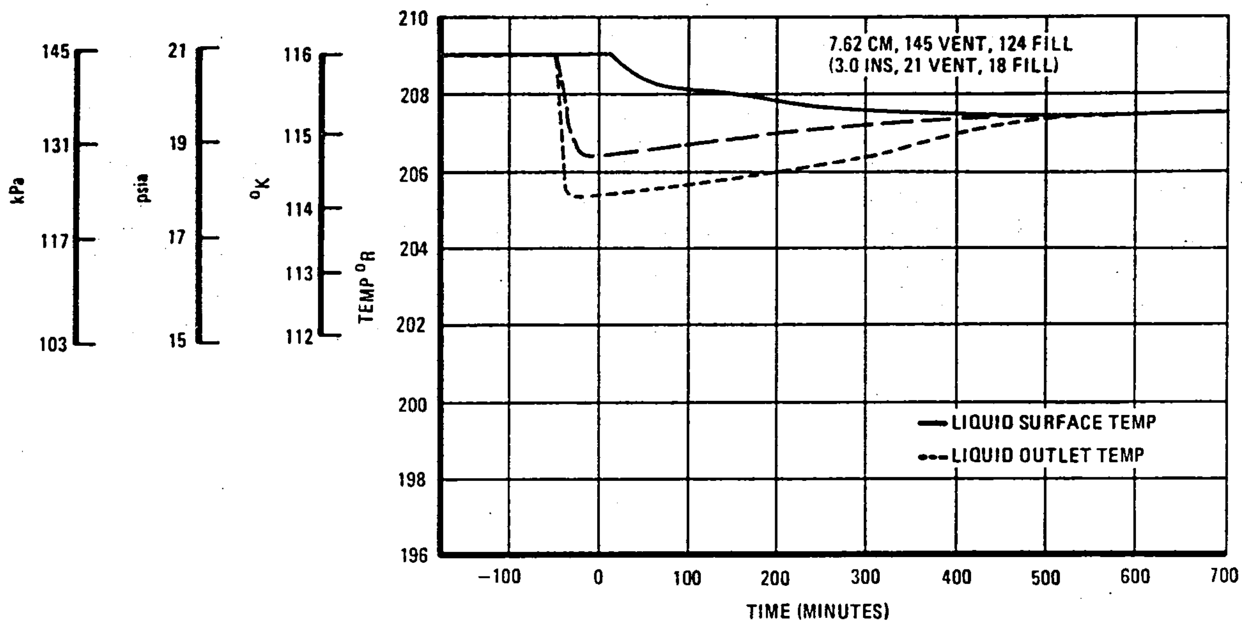

Figure 118. - Aft tank pressure and liquid temperature histories, 124 kPa (18 psia) fill, t_{ip} = 7.62 cm (3.0 inch).

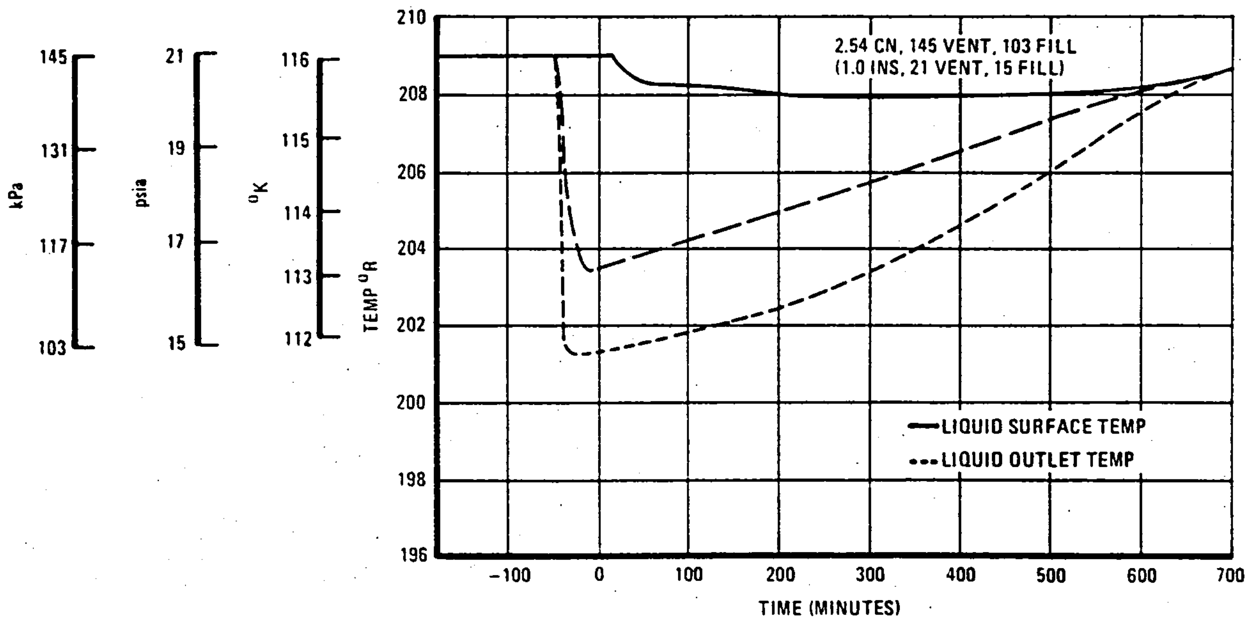

Figure 119. - Aft tank pressure and liquid temperature histories, 103 kPa (15 psia), t_{ip} = 2.54 cm (1.0 inch).

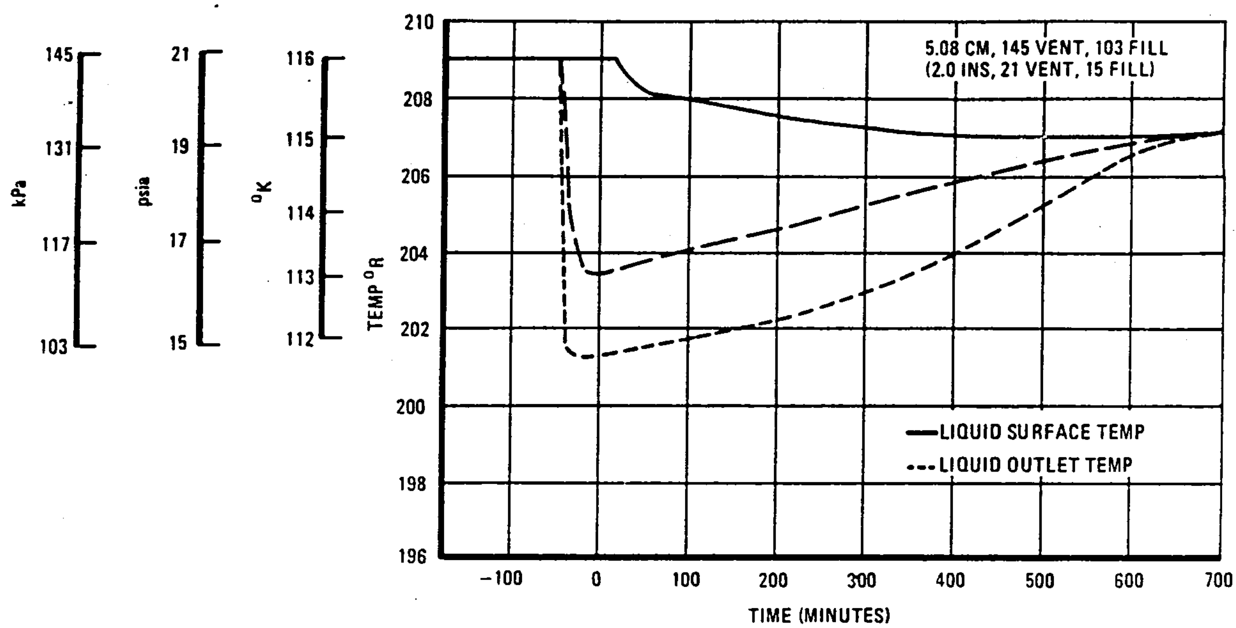

Figure 120. - Aft tank pressure and liquid temperature histories, 103 kPa (15 psia) fill, t_{ip} = 5.08 cm (2.0 inch).

As regards the effect of severe in-flight turbulence on tank pressure, two cases were studied. One was for turbulence during climb (15 minutes into flight) and one on landing. These represent the extremes of vapor volumes and tank wall temperatures. For climb, the vapor volume is small, and the mean vapor temperature is low. The vapor space average tank wall temperature is also low. At landing, vapor volume is large and mean vapor temperature is higher with a corresponding higher tank wall temperature. For 103 kPa (15 psia) fill conditions and t_{ip} = 5.08 cm (2.0 in.), tank pressure did not fall below 110 kPa (16 psia) for either case. At landing, a pressure rise was observed due to turbulence.

8.3.3.4 Fuel containment system temperatures.- Aft tank wall temperature distributions as a function of circumferential location, w/ℓ , for liquid fractions of 0.50 and 0.15 are given in table 46 for two fill conditions, 145 and 103 kPa (21 and 15 psia). At the top of the tank x/ℓ = 0. The gradient decreases with increasing insulation thickness, and the maximum gradient occurs at the liquid-vapor interface (x/ℓ = 0.5 for 50 percent liquid fraction and x/ℓ = 0.699 for 15 percent liquid draction). The temperature of the fill liquid has little influence on the gradient, as shown by comparing the 145 and 103 kPa (21 and 15 psia) results.

TABLE 45. - FORWARD TANK - SUMMARY OF FUEL AND INSULATION WEIGHTS AS A FUNCTION OF INSULATION THICKNESS AND FUEL SATURATION PRESSURE AT FILL

Saturation Pressure of Fuel at Fill kPa (psia)	145 (21)			124 (18)			103 (15)		
Insulation Thickness cm (in)	3.81 (1.5)	6.35 (2.5)	8.89 (3.5)	3.81 (1.5)	6.35 (2.5)	8.89 (3.5)	3.81 (1.5)	6.35 (2.5)	8.89 (3.5)
Fuel Vented during Ground Hold, kg (lb)	230 (506.9)	170 (380.1)	134 (296.0)	228 (502.4)	167 (367.4)	119 (262.0)	227 (500.8)	153 (338.2)	105 (231.5)
Fuel Vented during Fill, kg (lb)	138 (303.3)	134 (295.4)	129 (285.4)	132 (291.0)	128 (281.5)	126 (277.2)	128 (282.0)	124 (273.2)	122 (268.8)
Total Recoverable Fuel Vented on Ground, kg (lb)	368 (810.2)	306 (675.5)	264 (581.4)	360 (793.4)	294 (648.9)	245 (539.2)	355 (782.8)	277 (611.4)	227 (500.3)
Fuel Vented during Flight, kg (lb	168 (369.3)	63.5 (140.0)	3.6 (7.9)	23 (51.0)	6.4 (14.1)	5.8 (12.7)	8.8 (19.3)	5.9 (13.1)	4.6 (10.2)
Fuel Evaporated during Flight, kg (lb)	338 (745.1)	230 (507.6)	179 (394.0)	188 (414.1)	150 (330.1)	145 (320.3)	152 (334.9)	143 (314.5)	138 (304.3)
Insulation Weight*, kg (lb)	163 (359.7)	259 (571.9)	357 (787.9)	163 (359.7)	259 (571.9)	357 (787.9)	163 (359.7)	294 (571.9)	357 (787.9)
Weight of Insulation and Fuel Evaporated during Flight, kg (lb)	501 (1104.8)	490 (1079.5)	536 (1181.9)	164 (773.8)	414 (912.0)	503 (1108.2)	315 (694.6)	402 (886.4)	495 (1092.2)

*36.8 kg/m^3 (2.3 lb/ft^3) STEPAN foam plus MAAMF vapor barrier.

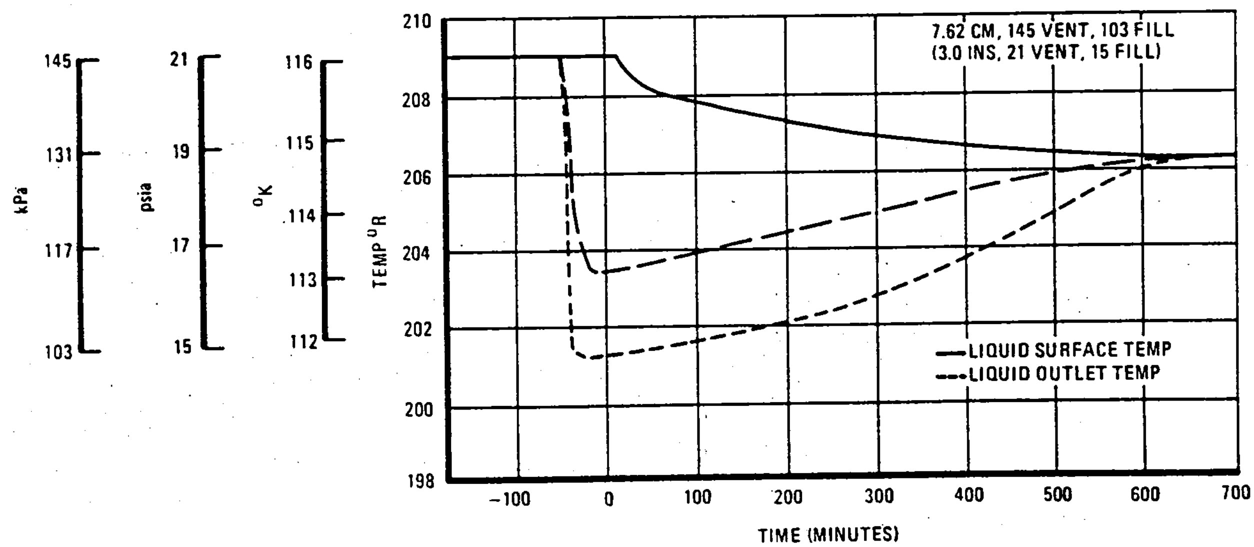

Figure 121. - Aft tank pressure and liquid temperature histories, 103 kPa (15 psia) fill, t_{ip} = 7.62 cm (3.0 inch).

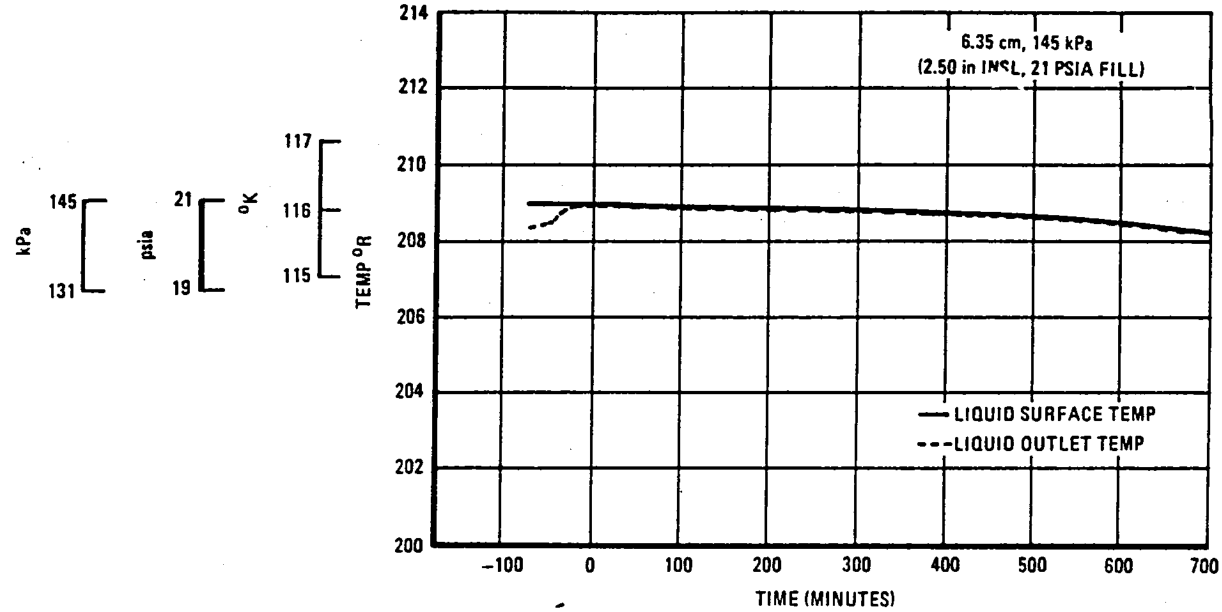

Figure 122. - Forward tank pressure and liquid temperature histories, 145 kPa (21 psia) fill, t_i = 6.35 cm (2.5 inch).

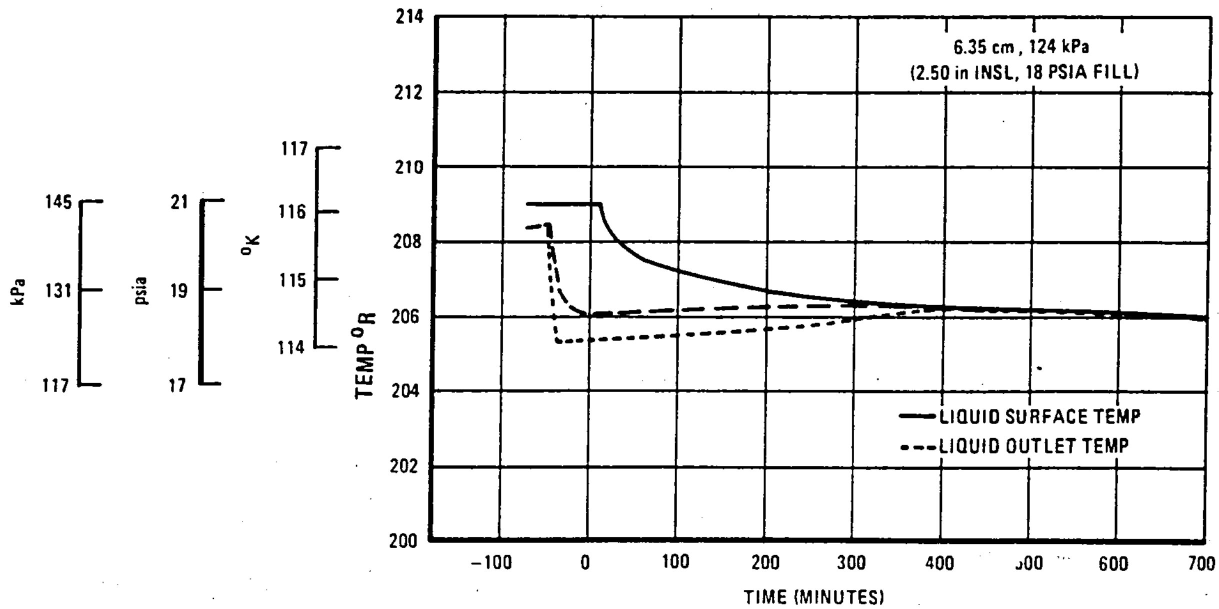

Figure 123. - Forward tank pressure and liquid temperature histories, 124 kPa (18 psia) fill, t_i = 6.35 cm (2.5 inch).

TABLE 46. - AFT TANK WALL TEMPERATURE DISTRIBUTION ^{o}K (^{o}R)

(a) Liquid Fraction = 0.50 (Tank Half Empty)

Fill Conditions, P_{SAT} kPa (psia)	145 (21)			103 (15)		
T_{ip} cm (inches)	2.54 (1)	5.08 (2)	7.62 (3)	2.54 (1)	5.08 (2)	7.62 (3)
x/ℓ = 0.101	197 (354)	184 (331)	176 (316)	198 (356)	184 (332)	176 (317)
0.177	192 (346)	179 (323)	171 (308)	193 (348)	180 (324)	172 (309)
0.230	188 (338)	175 (315)	167 (300)	188 (339)	175 (315)	167 (300)
0.275	183 (329)	170 (306)	162 (292)	183 (330)	170 (306)	162 (292)
0.315	177 (318)	164 (296)	157 (283)	177 (319)	164 (296)	157 (282)
0.351	169 (305)	158 (285)	152 (273)	170 (306)	158 (284)	152 (272)
0.386	162 (291)	151 (272)	145 (261)	162 (291)	151 (272)	144 (260)
0.419	152 (273)	143 (258)	138 (249)	152 (273)	143 (257)	138 (248)
0.452	140 (252)	134 (241)	131 (235)	140 (252)	133 (240)	129 (233)
0.484	126 (226)	123 (221)	122 (219)	125 (225)	122 (220)	121 (217)
0.500	117 (210)	116 (209)	116 (209)	116 (208)	115 (207)	115 (207)
1.000	117 (210)	116 (209)	116 (209)	114 (205)	113 (204)	113 (204)

(b) Liquid Fraction = 0.15 (Tank at Reserve Level)

0.128	209 (376)	194 (349)	184 (331)	209 (377)	194 (350)	184 (331)
0.224	206 (371)	191 (343)	181 (325)	207 (372)	191 (344)	181 (325)
0.294	203 (366)	187 (337)	177 (319)	203 (366)	188 (338)	177 (319)
0.353	199 (359)	183 (330)	173 (312)	199 (359)	183 (330)	173 (311)
0.407	195 (351)	179 (322)	169 (304)	195 (351)	179 (322)	168 (303)
0.452	189 (340)	173 (312)	163 (294)	189 (340)	173 (311)	163 (293)
0.510	182 (327)	167 (300)	157 (283)	182 (327)	161 (290)	157 (282)
0.561	172 (310)	158 (284)	150 (270)	172 (309)	157 (283)	149 (268)
0.613	159 (286)	147 (264)	141 (253)	158 (285)	146 (263)	139 (251)
0.669	137 (147)	131 (235)	127 (229)	137 (247)	130 (234)	126 (227)
0.699	117 (210)	117 (210)	116 (209)	117 (210)	116 (208)	115 (207)
1.000	117 (210)	117 (210)	116 (209)	117 (210)	116 (208)	114 (206)

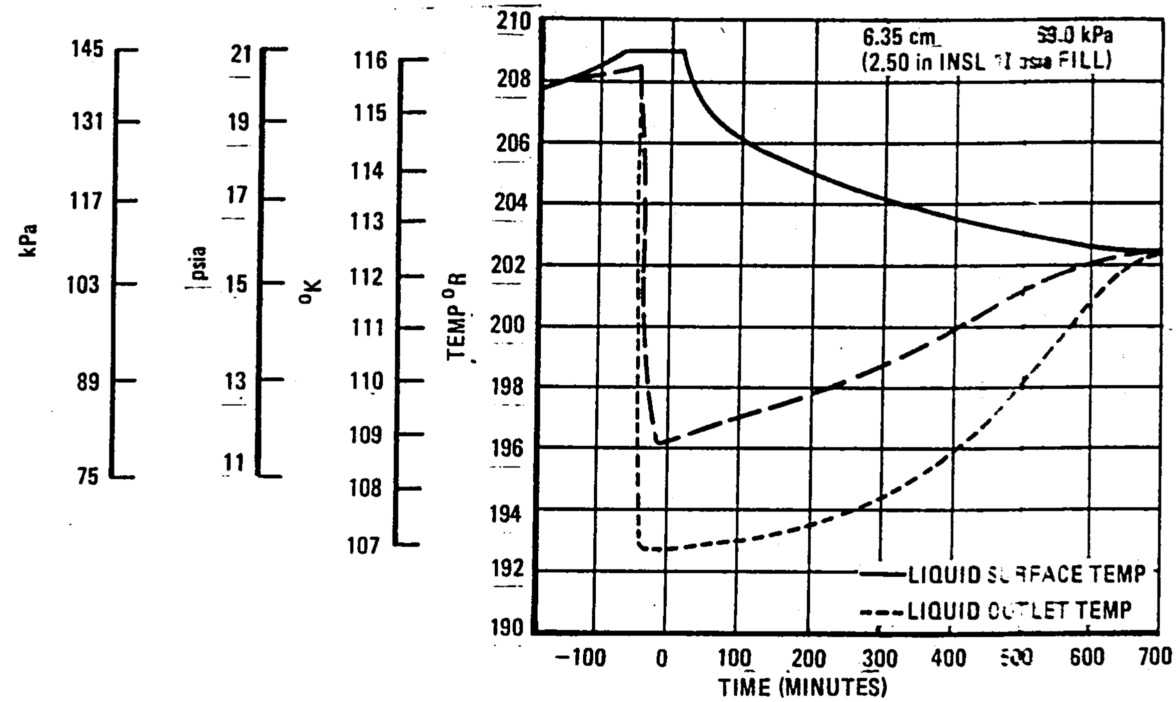

Figure 124. - Forward tank pressure and liquid temperature histories, 69.0 kPa (10 psia) fill, t_i = 6.35 cm (2.5 inch).

Circumferential temperature distributions along the vapor barrier and fuselage external surface as a function of insulation thickness are shown by table 47 for the two fill conditions. Again, the fill condition has a negligible effect on temperature. Also, for the small insulation thicknesses, 2.54 cm (1 in.), the exterior temperatures are identical with those for the thicker insulation, 2.62 cm (3 in.). As external temperature levels and the local gradients are not influenced by the fill conditions, the 2.54 cm (1 in.) insulation thickness is in the optimum region if tank filling can be done with 124 or 103 kPa (18 or 15 psia) saturated liquid.

The values for the forward spherical tank wall temperature distribution are given in table 48. As before, the model used is simply a section of the tank on a diameter. The points x/ℓ to which the numbers are referred are positions around the tank expressed in terms of π radians. Values are given for the landing condition which will be used as the design point. The temperature differences between that and the 50 percent full condition are small.

TABLE 47. - AFT TANK VAPOR BARRIER AND FUSELAGE EXTERIOR TEMPERATURE DISTRIBUTIONS °K (°R)

(a) Liquid Fraction = 0.50 (Tank Half Empty)

Fill Condition P_{SAT} kPa (psia)	145 (21)						103 (15)					
T_{ip} cm (inches)	2.54 (1)		5.08 (2)		7.62 (3)		2.54 (1)		5.08 (2)		7.62 (3)	
Location	VB	F	VB	F	VB	F	VB	F	VB	F	VB	F
x/ℓ = 0.101	224 (404)	247 (444)	229 (413)	247 (444)	233 (419)	247 (444)	225 (405)	247 (444)	229 (413)	224 (404)	233 (419)	224 (404)
0.177	223 (401)		228 (411)		232 (417)		223 (402)		228 (411)		232 (417)	
0.230	221 (398)		227 (409)		231 (416)		221 (398)		227 (410)		231 (416)	
0.275	219 (394)		226 (407)		230 (414)		219 (394)		226 (407)		230 (414)	
0.315	217 (390)		225 (404)		229 (413)		217 (390)		224 (404)		230 (314)	
0.351	214 (385)		223 (402)		228 (411)		214 (385)		223 (402)		228 (411)	
0.386	211 (379)	246 (443)	222 (399)		227 (409)		211 (379)		222 (399)		227 (409)	
0.419	207 (373)		220 (396)		226 (407)		207 (373)	246 (443)	220 (396)		226 (407)	
0.452	203 (366)		218 (393)		225 (406)		203 (366)		218 (392)		225 (405)	
0.484	199 (358)		217 (390)		224 (404)		199 (358)		215 (389)		224 (404)	
0.500	198 (356)		216 (389)		224 (404)		197 (355)		215 (388)		224 (404)	
1.000	197 (354)	246 (443)	215 (388)	246 (443)	224 (404)	247 (444)	196 (353)	246 (443)	215 (388)	246 (443)	224 (403)	247 (444)
(b) Liquid Fraction = 0.15 (Tank at Reserve Level)												
0.128	251 (452)	282 (507)	257 (463)	283 (509)	260 (468)	283 (510)	251 (452)	282 (507)	257 (463)	283 (509)	260 (468)	283 (510)
0.224	250 (450)		257 (462)		259 (467)		250 (450)		257 (462)		259 (467)	
0.294	248 (447)	281 (506)	256 (461)	283 (508)	259 (466)	283 (509)	249 (448)	281 (506)	256 (461)	283 (508)	259 (466)	283 (509)
0.353	247 (444)		255 (459)		258 (465)		247 (445)		255 (459)		258 (465)	
0.407	245 (441)	281 (505)	254 (457)		258 (464)		245 (441)	281 (505)	254 (457)		257 (463)	
0.452	243 (437)		252 (454)	282 (507)	257 (462)	282 (508)	243 (437)		252 (454)	282 (507)	257 (462)	
0.510	239 (431)	280 (504)	251 (451)		256 (460)		239 (431)	280 (504)	251 (451)		255 (460)	282 (508)
0.561	236 (425)		249 (448)	281 (506)	254 (458)		236 (425)	279 (502)	249 (448)	281 (506)	254 (458)	
0.613	231 (416)	278 (501)	247 (444)		253 (455)	282 (507)	231 (416)	278 (501)	247 (444)		253 (455)	
0.669	224 (404)		244 (439)	281 (505)	252 (453)		224 (404)	277 (499)	244 (439)	281 (505)	253 (456)	282 (507)
0.699	221 (397)	277 (498)	243 (437)	280 (504)	251 (452)		221 (397)	277 (498)	242 (436)	280 (504)	251 (452)	
1.000	219 (395)	277 (498)	242 (436)	280 (504)	251 (452)	282 (507)	219 (395)	277 (498)	242 (436)	280 (504)	251 (451)	282 (507)

TABLE 48. - FORWARD TANK WALL TEMPERATURE DISTRIBUTION FOR 15 PERCENT LIQUID LEVEL t_{ip} = 5.08 cm (2.0 inch)

x/L	°K (°R)
0.128	193 (348)
0.224	191 (343)
0.294	188 (338)
0.353	183 (330)
0.407	179 (322)
0.452	173 (312)
0.510	166 (298)
0.561	156 (281)
0.613	144 (259)
0.669	126 (226)
0.699	114 (205)

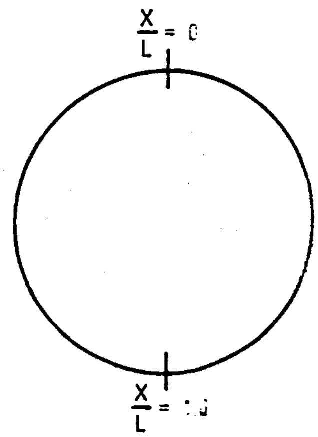

Tank Insulation is 5.08 cm (2.0 inch) of External Stepan Foam BX 250A at 36.8 kg/m^3 (2.3 pcf)

8.3.3.5 Engine feed and fueling/vent lines. - Stepan Foam BX250A was also selected for both engine feed lines and tank fueling and vent lines. This choice is based upon lower line weights and greater aircraft dispatch reliability over vacuum jacketed, multilayer insulated lines. Considering the 3.18 cm (1-1/4 in.) ID engine feed line, a vacuum jacketed line would weight 1.06 kg/m (0.712 lb/ft) of line length; the foam insulated line weights 0.659 kg/m (0.443 lb/ft). These weights do not include the weight of the fuel containing conduit itself. The two line concepts are shown diagrammatically in figure 125. The vacuum jacket thickness is based upon the minimum size recommended in reference 4.

A stainless steel vacuum jacket was selected to be consistent with commercial practices for cryogenic lines because of the nonactive pumping system concept. A metal jacket for the foam insulated line was selected to provide an impervious vapor barrier which would have a high degree of resistance to accidental puncture during servicing and would transfer line support point loads more uniformly to the foam.

Both concepts were considered to be made up of 6.096 m (20-ft) lengths of line with couplings for removal at each end. The couplings for the vacuum jacketed line was estimated to weigh 0.907 kg (2 lb) per section, whereas, the foam insulated line couplings are 0.454 kg (1 lb) per section. The higher vacuum jacketed line coupling weight is necessitated by the requirements of a re-entrant type of construction and long-life vacuum integrity for a non-actively pumped system.

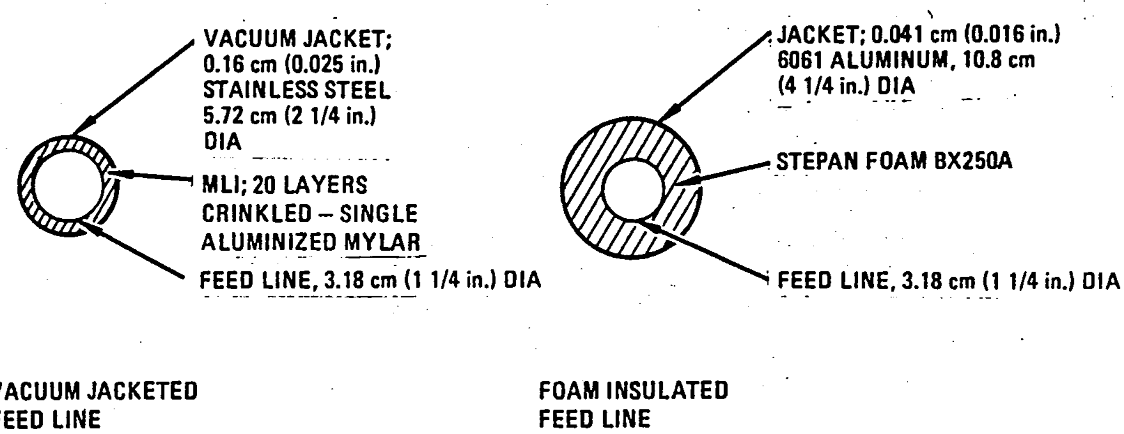

LINE WEIGHTS kg/m (lb/ft)

	VACUUM JACKET	FOAM INSULATED
JACKET	0.082 (0.594)	0.0257 (0.186)
INSULATION	0.002 (0.018)	0.0286 (0.207)
COUPLINGS	0.014 (0.100)	0.0069 (0.050)
	0.098 (0.712)	0.0612 (0.443)

Figure 125. - Comparison of feed line weights (inner line weight not included).

Loss of vacuum in a single section of line would not present a direct safety hazard. It would, however, require replacement during aircraft turnaround which would necessitate taking the aircraft out of service for inerting of the line and replacement. The foam insulated line may experience long-term degradation due to thermal cycling. The outer aluminum jacket will, however, prevent water and ice buildup within the insulation. This type of long-term degradation would be handled by scheduled servicing operations and would increase dispatch reliability.

The weight of the 10.16 cm (4 in.) fueling line is also greater for the vacuum jacketed-multilayer insulated line than for the foam concept. Weight estimates for these two concepts, excluding couplings, are 2.03 kg/m (1.364 lb/ft) and 1.31 kg/m (0.878 lb/ft), respectively. This weight difference is again due to the stainless steel vacuum jacket requirement. An aluminum jacket and coupling were considered and rejected because of vacuum integrity considerations. Problems associated with failures of welded aluminum joints (cracking) under long-term thermal and mechanical cycling resulted in the rejection of this concept.

The foam insulated lines will be subject to condensation during periods of operation at low ambient temperatures and high relative humidities; i.e., temperatures on the ground within the 278 to 289°K (500° to 520°R) range. Condensation will occur for relatively short period of time on the ground or at low altitudes. Water vapor will form as liquid rather than a solid because of the small temperature difference between ambient and the line exterior surface, considering the energy given up during condensation and the thermal resistance of the insulation. Condensation could be disposed of by suitable drains in the aircraft interior or eliminated by providing a dry air purge of the area adjacent to the lines during ground operations when the lines are chilled.

Foam insulation thicknesses were computed for the fueling and feed lines by equating the heat transfer to the liquid with a maximum permitted temperature rise for the length of line at the critical flow rate. For the feed system, this mass flow rate was the ground taxi rate (minimum fuel flow). For fill lines, it was the average mass flow rate in each section. Computations were performed in an iterative manner using:

$$\Delta T = \frac{q^* \ell}{m c_p}$$

where ΔT is the liquid temperature rise in the total line length/(ℓ), q^* is the liquid wall heat flux per unit length of line, m is the liquid mass flow rate, and C_p is the mean specific heat of the liquid.

Wall heat flux, q^*, is computed from:

$$q^* = \frac{T_{ambient} - T_{liquid}}{R_T}$$

where $R_T = R_o + R_i + R_e$, and R_o is the total resistance between ambient and the exterior surface of the line (radiation and convection), R_i is the resistance of the insulation and R_e is the resistance at liquid-wall interface. For R_o, the ambient and enclosure temperatures were considered to be equal for radiation and conduction computations, and the emittance of the enclosure was taken to be 0.8 and the line 0.1. As the resistances are functions of temperature and diameters, it was necessary to use an iterative procedure for convergence of the solution.

Insulation for the engine feed line was sized using a 63.5 m (208.33 ft) length of 3.18 cm (1-1/4 in.) line with the pressure at the engine feed pump end of the line at 276 kPa (40 psia). The liquid thermodynamic state from the boost pump corresponds to a saturated liquid at 145 kPa (21 psia). In order to keep the fuel at a saturation temperature below that of liquid at 276 kPa (40 psia) a ($6^{o}R$) temperature rise was permitted at a minimum flow rate of 0.057 kg/sec (0.126 lb/sec) while taxiing. The $3.3^{o}K$ ($6^{o}R$) rise provides a factor of safety of 2 to account for possible line insulation degradation or a lower mass flow rate.

Calculations of wall heat flux per unit line length as a function of insulation thickness for several ambient conditions were made, and the results are shown in figure 126a. Temperature differences between ambient and exterior line surface as a function of ambient temperatures are shown in figure 126b. These values are for a line surface emittance of 0.1. Increasing the emittance to 0.8 decreases the ΔT value by approximately 40 percent; i.e., at 3.18 cm (1-1/2 in.) insulation thickness for $T_{amb} = 289^{o}K$ ($500^{o}R$), $\Delta T_{\epsilon = 0.8} = 7.2^{o}K$ ($13^{o}R$) compared to $11.7^{o}K$ ($21^{o}R$) for $\epsilon = 0.1$. Increasing the surface emittance will raise the line surface temperature, but this will not eliminate surface condensation for all ambient conditions.

The fuel line insulation thickness was selected for a $289^{o}K$ ($500^{o}R$) ambient, with the fuel conditions from the preceding. This results in a 3.81 cm (1.5 in.) thickness. At cruise, ambient adiabatic wall temperature at the aft tank of $250^{o}K$ ($450^{o}R$), the heat rate is reduced nearly 50 percent from the design point providing an additional margin of safety for flight-idle conditions. Cooling of the fuel line is calculated to occur within 20 sec with boiling liquid in the line, and approximately 8.16 kg (18 lb) of liquid will be evaporated during this cooling period.

A similar sizing approach was used for the fill line which was divided into 50.3 m (165 ft) of 10.16 cm (4 in.) diameter line plus 5.34 m (17.5 ft) of 5.08 cm (2 in.) diameter line. Mass flow rate was reduced at each length segment corresponding to a tank compartment fill point. The insulation was sized to provide a maximum temperature rise of $0.027^{o}K$ ($0.05^{o}R$) for the liquid entering the forward compartment of the front tank. This rise was selected to minimize fuel heating during delivery to maximize heat storage capacity of the fuel if the tanks are filled with liquid saturated at a pressure less than tank venting pressure 145 kPa (21 psia). The results of the wall heat flux and ambient-to-wall temperature difference are shown in Figure 126 and 127 respectively. These results, combined with the fuel-heating criteria, give an insulation thickness of 4.45 cm (1-3/4 in.) for the 10.16 cm (4 in.) diameter segment and 2.23 cm (7/8 in.) for the 5.08 cm (2 in.) diameter portion of the line. The previous comments concerning line cover emittance also apply to this line.

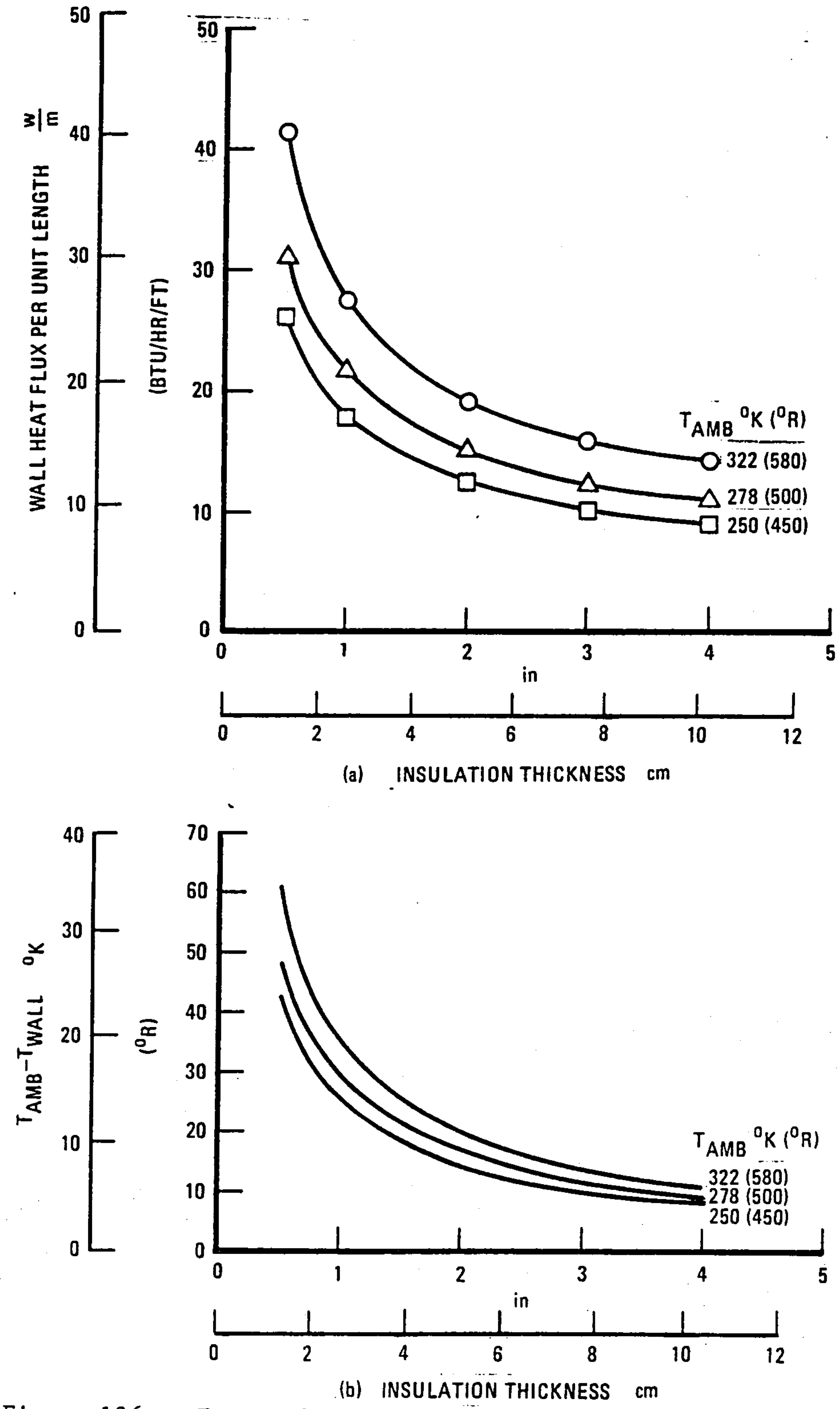

Figure 126. - Engine feed line 3.18 cm (1 1/4 inch) Stepan foam BX250A, outer cover ϵ = 0.1.

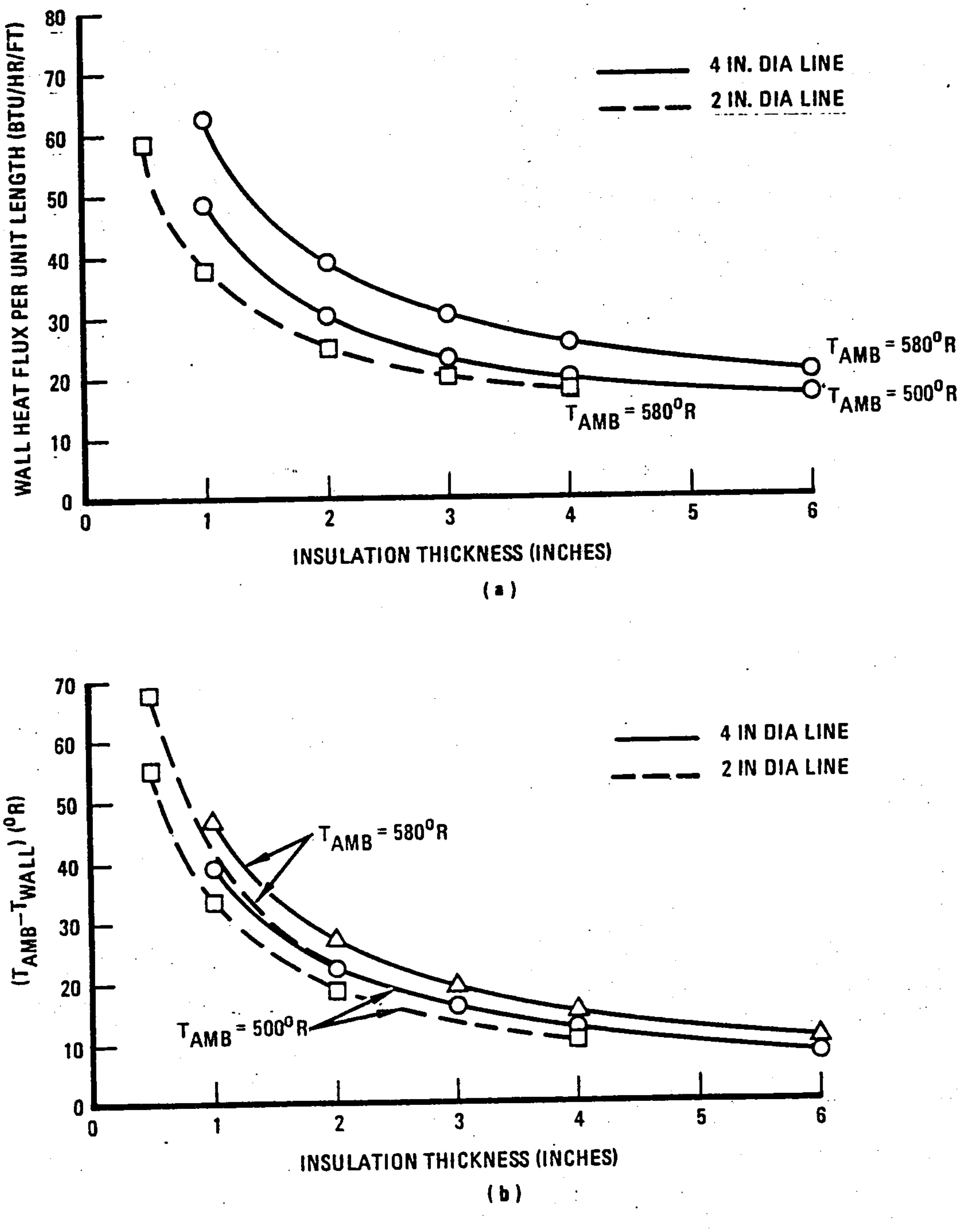

Figure 127. Tank fill and vent lines, Stepan foam BX250A, outer cover ϵ = 0.1.

9. AIRPORT FACILITY REQUIREMENTS

The objective of this task was to determine the requirements and design of the ground facilities, including liquefaction, storage, processing, and distribution system, such that the cost of liquid methane (LCH_4) as an aircraft fuel can be assessed. Further, the relative safety of the LCH_4 ground system was also evaluated.

Evaluation of the ground system for LCH_4 as fuel for subsonic aircraft included the following discrete task analyses:

Task 1. Develop the conceptual configuration of the ground systems

Task 1.1 Select a preferred liquefaction cycle and establish requirements

Task 1.2 Determine the requirements for LCH_4 storage

Task 1.3 Determine the LCH_4 distribution and aircraft refueling system requirements

Task 1.4 Determine LCH_4 processing requirements

Task 2. Assess ground system operating procedure

Task 3. Evaluate the relative safety of the LCH_4 ground system

Task 4. Evaluate the energy consumption of the ground system

Task 5. Estimate the capital and operating costs of the ground system.

The Lockheed-California Company previously analyzed the conceptual requirements of liquid hydrogen (LH_2) as a fuel for subsonic aircraft for NASA (reference 5). To the extent possible, the conceptual LH_2 ground system was modified rather than redesigned for LCH_4 service. The Lockheed study assessed the costs using fuel produced from coal. The present study utilized two feedstocks to produce the LCH_4: substitute natural gas (SNG) from a coal conversion facility and natural gas.

The ground system that was considered in this study had as its input a supply of pipeline natural gas or SNG at the San Francisco International Air Terminal (SFO) boundary. The output of the system is LCH_4, delivered into the aircraft fuel tanks. Consequently, the components of the ground system include the following:

- Liquefaction Facility - The liquefaction facility includes the equipment necessary to receive the feed gas (either natural gas or SNG) and to produce LCH_4 with only traces of other components.

- Storage Facility - The storage facilities include the tankage required to accommodate scheduled and unscheduled downtime of the liquefaction facility and aircraft LCH_4 demand.

- Processing Facility - The processing facilities include those that could be required to subcool the LCH_4 prior to loading of the aircraft fuel tanks in the event analysis herein performed indicated such subcooling to be worthwhile.

- Distribution Facility - The distribution facility includes the piping, pump systems, and hydrants required to deliver the LCH_4 from final processing or storage to the aircraft fuel tanks.

The initial inputs and outputs of the ground system are presented in table 49. The quantities of fuel for SFO are for wide body aircraft in the year 2000. The initial estimates of the quantity of LCH_4 required were based on a BTU equivalency of the requirements for LH_2 as specified in the "LH_2 Airport Requirements Study" (reference 5). A revision of these initial estimates was made as a result of the work that was concurrently being done on the methane aircraft design. The LCH_4-fueled aircraft is larger and heavier than the LH_2-fueled aircraft for the same payload/range. Consequently, the LCH_4 aircraft was determined to require 13 percent more specific energy (BTUs per seat nautical mile) than the LH_2 aircraft. However, the detailed analysis described in Section 10.1.4 explains that this difference in specific energy results in less than 1 percent change in required daily plant capacity.

The primary results of this study are as follows:

- The most appropriate liquefaction cycle, based on relative costs (capital and operating) and six other factors, such as operating flexibility, for the application is the propane-precooled multi-component refrigerant cycle similar to that which is commercially employed in several liquefied natural gas facilities. If the feed gas for the cycle is natural gas, a demethanizer would be required to produce LCH_4 rather than LNG. If the feed gas is SNG, no extensive modifications to the cycle are expected because of the lower boiling points to the feed gas components relative to the boiling point of methane.

- A single liquefaction module (train) sized at 2.41×10^6 m^3/day (85 million SCF/day) of LCH_4 production capacity with appropriate LCH_4 storage facilities was determined to be approximately \$8 million (1976 dollars) less expensive than a dual liquefaction module concept. Both concepts, when storage capacity and number of trains are accounted for, offer the same degree of overall system reliability.

TABLE 49. - INPUTS AND OUTPUTS OF THE GROUND SYSTEM

Input		Output Requirements		
Substitute Natural Gas		**Liquid Methane (LCH_4)**		
Composition, mol %		Composition, mol %		
Methane	94.7	Methane	~ 99	
Carbon Monoxide	0.1	All other	trace	
Carbon Dioxide	0.1	Higher Heating Value =	(23 900 Btu/lb)	
Hydrogen	4.4	Lower Heating Value =	(21 500 Btu/lb)	
Nitrogen	0.7			
or				
Natural Gas		Quantity Required Based on LHVs		
Composition, mol %			Original Estimate	Revised*
Methane	90	Total	($1\,012 \times 10^6$ lb/yr)	($1\,144 \times 10^6$ lb/yr)
Ethane	8	Peak Month	(114.0×10^6 lb)	(129.3×10^6 lb)
Propane	2	11-month Average	(81.6×10^6 lb/mo)	(92.2×10^6 lb/mo)
Quantity Available:	Unlimited	Outlet Pressure:	Unspecified	
Inlet Pressure:	(500 psig)	Outlet Temperature: $\geq$ (-259°)		
Inlet Temperature:	(65°F)			

$$* \; (LH_2 \text{ Req'd}) \times \frac{51\,600 \text{ Btu/lb}}{21\,500 \text{ Btu/lb}} \times 1.13$$

- LCH_4 storage requirements to accommodate schedule downtime, peak demand, and unscheduled downtime, were calculated at 125 900 m^3 (792 000 bbl, API). Based on the relative costs of LCH_4 storage tankage and the ground system requirements, three 42 100 m^3 (265 000 bbl) cylindrical tanks, each with an aluminum inner tank and a carbon steel outer tank, were selected. The minimum cost insulation system for the storage tanks uses perlite of 0.91 m (3-ft) thickness in the annulus formed by the double walled cylinders. The outer tanks are 57.9 m (190 ft) diameter.

- The ground distribution system to deliver the LCH_4 from storage to the aircraft is conceptually similar to the system developed in reference 5. The system consists of two 4878 m (16 000-ft) length, 25.4 cm (10-in.) diameter, 9 percent nickel-steel pipelines. The system will simultaneously accommodate the fueling of four aircraft within 22 minutes. The pipeline insulation consists of 5.08 cm (2-in.) thick polyurethane, which is adequate to minimize the heat infiltration into the pipeline system. Because the pipeline system is below ground (in a trench covered by open grating), expansion bellows rather than loops are required to accommodate thermal contraction and expansion.

- As the LCH_4 liquefaction facility is within the airport boundary, the pipeline distribution system is less costly than truck transport of the LCH_4. However, if the liquefaction facility were sited more than 15 miles from the airport, truck transport of the LCH_4 from storage to the aircraft would be economically preferable.

- If required the LCH_4 can be subcooled by exchange with liquid nitrogen. The extent of subcooling requirements is dependent on the aircraft fuel tank design. Consequently, the costs and requirements for subcooling the LCH_4 by as much as 11.1°C (20°F) were estimated. Costs were provided as input to determine if subcooling or gelling the LCH_4 might be advantageous to minimize the boil-off losses from the LCH_4 during aircraft flight.

- The energy consumption of the LCH_4 ground system is dependent on the composition of the feed gas to produce LCH_4 and the degree of subcooling required. Natural gas-feed requirements were calculated at 3.81×10^{12} J (36.13 trillion Btu/yr) (HHV) whereas SNG-feed requirements are 3.46×10^{12} J (32.78 trillion Btu/yr) (HHV). The difference is due to the greater mole percentage of methane in the SNG. Basic electricity requirements for the ground system are 6258 kW. Subcooling the LCH_4 by 20°F would increase electricity requirements to 16 000 kW.

- The total capital investment for the LCH_4 ground system ranges from $104.5 million (1976 dollars) to $144.2 million (1976 dollars), depending on the cost of the feed gas, which affects net receivables included in working capital and the degree of subcooling 0.55°C to 11.1°C (1°F to 20°F below -259°F) required.

- The total annual operating costs (excluding capitalization) of the ground system range from $105.5 million (1976 dollars) to $329.0 million (1976 dollars), depending on the feed gas composition, the cost of the feed gas taken from $2.85 to $8.54/GJ ($3 to $9/million Btu, HHV), and the degree of subcooling required.

- A review of the physical properties of LCH_4 and LH_2 indicate that both products can be safely used as aircraft fuel as long as the appropriate standards for their handling are followed. However, utilization of LCH_4 as aircraft fuel may be subject to public pressures resulting from the current controversy in the area of LNG safety.

Because the LNG industry is a relatively mature industry, utilization of LCH_4 as aircraft fuel would not be precluded by technological limitations on the ground system.

9.1 The Conceptual Physical Configuration of the Ground Systems

For the purposes of this study, a supply of pipeline-quality natural gas was assumed to be available at the boundary of SFO. The major facilities that are required for the ground system are as follows:

- Natural gas liquefaction plant and utilities
- LCH_4 storage system
- LCH_4 distribution and aircraft refueling system
- LCH_4 processing systems.

The major components of the ground system that are required for the supply of LCH_4 at the San Francisco airport are shown in figure 128.

9.1.1 Select a preferred liquefaction cycle and requirements.- Preliminary estimates indicated that a liquefaction plant design capacity of about 2.41×10^6 m^3 (85 million SCF/day) would be sufficient to meet the annual aircraft fuel requirements at SFO, in the year 2000. This capacity was arrived at by considering the annual aircraft fuel consumption, the expected fuel losses from the distribution and storage systems, and the annual availability of a liquefaction plant, which is assumed to be 340 stream-days/year (table 50). Even though the operating capacity of the liquefaction plant is set at 2.41×10^6 m^3 (85 million SCF/day), the plant would be capable of liquefying 10 percent in excess of this capacity.

To select the most economical and practical cycle for the application under study, a comparative analysis of the four basic natural gas

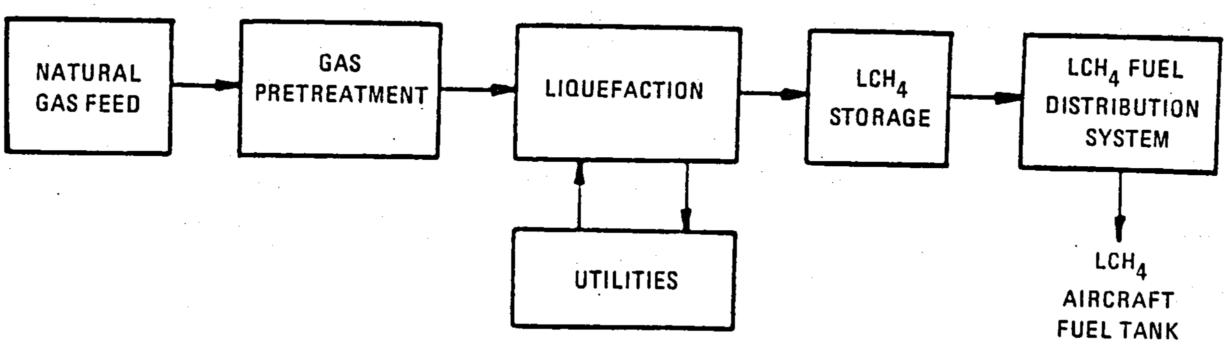

Figure 128. - Major facilities for SFO ground system.

TABLE 50. - PRELIMINARY ESTIMATE OF LIQUEFACTION FACILITY DESIGN CAPACITY

		Capacity, 10^6 kg (lb)/yr
Annual Quantity of LCH_4 to be loaded		459 (1 012)
Distribution Losses at 11%		56.7 (125)
Annual Quantity of LCH_4 into Distribution System		527 (1 137)
Storage Losses at 7%*		37.6 (81)
Annual Quantity into Storage		565 (1 218)
Annual Quantity of LCH_4 Required		565 (1 218)
Operating Days of Liquefaction Facility	340 days/year	
Daily Design Capacity of Liquefaction Facility	1.66×10^6 kg (3.58×10^6 lb)/day 2.39 m^3/day (84.4×10^6 SCF/day)	

*Estimated, based on storage boil-off of 0.05%/day and flash losses from return of LCH_4 from circulation in distribution system.

liquefaction cycles was conducted to establish the selection criteria values. The liquefaction cycles considered in this analysis are (1) the cascade cycle, which is the basis of the Phillips Petroleum Co. Improved Optimized Cascade Cycle (reference 29); (2) the propane-precooled multicomponent cycle, which is commercially available as the Air Products and Chemicals, Inc., MCR cycle (reference 30); (3) the multicomponent cycle, which is commercially available as the J. F. Pritchard Co. PRICO® process (reference 31); and (4) the expander cycle, which has not been used for baseload applications (reference 32). A description of the three commercially available liquefaction processes for baseload applications are presented in Appendix A. These cycles are utilized in the gas industry for production of liquefied natural gas (LNG) and would require modification for production of LCH_4. The implications of producing LCH_4 are discussed in Section 9.1.4, LCH_4 Processing Requirements. The basis of the selection was a plant design capacity of 2.41×10^6 m^3/day (85 million SCF/day). Throughout the comparison of the cycles, the plant was assumed to consist of a single liquefaction train. An economic trade-off analysis of a single vs. dual train facility was conducted under Task 5, Estimate the Capital and Operating Costs of the Ground System, because such a trade-off must also consider the storage capacity requirements. Essentially, the selection of the cycle was therefore based on the relative values of criteria for each cycle.

Although the primary considerations in establishing the most appropriate cycle for the application under study are the operating costs and the initial capital costs, a number of other factors are also considered on the basis of actual operating experience of liquefaction cycles. That is, in the LNG industry, the operating experience has been for plant design capacities of less than 0.71×10^6 m^3/day (25 million SCF/day) (for the peakshaving segment of the industry) or greater than 3.54×10^6 m^3/day (125 million SCF/day) for the baseload segment of the industry (reference 33). Because of the limitations in operating experience and the unique application of this liquefaction cycle, the following criteria were utilized in the cycle selection to ensure that the most economical and practical cycle was chosen:

- <u>Horsepower Requirements</u> - Minimum horsepower requirements per standard CF/day of gas liquefied directly affect both initial capital cost and operating costs.

- <u>Fuel Gas Requirements</u> - Fuel gas requirements directly affect operating costs.

- <u>Operating Flexibility</u> - Operating flexibility is the capability of the cycle to operate at less than design capacity without a loss in efficiency.

- <u>Design Simplicity</u> - Design simplicity, which is defined as fewer major components, is expected to decrease the probability of unscheduled downtime and also decreases working capital requirements as parts inventories are smaller.

- <u>Availability of Off-the-Shelf Turbomachinery</u> - Although future technologies can be considered for this application, the availability of off-the-shelf turbomachinery ensures that at least the actual design efficiency of the cycle can be obtained because overrating or underrating of the turbomachinery is avoided.

- <u>Relative Operating Costs</u> - The operating costs, including capitalization, are used to determine the most economical cycle.

- <u>Refrigerant Requirements</u> - Refrigerant requirements affect the operating cost and also the reliance of the cycle on outside vendors; therefore, the more self-sustaining the cycle, the more appropriate it is for this application.

- <u>Operating Experience</u> - The actual operating experience of commercially available liquefaction cycles was taken as an indication of the proven performance of the cycle.

The method of evaluating the four cycles consisted of the following steps:

- <u>Computer Simulation</u> - Computer simulation (reference 34) of the four basic cycles was used to determine the horsepower and fuel gas requirements. Simulation was used because the actual requirements for commercially available liquefaction cycles are not available as no liquefaction plants have been placed in operation at the design capacity as determined for this application. Because simulation was based on models of the major cycles and not on the specific design of the commercial processes, the horsepower requirements and fuel gas requirements are not necessarily the requirements that would result if a commercial vendor developed a specific design for this application. The results are, however, consistent with available information on operating liquefaction facilities.

- Literature Review and Evaluation - The available literature on commercially available processes were reviewed and commercial vendors were contacted to obtain information to evaluate the following criteria: operating flexibility, design simplicity, availability of off-the-shelf turbomachinery, refrigerant requirements, and operating experience. Based on the literature review and evaluation, each cycle was rated on each of the previously mentioned criteria on a scale from 1 to 4 (best to worst). The cycle with the minimum sum of criteria ratings was taken as being the most practical cycle.

- Comparison of Operating Costs - A comparison of the relative operating costs of the four cycles as a function of natural gas price was conducted.

9.1.1.1 Comparison of cycles. - A comparison of the liquefaction cycles by criteria follows.

Horsepower requirements: The results of the simulation of the cycles show that the propane-precooled process represents the lowest horsepower 11.8 W/m^3/day (447 hp/million SCF-day) requirement per 28.3 m^3/day (million SCF/day). The multicomponent process requires 19 percent more horsepower than the propane-precooled process and 9 percent more than the cascade process. These differences indicate a possible fuel cost and possible investment advantage for the propane-precooled process in particular. The expander cycle horsepower requirements were estimated at 22.4 kW/m^3-day (850 hp/million SCF-day).

These horsepower requirements are not based on proprietary data, and do not reflect any licensor's recommended refrigerant conditions or operating conditions. Each process vendor may come up with a specific design variation, thus reducing the total horsepower requirement. However, in general, it can be anticipated that the expander cycle, unless it employs several stages of expansion and cooling, will exhibit a higher power consumption than the other types of LNG cycles. Similarly, a multicomponent refrigerant cycle will tend to exhibit higher power consumption than either cascade or propane-precooled multicomponent cycles because it employs a single stage of cooling.

Fuel gas requirements: Fuel gas is used to supply all compressor power requirements and also the auxiliary electric power requirements for instrumentation and controls. The cascade process requires 11.1 x 10^{12} J/day (10.50 billion Btu/day) for fuel, while the propane-precooled and the multicomponent processes require 10.1 x 10^{12} J/day (9.6 billion Btu/day) and

12.1×10^{12} J/day (11.45 billion Btu/day), respectively. The expander cycle is estimated to require 20.3×10^{12} J/day (18.3 billion Btu/day).

The fuel gas requirement ranged from 12.0 percent to 14.0 percent of the net plant output, if an identical heating value is assigned to the product gas produced in the different liquefaction plants. The indicated difference between fuel requirements for cascade and multicomponent refrigerant processes represents an annual operating saving of $0.45 million for the cascade process, based on an inlet fuel cost of $1.33/GJ ($1.40/million Btu) and a 93-percent stream factor. The same comparison between multicomponent refrigerant and propane-precooled processes yields an annual saving of $0.88 million/year for the propane-precooled process. If the inlet gas price is escalated, the annual saving would increase accordingly for each comparison.

Operating flexibility: The operating flexibility of the liquefaction cycle is principally determined by three factors: turndown capability, changes in feed gas composition, and ease of start-up operations.

Plant turndown capabilities: As the demand for LCH_4 at an airport is expected to have a greater variation than would normally be encountered in a baseload LNG operation, the turndown capabilities of the cycles are considered important in minimizing the actual operating costs of the cycles. The turndown capability is evaluated in terms of the ability of the cycle to operate at less than design capacity without a loss in efficiency, where efficiency is defined as:

$$\text{energy output} \div \text{energy input}$$

The Phillips Petroleum process can be turned down to 80 percent of the design capacity without sacrificing efficiency. However, the liquefaction unit can be operated betwen 100 percent and 0 percent of the capacity by recycling a portion of the compressor refrigerant back into the compressor suction side (reference 35).

The Pritchard process can be turned down to 70 percent of product design capacity by controlling the compressor inlet guide vanes without a loss in efficiency. Further turndown can be achieved, but the fuel rate will remain constant. After 70 percent turndown of the compression capacity by controlling inlet guide vanes, further reduction is obtained by feeding a portion of compressor refrigerant back into the compressor suction side (reference 36).

The Air Products process is capable of being turned down to 70 percent of design capacity with a slight improvement in overall efficiency (reference 37). As with the Pritchard process, the fuel consumption rate would remain at the 70 percent level if the Air Products process is turned down lower. Turndown operation to 25 percent of capacity for extended periods has been achieved on the Brunei, Borneo, LNG facility (references 38 and 39).

Theoretically, the expander cycle should be capable of exhibiting some turndown capacity, depending on the design the turbo-expander. That is, if the expander blade positions can be adjusted for different flow rates, turndown without an efficiency loss could be accomplished (reference 40). The extent of such turndown capabilities is, however, not known.

Feed Gas Composition: The capability of the cycle to accommodate changes in feed gas compositions is considered important because the feed gas for the LCH_4 may originate from a coal-gasification facility. The composition of such a feed gas is different from the feed gas compositions normally encountered in LNG liquefaction.

Phillips' design is least flexible in handling changes in feed gas composition. Phillips' literature stresses the importance of first determining the limits of feed composition variation and designing the cryogenic exchangers accordingly (references 29 and 41). The design should be made with sufficient flexibility to anticipate future feed composition changes and normal day-to-day fluctuations, whether it be heavy or light components.

Air Products described experiences at the Brunei, Borneo, LNG facility where its process operated successfully over a wide variation in feed gas composition (references 38 and 39). Feed variations ranged from 38.7 to 40.9 GJ/m^3 (1040 to 1100 Btu/SCF). For the Das Island, Abu Dhabi, project, the same process will handle the full range from 38.7 (1040) to higher than 48.4 GJ/m^3 (1300 Btu/SCF) (reference 42). According to Air Products, the cryogenic heat exchanger regulates LNG production and the amount of refrigerant required. The refrigerant composition may be altered for a wider range of feed gas composition.

According to Pritchard information, the performance of the cryogenic heat exchanger is relatively insensitive to small changes in gas composition and precise control is not required (references 43 and 31).

Plant start-up: The three different commercially available cycles would be started by placing the gas treater, the gas dehydrator, and the utility system in operation, each in the same manner. However, the compressor start-up for each plant would not follow the same pattern since each plant uses a different refrigerant.

According to Pritchard descriptions, the only refrigerant required for start-up is dry natural gas in the refrigerant loop. Refrigerant is added to the system and exchanger cooldown proceeds. The cooldown and LNG production process takes about 3 to 6 hours. This start-up description assumes that auxiliary equipment - pretreatment units, boilers, etc. - are in operation and that the liquefaction system is purged and defrosted. Pritchard claims immediate, safe shutdown can easily be accomplished manually at the control center with the push of a button. From a cooldown condition, start-up may be accomplished in about 0.5 hours (reference 36).

The Phillips improved "optimized cascade" process requires that propane and ethylene refrigerant be purchased for operation. Storage must be provided for both refrigerants, including small, packaged refrigeration units for ethylene. The start-up time, based on previous experience gained at Kenai, runs around 4 to 8 hours (reference 41).

The Air Products cycle requires an initial charge of propane for start-up. The start-up time for LNG production from a hot start with all the equipment in operation is reported to be around 3 days (reference 38).

Design simplicity: Design simplicity is primarily affected by the two major components of a liquefaction cycle: the turbomachinery and the cryogenic heat exchangers.

Cryogenic heat exchangers: A list of cryogenic and other heat exchangers used in the different liquefaction processes considered is given in table 51. The cryogenic heat exchangers employed in the processes fit into two basic categories: spiral wound and the brazed plate-fin type. Air Products incorporates the wound aluminum tube design, while Phillips and Pritchard use the brazed aluminum plate-fin exchangers. The coil wound tube exchangers usually comprise a much larger single package in physical size and weight than the individual plate-fin cold boxes. Air Products' design will use one large cryogenic coil-wound heat exchanger. This unit will consist of two wound shell-and-tube bundles in a common pressure shell. Phillips' improved optimized cascade design will use nine cold boxes with four cores per box, and each core box will be installed vertically and connected in parallel. In addition to the main liquefaction exchangers, the Pritchard process employs brazed aluminum exchangers for two other services. These are relatively small units.

Other Heat Exchangers: Heat exchangers considered in this category include water coolers, flash gas, and flash liquid exchangers, and boilers or steam turbine condensers. The approximate square feet of heat transfer surface required in this service is presented in table 51.

TABLE 51. - CRYOGENIC HEAT EXCHANGERS

	(Air Products) Propane-Precooled	(Phillips) Cascade	(Pritchard) Multicomponent Refrigerant
Liquefaction Capacity/ Train (plant), million m^3(SCF) day	2.41 (85)	2.41 (85)	2.41 (85)
Number and Type of Cryogenic Heat Exchanger per Train	1 cold box* coil wound aluminum tubes	9 cold boxes plate-fin (aluminum)	8 parallel cold boxes aluminum plate and fin
$m^2(Ft^2)$ of Cryogenic Heat Exchanger Area per Tain	31 999 (344 450)	28 872 (310 787)	173 760 (1 870 400)
Other Heat Exchanger Area per Train, $m^2(Ft^2)$	8 706 (93 715)	13 415 (144 398)	9 694 (104 352)
Plant Cooling Water Requirement, m^3(gpm)	1049 (37 053) 8.3°c (15°F rise)	843 (29 789) 11.1°c (20°F rise)	1235 (43 608) 8.3°c (15°F rise)

*One cold box has two crogenic exchanger bundles.

Compressor and driver components: A list of compressors and drivers employed in the different liquefaction plants is given in table 52. The propane-precooled and cascade cycles are similar in that they both incorporate three compressors. In contrast, the multicomponent design employs a single axial compressor with two drivers. Both the cascade and propane-precooled designs use steam turbines as the compressor drivers, whereas the multicomponent design will use one turbine and a gas turbine to drive a single axial compressor. In selecting the steam turbines, wherever possible, a similar unit is recommended for driving the different compressors. This duplication of steam turbines helps reduce the size of the spare parts inventory.

TABLE 52. - LIST OF COMPRESSORS AND DRIVERS

	Cycle	
Cascade	Propane-Precooled	Multicomponent
4 Centrifugal	3 Centrifugal	1 Axial
Propane Service 1 Elliot 46M5 10 660 kW (14 291 hp)	Propane Service 1 Elliot 60M6 8 576 kW (11 496 hp)	1 Elliot 268A11 33 200 kW (44 505 hp)
Ethylene Service 1 Elliot 46M8 9 747 kW (13 066 hp)	MCR Low-Pressure Service 1 Elliot 60M5 10 668 kW (14 300 hp)	
Methane Service 1 Elliot 38M5 1 Elliot 29M6 10 052 kW (13 475 hp) (combined)	MCR High-Pressure Service 1 Elliot 38MB6 8 576 kW (11 496 hp)	
3 Condensing Steam Turbines	3 Condensing Steam Turbines	1 Condensing Steam Turbine
Propane Service 1 Elliot SQV8DF	Propane Service 1 Elliot 2SNV8DF	Elliot 2SNV9
Ethylene Service 1 Elliot SQV8DF	MCR Low-Pressure Service 1 Elliot 2SNV8DF	1 Gas Turbine GE Frame 5
Methane Service 1 Elliot SRV8DS	MCR High-Pressure Service 1 Elliot SRV8DF	

Availability of off-the-shelf turbomachinery: The number of compressor units and major drive system components required for different liquefaction and operating speed are recommended by Elliot Co. According to Elliot Co., all of the compressors and turbine drivers recommended are off-the-shelf machines (references 44 and 45). An economic comparison of steam turbine drivers, as opposed to gas turbine drivers, is outside the scope of this study. In most cases, the configuration of turbomachinery is kept similar to the one used in different existing or proposed baseline LNG plants (references 46, 47, 48).

Although the compressors for an expander cycle are off-the-shelf items, a condensing turboexpander rated at about 5640 kW (7560 hp) for LNG service is not available.

Refrigerant requirements: Air Products requires propane for the propane refrigeration section, as described in the process description in the Appendix, and a mixed refrigerant composed of 40 percent methane, 35 percent ethane, 15 percent propane, and 10 percent nitrogen (reference 30). Pritchard utilizes mixed refrigerant, but the specific details on the composition breakdown are not available. The Pritchard refrigerant would include methane, ethane, propane, butane, and pentane hydrocarbons along with nitrogen (reference (43) The Phillips improved optimized cascade design, uses three separate refrigerants: propane, ethylene, and flash gas. The flash gas, composed primarily of methane (about 83 percent) and nitrogen (about 17 percent), is produced continuously from LNG pressure letdown, and recycled to the feed gas being liquefied (reference 29).

For all the three liquefaction designs, nitrogen must be supplied to the plants. Generally, nitrogen is supplied from a package air separation unit.

The source and quantities of makeup refrigerants varies for different processes. Phillip's design needs approximately 419 kg (924 lb/day) of ethylene and 596 kg (1315 lb/day) of propane, and both of the refrigerants are assumed to be purchased (reference 29). Storage facilities for both propane and ethylene must be provided on site for Phillips. Pritchard has a smaller makeup requirement 161 kg (354 lb/day total) and most of these refrigerant components are to be obtained from the feed gas (reference 31). Information on the Air Products refrigerant makeup is not available, but it can be assumed that the refrigerant makeup is obtained from the light end fraction.*

Information on expander cycle refrigeration is not available but the cycle would require nitrogen if a closed cycle is employed and methane for either the closed or open cycle. It is expected that the refrigerant requirements for the expander cycle would, however, be less than the commercially available cycles since the expander cycle is essentially based on Joule-Thompson cooling (references 49, 50, and 51).

---

*If the feed gas is SNG, then all refrigerant requirements must be purchased from outside vendors

Operating experience: The operating experience of the commercially available liquefaction cycles is taken as an indication of the proven performance of these cycles. Of the international base-load liquefaction facilities in operation or under construction, eight utilize an Air Products cycle design, two utilize a Pritchard design, and one utilizes the Phillips optimized cascade design (reference 33). As previously mentioned, the expander cycle has not been utilized for base-load applications.

Relative operating cost comparison: To determine the most economical liquefaction cycle, a comparison of the relative operating costs including capitalization of the major components unique to each cycle was performed. The direct capital costs for each cycle are presented in tables 53 through 56.

As only a comparative analysis is required, the annualized capital cost of each cycle was taken as 5 percent of the total direct cost (which would be consistent with a nondiscounted straight-line depreciation expense over 20 years). Annual operating and maintenance costs were then added to the annualized capital cost to obtain an annual cost of operation for each cycle excluding the annual cost of fuel gas. A range of fuel gas prices was used to then determine the relative cost of operation of each cycle. The costs were normalized to the propane-precooled cycle at a fuel gas cost of \$0.95/GJ (\$1.00/million Btu).

The results of the comparative economic analysis, figure 129, show that the propane-precooled liquefaction cycle would be the most economical cycle for the application under study when fuel gas costs are greater than about \$0.33/GJ (\$0.35/million Btu).

Results: The results of the analyses undertaken in Task 1.1 show that the propane-precooled multicomponent cycle is the most economical cycle for this application and that it is as practical as the next least costly cycle, the multicomponent cycle, table 57. Consequently, the propane-precooled cycle is dominant and further analyses of LCH_4 for subsonic aircraft considered only that cycle.

9.1.2 Requirements for LCH_4 storage.- The methodology of this task included the following steps:

- Storage Capacity Requirements. Total storage capacity required for this application was determined by an analysis of the LCH_4 demand and supply cycle.

- Number and Size of Storage Tanks. The number and size of storage tanks is based on the expected operation at the airport in meeting aircraft LCH_4 demand.

- Type of Storage Tank. The analysis was restricted to aboveground storage tanks, consequently the type of storage tanks was based on an economic analysis of the tank cryogenic material: 9 percent nickel-steel, 5083-Aluminum, and prestressed concrete.

TABLE 53. - COST ESTIMATE, CASCADE CYCLE

Principal Components	Estimated Cost, $
Steam Turbine 10 668 kW (14 300 hp)	580 000
Steam Turbine 9 772 kW (13 100 hp)	580 000
Steam Turbine (13 500 hp)	526 500
Centrifugal Compressor 10 668 kW (14 300 hp)	415 000
Centrifugal Compressor 9 772 kW (13 100 hp)	534 000
Centrifugal Compressor 10 071 kW (13 500 hp, 2 frames)	774 500
Heat Exchangers	
Cryogenic Cold Box 28 872 m^2 (310 787 ft^2)(9 units)	1 865 000
Other 13 415 m^2 (144 398 ft^2)	723 000
Utility Area (steam Boilers, etc.)	6 500 000
Total Direct Cost	12 498 000
Annualized Capital Cost (0.05 X Total Direct Cost)	624 900
Annual Operating & Maintenance Expense (0.040 X Total Direct Cost)	499 920
Annual Cost (excluding fuel gas)	1 124 820

TABLE 54. - COST ESTIMATE, PROPANE-PRECOOLED MULTICOMPONENT

Principal Components	Estimated Cost, $
Steam Turbine 8 579 kW (11 500 hp)	522 000
Steam Turbine 8 579 kW (11 500 hp)	522 000
Steam Turbine 10 817 kW (14 500 hp)	566 000
Centrifugal Compressors 8 579 kW (11 500 hp)	403 000
Centrifugal Compressors 8 579 kW (11 500 hp)	403 000
Centrifugal Compressors 10 817 kW (14 500 hp)	420 000
Heat Exchangers	
Cryogenic Cold Box 32 050 m^2 (345 000 ft^2)(2 bundles)	2 070 000
Other 8 733 m^2 (94 000 ft^2)	470 000
Utility Area (steam boilers, etc.)	6 500 000
Total Direct Cost	11 876 000
Annualized Capital Cost (0.05 X Total Direct Cost)	593 800
Annual Operating & Maintenance Expense (0.028 X Total Direct Cost)	332 528
Annual Cost (excluding fuel gas)	926 328

TABLE 55. - COST ESTIMATE, MULTICOMPONENT CYCLE

Principal Components	Estimated Cost, $
Gas Turbine 22 529 kW (30 200 hp)	3 020 000
Steam Turbine 10 742 kW (14 400 hp)	520 000
Axial Compressor 24 765 kW (44 500 hp)	800 000
Heat Exchangers	
Cryogenic Cold Box 173 700 m^2 (1 870 000 ft^2)(8 units)	3 500 000
Other 9 694 m^3 (104 352 ft^2)	525 000
Utility Area (steam boilers, etc.)	3 400 000
Total Direct Cost	11 765 000
Annualized Capital Cost (0.05 X Total Direct Cost)	588 250
Annual Operating & Maintenance Expense (0.030 X Total Direct Cost)	352 950
Annual Cost (excluding fuel gas)	941 200

TABLE 56. - COST ESTIMATE, EXPANDER CYCLE

Principal Components	Estimated Cost, $
Turboexpander/Compressor 5 595 kW (7 500 hp)	635 000
Main Compressor 31 705 kW (42 500 hp)	2 380 000
Refrigeration Compressor 15 368 kW (20 600 hp)	830 000
Cold Gas Compressor 298 kW (400 hp)	120 000
Heat Exchanger 16 722 kW 180 000 ft^2	1 100 000
Steam Turbine 15 368 kW (20 600 hp)	824 000
Gas Turbine 31 705 kW (42 500 hp)	4 250 000
Utility Area (steam boilers, etc.)	3 400 000
Total Direct Cost	13 539 000
Annualized Capital Cost (0.05 X Total Direct Cost)	676 950
Annual Operating & Maintenance Expense (0.025 X Total Direct Cost)	388 475
Annual Cost (excluding fuel gas)	1 065 425

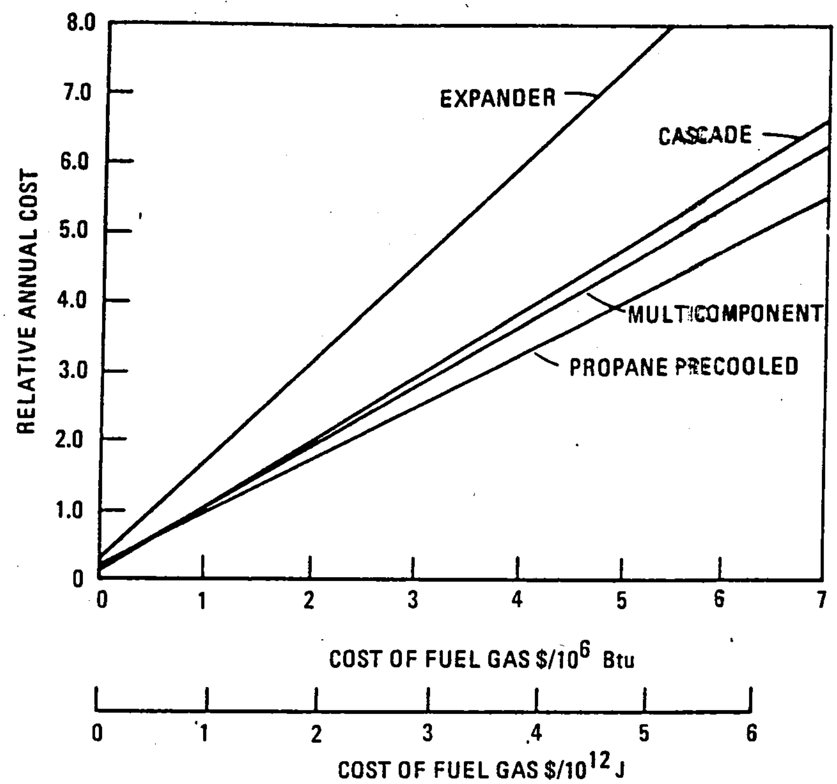

Figure 129. - Relative annual cost of liquefaction cycles.

TABLE 57. - COMPARISON OF LIQUEFACTION CYCLES

Characteristics	Cycle			
	Multicomponent	Propane Precooled	Cascade	Expander
Horsepower Requirements	15.1×10^6 m^3 (533 hp/10^6 SCF) day	12.7×10^6 m^3 (447 hp/10^6 SCF) day	13.8×10^6 m^3 (489 hp/10^6 SCF) day	24.1×10^6 m^3 (850 hp/10^6 SCF) day
Fuel Gas Requirements	12.1×10^9 kJ (11.45×10^9 Btu) day	10.1×10^9 kJ (9.6×10^9 Btu) day	11.1×10^9 kJ (10.5×10^9 Btu) day	19.3×10^9 kJ (18.3×10^9 Btu) day
Operating Flexibility	1	1	2	4
Design Simplicity	1	2	3	1
Availability of Off-the-Shelf Turbomachinery	1	1	1	4
Refrigerant Requirements	2	3	4	1
Operating Experience	3	1	2	4

- <u>Insulation Requirements</u>. The thickness of the insulation system was based on an economic analysis of the capital and operating costs of a boil-off compressor versus the increased capital cost of the tankage due to increased insulation thickness.

9.1.2.1 <u>Storage capacity requirements</u>.- The total storage capacity of the facility must be sufficient to provide for (1) the differences between peak and normal fueling operations, (2) scheduled downtime, and (3) unscheduled downtime. Based on the results of the LH_2 Airport Requirement Study, the annual quantity of the LH_2 loaded in the year 2000 is 191.2 x 10^6 kg (421.6 million lb) (reference 5). As the average day demand during the peak month is 697 tonnes/day (768 tons/day), the average daily demand during the off-peak months would be 508 tonnes/day (560 tons/day). Assuming a lower heating value Btu equivalency between LH_2 and LCH_4 requirements, the annual quantity of LCH_4 to be loaded would be .677 x 10^9 m^3 (23.9 billion SCF). The LCH_4 aircraft demand cycle consists of 31 days of peak demand at 2.46 x 10^6 m^3/day (86.7 million SCF/day) and 334 days of off-peak demand at 1.80 m^3/day (63.4 million SCF/day).

The production schedule of LCH_4 is dependent on the liquefaction cycle operation. That is, the production schedule depends on the number of trains (modules) employed in the liquefaction plant, the scheduled downtime requirements and unscheduled downtime. Although the liquefaction cycle selection of Section 9.1.1 was based on a single liquefaction train (as the selection was based on only a comparative analysis and the economics of scale are assumed continuous over the range of liquefaction capacities defined by dual versus single trains) the analysis of storage capacity was done for single and multiple liquefaction train facilities to facilitate the economic analysis as reported in Section 9.5 of this study.

9.1.2.2 <u>Single train liquefaction</u>.- For a single train liquefaction facility, the design capacity of the facility as set at 2.41 x 10^6 m^3/day (85 million SCF/day), which is based on a plant on-stream factor of 0.93 (340 days/year) and total distribution and storage system losses of 18 percent. The LCH_4 production and demand cycle for a single liquefaction train is presented in figure 130.

The area A is the quantity of LCH_4 required from storage during scheduled maintenance that would occur during off-peak operations. Area C is the quantity of LCH_4 provided from storage for peaking operations. Area B represents the quantity of LCH_4 available for storage during normal operations and is equal to the sum of areas A and C. The quantity of LCH_4 that must be in storage at the beginning of expected and unexpected downtime and the peak demand period is presented in table 58.

For scheduled downtime of the single train liquefaction facility, the quantity of LCH_4 that must be delivered to the aircraft is 44.9 x 10^6 m^3 (1585 million SCF) based on 25 days of downtime during the off-peak demand period. Including the estimated distribution and storage system losses of liquid to vapor, the total quantity of LCH_4 that must be in storage at the start of the scheduled liquefaction facility downtime is 54.7 x 10^6 m^3 (1933 million SCF).

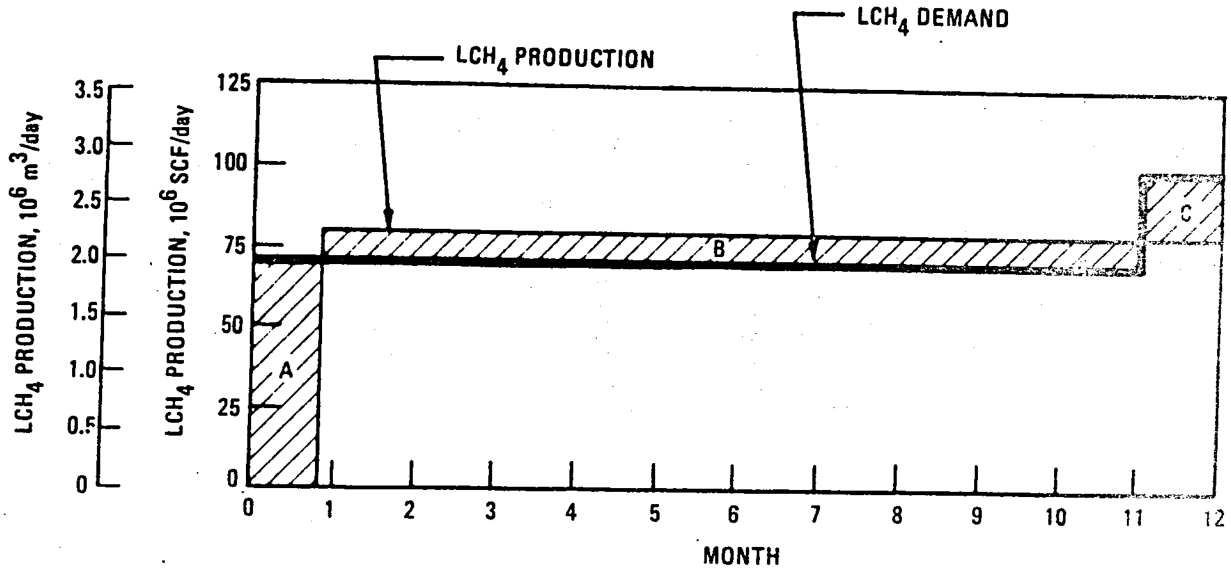

Figure 130. - LCH_4 production versus demand cycle (single train liquefaction).

TABLE 58. - LCH_4 DEMAND TO BE MET FROM STORAGE (SINGLE TRAIN)

	Storage	
	10^6 m^3 (Million SCF)	m^3 (bbl, API)
Unscheduled Downtime	24.1 (850.0)	38 474 (242 000)
Scheduled Downtime	54.7 (1933)	87 440 (550 000)
Peaking Operations	18.2 (643)	29 094 (183 000)

During the peak demand period of 31 days, 2.46 x 10^6 m^3/day (86.7 million SCF/day) of LCH_4 must be delivered to the aircraft. Of this quantity 1.97 x 10^6 m^3/day (69.7 million SCF/day) is estimated to be delivered from the liquefaction facility. Consequently, a total of 14.9 x 10^6 m^3/day (527 million SCF) of LCH_4 must be delivered to the aircraft from storage during the peak period. Adjusting for the estimated losses in the storage and distribution system, 18.2 m^3 (643 million SCF) of LCH_4 must be in storage at the beginning of the peak period.

For the single liquefaction train, storage for unscheduled downtime was arbitrarily set at 1.42 m^3 (50 million SCF) based on an assumed failure mode of 10 days' duration. "Rules-of-thumb" for sizing contingency storage for base-load LNG facilities are not appropriate for this application because contingency storage at base-load facilities is principally a function of the transportation (i.e., the LNG ships and expected travel time delays) rather than the probability of liquefaction plant outage (reference 33). However, for this application the delay of one aircraft is insignificant in the total system. Consequently, the principal need for contingency storage is the probability of failure in the liquefaction plant. Based on the operating history of the baseload LNG industry and the requirements for other storage at the facility (which could also be drawn down in the event of an outage exceeding 10 days); contingency storage of 1415 m^3 (50 million SCF) is believed to be sufficient (reference 52).

However, because the scheduled downtime could be arranged to occur during any period during the off-peak demand, maximum recycling of the actual storage tanks could be obtained. Consequently, the actual storage capacity required is equal to the maximum of the annual demand that must be supplied from storage during scheduled downtime or during the peak month plus additional storage for unscheduled operations. As the maximum quantity of LCH_4 that must be met from storage is the LCH_4 for scheduled downtime, the resultant physical storage capacity of the facility is 125.900 m^3 (792 000 bbl) including storage for unscheduled LCH_4 production outage.

9.1.2.3 Dual train liquefaction.- For a dual train liquefaction facility, the total storage capacity would be reduced by two effects: (1) the ability to schedule maintenance so that recycling of the storage tanks is greater than in the single train case, and (2) the reduction in contingency storage. The LCH_4 production versus demand schedule is presented in figure 131.

The quantity of LCH_4 that must be in storage for scheduled and unscheduled downtime and for peaking operations is presented in table 59. The quantity of LCH_4 that must be in storage at the beginning of the peak demand period is the same as that required for the single liquefaction train. LCH_4 in storage at the beginning of the scheduled downtime of each of the two liquefaction trains is 27.4 x 10^6 m^3 (966.5 million SCF).

For unscheduled downtime, the contingency storage is taken as 50 percent of that required for the single train facility. Although the actual contingency storage capacity would be based on the probabilities of failure, duration of failure, and the dependence of the operation of each train on the continued operation of the other train, sizing contingency storage at 50 percent of that for the single train is valid if the probabilities of failure are relatively low (i.e., odds of less than 1 in 10 of failure) and the operations of the trains are completely independent.

With maximum recycling of the storage tanks, a total of 62 950 m^3 (396 000 bbl) of storage would be required. This capacity is based on the maximum of the requirements for scheduled downtimes and peaking operations 43 720 m^3 (275 000 bbl) and the capacity required for unscheduled downtime 19 240 m^3 (121 000 bbl).

Based on the methodology of single versus dual train analysis of storage tankage required, storage tankage required as a function of the number of liquefaction trains is presented in figure 132. As the number of trains increases, the storage capacity required approaches the minimum of 29 090 m^3 (183 000 bbl), which is needed for peak-month operations.

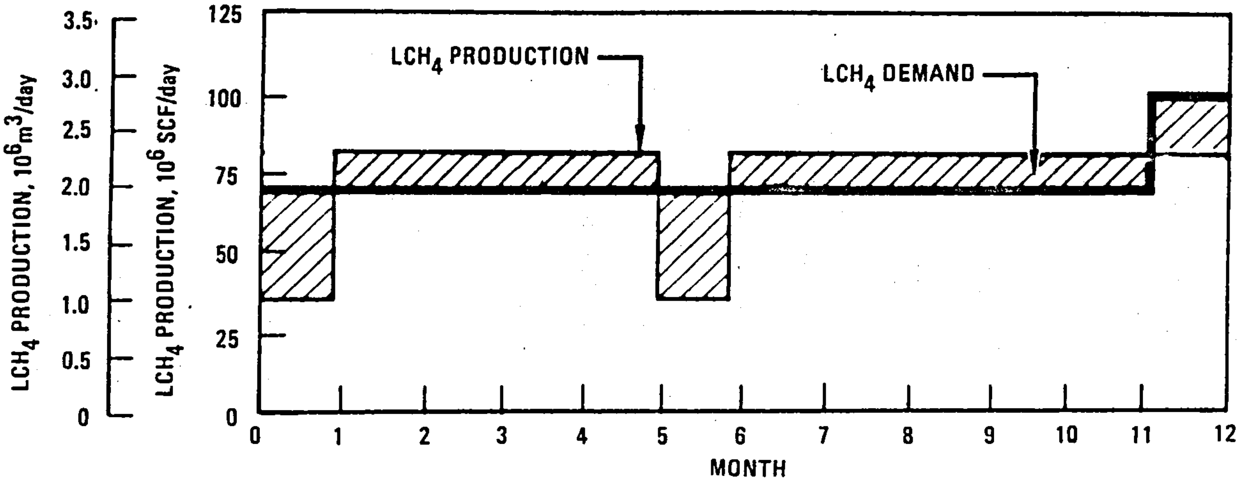

Figure 131. - LCH_4 production versus demand cycle (dual train).

TABLE 59. - LCH_4 DEMAND TO BE MET FROM STORAGE (DUAL TRAIN)

	Storage	
	10^6 m^3 (Million SCF)	m^3 (bbl, API)
Scheduled Downtime (Train A)	27.4 (966.5)	43 720 (275 000)
Scheduled Downtime (Train B)	27.4 (966.5)	43 720 (275 000)
Peaking Operations	18.2 (643.0)	29 094 (183 000)
Unscheduled Downtime	12.0 (425.0)	19 237 (121 000)

9.1.2.4 Number and size of storage tanks.- A minimum of three tanks is required for dispensing and receiving operations. One tank is used for dispensing. The second tank is used for receiving liquid from the natural gas liquefiers as well as excess liquid returned from the fueling circuit or from defueling of aircraft. The third tank serves as a full standby tank that can be ready for immediate switchover to dispensing service at the moment the dispensing tank becomes empty. In operation, the storage tanks would never be completely emptied so that they could be maintained in a cooldown condition except for maintenance operations. The need for the standby tank results from the near impossibility of scheduling, receiving, and dispensing operations in such a way that an empty dispensing tank and full receiving tank occur simultaneously. A three-tank system provides the necessary flexibility in operations and permits decoupling of storage tank filling and emptying operations from aircraft fueling schedules.

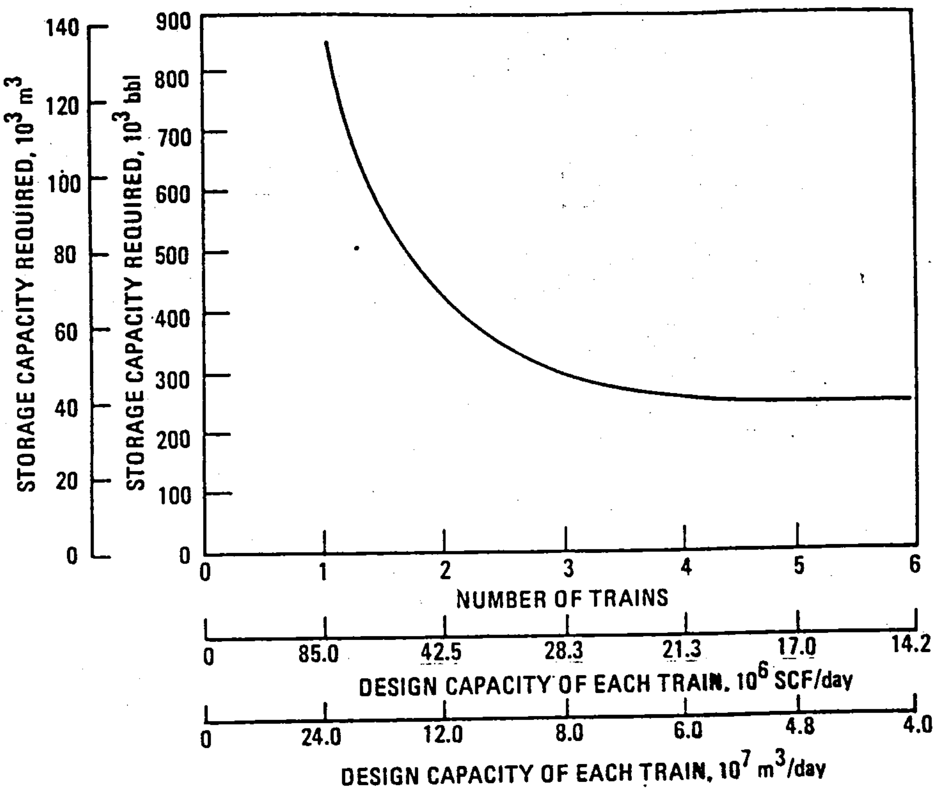

Figure 132. - Storage tankage capacity requirements as a function of liquefaction train capacity.

The capacity of each storage tank is set at 42 130 m^3 (265 000 bbl) as the economic tradeoff analysis of 9.5 shows that the most economical configuration results with a single liquefaction train design capacity of 2.41×10^6 m^3/day (85 million SCF/day) and a total capacity 125 900 m^3 (792 000 bbl).

9.1.2.5 Type of storage tank.- The type of LCH_4 storage tank selected was based on the direct cost of aboveground LNG storage tanks, figure 133 (reference 53). For a 42 130 m^3 (265 000 bbl) aboveground tank, the direct cost per barrel of capacity is lowest for aluminum tankage.

The storage tank will be an above ground, double-wall cylindrical tank. The inner tank will be aluminum. The outer wall is made of carbon steel and the annulus is filled with perlite insulation. To absorb differential movement between the outer and the inner wall due to temperature cycles, a fiberglass elastic blanket is installed around the outside of the inner wall, and the inside of the outer wall.

The inner tank stands on load-bearing insulation above a concrete foundation that is maintained above freezing by an electrical heating system.

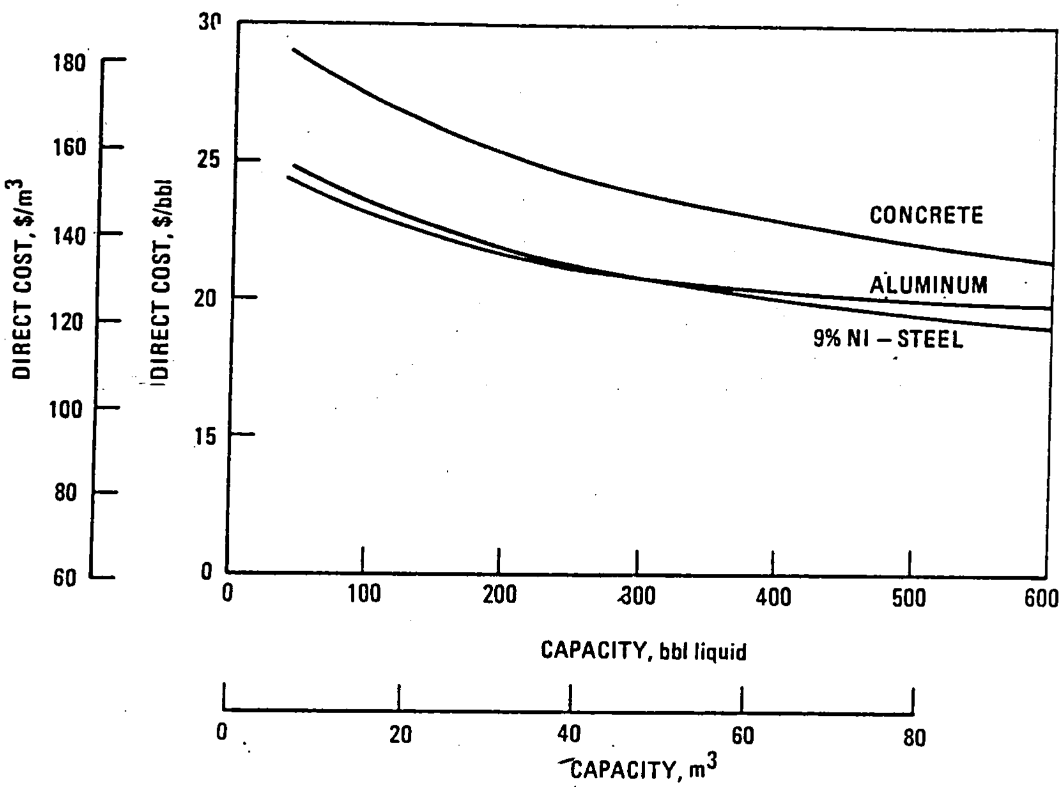

Figure 133. - Unit costs of LCH_4 storage tank.

The conventional double-wall tank included a complete double roof in the first LNG tank design. Recently, an alternative form of roof construction has been available in the suspended insulating deck concept. In this design concept, the inner tank has a suspended deck ceiling that eliminates the need for a self-supporting dome made of cryogenic material over the inner tank. The dome is replaced with a minimum thickness plate that is supported by hanger rods attached to the sealed outer tank. Mineral wool and/or perlite insulation is loosely filled on top of this deck. The use of a suspended deck ceiling allows the insulation space to be purged via the boil-off vapor in the storage tank. For a sketch of the configuration, see figure 152.

The cost components of a double-wall aluminum/carbon steel storage tank are presented in table 60. Standard accessories include piping penetrations and pressure relief valving. The insulation costs is based on standard thickness of 0.91 m (3 ft) for perlite insulation (reference 54).

9.1.2.6 <u>Insulation thickness</u>.- The standard insulation thickness for liquified natural gas storage tanks is generally about 0.91 m (3 ft) (reference 54). In order to determine the appropriate insulation thickness for the storage tanks in this application, an economic trade-off analysis was conducted.

TABLE 60. - COST COMPONENTS OF ALUMINUM, DOUBLE-WALL ABOVEGROUND TANKAGE FOR LCH_4

Component	% of Total Cost
Ringwall Foundation	6
Outer Tank (Carbon Steel)	33
Inner Tank (Aluminum) and Deck	49
Standard Accessories	5
Insulation	7

As shown in table 60, insulation accounts for about 7 percent of the direct cost of LCH_4 storage tankage. However, increasing or decreasing the thickness of the insulation will not only require more insulation, but will also require a larger ringwall foundation and a larger outer tank. The direct cost of LCH_4 tankage as a function of insulation thickness is presented in figure 134. Reduction of the insulation thickness from 0.91 m (3 ft) to 0.152 m (1/2 ft) would reduce the total direct cost of the three 42 130 m^3 (265 000-bbl) storage tanks by \$1.9 million.*

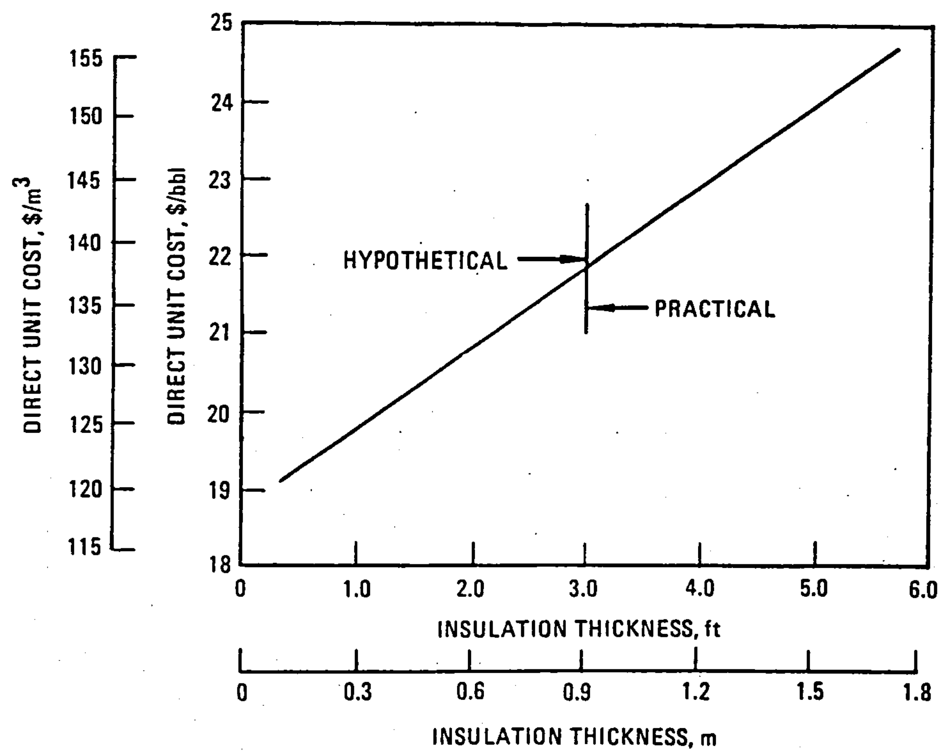

Figure 134. - Storage tank cost versus insulation thickness.

*Due to the practical considerations in constructing an aboveground double-wall tank, the minimum distance between the inner and outer wall is about 0.91 m (3 ft).

However, a reduction in the insulation thickness would result in an increased boil-off rate that would then require additional boil-off compressor capacity and additional liquefaction capacity.

Utilizing the following two equations, the maximum steady-state boil-off for the three LCH_4 storage tanks was calculated

$$Q = \lambda/d \, A \left(t_0 - t_1\right) \qquad (1)$$

where

Q = heat gain per unit time
λ = coefficient of thermal conductivity of perlite
A = surface area of the inner storage tank
t_0 = outside ambient temperature
t_1 = temperature of the LCH_4

$$\text{Boil-off Rate} = \dot{Q}/h \qquad (2)$$

where,

Q = heat gain per lbm of LCH_4 per unit time
h = enthalpy of LCH_4 at t_1

The resulting total (all three tanks) maximum steady-state boil-off for LCH_4 storage as a function of insulation thickness is presented in figure 135.

From the economic analysis of Section 9.5, the effect of insulation thickness on the direct operating cost (including capitalization) of the LCH_4 facility was calculated. The results of the calculation are presented in figure 136. As shown in the figure, the direct operating costs associated with the storage tankage increases as insulation thickness increases, the direct operating costs associated with the liquefaction train and the boil-off compressor/driver decrease as insulation thickness increases. The minimum cost insulation thickness is 0.76 m (2-1/2 ft). The total direct operating cost curve of figure 136 was based on a fuel gas cost of zero. The effect of insulation thickness on direct operating cost for different values of the fuel gas cost is presented in figure 137. Obviously, as the cost of energy to recompress and reliquefy the boil-off increases, the insulation thickness associated with the minimum direct operating cost increases.

Although there are conceivably other uses for the LCH_4 boil-off (e.g., fuel for the liquefaction plant), it must be remembered that boil-off from the storage tanks is also a function of the outside ambient temperature. Whereas the boil-off compressor must be designed for the maximum

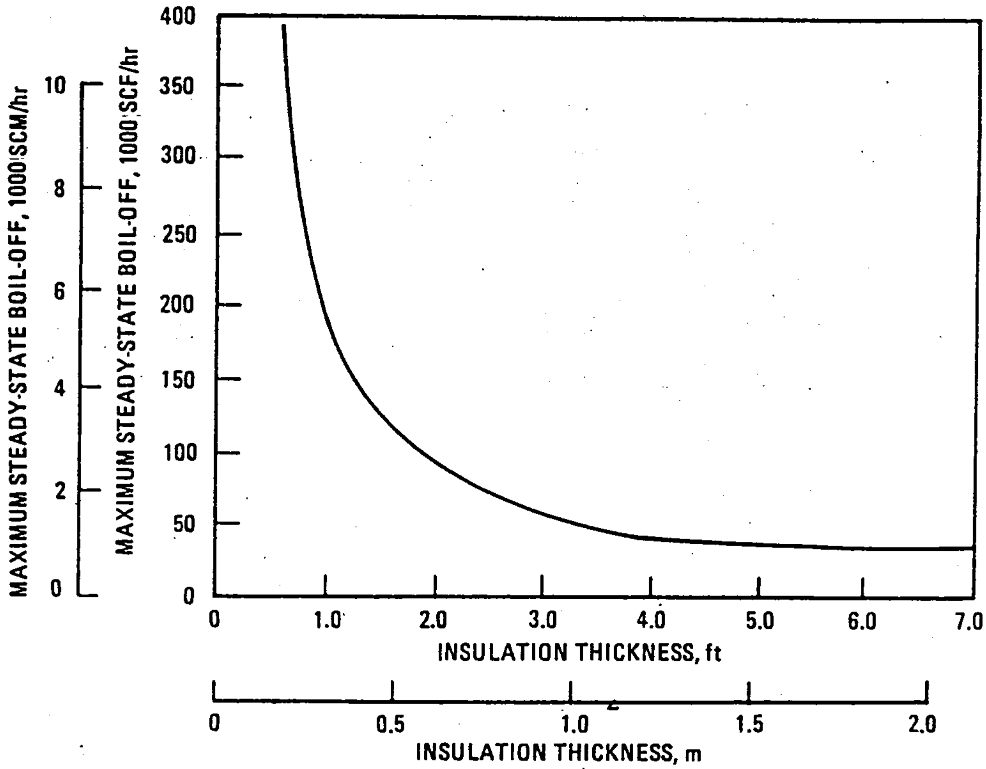

Figure 135. - Maximum storage tank steady-state boil-off versus insulation thickness.

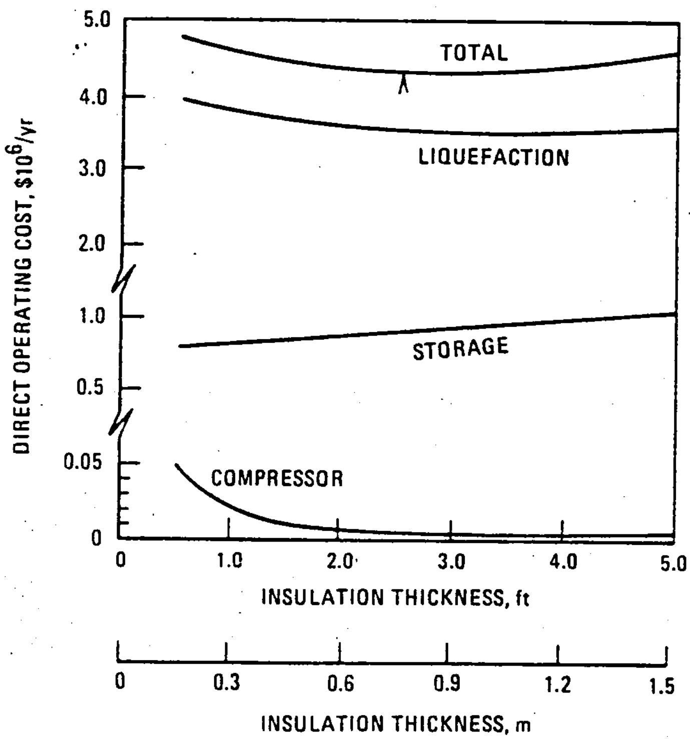

Figure 136. - Ground system direct operating cost versus insulation thickness.

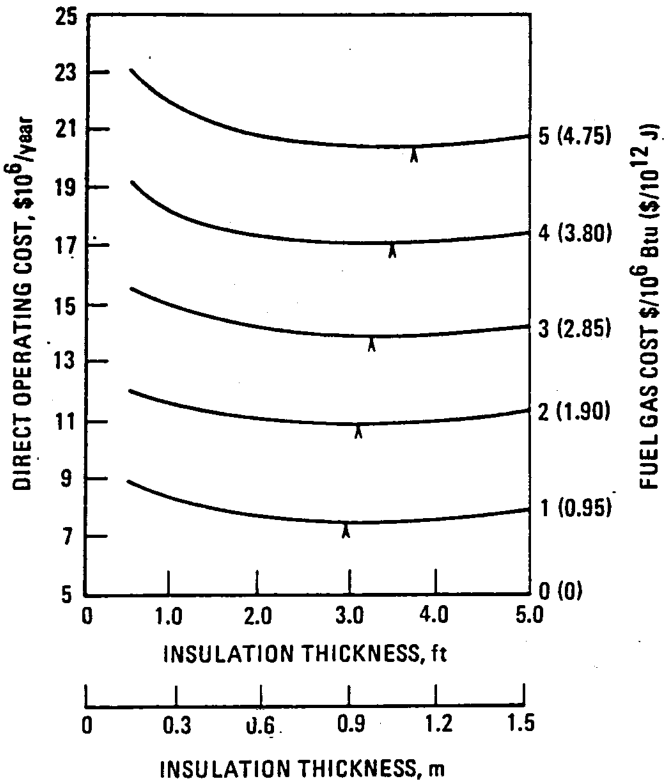

Figure 137. - Insulation thickness versus direct operating cost at different fuel gas costs.

expected boil-off, the use of boil-off for liquefaction fuel could reduce the size of the compressor but not eliminate the need for a compressor. Further, regardless of the use of the boil-off, the liquefaction plant design capcity must be increased as the boil-off rate increases. As the cost of liquefaction (either increased capacity or reliquefaction) is the overriding cost element, the appropriate economic trade-off analysis is that which has been conducted because the actual method of use of the boil-off will have little effect on the direct operating cost. In essence, the existence of boil-off imposes an economic penalty, not the method of utilizing the boil-off.

Because the change in direct operating cost is not substantial as the insulation thickness increases beyond 0.91 m (3 ft) (regardless of the fuel gas cost), an insulation thickness of 0.91 m (3 ft) has been selected.

9.1.2.7 Results.- The results of the storage analysis are that three aboveground double-wall aluminum/carbon steel storage tanks, each tank with a capacity of 42 130 m (265 000 bbl), will provide the most economical storage concept. The minimum cost insulation for the storage tank is perlite of 0.91 m (3-ft) thickness.

Low profile storage tanks of this capacity would have the following profile dimensions: height 30.5 m (100 ft); outer diameter 57.9 m (190 ft). For a discussion of tank spacing and diking requirements see section 9.3.4.

9.1.3 LCH_4 distribution and aircraft refueling system requirements.- The analyses of the ground LCH_4 distribution and refueling system included the following:

- Review and modify, where necessary, the LH_2 ground distribution pipeline system developed and conceptualized in the previous Lockheed Study (reference 5).

- Conduct a comparative economic analysis of pipeline versus truck ground distribution for LCH_4.

9.1.3.1 LCH_4 pipeline system (modified LH_2 system).- The liquid methane ground pipeline distribution system and the aircraft fueling systems are based on the concept developed for handling liquid hydrogen at San Francisco airport. In the concept, the fueling operation is performed at the terminal gate by a fueler vehicle equipped to provide all necessary interfaces between a hydrant point-of-supply and the aircraft fuel system. Each of the 19-gate fueling stations considered for supplying liquid methane fuel will consist of a hydrant pit containing interface connect points for LCH_4 supply and vent gas collection. A typical hydrant pit based on that designed for liquid hydrogen fuel is shown in figure 138. This hydrant would operate in a similar fashion when used for supplying liquid methane fuel. As shown in the figure, the hydrant pit is equipped with a riser from each of the fuel supply loops. The risers are connected through service isolation valves to a hydrant shut-off valve and a fuel transfer disconnect device. The vent gas displaced from the aircraft tanks during refueling would be routed through the fueler vehicle to a vent disconnect device to the vent collection header. This equipment will be situated in a pit located in the apron below the tail of the aircraft.

The refueling operation will be carried out by a hydrant fueler vehicle equipped to provide the fluid and operational interfaces between a hydrant pit and the aircraft. A flow schematic of the hydrant fueling operation is illustrated in figure 139. A detailed procedure for the hydrant fueling operation is given in the LH_2 airport requirements study (reference 5). This concept would not require any modification for transferring LCH_4 to the aircraft rather than LH_2.

9.1.3.2 Ground distribution and refueling system.- The distribution of liquid methane throughout the terminal area to the 19 gates at San Francisco airport uses a similar concept as developed for LH_2 in a previous study. This concept is depicted schematically in figure 140. The basic system is a circulating liquid methane distribution loop which is fed with a saturated or a relatively subcooled* liquid methane from a storage tank. The liquid loop, as shown in figure 140, is routed past each of the 19 hydrant pits (one for

*Depends on the degree of subcooling required to reduce the aircraft tank flash boil-off losses.

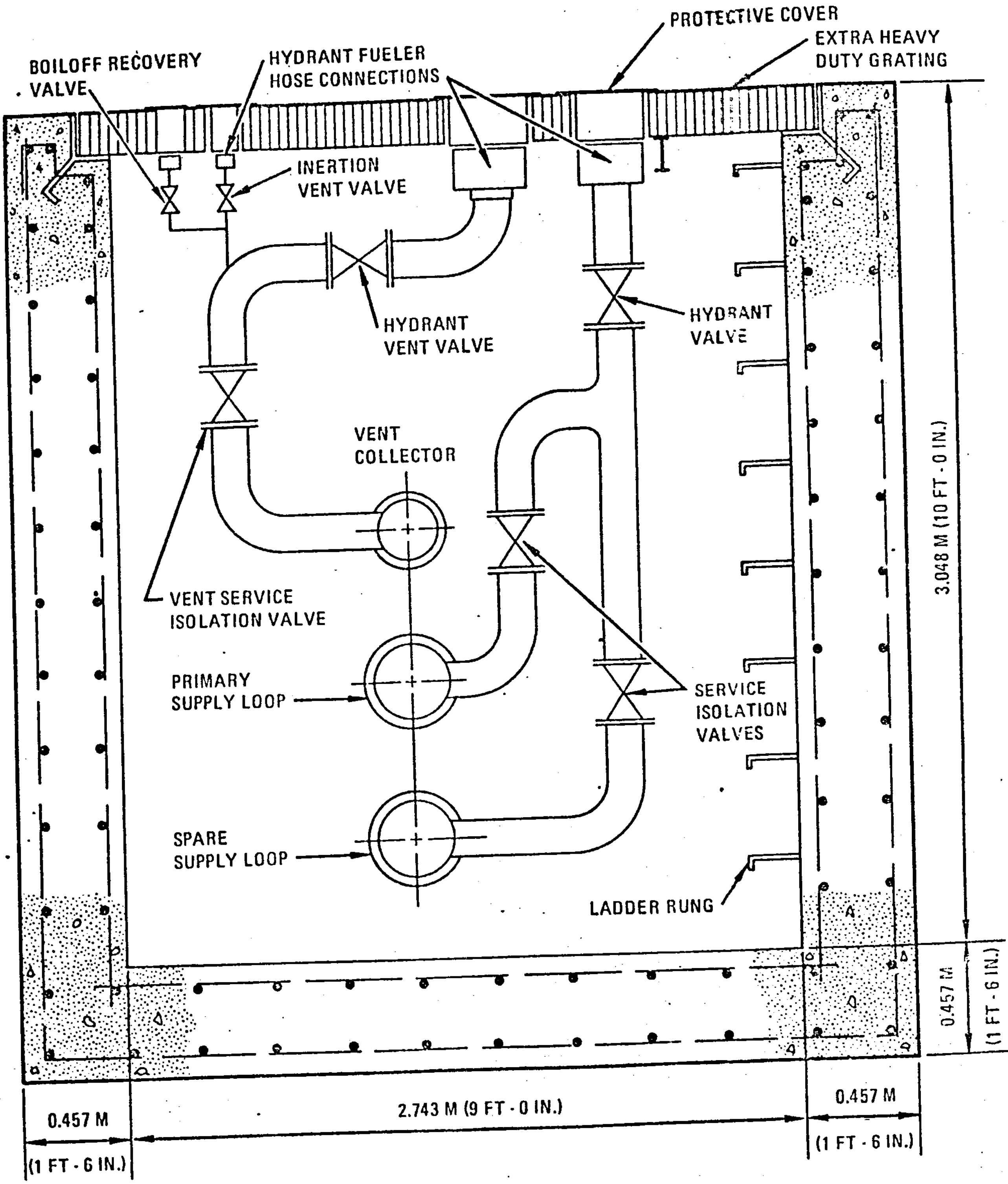

Figure 138. - Typical LCH_4 hydrant pit.

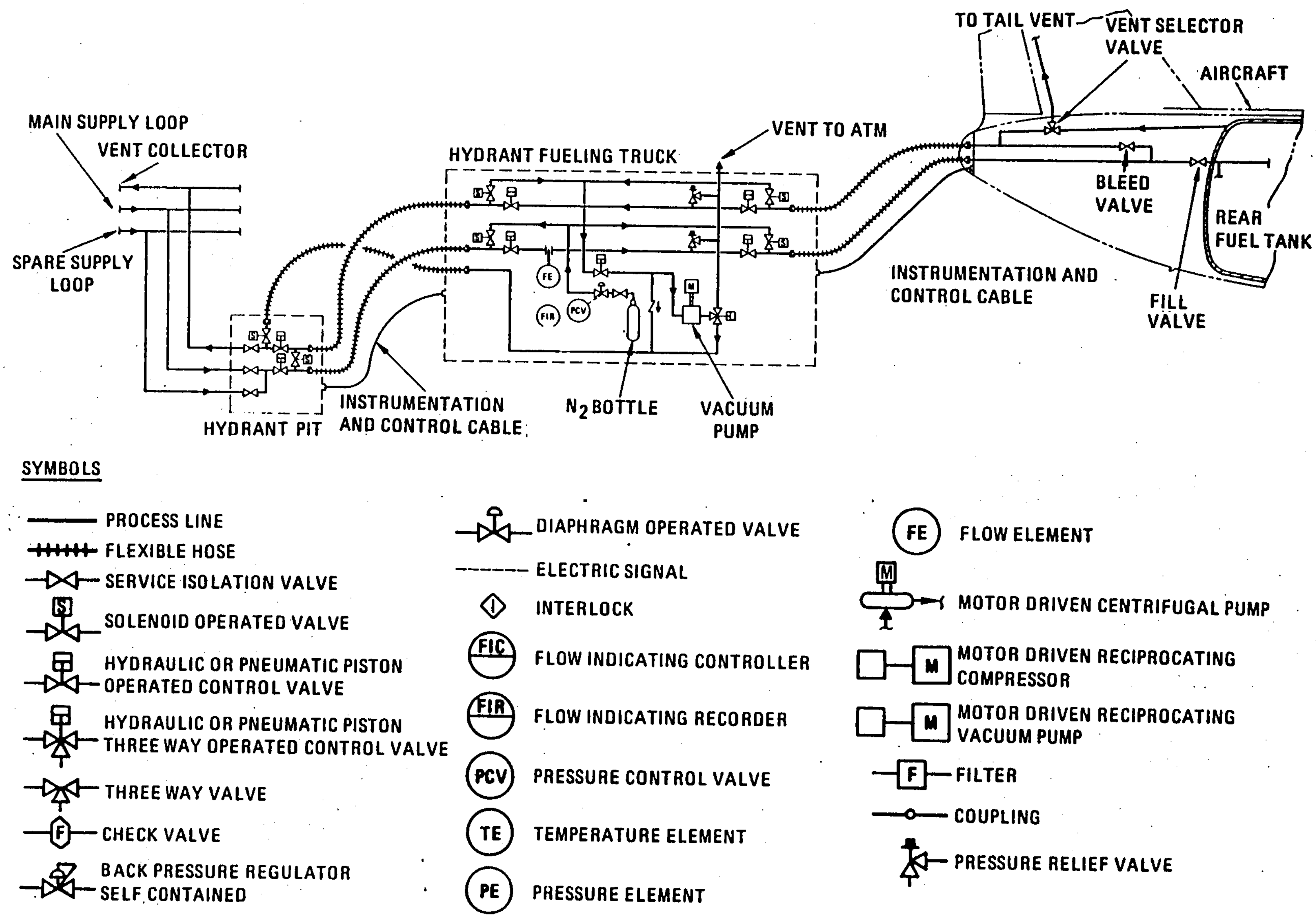

Figure 139. - Flow schematic, hydrant fueling.

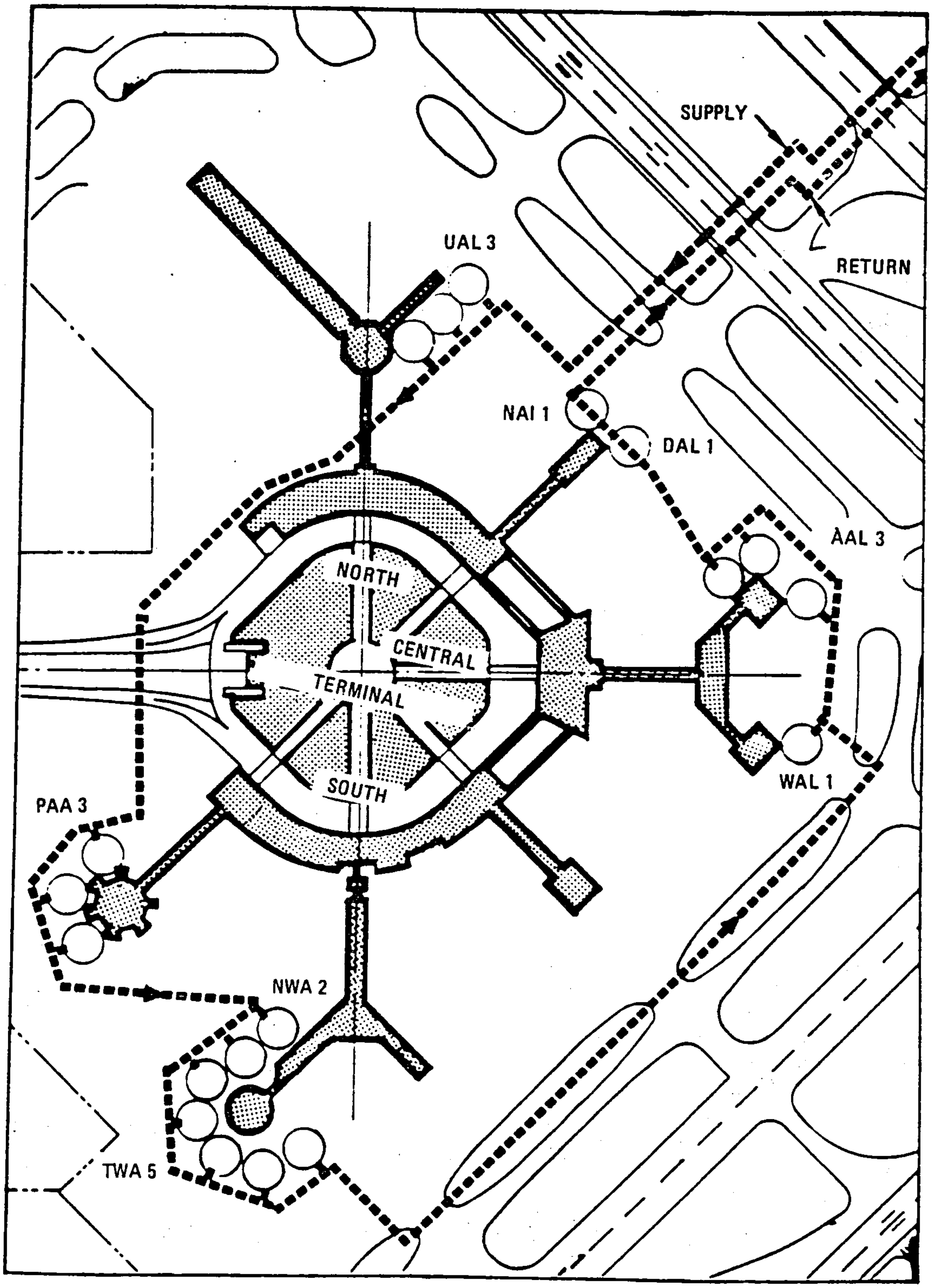

Figure 140. - Distribution loop concept plan.

each gate), then returned to the storage system. This liquid methane constant fuel circulating system keeps the distribution lines and the fueling system cool, and the chilldown time is virtually eliminated. In this way, the aircraft will obtain fuel upon arrival at its assigned gate without extensive planning and scheduling or elaborate communications with LCH_4 facility operations.

9.1.3.3 Design considerations for liquid methane ground distribution and fueling systems.- The liquid methane ground distribution system considered here consists of two distribution lines. A main distribution line and a spare distribution line. During an average fuel demand period, where as many as two aircraft might be fueling at the same time, the main distribution line alone will be sufficient to meet the fuel demand. The spare distribution line will then provide the required redundancy in the distribution system to ensure an uninterrupted supply of liquid methane fuel. In case of a peak day operation, where as many as four aircraft might be fueling at the same time, both liquid methane distribution lines will be used. In other words, the required redundancy in the distribution system is not available during the peak fueling operation. But, considering the short duration of peak fuel demand period, it is safe to assume that a dual line distribution system will be adequate to ensure an uninterrupted supply of liquid methane fuel.

The total length of the cryogenic piping used in the distribution system at San Francisco airport can be broken down approximately as follows:

	Approximate Length m, (ft)
Supply Line	1524 (5 000)
Distribution Line	1829 (6 000)
Return Line	1524 (5 000)
Total Length of Cryogenic Piping	4877 (16 000)

As shown above, each distribution line will use approximately 4877 m (16 000 ft) of cryogenic piping. A 25.4 cm (10-in.) nominal diameter pipeline is considered in the above conceived distribution system (reference 55). The maximum operating pressure of the distribution lines is set by considering the following design constraints:

- Maximum flow rate through the distribution lines
- Total pressure drop due to the frictional losses (a reasonable allowance is made to account for the pressure drop due to valves, pipefittings, and bends, etc.)
- Pressure drop through hydrant pit and the hydrant fueler vehicle

- The pressure at the end of the last hydrant is set to a value, so that the liquid returning to the storage system is saturated in spite of the temperature rise due to heat infiltration and frictional losses in the distribution lines.

The minimum flow rate of liquid methane through the distribution lines is kept at 0.139 m^3/s (2200 gpm).* At this flow rate, a single aircraft can be fueled. At a maximum flow rate of 0.278 m^3/s (4400 gpm), each distribution line is capable of fueling two aircraft, thus, supplying the expected peak fuel demand at San Francisco airport. The liquid methane circulation rate, required to keep the distribution lines cool during the idle periods could be less than 0.139 m^3/s (2200 gpm), but to keep the distribution system simple (avoid additional transfer pumps), the idle period liquid methane circulation rate is also set at 0.139 m^3/s (2200 gpm).

The total pressure drop due to frictional losses through the supply distribution and return lines 4877 m of 25.4 cm (16 000 ft of 10 in.) pipeline is approximately 641.2 kPa (93 psi) for a flow rate of 0.139 m^3/s (2200 gpm) and 1972 kPa (286 psi) for a flow rate of 0.278 m^3/s (4400 gpm). These pressure drop calculations are carried out by using the Darcy-Weisbach equation as given below for flow of incompressible fluids in pipes.

$$\Delta P = \frac{f \rho \bar{v}^2 L}{2 g_c Di} \tag{3}$$

where,

ΔP = Pressure drop, lbf/ft^2
f = Friction factor, dimensionless
ρ = Density of liquid methane, lbm/ft^3
$\bar{v}$ = Velocity of flow, ft/sec
L = Total length of piping used in the distribution lines
g_c = Conversion factor, $\frac{ft\text{-}lbm}{sec^2\text{-}lbf}$
Di = Internal diameter of pipeline, ft.

The pressure drop through the hydrant pit valves and fueler vehicle is taken as 82.7 kPa (12 psi). Of this, 41.4 kPa (6 psi) represents the pressure drop incurred in lifting the liquid methane from the hydrant pit level to the fueling point located in the tail of the aircraft. The temperature as a function of liquid methane distribution line length is presented by the following relationship

*The fuel circulation rate is set to accomplish the aircraft fueling operation in 20 minutes.

$$L = \frac{WC\ (Tb - Ta)}{\dfrac{Tb - Ta}{(R_{23} + R_{34})\ \ln \dfrac{(T_4 - Ta)}{T_4 - Tb}} + \dfrac{\rho f\ \bar{v}^{\,2}}{2g_c\ Di\ J}} \tag{4}$$

where,

L	=	Total length of distribution line, ft
W	=	Liquid methane flow rate, lb/sec
C	=	Specific heat, Btu/(lb)(^{o}F)
Tb	=	Temperature at pipeline outlet, ^{o}F
Ta	=	Temperature at pipeline inlet, ^{o}F
Tb-Ta	=	Temperature rise over length L of the distribution line
R_{23}	=	Heat transfer resistance of the pipe insulation, (sec)(ft)(^{o}F)/Btu
R_{34}	=	Heat transfer resistance of the ground, (sec) (ft) (^{o}F)/Btu. (Used only when the distribution line is underground. For aboveground distribution lines, R_{34} = 0.)
T_4	=	Mean ambient temperature, ^{o}F
ρ	=	Density of liquid methane, lbm/ft^3
f	=	Friction factor
$\bar{v}$	=	fluid velocity, ft/sec
g_c	=	Gravitational conversion factor $\dfrac{ft - lbm}{lbf - sec^2}$
Di	=	Inside diameter of the distribution line, ft
J	=	Conversion factor, 778 ft-lb/Btu.

This relationship gives the temperature profile along the distribution lines. It takes into account the temperature rise due to both the ambient heat infiltration through pipe insulation and the frictional losses converted to heat.

Equation 4 is used to establish the temperature rise along the liquid methane supply, distribution, and return lines. Above ground insulated pipelines are considered for the ground distribution system. Generally, two types of insulation systems can be used for liquid methane pipelines. These are (1) a high vacuum superinsulation system, and (2) a nonvacuum system using polyurethane foam insulation. In the case of a high vacuum superinsulation system, a cryogenic pipeline would be suspended within a concentric external carbon steel pipe, and a 10^{-3} to 10^{-4} mm Hg vacuum would be maintained in the annulus between the two pipes. The use of multilayered superinsulation in the vacuum annuler space is necessary to reduce radiant heat transfer. In the case of a nonvacuum polyurethane system, the insulation is fabricated by shaping and filling pieces of insulation to cover the pipe; the seams between the pieces can be sealed by a suitable mastic, epoxy, etc., or by an external covering (references 56 and 57).

Although the vacuum insulation system has superior thermal performance characteristics than the nonvacuum polyurethane foam insulation system, the high cost and maintenance difficulties of a vacuum insulation system makes its choice unfavorable, whereas, the use of polyurethane foam mechanical insulation appears preferable, since it would circumvent many of the installation and maintenance difficulties of a vacuum insulation system. The polyurethane foam is a rigid plastic material with an ideal combination of thermal-performance characteristics, strength, ease of fabrication, and low cost.

It was found that a 5.08 cm (2-in.) thick polyurethane insulation was adequate to minimize the ambient heat infiltration into an LNG pipeline (reference 58). Increasing the insulation thickness over 5.08 cm (2 in.) resulted in only a marginal improvement in the thermal performance. In accordance with the above, we have selected a 5.08 cm (2-in.) thick polyurethane insulation for the liquid methane lines employed in the ground fuel distribution system. For a 5.08 cm (2-in.) thick polyurethane insulation, when used in a 25.4 cm (10-in.) nominal size aboveground liquid methane line, the temperature rise due to heat leakage and fluid friction is calculated to be about 2.2°C (4°F) for both the minimum and maximum rates. It is interesting to note that temperature rise does not decrease when the fuel circulating rate is increased from 0.139 m^3/s (2200 gpm) to 0.278 m^3/s (4400 gpm). This results from the increased frictional losses encountered at higher fuel circulating rate, which negate any gain in the heat sink capacity provided by the additional mass of liquid fuel. In either case, the minimum pressure required to keep the methane fuel a saturated liquid at the end of the return line, will depend on the inlet temperature of the liquid fuel fed into the distribution system. For example, if the inlet temperature of liquid methane at the supply line is set at -162°C (-259°F), then the methane fuel returning to the ground storage areas will be around -160°C (-255°F). At this terminal temperature, a pressure of 138 kPa (20 psia) is required to keep the methane fuel as saturated liquid. This saturated liquid is introduced into a vented storage tank and flashed back to saturation conditions at the storage tank pressure of 103 kPa (15 psia).

Based on the design constraints, the maximum design pressure of the liquid methane lines is set at 2137 kPa (310 psia). This maximum pressure will be encountered during the peak fuel demand 0.278 m^3/s (4400 gpm), when as many as four aircraft might be refueling at the same time. Whereas, during the low fuel demand 0.139 m^3/s (2200 gpm) or idle period, the liquid methane lines are subjected to a maximum pressure of 793 kPa (115 psia). The ground distribution system operating flexibility is ensured by a pressure control system that provides constant LCH_4 pressure to all the hydrants (19 gates) and fueler vehicle at San Francisco airport. Each hydrant will see a constant LCH_4 pressure of 276 kPa (40 psia). Allowing a pressure drop of 82.7 kPa (12 psi) through the hydrant valves and fueler vehicle, an aircraft interface pressure of 193 kPa (28 psia) is maintained when fueling at the design rate of 0.139 m^3/s (2200 gpm). The aircraft tank nominal operating pressure is 145 kPa (21 psia).

The pressure in the line is controlled by a back pressure regulator located at the storage area end of the LCH_4 return line. This valve is controlled by a pressure sensor located at the last hydrant on the distribution line. As the back pressure regulator reaches the extreme of its available control range, transfer pumps are either brought on line or dropped off line, as required to maintain a constant LCH_4 pressure. During the idle periods, one transfer pump remains on line to ensure the availability of liquid methane and to maintain constant supply pressure.

9.1.3.4 Pipe material.- Depending on the required degree of subcooling, the cryogenic piping employed in the ground distribution system will encounter temperatures as low as -173°C (-279°F). There are a large number of materials that are either acceptable or potentially acceptable for construction of a liquid methane line. A detailed discussion and economic comparison of these materials is out of the scope of this study, however, a brief discussion of some of the important considerations in the selection of pipe material is presented below.

A major problem from a material standpoint in the construction of a liquid methane pipeline is the loss of ductility exhibited by some materials at low temperatures. Generally, metals that have a face-centered-cubic lattice, such as copper and aluminum, show no loss of ductility at low temperatures. Members of the body-centered-cubic class, such as iron, will generally fail with limited ductility below a certain transition temperature range. Austenitic stainless steels have a face-centered-cubic lattice and therefore, have no ductile-brittle transition temperature. In other ferrous alloys, the transition temperature is lowered by reducing carbon content or by increasing nickel content.

In general, the following items must be considered in the selection of materials for liquid methane pipelines.

- Strength
- Resistance to crack initiation
- Coefficient of thermal expansion
- Weldability or joining
- Minimum wall thickness permitted by the pipeline code
- Surface friction factor
- Thermal conductivity
- Cost.

At the present time, austenitic stainless steels, aluminum alloys, and nickel steels are the most suitable pipe materials. An extensive comparison of all the items listed above for different suitable pipe materials is reported in the literature (references 59 and 60). Based on the conclusions reached in these previous studies, we have selected a 9 percent nickel steel as a pipe material for the liquid methane lines used in the ground distribution system.

Once the pipe size and pipe material are selected, an important factor is providing for thermal contraction by flexibility of the system. This thermal contraction is a result of the temperature range encountered, ambient to about -162°C (-259°F) in the liquid methane pipeline transfer operation. There are several methods of relieving the longitudinal thermal contraction of the line. For example, this can be accomplished by using either Invar (36 percent nickel) steel), expansion loops, or expansion joints (bellows) (references 54, 61 and 62).

The major advantage of Invar over the other cryogenic pipe materials is its low coefficient of expansion, which is low enough to allow the use of Invar pipe without expansion loops or joints. But Invar is a very expensive material, and its use does not appear to be justified from economic considerations.

The expansion-loop design for the liquid methane lines at San Francisco airport might require construction of a chamber to allow free movement of the loop piping. For a -25.4 cm (10-in.) line and a specified loop height of 6.1m (20 ft) and loop width of 3.05m (10 ft), the number of expansion loops required for a 9 percent nickel steel might run as high as 26. Expansion loops are generally recommended for long distance 1608 km (1000 mi) and high pressure 6.90 mPa (1000 psi) cryogenic pipelines. Considering the ground fuel distribution system at San Francisco airport, which contains approximately 4.8 km (3 mi) of cryogenic pipeline and has a maximum operating pressure of approximately 2.07 mPa (300 psia), the use of expansion loops may be impractical. Moreover, construction of chambers to allow free movement of the loop piping along the airport fuel distribution line might complicate the layout of the ground fuel distribution system. Therefore, expansion loops are not a suitable method of relieving axial stresses in the conceived ground fuel distribution system

In-line expansion joints of stainless steel bellows construction are available for cryogenic service. For short distances 16.1 to 24.1 km (10 to 15 mi or less), where the liquid methane line is operating at or around a pressure of 2.07 mPa (300 psia), the use of bellows is justified due to the possible greater maximum deflections of the expansion joints at this pressure. A maximum axial deflection of 2.94 in. is obtained for a 6-convolution, Tube-Turns, Serial R bellows joint operating at a pressure of 2.07 mPa (300 psia). The approximate longitudinal contraction for a temperature drop from 15.5°C to -162°C (60°F to -259°F) would be 167 cm/km (107 in./mi) for 9 percent nickel steel. Since the total length of cryogenic fuel line is approximately 4.8 km (3 mi), the total longitudinal contraction in each liquid fuel line is estimated to be about 815 cm (321 in.).

To compensate for this longitudinal contraction, approximately 110 expansion bellows are required for each liquid methane fuel distribution line. The liquid methane line using expansion joints (bellows) only would have the bellows located in the line back-to-back as shown below.

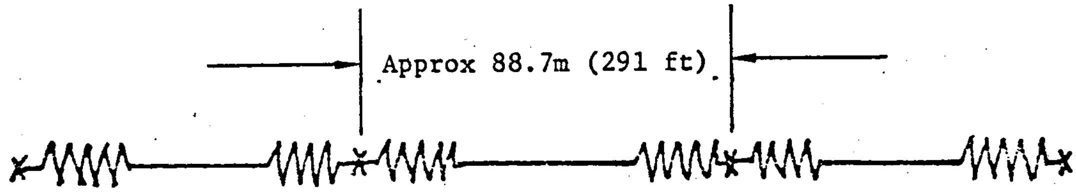

where,

x = intermediate anchor
= expansion joint

Figure 141 shows details of a possible expansion joint, anchor, and concrete enclosure.

9.1.3.5 Pipe thickness calculation.- The design pipe wall thickness of the liquid methane lines is calculated from the allowable design stress. For the majority of the materials, the USASI B31.1 allowable stress corresponds to approximately 60 percent of Specified Minimum Yield Strength (SMYS) (reference 59). The only exception is 9 percent nickel, which has an allowable stress equal to 50 percent of SMYS.

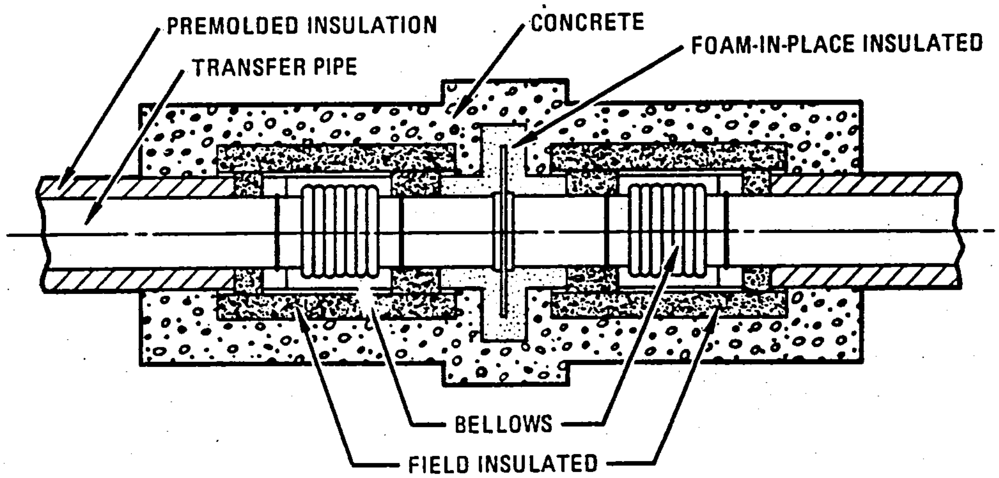

Figure 141. - Expansion joint with concrete enclosure.

The approximate thickness of the pipe is calculated by the following equation:

$$t = \frac{P_1 \times Do}{2 \times 0.5 \times S} \tag{5}$$

where,

t = Pipe wall thickness, in.

P_1 = Internal pressure, psi

Do = Outside pipe diameter, in.

S = Specified minimum yield strength (0.5S = allowable design stress).

The minimum specified yield strength for 9 percent nickel steel may be taken as 414 MPa (60 000 psi). If the maximum operating pressure of the liquid methane fuel line is taken as 2.14 MPa (310 psi), then the design thickness of the pipeline will be 0.13 cm (0.052 in.). This design thickness is considerably below the least nominal thickness of 0.26 cm (0.104 in.) specified in ANSI B31.8 for a 25.4 cm (10-in.) nominal size pipe. Therefore, the actual thickness of the pipe used in the liquid methane line should be 0.26 cm (0.104 in.).

9.1.3.6 $\underline{LCH_4 \text{ transfer method}}$.- The methane fuel transfer method considered in our study is similar to the LH_2 transfer method, proposed in a previous study. In this proposed transfer method, liquid pumps are employed to move methane fuel on an uninterrupted basis from the storage tanks through the distribution lines. The rationale for selecting a pump-fed system is presented in the LH_2 fuel study referred to above (reference 5). In order to compensate for the poor reliability and demand flexibility of transfer pumps, multiple units are provided in the system. Each of these units is a four-stage, two-speed, cryogenic pump. According to J.C. Carter Company, this pump, when operating at higher design speed, will be capable of delivering 0.278 m^3/s (4400 gpm) of liquid methane at a differential head of 2.55 MPa (370 psi) (reference 63). The approximate horsepower requirement at this flow rate will be around 933 kw (1250 hp). At the lower speed, the same pump will be capable of delivering 0.139 m^3/s (2200 gpm) of liquid methane with a corresponding differential head of 655 kPa (95 psi). The horsepower requirement at this low flow rate operation amount to approximately 276 kw (370 hp). Thus, each of the variable speed pumps is capable of fueling a single aircraft at the lower design flow rate 0.139 m^3/s (2200 gpm), whereas, the higher flow rate 0.278 m^3/s (4400 gpm) has the capacity to fuel two aircrafts simultaneously. These are submerged motor pumps, which are mounted in a suction pot, thus, avoiding the net positive suction head (NPSH) requirement. Moreover, these pumps are close-coupled to the storage tanks to minimize heat leak into the suction pot piping. The close-coupled configuration limits flexibility to the extent that a pump can be utilized only to withdraw LCH_4 from the storage tank to which it is mated. In normal conditions, all fueling operations are supplied from one storage tank. Thus, all three storage tanks require a set of liquid pumps so that all may provide fuel distribution. At the design peak, four aircraft may require fuel simultaneously. Thus, two variable speed, multistage pumps are required per storage tank. This provides 100 percent pump capacity redundancy during normal operation (two aircraft fueling). However, during peak periods, a pump outage will require that one of the reserve storage tanks be brought on line to provide sufficient pump capacity.

9.1.3.6 Trade-off analysis, truck versus pipeline transport.- As the volumetric energy content of LCH_4 21.2 MJ/liter (76 132 Btu/gal) exceeds that of LH_2 [8.51 MJ/liter (30 550 Btu/gal)], the trade-off analysis concerning truck versus pipeline transport for LH_2 in the previous study is not directly applicable to the transport of LCH_4. Essentially, the LH_2 study showed that the breakdown distance for truck versus pipeline transport was 80.5 km (50 mi), figure 142 (reference 5). The transportation distance is the distance that the liquefaction unit is located away from the airport.

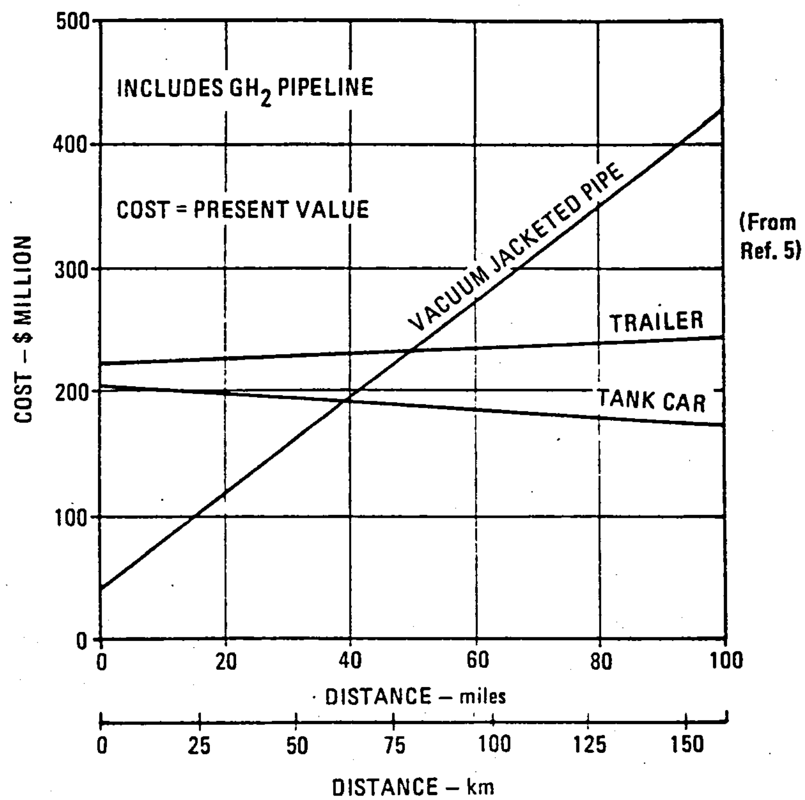

Figure 142. - Cost of LH_2 transport by pipeline, truck, and rail tank car.

Based on the LH_2 analysis and the energy content differences of LH_2 and LCH_4, the number of LCH_4 trucks required to meet the aircraft fuel demand schedule as a function of one-way trip distance is presented in table 61. Each trailer can carry 51,100 liters (13 500 gallons) of LCH_4.

If the LCH_4 is transported by truck, there are additional components that must also be accounted for. These include a maintenance building for the fleet of vehicles, filling stations at both the liquefaction and airport sites, and changes in storage tank configuration. That is, if the liquefaction plant is remote to the airport, then two sets of storage tanks are required at each site. The total storage capacity requirements do not change, but rather, there is an economic penalty for a loss in the economies of scale for LCH_4 tankage, figure 133. Rather than provide three tanks, each with a capacity of 42 130 m^3 (265 000 bbl), as in the case of LCH_4 pipeline distribution, two tanks, each with a capacity of 31 780 m^3 (200 000 bbl), must be provided at the liquefaction site and the airport terminal. The new storage configuration results in a direct cost increase of $800 000, which is attributable to the truck transport system. In addition, fuel losses from truck transport exceed the fuel losses from pipeline distribution by about 10 percent. The increase in fuel losses (due to boil-off during loading/ unloading and transport by truck of the LCH_4) would require a 10 percent increase in the design liquefaction capacity relative to the pipeline distribution system. Accounting for these modifications to the ground distribution system, the costs attributable to truck transport of LCH_4 are presented in table 62.

For long-distance transmission of LCH_4, the principal changes in cost of the distribution system result from (1) increased pipeline costs, (2) additional pumping capacity for the supply and vapor return lines, and (3) cooling stations to maintain the LCH_4 in the liquid phase regime (reference 61). The costs attributable to pipeline transport of LCH_4 are presented in table 63.

Based on the information of tables 62 and 63, figure 143 was constructed. The figure shows that if the liquefaction site is more than 27.8 km (15 mi) from the airport truck transport would be less costly than pipeline transport.

TABLE 61. - LCH_4 TRAILER TRUCK REQUIREMENTS

One-Way Distance, km (miles)	Number of Trailers
1.85 (1)	36
9.26 (5)	39
18.5 (10)	44
92.6 (50)	84
185 (100)	132

TABLE 62. - COST OF TRUCK TRANSPORT OF LCH_4

Distance, km (miles)	0*	1.85 (1)	9.26 (5)	18.5 (10)	92.6 (50)	185 (100)
	Millions of Dollars					
Investment						
Storage (Change)	0	1.2	1.2	1.2	1.2	1.2
Liquefaction (Change)	8.5	8.5	8.5	8.5	8.5	8.5
Building	1.2	1.2	1.2	1.2	1.2	1.2
Filling Station	0.3	0.6	0.6	0.6	0.6	0.6
Vehicles	1.6	1.6	1.7	2.0	6.2	9.8
Total	11.6	13.1	13.2	13.5	17.7	21.3
Operating Costs						
Liquefaction† (Change)	1.0	1.0	1.0	1.0	1.0	1.0
Vehicles	2.0	2.0	2.2	2.5	4.6	7.4
Total	3.0	3.0	3.2	3.5	5.6	8.4

* Liquefaction plant is located inside airport, but trucks are used to fuel aircraft directly. Tankage configuration is similar to pipeline concept and only one filling station required.

† Cost of fuel gas taken at $3/million Btu.

TABLE 63. - COST OF PIPELINE TRANSPORT OF LCH_4

Distance, km (miles)	0	1.85 (1)	9.26 (5)	18.5 (10)	92.6 (50)	185 (100)
	Millions of Dollars					
Investment						
Trenching System*	5.8	5.8	5.8	5.8	5.8	5.8
Pipeline System	1.8	2.2	3.4	5.0	17.8	33.8
Compressor/Pumping Capacity	0.1	0.1	0.5	1.0	5.0	10.0
Cooling Units†	0.0	0.0	1.0	2.0	10.0	20.0
Total	7.7	8.1	10.7	13.8	38.6	69.6
Operating Costs						
Pipeline	6.4	0.4	1.6	2.0	8.6	16.5

* In airport only. Long distance transmission is aboveground.

† Approximately 1 cooling unit per 9.26 km (5 mi) of supply line.

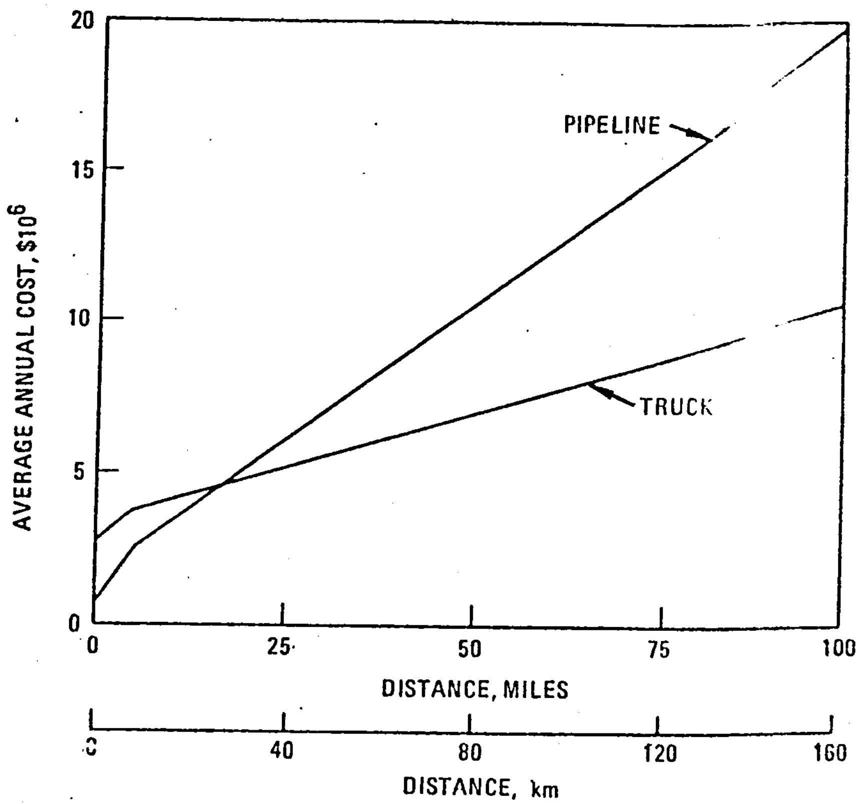

Figure 143. - Average cost of LCH_4 transport.

9.1.3.7 Results.-The results of the analysis of the distribution system are that the leastcost distribution concept is the pipeline distribution concept, unless the liquefaction facility is located at a distance greater than 27.8 km (15 mi) from the airport. In addition if truck transport were used exclusively surface traffic would be excessive and there would be no vent recovery. Further, review of the appropriate safety standards for design of liquefied natural gas facilities have not resulted in any modification to the proposed pipeline distribution concept (reference 30).

9.1.4 LCH_4 processing requirements.- The method of this task included a review of typical pretreatment processes to remove water, acid gases, and heavier hydrocarbons from the feed stream; contact with process designers to determine the requirements for pure LCH_4 production; and literature and patent reviews to determine processes for subcooling and gelling LCH_4.

9.1.4.1 Feed gas pretreatment.- Liquefaction of natural gas requires process temperatures as low as -162°C (-260°F). Any constituents of the inlet gas stream that may become solid at these temperatures must be removed to the extent that they will either remain in solution in the LCH_4 or be of such low concentrations as to create no significant fouling or plugging problems. The two constituents typically found in natural gas from a distribution pipeline that must be reduced in concentration are water (H_2O) and carbon dioxide (CO_2) and, in some cases, small amounts of H_2S (reference 63). Typical feed gas specifications for natural gas liquefaction include:

50 ppm (v) for CO_2, and 1 ppm (v) H_2O.

Any heavier hydrocarbons present must also be removed prior to entering the cryogenic heat exchanger. The most frequently used pretreatment processes are summarized below and are included in the discussion of commercially available liquefaction processes in Appendix A.

	APCI	Phillips	Pritchard
Acid-Gas Removal	MEA	Amine Treater	DEA
Dehydration	Molecular Sieve	Molecular Sieve	Molecular Sieve
Heavy Ends Removal	Condensate Side Stream Removal	Heavier Hydrocarbons Draw From Ethylene Section	Condensate Side Stream Removal

9.1.4.2 Production of pure methane: substitute natural gas.- If the feed stream for the liquefaction plant is substitute natural gas, it will consist of methane (CH_4), carbon monoxide (CO), carbon dioxide (CO_2) hydrogen (H_2), and nitrogen (N_2). Although none of the existing liquefied natural gas facilities have liquefied SNG, liquefaction of SNG is not expected to cause any unusual problems. The CO_2 can be removed in the pretreatment process. The resulting gas stream can then be refrigerated down to the boiling point of CH_4. As the boiling points of CO, H_2, and N_2 are lower than that of CH_4, the LCH_4 can be drawn off with only trace amounts of the other constituents. The vapor stream consisting of H_2, CO, and N_2 could then be utilized as fuel supplement to the liquefaction facility.

In the case of SNG, all refrigerant makeup requirements, such as ethane, propane, butanes, and pentanes would have to be purchased from outside vendors and stored at the liquefaction facility.

Natural Gas: The front end processing (pretreatment) of natural gas will remain unchanged, irrespective of the desired product, LNG or pure liquid methane (references 64, 65 and 66). However, in the case of liquid methane production from a natural gas feed, a distillation column (demethanizer) will be supplied in the cryogenic section of the liquefaction plant. In general, the operation of a pure liquid methane production plant can be briefly described as follows (reference 67 and 68).

The natural gas feed after necessary pretreatment is chilled to -37.2°C (-35°F). About half the recoverable heavier hydrocarbons are condensed at this point. They are separated from the balance of the feed gas and pumped to the demethanizer. The remaining vapor is further cooled to between approximately $-92.8^{o}C$ (-135^{o}) and $-95.6^{o}C$ ($-140^{o}F$). At this stage, nearly 99 percent of the propane and practically all the butane and other heavier hydrocarbons, if present, are condensed with the ethane. This partially condensed feed gas enters a separator and the vapors (nearly pure methane) from the separator are sent to a final stage of refrigeration, while the liquid is warmed against the feed vapor and pumped to the demethanizer tower. Operating conditions of the demethanizer are controlled to permit the stripping of sufficient methane from the bottoms liquid to reduce the loss of methane fuel, while minimizing ethane leakage in the column overhead vapor.

If the demethanizer operates at about 3.45 MPa (500 psi, $-140^{o}F$), ethylene can be used as the overhead condenser coolant and condensing propane as the main heating medium for the reboiler. This will significantly cut refrigeration horsepower needs and plant operating costs (reference 68). The overhead methane vapors will be further cooled in the final stage of cryogenic heat exchangers. The liquid product exiting the cryogenic heat exchanger is essentially pure liquid methane, is throttled down to the storage tank, and is transferred to the fuel storage subsystem. The bottoms liquid from the demethanizer can be further fractionated into pure propane or ethane fractions (and sold as byproducts), or else, burned to supply the fuel requirements of the liquefaction plants (references 70, 71, and 72).

Subcooling: The amount of subcooling desired to optimize the tradeoff of boil-off from aircraft fuel tanks as the airplane climbs to high altitude vs. system cost, depends on the aircraft fuel tank design pressure. The LCH_4 boils off until the liquid temperature is lowered to the corresponding saturation temperature at the pressure of the particular altitude level. To prevent this, either the tank pressure must be increased on the LCH_4 may be subcooled to a point where its vapor pressure is below the ambient pressure (reference 73).

The extent of boil-off from the aircraft fuel tank, during the aircraft climb schedule was estimated as a function of subcooling and aircraft fuel tank design pressure, figure 144. The cruising altitude for the subsonic aircraft was assumed to be 9754 m (32 000 ft) for purposes of this exercise, and the ambient pressure corresponding to this altitude was taken as 27.6 kPa (4 psia). As mentioned earlier, the LCH_4 boils off during the time from takeoff until the cruising altitude is reached. At the cruising altitude, a new saturation pressure and temperature will be established, and the LCH_4 will come in equilibrium with the vapor. This is the amount of vapor produced, due to the reduction in atmospheric pressure with the increasing altitude. The vapors that might be produced by the atmospheric frictional heating, are not included. The amount of vapor produced by the frictional heating will be very small when compared with the vapor produced by ambient pressure reduction.

As shown in figure 144, increasing the aircraft fuel tank pressure from 20.7 to 82.7 kPa (3 psi to 12 psi), reduced the LNG boil-off from 7.1 percent to 1.0 percent, without any initial subcooling. The figure

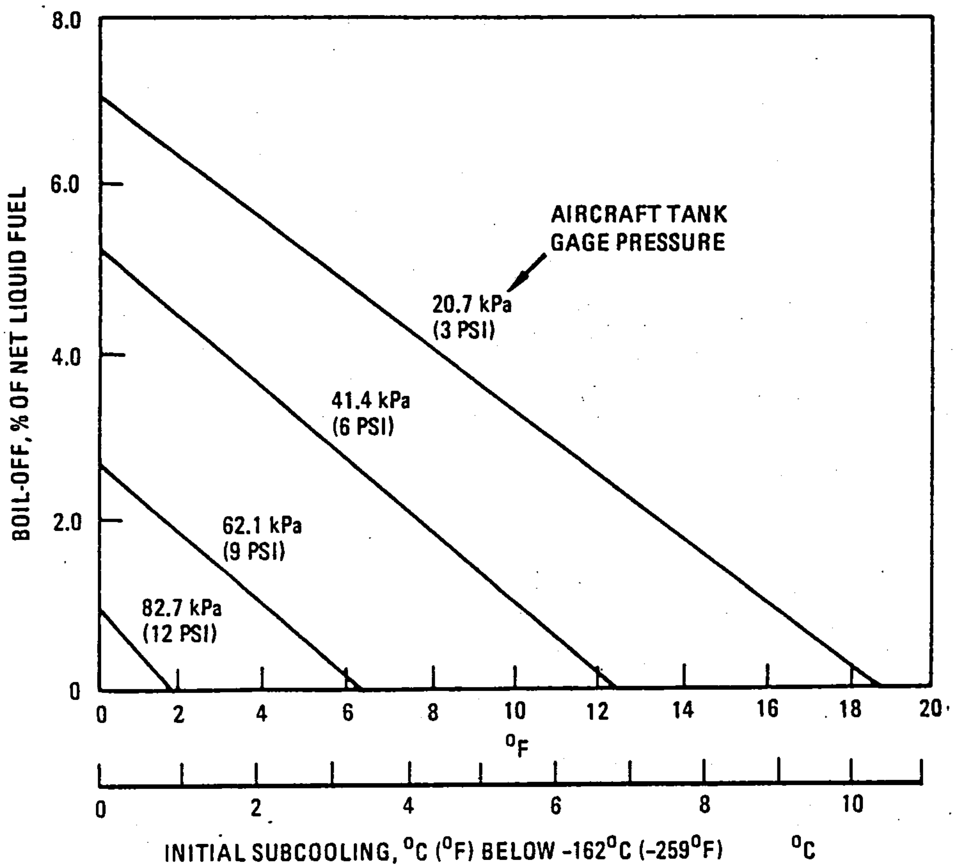

Figure 144. - LCH_4 boil-off vs. LCH_4 temperature and aircraft tank design pressure.

also shows that, to eliminate boil-off entirely, with an internal tank pressure of 20.7 kPa (3 psi), the fuel would have to be initially subcooled -7.2°C to -172°C (19°F to -278°F). Maximum subcooling is limited to -183°C (-297°F), the normal freezing point of methane (reference 54).

Subcooling the LCH_4 would require additional refrigeration horsepower. An estimate of additional refrigeration horsepower required at various initial subcooling levels is presented in figure 145 (reference 74). The bulk of the additional horsepower requirement goes for supplying the initial subcooling. For example, approximately 140 kw (188 hp) are required in additional refrigeration work to subcool liquid methane at 25.3 kw (-259°F) by 1°F. Whereas, the increased horsepower required to pump LCH_4, when the aircraft tank pressure changed from 20.7 to 82.7 kPa (3 psi to 12 psi) is only 25.3 kw (34 hp).

This subcooling of LCH_4, if required, can be accomplished by providing a final stage of heat exchange with liquid nitrogen (reference 75).

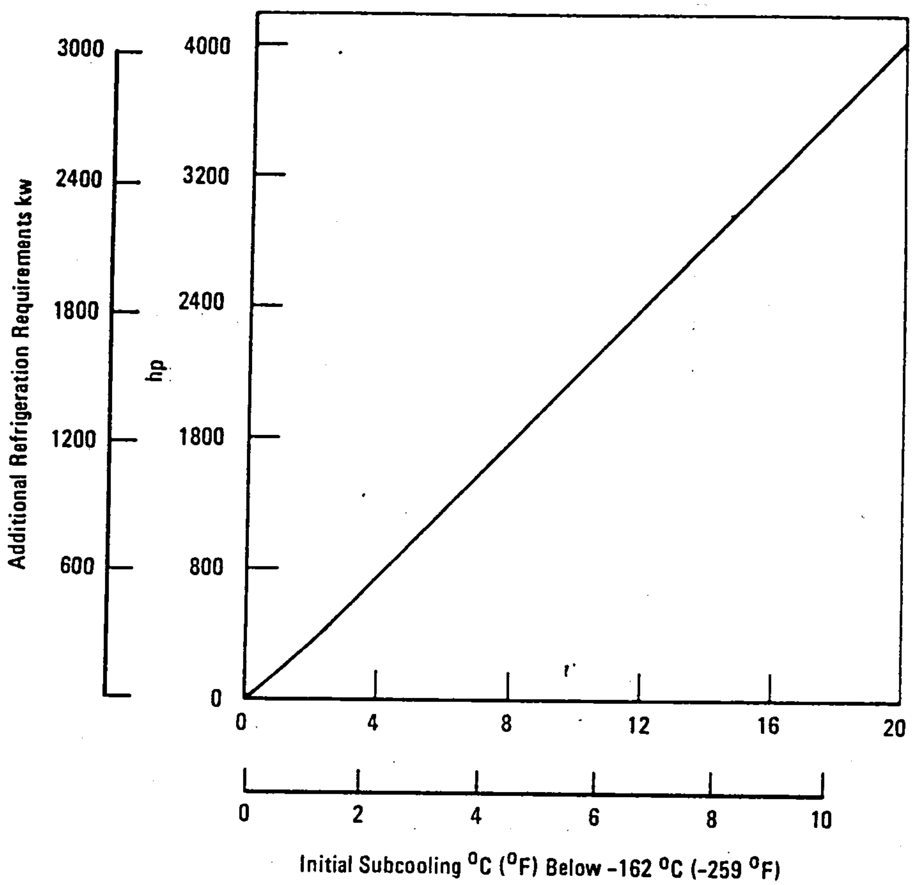

Figure 145. - Refrigeration horsepower requirements for subcooling.

If the LCH_4 were to be stored as a subcooled liquid, an inert pressurant gas (i.e., helium) would be required to maintain a positive pressure in the LCH_4 storage tanks as the vapor pressure of subcooled LCH_4 is below atmospheric (reference 73). This condition would develop a vacuum in the storage tank that could cause a tank roof failure. Rather than store the LCH_4 as a subcooled liquid, the subcooler could be placed between the storage tanks and the distribution system. In this manner, the LCH_4 would be stored as a saturated liquid without requiring any modifications to the LCH_4 tankage system. However, location of the subcooler after the storage tanks would result in constant recooling the LCH_4 that is circulating through the distribution system. Depending on the degree of subcooling required, two separate subcoolers could be required. That is, one subcooler to subcool the LCH_4 down to the required temperature, and then another subcooler to compensate for the -2.2°C (4°F) temperature rise in the LCH_4 due to heat gain and fluid friction in the distribution system. The concept is depicted in figure 146. In this manner, the advantages are that the storage system does not need to be pressurized by an inert pressurant and the extensive refrigeration horsepower

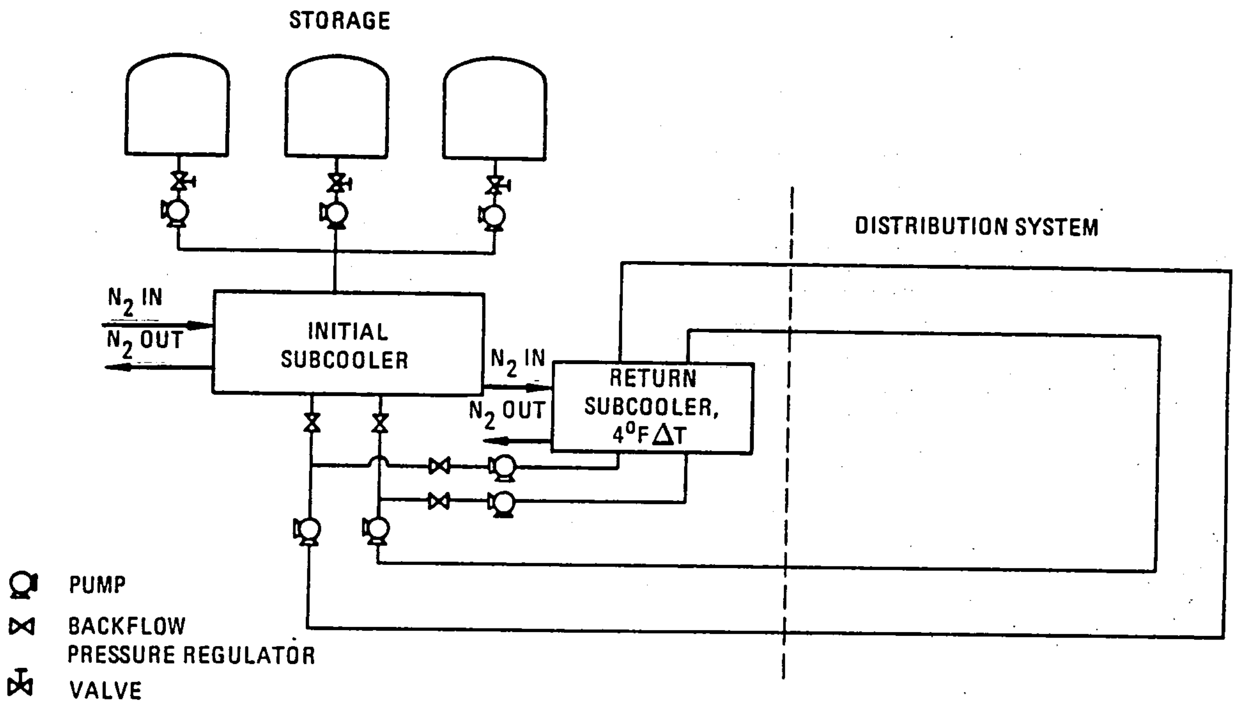

Figure 146. - Subcooling concept.

required for initial subcooling is limited to only the flow rate of the LCH_4 consistent with the aircraft fuel demand schedule rather than constant total subcooling of the recirculating LCH_4 in the distribution system.

Further, since the conceptual subcooler is primarily an N_2 coil immersed in an LCH_4 bath, the three sets of variable speed multistage pumps required with subcooling before storage are reduced to two sets (one after each subcooler). However, three single speed pumps would be required to deliver the LCH_4 from storage to the initial subcooler.

The principal disadvantage of this concept would be the extensive control system and instrumentation required to ensure LCH_4 feed from the initial subcooler to the distribution system consistent with the draw by the LCH_4 aircraft. However, if the LCH_4 were subcooled prior to injection into storage, an extensive control system and instrumentation would also be required to maintain the appropriate pressure with an inert pressurant during the complete cycle of storage from empty to full. Therefore, the primary difference between subcooling the LCH_4 either before storage or prior to entering the distribution system is that the need for pressurized storage is eliminated with the initial subcooler located after the storage system.

The required trade-off analysis to determine the appropriate degree of subcooling involves evaluating the cost incurred in increasing the aircraft LCH_4 tank design pressure relative to the increased costs of decreasing boil-off by subcooling. The costs of subcooling as a function of degree below -162°C (-259°F) are estimated in Section 9.5.

Subcooling of LNG is not a common practice in LNG production and handling operations. To this date, there has been no attempt made to subcool LNG in large quantities. But, at the same time, we do not see any technical barrier to the use of a liquid nitrogen heat exchanger subcooler. The liquid methane fuel subcooler, in its simplest configuration (figure 147), will consist of a spiral wound coil, through which liquid nitrogen is passed (reference 75). This liquid nitrogen-carrying coil is submerged in the saturated LCH_4, which is contained in the subcooler. The saturated LCH_4 entering the subcooler exits as a subcooled liquid and is sent to the distribution system. The normal boiling point of liquid nitrogen is well below the freezing point of liquid methane, thus, requiring a controlled liquid nitrogen flow, through the subcooler, to avoid freezing of the LCH_4.

As previously mentioned in conjunction with the LCH_4 ground system storage tanks, the vapor pressure of subcooled LCH_4 will be below atmospheric, which would result in a vacuum inside the tanks. This same condition applies to the aircraft fuel tanks. If subcooled LCH_4 is utilized as aircraft fuel, a suitable pressurant that is as insoluble as possible in LCH_4 is required. Pressurants that have been considered include nitrogen, helium, warm methane, and hydrogen (reference 73).

Nitrogen is undesirable because of its high solubility (about 5 percent by weight in liquid methane subcooled 9.4°C (17°F). This high solubility of nitrogen can create an intolerable weight penalty. Helium is a possible

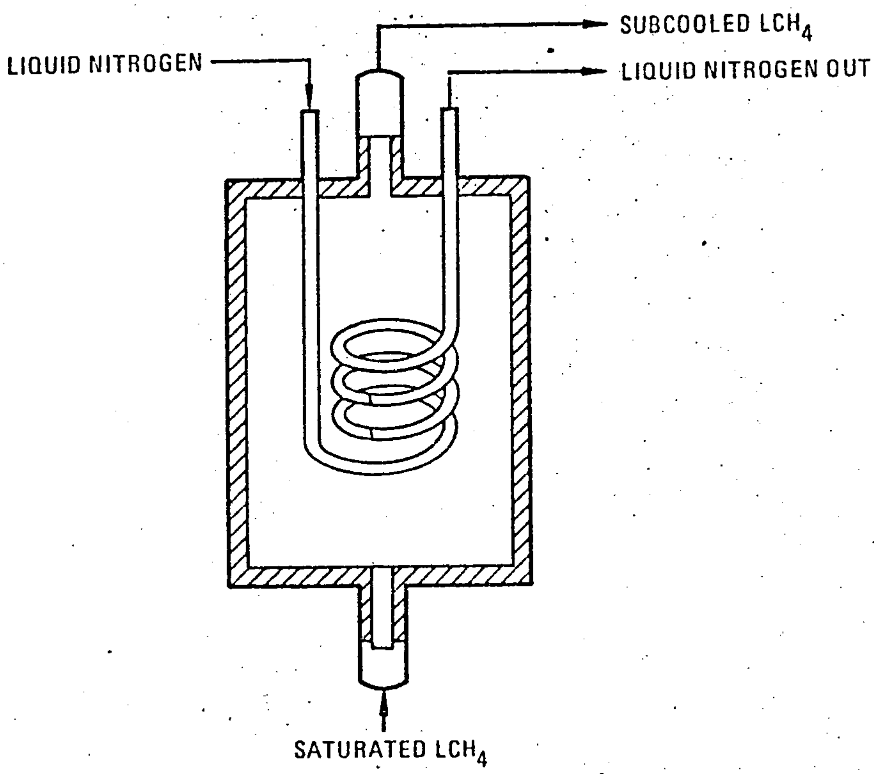

Figure 147. - Liquid N_2 subcooler.

pressurant because its solubility is very low. Warm methane gas is another possibility as a pressurant, but mixing and the subsequent heat transfer from the warm gas to the subcooled liquid fuel might result in the condensation of some of the gas, thereby, causing a rapid reduction in the tank pressure. Hydrogen gas might also be used as pressurant, but is difficult to contain and could present a safety hazard. Of the possibilities mentioned, helium would be the most satisfactory pressurant. If a flexible membrane can be devised to separate the LCH_4 from the pressurizing gas, air (with its moisture and carbon dioxide removed) should be a satisfactory pressurant.

Another method for making use of soluble or condensable pressuring gases is to reduce the area of gas in contact with the liquid methane. This can be achieved either by covering the liquid surface with floating objects, such as balls, or a full tank can be pressurized using a standpipe. These methods will expose only a small area to the pressurizing gas. A detailed discussion of different techniques employed in handling subcooled liquid methane fuel is presented in NASA technical memorandums (references 7, 76, 77, 78, and 79).

While raising the minimum tank pressure reduces the total boil-off, it does not stop the boil-off at altitudes lower than the altitude equivalent of the tank pressure. If it is possible to compensate for the weight penalty incurred in pressurizing the tanks at 101.4 kPa (14.7 psia), the boil-off due to higher amibent pressure reduction, could be eliminated with no initial subcooling. The boil-off that would occur at this point would be the result of only atmospheric frictional heating. A reasonable subcooling (i.e., less than 2.8°C (5°F) of the liquid methane fuel should compensate for this atmospheric frictional heating, so that the boil-off is eliminated over the entire flight.

<u>Gelled LCH_4</u>: The concept of gelling methane has been studied specifically in connection with the use of liquid methane as an aircraft fuel (reference 80). Gelling the LCH_4 can reduce the solubility of pressurant gas in LCH_4 to an extent where nitrogen or air can be used without causing any excessive weight penalities.

Research programs are under way at Aerojet Liquid Rocket Company, Sacramento, California, to determine the suitability of using gelled methane as a fuel for a jet engine. The overall conclusions reached during the course of the Aerojet study are presented below:

1. Gelation of liquid methane with either water or methanol particles provides a satisfactory method to reduce the rate of nitrogen absorption in subcooled liquid methane to an insignificant value. Less than 1.5 weight percent of methanol is sufficient to reduce the nitrogen absorption rate to an insignificant value.
2. The increased specific fuel consumption will not be excessive due to the gelant required.
3. Gelled liquid methane is storable for periods exceeding 100 hours near the normal boiling point of liquid methane. No significant gel structure degradation occurs during this time span.

4. The gels can be transferred through properly designed heat exchangers at comparatively high flow rates 4.5 kg/hr, (10 lb/hr) without clogging by proper selection of the operating conditions. Formation of methane hydrates does not appear to be a problem in the heat exchanger.

Summary of Results: In Section 9.1, the overall objective was to develop the conceptual LCH_4 ground system components. In order to proceed with the analyses, certain input assumptions with regard to boil-off losses in the distribution and storage system were made. As a result of the previous analyses, the actual boil-off losses are now determinable and are used to identify major changes in the conceptual ground system components. In addition, in this summary, the aircraft efficiency factor, which was determined concurrently in the design of the LCH_4 aircraft, is used to identify modifications to the conceptual ground system.

Ground System Boil-Off Losses: There are four sources of boil-off in the conceptual ground system. These are heat gain in the distribution system, heat gain in the storage system, and flash losses due to the pressure difference in the distribution and storage systems as the LCH_4 is circulated from storage through the distribution system and then back to storage, and vapor losses during the filling of the LCH_4 storage tanks from the liquefaction facility.

The temperature rise of the LCH_4 in the distribution system has been calculated as 2.2°C (4°F). (See Section 9.1.3.) Consequently, the maximum exit temperature of the LCH_4 from the distribution system back into storage is -159°C (-255°F). As the operating pressure of the distribution system exceeds the vapor pressure of the LCH_4 throughout the distribution system, boil-off in the distribution system is zero.

Because of the difference in the pressure of the distribution system and the storage system, flash-off of the LCH_4 upon return to storage is expected to occur. The maximum expected flash losses were calculated based on a distribution system discharge pressure of 138 kPa (20 psia) and a storage system pressure of 103 kPa (15 psia). The temperature of the LCH_4 entering storage from the distribution system is -159°C (-255°F). Under these conditions, 0.92 percent of the returning LCH_4 would flash to vapor. During the off-peak aircraft LCH_4 demand period, 0.139 m^3/s (2200 gpm) of LCH_4 are constantly recirculating in each line of the distribution system. Therefore, the total annual quantity of flash vapor produced during the 11-month off-peak period upon return to storage is 31.3 x 10^6 kg/yr (69 million lb/yr). During the peak aircraft LCH_4 demand period of 31 days, each line of the distribution system is operating at 0.278 m^3/s (4400 gpm) for about 6 hours each day and at 0.139 m^3/s (2200 gpm) for 18 hours each day. The resultant flash vapor produced from the distribution/storage return interface during the peak demand period is 3.3 x 10^6 kg (7.3 million lb/yr). During a peak demand hour the quantity of flash vapor produced is 11,440 m^3/hr (404 000 SCF/hr).

Heat gain in the storage system is estimated to result in a maximum boil-off rate of 0.05 percent per day. As the total storage capacity of the ground system is 126 400 m^3 (795 000 bbl) (10.1.2), the total annual boil-off from heat gain in the storage system is 4.85 x 10^6 kg (10.7 million lb/yr) assuming that on the average the storage system is half full. The maximum daily storage system boil-off would be 25,595 kg (58 630 lb) equivalent to 1643 m^3/hr (58 000 SCF/hr).

The quantity of vapor produced upon filling the LCH_4 storage tanks from the liquefaction facility is calculated as 2.34 kg/yr (5.2 million lb/yr) based on the LCH_4 production capacity of 1.62 x 10^6 kg/day (3.58 million lb/day) for 340 days each year (Section 9.1.1), pressure differentials of 13.8 kPa (2 psia) at the storage tank/liquefaction facility interface, and an initial LCH_4 temperature of -159°C (-257°F). The maximum hourly flash vapor produced by filling the storage tanks is therefore 15 000 SCF/hr).

The results of the above calculations are summarized in Table 10-16. Starting with an annual quantity of 519 x 10^6 kg/yr (1144 million lb/yr) of LCH_4 to be loaded into the aircraft fuel tanks and adjusting for vapor losses, the liquefaction facility must produce 2.46 x 10^6 m^3/day (85.8 million SVF/day). The initial assumptions in the analyses of Section 9.1 resulted in an expected liquefaction capacity of 2.41 x 10^6 m^3/day (85 million SCF/day). Consequently, the initial assumptions resulted in an error of less than 1 percent. Therefore, no modifications to the previous analyses are warranted.

The conceptual ground system is depicted in figure 147. The concept is shown with the initial subcooler and cooler. If subcooling is not required, the LCH^4 would simply cycle from storage through distribution and back. Depending on the type of gas feed (natural gas or SNG), products will result from the liquefaction of the feed to pure LCH_4 that can be used as either fuel gas or refrigerant makeup. Boil-off of LCH_4 to CH_4 in the system will be either reliquefied or used as fuel gas depending on the quantity of vent gas relative to the total system fuel gas requirements. (Refer to Section 9.4.) The air separation plant will be required to produce LN_2 for subcooling.

Defueling of an aircraft would be accomplished on an apron near the ground system storage facilities so that the LCH_4 could be placed directly into storage (reference 5). Vent CH_4 from the aircraft during fueling operations will be collected in a vent gas distribution system and will either be reliquefied or used as plant fuel.

9.2 Assessment of the Ground System Operating Procedure

Provided in the following paragraphs is a description of the liquefaction and storage subsystems of the LCH_4 ground system such that personnel requirements can be delineated. This includes a description of the generic ground

TABLE 64. - SUMMARY OF ACTUAL VAPOR LOSSES IN CONCEPTUAL SYSTEM, KG(LB)/YR

Annual Quantity of LCH_4 to be Loaded	519 X 10^6 kg (1144 X 10^6 lb/yr)
Distribution System Losses	
Heat Gain	0
Circulating Return to Storage Flash	
Peak Demand Period	3.3 X 10^6 kg (7.3 X 10^6 lb/yr)
Off-Peak Period	31.3 X 10^6 kg (69.0 X 10^6 lb/yr)
Storage System Losses	
Heat at 0.05%/day	4.85 X 10^6 kg (10.7 X 10^6 lb/yr)
Flash into Storage	2.36 X 10^6 kg (5.2 X 10^6 lb/yr)
Annual Quantity of LCH_4 to be Produced	561 X 10^6 kg (1236.2 X 10^6 lb/yr)
Operating Days of Liquefaction Facility	340 days/yr
Daily Design Capacity of Liquefaction Facility	1.65 X 10^6 kg (3.64 X 10^6 lb/yr)

1.65 X 10^6 kg (3.64 X 10^6 lb/day)= 2.43 X 10^6 m^3 (85.8 X 10^6 SCF/day)

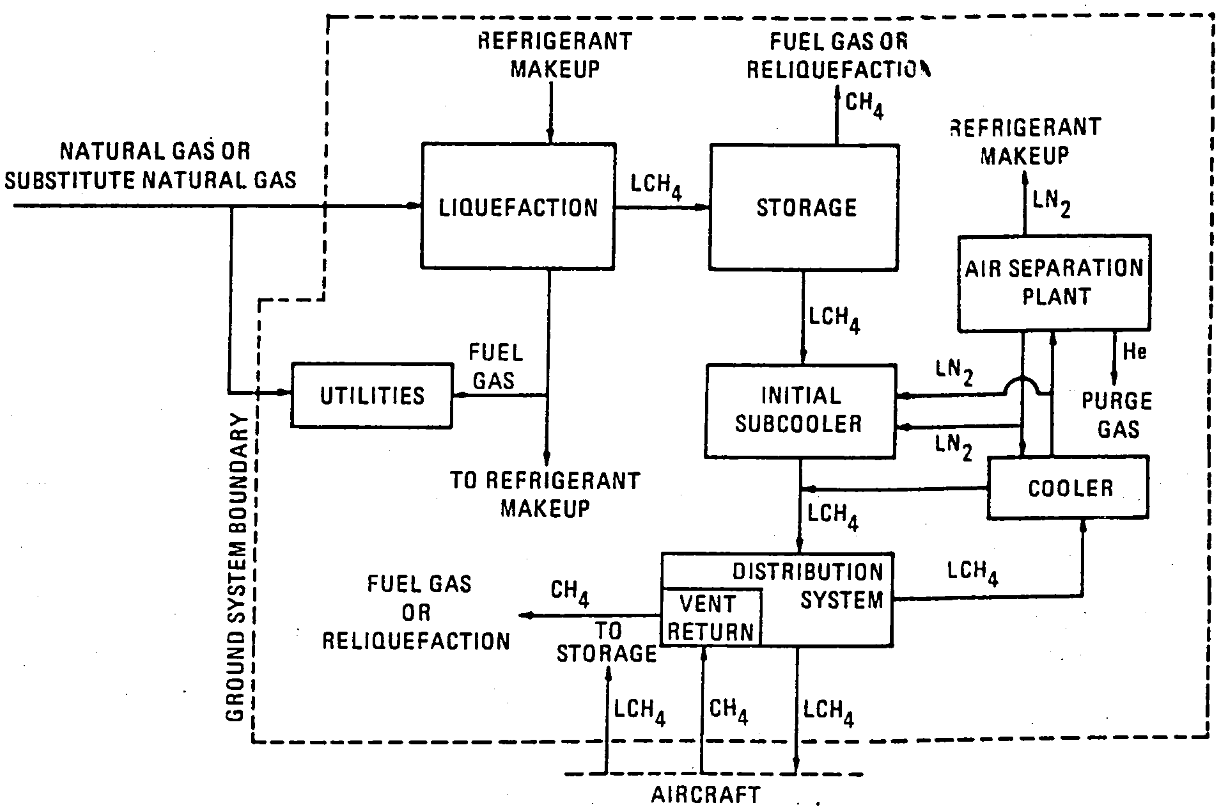

Figure 148. - Conceptual ground system.

system operating procedures based on the work presented in the Introduction. Determination of personnel requirements is based on the similarities and comparative size of the liquefaction and storage subsystems relative to operating LNG facilities.

There are four primary operations of concern within the liquefaction and storage subsystems. They are (1) receipt of gas for liquefaction, (2) liquefaction, (3) storage, and (4) delivery of LCH_4 storage.

Except for the scheduled downtime (25 days each year), the ground system is a continuous operation. Operations would be very similar to those of a baseload LNG facility with the exception of withdrawal of the LCH_4 from storage. Withdrawal of the LCH_4 from storage must be consistent with the aircraft fuel demand schedule. Providing for consistency between the aircraft fuel demand and the LCH_4 storage system will require additional instrumentation at the LCH_4 hydrant fueler pits. That is, the operation of fueling the aircraft must be coordinated with the delivery of LCH_4 from the storage tanks into the ground distribution system. Although normal LNG operations would not require coordination of a discontinuous stochastic event such as aircraft fueling, instrumentation to coordinate the operation is available. It is expected that the coordination would require electronic communication between the LCH_4 fueler valves in the hydrant pits and the storage system pumps and also pressure sensors throughout the distribution system to monitor both a loss of LCH_4 in the system (low-pressure sensor) and also an increase in operating pressure resulting from possible flashing (high-pressure sensor) in the LCH_4 distribution system. Pressure monitoring of LNG distribution systems is typically employed when recirculation of LNG within the in-plant distribution lines is used to avoid cooldown procedures. This type of operation is very similar to that employed in the LCH_4 ground system, where LCH_4 is constantly recirculating through the ground distribution system.

Due to the stochastics of the aircraft fuel demand, it is expected that the LCH_4 ground system would require two persons/shift to monitor fueling operations and instrumentation that coordinates the fueling operations with delivery of LCH_4 from storage.

Typically, a baseload 28.3×10^6 m^3/day (1 billion CF/day) LNG liquefaction facility will employ about 160 persons, including 96 operators, 20 administrators, 32 engineering and maintenance personnel, and 12 supervisors (reference 81). Since 28.3×10^6 m^3/day (1 billion CF/day) facility would typically include four liquefaction trains, the personnel requirements for the LCH_4 ground system are reduced to 25 percent of those for the baseload LNG system. A further reduction would not be warranted because normal operations for a single liquefaction train of 2.41×10^6 m^3/day (85 million SCF/day) are expected to require the same personnel as the operations for a single train of 7.08×10^6 m^3/day (250 million SCF/day). For example, lubricants on the turbomachinery for a single train must be checked on a relatively consistent bases regardless of the size of the train (reference 82).

Consequently, the total personnel requirements for the LCH_4 ground system (excluding those required for the hydrant fueler vehicle operations) are as follows:

Operators	24
Administrators	4
Engineering and Maintenance	8
Supervisors*	4

As the coordination and monitoring of the aircraft fueling operations as previously mentioned would require two additional operators per shift, the total requirements is 48 persons to provide for continuous operation of the ground system.

Operators	32
Administrators	4
Engineering and Maintenance	8
Supervisors	4

Each shift at the facility would comprise 12 persons based on a 44-hour work week and 2 weeks vacation per person.

9.3 Evaluation of the Energy Consumption of the Ground System

The overall energy consumption of the ground system depends on the feedgas composition available for liquefaction and the degree of subcooling required. Further, the energy consumption is also dependent on the inlet feedgas temperature and pressure. Therefore, the method involved first, estimating the energy consumption for the ground system based on a natural gas feed without subcooling; second, estimating the energy consumption for the ground system based on substitute natural gas feed without subcooling; third, estimating the effect of feedgas inlet temperature and pressure on energy consumption; and fourth, estimating the additional energy consumption as a function of degree of subcooling.

9.3.1 Energy consumption of the natural gas feed ground system.- The conceptual gas energy balance of the natural gas, feed-based ground system is presented in figure 153. The liquefaction facility was estimated to require about 3.61×10^{15} J/yr (3.427 trillion Btu/yr) of fuel gas. This is 10 percent greater than the fuel gas requirements for the substitute natural gas feed concept because of the need for a cryogenic distillation column to produce LCH_4 rather than LNG. This quantity of fuel gas can be met from the propane and ethane that would be separated from the methane in the production of LCH_4. After accounting for refrigerant makeup, the total quantity of natural gas that must be supplied as imput to the liquefaction complex to produce the required 519×10^6 kg/yr (1144×10^6 lb/yr of LCH_4 is 38.1×10^{15} J/yr (36.13 trillion Btu/yr). Production of LCH_4 from the natural gas feed will result in an excess quantity of 63.3×10^6 kg/yr (139.6 million lb/yr) of ethane.

*A 25-percent reduction would be three supervisors; however, a minimum of four are needed to provide for continuous operation with about a 44-hour work week per supervisor.

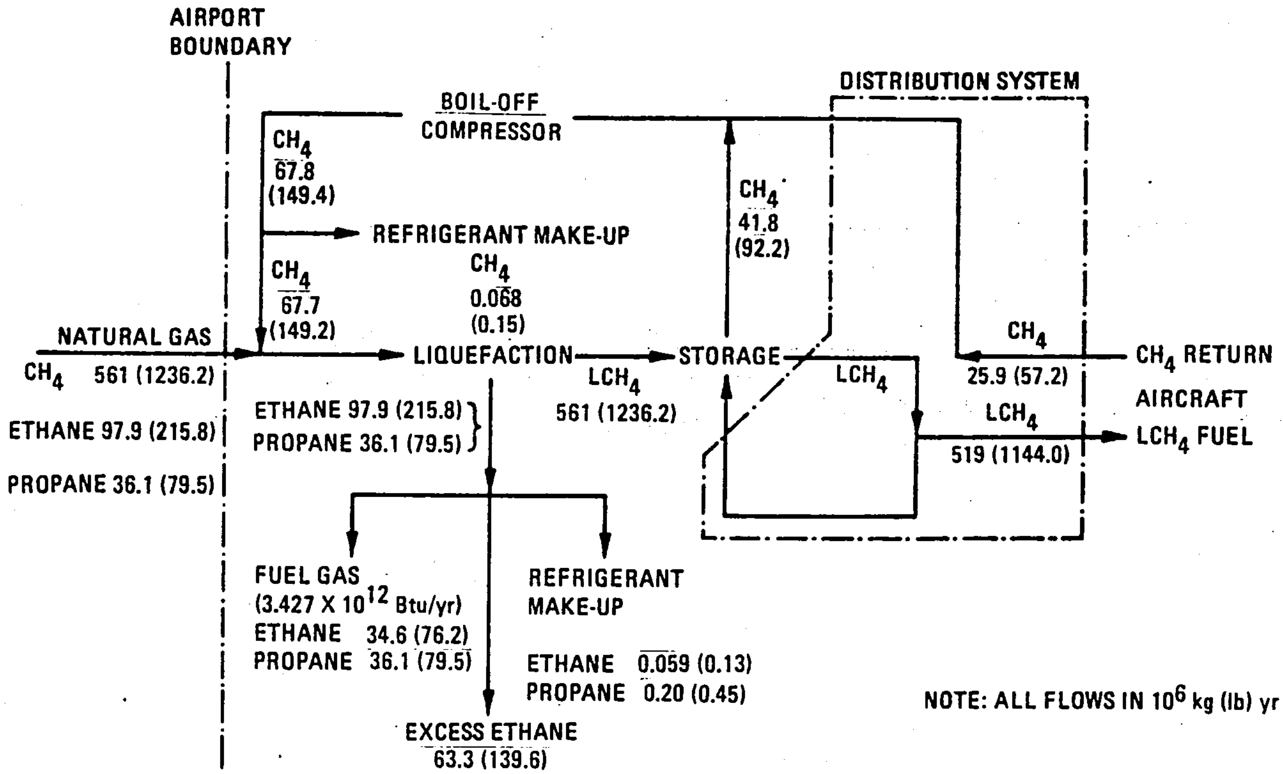

Figure 149. - Natural Gas system energy consumption.

Electricity requirements for this ground system concept are presented in table 67. Total electricity requirements are estimated at 6258 kW. The electricity requirements for the boil-off compressor are based on a 933 kW (1250 hp) compressor/driver that would compress up to 14 160 m^3/hr (500 000 SCF/hr) (the maximum hourly boil-off rate) for reliquefaction (reference 93). However, the compressor/driver would operate at an average annual capacity of 55 percent. The electricity requirements are based on one set of the multi-stage two-speed pumps operating continuously to maintain the circulation rate of 0.139 m^3/s (2200 gpm) in the two LCH_4 distribution lines except for the 6 hours/day that the lines operate at a circulation rate of 0.278 m^3/s (4400 gpm) during the peak month. The pumping requirements for cooling water makeup and water supply are based on cooling water makeup of 0.063 m^3/s (1000 gpm), water makeup of approximately 0.0063 m^3s (100 gpm) for steam generation, and cooling water for lube systems and packing glands at about 0.00473 m^3 (75 gpm). Auxiliary lighting electricity requirements are taken from the previous Lockheed study (reference 5).

9.3.2 Energy consumption of the substitute natural gas feed ground system.- The conceptual gas energy balance of the substitute natural gas feed based ground system is presented in figure 154. The liquefaction facility was estimated to require about 3.44 x 10^{15} J/yr (3.264 trillion Btu/yr) of fuel

TABLE 65. - ESTIMATED ENERGY CONSUMPTION OF LCH_4 GROUND SYSTEM WITH NATURAL GAS FEED*

Feed Gas Requirements, Btu/yr	38.08×10^{12} (36.13×10^{12}) (HHV)
Electricity Requirements, kW	
Boil-Off Compressor	492
Distribution System Pumps	558
Cooling Tower and Water Supply	3860
Road and Exterior Lighting	300
Building Lighting and Space Conditioning	750
Subtotal	5960
Process Contingency (5%)	298
Total	6528

*Based on average daily liquefaction capacity of 1.65×10^6 kg (3.64×10^6) day of LCH_4 and delivery of saturated LCH_4 to the aircraft. No sub-cooling.

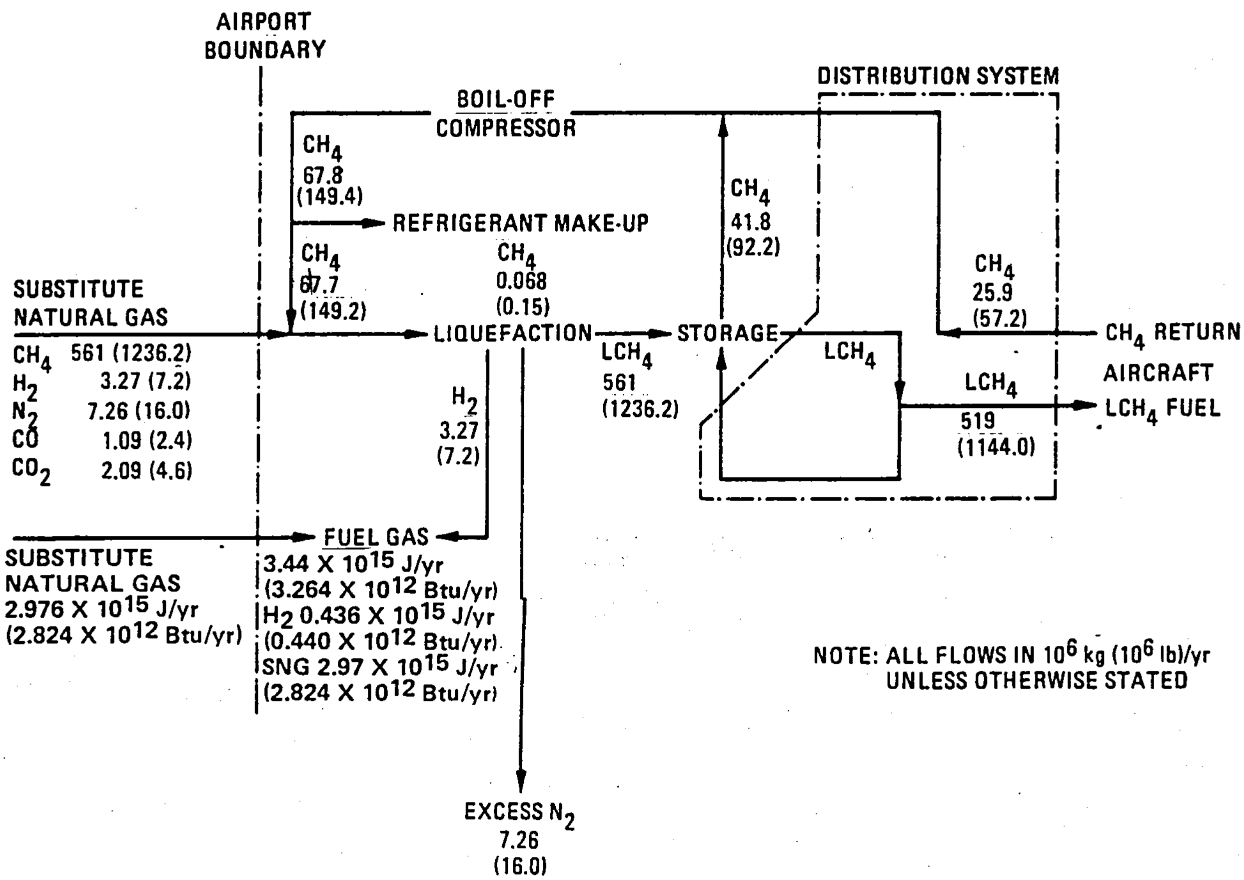

Figure 150. - Substitute natural gas system energy consumption.

gas. Of this quantity, approximately 0.464 x 10^{15} J/yr (0.440 trillion Btu/yr) can be made up from the H_2 that will remain in the vapor phase as the SNG is liquefied to produce LCH_4, due to the difference in the boiling points in H_2 and CH_4. Therefore, an additional 2.98 x 10^{15} J/yr (2.824 trillion Btu/yr) of SNG for fuel gas will be required.

Furthermore, the quantity of SNG for liquefaction is 31.6 x 10^{15} J/yr (29.959 trillion Btu/yr) that is 0.646 x 10^{15} J/yr (0.613 trillion Btu/yr) less than the natural gas feed concept due to the lower heating value of the SNG feedgas and greater mole percentage of CH_4 in the SNG feedgas. Total feedgas requirement for the SNG-based concept is 3.46 x 10^{15} J/yr (3.278 trillion Btu/yr).

Electricity requirements remain unchanged from the natural gas based concept.

9.3.3 Effect of feedgas inlet conditions on fuel gas requirements.- In this study, the inlet temperature of the feedgas is assumed at 18.3°C (65°F) and the inlet pressure is assumed at 3448 kPa (500 psig). The effect of the inlet temperature and pressure in the annual fuel gas requirements of the liquefaction cycle are presented in figure 155. A reduction in the inlet pressure of 40 percent and an increase in temperature to 26.7°C (80°F) would increase the gas requirements by about 6 percent.

9.3.4 Energy consumption as a function of degree of subcooling.- Subcooling the LCH_4 will directly affect the energy consumption of the ground system. The conceptual subcooling system was presented in figure 146. Essentially, the subcooling concept will require two subcoolers; one for initial subcooling and one for maintaining the subcooled LCH_4 that is circulating in the distribution system at the subcooled temperature i.e., a cooler to compensate for the 2.2°C (4°) ΔT in the LCH_4 as it circulates.

Conceptually, both of these subcoolers would be LN_2/LCH_4 heat exchangers. Makeup quantities of LN_2 would be supplied from an air separation plant including an N_2 liquefier. Based on the heat capacities of LCH_4 and LN_2 and an assumed exchanger efficiency of 80 percent, the quantity of LN_2 that would have to be supplied to the initial heat exchanger for an LCH_4 flow rate of 519 x 10^6 kg/yr (1144 million lb/yr) is presented in figure 156. As shown, the total quantity of LN_2 required for each 2.8°C (5°F) of subcooling is about 34 x 10^6 kg (75 million lb). In addition to the LN_2 required for the initial subcooler, the coolant required to compensate for the 2.2°C (4°) ΔT in the distribution lines would require about 27.2 x 10^6 kg (60 million lb of LN_2). The total quantity of LCH_4 to be supplied to the aircraft will circulate through the distribution system approximately 7.2 times each year. Consequently, the air separation plant and N_2 liquefier must produce approximately 16.6 x 10^6 kg/yr (36.7 million lb/yr) of LN_2 for coolant makeup. The total quantity, including 2.2°C (4°) ΔT coolant, of LN_2 that must be supplied from the air separation plant and N_2 liquefier each year is presented in figure 157.

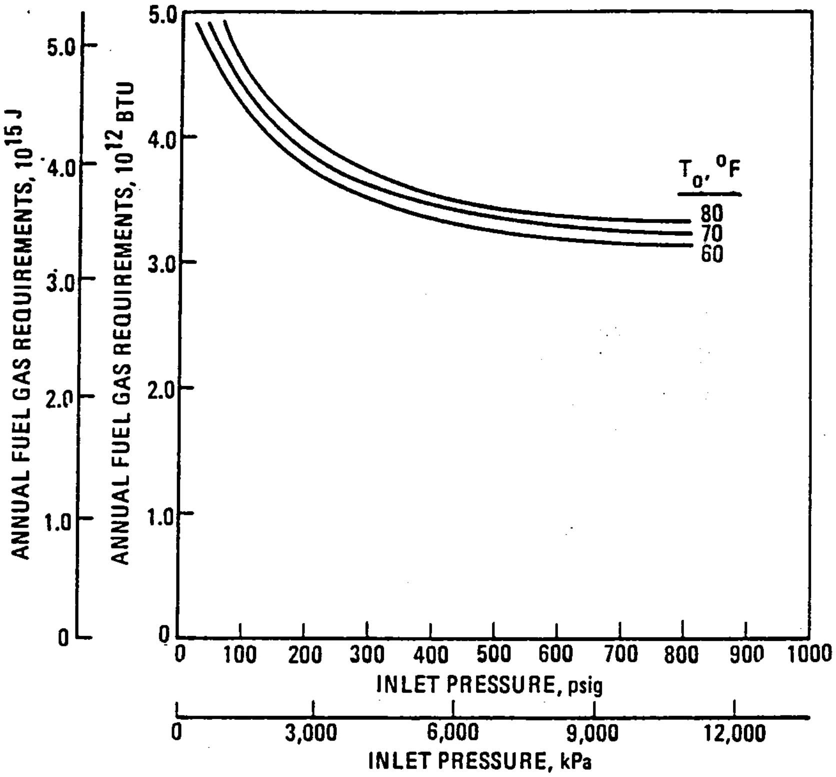

Figure 151. - Effect of feedgas temperature and pressure on fuel-gas requirements.

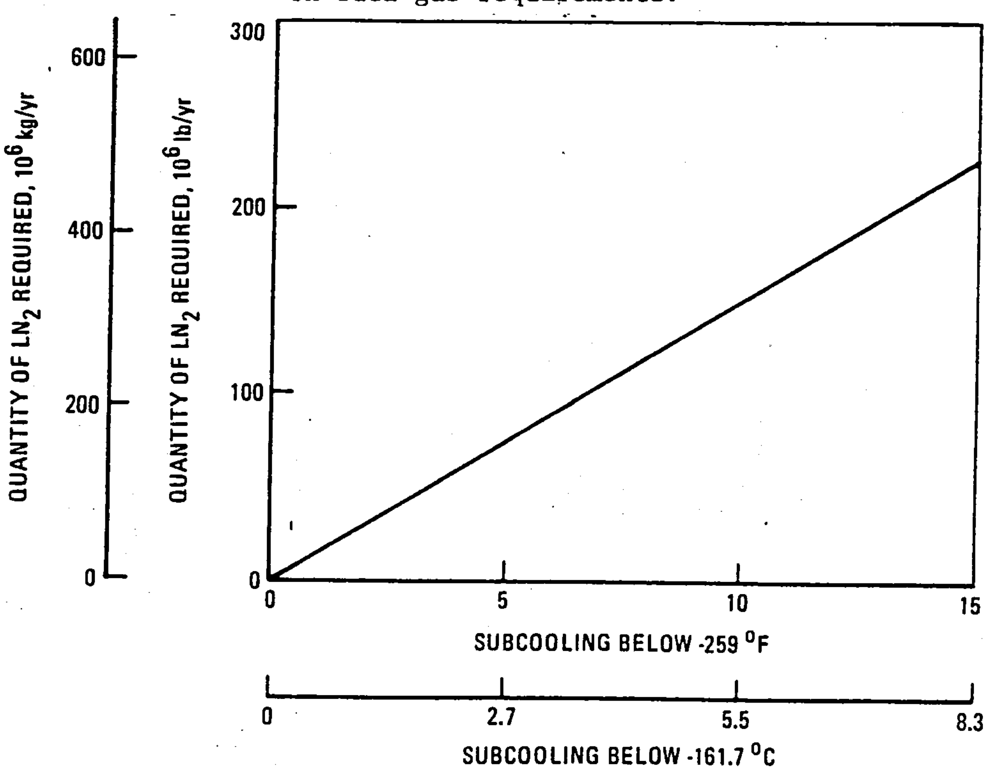

Figure 152. - Quantity of LN_2 required for LCH_4 subcooling.

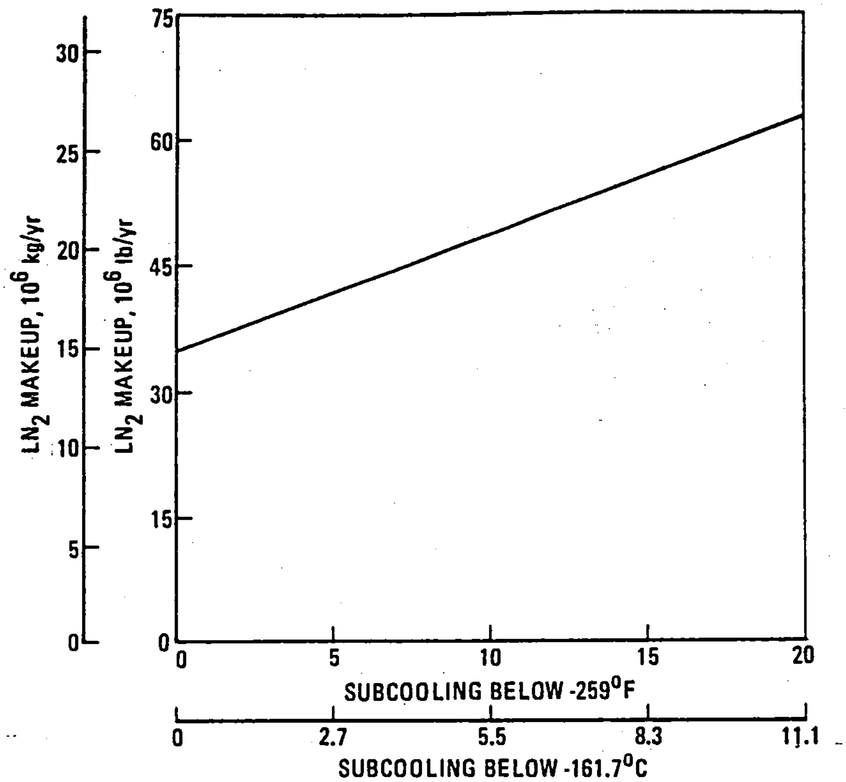

Figure 153. - Quantity of makeup LN_2 required for LCH_4 subcooling.

TABLE 66. - EQUIPMENT REQUIREMENTS FOR SUBCOOLING CONCEPT

Equipment	Capacity	
	Distribution System Cooler 2.2°C (4° ΔT)	Initial Subcooler Capacity 2.8°C (5F°) Subcooling
Air Separation Cold Box, m^3 (SCF)hr	56 000	10 000
Forecooling Refrigeration Unit, kW	645	108
N_2 Recycle Compressor, kW	3 889	648
N_2 Centrifugal Feed Compressor, kW	457	76
Air Plant Centrifugal Compressor, kW	269	45
Cooling Water Makeup Pumps, kW	521	87
Cooling Water Makeup, $m^{3/s}$ (gpm)	0.0119 (189)	0.002 (32)

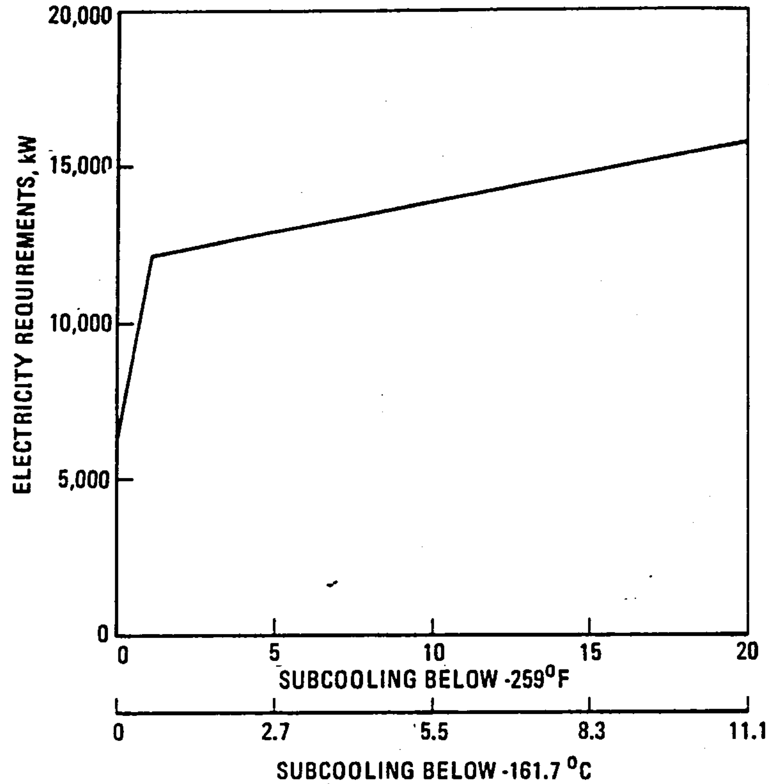

Figure 154. - Ground system electricity requirement as a function of subcooling.

Based on the air separation plant and N_2 liquefier concept presented in the previous Lockheed study (reference 5), subcooling of the LCH_4 would require the additional equipment presented in table 68.

The total electricity energy requirements as a function of degree of subcooling are presented in figure 158. The electricity requirements in figure 158 also include the balance of plant requirements of 6258 kW.

These results show that the annual fuel gas requirements for LCH_4 ground system depend on the composition of the feedgas for liquefaction. For example, the natural gas feed requirements are 38.1×10^{12} kJ (36.13 trillion Btu/yr) (HHV) whereas the substitute natural gas feed requirements are 34.56×10^{12} kJ (32.78 trillion Btu/yr).

Basic electricity requirements for the ground system are 6258 kW with no subcooling of the LCH_4. However, subcooling of the LCH_4 by 11.1°C (20°F) would increase electricity requirements to almost 16,000 kW.

9.4 Estimate of the Capital and Operating Costs of the Ground System

The capital and annual operating costs of the LCH_4 ground system are dependent on the degree of subcooling required, the feedgas composition, and the cost of the feedgas. Therefore, the methodology employed in this task was first, to estimate the total plant investment, including working capital, for the ground system with no subcooling; second, to estimate the total plant investment as a function of degree of subcooling and feedgas cost; third, to estimate the total operating cost of the natural-gas-based ground system and the substitute-natural-gas-based ground system with no subcooling; and fourth, to estimate the total annual operating cost of the two feedgas-based ground systems as a function of degree of subcooling and feedgas cost.

In addition, because the economic analysis to determine the most cost-effective number of liquefaction trains to be employed in the ground system concept required input information from Section 9.1 and 9.2, the trade-off analysis is documented here.

9.4.1 Economic trade-off analysis (number of liquefaction trains).- Based on the information of 9.1, the major components of a propane-precooled liquefaction facility, i.e., a single train at 2.41×10^6 m^3/day (85 million SCF/day) design capacity, will result in a direct cost of $11 876 000. These costs include $6.5 million for the utility area. The direct cost of the major components of the liquefaction train are, therefore, $5 376 000. The direct cost of the major components is, however, only about 20 percent of the total direct cost of the liquefaction train. The other 80 percent includes piping and valves, control equipment, design of the cycle, and designer's burden and profit. Whereas the direct cost of the major components is the direct cost of the component manufacturers, the direct cost of the actual liquefaction plant will be the direct cost from the designer of the cycle. Similarly, the direct costs of the utility area are the direct costs of major components and only account for about 25 percent of the total direct cost of the utility area (reference 94 and 95).

To estimate the cost of the liquefaction train as a function of train design capacity, a power factor of 0.9 was utilized. This factor is based on the actual costs of liquefaction trains ranging in design capacity from 2.83×10^6 m^3/day (100 million SCF/day) to 7.79×10^6 m^3/day (275 million SCF/day) (references 53 and 96). As previously mentioned, train capacities of less than 2.83×10^6 m^3/day (100 million SCF/day) are not being designed for baseload LNG operations. The same power factor is also applicable to the utility area costs. The total direct cost per liquefaction train is presented in figure 159.

Utilizing the costs as presented in figure 159, and direct costs for storage of $138/$m^3$ ($22/bbl) (direct cost from the designer and constructor), the total direct cost of the liquefaction and storage facilities for the SFO application was calculated as a function of liquefaction train capacity. The results, which are presented in figure 160, show that the single train

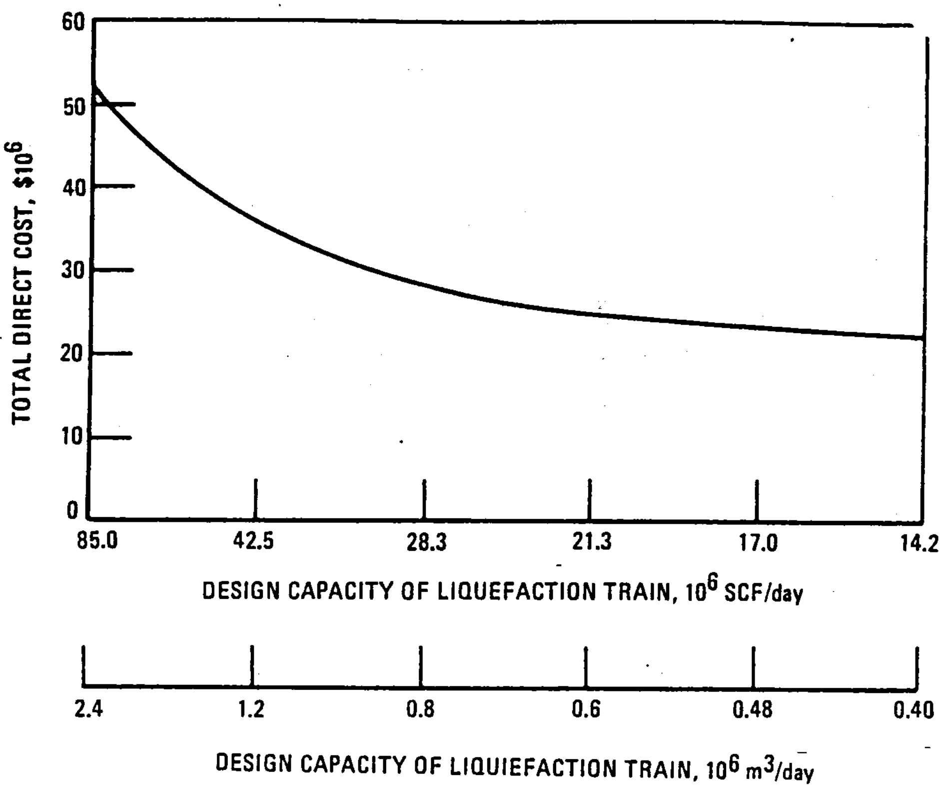

Figure 155. - Liquefaction train direct cost vs. design capacity.

concept, 2.41 x 10^6 m^3/day one train at 85.0 million SCF/day is the least-cost alternative relative to the multiple trains concept. Furthermore, the single train concept offers the same degree of reliability as the multiple train concept in that storage capacity is increased as train size increases to maintain a constant system reliability as calculated in 9.2.

9.4.2 Capital costs.- Unless otherwise specified, cost assumptions are as presented in Table 69.

Utilizing information from Section 9.1, the major equipment and components of the LCH_4 ground system are summarized in Table 70. This table does not include equipment requirements for subcooling the LCH_4, which were presented in Table 68.

The total capital investment of the LCH_4 ground system, exclusive of capital required for subcooling the LCH_4, is estimated at $104.5 million. See Table 71. Of this total, about $4 million is attributable to the net receivables of product LCH_4 (valued at $3.00/million Btu) included in the working capital requirements. If the product LCH_4 is doubled in value, the total capital investment for the ground system increases by 3.8 percent.

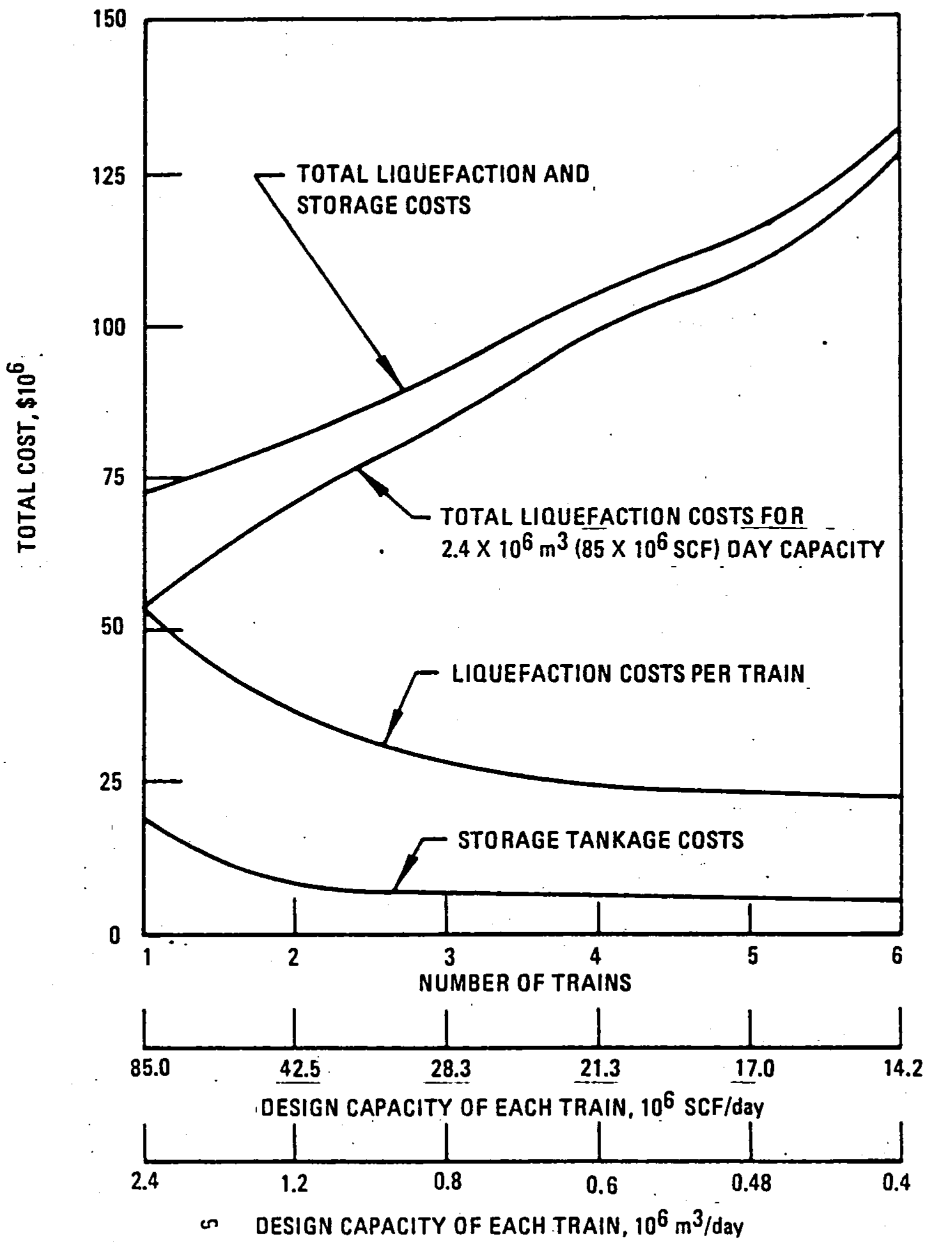

Figure 156. - Total cost of liquefaction and storage as a function of number of liquefaction trains.

TABLE 67. - COST ASSUMPTION, LCH_4 GROUND SYSTEM

- Investment includes all equipment costs except LCH_4 fueler/defueler trucks, fuel/defuel apron, utility right-of-way and pipeline to airport.
- Land assumed available at no cost.
- Cost of site preparation is included in LCH_4 liquefaction facility costs.
- Costs are 1976 dollars.
- Average LCH_4 operating capacity is 1.65×10^6 kg (3.64 million lb) day
- Liquefaction plant operates 340 days per year.
- Electricity costs are $0.025/kWhr.
- Cooling water makeup costs are $\$0.0925/m^3$ ($0.35/1000 gal.)
- Potable water makeup costs are $\$0.0145/m^3$ ($0.55/1000) gal.
- Propane costs are $0.13/kg ($0.059/lb) (Reference 96).
- Ethane costs are $0.14/kg ($0.064/lb) (Reference 96).
- Operating labor rate is $7.00/hr.
- Administrative labor rate is $7.50/hr.
- Engineering and maintenance labor rate is $11.00/hr.
- Supervisory labor rate is $30 000/yr.
- Overhead costs are 60% of labor plus supervision.
- Operating supplies are 30% of operating labor.
- Maintenance supplies are 1.5% of total plant investment.
- Taxes and insurance are 1.5% of total plant investment.

If the LCH_4 delivered to the aircraft is required to be subcooled, the total investment for the ground system will increase due to the need for an air separation plant to supply the requisite LN_2 makeup as calculated in Task 4 (figure 157). The estimated direct capital cost of the additional equipment required for subcooling the LCH_4 is presented in figure 161 and was estimated based on the air separation plant costs of the previous Lockheed study. The discontinuity in the graph, i.e., the substantial direct cost at 0.55^oC (1^oF) subcooling, is associated with the initial requirements for a distrubtion system cooler to compensate for the 2.2^oC (4^o) ΔT in the distrubution system.

The total capital investment for the LCH_4 ground system as a function of degree of subcooling and as a function of feedgas cost, which affects net receivables. is presented in figure 162. At a feedgas cost of 2.85/GJ ($3.00/million Btu), the total capital investment for the LCH_4 ground system ranges from $104.5 million to $140.2 million depending on the degree of subcooling required. At a feedgas cost of $5.69/GJ ($6.00/million Btu), the total capital investment ranges from $108.5 million to $144.2 million.

TABLE 68. - EQUIPMENT LIST OF MAJOR ITEMS: LCH_4 GROUND SYSTEM

Item	No. Required	Description
1	1	Elliot 60M6 8 579 kW (11 500 hp) centrifugal compressor, LCH_4 cycle 4.9 X 9.1 X 2.4 m (16 ft X 30 ft X 8 ft)
2	1	Elliot 60M5 10 670 kW (14 300 hp) centrifugal compressor, LCH_4 cycle 4.9 X 9.1 X 2.4 m (16 ft X 30 ft X 8 ft)
3	1	Elliot 38MB6 8 579 kW (11 500 hp) centrifugal compressor, LCH_4 cycle 4.6 X 7.62 X 3.1 m (15 ft X 25 ft X 10 ft)
4	2	Elliot 2SNV8DF condensing steam turbine, LCH_4 cycle 4.9 X 9.1 X 2.7 m (16 ft X 30 ft X 9 ft)
5	1	Elliot SRV8DF condensing steam turbine, LCH_4 cycle 4.6 X 7.62 X 2.4 m (15 ft X 25 ft X 8 ft)
6	1	LCH_4 liquefied cold box, LCH_4 capacity 3.66 X 30.5 m (12 ft diameter X 100 ft)
7	3	LCH_4 storage tank (265 000 API bbl) capacity 57.9 X 30.5 m (190 ft diameter X 100 ft)
8	2	4-stage, two-speed, cryogenic pump
9	4877 m (16 000 feet)	9% nickel steel, 25.4 Cm (10-inch diameter) LCH_4 distribution pipe
10	330	Expansion bellows for distribution system
11	1	Cooling tower, 2.8 m^3/s (45 000 gpm) 25 X 53 X 18 m (82 ft X 175 ft X 60 ft)
12	1	Boil-off compressor, 236 m^3/s (500 000 SCF) hr, 895 kW (1200 hp) 3.05 X 4.57 X 1.83 m (10 ft X 15 ft X 6 ft)
13	1	Maintenance building, 1394 m^2 (15 000 ft^2) 22.9 X 61 X 7.6 m (75 ft X 200 ft X 25 ft)
14	1	Control room (1394 m^2) (22.9 X 61 X 7.6 m) (75 ft X 200 ft X 25 ft)
15	1	Office building, (502 m^2) (18.3 X 27.4 X 4.6 m) (5400 ft^2) (60 ft X 90 ft X 15 ft)
16	1	Electrical substation and switchgear center, 28 000 kW (30.5 X 71.9 X 7.6 m) (100 ft X 235 ft X 25 ft)
17	1	Utility area (i.e., steam boilers)

9.4.3 Operating costs.- Unless otherwise specified, cost assumptions are as presented in table 69.

Based on the analyses of Section 9.1, 9.2 and 9.4, the annual operating costs for the natural gas feed-based LCH_4 ground system are $106.6 million without any subcooling (table 72). Refrigerant makeup and fuel gas for the natural gas based ground system are extracted from the natural gas feedstock such that additional refrigerant makeup or fuel gas is not required (figure 163). Although the substitute natural gas based system requires less feedstock than the natural-gas-based system due to the greater mole percentage of CH_4 in the SNG feedgas, refrigerant makeup and addtional fuel gas must be purchased. The annual operating cost of the SNG-based ground system with no subcooling is estimated at $105.5 million (Table 73).

TABLE 69. - EQUIPMENT LIST OF MAJOR ITEMS: LCH_4 GROUND SYSTEM

Component	Total Direct Cost (1976 \$), \$10[6]
Liquefaction Facility(1)	52.4
Storage Facilities	21.4
Distribution System(2)	11.2
Total Plant Investment	85.0
Interest During Construction(3)	15.3
Working Capital(4)	4.2
Total Capital Investment	104.5

Notes:

(1) Includes liquefaction train, utility area, maintenance, and control buildings and cooling tower.

(2) Includes piping, valves, pumps, bellows, boil-off compressor, trench, and hydrant pits.

(3) At 12% interest rate on total plant investment and a 2-year construction period.

(4) Sum of 1) materials and supplies at 0.9% of total plant investment plus 2) net receivables of product LCH_4 at 1/24 of annual delivered production at \$3.00/million Btu (HHV).

The total annual operating costs of the LCH_4 ground systems as a function of degree of subcooling and feedgas cost are presented in figure 163. The total annual operating costs of the natural gas feedstock-based ground system are increasingly higher at each level of feedgas cost due to the increased quantity of natural gas required to produce the required LCH_4 relative to the quantity of SNG required.

9.4.4 Results.- The results show that the total investment for the LCH_4 ground system ranges from \$104.5 million to \$144.2 million, depending on the cost of the feedgas, which affects net receivables included in working capital, and the degree of subcooling required prior to delivery of the LCH_4 to the aircraft. The total annual operating costs of the ground system range from \$105.5 million to \$329.0 million, depending on the feedgas composition, the cost of the feedgas, and the degree of subcooling required.

9.4.5 Additional costs for storing, distributing, and fueling of aircraft with LH_2, LCH_4 and Jet A.- The net cost of storing, distributing and loading fuel into the aircraft has been estimated for LH_2 and LCH_4. The data for Jet A has been obtained from the actual operating experience of Lockheed Air Terminal, Inc. (LAT) at the San Francisco Airport.

The additional or net cost is defined as the annual operating cost to perform the storing, distributing and loading functions excluding the capital cost of the basic liquefaction plant and also excluding the feed gas for liquefaction. In the case of LCH_4 the impact of feed gas on capital cost is illustrated in figure 162.

Beginning with LCH_4, the method used was to derive the capital investment costs from table 71. Working capital and interest costs were apportioned on a prorata basis according to the cost of the major elements constructed, liquefaction, storage and distribution. Operating costs were derived by the Institute of Gas Technology from table 73 and include labor, operating and maintenance, electricity and fueling vehicles.

The results for LCH_4 are:

LCH_4 Costs - 10^6 dollar

	Capital Investment	Annual Operating Cost	$\frac{\text{Operating Cost}}{\text{Capital Invest}}$,%
Storage	26.3	1.13	4.2
Distribution	13.8	2.74	19.8
TOTAL	40.1	3.87	

For LH_2 the premise is taken that the percentage relationship between operating and capital cost, i.e., 4.2% and 19.8%, for storage and distribution of liquid methane is also a valid relationship between LH_2 operating costs and capital investment for storage and distribution if both facilities are located at the same airport (with the same distances involved). That is the case here since both were sited at SFO. At the same time it should be pointed out that the total capital investment for the two complete facilities is greatly different, \$340.4 million for LH_2 (reference 5) compared with \$104.5 million for LCH_4, (table 71).

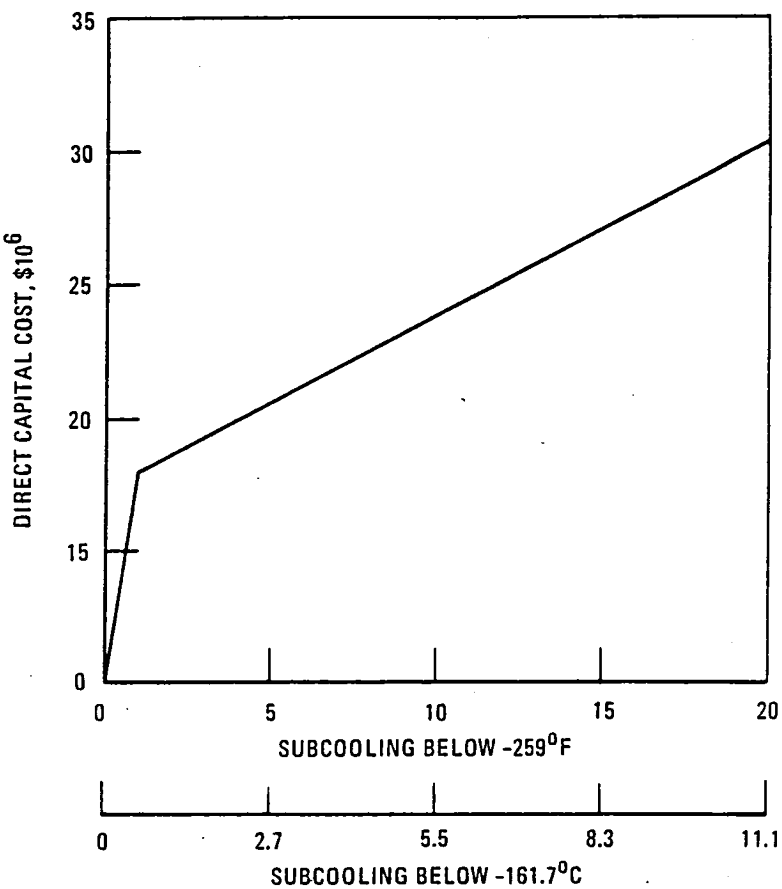

Figure 157. - Air separation plant and subcooler direct cost as a function of degree of subcooling.

The results for LH_2 using the percentages shown above are:

LH_2 COSTS - 10^6 DOLLAR

	Capital Investment	Annual Operating Cost	$\frac{\text{Operating Cost}}{\text{Capital Invest}}$, %
Storage	77.0	3.23	4.2
Distribution	31.8	6.20	19.8
TOTAL	108.8	9.43	

Comparable costs for Jet A as obtained from Lockheed Air Terminal, Inc. for SFO are:

Storage	0.0045	cents/gallon
Distribution	0.5	cents/gallon
Total (into aircraft)	0.5045	cents/gallon

Converting to a common base figure, dollars per gigajoule, using the annual quantity of methane to be loaded, table 50, and of hydrogen, reference 5, the results are:

LH_2 $$\frac{\$9.43 \times 10^6}{421.6 \times 10^6 \text{ lbs}} = 0.0224 \text{ \$/lb or } 0.41 \text{ \$/GJ}$$

LCH_4 $$\frac{\$3.87 \times 10^6}{1012 \times 10^6 \text{ lbs}} = \; = 0.00382 \text{ \$/lb or } 0.168 \text{ \$/GJ}$$

Jet A $$\frac{0.005045 \text{ \$/gal}}{6.90 \text{ lb/gal}} = 0.00073 \text{ \$/lb or } 0.038 \text{ \$/GJ}$$

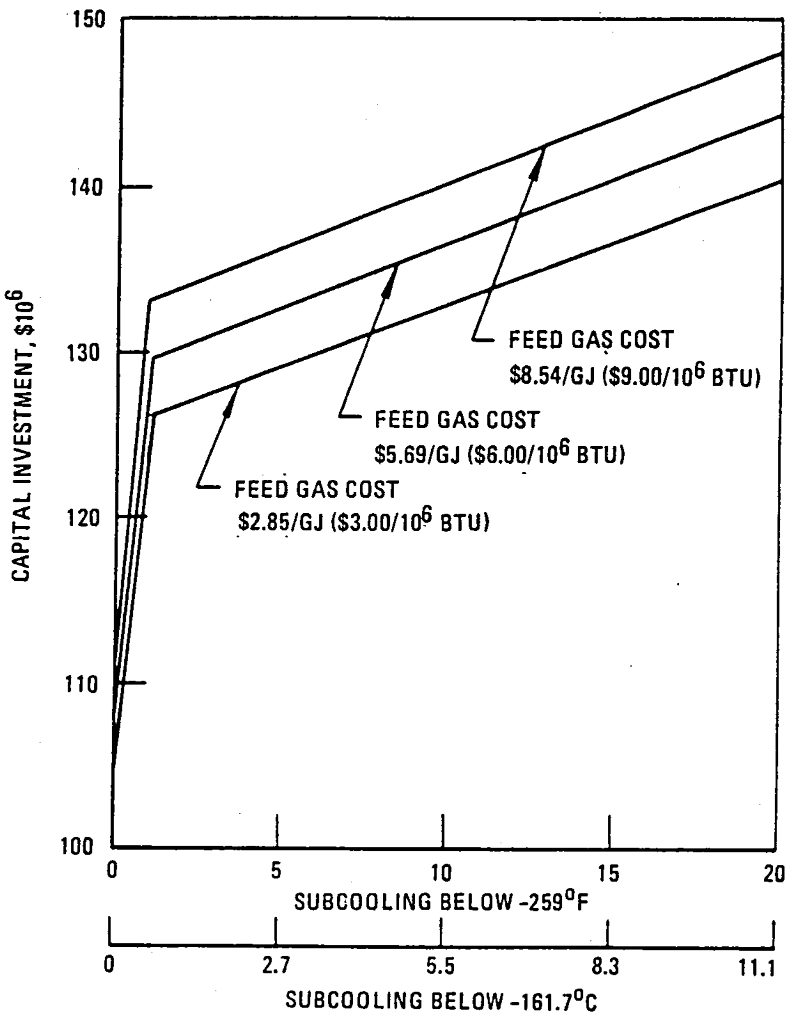

Figure 158. - Total capital investment as a function of degree of subcooling and feedgas cost.

TABLE 70. - ANNUAL OPERATING COSTS, LCH_4 GROUND SYSTEM, NATURAL GASFEED, NO SUBCOOLING

	Cost, $
Raw Materials	
Feedstock (3.613×10^{13} Btu/yr at $3.00/$10^6$ Btu)	108 390 000
Chemicals	
Refrigerant Makeup	
Propane	0
Ethane	0
Other	
Dessicants, absorbents, and catalysts	1 000 000
Utilities	
Fuel Gas	0
Electricity, 6258 kW	1 370 502
Cooling Water Makeup, 1000 gpm	171 360
Potable Water, 25 000 gal/day	3 194
Labor	
Operating Labor, 32 persons	490 560
Supervision, 4 persons	120 000
Administrative, 4 persons	65 700
Engineering and Maintenance, 8 persons	192 720
Administration and Overhead	481 968
Supplies	
Operating	147 168
Maintenance	1 567 500
Taxes and Insurance	1 567 500
Total Annual Operating Cost	115 568 172
Credit for Excess Ethane*	-8 934 400
Net Total Annual Operating Cost	106 633 772

*Taken at 20% of the market value of ethane.

TABLE 71. - ANNUAL OPERATING COSTS, LCH_4 GROUND SYSTEM, SUBSTITUTE NATURAL GASFEED, NO SUBCOOLING

	Cost, $
Raw Materials	
Feedstock (2.996×10^{13} Btu/yr at $3.00/$10^6$ Btu)	89 877 000
Chemicals	
Refrigerant Makeup	
Propane	26 550
Ethane	8 320
Other	
Dessicants, absorbents, and catalysts	1 000 000
Utilities	
Fuel Gas, 2.824×10^{12} Btu/yr	8 472 000
Electricity, 6258 kW	1 370 502
Cooling Water Makeup, 1000 gpm	171 360
Potable Water, 25 000 gal/day	3 194
Labor	
Operating Labor, 32 persons	490 560
Supervision, 4 persons	120 000
Administrative, 4 persons	65 700
Engineering and Maintenance, 8 persons	192 720
Administrative and Overhead	481 968
Supplies	
Operating	147 168
Maintenance	1 567 500
Taxes and Insurance	1 567 500
Total Annual Operating Costs	105 562 042

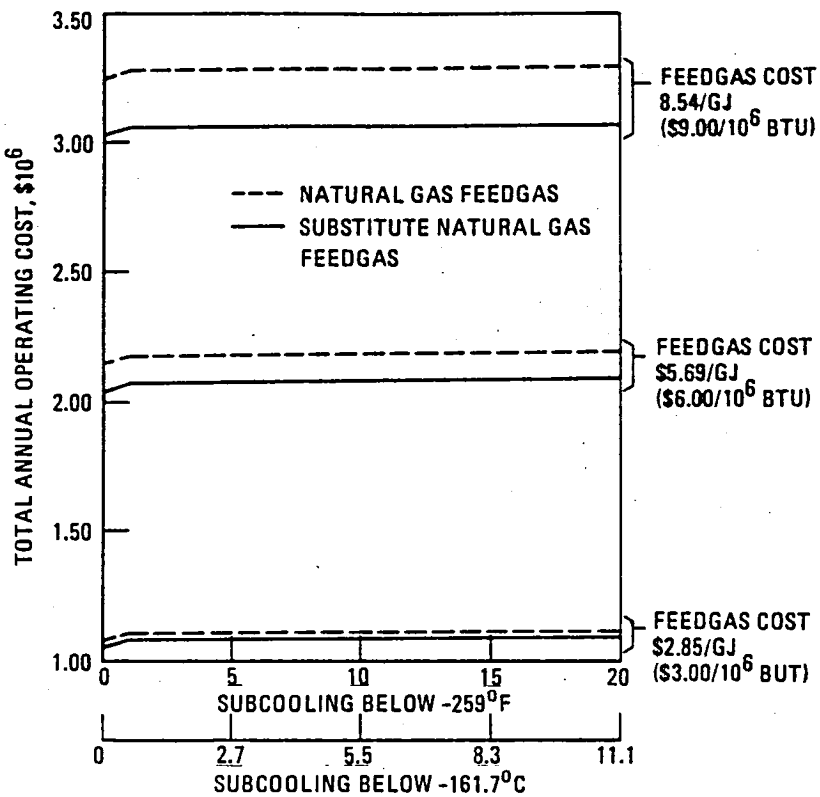

Figure 159. - Total annual operating cost of ground system as a function of feedgas cost and subcooling.

9.5 Evaluation of the Relative Safety of the LCH_4 Ground System

Provided in the following paragraphs is an assessment of the safety of LCH_4 and its associated ground system requirements relative to LH_2. To accomplish this, a comparison of the physical properties of LCH_4 and LH_2, a comparison of the combustion-related properties, and a summary of the relative hazards of LCH_4 and LH_2 are provided. In addition, the requirements of the NFPA Standard 59A were reviewed to identify particular modifications required for the LCH_4 ground system. The spacing requirements of NFPA 59A were examined to determine compliance with spacing requirements for this application. Because safety has become a controversial issue in the LNG industry, the most stringent recommendations for LNG facility siting were also reviewed to identify possible future changes in siting regulations that could affect the siting of an LCH_4 facility within an airport. Federal legislation introduced in Congress that could also affect the utilization of LCH_4 as aircraft fuel was also examined. Finally, because of the controversy concerning LNG, the operating history of the LNG industry was reviewed.

9.5.1 Physical properties. - Table 65 compares the physical properties of methane and hydrogen. Values for hydrogen are based on the para form (reference 83). It is difficult to weigh the contributions to a hazard of each property since the effect on safety is related to the actual accident situation occurring.

One of the physical parameters that affects safety is vapor or gaseous density. Both LCH_4 and LH_2 vapors and gases are lighter than air under most conditions. Specific gravity as a function of temperature is shown for methane in figure 149 and for hydrogen in figure 150. Methane is less dense than ambient air at methane temperatures above -108°C (-162°F). Hydrogen is less dense than air at temperatures above -251°C (-420°F). When vapors or gases are denser than air, they tend to layer, or settle near the ground. Under these conditions, vapors or gases can form flammable mixtures with air extending over a considerable distance. The vapors of many hydrocarbon fuels are denser than air and would be expected to layer significantly; flammable mixtures of fuel and air could exist a considerable distance from a spill. For both methane and hydrogen this phenomenon is less likely to occur since the vapors are quickly warmed to near ambient temperature where gas densities are much less than air, and the gases can rise, diffuse, and disperse. As may be observed by comparing figures 149 and 150, layering will be far less extensive with LH_2 than with LCH_4.

TABLE 72. - PHYSICAL PROPERTIES OF METHANE AND HYDROGEN

Property	Methane	Hydrogen
Molecular Weight	16.04	2.02
Normal Boiling Point (NBP), °C (°F)	-162 (-259)	-253 (-423)
Critical Temperature, °C (°F)	-82.8 (-117)	-240 (-400)
Critical Pressure, kPa (psia)	4599 (667)	1296 (188)
Density of Liquid at NBP, kg/m^3 (lb/gal)	423 (3.53)	70.8 (0.591)
Specific Gravity of Liquid (Water = 1.0)	0.44	0.07
Density of Vapor at NBP, kg/m^3 (lb/ft^3)	1.83 (0.114)	1.34 (0.0837)
Specific Gravity of Vapor (Air at 60°F = 1.0)	1.5	1.1
Density of Gas, kg/m^3 (lb/SCF)	0.642 (0.0401)	0.0826 (0.00516)
Specific Gravity of Gas (Air = 1.0)	0.53	0.068
Diffusion Velocity in Air, m/s (ft/s)	(<0.017)	(0.066)
Buoyant Velocity in Air, m/s (ft/s)	0.79 to 6.1 (2.6 to 20)	1.19 to 9.14 (3.9 to 30)
Heat of Vaporization at NBP, kJ/kg (Btu/lb)	510 (219.4)	446 (191.7)
Toxicity	simple asphyxiant	simple asphyxiant

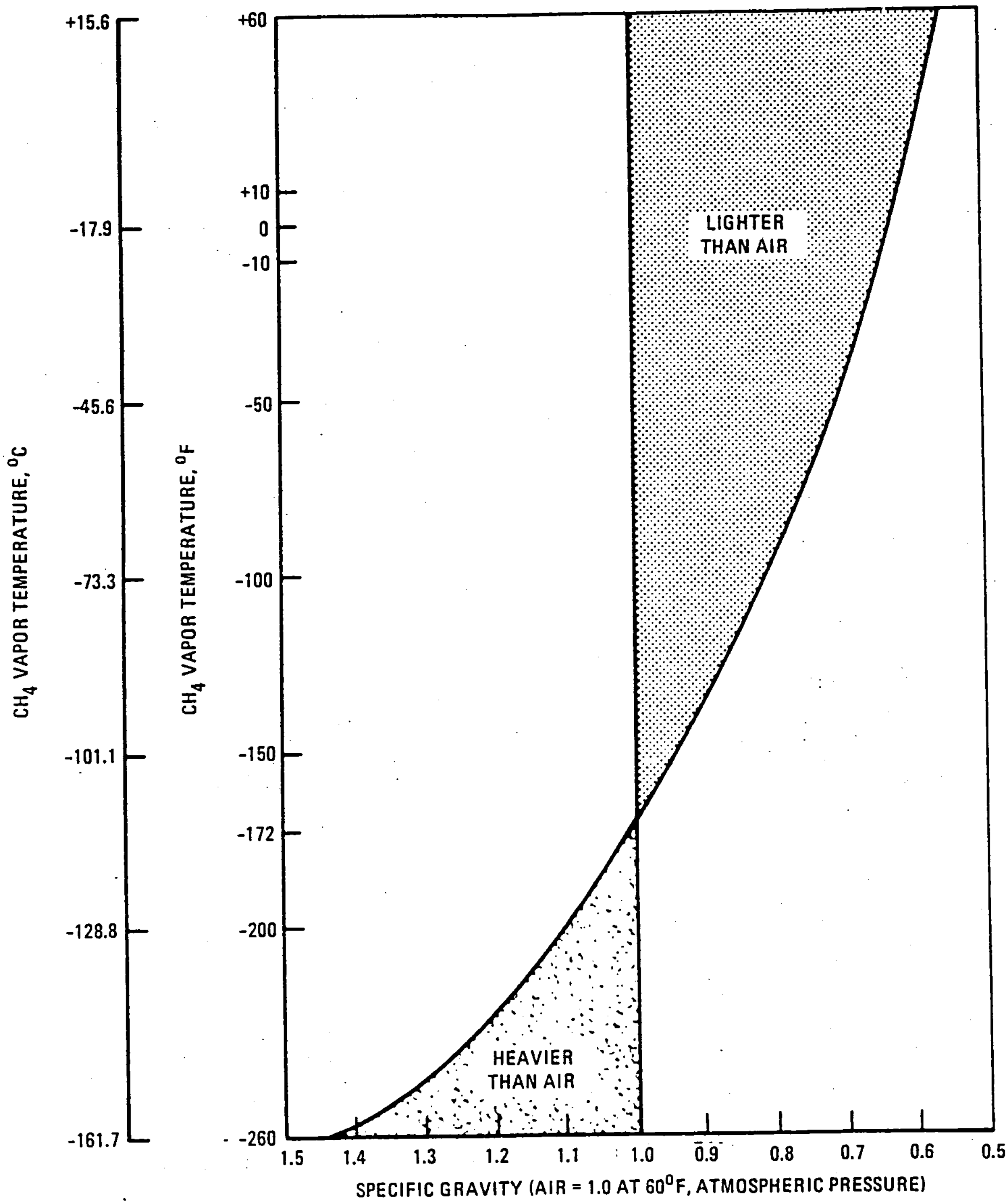

Figure 160. - Effect of temperature on specific gravity of methane vapor.

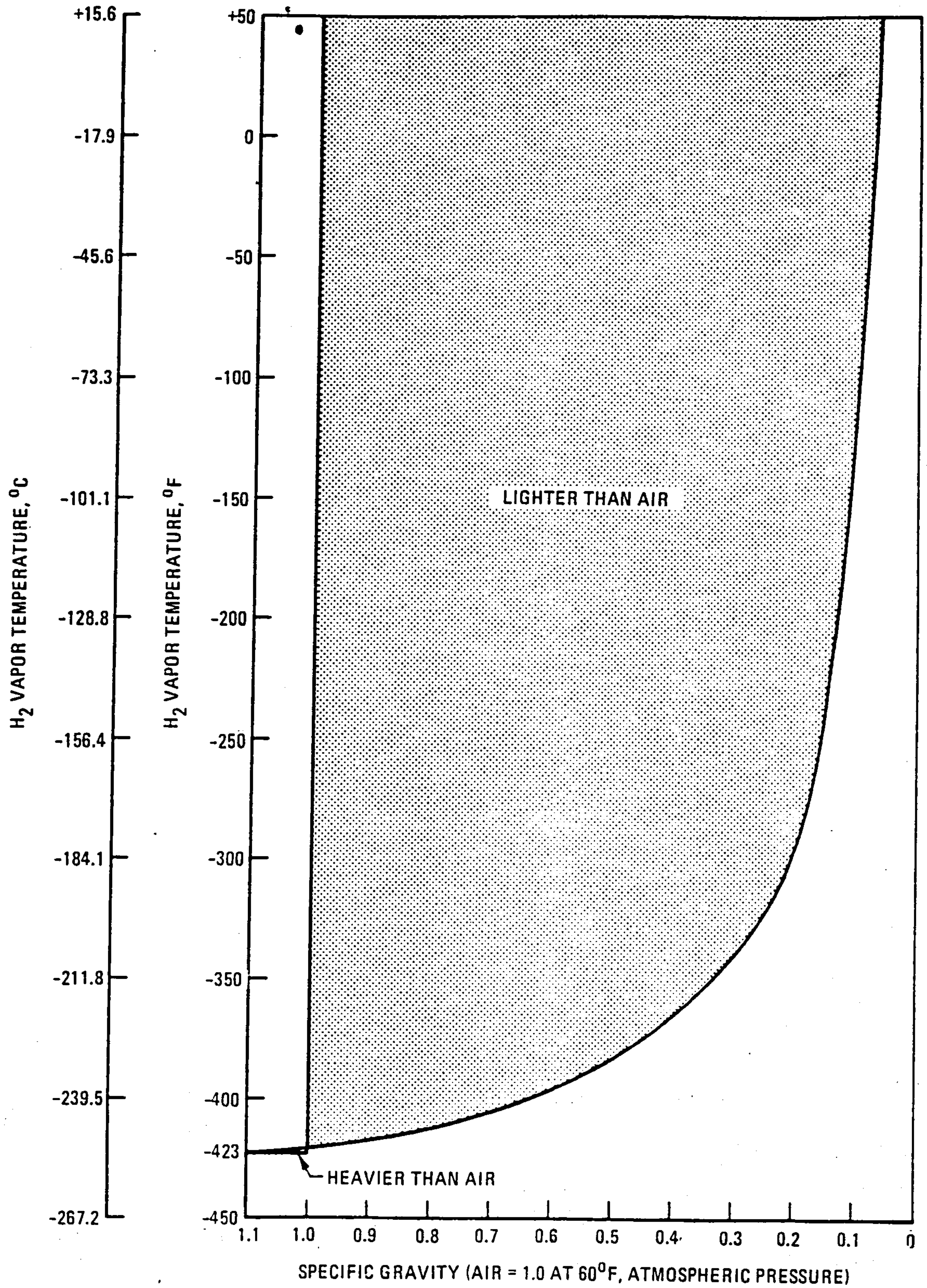

Figure 161. - Effect of temperature on specific gravity of hydrogen vapor.

Density must be considered along with diffusion and buoyant velocities, important parameters for dispersing fuel vapors and gases, in evaluating safety. Diffusion velocity is the speed at which vapors or gases diffuse through air with both components at ambient pressure and temperature. The velocity specified in table 65 is based on a concentration gradient varying from 0.9999 fuel volume fraction to 0.00 over distances of 2.54 cm (1 in.) to 30.5 m (100 ft.) (reference 83). Buoyant velocity is the speed at which a light vapor or gas rises in air. The value is not simple to determine since it depends on atmospheric turbulence and the size and shape of the rising volume. The velocity in table 65 has been calculated from fundamental dynamic principles and empirical data. Diameters of buoyant gas volumes were assumed to vary from 5.08 cm (2 in.) to 1.52 m (5 ft.) (reference 83).

Methane vapor or gas is denser than hydrogen at all temperatures. It also has slower diffusion and buoyant velocities.

These characteristics add up to a seriously adverse assessment of the safety of liquid methane insofar as large-scale spills are concerned. For example, in the event of a catastrophic spill of a large quantity of fuel, e.g., rupture of a storage tank by earthquake, sabotage, etc., or in the event of a crash, airline passengers who survive the impact, as well as people and property in the immediate area, will be considerably safer if the fuel is LH_2 rather than LCH_4.

Liquid methane is rated hazardous because, when spilled in large quantities, it can lay on the ground for an extended period before its temperature increases sufficiently that it will rise and dissipate in the atmosphere. The temperature of the gaseous methane must increase nearly 56°C (100°F) before its density becomes lighter than that of air. All of the area traversed by the cloud under these conditions is susceptible to fire and explosion damage comparable to that experienced in Cleveland in 1944 (Reference 92). This unfortunate characteristic is largely responsible for the severity of laws and regulations which have been passed by various municipalities, states, and even the federal government in the United States regarding shipment and storage of LNG. In view of these governmental restrictions, it is considered unlikely that storage of large quantities of LCH_4 would be permitted at airports of major air terminals.

By contrast, liquid hydrogen need gain only 2.8°C (5°F) to achieve buoyancy in air at standard atmospheric conditions. Considering this in conjunction with hydrogen's much greater temperature differential between the saturated liquid condition at one atmosphere (-253°C (-423°F) for hydrogen and 161°C (-258°F) for methane at standard atmosphere, it is clear that a cloud of spilled hydrogen would not persist for long on the ground.

The probability of a fire is about equal for either fuel. A large spill usually means fractured metal and the release of sufficient energy to cause ignition. With hydrogen, the ensuing deflagration would be about one-tenth the duration and lateral radiation from the flame would be significantly less.

The result would be a hazard to a far smaller area than would be the case for an equal-energy spill of methane.

9.5.2 Combustion-related properties.- The more important combustion-related properties that affect safety are listed in table 66. It can be seen that the flammable and detonable limits of methane are much narrower than those of hydrogen (5.3 percent to 15 percent and 4 percent to 75 percent, respectively). However, it should be recognized that for the majority of cases, i.e., for small leaks of flammable gases into the open air, the lower limit of flammability is reached first and is more indicative of a fire hazard. For methane and hydrogen, these values are roughly the same (5 percent for methane and 4 percent for hydrogen).

The limiting oxygen index is the minimum volume percent of oxygen that will propogate a flame in an unknown composition of a flammable vapor or gas. For example, a mixture of methane in air does not exist that will allow a flame to spread if the oxygen percentage is less than 12.1 percent. The index for hydrogen is 5.0 percent.

The minimum ignition energy is the least amount of spark energy required to ignite the most easily ignitable mixture of vapor or gas in air. The value for methane is 0.29 mJ and for hydrogen it is 0.02. The large difference in minimum ignition energy is not too significant because most all common sources of ignition, such as sparks, matches, or open flame have

TABLE 73. - COMBUSTION-RELATED PROPERTIES OF METHANE AND HYDROGEN

Property	Methane	Hydrogen
Gross Heat of Combustion (Higher Heating Value), kJ/kg Btu/lb	55 520 (23 890)	141 830 (61 030)
Net Heat of Combustion (Lower Heating Value), kJ/kg Btu/lb	49 970 (21 500)	119 900 (51 590)
Flammability Limits, vol % in air	5.3 – 15.0	4.0 – 75.0
Detonability Limits, vol % in air	6.3 – 13.5	18.3 – 59.0
Limiting Oxygen Index, vol %	12.1	5.0
Minimum Ignition Energy, mj	0.29	0.02
Autoignition Temperature, °C (°F)	538 (1 000)	585 (1 085)
Hot-Air Ignition Temperature, °C (°F)	1 221 (2 230)	671 (1 240)
Flame Temperature in Air, °C (°F)	1 877 (3 410)	2 043 (3 710)
Radiative Heat Transfer From Flame, %	23 to 33	17 to 25
Maximum Safe Gap, cm (in.)	0.127 (0.05)	0.0076 (0.003)
Burning Velocity in Air, m/s (ft/s)	0.36 to 0.48 (1.2 to 1.5)	2.7 to 3.4 (8.7 to 11)
Detonation Velocity in Air, m/s (ft/s)	1390 to 1640 (4560 to 5380)	1481 to 2149 (4860 to 7050)
Energy of Explosion, kg TNT/10^6 kJ (lb TNT/10^6 Btu) fuel	215 (500)	172 (400)

sufficient energy to cause ignition. Even weak sparks of static electricity from a human body contain about 10 mJ of energy, which is sufficient to ignite certain mixtures of methane or hydrogen (reference 83).

The autoignition temperature is the minimum temperature of a hot surface that causes spontaneous combustion upon contact with a vapor or gas. The value for methane is 538°C (1000°F), slightly less than the hydrogen value of 585°C (1085°F). The hot air ignition temperature is the temperature of a jet of air that causes a mixture of pure fuel vapor or gas to ignite. The values in table 66 are based on a jet diameter of 0.41 cm (0.16 in.) The value for methane 1221°C (2230°F) is much higher than that for hydrogen 671°C (1240°F) indicating methane is more difficult to ignite in this manner (reference 83).

Flame temperature in air is observed in a burning mixture of premixed air and fuel. Actual flame temperature of a fire at a spill is expected to be less. Experimental flame temperatures in air for methane and hydrogen are about the same, 1871°C and 2038°C (3400° and 3700°F), respectively. About one-fourth of the heat from these methane and hydrogen flames is transferred by radiation. Water vapor in the air tends to absorb some of this radiation, with radiation from methane flames being absorbed less than that from hydrogen (reference 83).

The maximum safe gap is the maximum distance between parallel steel surfaces that prevents flame propagation. It is experimentally measured using laboratory apparatus and is an important parameter in the design of explosion-proof equipment. The values appearing in table 66 for hydrogen and methane are not strictly comparable because they were obtained from different experimental apparatus.

The burning velocity is the rate at which a flame propagates through a flammable mixture of vapors or gas in free air. Its value is a design parameter for flame arresters. Substances with high burning velocities can more easily transform simple deflagrations into explosive detonations in a confined space. On the average, the burning velocity of methane is seven times slower than that of hydrogen (table 66). The detonation velocity is the speed at which a shock wave travels in a detonation. The detonation velocity for methane is slightly less than that for hydrogen.

Energy of explosion is the maximum amount of energy released in detonation. This yield is described as a ratio of the weight of TNT (2, 4, 6, or symmetrical, trinitrotoleune) equivalent to the higher heating value of the fuel in millions of Btu. The value listed in table 66 is the theoretical maximum. Actual yield from explosions commencing from spills would be on the order of 10 percent of the theoretical yeild. Another difficulty in utilizing TNT for comparison is the difference in overpressure and impulse values of fuel/air mixtures and TNT at distances close to the center of the explosion. Fuel/air mixtures generally have less overpressure, but greater impulses than TNT. Thus, methane or hydrogen are expected to have less of a crushing effect on structures, but greater ability to overturn objects than TNT (reference 83).

9.5.3 Overview of relative hazards.- The actual hazard that develops from using any of the high energy fuels depends on the specific details of the storage/distribution system and the type of accident that occurs. Generalized safety comparisons such as the foregoing are of limited interest and usefulness. Conclusions that can be universally applied cannot be made from discussion of general, nonspecific hazards. However, some important safety items which have been identified relative to LH_2 and LCH_4 are the following (reference 84).

LCH_4 presents more of a hazard in event of a major spill because its vapors are harder to disperse than those of LH_2. Both fuels are easily ignitable, but the fire hazard would linger longer for LCH_4. LH_2 probably has the greater explosion hazard because of its sensitivity to confinement.

Both LH_2 and LNG (principally LCH_4) are stored and used commercially today. Safety problems have not precluded their use. However, because of the potential hazard resulting from a large spill previously referred to, and because of the widespread opposition which has developed in recent years relative to storage of large quantities of LNG in or near populated areas (see Federal Legislation) it must be considered unlikely that storage of necessary volumes of LCH_4 at airports will be permitted.

9.5.4 Spacing requirement.- Based on existing standards, and assuming legislation currently pending in Congress to severely restrict storage is not enacted, the following discussion provides information about design and spacing of LNG facilities.

Minimum distances between LNG storage tanks, dike walls, process equipment and property lines can be determined from equations given in the National Fire Protection Association (NFPA) Standard 59A-1975, "Production, Storage and Handling of Liquefied Natural Gas" (reference 85). This standard would certainly be applicable to LCH_4 production, storage, and handling. Spacing requirements related to the storage tanks have the greatest impact on the land area of the storage facility.

A "low-profile" storage tank was assumed to be better suited to an airport site; conventional tanks have larger height-to-diameter ratios. It was further assumed that the tanks would not be located in a seismic zone; special tanks must be designed for these areas.

Approximate tank dimensions for the 42 130 m^3 (256 000 bbl) containers conceived in this study were provided by Chicago Bridge and Iron Company (reference 86). The inner tank is 55.5 m (182 ft) in diameter and 18.9 m (62 ft high). The outer tank is 57.9 m (190 ft) in diameter and 30.5 m (100 ft) high.

The three tanks could be arranged in either a row or triangle configuration. Based upon the NFPA standard for minimum clear distances, it was determined that the row arrangement requires the least amount of land space. A plan view of the area is shown in figure 151.

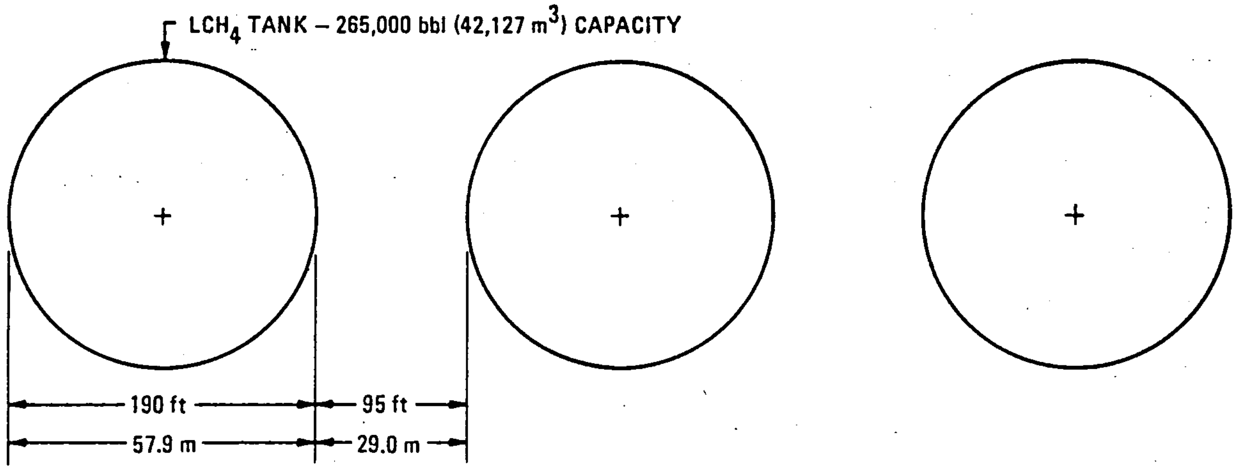

Figure 162. - Plan view of the LCH_4 storage tanks.

Impounding, or diking, areas can also be determined by use of NFPA Standard 59A. A nominal dike size could be estimated for the LCH_4 storage facility by using this standard, however, the resulting dike may not necessarily be the minimally priced one. Engineering design work is required to properly size the dike; parameters include safety, materials of construction (e.g., concrete or earth), and available land area.

Minimum dike dimension can be estimated from figure 152, its accompanying note, and the minimum volume requirement. A most conservative minimum volume requirement is to specify that the dike volume equals the sum of the maximum storage capacity of all tanks within the dike. If it can be ensured that a leak from one tank will not cause others to leak, the required dike volume may be just that of the largest tank. For a storage facility sited near an airport, the more conservative requirement mentioned first would be prudent.

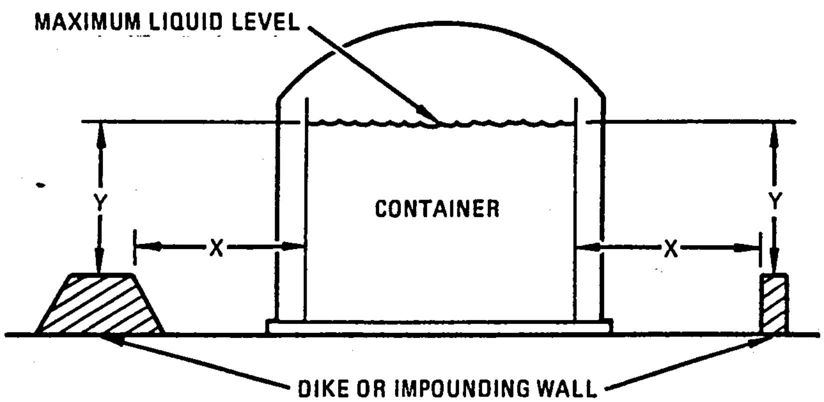

NOTES

DIMENSION "X" MUST EQUAL OR EXCEED 0.6 TIMES DIMENSION "Y".

DIMENSION "X" IS THE DISTANCE FROM THE INNER WALL OF THE CONTAINER TO THE CLOSEST FACE OF THE DIKE OR IMPOUNDING WALL.

DIMENSION "Y" IS THE DISTANCE FROM THE MAXIMUM LIQUID LEVEL IN THE CONTAINER TO THE TOP OF THE DIKE OR IMPOUNDING WALL.

Figure 163. - Dike or impounding wall proximity to containers (reference 71).

Distances from the facility to a property line that can be built upon are based on provisions that limit the heat flux from a fire contained by a dike or that minimize the possibility of a design spill forming a flammable mixture at the property line.

The minimum distance to the SFO property line from the LCH_4 storage facility is 610 m (2000 ft). This distance is more than sufficient to provide for conventional dike configuration and be within NFPA 59A specifications (reference 85). For example, if the dike height were 3.65 m (12 ft) the impoundment area for each storage tank would be about 111.2 x 111.2 m (365 x 365 ft). The minimum allowable distance to the property line under this configuration would be 89 m (292 ft), which is 521 m (1708 ft) less than the actual minimum distance to the SFO property line.

9.5.5 Additional safety standard requirements.- Besides spacing requirements, NFPA 59A also gives safety criteria for other facets of LNG operations. The standard was examined for specific issues that might affect LCH_4 fueling of aircraft.

During aircraft fueling operations, the engines would be required to be shut off. Traffic around the fueling aircraft could not come within 7.62 m (25 feet) which is an NFPA 59A standard. Monitoring of the oxygen content of the empty tank may be required. If it exceeds 2 percent by volume, it must be suitably purged before filling.

The standard calls for ways to prevent spills from endangering structures, equipment, or surrounding property, during LCH_4 transfer operations. This may require drainage channels around the LCH_4 fueling areas. These channels could be covered with steel grates to allow traffic above them. Such channels or other drainage methods are not incorporated into fueling areas of airports today (reference 87). Enclosed drainage channels are specifically prohibited by the NFPA 59A standard.

Other safety criteria in Standard 59A would be applicable to LCH_4 production, storage, and handling and include items such as recommended materials of construction, piping, types of pressure-relief valves, electrical equipment, welding procedures, corrosion control, assurance of competent designers, and fabricators, etc. (reference 85).

9.5.6 Possible safety standard changes.- The United States General Accounting Office (GAO) has recently issued a comprehensive report to Congress on the safety of liquefied energy gases (LEG) (reference 88). The report is critical of current methods of storing and handling LNG. While it is uncertain that the recommendations of this report will be put into effect, they are receiving widespread attention in the industry, and may cause changes to existing standards.

A major recommendation is to site LEG storage facilities in remote areas. This could be accomplished by requiring exclusion zones around storage facilities similar to those of nuclear power plants. The owner would be required to purchase all land within a specified radius of the storage tank(s). Remote area means a nonurban area. Probably a majority of airports are considered to be located in urban areas and would require an exemption from this possible change in the safety standard in order to store and handle LCH_4 within the airport.

The report also suggests that LNG storage tanks be built underground with the maximum liquid height below ground level. Many LNG storage tanks in Japan are constructed this way (reference 89). LNG storage tanks in the United States are usually built aboveground, as constructing underground tanks would be more expensive.

GAO recommends the use of nuclear plant construction codes instead of the Uniform Building Code (UBC), to which most LNG facilities are built today (reference 90). The nuclear construction codes are more restrictive and require greater safety factors. (For example, facilities must be designed to withstand greater natural disasters than those specified by the UBC.)

Another significant recommendation of the report is to require LNG facilities to employ armed guards. LNG facilities in the United States generally do not employ armed guards, with some small storage facilities often operating unattended. The addition of security guards would increase operating costs. For LCH_4 facilities at an airport, the additional cost for guards might not be as restrictive, since a base security system will already exist.

9.5.7 Federal legislation.- Because of the large quantities of LNG that may be imported into the United States, public opposition to the siting of LNG receiving terminals has occurred in some areas of the country. In response to this public opposition, various Congressmen have introduced legislation that could affect the utilization of LCH_4 as aircraft fuel.

Four pieces of legislation, introduced in the first session of the 95th Congress, could have a direct impact on the implementation of LCH_4 as aircraft fuel. These are described as follows:

- S. 2273, "Liquefied Natural Gas Siting and Safety Act." - Introduced by Mr. Pell (D-R.I.), November 1, 1977. This bill gives the Secretary of Energy jurisdiction over construction permits and operating licenses for LNG facilities and directs the Secretary of Energy (hereafter referred to as "Secretary") to promulgate such regulations as may be necessary to establish minimum standards for the location, design, operation, and construction of LNG facilities. S. 2273 provides that after June 30, 1977, an LNG facility cannot be constructed without a permit issued by the Secretary.

  Under the terms of S. 2273, in order for the Secretary to issue any LNG construction permit, the Governor or a responsible agency of the affected State must approve the specific location of the proposed facility. However, the bill allows the Secretary to issue a construction permit without this approval if the Secretary determines that S. 2273 mandates that a hearing be held in the affected local district on an application to build an LNG facility.

  S. 2273 directs the Secretary to report to Congress his recommendations concerning creation of a compensation and liability fund to protect the public against risks associated with construction and operation of LNG facilities.

  The Secretary, in consultation with other Federal agencies, must report to Congress on the adequacy of current federal research and development efforts relating to health, safety, and environmental control in connection with LNG facilities. S. 2273 charges the Secretary with primary responsibility for federal research and development relating to health, safety, and environmental control in connection with LNG facilities. This bill also names the Secretary as coordinator of federal research and development activities in this area.

- H.R. 6844, "Liquefied Natural Gas Facility Safety Act." - Introduced by Mr. Dingell (D-Mich.) and Mr. Markey (D-Mass.), May 3, 1977. This bill affects the siting, design, construction, and operation of facilities used in the transportation, storage, and conversion of LNG. H.R. 6844 directs the Secretary of Transportation (hereafter referred to as "Secretary") to prescribe minimum standards for determining the location of any new LNG facility and standards for their design, construction, and operation. The Secretary is directed to prescribe standards for the location and operation of existing LNG facilities.

  H.R. 6844 mandates that no new LNG facility may be constructed unless a permit has been issued by the Secretary. The bill also specifies that, except for certain exemptions, no new or existing LNG facility may be operated unless a permit has been issued by the Secretary. A permit may not be issued unless an adequate contingency plan setting forth steps to be taken in the event of an LNG accident is provided to Secretary. In addition, assurances must be given that there is adequate financial coverage to satisfy claims for personal injury and property damage resulting from the most severe LNG accident which could be expected.

  H.R. 6844 prohibits the Secretary from issuing a permit in the case of the construction of (or with respect to) any LNG facility that is stationary and:

  - Any portion of such facility located within 610 m (2000 ft) of any residential structure

  - The population density of the area within 14.8 km (8 mi) of such facility averages 10 or more persons per square mile (taking into account those who either work or reside within the area).

  The governor of the state in which such a facility is to be located notifies the Secretary in writing that he does not object to such construction. The bill also provides civil penalties for certain violations pertaining to the construction or operation of LNG facilities.

  H.R. 6844 states that a political subdivision shall not have its laws or regulations pertaining to LNG facility standards preempted (under this bill) unless these standards are incompatible with the standards set forth in this bill. The Secretary of Transportation is also directed to coordinate his actions under this proposed Act with those taken by other Federal agencies.

  H.R. 6844 also directs the President to determine tentatively the maximum amount of imported LNG to be authorized during each of the following 10 years and to determine the number, size, and type of additional LNG facilities needed to accommodate this fuel. The bill authorizes $4 million for the Secretary to conduct an LNG safety study.

- H.R. 9731, Amends the Natural Gas Act. - Introduced by Mr. St. Germain (D-R.I.), October 25, 1977. H.R. 9731 amends the Natural Gas Act so that a certificate for the construction or extension of any LNG facility may not be issued "unless the Governor of the State and the legislative body or bodies of that State in which such facility is to be located has approved in writing such facility."

- H.R. 9773, Amends the Natural Gas Act. - Introduced by Mr. Beard (D-R.I.), October 27, 1977. This bill amends the Natural Gas Act to provide that no certificate for the construction or extension of any LNG facility may be granted unless approved by the affected states. H.R. 9773 specifies that "no standard or requirement imposed by the State as a condition of its approval (other than a requirement solely relating to facility location) may be inconsistent with any standard or requirement applicable to such facility . . ." to the Natural Gas Act.

Although none of the above proposed legislation was enacted by Congress, the legislation could be reintroduced in the next Congress. In fact, Congress has maintained its interest and will hold hearings on LNG safety. The outcome of the hearings are, of course, unpredictable, but the legislation that has previously been proposed indicates that siting of an LCH_4 facility in an airport may have substantial political opposition.

9.5.8 Review of the LNG industry safety record.- The first LNG peakshaving facility was a pilot plant built by Hope Natural Gas Company, a subsidiary of Consolidated Natural Gas System, in Cornwell, West Virginia, in 1939 (reference 54). This plant had a liquefaction capacity of 8490 m^3 (300 000 CF/day) and a storage capacity of 34 x 10^3 m^3 (1.2 million C.F). In 1941, the East Ohio Gas Company, another Consolidated subsidiary, built a peakshaving plant in Cleveland that had a 113.2 x 10^3 m^3/day (4 million CF/day) liquefaction capacity and three tanks, which together would hold 4.75 x 10^6 m^3 (168 million CF). After 2-1/2 years of successful operation, a fourth storage tank with a capacity of 2.83 x 10^6 m^3 (100 million CF) was added. It was this tank that failed in 1944, resulting in a disastrous fire and considerable loss of life. In view of the recent controversy over LNG safety, it is interesting to note that the report of the U.S. Bureau of Mines investigation team concluded that, regardless of the cause of the disaster (probably the use of 3.5 nickel steel for the inner shell, which has low impact resistance, "the application of the system of liquefying and storing large quantities of natural gas is not invalidated, provided proper precautions are observed." Nonetheless, this accident had a dampening effect on the use of LNG for peakshaving, and it was not until 1965 when peakshaving facilities built by Wisconsin Natural Gas Company, San Diego Gas and Electric Company, and Alabama Gas Corporation went onstream that the concept was again used in the United States. The first satellite facility, built in 1969 by Northern States Power Company in Wisconsin, had a storage capacity of 3.7 x 10^6 m^3 (130 million CF). In the following years, the number of LNG plants increased rapidly and dramatically to the present level.

Currently in the United States and Canada, there are 118 peakshaving LNG facilities in operation. The peakshaving facilities have a total storage capacity of about 2.12×10^6 m^3 (75 billion SCF). In addition, there are three operational LNG import terminals and one operating base-load liquefaction facility that have a total storage capacity of about 0.425×10 m^3 (15 billion SCF) (reference 33, 91, and 32).

The safety record of the LNG industry is exemplary. In the aggregate, the facilities have achieved some 6.2 million hours (708 years) of safe operation without incident. None of the LNG facilities have experienced accidents that resulted in hazards outside the plant boundary since the Cleveland accident (reference 92).

These results indicate that the existing safety standards for storage and handling of LNG (NFPA 59A) should be sufficient to ensure safe utilization of LCH_4 as an aircraft fuel. Certainly the operating history of the United States LNG industry supports the adequacy of NFPA 59A and the industry in ensuring safety. Nonetheless, the current controversy over LNG safety has resulted in the possibility of the development of more stringent siting regulations for LNG facilities that would certainly affect the utilization of LCH_4 as an aircraft fuel.

9.6 Conclusions of Study of Ground Facilities

The results of this study show that substitute natural gas derived from coal can be utilized as a feedstock to produce LCH_4 as subsonic aircraft fuel. Utilization of LCH_4 as aircraft fuel is not precluded by technological limitations on the ground system that would supply the fuel.

Liquid methane is considered to present a significantly greater hazard than LH_2 in event of a massive spill as might result from rupture of ground storage tanks or from crash of an aircraft. This, plus the present public controversy over safeguards required for LNG shipment, handling, and storage, plus resulting pending legislation, make it unlikely that storage of large quantities of LCH_4 will be permitted at airports. However, if the question of safety of methane can be satisfactorily resolved, the fuel is very attractive because of its cost advantages.

10. TECHNOLOGY DEVELOPMENT REQUIRED

10.1 Airport Facility Requirements

With respect to materials and equipment requirements for the ground system as studied in Section 9, there are no requirements that cannot be satisfied with existing technology. There are no technical barriers that would preclude the implementation of liquid methane as a fuel for subsonic transport aircraft.

10.2 Aircraft Component and Systems Development

To proceed from conceptual preliminary designs, a technology base must be established and confirmation of design concepts must take place. Starting with the simplest structural element tests and functional equipment tests, as the program progressed, these elements would be integrated into the next higher level subassemblies until a flight-worthy system was arrived at. As one proceeds through Sections 5, 6, 7, and 8 of this study, the lines of required development become quickly delineated. The cryogenic fuel system is the heart of the matter, and determination of the behavior of the elements of this system under static and dynamic (and cyclic) conditions is the route of investigation that should be undertaken.

10.2.1 Structural element tests.- Several materials have been recommended in Sections 5 and 8 for both the fore and aft tanks:

- Kevlar aerodynamic fairing
- A flexible open cell foam
- Mylar-aluminum (MAAMF) Vapor Barrier
- A closed cell foam insulation, Stepan Foam BX250A
- Primary tank material of 2219 aluminum
- A tank wall-to-insulation adhesive.

The mechanical properties of these materials in their real temperature environment under the appropriate loadings must be determined as a first step. The design allowable stresses in tension, compression, fatigue, bending, and peel strength at cryogenic temperatures will result from these efforts.

10.2.2 Small component tests.- At this point, buildup combinations of these materials into cross sections representing sections of the tank and/or insulation can proceed. A rather detailed design of the integral aft tank is presented in figures 164 and 165 as an aid to describing what the potential development tasks are. Several sections and views have been taken, and any one of them could be evaluated as a necessary test specimen. However, the composite truss member with titanium fittings and its lug attachments, shown in View G of figure 164, along with the elements of the attachment structure at the tank end, is an obvious choice for a life cycle fatigue test program. Relatively large panel tests would also be required for the structural-insulation concept, with the load and temperature environment being that of the actual flight environment with a cryogenic fuel on board.

10.2.3 Large-Scale Tank Fabrication and Test.- The purpose here would be to design, fabricate, and test a half-scale aft tank complete with its insulation system. The program would be in two major parts:

- Structural Development and Producibility
  - Develop fabrication methods
  - Install insulation concept
  - Install structural support with trusses
  - Develop inspection and repair provisions
- Fuel System Simulation
  - Install functional equipment
  - Develop filling procedures
  - Verify design of plumbing system
  - Check sensing devices
  - Conduct flow rate tests
  - Simulate engine consumption and aircraft attitudes
  - Establish operating and maintenance procedures

10.2.4 Pumps and other functional equipment development.- The design and development of the equipment items that must function at cryogenic temperatures is a major requirement. The more important of these are:

- Tank boost pumps
- Engine-mounted, high-pressure pumps

- Engine fuel control system
- Tank pressure vent valves
- Tank and engine crossfeed valves
- Sensors and instrumentation to crew station
- Engine-mounted heat exchangers

The order in which these recommendations are made should not be construed as a listing of relative importance but taken only as a sequence in which these events could occur. Ideally, in fact, the functional equipment development should parallel the tank structural development of the preceding Section 10.2.3 so that the fuel system simulator can be operable as the immediate next step.

11. CONCLUSIONS

Major Conclusions

- Methane is competitive as an alternate fuel in all major performance factors such as DOC, gross weight, initial cost and energy utilization.
- The mission range in which methane is competitive is, however, limited to ranges of 2778 km (1500 n.mi.) to about 10186 km (5500 n.mi.). Neither LCH_4 nor LH_2 are competitive with Jet A at the shorter ranges. At the very long ranges, i.e., above 10.186 km (5500 n.mi.), methane becomes noncompetitive to both Jet A and LH_2. The advantages of LH_2 in terms of DOC, weight, cost and energy utilization become even more pronounced at very long ranges.
- The best fuel tank locations for the LCH_4 fueled airplane was found to be fore and aft of the cabin in the fuselage as it was in the LH_2 aircraft studied previously.
- The cryogenic tanks for LCH_4 were found to be producible by present methods using an all welded structure of 2219 aluminum.
- Considerations of safety, design complexity and maintenance weighed as heavily in the choice of the LCH_4 aircraft configuration as did the major performance factors.

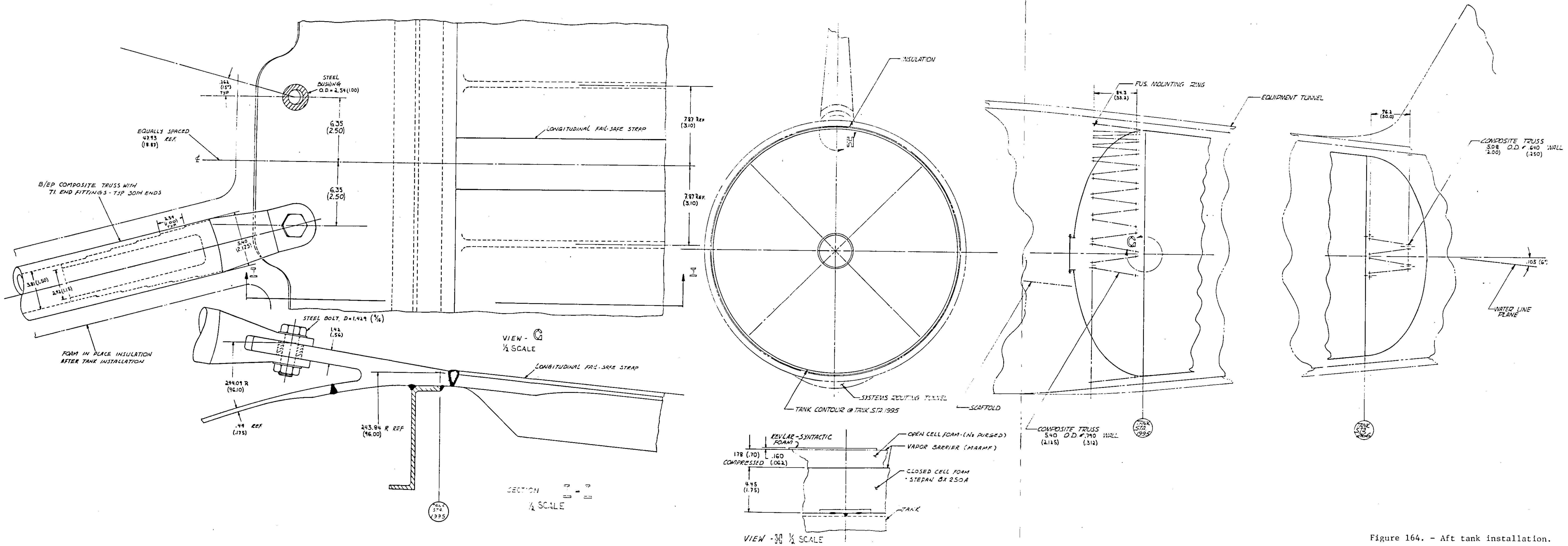

Figure 164. - Aft tank installation.

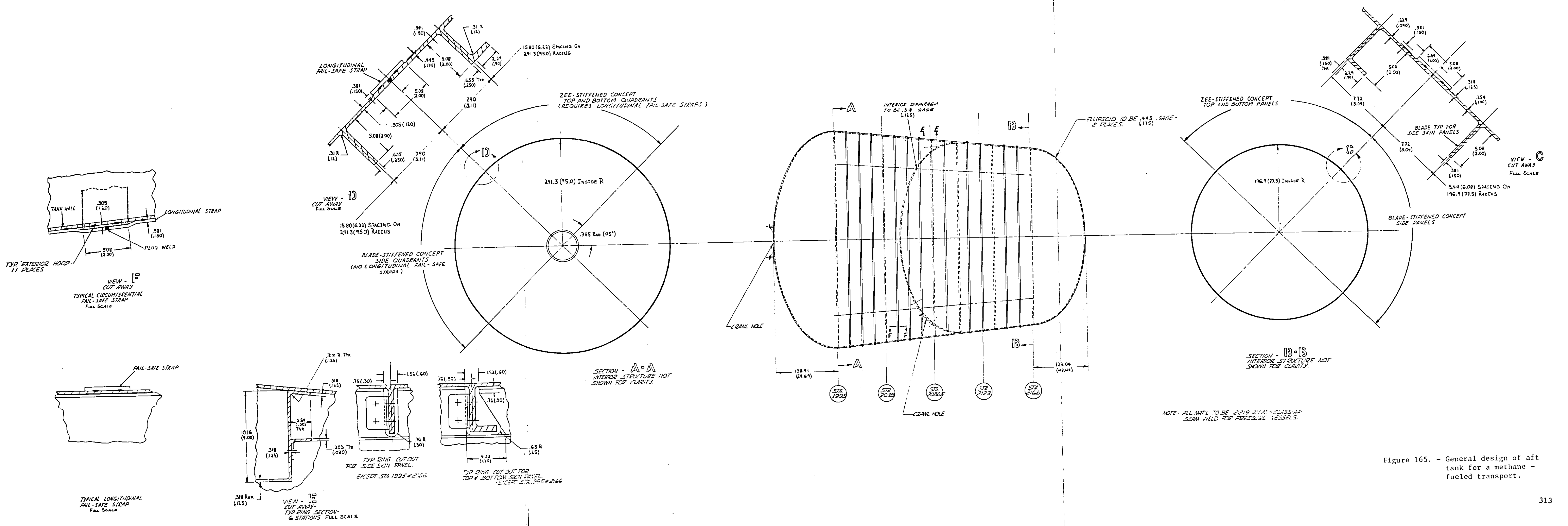

Figure 165. - General design of aft tank for a methane - fueled transport.

- The present public controversy about the safety of LNG shipment, storage and handling bears directly and with equal emphasis on the production and distribution of liquid methane at air terminals. **It is unlikely, under currently proposed legislation, that the storage of large quantities of liquid methane would be permitted at airports.**

- If the question of safety can be satisfactorily resolved, there are no technical barriers in the design of the ground system or of the airplane that would prevent the use of methane as an alternate fuel.

Subcooling

Subcooling of the fuel used for aircraft refueling can result in reduced fuel losses and reduction of venting during flight. A totally nonventing state could be maintained from the termination of fill operations to some time after landing by controlled mixing of the stratified liquid in the tank. The degree of mixing would be controlled by a system using instantaneous tank pressure as the control input. Some economic benefit, from an operational standpoint, may be derived by nonventing when considering ground servicing aspects. However, this was not examined during this study. Subcooling will also reduce tank insulation thickness requirements, and the corresponding system weight and volume reductions will favorably influence DOC.

Although subcooling reduces the amount of fuel vented during a flight, the fuel cost savings do not balance the additional capital equipment expense. The maximum fuel savings would result from the condition of constant weight, i.e., increase insulation thickness for the subcooled case to equal the decrease in weight of fuel evaporated. From figures 110 and 113, subcooling to the 103 kPa (15 psia) state would result in a savings, per 10 186 km (5500 n.mi.) flight, of 259 kg (571 lb) in fuel evaporated over the design point of 148 kPa (21 psia) fill, which is 4.45 cm (1.75-in.) aft tank insulation thickness and 5.08 cm (2.00-in.) forward tank insulation thickness. The yearly fuel loaded figure of 0.459×10^9 kg (1.012×10^9 lb)/yr for the base line terminal liquefication facility corresponds to 7793 flights per year of the 10 186 km (5500 n.mi.) range.

At 259 kg (571 lb) saving per flight the fuel cost reduction is $383,000 per year, based upon $3.79/GJ ($4/10^6 Btu). For 4.44°C (8°F) of subcooling the added capital cost is $33,000,000. This corresponds to a 20-year write-off of $1,650,000/year, or four times the yearly fuel cost savings.

A more optimum case would be to reduce insulation thickness for the subcooled condition, to 1-inch for both tanks, and benefit from lower gross weight. The fuel savings would be 219 kg (482 lb)/flight and insulation system weight reduction would be 166 kg (366 lb) for a net weight reduction of 385 kg (848 lb). Although no DOC weight sensitivity studies were conducted for the fuel system, an approximation of this may be made using the data of Table 5-1. Considering DOC in terms of gross weight as 3.602 cents/seat km - kg(3.026×10^{-6} cents/seat n.mi-lb,) an approximation of DOC benefit is $446,000 per year with an additional $383,000 from fuel cost reduction. This total annual saving is still less than one-half of the capital expense of $1,650,000/year. Therefore, subcooling has not been included in the design.

APPENDIX A

DESCRIPTION OF COMMERCIALLY AVAILABLE BASELOAD LNG LIQUEFACTION PROCESSES

AIR PRODUCTS' MCR PROCESS DESCRIPTION

Air Products and Chemicals, Inc., has patented a multicomponent refrigerant (MCR) process for the liquefaction of natural gas (reference 98). This process is based on a mixed refrigerant, circulated in a closed circuit. It has been used in two operational baseload LNG plants, at Brunei, Borneo, and at Marsa El Brega, Libya, and will be employed in several other installations currently under construction or in the planning stage (references 32 and 99). The earlier installation at Marsa El Brega employed a single mixed refrigerant system, while Brunei and later plants employed a propane-precooled mixed refrigerant system. The refrigerant requirements of a propane-precooled mixed refrigerant system are fulfilled by two major closed-loop circuits: a multi-level propane cascade and a mixed refrigerant service. The mixed refrigerant is composed of nitrogen, methane, ethane, and propane. A process flow diagram of a typical propane-precooled mixed refrigerant process is presented in figure 166. The refrigerant makeup system includes a single fractionation system to provide ethane and propane, and a cryogenic air separation plant to supply nitrogen. The air separation unit also supplies purge and utility nitrogen. The process systems operate as follows:

- <u>LNG Circuit</u> - The feed gas, after pretreatment for removal of entrained condensate, carbon dioxide, and some water, is cooled to about -35°C in three levels of propane refrigeration in evaporators X-1, X-2, and X-3. The gas is dried after heat exchange with high-level propane, X-1, and then cooled in evaporators X-2 and X-3. The heavier components in the feed are removed in a scrub column, D-1, for LPG recovery and refrigerant makeup. Final cooling of the feed to the required LNG temperature is carried out by a single mixed refrigerant stream in the MCR Cryogenic Heat Exchanger, X-5.

- <u>Mixed Refrigerant System</u> - The low-pressure refrigerant stream leaving the MCR Cryogenic Heat Exchanger is compressed to a high pressure in a compressor system, C-1, and cooled to about -35°C by propane refrigeration in evaporators X-6, X-7, and X-8. The partially condensed stream is separated into liquid and vapor fractions in a phase separator, V-1. The liquid is cooled in the warm bundle (WB) of the MCR Cryogenic Heat Exchanger, flashed across a pressure letdown valve, JT-1, and distributed over the shell side of the exchanger. The vapor stream is condensed and subcooled in both the warm bundle and the cold bundle (CB) flashed across a letdown valve, JT-2, and distributed over the shell side of the cold bundle. The stream from the bottom of the cold bundle mixes with the low-pressure stream from JT-1 before redistribution over the warm bundle.

- <u>Propane System</u> - The propane streams from the high-, medium-, and low-level evaporators in the plant are compressed in a single, multistage compressor system, C-2. The high-pressure propane is cooled and condensed against cooling water and stored in an accumulator that supplies propane to the evaporators.

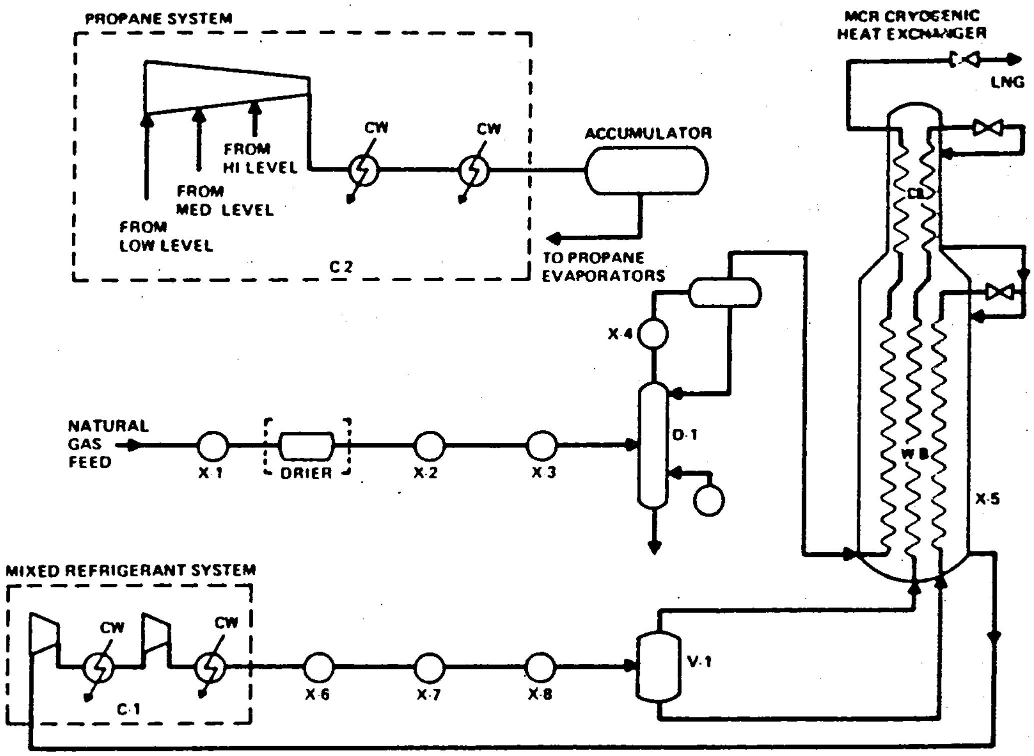

Figure 166. - Propane precooled MCR process - schematic (Reference 36).

- Refrigerant Makeup - The liquid bottoms from the scrub column are the feed to the fractionation system. A series of distillation columns process this feed to provide makeup for the mixed refrigerant and propane systems, LPG and heavier hydrocarbon recovery, plant fuel, etc. Excess hydrocarbon liquids can be reinjected into the LNG. (reference 37).

PRICO® PROCESS DESCRIPTION

A natural gas processing scheme incorporating the PRICO liquefaction process is presented in figure 167. This process is the one that has been chosen for Algeria's Skikda liquefaction facility (Reference 35). The refrigerant mixture consists of nitrogen and a combination of hydrocarbon components of methane through pentane. The refrigerant mixture is circulated by means of a single casing refrigerant compressor. The refrigerant compressor operates at a relatively low discharge temperature of 121°C to 149°C (250° to 300°F) and ambient suction temperatures. There are no cryogenic temperature considerations required for any part of the refrigerant loop outside of the refrigerant exchanger cold boxes with the exception of the cold refrigerant expansion valves and associated piping.

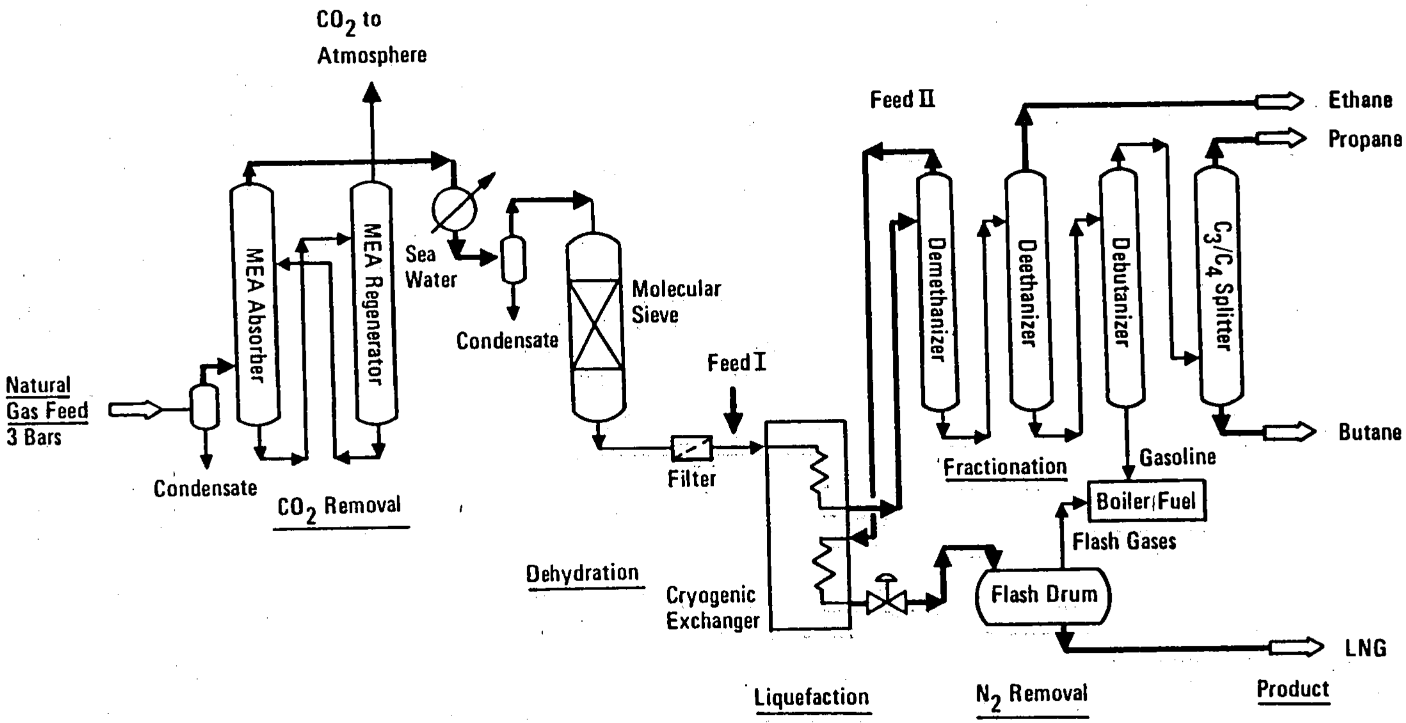

Figure 167. - Natural gas processing scheme incorporating the Prico process.

Feed Gas Treatment

The PRICO liquefaction process requires feed gas preparation no more stringent than any other natural gas liquefaction process. Solid particles and heavy hydrocarbons are removed to prevent deposition on the cold heat transfer surfaces. Moisture, carbon dioxide, and sulfur compounds are removed to avoid solids formation at the low refrigeration temperatures employed.

Liquids in the feed gas are removed prior to absorption of carbon dioxide by monoethanolamine. Then water vapour is first partially condensed by sea water and separated out prior to completing dehydration over a molecular sieve desiccant. The treated gas now contains less than 100 ppm of CO_2 and 1 ppm of water vapour to avoid solids formation by these components in the cryogenic exchangers.

Products. - In the first pass through the cryogenic exchangers (Feed I) the feed gas is partially condensed prior to entering the demethaniser. The overhead vapour (Feed II) is condensed in the cold end to produce nitrogen rich LNG. This nitrogen is flashed off and the LNG product sent to storage. The demethaniser liquids are fractionated into ethane, propane and butane products. The gasoline remaining and nitrogen rich flash gases are used as boiler fuel.

Liquefaction. - The process consists of a single refrigeration loop, figure 168, containing:

- One single casing axial compressor
- One refrigerant sea water cooled condenser
- One multicore cryogenic exchanger.

Thus, the natural gas is cooled over the full temperature range in a single exchanger.

The multicomponent refrigerant is a mixture of nitrogen and hydrocarbons up to pentane. The full mixture circulates around the whole loop.

Refrigerant components are extracted from the feedstock, except for nitrogen which is produced from an air separation unit (Reference 42).

PHILLIPS' "IMPROVED OPTIMIZED CASCADE" PROCESS DESCRIPTION

The Phillips Cascade Cycle consists of propane, ethylene, and methane refrigerant systems. The Kenai, Alaska, LNG installation is currently the only baseload plant that uses the Phillips optimized cascade process (reference 41). The improved version of this process was planned for incorporation into El Paso's Gravinia Point, Alaska, LNG facility (reference 32).

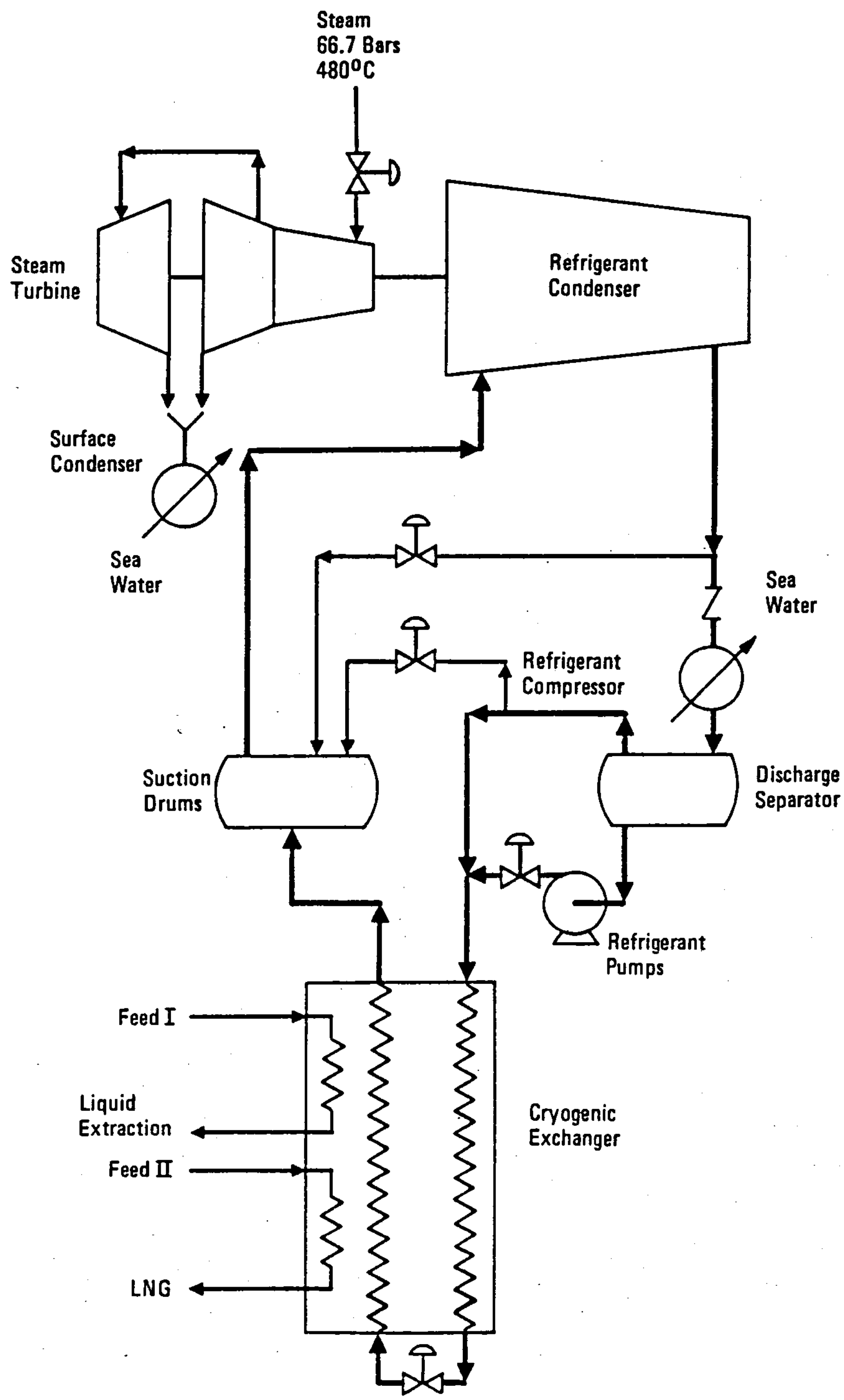

Figure 168. - Prico process (Reference 42).

The improved version of the "optimized cascade" is similar to the Kenai plant in that it uses propane, ethylene, and methane as the refrigerants. A flow sheet of a single unit of the improved optimized cascade cycle is given in figure 169.

Feed Gas Flow

Gas entering the liquefaction unit flows through three stages of propane cooling, three stages of ethylene cooling, and, finally, three stages of methane cooling. In the ethylene portion, a heavy hydrocarbon draw is made. This provides feed for the LPG fractionators and eliminates the heavy hydrocarbons which would form solids in LNG. The draw point was selected for ethane recovery. In plants where a high recovery of ethane is not desired, the draw point would be a warmer temperature. This is another advantage in the cascade cycle. The draw point can be varied or the temperature controlled to accommodate the desired hydrocarbon removal without changing the design or operating scheme of the liquefaction unit.

Nitrogen is removed from the feed gas in the methane refrigeration system as a portion of the fuel stream. The nitrogen content in the feed gas determines the volume of fuel drawn. Here again the system is adjusted to accommodate the feed gas nitrogen content without changing the control scheme.

Propane Refrigeration System

Feed gas leaving the gas treater is chilled to (60°F) by use of high stage propane (X-1). After leaving the high stage chiller it passes through the dehydrator and is then cooled in successive stages with intermediate (X-2) and low pressure propane (X-3). The vapors from each of the propane evaporators flow to the propane compressors (C-1) and, after compression, are cooled and condensed with water (CWI).

Ethylene Refrigeration System

Feed gas from the low stage propane refrigeration system is chilled with high stage ethylene refrigerant to -53.9°C (-65°F) (X-4). About 15 percent of the stream is condensed. The liquid is removed from the separator (H-1) and flashed into the top of a stripper column (H-2). The methane is removed and the liquids, ethane and heavier hydrocarbons, sent to LPG fractionators. The methane joins the high stage methane refrigerant vapors, as discussed later. Vapors from the separator (H-1) are joined by the methane discharge stream and passed through interstage and low stage ethylene chillers (X-5). The feed-methane stream leaves the low stage chiller totally condensed, at -88.3°C and 4137 kPa (-127°F and 600 psia).

Ethylene vapors from the liquefaction unit at their respective pressures are passed through economizing heat exchangers (X-6, X-7, and X-8), then on to the compressors (C-2 and C-3). Each of the interstage streams is cooled

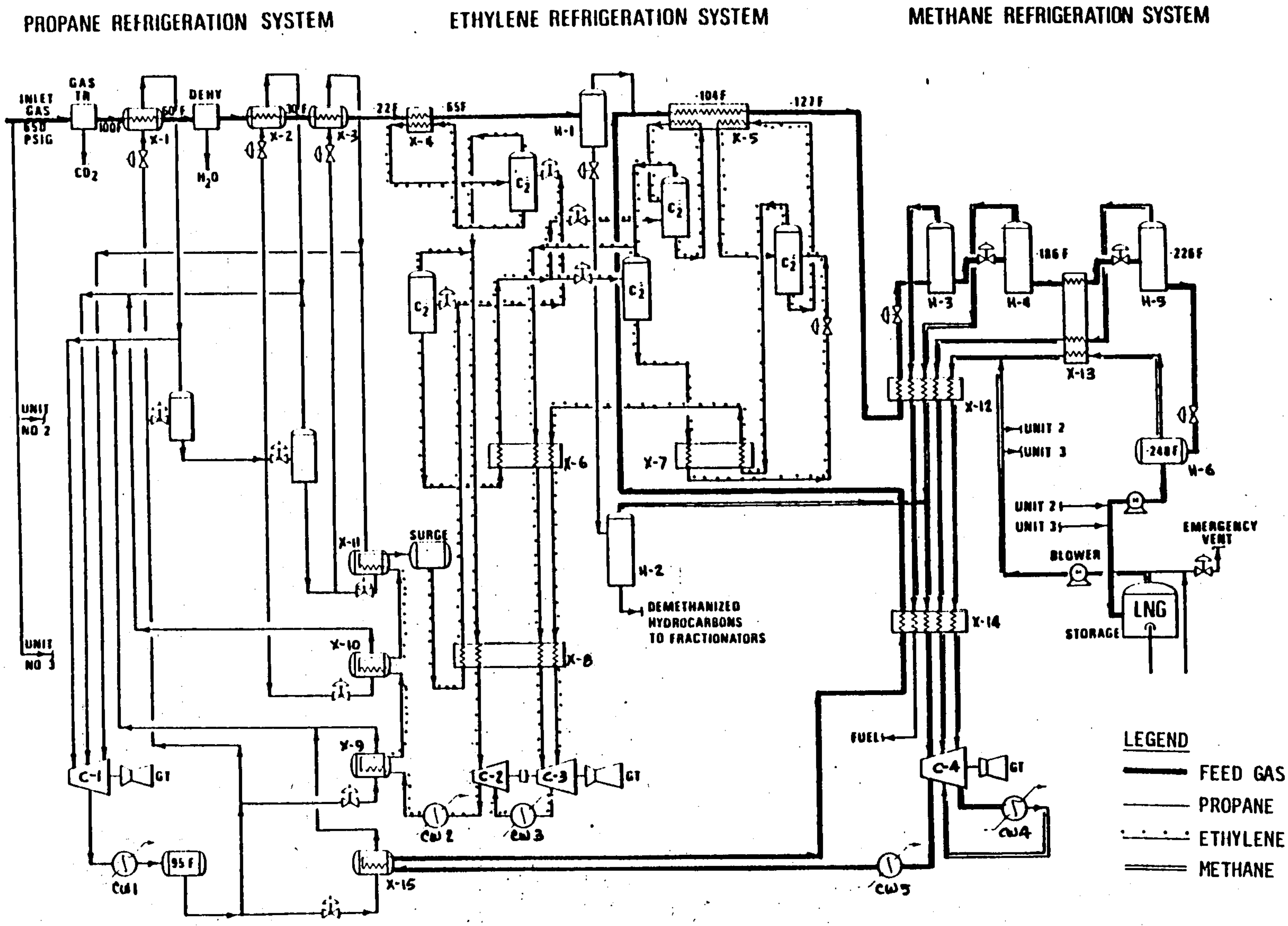

Figure 169. - Phillips improved optimized cascade liquefaction cycle (Reference 28).

after compression and joins the stream from the liquefaction unit. The final discharge is water cooled (CW-2 and CW-3), precooled with high stage propane (X-9 and X-10), and then condensed by low stage propane (X-11) before entering the ethylene surge tank at (-22°F and 300 psia).

Methane System and LNG Storage

The combined feed gas-methane stream enters the methane refrigeration system as a liquid at 88.3°C (-127°F). The stream is first passed through an economizer (X-12), then flashed at a reduced pressure to remove about 10 percent of the feed gas volume (H-3). This vapor stream, after passing through economizers (X-12 and X-14), is sent to the fuel system.

Liquid from the fuel flash drum is reduced in pressure to (180 psia) (H-4) and the flashed vapors become the high stage methane refrigerant. The high stage liquid is passed through a final economizing heat exchanger (X-13), and then flashed in two successive stages (H-5 and H-6) to produce intermediate and low stage methane refrigerant vapors. Each of the methane vapor refrigerant streams then enters the methane compressor (C-4) at its respective pressure.

A methane recycle system identical to that discussed for the ethylene system is provided. This ensures continuous operation regardless of liquefaction unit feed gas flow.

The methane vapors from the demethanizer (H-2), discussed in the ethylene system, enter the high stage methane vapor stream ahead of the final methane economizer (X-14) and become part of the methane refrigerant and compressor discharge stream. The methane compressor discharge is cooled first with water (CW-5), then high stage propane (X-15), is passed back through the methane economizer (X-14) and joins the feed gas stream ahead of the interstage ethylene chiller (X-5).

Liquid produced in the low stage methane flash drum (H-6) is pumped to LNG storage tanks. Here it reaches its lowest pressure and temperature. Storage vapors produced due to reduction in pressure, heat leak, and vapor displacement are returned by means of a blower to the low stage methane refrigeration system ahead of the economizers (X-12 and X-13) (reference 29).

APPENDIX B

COMPUTER PRINTOUT PAGES

FOR FINAL DESIGNS OF

LH_2, LCH_4, AND JET A AIRCRAFT

Computer printout pages for final designs of LH_2, LCH_4, and Jet A Aircraft consisting of:

- Configuration Geometry
- Weight Summary
- Cost Summary
- Mission Summary
- Point Design.

All aircraft are designed for:

400 Passengers

Mach 0.85

Range 10,190 (5500 n.mi.)

TOFL 3200 m (10,500 ft)

Approach speed 72 m/s (140 kt).

LIQ. HYD. 69000 LB P/L / 5500NMI. - 400 PAX / M .85 0001

T/C=10.00 AR= 9.00 W/S=119.00 T/W=0.303

C O N F I G U R A T I O N   G E O M E T R Y

BASIC WING--	AREA(SQ FT)	SPAN(FT)	TAPER RATIO	C/4 SWEEP	L.E. SWEEP	MAC(FT)	
	3096.2	166.93	0.300	30.000	32.504	20.34	
WING PANELS--	AREA(SQ FT)	EXP. AREA	AVG T/C	L.E. SWEEP	SFLE(SQ FT)	REF L(FT)	
	1686.9	1085.0	11.11	32.250	0.0	23.45	
	921.6	921.6	10.23	32.250	0.0	19.01	
	814.7	814.7	9.20	32.250	0.0	16.31	
TOTAL WING--	AREA(SQ FT)	EFF AR	AVG T/C	CR(FT)	CT(FT)	MAC(FT)	L(FT)
	3423.2	8.14	10.52	29.06	14.95	21.30	67.61
FUSELAGE--	LENGTH(FT)	S WET(SQ FT)	BWW(FT)	EQUIV D(FT)	SPI(SQ FT)		
	215.60	13775.0	21.75	23.19	422.44		
	BW(FT)	BH(FT)	SBH(SQ FT)				
	21.75	25.00	13775.00				
HORZ. TAIL 1--	SHT1(SQ FT)	SHX1(SQ FT)	REF L1(FT)	L HT1(FT)	HT1 VOL COEF		
	569.84	406.28	11.47	101.05	0.9143		
HORZ. TAIL 2--	SHT2(SQ FT)	SHX2(SQ FT)	REF L2(FT)	L HT2(FT)	HT2 VOL COEF		
	0.0	0.0	0.0	215.60	0.0		
VERT. TAIL 1--	SVT1(SQ FT)	SVX1(SQ FT)	REF L1(FT)	L VT1(FT)	VT1 VOL COEF		
	263.24	263.24	14.07	100.53	0.0512		
VERT. TAIL 2--	SVT2(SQ FT)	SVX2(SQ FT)	REF L2(FT)	L VT2(FT)	VT2 VOL COEF		
	0.0	0.0	0.0	215.60	0.0		
PROPULSION--	ENG L(FT)	ENG D(FT)	POD L(FT)	POD D(FT)	POD S WET	NO. PODS	INLET L(FT)
	9.59	6.12	16.49	6.86	1421.87	4.	0.0
FUEL TANKS--	WING(CU FT)	BOX(CU FT)	FUS(CU FT)				
	26.31	0.0	15006.00				
WETTED VOLUMES--	BODY	WING	TAILS	PODS	PYLONS	PONTOONS	TOTAL
	55512.79	2923.51	408.79	2438.43	54.19	0.0	61337.70

B-1

FINAL DESIGN

LH_2 MACH 0.85

400 PASSENGER

10,190 Km (5500 n.mi)

TOFL 3200 m (10,500 ft)

APP SPEED 72 m/s (140 Kt)

LIQ. HYD. 88000 LB P/L / 5500NMI. - 400 PAX / M .85 0001

T/C=10.00 AR= 9.00 W/S=119.00 T/W=0.303

W E I G H T   S T A T E M E N T

	WEIGHT(POUNDS)	WEIGHT FRACTION	(PERCENT)
GROSS WEIGHT	(368443.)		
FUEL AVAILABLE	56164.	FUEL	15.24
EXTERNAL	0.		
INTERNAL	56163.		
ZERO FUEL WEIGHT	312280.		
PAYLOAD	88000.	PAYLOAD	23.88
PASSENGERS	80000.		
BAGGAGE	0.		
CARGO	8000.		
STORES	0.		
OPERATIONAL EMPTY WEIGHT	224280.		
OPERATIONAL ITEMS	15732.	OPERATIONAL ITEMS	5.57
STANDARD ITEMS	4796.		
EMPTY WEIGHT	203752.		
STRUCTURE	118827.	STRUCTURE	32.25
WING	36239.		
ROTOR	0.		
TAIL	3377.		
BODY	53477.		
ALIGHTING GEAR	19948.		
ENGINE SECTION AND NACELLE	5786.		
PROPULSION	32120.	PROPULSION	8.72
CRUISE ENGINES	15393.		
LIFT ENGINES	0.		
THRUST REVERSER	1206.		
EXHAUST SYSTEM	0.		
ENGINE CONTROL	145.		
STARTING SYSTEM	262.		
PROPELLERS	0.		
LUBRICATING SYSTEM	0.		
FUEL SYSTEM	15115.		
DRIVE SYSTEM (POWER TRANS)	0.		
SYSTEMS	52805.		
FLIGHT CONTROLS	4737.		
AUXILIARY POWER PLANT	1116.		
INSTRUMENTS	1174.		
HYDRAULIC AND PNEUMATIC	2765.		
ELECTRICAL	5390.		
AVIONICS	2261.	SYSTEMS	14.33
ARMAMENT	0.		
FURNISHINGS AND EQUIPMENT	28492.		
AIR CONDITIONING	6504.		
ANTI-ICING	345.		
PHOTOGRAPHIC	0.		
LOAD AND HANDLING	0.		
		TOTAL	(100.)

COST SUMMARY

RDT AND E

	TOTAL *
DEVELOPMENT - NONRECURRING	
ENGINEERING	959.23
TOOLING	589.69
TEST ARTICLES	56.79
DATA	0.0
SYSTEMS ENG/MNGMT	0.0
CRUISE ENGINE	0.0
LIFT ENGINE	0.0
FAN	0.0
AVIONICS	0.0
OTHER SYSTEMS	0.0
FACILITIES	0.0
TOTAL AIR VEHICLE	1605.92
INTEGR LOGISTICS SUPPORT	
PLANNING	10.21
TRAINING	3.47
HANDBOOKS	18.42
SSE	5.00
TOTAL ILS	37.10
TOTAL DVLPMNT-NONREC	1643.02
DEVELOPMENT - RECUR(PROTOTYPES)	
AIR VEHICLE	581.19
SPARES	111.80
TOTAL DVLPMNT-RECUR	692.99
GOVMNT DVLPMNT COST	0.0
TOTAL DVLPMNT COST	2336.01

PRODUCTION

	MATERIAL	LABOR	TOTAL PER PROD A/C**
STRUCTURE	3741.61	8306.11	12047.72
WING	1228.08	1974.51	3202.60
ROTOR	0.0	0.0	0.0
TAIL	110.92	273.53	384.45
BODY	1530.04	4766.95	6296.99
ALIGHTING GEAR	624.07	31.60	655.67
ENG SECT + NACELLE	248.50	1259.52	1508.02
ENG SECTION	0.0	0.0	0.0
NACELLE	212.41	1171.17	1383.58
AIR INDUCTION	36.08	88.35	124.43
PROPULSION	344.03	1251.15	1595.18
ENGINE INSTALL	0.0	19.35	19.35
THRUST REVERSER	0.0	1.52	1.52
EXHAUST SYSTEM	0.0	0.0	0.0
ENGINE CONTROLS	2.48	3.86	6.33
STARTING SYSTEM	26.00	4.76	30.76
PROPELLER INSTALL	0.0	0.0	0.0
LUBRICATING SYSTEM	0.0	0.0	0.0
FUEL SYSTEM	315.55	1221.67	1537.22
DRIVE SYS(PWR TRN)	0.0	0.0	0.0
SYSTEMS	2388.46	5694.57	8083.03
FLIGHT CONTROLS	560.38	410.52	970.90
AUX POWER PLANT	124.14	21.95	146.09
INSTRUMENTS	96.38	91.33	187.71
HYDRAULIC + PNEUM	137.30	361.67	498.97
ELECTRICAL	404.00	1112.85	1516.85
AVIONIC INSTALL	30.00	326.39	356.39
ARMAMENT	0.0	0.0	0.0
FURN AND EQUIP	680.49	2909.38	3589.87
AIR CONDITIONING	337.85	437.28	775.13
ANTI-ICING	17.93	23.20	41.13
PHOTOGRAPHIC	0.0	0.0	0.0
LOAD AND HANDLING	0.0	0.0	0.0
SYSTEMS INTEGR	436.01	494.06	930.08
TOTAL COST	6910.11	15745.90	22656.00
TOTAL HRS **		563.69	563.69
ENG CHANGE ORDERS			741.09
SUSTAINING ENG COST			1575.63
PROD TOOLING COST			1159.38
QUALITY ASSURANCE			2121.12
MISCELLANEOUS ***			733.07
TOTAL AIRFRAME COST			28986.27
ENGINE COST			5529.57
AVIONICS COST			750.89
TOTAL MANUFACTURING COST			35266.72
WARRANTY			176.86
TOTAL PRODUCTION COST			35443.57

PROCUREMENT

	PER PROD A/C**
TOTAL PRODUCTION	35443.57
INTEGR LOGISTICS SUPPORT	
PLANNING	27.97
TRAINING	9.51
TRAINERS	308.41
HANDBOOKS	35.54
FACILITIES	0.0
SSE - CFE	17.72
SSE - GFE	924.99
TOTAL ILS	1324.13
INITIAL SPARES COST	5164.37
PRODUCTION DEVELOPMENT	
ENGINEERING	314.56
TOOLING	192.03
ENGINES	0.0
TOTAL PROD DEV	506.60
TOTAL PROCUREMENT	42438.65

* - MILLIONS OF DOLLARS

** -1000 OF DOLLARS OR HOURS PER PROD A/C

*** - INCLUDES PROD DATA, SYSTEMS ENGR AND OTHER SYSTEMS

MISSION SUMMARY

LIQ. HYD. 88000 LB P/L / 5500NMI. - 400 PAX / M .85 0001

SEGMENT	INIT ALTITUDE (FT)	INIT MACH NO	INIT WEIGHT (LB)	SEGMT FUEL (LB)	TOTAL FUEL (LB)	SEGMT DIST (N MI)	TOTAL DIST (N MI)	SEGMT TIME (MIN)	TOTAL TIME (MIN)	EXTERN STORE TAB ID	ENGINE THRUST TAB ID	EXTERN F TANK TAB ID	AVG L/D RATIO	AVG SFC (FF/T)	MAX OVER PRES
TAKEOFF POWER 1	0.	0.0	368443.	149.	149.	0.	0.	14.0	14.0	0.	395501.	0.	0.0	0.089	0.0
POWER 2	0.	0.0	368294.	177.	326.	0.	0.	1.0	15.0	0.	304401.	0.	0.0	0.102	0.0
CLIMB	0.	0.378	368117.	605.	931.	17.	17.	3.9	18.9	0.	304201.	0.	17.55	0.159	0.0
ACCEL	10000.	0.456	367512.	208.	1139.	8.	26.	1.4	20.3	0.	304201.	0.	15.93	0.178	0.0
CLIMB	10000.	0.638	367304.	3313.	4452.	244.	269.	30.1	50.3	0.	304201.	0.	14.77	0.205	0.0
CRUISE	37000.	0.850	363991.	41646.	46098.	5031.	5300.	619.1	669.4	0.	-304101.	0.	17.15	0.202	0.0
DESCENT	39000.	0.850	322345.	260.	46358.	82.	5382.	10.4	679.9	0.	304301.	0.	13.62	0.471	0.0
DECEL	10000.	0.638	322085.	59.	46417.	12.	5394.	2.0	681.9	0.	304301.	0.	15.33	0.362	0.0
DESCENT	10000.	0.456	322026.	391.	46808.	54.	5448.	12.0	693.9	0.	304301.	0.	17.23	0.249	0.0
CRUISE	39000.	0.850	321635.	409.	47216.	52.	5500.	6.4	700.3	0.	-304101.	0.	17.07	0.202	0.0
LOITER	1500.	0.350	321226.	332.	47548.	0.	5500.	6.0	706.3	0.	-304101.	0.	17.35	0.179	0.0
RESET	0.	0.0	320895.	0.	47548.	-5500.	0.	0.0	706.3	0.	0.	0.	0.0	0.0	0.0
RESET	0.	0.0	320895.	0.	47548.	0.	0.	0.0	706.3	0.	0.	0.	0.0	0.0	0.0
CRUISE	39000.	0.850	320895.	4455.	52003.	0.	0.	70.6	777.0	0.	-304101.	0.	17.02	0.202	0.0
TAKEOFF POWER 1	0.	0.0	316439.	0.	52003.	0.	0.	0.0	777.0	0.	395501.	0.	0.0	0.089	0.0
POWER 2	0.	0.0	316439.	177.	52181.	0.	0.	1.0	778.0	0.	304401.	0.	0.0	0.102	0.0
CLIMB	0.	0.378	316262.	487.	52668.	14.	14.	3.1	781.1	0.	304201.	0.	17.12	0.159	0.0
ACCEL	10000.	0.456	315775.	74.	52742.	3.	17.	0.5	781.6	0.	304201.	0.	16.09	0.170	0.0
CLIMB	10000.	0.547	315701.	1060.	53802.	58.	75.	8.8	790.3	0.	304201.	0.	15.21	0.187	0.0
CRUISE	30000.	0.730	314640.	0.	53802.	0.	75.	0.0	790.3	0.	-304101.	0.	16.43	0.192	0.0
DESCENT	30000.	0.700	314640.	274.	54076.	70.	145.	10.6	800.9	0.	304301.	0.	15.26	0.369	0.0
DECEL	10000.	0.547	314367.	34.	54110.	6.	151.	1.2	802.1	0.	304301.	0.	16.15	0.297	0.0
DESCENT	10000.	0.456	314333.	322.	54432.	45.	196.	10.0	812.1	0.	304301.	0.	17.12	0.251	0.0
CRUISE	30000.	0.730	314011.	31.	54463.	4.	200.	0.5	812.6	0.	-304101.	0.	16.42	0.192	0.0
LOITER	1500.	0.343	313979.	1616.	56079.	0.	200.	30.0	842.6	0.	-304101.	0.	17.29	0.178	0.0

WTO = 368443.1 FUEL A= 56163.5 FUEL R= 56079.3

SUMMARY . . NO. 1 ASSET PARAMETRIC ANALYSIS MAY 29 1979

AIRCRAFT MODEL --L 1317-1-1
I.O.C. DATE --1995
DESIGN SPEED --SUBSONIC

ENGINE I.D. -- 304000
SLS SCALE 1.0 = 33000
NUMBER OF ENGINES = 4.

WING QUARTER CHORD SWEEP = 30.00 DEG
WING TAPER RATIO = 0.300

1 W/S	119.0	0.0	0.0	0.0	0.0	0.0	0.0	0.0	0.0	0.0	0.0	0.0	0.0	0.0	0.0	0.0
2 T/W	0.303	0.0	0.0	0.0	0.0	0.0	0.0	0.0	0.0	0.0	0.0	0.0	0.0	0.0	0.0	0.0
3 AR	9.00	0.0	0.0	0.0	0.0	0.0	0.0	0.0	0.0	0.0	0.0	0.0	0.0	0.0	0.0	0.0
4 T/C	10.00	0.0	0.0	0.0	0.0	0.0	0.0	0.0	0.0	0.0	0.0	0.0	0.0	0.0	0.0	0.0
5 SWEEP	30.00	0.0	0.0	0.0	0.0	0.0	0.0	0.0	0.0	0.0	0.0	0.0	0.0	0.0	0.0	0.0
6 FPR	0.0	0.0	0.0	0.0	0.0	0.0	0.0	0.0	0.0	0.0	0.0	0.0	0.0	0.0	0.0	0.0
7 OPR	0.0	0.0	0.0	0.0	0.0	0.0	0.0	0.0	0.0	0.0	0.0	0.0	0.0	0.0	0.0	0.0
8 TIT	0.	0.	0.	0.	0.	0.	0.	0.	0.	0.	0.	0.	0.	0.	0.	0.
9 NPR	0.0	0.0	0.0	0.0	0.0	0.0	0.0	0.0	0.0	0.0	0.0	0.0	0.0	0.0	0.0	0.0
10 AUG T	0.	0.	0.	0.	0.	0.	0.	0.	0.	0.	0.	0.	0.	0.	0.	0.
11 RADIUS N. MI	5500	0	0	0	0	0	0	0	0	0	0	0	0	0	0	0
12 GROSS WEIGHT	368443	0	0	0	0	0	0	0	0	0	0	0	0	0	0	0
13 FUEL WEIGHT	56164	0	0	0	0	0	0	0	0	0	0	0	0	0	0	0
14 OP. WT. EMPTY	224280	0	0	0	0	0	0	0	0	0	0	0	0	0	0	0
15 ZERO FUEL WT.	312280	0	0	0	0	0	0	0	0	0	0	0	0	0	0	0
16 THRUST/ENGINE	27910	0	0	0	0	0	0	0	0	0	0	0	0	0	0	0
17 ENGINE SCALE	0.846	0.0	0.0	0.0	0.0	0.0	0.0	0.0	0.0	0.0	0.0	0.0	0.0	0.0	0.0	0.0
18 WING AREA	3096.	0.	0.	0.	0.	0.	0.	0.	0.	0.	0.	0.	0.	0.	0.	0.
19 WING SPAN	166.9	0.0	0.0	0.0	0.0	0.0	0.0	0.0	0.0	0.0	0.0	0.0	0.0	0.0	0.0	0.0
20 H. TAIL AREA	569.8	0.0	0.0	0.0	0.0	0.0	0.0	0.0	0.0	0.0	0.0	0.0	0.0	0.0	0.0	0.0
21 V. TAIL AREA	263.2	0.0	0.0	0.0	0.0	0.0	0.0	0.0	0.0	0.0	0.0	0.0	0.0	0.0	0.0	0.0
22 ENG. LENGTH	9.59	0.0	0.0	0.0	0.0	0.0	0.0	0.0	0.0	0.0	0.0	0.0	0.0	0.0	0.0	0.0
23 ENG. DIAMETER	6.12	0.0	0.0	0.0	0.0	0.0	0.0	0.0	0.0	0.0	0.0	0.0	0.0	0.0	0.0	0.0
24 BODY LENGTH	215.6	0.0	0.0	0.0	0.0	0.0	0.0	0.0	0.0	0.0	0.0	0.0	0.0	0.0	0.0	0.0
25 WING FUEL LIMIT	0.002	0.0	0.0	0.0	0.0	0.0	0.0	0.0	0.0	0.0	0.0	0.0	0.0	0.0	0.0	0.0
COST DATA																
26 RDTE - BIL.	2.336	0.0	0.0	0.0	0.0	0.0	0.0	0.0	0.0	0.0	0.0	0.0	0.0	0.0	0.0	0.0
27 FLYAWAY - MIL.	42.62	0.0	0.0	0.0	0.0	0.0	0.0	0.0	0.0	0.0	0.0	0.0	0.0	0.0	0.0	0.0
28 INVESTMNT-BIL.	0.992	0.0	0.0	0.0	0.0	0.0	0.0	0.0	0.0	0.0	0.0	0.0	0.0	0.0	0.0	0.0
29 DOC - C/SM	1.591	0.0	0.0	0.0	0.0	0.0	0.0	0.0	0.0	0.0	0.0	0.0	0.0	0.0	0.0	0.0
30 IOC - C/SM	1.262	0.0	0.0	0.0	0.0	0.0	0.0	0.0	0.0	0.0	0.0	0.0	0.0	0.0	0.0	0.0
31 ROI A.T. - 0/0	21.99	0.0	0.0	0.0	0.0	0.0	0.0	0.0	0.0	0.0	0.0	0.0	0.0	0.0	0.0	0.0
MISSION PARAMETERS																
32 MISN V1(1,1)	37000	0	0	0	0	0	0	0	0	0	0	0	0	0	0	0
33 MISN V2(1,1)	47548	0	0	0	0	0	0	0	0	0	0	0	0	0	0	0
CONSTRAINT OUTPUT																
34 TAKEOFF DST(1)	10460	0	0	0	0	0	0	0	0	0	0	0	0	0	0	0
35 CLIMB GRAD(1)	0.0834	0.0	0.0	0.0	0.0	0.0	0.0	0.0	0.0	0.0	0.0	0.0	0.0	0.0	0.0	0.0
36 TAKEOFF DST(2)	9812	0	0	0	0	0	0	0	0	0	0	0	0	0	0	0
37 CLIMB GRAD(2)	0.0374	0.0	0.0	0.0	0.0	0.0	0.0	0.0	0.0	0.0	0.0	0.0	0.0	0.0	0.0	0.0
38 CTOL LNDG D(1)	5901	0	0	0	0	0	0	0	0	0	0	0	0	0	0	0
39 AP SPEED-KT(1)	139.8	0.0	0.0	0.0	0.0	0.0	0.0	0.0	0.0	0.0	0.0	0.0	0.0	0.0	0.0	0.0
40 SEP(1) - FPS	6	0	0	0	0	0	0	0	0	0	0	0	0	0	0	0
41 SEP(2) - FPS	3	0	0	0	0	0	0	0	0	0	0	0	0	0	0	0

METHANE /88000 LB P/L / 5500 NMI RNG / M .85 MISS

T/C = 9.73 AR = 9.00 W/S = 135.0 T/W = 0.30

C O N F I G U R A T I O N   G E O M E T R Y

BASIC WING--	AREA(SQ FT)	SPAN(FT)	TAPER RATIO	C/4 SWEEP	L.E. SWEEP	MAC(FT)	
	3618.3	180.46	0.300	30.000	32.504	21.99	
WING PANELS--	AREA(SQ FT)	EXP. AREA	AVG T/C	L.E. SWEEP	SFLE(SQ FT)	REF L(FT)	
	1976.2	1370.9	10.90	32.250	0.0	25.64	
	1142.1	1142.1	9.67	32.250	0.0	18.77	
	550.0	550.0	8.79	32.250	0.0	12.43	
TOTAL WING--	AREA(SQ FT)	EFF AR	AVG T/C	CR(FT)	CT(FT)	MAC(FT)	L(FT)
	3668.3	8.88	10.32	31.56	9.25	22.29	66.18
FUSELAGE--	LENGTH(FT)	S WET(SQ FT)	BWW(FT)	EQUIV D(FT)	SPI(SQ FT)		
	201.30	11686.0	20.00	22.37	393.00		
	BW(FT)	BH(FT)	SBW(SQ FT)				
	20.00	25.00	11686.00				
HORZ. TAIL 1--	SHT1(SQ FT)	SHX1(SQ FT)	REF L1(FT)	L HT1(FT)	HT1 VOL COEF		
	741.33	592.76	12.23	94.61	0.8815		
HORZ. TAIL 2--	SHT2(SQ FT)	SHX2(SQ FT)	REF L2(FT)	L HT2(FT)	HT2 VOL COEF		
	0.0	0.0	0.0	201.30	0.0		
VERT. TAIL 1--	SVT1(SQ FT)	SVX1(SQ FT)	REF L1(FT)	L VT1(FT)	VT1 VOL COEF		
	391.82	391.82	16.75	95.34	0.0572		
VERT. TAIL 2--	SVT2(SQ FT)	SVX2(SQ FT)	REF L2(FT)	L VT2(FT)	VT2 VOL COEF		
	0.0	0.0	0.0	201.30	0.0		
PROPULSION--	ENG L(FT)	ENG D(FT)	POD L(FT)	POD D(FT)	POD S WET	NO. PODS	INLET L(FT)
	10.24	6.98	21.30	8.38	2242.30	4.	0.0
FUEL TANKS--	WING(CU FT)	BOX(CU FT)	FUS(CU FT)				
	29.35	0.0	6065.00				
WETTED VOLUMES--	BODY	WING	TAILS	PODS	PYLONS	PONTOONS	TOTAL
	53625.75	3260.84	677.39	4696.76	148.71	0.0	62409.44

B-2

FINAL DESIGN

LCH_4 MACH 0.85

400 PASSENGER

10,190 km (5500 n.mi)

APP SPEED 72 m/s (140 kt)

TOFL 3200 m (10,500 ft)

COST SUMMARY

RDT AND E

	TOTAL *
DEVELOPMENT - NONRECURRING	
ENGINEERING	1119.41
TOOLING	647.43
TEST ARTICLES	61.48
DATA	0.0
SYSTEMS ENG/MNGMT	0.0
CRUISE ENGINE	0.0
LIFT ENGINE	0.0
FAN	0.0
AVIONICS	0.0
OTHER SYSTEMS	0.0
FACILITIES	0.0
TOTAL AIR VEHICLE	1828.31
INTEGR LOGISTICS SUPPORT	
PLANNING	11.57
TRAINING	3.93
HANDBOOKS	23.62
SSE	5.67
TOTAL ILS	44.79
TOTAL DVLPMNT-NONREC	1873.11
DEVELOPMENT - RECUR(PROTOTYPES)	
AIR VEHICLE	632.46
SPARES	121.74
TOTAL DVLPMNT-RECUR	754.19
GOVMNT DVLPMNT COST	0.0
TOTAL DVLPMNT COST	2627.30

PRODUCTION

	MATERIAL	LABOR	TOTAL PER PROD A/C**
STRUCTURE	4307.84	9346.62	13654.46
WING	1692.24	2707.76	4400.00
ROTOR	0.0	0.0	0.0
TAIL	130.14	319.39	449.53
BODY	1501.70	4656.22	6157.91
ALIGHTING GEAR	659.84	33.25	693.10
ENG SECT + NACELLE	323.92	1630.01	1953.92
ENG SECTION	0.0	0.0	0.0
NACELLE	275.60	1512.28	1787.88
AIR INDUCTION	48.31	117.72	166.04
PROPULSION	356.72	1270.00	1626.72
ENGINE INSTALL	0.0	24.99	24.99
THRUST REVERSER	0.0	1.80	1.80
EXHAUST SYSTEM	0.0	0.0	0.0
ENGINE CONTROLS	3.22	4.98	8.19
STARTING SYSTEM	33.74	6.15	39.88
PROPELLER INSTALL	0.0	0.0	0.0
LUBRICATING SYSTEM	0.0	0.0	0.0
FUEL SYSTEM	319.77	1232.08	1551.85
DRIVE SYS(PWR TRN)	0.0	0.0	0.0
SYSTEMS	2554.58	5812.60	8367.18
FLIGHT CONTROLS	712.04	519.13	1231.17
AUX POWER PLANT	123.94	21.81	145.75
INSTRUMENTS	96.13	90.66	186.80
HYDRAULIC + PNEUM	153.21	401.66	554.86
ELECTRICAL	402.77	1104.13	1506.90
AVIONIC INSTALL	29.95	324.32	354.27
ARMAMENT	0.0	0.0	0.0
FURN AND EQUIP	679.43	2890.90	3570.32
AIR CONDITIONING	337.32	434.51	771.83
ANTI-ICING	19.79	25.49	45.28
PHOTOGRAPHIC	0.0	0.0	0.0
LOAD AND HANDLING	0.0	0.0	0.0
SYSTEMS INTEGR	485.08	547.03	1032.12
TOTAL COST	7704.23	16976.24	24680.46
TOTAL HRS **		607.74	607.74
ENG CHANGE ORDERS			806.62
SUSTAINING ENG COST			1758.87
PROD TOOLING COST			1249.97
QUALITY ASSURANCE			2286.86
MISCELLANEOUS ***			790.35
TOTAL AIRFRAME COST			31573.10
ENGINE COST			6072.82
AVIONICS COST			750.89
TOTAL MANUFACTURING COST			38396.80
WARRANTY			192.38
TOTAL PRODUCTION COST			38589.17

PROCUREMENT

	PER PROD A/C**
TOTAL PRODUCTION	38589.17
INTEGR LOGISTICS SUPPORT	
PLANNING	30.83
TRAINING	10.48
TRAINERS	308.41
HANDBOOKS	41.14
FACILITIES	0.0
SSE - CFE	19.29
SSE - GFE	924.99
TOTAL ILS	1335.14
INITIAL SPARES COST	5632.32
PRODUCTION DEVELOPMENT	
ENGINEERING	346.70
TOOLING	150.55
ENGINES	0.0
TOTAL PROD DEV	497.25
TOTAL PROCUREMENT	46053.87

* - MILLIONS OF DOLLARS

** -1000 OF DOLLARS OR HOURS PER PROD A/C

*** - INCLUDES PROD DATA, SYSTEMS ENGR AND OTHER SYSTEMS

METHANE /88000 LB P/L / 5500 NMI RNG / M .85 MISS

T/C = 9.73 AR = 9.00 W/S = 135.0 T/W = 0.30

W E I G H T S T A T E M E N T

	WEIGHT(POUNDS)	WEIGHT FRACTION	(PERCENT)
GROSS WEIGHT	(488470.)		
FUEL AVAILABLE	152326.	FUEL	31.18
EXTERNAL	0.		
INTERNAL	152326.		
ZERO FUEL WEIGHT	336144.		
PAYLOAD	88000.	PAYLOAD	18.02
PASSENGERS	80000.		
BAGGAGE	0.		
CARGO	8000.		
STORES	0.		
OPERATIONAL EMPTY WEIGHT	248144.		
OPERATIONAL ITEMS	15774.	OPERATIONAL ITEMS	4.32
STANDARD ITEMS	5330.		
EMPTY WEIGHT	227039.		
STRUCTURE	135277.	STRUCTURE	27.69
WING	50015.		
ROTOR	0.		
TAIL	3969.		
BODY	52569.		
ALIGHTING GEAR	21125.		
ENGINE SECTION AND NACELLE	7600.		
PROPULSION	37311.	PROPULSION	7.64
CRUISE ENGINES	20003.		
LIFT ENGINES	0.		
THRUST REVERSER	1439.		
EXHAUST SYSTEM	0.		
ENGINE CONTROL	189.		
STARTING SYSTEM	340.		
PROPELLERS	0.		
LUBRICATING SYSTEM	0.		
FUEL SYSTEM	15341.		
DRIVE SYSTEM (POWER TRANS)	0.		
SYSTEMS	54451.		
FLIGHT CONTROLS	6028.		
AUXILIARY POWER PLANT	1116.		
INSTRUMENTS	1173.		
HYDRAULIC AND PNEUMATIC	3113.		
ELECTRICAL	5382.		
AVIONICS	2261.	SYSTEMS	11.15
ARMAMENT	0.		
FURNISHINGS AND EQUIPMENT	28492.		
AIR CONDITIONING	6504.		
ANTI-ICING	382.		
PHOTOGRAPHIC	0.		
LOAD AND HANDLING	0.		
		TOTAL	(100.)

M I S S I O N   S U M M A R Y

METHANE /88000 LB P/L / 5500 NMI RNG / M .85 MISS

SEGMENT	INIT ALTITUDE (FT)	INIT MACH NO	INIT WEIGHT (LB)	SEGMT FUEL (LB)	TOTAL FUEL (LB)	SEGMT DIST (N MI)	TOTAL DIST (N MI)	SEGMT TIME (MIN)	TOTAL TIME (MIN)	EXTERN STORE TAB ID	ENGINE THRUST TAB ID	EXTERN F TANK TAB ID	AVG L/D RATIO	AVG SFC (FF/T)	MAX OVER PRES
TAKEOFF POWER 1	0.	0.0	488470.	394.	394.	0.	0.	14.0	14.0	0.	395501.	0.	0.0	0.182	0.0
POWER 2	0.	0.0	488076.	496.	890.	0.	0.	1.0	15.0	0.	395402.	0.	0.0	0.251	0.0
CLIMB	0.	0.378	487580.	1971.	2861.	18.	18.	4.1	19.1	0.	395201.	0.	18.24	0.387	0.0
ACCEL	10000.	0.456	485609.	636.	3497.	8.	27.	1.4	20.5	0.	395201.	0.	17.92	0.434	0.0
CLIMB	10000.	0.638	484973.	8093.	11591.	195.	221.	24.1	44.6	0.	395201.	0.	17.06	0.498	0.0
CRUISE	37000.	0.850	476879.	114277.	125867.	5079.	5300.	624.7	669.4	0.	-395101.	0.	18.70	0.492	0.0
DESCENT	42000.	0.850	362603.	373.	126240.	58.	5358.	7.3	676.7	0.	312301.	0.	15.08	-0.309	0.0
DECEL	10000.	0.638	362229.	71.	126311.	6.	5364.	1.0	677.7	0.	312301.	0.	16.20	-0.322	0.0
DESCENT	10000.	0.456	362159.	387.	126697.	22.	5386.	5.0	682.7	0.	312301.	0.	18.24	-0.503	0.0
CRUISE	42000.	0.850	361772.	2251.	128948.	114.	5500.	14.0	696.7	0.	-395101.	0.	18.51	0.495	0.0
LOITER	1500.	0.350	359521.	904.	129852.	0.	5500.	6.0	702.7	0.	-395101.	0.	18.33	0.461	0.0
RESET	0.	0.0	358618.	0.	129852.	-5500.	0.	0.0	702.7	0.	0.	0.	0.0	0.0	0.0
RESET	0.	0.0	358618.	0.	129852.	0.	0.	0.0	702.7	0.	0.	0.	0.0	0.0	0.0
CRUISE	42000.	0.850	358618.	11089.	140941.	0.	0.	70.3	773.0	0.	-395101.	0.	18.45	0.495	0.0
TAKEOFF POWER 1	0.	0.0	347528.	0.	140941.	0.	0.	0.0	773.0	0.	395501.	0.	0.0	0.182	0.0
POWER 2	0.	0.0	347528.	496.	141437.	0.	0.	1.0	774.0	0.	395402.	0.	0.0	0.251	0.0
CLIMB	0.	0.378	347032.	1210.	142647.	11.	11.	2.5	776.5	0.	395201.	0.	17.90	0.387	0.0
ACCEL	10000.	0.456	345823.	179.	142826.	2.	13.	0.4	776.9	0.	395201.	0.	16.89	0.414	0.0
CLIMB	10000.	0.547	345643.	2623.	145449.	49.	63.	7.4	784.3	0.	395201.	0.	16.10	0.453	0.0
CRUISE	30000.	0.725	343020.	823.	146273.	37.	100.	5.2	789.6	0.	-395101.	0.	17.30	0.476	0.0
DESCENT	30000.	0.700	342196.	300.	146573.	37.	137.	5.6	795.2	0.	312301.	0.	15.96	-0.268	0.0
DECEL	10000.	0.547	341896.	37.	146610.	3.	140.	0.6	795.8	0.	312301.	0.	16.87	-0.359	0.0
DESCENT	10000.	0.456	341859.	308.	146917.	19.	159.	4.1	799.9	0.	312301.	0.	17.96	-0.487	0.0
CRUISE	30000.	0.720	341552.	906.	147824.	41.	200.	5.8	805.7	0.	-395101.	0.	17.36	0.474	0.0
LOITER	1500.	0.330	340645.	4299.	152122.	0.	200.	30.0	835.7	0.	-395101.	0.	18.26	0.464	0.0
CRUISE	1500.	0.378	336347.	301.	152423.	0.	200.	2.0	837.7	0.	-395101.	0.	18.10	0.487	0.0

WTO = 488469.9   FUEL A=152326.3   FUEL R=152423.4

METHANE /88000 LB P/L / 5500 NMI RNG / M .85 MISS

T/C = 9.73 AR = 9.00 W/S = 135.0 T/W = 0.30

W E I G H T   S T A T E M E N T

	WEIGHT(POUNDS)
GROSS WEIGHT	(488470.)
FUEL AVAILABLE	152326.
EXTERNAL	0.
INTERNAL	152326.
ZERO FUEL WEIGHT	336144.
PAYLOAD	88000.
PASSENGERS	80000.
BAGGAGE	0.
CARGO	8000.
STORES	0.
OPERATIONAL EMPTY WEIGHT	248144.
OPERATIONAL ITEMS	15774.
STANDARD ITEMS	5330.
EMPTY WEIGHT	227039.
STRUCTURE	135277.
WING	50015.
ROTOR	0.
TAIL	3969.
BODY	52569.
ALIGHTING GEAR	21125.
ENGINE SECTION AND NACELLE	7600.
PROPULSION	37311.
CRUISE ENGINES	20003.
LIFT ENGINES	0.
THRUST REVERSER	1439.
EXHAUST SYSTEM	0.
ENGINE CONTROL	189.
STARTING SYSTEM	340.
PROPELLERS	0.
LUBRICATING SYSTEM	0.
FUEL SYSTEM	15341.
DRIVE SYSTEM (POWER TRANS)	0.
SYSTEMS	54451.
FLIGHT CONTROLS	6028.
AUXILIARY POWER PLANT	1116.
INSTRUMENTS	1173.
HYDRAULIC AND PNEUMATIC	3113.
ELECTRICAL	5382.
AVIONICS	2261.
ARMAMENT	0.
FURNISHINGS AND EQUIPMENT	28492.
AIR CONDITIONING	6504.
ANTI-ICING	382.
PHOTOGRAPHIC	0.
LOAD AND HANDLING	0.

WEIGHT FRACTION	(PERCENT)
FUEL	31.18
PAYLOAD	18.02
OPERATIONAL ITEMS	4.32
STRUCTURE	27.69
PROPULSION	7.64
SYSTEMS	11.15
TOTAL	(1C0.)

SUMMARY ID NO. 1 **A S S E T   P A R A M E T R I C   A N A L Y S I S** FEBRUARY 14 1979

AIRCRAFT MODEL --CL1341-1-1
I.O.C. DATE --1995
DESIGN SPEED --SUBSONIC

ENGINE I.D. -- 395000
SLS SCALE 1.0 = 33000
NUMBER OF ENGINES = 4.

WING QUARTER CHORD SWEEP = 30.00 DEG
WING TAPER RATIO = 0.300

1 W/S	135.0	0.0	0.0	0.0	0.0	0.0	0.0	0.0	0.0	0.0	0.0	0.0	0.0	0.0	0.0	0.0
2 T/W	0.297	0.0	0.0	0.0	0.0	0.0	0.0	0.0	0.0	0.0	0.0	0.0	0.0	0.0	0.0	0.0
3 AR	9.00	0.0	0.0	0.0	0.0	0.0	0.0	0.0	0.0	0.0	0.0	0.0	0.0	0.0	0.0	0.0
4 T/C	9.73	0.0	0.0	0.0	0.0	0.0	0.0	0.0	0.0	0.0	0.0	0.0	0.0	0.0	0.0	0.0
5 SWEEP	30.00	0.0	0.0	0.0	0.0	0.0	0.0	0.0	0.0	0.0	0.0	0.0	0.0	0.0	0.0	0.0
6 FPR	0.0	0.0	0.0	0.0	0.0	0.0	0.0	0.0	0.0	0.0	0.0	0.0	0.0	0.0	0.0	0.0
7 OPR	0.0	0.0	0.0	0.0	0.0	0.0	0.0	0.0	0.0	0.0	0.0	0.0	0.0	0.0	0.0	0.0
8 TIT	0.	0.	0.	0.	0.	0.	0.	0.	0.	0.	0.	0.	0.	0.	0.	0.
9 NPR	0.0	0.0	0.0	0.0	0.0	0.0	0.0	0.0	0.0	0.0	0.0	0.0	0.0	0.0	0.0	0.0
10 AUG T	0.	0.	0.	0.	0.	0.	0.	0.	0.	0.	0.	0.	0.	0.	0.	0.
11 RADIUS N. MI	5500	0	0	0	0	0	0	0	0	0	0	0	0	0	0	0
12 GROSS WEIGHT	488470	0	0	0	0	0	0	0	0	0	0	0	0	0	0	0
13 FUEL WEIGHT	152326	0	0	0	0	0	0	0	0	0	0	0	0	0	0	0
14 OP. WT. EMPTY	248144	0	0	0	0	0	0	0	0	0	0	0	0	0	0	0
15 ZERO FUEL WT.	336144	0	0	0	0	0	0	0	0	0	0	0	0	0	0	0
16 THRUST/ENGINE	36269	0	0	0	0	0	0	0	0	0	0	0	0	0	0	0
17 ENGINE SCALE	1.099	0.0	0.0	0.0	0.0	0.0	0.0	0.0	0.0	0.0	0.0	0.0	0.0	0.0	0.0	0.0
18 WING AREA	3618.	0.	0.	0.	0.	0.	0.	0.	0.	0.	0.	0.	0.	0.	0.	0.
19 WING SPAN	180.5	0.0	0.0	0.0	0.0	0.0	0.0	0.0	0.0	0.0	0.0	0.0	0.0	0.0	0.0	0.0
20 H. TAIL AREA	741.3	0.0	0.0	0.0	0.0	0.0	0.0	0.0	0.0	0.0	0.0	0.0	0.0	0.0	0.0	0.0
21 V. TAIL AREA	391.8	0.0	0.0	0.0	0.0	0.0	0.0	0.0	0.0	0.0	0.0	0.0	0.0	0.0	0.0	0.0
22 ENG. LENGTH	10.24	0.0	0.0	0.0	0.0	0.0	0.0	0.0	0.0	0.0	0.0	0.0	0.0	0.0	0.0	0.0
23 ENG. DIAMETER	6.98	0.0	0.0	0.0	0.0	0.0	0.0	0.0	0.0	0.0	0.0	0.0	0.0	0.0	0.0	0.0
24 BODY LENGTH	201.3	0.0	0.0	0.0	0.0	0.0	0.0	0.0	0.0	0.0	0.0	0.0	0.0	0.0	0.0	0.0
25 WING FUEL LIMIT	0.005	0.0	0.0	0.0	0.0	0.0	0.0	0.0	0.0	0.0	0.0	0.0	0.0	0.0	0.0	0.0
COST DATA																
26 RDTE - BIL.	2.627	0.0	0.0	0.0	0.0	0.0	0.0	0.0	0.0	0.0	0.0	0.0	0.0	0.0	0.0	0.0
27 FLYAWAY - MIL.	46.59	0.0	0.0	0.0	0.0	0.0	0.0	0.0	0.0	0.0	0.0	0.0	0.0	0.0	0.0	0.0
28 INVESTMNT-BIL.	1.071	0.0	0.0	0.0	0.0	0.0	0.0	0.0	0.0	0.0	0.0	0.0	0.0	0.0	0.0	0.0
29 DOC - C/SM	1.510	0.0	0.0	0.0	0.0	0.0	0.0	0.0	0.0	0.0	0.0	0.0	0.0	0.0	0.0	0.0
30 IOC - C/SM	1.284	0.0	0.0	0.0	0.0	0.0	0.0	0.0	0.0	0.0	0.0	0.0	0.0	0.0	0.0	0.0
31 ROI A.T. - 0/0	21.15	0.0	0.0	0.0	0.0	0.0	0.0	0.0	0.0	0.0	0.0	0.0	0.0	0.0	0.0	0.0
MISSION PARAMETERS																
32 MISN V1(1,1)	37000	0	0	0	0	0	0	0	0	0	0	0	0	0	0	0
33 MISN V2(1,1)	129852	0	0	0	0	0	0	0	0	0	0	0	0	0	0	0
34 MISN V1(2,1)	42000	0	0	0	0	0	0	0	0	0	0	0	0	0	0	0
35 MISN V2(2,1)	45972	0	0	0	0	0	0	0	0	0	0	0	0	0	0	0
CONSTRAINT OUTPUT																
36 TAKEOFF DST(1)	10433	0	0	0	0	0	0	0	0	0	0	0	0	0	0	0
37 CLIMB GRAD(1)	0.0792	0.0	0.0	0.0	0.0	0.0	0.0	0.0	0.0	0.0	0.0	0.0	0.0	0.0	0.0	0.0
38 TAKEOFF DST(2)	10336	0	0	0	0	0	0	0	0	0	0	0	0	0	0	0
39 CLIMB GRAD(2)	0.0300	0.0	0.0	0.0	0.0	0.0	0.0	0.0	0.0	0.0	0.0	0.0	0.0	0.0	0.0	0.0
40 CTOL LNDG D(1)	5761	0	0	0	0	0	0	0	0	0	0	0	0	0	0	0
41 AP SPEED-KT(1)	136.7	0.0	0.0	0.0	0.0	0.0	0.0	0.0	0.0	0.0	0.0	0.0	0.0	0.0	0.0	0.0
42 SEP(1) - FPS	9	0	0	0	0	0	0	0	0	0	0	0	0	0	0	0
43 SEP(2) - FPS	5	0	0	0	0	0	0	0	0	0	0	0	0	0	0	0

JETA /88000 LB P/L / 5500 NMI RNG / M .85 MISS

T/C=10.00 AR= 9.00 W/S=130.00 T/W=0.297

C O N F I G U R A T I O N   G E O M E T R Y

BASIC WING--

AREA(SQ FT)	SPAN(FT)	TAPER RATIO	C/4 SWEEP	L.E. SWEEP	MAC(FT)
3787.1	184.62	0.300	30.000	32.504	22.50

WING PANELS--

AREA(SQ FT)	EXP. AREA	AVG T/C	L.E. SWEEP	SFLE(SQ FT)	REF L(FT)
542.5	0.0	11.80	32.250	0.0	42.61
1739.3	1712.6	11.22	32.250	0.0	32.92
1911.3	1911.3	10.01	33.250	0.0	17.68
37.6	37.6	8.55	32.250	0.0	9.70

TOTAL WING--

AREA(SQ FT)	EFF AR	AVG T/C	CR(FT)	CT(FT)	MAC(FT)	L(FT)
4230.7	8.06	10.73	44.24	9.47	27.12	69.12

FUSELAGE--

LENGTH(FT)	S WET(SQ FT)	BWW(FT)	EQUIV D(FT)	SPI(SQ FT)
197.00	10519.5	13.39	21.36	358.40

BW(FT)	BH(FT)	SBW(SQ FT)
19.17	23.75	10519.50

HORZ. TAIL 1--

SHT1(SQ FT)	SHX1(SQ FT)	REF L1(FT)	L HT1(FT)	HT1 VOL COEF
728.49	541.58	13.18	101.35	0.8666

HORZ. TAIL 2--

SHT2(SQ FT)	SHX2(SQ FT)	REF L2(FT)	L HT2(FT)	HT2 VOL COEF
0.0	0.0	0.0	197.00	0.0

VERT. TAIL 1--

SVT1(SQ FT)	SVX1(SQ FT)	REF L1(FT)	L VT1(FT)	VT1 VOL COEF
340.93	340.93	16.01	97.15	0.0474

VERT. TAIL 2--

SVT2(SQ FT)	SVX2(SQ FT)	REF L2(FT)	L VT2(FT)	VT2 VOL COEF
0.0	0.0	0.0	197.00	0.0

PROPULSION--

ENG L(FT)	ENG D(FT)	POD L(FT)	POD D(FT)	POD S WET	NO. PODS	INLET L(FT)
10.26	7.01	18.14	8.76	1997.83	4.	0.0

FUEL TANKS--

WING(CU FT)	BOX(CU FT)	FUS(CU FT)
3658.03	846.62	99999.00

WETTED VOLUMES--

BODY	WING	TAILS	PODS	PYLONS	PONTOONS	TOTAL
53441.25	4896.84	616.20	4376.20	83.76	0.0	63414.25

<u>B-3</u>

FINAL DESIGN

JET A MACH 0.85

400 PASSENGER

10,190 km (5500 n.mi.)

APP SPEED 72 m/s (140 Kt)

TOFL 3200 m (10,500 ft)

JETA /88000 LB P/L / 5500 NMI RNG / M .85 MISS

T/C=10.00 AR= 9.00 W/S=130.00 T/W=0.297

W E I G H T   S T A T E M E N T

	WEIGHT(POUNDS)	WEIGHT FRACTION	(PERCENT)
GROSS WEIGHT	(492318.)		
FUEL AVAILABLE	179698.	FUEL	36.50
EXTERNAL	0.		
INTERNAL	179699.		
ZERO FUEL WEIGHT	312620.		
PAYLOAD	88000.	PAYLOAD	17.87
PASSENGERS	80000.		
BAGGAGE	0.		
CARGO	8000.		
STORES	0.		
OPERATIONAL EMPTY WEIGHT	224620.		
OPERATIONAL ITEMS	15776.	OPERATIONAL ITEMS	3.98
STANDARD ITEMS	3833.		
EMPTY WEIGHT	205011.		
STRUCTURE	126129.	STRUCTURE	25.62
WING	49200.		
ROTOR	0.		
TAIL	3796.		
BODY	44180.		
ALIGHTING GEAR	21291.		
ENGINE SECTION AND NACELLE	7662.		
PROPULSION	24364.	PROPULSION	4.95
CRUISE ENGINES	20160.		
LIFT ENGINES	0.		
THRUST REVERSER	1447.		
EXHAUST SYSTEM	0.		
ENGINE CONTROL	190.		
STARTING SYSTEM	343.		
PROPELLERS	0.		
LUBRICATING SYSTEM	0.		
FUEL SYSTEM	2224.		
DRIVE SYSTEM (POWER TRANS)	0.		
SYSTEMS	54518.	SYSTEMS	11.07
FLIGHT CONTROLS	6069.		
AUXILIARY POWER PLANT	1116.		
INSTRUMENTS	1172.		
HYDRAULIC AND PNEUMATIC	3135.		
ELECTRICAL	5381.		
AVIONICS	2261.		
ARMAMENT	0.		
FURNISHINGS AND EQUIPMENT	28492.		
AIR CONDITIONING	6504.		
ANTI-ICING	387.		
PHOTOGRAPHIC	0.		
LOAD AND HANDLING	0.		
		TOTAL	(100.)

COST SUMMARY

RDT AND E

	TOTAL *
DEVELOPMENT - NONRECURRING	
ENGINEERING	1014.62
TOOLING	588.40
TEST ARTICLES	54.69
DATA	0.0
SYSTEMS ENG/MNGMT	0.0
CRUISE ENGINE	0.0
LIFT ENGINE	0.0
FAN	0.0
AVIONICS	0.0
OTHER SYSTEMS	0.0
FACILITIES	0.0
TOTAL AIR VEHICLE	1657.71
INTEGR LOGISTICS SUPPORT	
PLANNING	10.94
TRAINING	3.72
HANDBOOKS	22.95
SSE	5.36
TOTAL ILS	42.98
TOTAL DVLPMNT-NONREC	1700.69
DEVELOPMENT - RECUR(PROTOTYPES)	
AIR VEHICLE	569.15
SPARES	109.84
TOTAL DVLPMNT-RECUR	678.99
GOVMNT DVLPMNT COST	0.0
TOTAL DVLPMNT COST	2379.68

PRODUCTION

	MATERIAL	LABOR	TOTAL PER PROD A/C**
STRUCTURE	4019.97	8518.75	12538.72
WING	1667.14	2679.70	4346.84
ROTOR	0.0	0.0	0.0
TAIL	124.67	307.34	432.01
BODY	1235.14	3845.13	5080.27
ALIGHTING GEAR	666.03	33.72	699.74
ENG SECT + NACELLE	327.00	1652.87	1979.86
ENG SECTION	0.0	0.0	0.0
NACELLE	278.18	1533.39	1811.57
AIR INDUCTION	48.81	119.48	168.29
PROPULSION	127.76	142.44	270.20
ENGINE INSTALL	0.0	25.34	25.34
THRUST REVERSER	0.0	1.82	1.82
EXHAUST SYSTEM	0.0	0.0	0.0
ENGINE CONTROLS	3.25	5.05	8.29
STARTING SYSTEM	34.05	6.23	40.29
PROPELLER INSTALL	0.0	0.0	0.0
LUBRICATING SYSTEM	0.0	0.0	0.0
FUEL SYSTEM	90.46	104.00	194.46
DRIVE SYS(PWR TRN)	0.0	0.0	0.0
SYSTEMS	2564.44	5854.12	8418.55
FLIGHT CONTROLS	717.90	525.77	1243.67
AUX POWER PLANT	124.13	21.94	146.07
INSTRUMENTS	96.26	91.19	187.45
HYDRAULIC + PNEUM	154.54	406.97	561.51
ELECTRICAL	403.26	1110.49	1513.74
AVIONIC INSTALL	30.00	326.27	356.27
ARMAMENT	0.0	0.0	0.0
FURN AND EQUIP	680.43	2908.32	3588.75
AIR CONDITIONING	337.82	437.13	774.94
ANTI-ICING	20.11	26.03	46.14
PHOTOGRAPHIC	0.0	0.0	0.0
LOAD AND HANDLING	0.0	0.0	0.0
SYSTEMS INTEGR	438.67	496.94	935.61
TOTAL COST	7150.83	15012.25	22163.07
TOTAL HRS **		537.43	537.43
ENG CHANGE ORDERS			723.44
SUSTAINING ENG COST			1633.88
PROD TOOLING COST			1105.36
QUALITY ASSURANCE			2022.29
MISCELLANEOUS ***			698.91
TOTAL AIRFRAME COST			28346.93
ENGINE COST			5689.02
AVIONICS COST			750.89
TOTAL MANUFACTURING COST			34786.83
WARRANTY			173.02
TOTAL PRODUCTION COST			34959.84

PROCUREMENT

	PER PROD A/C**
TOTAL PRODUCTION	34959.84
INTEGR LOGISTICS SUPPORT	
PLANNING	29.52
TRAINING	10.04
TRAINERS	308.41
HANDBOOKS	40.30
FACILITIES	0.0
SSE - CFE	17.48
SSE - GFE	924.99
TOTAL ILS	1330.73
INITIAL SPARES COST	5133.88
PRODUCTION DEVELOPMENT	
ENGINEERING	331.98
TOOLING	252.92
ENGINES	0.0
TOTAL PROD DEV	584.90
TOTAL PROCUREMENT	42009.32

* - MILLIONS OF DOLLARS

** -1000 OF DOLLARS OR HOURS PER PROD A/C

*** - INCLUDES PROD DATA, SYSTEMS ENGR AND OTHER SYSTEMS

MISSION SUMMARY

JETA /88000 LB P/L / 5500 NMI RNG / M .85 MISS

SEGMENT	INIT ALTITUDE (FT)	INIT MACH NO	INIT WEIGHT (LB)	SEGMT FUEL (LB)	TOTAL FUEL (LB)	SEGMT DIST (N MI)	TOTAL DIST (N MI)	SEGMT TIME (MIN)	TOTAL TIME (MIN)	EXTERN STORE TAB ID	ENGINE THRUST TAB ID	EXTERN F TANK TAB ID	AVG L/D RATIO	AVG SFC (FF/T)	MAX OVER FRES
TAKEOFF POWER 1	0.	0.0	492318.	1707.	1707.	0.	0.	14.0	14.0	0.	315501.	0.	0.0	0.780	0.0
POWER 2	0.	0.0	490612.	688.	2394.	0.	0.	1.0	15.0	0.	315401.	0.	0.0	0.304	0.0
CLIMB	0.	0.378	489924.	2368.	4762.	18.	18.	4.0	19.0	0.	315201.	0.	18.93	0.474	0.0
ACCEL	10000.	0.456	487556.	767.	5529.	8.	26.	1.4	20.4	0.	315201.	0.	18.31	0.531	0.0
CLIMB	10000.	0.638	486789.	10152.	15681.	202.	229.	25.1	45.5	0.	315201.	0.	17.37	0.608	0.0
CRUISE	38000.	0.850	476637.	133412.	149093.	5071.	5300.	623.8	669.3	0.	-315101.	0.	19.00	0.600	0.0
DESCENT	42000.	0.850	343225.	353.	149447.	55.	5355.	7.0	676.3	0.	312301.	0.	14.62	-0.305	0.0
DECEL	10000.	0.638	342872.	67.	149514.	6.	5361.	1.0	677.3	0.	312301.	0.	15.91	-0.316	0.0
DESCENT	10000.	0.456	342804.	375.	149888.	22.	5383.	4.9	682.3	0.	312301.	0.	18.27	-0.493	0.0
CRUISE	42000.	0.850	342430.	2654.	152543.	117.	5500.	14.4	696.6	0.	-315101.	0.	18.59	0.603	0.0
LOITER	1500.	0.335	339775.	1064.	153607.	0.	5500.	6.0	702.6	0.	-315101.	0.	18.83	0.591	0.0
RESET	0.	0.0	338711.	0.	153607.	-5500.	0.	0.0	702.6	0.	0.	0.	0.0	0.0	0.0
RESET	0.	0.0	338711.	0.	153607.	0.	0.	0.0	702.6	0.	0.	0.	0.0	0.0	0.0
CRUISE	42000.	0.850	338711.	12731.	166338.	0.	0.	70.3	772.9	0.	-315101.	0.	18.46	0.604	0.0
TAKEOFF POWER 1	0.	0.0	325980.	0.	166338.	0.	0.	0.0	772.9	0.	315501.	0.	0.0	0.780	0.0
POWER 2	0.	0.0	325980.	688.	167026.	0.	0.	1.0	773.9	0.	315401.	0.	0.0	0.304	0.0
CLIMB	0.	0.378	325292.	1357.	168382.	10.	10.	2.3	776.2	0.	315201.	0.	17.81	0.474	0.0
ACCEL	10000.	0.456	323935.	201.	168583.	2.	12.	0.4	776.6	0.	315201.	0.	16.58	0.507	0.0
CLIMB	10000.	0.547	323735.	2887.	171470.	44.	56.	6.6	783.1	0.	315201.	0.	15.65	0.554	0.0
CRUISE	30000.	0.700	320848.	1126.	172596.	44.	100.	6.4	789.5	0.	-315101.	0.	17.53	0.578	0.0
DESCENT	30000.	0.700	319722.	283.	172879.	36.	136.	5.4	794.9	0.	312301.	0.	15.49	-0.262	0.0
DECEL	10000.	0.547	319438.	35.	172914.	3.	138.	0.5	795.4	0.	312301.	0.	16.54	-0.352	0.0
DESCENT	10000.	0.456	319404.	294.	173208.	18.	156.	4.8	799.4	0.	312301.	0.	17.79	-0.478	0.0
CRUISE	30000.	0.700	319109.	1115.	174323.	44.	200.	6.4	805.8	0.	-315101.	0.	17.49	0.578	0.0
LOITER	1500.	0.323	317994.	5023.	179346.	0.	200.	30.0	835.8	0.	-315101.	0.	18.74	0.597	0.0
CRUISE	1500.	0.378	312971.	366.	179712.		800	2.0	837.8	0.	-315101.	0.	17.97	0.630	0.0

WTO = 492318.3 FUEL A=179698.1 FUEL R=179711.6

SUMMARY ID NO. 1 — **A S S E T   P A R A M E T R I C   A N A L Y S I S** — JUNE 01 1979

AIRCRAFT MODEL --CL1317-4-1
I.O.C. DATE --1995
DESIGN SPEED --SUBSONIC

ENGINE I.D. -- 315000
SLS SCALE 1.0 = 33000
NUMBER OF ENGINES = 4.

WING QUARTER CHORD SWEEP = 30.00 DEG
WING TAPER RATIO = 0.300

1 W/S	130.0	0.0	0.0	0.0	0.0	0.0	0.0	0.0	0.0	0.0	0.0	0.0	0.0	0.0	0.0	0.0
2 T/W	0.297	0.0	0.0	0.0	0.0	0.0	0.0	0.0	0.0	0.0	0.0	0.0	0.0	0.0	0.0	0.0
3 AR	9.00	0.0	0.0	0.0	0.0	0.0	0.0	0.0	0.0	0.0	0.0	0.0	0.0	0.0	0.0	0.0
4 T/C	10.00	0.0	0.0	0.0	0.0	0.0	0.0	0.0	0.0	0.0	0.0	0.0	0.0	0.0	0.0	0.0
5 SWEEP	30.00	0.0	0.0	0.0	0.0	0.0	0.0	0.0	0.0	0.0	0.0	0.0	0.0	0.0	0.0	0.0
6 FPR	0.0	0.0	0.0	0.0	0.0	0.0	0.0	0.0	0.0	0.0	0.0	0.0	0.0	0.0	0.0	0.0
7 OPR	0.0	0.0	0.0	0.0	0.0	0.0	0.0	0.0	0.0	0.0	0.0	0.0	0.0	0.0	0.0	0.0
8 TIT	0.	0.	0.	0.	0.	0.	0.	0.	0.	0.	0.	0.	0.	0.	0.	0.
9 NPR	0.0	0.0	0.0	0.0	0.0	0.0	0.0	0.0	0.0	0.0	0.0	0.0	0.0	0.0	0.0	0.0
10 AUG T	0.	0.	0.	0.	0.	0.	0.	0.	0.	0.	0.	0.	0.	0.	0.	0.
11 RADIUS N. MI	5500	0	0	0	0	0	0	0	0	0	0	0	0	0	0	0
12 GROSS WEIGHT	492318	0	0	0	0	0	0	0	0	0	0	0	0	0	0	0
13 FUEL WEIGHT	179698	0	0	0	0	0	0	0	0	0	0	0	0	0	0	0
14 OP. WT. EMPTY	224620	0	0	0	0	0	0	0	0	0	0	0	0	0	0	0
15 ZERO FUEL WT.	312620	0	0	0	0	0	0	0	0	0	0	0	0	0	0	0
16 THRUST/ENGINE	36555	0	0	0	0	0	0	0	0	0	0	0	0	0	0	0
17 ENGINE SCALE	1.108	0.0	0.0	0.0	0.0	0.0	0.0	0.0	0.0	0.0	0.0	0.0	0.0	0.0	0.0	0.0
18 WING AREA	3787.	0.	0.	0.	0.	0.	0.	0.	0.	0.	0.	0.	0.	0.	0.	0.
19 WING SPAN	184.6	0.0	0.0	0.0	0.0	0.0	0.0	0.0	0.0	0.0	0.0	0.0	0.0	0.0	0.0	0.0
20 H. TAIL AREA	728.5	0.0	0.0	0.0	0.0	0.0	0.0	0.0	0.0	0.0	0.0	0.0	0.0	0.0	0.0	0.0
21 V. TAIL AREA	340.9	0.0	0.0	0.0	0.0	0.0	0.0	0.0	0.0	0.0	0.0	0.0	0.0	0.0	0.0	0.0
22 ENG. LENGTH	10.26	0.0	0.0	0.0	0.0	0.0	0.0	0.0	0.0	0.0	0.0	0.0	0.0	0.0	0.0	0.0
23 ENG. DIAMETER	7.01	0.0	0.0	0.0	0.0	0.0	0.0	0.0	0.0	0.0	0.0	0.0	0.0	0.0	0.0	0.0
24 BODY LENGTH	197.0	0.0	0.0	0.0	0.0	0.0	0.0	0.0	0.0	0.0	0.0	0.0	0.0	0.0	0.0	0.0
25 WING FUEL LIMIT	1.253	0.0	0.0	0.0	0.0	0.0	0.0	0.0	0.0	0.0	0.0	0.0	0.0	0.0	0.0	0.0
COST DATA																
26 RDTE - BIL.	2.380	0.0	0.0	0.0	0.0	0.0	0.0	0.0	0.0	0.0	0.0	0.0	0.0	0.0	0.0	0.0
27 FLYAWAY - MIL.	42.34	0.0	0.0	0.0	0.0	0.0	0.0	0.0	0.0	0.0	0.0	0.0	0.0	0.0	0.0	0.0
28 INVESTMNT-BIL.	0.976	0.0	0.0	0.0	0.0	0.0	0.0	0.0	0.0	0.0	0.0	0.0	0.0	0.0	0.0	0.0
29 DOC - C/SM	1.611	0.0	0.0	0.0	0.0	0.0	0.0	0.0	0.0	0.0	0.0	0.0	0.0	0.0	0.0	0.0
30 IOC - C/SM	1.293	0.0	0.0	0.0	0.0	0.0	0.0	0.0	0.0	0.0	0.0	0.0	0.0	0.0	0.0	0.0
31 ROI A.T. - O/O	21.64	0.0	0.0	0.0	0.0	0.0	0.0	0.0	0.0	0.0	0.0	0.0	0.0	0.0	0.0	0.0
MISSION PARAMETERS																
32 MISN V1(1,1)	38000	0	0	0	0	0	0	0	0	0	0	0	0	0	0	0
33 MISN V2(1,1)	153607	0	0	0	0	0	0	0	0	0	0	0	0	0	0	0
CONSTRAINT OUTPUT																
34 TAKEOFF DST(1)	10482	0	0	0	0	0	0	0	0	0	0	0	0	0	0	0
35 CLIMB GRAD(1)	0.0846	0.0	0.0	0.0	0.0	0.0	0.0	0.0	0.0	0.0	0.0	0.0	0.0	0.0	0.0	0.0
36 TAKEOFF DST(2)	9352	0	0	0	0	0	0	0	0	0	0	0	0	0	0	0
37 CLIMB GRAD(2)	0.0366	0.0	0.0	0.0	0.0	0.0	0.0	0.0	0.0	0.0	0.0	0.0	0.0	0.0	0.0	0.0
38 CTOL LNDG D(1)	5356	0	0	0	0	0	0	0	0	0	0	0	0	0	0	0
39 AP SPEED-KT(1)	129.9	0.0	0.0	0.0	0.0	0.0	0.0	0.0	0.0	0.0	0.0	0.0	0.0	0.0	0.0	0.0
40 SEP(1) - FPS	10	0	0	0	0	0	0	0	0	0	0	0	0	0	0	0
41 SEP(2) - FPS	6	0	0	0	0	0	0	0	0	0	0	0	0	0	0	0

REFERENCES

1. Hubbert, M. King, "The Energy Resources of the Earth," Scientific American, September 1971, p. 149.

2. Parent, Joseph D., "A Survey of U.S. and Total World Production, Proved Reserves and Remaining Recoverable Reserves of Fossil Fuels and Uranium," Institute of Gas Technology, Chicago, March 1979.

3. Brewer, G.D. et al., "Study of the Application of Hydrogen Fuel to Long Range Subsonic Transport Aircraft," NASA CR-132559 by Lockheed-California Company and Lockheed-Georgia Company under contract NAS 1-12972, January 1975.

4. Brewer, G.D. et al., "Study of Fuel Systems for LH_2 Fueled Subsonic Transport Aircraft," NASA CR-145369 by Lockheed-California Company under contract NAS 1-14614, July 1978.

5. Brewer, G.D., et al., "LH_2 Airport Requirements Study," NASA CR-2700 by Lockheed-California Company under contract NAS 1-14137, March 1976.

6. Brewer, G.D. and Morris, R.E., "Study of LH_2 Fueled Subsonic Passenger Transport Aircraft," NASA CR-144935 by Lockheed-California under contract NAS 1-12972 (MOD 4), January 1976.

7. Eisenberg, J.D. and Chambellan, R.E., "Tankage Systems for a Methane-Fueled Supersonic Transport," NASA Technical Memorandum NASA TMX-1591, Cleveland: Lewis Research Center, May 1968.

8. Horeff, T.G., Presented to the FAA Special Aviation Fire and Explosion Advisory Committee (SAFER Committee) at the Aerospace Corporation, El Segundo, Calif., on 5 March 1980.

9. Louthan, M.R., Caskey, G.R., Hydrogen Transport and Embrittlement in Structural Metals. First World Hydrogen Energy Conference, Miami Beach, Florida, Paper DP-MS-75-54X, Volume 1, March 1976.

10. Gray, H.R., et al, Potential Structural Material Problems in a Hydrogen Energy System. First World Hydrogen Energy Conference, Miami Beach, Florida, Volume 1, March 1976.

11. Anonymous, Engineering Structural Life-Assurance Manual, Lockheed-California Company, latest revision date - April 15, 1980.

12. Roark, R.J., Formulas for Stress and Strain, Third Edition, McGraw-Hill Book Company, Inc., 1954.

13. Anonymous, Engineering Stress Memo Manual, Lockheed-California Company, latest revision date - Dec. 8, 1978.

14. Maddux, G.E., et al, Stress Analysis Manual, AFFDL-TR-69-42, Feb. 1970.

15. Timoshenko, S.P., and Gere, J.M.: Theory of Elastic Stability. Second Edition, McGraw-Hill Book Company, Inc., 1961.

16. Shanley, F.R.: Weight-Strength Analysis of Aircraft Structures. Second Edition, Dover Publications, Inc., 1960.

17. Pleban, E.J., "Analytical Heat Transfer Investigation of Insulated Liquid Methane Tanks for Supersonic Cruise Aircraft," NASA TN D-5641 (1970).

18. Johnson, V.J., ed., "A Compendium of the Properties of Materials at Low Temperature," WADD Technical Report 60-56 Part II, Wright Air Development Division, Wright-Patterson Air Force Base (Oct 1960).

19. Sindt, C.F., et al., "Slush and Boiling Methane Characterization," NBS Report 9758, U.S. Dept. of Commerce, National Bureau of Standards (1970).

20. Parmley, R.T.,: Handbook of Thermal Design Data for Multilayer Insulation Systems. LMSC A847882, Vol. II, Contract NAS 8-20353, Lockheed Missiles and Space Company, Inc. (June 1967).

21. Childs, G.E.; et al: Thermal Conductivity of Solids at Room Temperature and Below. NBS Monograph 131, National Bureau of Standards, U.S. Department of Commerce (Sept. 1973).

22. Barker, H.H.; et al: Internal Insulation Systems for LH_2 Tanks - Gas Layer and Reinforced Foam. Proceedings Space Transportation System Propulsion Technology Conference, Vol IV, NASA George C. Marshall Space Flight Center (April 1971) pp 1455-1480.

23. Tatro, R.E. and Bennett, F.O. Jr, "Internal Insulation for LNG," Advances in Cryogenic Engineering, Vol. 20, Plenum Press, New York (1975) pp 315-326.

24. Yates, G.B. and Tatro, R.E.: PPO Foam Internal Insulation. Proceedings Space Transportation System Propulsion Technology Conference, Vol IV. NASA George C. Marshall Space Flight Center (April 1971) pp 1439-1452.

25. Barber, J.R.: Cryogenic Insulation Technology Review for the Space Shuttle. NASA TMX-52876, Vol V (July 1974) pp 146-166.

26. Cunnington, G.R., and Tien, C.L.: Advances in Cryogenic Engineering, Vol 22, Plenum Press, New York (1976) pp 263.

27. --: Development and Design Application of Rigidized Surface Insulation Thermal Protection Systems. LMSC D282673, Vol. I, Contract NAS 9-12856, Lockheed Missiles and Space Company, Inc. (Dec. 1972).

28. Harper, E.Y., et al: Analytical and Experimental Study of Stratification and Liquid Ullage Coupling. LMSC 2-05-65-1, Contract NAS 8-11525, Lockheed Missile and Space Company, Inc. (Aug. 1965).

29. Harper, E.A., Rust, J.R. and Dean, L.E., "Trouble Free LNG or An Improved Cascade Liquefaction Cycle," Bartlesville, Oklahoma: Phillips Petroleum Co., n.d.

30. Speir, G.A., "Indonesia's Badak LNG Project Sets New Records," Pipeline and Gas Journal, 22-24 (1978) June.

31. Swenson, L.K. and Peterson, J.L., "The Pritchard Mixed Refrigerant Process," Session II Paper 1, the The third International Conference and Exhibition on Liquefied Natural Gas, Washington, D.D., September 24-28, 1972.

32. "Scorecard," Pipeline and Gas Journal, 19-21 (1978) June.

33. Anderson, P.J. and Daniels, E.J., "The LNG Industry: Past, Present, Future," IGT Project 8988 Final Report to the U.S. Energy Research and Development Administration, Chicago: Institute of Gas Technology, July 1977.

34. Kao, R.L., Waterman, W.W. and Bukacek, R.F., "Computer Simulation of LNG Cycles," Chicago: Institute of Gas Technology, n.d.

35. Culbertson, L. and Emery, W.B., "Liquefaction Plant Experience at Kenai," Session V Paper 7, Third International Conference and Exhibition on Liquefied Natural Gas, Washington, D.C., September 24-28, 1972.

36. Dolle, J. and Gilbourne, D., "LNG: Startup of the Skikda LNG Plant," Chemical Engineering Progress, 39-43 (1976) January.

37. Chatterjee, N., Gaumer, L.S. and Geist, J.M., "Operational Flexibility of LNG Plants Using the Propane Precooled Multicomponent Refrigerant MCR® Process," Session II Paper 3, Fifth International Conference on Liquefied Natural Gas, Dusseldorf, Germany, August 29, 1977 - September 1, 1977.

38. Jenkins, J.E., Friesman, F. and Prew, L.R., "Early Operating Experience with the Brunei - Japan LNG Project," Session II Paper 2, Fourth International Conference on Liquefied Natural Gas, Algiers, Algeria, June 24-27, 1974.

39. Ploum, A.J.W., "The Brunei Liquefied Natural Gas Plant," Session II Paper 1, Fifth International Conference on Liquefied Natural Gas, Dusseldorf, Germany, August 29, 1977 - September 1, 1977.

40. Swearingen, J.S., "Design Consideration in LNG Expansion Liquefaction Cycles," Reprint from Oil and Gas Journal, (1969) October 6.

41. Horn, J., Tucher, P.W. and Emery, W.B., II, "Alaska to Japan LNG Project - Kenai Revisited," Session II, Paper 1, Fourth International Conference on Liquefied Natural Gas, Algiers, Algeria, June 24-27, 1974.

42. Stokes, E.C., "Abu Dhabi Facility 'On Stream'," Pipeline and Gas Journal, 41-46 (1977) August.

43. Stebbing, R. and O'Brien, J., "An Up-dated Report on the Prico Process for LNG Plants," Gastech 75 Proceeding, 151-153, Paris, France, September 30- October 3, 1975.

44. Elliott Company, Division of Carrier Corporation, "Large Gas Compressors: A State-of-the-Art Report," Reprint 118, Jeannette, Pennsylvania, February 1973.

45. Elliott Company, Division of Carrier Corporation, "Turbines - With Known Components," Reprint 123, Jeannette, Pennsylvania, February 1973.

46. Naegeli, J.P., Spechtenhauser, A. and Aicher, W., "Turbomachinery in Base Load Natural Gas Liquefaction Plants," Paper No. IGU/A23-73, 12th World Gas Conference, Nice, France, 1973.

47. Tanner, A.L. *et al.*, "Economic Comparison of Compressor Drivers for LNG Plants," Session III Paper 7, Fourth International Conference on Liquefied Natural Gas, Algiers, Algeria, June 24-27, 1974.

48. Hallock, D.C., Farber, R.M. and Davis, C.C., "Compressors and Drivers for Base Load LNG Plants," AIChE Reprint 10a. Presented at the 71st National Meeting, American Institute of Chemical Engineers, Dallas, Texas, February 21, 1972.

49. Dodge, B.F., "Comparison of Expander and Cascade Cycles for LNG," Reprint from Oil and Gas Journal, (1972) June 12.

50. Sarkes, L.A. and Mann, D.B., "A Survey of LNG Technological Needs in the U.S.A. 1974 to Beyond 2000," Session VII Paper 1, Fourth International Conference on Liquefied Natural Gas, Algiers, Algeria, June 24-27, 1974.

51. Swearingen Brothers, Inc., Affiliate of Rotoflow Corporation, "Rotoflow Expander Turbines for Methane Liquefaction," Los Angeles, n.d.

52. Daniels, E.J. and Anderson, P.J., "Economic Considerations and Operating History of Base-Load LNG Projects." Paper presented at the West Coast LNG Symposium, Nedlands, West Australia, December 15-16, 1977.

53. DiNapoli, R.N., "Capital and Operating Costs in Base Load LNG Projects." Paper presented at the LNG Fundamentals Course, Chicago: Institute of Gas Technology, October 20, 1978.

54. American Gas Association, LNG Information Book, 1973. Arlington, Virginia, 1974.

55. Murphy, M.V.K., Rao, R.V.S. and Srinirasa, K., "Dimensioning of Cryogenic Transfer Lines," Cryogenics, 220-223 (1974) April.

56. Isaacs, M., "Selecting Efficient, Economical Insulation," Chemical Engineering, 143-150 (1969) March 24.

57. Anderson, P.J. and Eakin, B.E., "Insulation Essentials for Cryogenic Systems," Chicago: Institute of Gas Technology, September 1970.

58. Abramovitz, J.L., "Economic Pipe Insulation for Cold Systems," Chemical Engineering, 104-112 (1976) October 25.

59. Dainora, J., Duffy, A.R. and Atterbury, T.J., "Materials of Construction for Use in an LNG Pipeline," Final Report A.G.A. Project PR-3-42, Catalogue No. L40000, April 1968.

60. Duffy, A.R. and Dainora, J., "Considerations for LNG Pipe Material Selection," Proceedings First International Conference on LNG, Chicago, April 7-12, 1968.

61. Canuck Engineering Ltd., "LNG Pipelines - A Technology Assessment," 2 Volumes, Final Report for Government of Canada Department of Supply and Services, D.S.S. File No. 17-SQ-23440-6-9014, Calgary, Alberta, Canada: Canuck Engineering Ltd., 1977.

62. "Development of LNG Pipeline Technology," Cryogenics and Industrial Gases, 29-36 (1971) September/October.

63. J.C. Carter Company, Subsidiary of International Telephone and Telegraph Corporation, "Submerged Motor Pumps," Costa Mesa, California, 1974.

64. DiNapoli, R.N., "Pick LNG Gas Pre-Treat With Care," Hydrocarbon Processing, 93-96 (1970) December.

65. Jordan, C.H., "Natural Gas Processing at Low Temperatures," Chemical Engineering Progress, 53-55 (1972) September.

66. Kinney, G.T., "World's Biggest Helium Plant Opens," Reprint from Oil and Gas Journal, (1963) September 30.

67. Lam W.K., Fischer, G.I. and Clavey, G.M., "Low-Pressure Demethanization Techniques for Ethylene Plants," Oil and Gas Journal, 111-118 (1970) May 18.

68. Rosenzweig, M.O., "Cryogenics for Natural Gas Extraction/Fractionation," Chemical Engineering, 74-76 (1970) January 12.

69. Edwards, B.H., "Joule-Thompson Plant Gas Processing Role," Oil and Gas Journal, 139-143 (1978) May 13.

70. Bacon, K.H. (assigned to Gulf Oil Corp.), "Separation of Liquid Hydrocarbons From Natural Gas," U.S. Patent 4,022,597 (1977) May 10.

71. Child, E.F. and Robeir, A.M. (assigned to Texaco, Inc.), "Production of Methane," U.S. Patent 3,888,043 (1975) June 10.

72. Pryor, J.A. and Rowles, H.C. (assigned to Air Products and Chemicals, Inc.), "Recovery of C_2+ Hydrocarbons by Plural Stage Rectification and First Stage Dephlegmation," U.S. Patent 4,002,042 (1977) February 11.

73. Foster, R.B. et al., "Liquefied Natural Gas - An Evaluation of Aircraft Fuel and Other Potential Markets," Final Report S-377, Chicago: Institute of Gas Technology, October 1967.

74. Kniel, L., "Energy Systems for LNG Plants," Chemical Engineering Progress, 77-84 (1973) October.

75. Proctor, R.C. and Parish, R.W. (assigned to Conch International Methane Ltd.), "Means for Maintaining the Substitutability of LNG," U.S. Patent 3,302,416 (1967) February 7.

76. Eisenberg, J.D. et al., "Tankage Systems for Methane Fueled Supersonic Transport," NASA Technical Memorandum NASA TMX-52378, Cleveland: Lewis Research Center, 1967.

77. Van Dyke, B.H., "Considerations for Design and Selection of Low Temperature Piping Insulations Systems," American Gas Association Operating Section Proceedings Paper No. 76-T-43, Arlington, Virginia, 1976.

78. Weber, R.J., "The Boiloff Problem with Methane Fuel in Supersonic Aircraft," NASA Technical Memorandum NASA TM X-1604, Cleveland: Lewis Research Center, July 1968.

79. Weber, R.J., "A Review of the Potential of Liquid Methane Fuel for Supersonic Transports," Report N 68-33584, Cleveland: Lewis Research Center, 1968.

80. Vander Wall, E.M., "Investigation of the Suitability of Gelled Methane for Use in a Jet Engine," Final Report NASA CR-72876, Cleveland: NASA Lewis Research Center, March 1971.

81. Souidi, M., "Policies for Training Operating Personnel of Future Liquefaction Plants in Algeria," Session VIII Paper 3, Fourth International Conference on Liquefied Natural Gas, Algiers, Algeria, June 24-27, 1974.

82. Sipple, P.A., "LNG Peakshaving Plant - Operating Experience," Session IV Paper 5, Fourth International Conference on Liquefied Natural Gas, Algiers, Algeria, June 24-27, 1974.

83. Dean, J.W., "A Tabulation of the Thermodynamic Properties of Normal Hydrogen," NBS Technical Note 120, Boulder, Colorado: National Bureau of Standards, November 1961.

84. Hord, J., "Is Hydrogen Safe?" NBS Technical Note 690, Boulder, Colorado: National Bureau of Standards, October 1976.

85. National Fire Protection Association, "Standard for the Production, Storage and Handling of Liquefied Natural Gas (LNG)," NFPA No. 59A-1975, New York, 1975.

86. Deleted.

87. Deleted.

88. Staats, E.B., Comptroller General, "Liquefied Energy Gases Safety," EMD-78-28, Washington, D.C.: General Accounting Office, July 31, 1978.

89. Anderson, P.J. and Bodle, W.W., "Safety Considerations in the Design and Operation of LNG Terminals," Session V Paper 4, Fourth International Conference on Liquefied Natural Gas, Algiers, Algeria, June 24-27, 1974.

90. Allan, D. et al., "Technology and Current Practices for Processing, Transferring and Storing Liquefied Natural Gas," Final Report C-76971, Washington, D.C.: Office of Pipeline Safety, Department of Transportation, December 1974.

91. Daniels, E.J. and Anderson, P.J., "LNG Terminals: Existing and Proposed Systems Compared," Pipeline and Gas Journal, 44-66 (1975) September.

92. Office of Technology Assessment, "Transportation of Liquefied Natural Gas," Washington, D.C.: U.S. Government Printing Office, Stock No. 052-003-00436-4, September 1977.

93. Ebara Corporation, "Elliot-Carrier Boil Off Gas Compressor; Return Gas Blower for LNG Projects," San Francisco, n.d.

94. Daniels, E.J., Anderson, P.J. and Seay, J.G., "The LNG Industry: An Overview of Projects and Costs." Paper presented at the ASME Annual Conference, Houston, Texas, November 5-9, 1978.

95. DiNapoli, R.N., "Trends in Base Load LNG Plants," Hydrocarbon Processing, 87-90 (1975) December.

96. DiNapoli, R.N., "LNG Peakshaving Plants Require Careful Cost Estimation," Pipeline and Gas Journal 205 No. 6, 28-34 (1978) May.

97. Seay, J.G., "A Study to Ascertain the Potential for Increased Production of Natural Gas Liquids From Natural Gas," Final Report IGT Project 8972, Washington, D.C.: Federal Energy Administration, February 1976.

98. Air Products and Chemicals, Inc., "Gas Processing Systems to Liquefy, Purify, Separate," Allentown, Pennsylvania, n.d.

99. Seaton, E., "Indonesia's Arun LNG Plant Nears Completion," Oil and Gas Journal, 62-64 (1976) March 13.

100. Barlett, D.W., "Wind Tunnel Investigation of Several High Aspect-Ratio Supercritical Wing Configuration on a Wide-Body Type Fuselage," NASA TMX 71996, July 1977.

101. Butze, H.F. and Smith, A.L., "Effect of Fuel Properties on the Performance of a Single Aircraft Turbojet Combustor at Simulated Idle, Cruise and Takeoff Conditions," NASA TMX 73780, Lewis Research Center, September 1977.

1. REPORT NO. NASA CR-159320	2. GOVERNMENT ACCESSION NO.	3. RECIPIENT'S CATALOG NO.
4. TITLE AND SUBTITLE Study of Methane Fuel for Subsonic Transport Aircraft		5. REPORT DATE September, 1980
		6. PERFORMING ORG CODE
7. AUTHOR(S) L.K. Carson, G.W. Davis, E.F. Versaw, G.R. Cunnington, Jr. and E.J. Daniels		8. PERFORMING ORG REPORT NO. LR 29157
9. PERFORMING ORGANIZATION NAME AND ADDRESS LOCKHEED-CALIFORNIA COMPANY P.O. BOX 551 BURBANK, CALIFORNIA 91520		10. WORK UNIT NO.
		11. CONTRACT OR GRANT NO. NAS 1-15239
12. SPONSORING AGENCY NAME AND ADDRESS National Aeronautics and Space Administration Washington, D.C. 20546		13. TYPE OF REPORT AND PERIOD COVERED Contractor Final Report 1/78-8/79
		14. SPONSORING AGENCY CODE

15. SUPPLEMENTARY NOTES

Langley Technical Monitor: Robert D. Witcofski
Final Report

16. ABSTRACT

This investigation was undertaken to define the cost and performance of a commercial transport using liquid methane including its fuel system and the ground facility complex required for the processing and storage of methane. A cost and performance comparison was made with Jet A and hydrogen powered aircraft of the same payload and range capability. Extensive design work has been done on cryogenic fuel tanks, insulation systems, as well as the fuel system itself. Three candidate fuel tank locations were evaluated, i.e., fuselage tanks, wing tanks or external pylon tanks.

17. KEY WORDS (SUGGESTED BY AUTHOR(S))	18. DISTRIBUTION STATEMENT
Methane, alternate fuels, cryogenic fuels, cryogenic insulation, tank structure, fuel system, methane fueled aircraft	Unclassified - Unlimited

19. SECURITY CLASSIF. (OF THIS REPORT)	20. SECURITY CLASSIF. (OF THIS PAGE)	21. NO. OF PAGES	22. PRICE*
Unclassified	Unclassified	352	

For sale by the National Technical Information Service, Springfield, Virginia 22161.

End of Document